

**NON-DESTRUCTIVE DAMAGE EVALUATION BASED ON  
POWER METHOD WITH TIME COLLOCATION**

A Dissertation

by

RAN LI

Submitted to the Office of Graduate and Professional Studies of  
Texas A&M University  
in partial fulfillment of the requirements for the degree of

DOCTOR OF PHILOSOPHY

Chair of Committee,	Peter B. Keating
Committee Members,	Luciana R. Barroso
	Stefan Hurlebaus
	Alan B. Palazzolo
Head of Department,	Robin Autenrieth

May 2016

Major Subject: Civil Engineering

Copyright 2016 Ran Li

## **ABSTRACT**

The objective of this dissertation is to develop a nondestructive evaluation (NDE) method that could accurately locate and evaluate damage in mass, stiffness and damping properties of structural members. The method is based on the power (Refer to the definition in Section 2.2) equilibrium between the undamaged and damaged structural systems. The method is applicable to a variety of structures and has high tolerance capacity to noise. To demonstrate the above characteristics of the proposed method, the following several tasks will be addressed: (1) the application of the proposed method to different discrete systems with exact deformation data; (2) the application of the proposed method to different continuous systems with exact deformation data; (3) the application of the proposed method to discrete and continuous systems with noise-polluted inputs; (4) the validation of the proposed method using field data. The damage detection results from Task #1 and Task #2 indicated that the proposed method can accurately locate and evaluate damage in mass, stiffness and damping of the structure if exact deformation data were given. The results from Task #3 indicated that the proposed method is proved to be effective in locating and evaluating damage at least fewer than 5% white noise. The damage evaluation results from the field experiment showed that the proposed method is applicable to real-world damage detection by providing damage locations and estimations of damage severities.

## DEDICATION

I dedicate this dissertation to:

My mother, 闫秀平 (Yan, Xiuping) and father, 李文勇 (Li, wenyong)

who gave me the chance to experience the life that I wanted.

To my late professor, Dr. Norris Stubbs,

who helped me launched my journey in the Non-destructive Evaluation field. Without the inspiration and the enthusiasm he instilled in me, this work wouldn't have happened.

Suddenly and unexpectedly, he passed away on August 9th, 2014.

He will forever be missed.

To my professor, Dr Peter B. Keating,

who offered me great care, help, and guidance in both my academic life and my personal life. Without his knowledge and support, this work would not have been completed.

To my research fellows in the NDE field and to the people who may find this work useful and who will bring this topic on. You have my best wishes!

## **ACKNOWLEDGMENTS**

I would like to send my sincere appreciation to my advisor and chairman of my advisory committee, Dr. Peter B. Keating, for offering me tremendous help and encouragement. Without my advisor, my doctoral life would be filled with obstacles and finishing my research work would only be a dream. I would like to express my gratitude, once again, to Dr. Luciana R. Barroso, for her consistent help to both my master study and doctoral study here in Texas A&M University. With her illuminative instructions in dynamic field, I was well equipped before I started my research in the non-destructive evaluation field. I would like to thank Dr. Stefan Hurlebaus and Dr. Alan B. Palazzolo for their invaluable advice and supports, which make the proposed method become more sophisticated and practical.

With this chance, I would like to put the name of my former advisor, Dr. Norris Stubbs, here to acknowledge his irreplaceable contribution to this work and also to remind myself to express my appreciation to the important individuals around me before it becomes too late.

I gratefully acknowledge the support of California Department of Transportation (under Agreement #65A0401) and the advice from Dr. Charles Sikorsky. I would also acknowledge the help of Dr. Gianmario Benzoni from University of California, San Diego. Without their help, the research wouldn't be complete.

Finally, my deepest appreciation goes to my parents, for offering me a clear mind to see my goal and providing me a strong and enduring body to overcome all the obstacles set in



the path. By becoming a valuable individual in the society, I wish I could make them live in a proud and happy life.

# TABLE OF CONTENTS

	Page
ABSTRACT .....	ii
DEDICATION.....	iii
ACKNOWLEDGMENTS.....	iv
TABLE OF CONTENTS .....	vi
LIST OF FIGURES.....	x
LIST OF TABLES.....	xxvii
1 INTRODUCTION.....	1
1.1 Problem Statement .....	1
1.2 Background on Non-Destructive Evaluation Method .....	2
1.3 Limitations of Current Non-Destructive Evaluation Techniques.....	15
1.4 Research Objectives .....	18
1.5 Significance of This Work.....	20
2 THEORY OF DAMAGE EVALUATION ON MASS, STIFFNESS, AND DAMPING FOR DISCRETE SYSTEMS .....	22
2.1 Introduction .....	22
2.2 Development of the General Power Method .....	22
2.3 Theory for 1-DOF Spring-Mass-Damper Systems .....	25
2.4 Theory for 2-DOF Spring-Mass-Damper Systems .....	29
2.5 Theory for N-DOF Spring-Mass-Damper Systems.....	37
2.6 Theory for Isolated Spring-Mass-Damper Systems .....	51
2.7 Overall Solution Procedure .....	56
2.8 Summary .....	57

	Page
3 CASE STUDIES OF DAMAGE EVALUATION FOR DISCRETE SYSTEMS.....	58
3.1 Introduction .....	58
3.2 Damage Evaluation for a 1-DOF Spring-Mass-Damper System .....	59
3.3 Damage Evaluation for a 2-DOF Spring-Mass-Damper System .....	64
3.4 Damage Evaluation for an N-DOF Spring-Mass-Damper System .....	70
3.5 Damage Evaluation for Isolated Spring-Mass-Damper Systems .....	77
3.6 Summary .....	82
4 THEORY OF DAMAGE EVALUATION ON MASS AND STIFFNESS FOR CONTINUOUS SYSTEMS .....	83
4.1 Introduction .....	83
4.2 Theory for Rods.....	83
4.3 Theory for Euler-Bernoulli Beams .....	108
4.4 Theory for Plane Frames .....	117
4.5 Theory for Space Trusses .....	126
4.6 Overall Solution Procedure .....	137
4.7 Summary .....	138
5 CASE STUDIES OF DAMAGE EVALUATION FOR CONTINUOUS SYSTEMS .....	140
5.1 Introduction .....	140
5.2 Damage Evaluation for a Rod .....	141
5.3 Damage Evaluation for a Rod as a Whole System.....	149
5.4 Damage Evaluation for an Euler-Bernoulli Beam .....	156
5.5 Damage Evaluation for a Plain Frame .....	164
5.6 Damage Evaluation for a Space Truss.....	177
5.7 Summary .....	185
6 STUDIES OF NOISE INFLUENCE TO THE PERFORMANCE OF THE POWER METHOD.....	186
6.1 Introduction .....	186

	Page
6.2 Studies of Noise Influence to a Discrete System Using Integral Method .....	190
6.3 Studies of Noise Influence to a Discrete System Using Isolation Method .....	209
6.4 Studies of Noise Influence to a Continuous System Using Integral Method .....	231
6.5 Studies of Noise Influence to a Continuous System Using Isolation Method .....	248
6.6 Evaluation of Results .....	270
7 REANALYSIS .....	283
7.1 Introduction .....	283
7.2 Study of Nodes without External Loads (Case #7.1) .....	283
7.3 Study of Efficiency of Noise-Influence Reduction by Repeating the Experiment (Case #7.2).....	298
7.4 Study of Damage Detection in Continuous Structures with Proportional Damping (Case #7.3) .....	307
8 APPLICATION OF THE METHOD TO SHAKE TABLE TESTS.....	335
8.1 Introduction .....	335
8.2 Description of the Structure and Test Setup .....	335
8.3 Theory of Approach.....	342
8.4 Experimental Data Processing.....	353
8.5 Damage Evaluation of the Shake Table Tests .....	362
8.6 Evaluation of Designed Damage Extent .....	370
8.7 Results Discussion.....	376
8.8 Damage Evaluation with Element Damping Effect .....	378
8.9 Conclusion.....	386
9 SUMMARY AND CONCLUSIONS .....	387
9.1 Summary .....	387
9.2 Findings .....	388
9.3 Originality of This Work .....	391

	Page
9.4 Contribution of This Work .....	392
9.5 Conclusion.....	393
9.6 Future Work.....	393
REFERENCES.....	396
APPENDIX .....	402

## LIST OF FIGURES

	Page
Figure 2.1. 1-DOF Spring-Mass-Damper System.....	26
Figure 2.2. 2-DOF Spring-Mass-Damper System.....	30
Figure 2.3. 5-DOF Spring-Mass-Damper System.....	38
Figure 2.4. Isolated Spring-Mass-Damper System .....	51
Figure 3.1. Property Definition and Load Case of the 1-DOF Spring-Mass-Damper System .....	60
Figure 3.2. Applied External Load for Both the Undamaged and Damaged Cases .....	61
Figure 3.3. Displacements of the Mass Block under the Given External Load .....	61
Figure 3.4. Velocities of the Mass Block under the Given External Load .....	62
Figure 3.5. Accelerations of the Mass Block under the Given External Load .....	62
Figure 3.6. Element Damage Indices ( $\beta_i$ ) for 1-DOF Spring-Mass-Damper System .....	63
Figure 3.7. Element Damage Severities ( $a_i$ ) for 1-DOF Spring-Mass-Damper System .....	64
Figure 3.8. Property Definition and Load Case of the 2-DOF Spring-Mass-Damper System .....	65
Figure 3.9. Applied External Load for Both the Undamaged and Damaged Cases .....	66
Figure 3.10. Displacements of the Mass Block 1 under the Given External Load .....	67
Figure 3.11. Velocities of the Mass Block 1 under the Given External Load .....	67

	Page
Figure 3.12. Accelerations of the Mass Block 1 under the Given External Load .....	68
Figure 3.13. Element Damage Indices ( $\beta_i$ ) for 2-DOF Spring-Mass-Damper System .....	69
Figure 3.14. Element Damage Severities ( $a_i$ ) for 2-DOF Spring-Mass-Damper System .....	69
Figure 3.15. Property Definition and Load Case of the 5-DOF Spring-Mass-Damper System .....	71
Figure 3.16. Applied External Load for Both the Undamaged and Damaged Cases .....	73
Figure 3.17. Displacements of the Mass Block 1 under the Given External Load .....	73
Figure 3.18. Velocities of the Mass Block 1 under the Given External Load .....	74
Figure 3.19. Accelerations of the Mass Block 1 under the Given External Load .....	74
Figure 3.20. Element Damage Indices ( $\beta_i$ ) for 5-DOF Spring-Mass-Damper System .....	76
Figure 3.21. Element Damage Severities ( $a_i$ ) for 5-DOF Spring-Mass-Damper System .....	76
Figure 3.22. Property Definition and Load Case of the Isolated Spring-Mass-Damper System .....	78
Figure 3.23. Element Damage Indices ( $\beta_i$ ) for Isolated Spring-Mass-Damper System .....	80
Figure 3.24. Element Damage Severities ( $a_i$ ) for Isolated Spring-Mass-Damper System .....	81
Figure 4.1. Two nearby Rod Elements .....	84
Figure 4.2. Free Body Diagram of Node $i$ under Axial and Torsional Effects .....	85

	Page
Figure 4.3. Two nearby Rod Elements .....	95
Figure 4.4. Free Body Diagram of Node $i$ under Axial Effects.....	95
Figure 4.5. Two nearby Euler–Bernoulli Beam Elements Considering Shear Force and Bending Moment.....	109
Figure 4.6. Free Body Diagram of Node $i$ Considering Shear Force and Bending Moment .....	109
Figure 4.7. Two nearby Plane Frame Elements.....	118
Figure 4.8. Free Body Diagram of Node $i$ Considering Axial, Shear Forces, and Bending Moment.....	118
Figure 4.9. One Joint from a Space Truss with All Bars Joined to the Joint $\gamma$ .....	127
Figure 4.10. Free Body Diagram of Joint $\gamma$ in Space .....	128
Figure 5.1. Geometry, Damage Scenario, and Finite Element Discretization of the Rod .....	143
Figure 5.2. Geometry of the Cross-Section of the Rod.....	144
Figure 5.3. Displacements in Axial Direction of the Node 13 of the Undamaged and Damaged Rods under the Given External Load .....	144
Figure 5.4. Velocities of the Node 13 in Axial Direction of the Undamaged and Damaged Rods under the Given External Load.....	145
Figure 5.5. Accelerations of the Node 13 in Axial Direction of the Undamaged and Damaged Rods under the Given External Load .....	145
Figure 5.6. Damage Indices of Nodal Mass ( $\beta_{mi}$ ) for the Rod under Axial and Torsional Vibrations .....	147



	Page
Figure 5.7. Damage Severities of Nodal Mass ( $a_{mi}$ ) for the Rod under Axial and Torsional Vibrations .....	147
Figure 5.8. Damage Indices of Element Stiffness ( $\beta_{ki}$ ) for the Rod under Axial and Torsional Vibrations.....	148
Figure 5.9. Damage Severities of Element Stiffness ( $a_{ki}$ ) for the Rod under Axial and Torsional Vibrations.....	148
Figure 5.10. Geometry, Damage Scenario, and Finite Element Discretization of the Rod .....	151
Figure 5.11. Displacements in Axial Direction of Node 13 of the Undamaged and Damaged Rods under the Given External Load .....	151
Figure 5.12. Velocities of Node 13 in Axial Direction of the Undamaged and Damaged Rods under the Given External Load.....	152
Figure 5.13. Accelerations of Node 13 in Axial Direction of the Undamaged and Damaged Rods under the Given External Load .....	152
Figure 5.14. Damage Indices of Nodal Mass ( $\beta_{mi}$ ) for the Rod under Axial and Torsional Vibrations .....	154
Figure 5.15. Damage Severities of Nodal Mass ( $a_{mi}$ ) for the Rod under Axial and Torsional Vibrations.....	154
Figure 5.16. Damage Indices of Element Stiffness ( $\beta_{ki}$ ) for the Rod under Axial and Torsional Vibrations.....	155
Figure 5.17. Damage Severities of Element Stiffness ( $a_{ki}$ ) for the Rod under Axial and Torsional Vibrations.....	155
Figure 5.18. Geometry, Damage Scenario, and Load Case for the Propped Cantilever .....	158
Figure 5.19. Geometry of the Cross-Section of the I Beam .....	158

	Page
Figure 5.20. Deflection of the Node 7 of the Undamaged and Damaged Cases under the Given External Load .....	159
Figure 5.21. Velocities in Transverse Direction of the Node 7 of the Undamaged and Damaged Cases under the Given External Load .....	159
Figure 5.22. Accelerations in Transverse Direction of the Node 7 of the Undamaged and Damaged Cases under the Given External Load.....	160
Figure 5.23. Damage Indices of Nodal Mass ( $\beta_{mi}$ ) for the Propped Cantilever .....	162
Figure 5.24. Damage Severities of Nodal Mass ( $a_{mi}$ ) for the Propped Cantilever .....	162
Figure 5.25. Damage Indices of Element Stiffness ( $\beta_{ki}$ ) for the Propped Cantilever .....	163
Figure 5.26. Damage Severities of Element Stiffness ( $a_{ki}$ ) for the Propped Cantilever .....	163
Figure 5.27. Geometry, Damage Scenario, and Finite Element Discretization for the Two-Bay Frame .....	167
Figure 5.28. Cross Sectional Geometries of the Three Elastic Isolators .....	167
Figure 5.29. Displacements of the Node 61 on the Continuous Beam for Both the Undamaged and Damaged Cases under the Given External Load .....	168
Figure 5.30. Velocities of the Node 61 on the Continuous Beam for Both the Undamaged and Damaged Cases under the Given External Load.....	168
Figure 5.31. Accelerations of the Node 61 on the Continuous Beam for Both the Undamaged and Damaged Cases under the Given External Load.....	169
Figure 5.32. Damage Indices of Nodal Mass ( $\beta_{mi}$ ) for the Continuous Beam from the Two-Bay Frame .....	169

	Page
Figure 5.33. Damage Severities of Nodal Mass ( $a_{mi}$ ) for the Continuous Beam from the Two-Bay Frame .....	170
Figure 5.34. Damage Indices of Element Stiffness ( $\beta_{ki}$ ) for the Continuous Beam from the Two-Bay Frame .....	170
Figure 5.35. Damage Severities of Element Stiffness ( $a_{ki}$ ) for the Continuous Beam from the Two-Bay Frame .....	171
Figure 5.36. Damage Indices of Nodal Mass ( $\beta_{mi}$ ) for the Isolator and Column A from the Two-Bay Frame .....	171
Figure 5.37. Damage Severities of Nodal Mass ( $a_{mi}$ ) for the Isolator and Column A from the Two-Bay Frame .....	172
Figure 5.38. Damage Indices of Element Stiffness ( $\beta_{ki}$ ) for the Isolator and Column A from the Two-Bay Frame .....	172
Figure 5.39. Damage Severities of Element Stiffness ( $a_{ki}$ ) for the Isolator and Column A from the Two-Bay Frame .....	173
Figure 5.40. Damage Indices of Nodal Mass ( $\beta_{mi}$ ) for the Isolator and Column B from the Two-Bay Frame .....	173
Figure 5.41. Damage Severities of Nodal Mass ( $a_{mi}$ ) for the Isolator and Column B from the Two-Bay Frame .....	174
Figure 5.42. Damage Indices of Element Stiffness ( $\beta_{ki}$ ) for the Isolator and Column B from the Two-Bay Frame .....	174
Figure 5.43. Damage Severities of Element Stiffness ( $a_{ki}$ ) for the Isolator and Column B from the Two-Bay Frame .....	175
Figure 5.44. Damage Indices of Nodal Mass ( $\beta_{mi}$ ) for the Isolator and Column C from the Two-Bay Frame .....	175

	Page
Figure 5.45. Damage Severities of Nodal Mass ( $a_{mi}$ ) for the Isolator and Column C from the Two-Bay Frame.....	176
Figure 5.46. Damage Indices of Element Stiffness ( $\beta_{ki}$ ) for the Isolator and Column C from the Two-Bay Frame.....	176
Figure 5.47. Damage Severities of Element Stiffness ( $a_{ki}$ ) for the Isolator and Column C from the Two-Bay Frame .....	177
Figure 5.48. Geometry, Damage Scenario, and Finite Element Discretization for the Space Truss.....	179
Figure 5.49. Displacements of the Joint 6 in Global X Direction for Both the Undamaged and Damaged Systems under the Given External Load.....	180
Figure 5.50. Velocities of the Joint 6 in Global X Direction for Both the Undamaged and Damaged Systems under the Given External Load.....	180
Figure 5.51. Accelerations of the Joint 6 in Global X Direction for Both the Undamaged and Damaged Systems under the Given External Load.....	181
Figure 5.52. Damage Indices of Joint Mass ( $\beta_{mi}$ ) for the Space Truss.....	183
Figure 5.53. Damage Severities of Joint Mass ( $a_{mi}$ ) for the Space Truss.....	183
Figure 5.54. Damage Indices of Member Stiffness ( $\beta_{ki}$ ) for the Space Truss .....	184
Figure 5.55. Damage Severities of Member Stiffness ( $a_{ki}$ ) for the Space Truss .....	184
Figure 6.1. Property Definition and Load Case of the 5-DOF Spring-Mass-Damper System .....	191
Figure 6.2. Applied External Excitation Forces at Each Mass Block .....	193

	Page
Figure 6.3. Noise-Polluted Accelerations of Mass Block 2 for the Undamaged and Damaged Models of Case #6.1 (1% Noise): (a) Full Plot and (b) Zoomed in Plot .....	194
Figure 6.4. Filtered Noise-Polluted Accelerations of Mass Block 2 for the Undamaged and Damaged Models of Case #6.1 (1% Noise): (a) Full Plot and (b) Zoomed in Plot .....	195
Figure 6.5. Estimated Velocities of Mass Block 2 for the Undamaged and Damaged Models of Case #6.1 (1% Noise): (a) Full Plot and (b) Zoomed in Plot .....	196
Figure 6.6. Estimated Displacements of Mass Block 2 for the Undamaged and Damaged Models of Case #6.1 (1% Noise): (a) Full Plot and (b) Zoomed in Plot.....	197
Figure 6.7. Damage Indices ( $\beta_i$ ) for 5-DOF Spring-Mass-Damper System with Noise-Polluted Accelerations (1% Noise).....	199
Figure 6.8. Damage Severities ( $a_i$ ) for 5-DOF Spring-Mass-Damper System with Noise-Polluted Accelerations (1% Noise).....	199
Figure 6.9. Normalized Damage Indices ( $\beta_{n,i}$ ) for 5-DOF Spring-Mass-Damper System with Noise-Polluted Accelerations (1% Noise) .....	200
Figure 6.10. Probability Damage Indices ( $\beta_{p,i}$ ) for 5-DOF Spring-Mass-Damper System with Noise-Polluted Accelerations (1% Noise) .....	200
Figure 6.11. Noise-Polluted Accelerations of Mass Block 2 for the Undamaged and Damaged Models of Case #6.2 (5% Noise): (a) Full Plot and (b) Zoomed in Plot.....	202
Figure 6.12. Filtered Noise-Polluted Accelerations of Mass Block 2 for the Undamaged and Damaged Models of Case #6.2 (5% Noise): (a) Full Plot and (b) Zoomed in Plot .....	203

	Page
Figure 6.13. Estimated Velocities of Mass Block 2 for the Undamaged and Damaged Models of Case #6.2 (5% Noise): (a) Full Plot and (b) Zoomed in Plot.....	204
Figure 6.14. Estimated Displacements of Mass Block 2 for the Undamaged and Damaged Models of Case #6.2 (5% Noise): (a) Full Plot and (b) Zoomed in Plot.....	205
Figure 6.15. Damage Indices ( $\beta_i$ ) for 5-DOF Spring-Mass-Damper System with Noise-Polluted Accelerations (5% Noise).....	207
Figure 6.16. Damage Severities ( $a_i$ ) for 5-DOF Spring-Mass-Damper System with Noise-Polluted Accelerations (5% Noise).....	207
Figure 6.17. Normalized Damage Indices ( $\beta_{n,i}$ ) for 5-DOF Spring-Mass-Damper System with Noise-Polluted Accelerations (5% Noise).....	208
Figure 6.18. Probability Damage Indices ( $\beta_{p,i}$ ) for 5-DOF Spring-Mass-Damper System with Noise-Polluted Accelerations (5% Noise).....	208
Figure 6.19. Noise-Polluted Accelerations of Mass Block 2 for the Undamaged and Damaged Models of Case #6.3 (1% Noise): (a) Full Plot and (b) Zoomed in Plot.....	212
Figure 6.20. Filtered Noise-Polluted Accelerations of Mass Block 2 for the Undamaged and Damaged Models of Case #6.3 (1% Noise): (a) Full Plot and (b) Zoomed in Plot .....	213
Figure 6.21. Estimated Velocities of Mass Block 2 for the Undamaged and Damaged Models of Case #6.3 (1% Noise): (a) Full Plot and (b) Zoomed in Plot.....	214
Figure 6.22. Estimated Displacements of Mass Block 2 for the Undamaged and Damaged Models of Case #6.3 (1% Noise): (a) Full Plot and (b) Zoomed in Plot.....	215

	Page
Figure 6.23. Damage Indices ( $\beta_i$ ) for the 5 Isolated Spring-Mass-Damper System with Noise-Polluted Accelerations (1% Noise).....	217
Figure 6.24. Damage Severities ( $a_i$ ) for 5-DOF Spring-Mass-Damper System with Noise-Polluted Accelerations (1% Noise).....	218
Figure 6.25. Normalized Damage Indices ( $\beta_{n,i}$ ) for 5-DOF Spring-Mass-Damper System with Noise-Polluted Accelerations (1% Noise).....	219
Figure 6.26. Damage Possibility Indices ( $\beta_{p,i}$ ) for 5-DOF Spring-Mass-Damper System with Noise-Polluted Accelerations (1% Noise).....	220
Figure 6.27. Noise-Polluted Accelerations of Mass Block 2 for the Undamaged and Damaged Models of Case #6.4 (5% Noise): (a) Full Plot and (b) Zoomed in Plot .....	222
Figure 6.28. Filtered Noise-Polluted Accelerations of Mass Block 2 for the Undamaged and Damaged Models of Case #6.4 (5% Noise): (a) Full Plot and (b) Zoomed in Plot .....	223
Figure 6.29. Estimated Velocities of Mass Block 2 for the Undamaged and Damaged Models of Case #6.4 (5% Noise): (a) Full Plot and (b) Zoomed in Plot.....	224
Figure 6.30. Estimated Displacements of Mass Block 2 for the Undamaged and Damaged Models of Case #6.4 (5% Noise): (a) Full Plot and (b) Zoomed in Plot.....	225
Figure 6.31. Damage Indices ( $\beta_i$ ) for the 5 Isolated Spring-Mass-Damper System with Noise-Polluted Accelerations (5% Noise).....	227
Figure 6.32. Damage Severities ( $a_i$ ) for 5-DOF Spring-Mass-Damper System with Noise-Polluted Accelerations (5% Noise).....	228
Figure 6.33. Normalized Damage Indices ( $\beta_{n,i}$ ) for 5-DOF Spring-Mass-Damper System with Noise-Polluted Accelerations (5% Noise).....	229

	Page
Figure 6.34. Damage Possibility Indices ( $\beta_{p,i}$ ) for 5-DOF Spring-Mass-Damper System with Noise-Polluted Accelerations (5% Noise) .....	230
Figure 6.35. Geometry and Damage Scenario for the Fixed-Fixed Beam .....	233
Figure 6.36. Noise-Polluted Accelerations of Node 2 for the Undamaged and Damaged Models of Case #6.5 (1% Noise): (a) Full Plot and (b) Zoomed in Plot .....	234
Figure 6.37. Filtered Noise-Polluted Accelerations of Node 2 for the Undamaged and Damaged Models of Case #6.5 (1% Noise): (a) Full Plot and (b) Zoomed in Plot .....	235
Figure 6.38. Estimated Velocities of Node 2 for the Undamaged and Damaged Models of Case #6.5 (1% Noise): (a) Full Plot and (b) Zoomed in Plot .....	236
Figure 6.39. Estimated Displacements of Node 2 for the Undamaged and Damaged Models of Case #6.5 (1% Noise): (a) Full Plot and (b) Zoomed in Plot .....	237
Figure 6.40. Damage Indices ( $\beta_i$ ) for the Fixed-Fixed Beam with Noise-Polluted Accelerations (1% Noise).....	238
Figure 6.41. Damage Severities ( $a_i$ ) for the Fixed-Fixed Beam with Noise-Polluted Accelerations (1% Noise).....	239
Figure 6.42. Normalized Damage Indices ( $\beta_{n,i}$ ) for the Fixed-Fixed Beam with Noise-Polluted Accelerations (1% Noise).....	239
Figure 6.43. Probability Damage Indices ( $\beta_{p,i}$ ) for the Fixed-Fixed Beam with Noise-Polluted Accelerations (1% Noise).....	240
Figure 6.44. Noise-Polluted Accelerations of Node 2 for the Undamaged and Damaged Models of Case #6.6 (5% Noise): (a) Full Plot and (b) Zoomed in Plot .....	241



Figure 6.45. Filtered Noise-Polluted Accelerations of Node 2 for the Undamaged and Damaged Models of Case #6.6 (5% Noise): (a) Full Plot and (b) Zoomed in Plot .....	243
Figure 6.46. Estimated Velocities of Node 2 for the Undamaged and Damaged Models of Case #6.6 (5% Noise): (a) Full Plot and (b) Zoomed in Plot .....	244
Figure 6.47. Estimated Displacements of Node 2 for the Undamaged and Damaged Models of Case #6.6 (5% Noise): (a) Full Plot and (b) Zoomed in Plot .....	245
Figure 6.48. Damage Indices ( $\beta_i$ ) for the Fixed-Fixed Beam with Noise-Polluted Accelerations (5% Noise).....	246
Figure 6.49. Damage Severities ( $a_i$ ) for the Fixed-Fixed Beam with Noise-Polluted Accelerations (5% Noise).....	247
Figure 6.50. Normalized Damage Indices ( $\beta_{n,i}$ ) for the Fixed-Fixed Beam with Noise-Polluted Accelerations (5% Noise).....	247
Figure 6.51. Probability Damage Indices ( $\beta_{p,i}$ ) for the Fixed-Fixed Beam with Noise-Polluted Accelerations (5% Noise).....	248
Figure 6.52. Noise-Polluted Accelerations of Node 2 for the Undamaged and Damaged Models of Case #6.7 (5% Noise): (a) Full Plot and (b) Zoomed in Plot.....	251
Figure 6.53. Filtered Noise-Polluted Accelerations of Node 2 for the Undamaged and Damaged Models of Case #6.7 (5% Noise): (a) Full Plot and (b) Zoomed in Plot .....	252
Figure 6.54. Estimated Velocities of Node 2 for the Undamaged and Damaged Models of Case #6.7 (5% Noise): (a) Full Plot and (b) Zoomed in Plot .....	253

	Page
Figure 6.55. Estimated Displacements of Node 2 for the Undamaged and Damaged Models of Case #6.7 (5% Noise): (a) Full Plot and (b) Zoomed in Plot .....	254
Figure 6.56. Damage Indices ( $\beta_i$ ) for the Fixed-Fixed Beam with Noise-Polluted Accelerations Using Isolated Beam Element Analysis Method (1% Noise).....	256
Figure 6.57. Damage Severities ( $a_i$ ) for the Fixed-Fixed Beam with Noise-Polluted Accelerations Using Isolated Beam Element Analysis Method (1% Noise) .....	257
Figure 6.58. Normalized Damage Indices ( $\beta_{n,i}$ ) for the Fixed-Fixed Beam with Noise-Polluted Accelerations Using Isolated Beam Element Analysis Method (1% Noise) .....	258
Figure 6.59. Probability Damage Indices ( $\beta_{p,i}$ ) for the Fixed-Fixed Beam with Noise-Polluted Accelerations Using Isolated Beam Element Analysis Method (1% Noise) .....	259
Figure 6.60. Noise-Polluted Accelerations of Node 2 for the Undamaged and Damaged Models of Case #6.8 (5% Noise): (a) Full Plot and (b) Zoomed in Plot .....	261
Figure 6.61. Filtered Noise-Polluted Accelerations of Node 2 for the Undamaged and Damaged Models of Case #6.8 (5% Noise): (a) Full Plot and (b) Zoomed in Plot .....	262
Figure 6.62. Estimated Velocities of Node 2 for the Undamaged and Damaged Models of Case #6.8 (5% Noise): (a) Full Plot and (b) Zoomed in Plot .....	263
Figure 6.63. Estimated Displacements of Node 2 for the Undamaged and Damaged Models of Case #6.8 (5% Noise): (a) Full Plot and (b) Zoomed in Plot .....	264

	Page
Figure 6.64. Damage Indices ( $\beta_i$ ) for the Fixed-Fixed Beam with Noise-Polluted Accelerations Using Isolated Beam Element Analysis Method (5% Noise) .....	266
Figure 6.65. Damage Severities ( $a_i$ ) for the Fixed-Fixed Beam with Noise-Polluted Accelerations Using Isolated Beam Element Analysis Method (5% Noise) .....	267
Figure 6.66. Normalized Damage Indices ( $\beta_{n,i}$ ) for the Fixed-Fixed Beam with Noise-Polluted Accelerations Using Isolated Beam Element Analysis Method (5% Noise) .....	268
Figure 6.67. Damage Possibility Indices ( $\beta_{p,i}$ ) for the Fixed-Fixed Beam with Noise-Polluted Accelerations Using Isolated Beam Element Analysis Method (5% Noise) .....	269
Figure 7.1. Two nearby Plane Frame Elements.....	285
Figure 7.2. Free Body Diagram of Node $i$ Considering Axial, Shear Forces, and Bending Moment .....	285
Figure 7.3. Geometry and Damage Scenario for the Cantilever Beam.....	291
Figure 7.4. Applied External Load at the Free End of the Cantilever.....	292
Figure 7.5. Displacements in Axial Direction of Node 7 of the Cantilever under the Given External Load: (a) Full Plot and (b) Zoomed in Plot.....	293
Figure 7.6. Velocities in Axial Direction of the Node 7 of the Cantilever under the Given External Load: (a) Full Plot and (b) Zoomed in Plot.....	294
Figure 7.7. Accelerations in Axial Direction of Node 7 of the Cantilever under the Given External Load: (a) Full Plot and (b) Zoomed in Plot.....	295
Figure 7.8. Damage Indices ( $\beta_i$ ) for the Fixed-Fixed Beam with Proportional Damping Using Isolated Beam Element Analysis Method .....	296

	Page
Figure 7.9. Damage Severities ( $a_i$ ) for the Fixed-Fixed Beam with Proportional Damping Using Isolated Beam Element Analysis Method .....	297
Figure 7.10. Averaged Damage Indices ( $\beta_i$ ) for 5-DOF Spring-Mass-Damper System with Noise-Polluted Accelerations (5% Noise, Ten Tests) .....	301
Figure 7.11. Averaged Damage Severities ( $a_i$ ) for 5-DOF Spring-Mass-Damper System with Noise-Polluted Accelerations (5% Noise, Ten Tests) .....	301
Figure 7.12. Normalized Averaged Damage Indices ( $\beta_{n,i}$ ) for 5-DOF Spring-Mass-Damper System with Noise-Polluted Accelerations (5% Noise, Ten Tests).....	302
Figure 7.13. Probability Damage Indices ( $\beta_{p,i}$ ) for 5-DOF Spring-Mass-Damper System with Noise-Polluted Accelerations (5% Noise, Ten Tests) .....	302
Figure 7.14. Damage Indices ( $\beta_i$ ) for 5-DOF Spring-Mass-Damper System with Averaged Noise-Polluted Accelerations (5% Noise, Ten Tests).....	305
Figure 7.15. Damage Severities ( $a_i$ ) for 5-DOF Spring-Mass-Damper System with Averaged Noise-Polluted Accelerations (5% Noise, Ten Tests).....	305
Figure 7.16. Normalized Damage Indices ( $\beta_{n,i}$ ) for 5-DOF Spring-Mass-Damper System with Averaged Noise-Polluted Accelerations (5% Noise, Ten Tests).....	306
Figure 7.17. Probability Damage Indices ( $\beta_{p,i}$ ) for 5-DOF Spring-Mass-Damper System with Averaged Noise-Polluted Accelerations (5% Noise, Ten Tests).....	306
Figure 7.18. Free Body Diagram of Node i Considering Axial, Shear Forces, and Bending Moment .....	308
Figure 7.19. Geometry of the Fixed-Fixed Beam with Proportional Damping .....	327

	Page
Figure 7.20. Displacements in Transverse Direction of Node 4 of the Fixed-Fixed Beam under the Given External Load: (a) Full Plot and (b) Zoomed in Plot.....	328
Figure 7.21. Velocities in Transverse Direction of the Node 4 of the Fixed-Fixed Beam under the Given External Load: (a) Full Plot and (b) Zoomed in Plot.....	329
Figure 7.22. Accelerations in Transverse Direction of Node 4 of the Fixed-Fixed Beam under the Given External Load: (a) Full Plot and (b) Zoomed in Plot.....	330
Figure 7.23. Damage Indices ( $\beta_i$ ) for the Fixed-Fixed Beam with Proportional Damping Using Isolated Beam Element Analysis Method .....	332
Figure 7.24. Damage Severities ( $a_i$ ) for the Fixed-Fixed Beam with Proportional Damping Using Isolated Beam Element Analysis Method .....	333
Figure 8.1. Test Setup and Global Coordinate System (Benzoni et al. 2012).....	338
Figure 8.2. Geometry of the Structure under Testing: (a) Geometry of Columns and (b) Geometry of Deck (Benzoni et al. 2012).....	339
Figure 8.3. Locations of Accelerometers and Damage Scenarios .....	341
Figure 8.4. Locations of String Pots (Benzoni et al. 2012).....	341
Figure 8.5. Comparison of the Measured Accelerations from Tri-Axis and Single-Axis Accelerometers (Test #11).....	343
Figure 8.6. Simplified Numerical Model for the Bridge Model .....	344
Figure 8.7. Free Body Diagram Analysis of the Deck (Element #2) .....	344
Figure 8.8. Measured Displacement Time Histories by String Pots from Test #01: (a) Full Plot and (b) Zoomed in Plot .....	354

	Page
Figure 8.9. Measured Displacement Time Histories by String Pots from Test #03: (a) Full Plot and (b) Zoomed in Plot.....	356
Figure 8.10. Measured Displacement Time Histories by String Pots from Test #11: (a) Full Plot and (b) Zoomed in Plot.....	357
Figure 8.11. Measured Displacement Time Histories by String Pots from Test #16: (a) Full Plot and (b) Zoomed in Plot.....	358
Figure 8.12. Power Spectrum Density Analysis of Displacements from String Pots from Test#11: (a) Full Plot and (b) Zoomed in Plot .....	365
Figure 8.13. Filtered Displacement Time Histories Recorded By String Pots from Test#11: (a) Full Plot and (b) Zoomed in Plot .....	367
Figure 8.14. Filtered Velocity Time Histories at the Locations of the String Pots from Test#11: (a) Full Plot and (b) Zoomed in Plot .....	368
Figure 8.15. Filtered Acceleration Time Histories at the Locations of the String Pots from Test#11: (a) Full Plot and (b) Zoomed in Plot .....	369
Figure 8.16. Layout of the Cross Section of the Column of the Bridge Model .....	371

## LIST OF TABLES

	Page
Table 3.1. Physical Properties of the 1-DOF Spring-Mass-Damper System .....	60
Table 3.2. Damage Detection Results for the 1-DOF Spring-Mass-Damper System .....	63
Table 3.3. Physical Properties of the 2-DOF System .....	66
Table 3.4. Damage Detection Results for the 2-DOF Spring-Mass-Damper System .....	68
Table 3.5. Physical Properties of the 5-DOF System .....	72
Table 3.6. Damage Detection Results for the 5-DOF Spring-Mass-Damper System .....	75
Table 3.7. Physical Properties of the Isolated Spring-Mass-Damper System .....	78
Table 3.8. Damage Detection Results for the Isolated Spring-Mass-Damper System .....	79
Table 5.1. Damage Detection Results for the Rod under Axial and Torsional Vibrations .....	146
Table 5.2. Damage Detection Results for the Analysis of Rod under Axial As a Whole .....	153
Table 5.3. Damage Detection Results for the Propped Cantilever .....	161
Table 5.4. Damage Detection Results for the Space Truss.....	182
Table 6.1. Physical Properties of the 5-DOF System for Noise Study.....	192

	Page
Table 6.2. Damage Detection Results for the 5-DOF Spring-Mass-Damper System (1% Noise Pollution) .....	198
Table 6.3. Damage Detection Results for the 5-DOF Spring-Mass-Damper System (5% Noise Pollution) .....	206
Table 6.4. Physical Properties of the 5 Isolated Spring-Mass-Damper Systems for Noise Study.....	211
Table 6.5. Damage Detection Results for the 5 Isolated Spring-Mass-Damper System (1% Noise Pollution) .....	216
Table 6.6. Damage Detection Results for the 5 Isolated Spring-Mass-Damper System (5% Noise Pollution) .....	226
Table 6.7. Damage Detection Results for the Fixed-Fixed Beam (1% Noise Pollution).....	238
Table 6.8. Damage Detection Results for the Fixed-Fixed Beam (5% Noise Pollution).....	246
Table 6.9. Damage Detection Results for the Fixed-Fixed Beam Using Isolated Method (1% Noise Pollution) .....	255
Table 6.10. Damage Detection Results for the Fixed-Fixed Beam Using Isolated Method (1% Noise Pollution) .....	265
Table 6.11. Results Evaluation for Discrete System with 1% Noise Pollution Using Integral Method .....	271
Table 6.12. Results Evaluation for Discrete System with 5% Noise Pollution Using Integral Method .....	272
Table 6.13. Results Evaluation for Discrete System with 1% Noise Pollution Using Isolated Method .....	274



	Page
Table 6.14. Results Evaluation for Discrete System with 5% Noise Pollution Using Isolated Method .....	276
Table 6.15. Results Evaluation for Continuous System with 1% Noise Pollution Using Integral Method .....	278
Table 6.16. Results Evaluation for Continuous System with 5% Noise Pollution Using Integral Method .....	279
Table 6.17. Results Evaluation for Continuous System with 1% Noise Pollution Using Isolated Method .....	281
Table 6.18. Results Evaluation for Continuous System with 5% Noise Pollution Using Isolated Method .....	282
Table 7.1. Damage Detection Results for the Cantilever under Axial Vibrations .....	296
Table 7.2. Summary of Damage Detection Results for the 5-DOF Spring-Mass-Damper System (5% Noise Pollution, Ten Tests).....	300
Table 7.3. Damage Detection Results for the 5-DOF Spring-Mass-Damper System Based on Averaged Inputs (5% Noise Pollution, Ten Tests) .....	304
Table 7.4. Designed Damage Scenario for the Fixed-Fixed Beam .....	327
Table 7.5. Damage Detection Results for the Fixed-Fixed Beam with Proportional Damping .....	331
Table 8.1. Locations of Bending Mode and Selected Pass Band of Digital Filters.....	370
Table 8.2. Damage Indices and Damage Severities for the Bridge Model .....	370
Table 8.3. Cross-Sectional Properties of the Tube and Channel Sections.....	372
Table 8.4. Moment of Inertia of the Cross Section of Column .....	376
Table 8.5. Evaluation of Damage Indices and Damage Severities.....	376

	Page
Table 8.6. Damage Indices and Damage Severities for the Bridge Model with Element Damping Effects .....	384

# **1 INTRODUCTION**

Damage in civil infrastructure can be caused by either aging from daily use or extreme loads from natural or man-made disasters. It's important to be able to measure damage in structures as well as protect life and property from the potential losses due to the existing damage in the structure. Thus, it's necessary to have an efficient non-destructive evaluation method which can locate and evaluate damage accurately. When compared to the local damage detection techniques, such as visual and ultrasonic inspection, global damage detection techniques are more efficient for use on civil infrastructures. Frequency-domain damage detection and time-domain damage detection techniques are two major categories of global damage detection techniques. Compared to the frequency-domain global damage detection techniques, the time-domain global damage detection techniques can be used to detect not only stiffness damage, but also damping and mass damage. Also, it's more convenient to apply the time-domain global damage detection techniques, since this type of global damage detection techniques is based on response time history, which can be measured directly from field experiments.

## **1.1 PROBLEM STATEMENT**

Since the failure of the civil infrastructures may result in serious life and property loss, the prediction and evaluation of existing damage in civil structures is critical. Non-destructive damage evaluation (NDE) techniques can play a key role.

Efficient non-destructive damage detection technique can save human lives, protect property and reduce maintenance costs and time. Because of this, non-destructive

damage detection techniques have been very well focused over the past few decades.

Non-destructive damage detection method can be categorized as either local methods or global methods. Local methods are generally based on ultrasonic, visual, or radiograph inspection. Global methods include damage detection methods based on modal information or the vibration time history of structures. Local NDE methods have two critical limitations: (i) the general damage locations need to be known beforehand; (ii) the general damage locations are accessible. Compared to local NDE methods, the global NDE methods are more economical and applicable to some specific purposes, such as life-cycle automated health monitoring.

The global method can also be classified into two sub-categories: (1) global method in time domain; (2) global method in frequency domain. Compared to the global NDE method in frequency domain, the global NDE method in time domain is able to directly use the measured time histories to detect damage in mass, stiffness, and damping without going through modal analysis.

This study presents a global NDE method in time domain which can be used to detect, locate, and evaluate the damage in the structure. Further, the structural damage may be defined as the changes of mass, stiffness, and damping.

## **1.2 BACKGROUND ON NON-DESTRUCTIVE EVALUATION METHOD**

### **1.2.1 Review of Frequency-Domain Methods**

In the past two decades, much research work focusing on damage detection in existed structures has been carried out. The following discussion briefly reviews significant

research findings.

Adams et al. (1975) proposed a method using the changes of natural frequencies and damping ratios as indications of damage. The theory is based on the assumption that any damage in the material could result in shifts of natural frequencies and damping ratios. The proposed theory has been demonstrated by its application to complex composite structures.

Loland and Dodds (1976) tried to detect the existences of damage by observing the changes of frequencies. Since the natural frequencies of a structure are determined by the geometry, stiffness, and mass of the structure, the natural frequencies may change if stiffness of members is changed. The proposed method was also validated using the acceleration records from three different offshore platforms in the southern sector of the North Sea. The advantages of this method are: (1) the instruments required by the method is only accelerometers; (2) the post analysis after the data collection is simple and can be performed automatically by computer. One of the limitations of this method is that it is hard to locate damaged area only by observing the changes of the frequencies. Also, the changes of the natural frequencies are controlled by the mass of the structure as well. If both mass and stiffness of a structure are changed, detect and locate damage may even harder. Moreover, the sensitivity of this method to the initial stage of members' damage is unknown. This method cannot provide evaluations to the damage severities.

Cawley and Adams (1979) presented a further study of the NDE method by investigating the changes of frequencies. Based on the idea that the ratio of the frequency changes in two modes is only a function of the damage location, the locations of damage can be

found by matching the experimentally measured ratio of frequency changes with the theoretically determined ratio, which is corresponded to a specified damage location. The major advantage of this method is that natural frequencies and damping of a structure need only be measured at any one location of the structure. However, since the method uses a passive procedure to locate and evaluate the damage by matching the measured values with the computer simulated values, the amount of computation time can be significant.

Allemang and Brown (1982) proposed a criterion to detect the existence of damage in structures by checking the consistency of mode shapes between the damaged and undamaged structures. The proposed criterion is known as the Modal Assurance Criterion (MAC). The MAC varies from zero to one, which is determined by the expression of the MAC. When the MAC is equal to zero, it means no linearly dependent relationship existed in the mode shapes from the undamaged and damaged structures, which means the structure may suffer severe damage. On the other hand, when the MAC is equal to one, it means the mode shapes from the damaged structure is linearly dependent to the mode shapes from the undamaged structure, which may indicates no damage or insignificant damage in the structure. This method can be easily performed if the mode shapes from the damaged and undamaged structures are given. However, the MAC criterion can only be an approximate primary check, because (1) the differences between the mode shapes from the undamaged and damaged structures can be so small that the computed MAC will still be closed to one; (2) this criterion cannot be used to locate and evaluate damage.

Lieven and Ewins (1988) proposed a similar criterion to detect damage, the Co-ordinate

Modal Assurance Criterion, known as COMAC. The COMAC showed the correlation between the mode shapes at a selected measurement point of the structure instead of the overall difference of the two groups of mode shapes. Unlike MAC, COMAC is said to be able to not only detect the existences of damage but also be able to locate damage. However, as stated previously, the sensitivity of the mode shapes to small physical property changes is questionable. With the uncertainty caused by the existence of noise in the measured data, the COMAC can be impractical to the detections of small physical property changes in in-service structures.

Rizos et al. (1990) proposed a NDE method based on the flexural vibration. At one of the natural mode of the structure, based on the recorded vibration amplitudes at two separated locations, the vibration frequency and an analytical solution of the dynamic response, the crack can be located and the depth of the crack can be closely estimated. The theory was validated using a cantilever beam which is 300 mm long and is clamped to a vibrating table. The damage was simulated as a thin saw cut. Five specimens with different damage locations and cut depths were tested. The difference between the measured and the computed values of the crack locations and depth were not larger than 8% for all tests.

Pandey et al. (1991) proposed a damage detection method based on changes of mode shape curvatures. The method could detect and locate damage according to the indication from the absolute difference of the mode shape curvatures between the damaged and undamaged structures. According to this study, the mode shape curvatures possessed higher sensitivity to damage than the mode shapes. The method was validated using a finite element cantilever beam model.

Raghavendrachar and Aktan (1992) applied the NDE method based on modal flexibility to a three-span reinforced concrete bridge. According to the study, the flexibility coefficients were found to be more sensitive to local damage than natural frequencies and mode shapes.

Stubbs et al. (1992) proposed a NDE method, known as the Damage Index Method (DIM), to detect and locate damage in the given structure. The proposed method was based on equality of the energy fractions between the undamaged and damaged structures. Mode shape curvatures were used to estimate the element strain energy for each element. The proposed method required no baseline model and was applicable to multi-damage locations. The method was validated using a numerical model of an offshore jacket platform.

Peterson et al. (1993) presented a damage detection method to locate both mass and stiffness damage. The method worked in modal domain and is based on changes in measured stiffness and mass matrix which was constructed using Eigen-system Realization Algorithm and the Common Basis Structural Identification Algorithm. The method was validated using numerical examples and experimental data.

Pandey and Biswas (1994) presented a NDE method based on the modal flexibility matrix. The flexibility matrix for the given structure was estimated using a few low-frequency modes and related frequencies. The damage was indicated by the plot of the maximum absolute value of the difference flexibility matrix between the damaged and undamaged structures. Numerical cantilever, simply supported, and free-free ends



beam models were employed to validate the method.

Ko et al. (1994) reported an application of the sensitivity study and MAC/COMAC analysis to a steel portal frame. The reports stated that the COMAC analysis can be used as a reliable indicator of the location of damage if the most sensitive correlated mode shape pairs were used.

Choy et al. (1995) proposed a fault-identification procedure to identify the defect in the stiffness of beam and the defect in the stiffness and damping characteristics in damping of the supporting foundation under the beam. The proposed methodology was based on the measurement of natural frequencies of the system and was limited to detecting the existences of damage.

Zhang and Aktan (1995) suggested using the changes of uniform flexibility shape curvatures to detect damage. Instead of computing the curvatures of the mode shapes, the proposed method computes the flexibility matrices for both the damaged and undamaged structures and used the difference of curvatures of each column vector from the flexibility matrices as the damage indicators.

Sheinman (1996) proposed a new damage detection algorithm based on updating the stiffness and mass matrices using mode data. By comparing the difference between the undamaged and damaged ones, the damage can be located, and then subsequent algorithm was required to evaluate the damage. The method was validated using several numerical examples.

Hjelmstad and Shin (1996) proposed a damage detection method based on system identification and measured modal response of a structure. The parameters of the damaged structure were estimated from the modal data by using modal displacement error method. A data perturbation scheme, based on Monte Carlo method, was used to assess the damage. The method was validated using a cantilever beam model and a plane stress model.

Stubbs and Kim (1996) presented a damage detection method to locate and estimate the severities of damage in structures. The method required only a few modal parameters from damaged structures and a finite element model. The modal parameters of the undamaged structure would be provided by the system identification technique by combining the post-damage modal parameters and modal parameters from the finite element model. The method was validated using a continuous beam model with only post-damage modal parameters available.

Cornwell et al. (1999) presented a damage detection method for plate-like structures. The proposed damage detection was an extension of the Damage Index Method (Stubbs et al. 1992). The method uses only mode shapes of the undamaged and damaged plate-like structures and requires no mass-normalization process. The method was validated using numerical and experimental 2-D plates.

Catbas et al. (2006) proposed a NDE method based on modal flexibility. The method detected the damage by comparing the displacement profiles of the undamaged and damaged structure. The displacement profiles were estimated from the frequency response function measurements of the structure. The method was demonstrated

experimentally on two in-service bridges.

Just et al. (2006) detected the damage in a sandwich composite aluminum beams by comparing the damping matrix in the damaged case with the one in the undamaged case, by acknowledging that damping characteristics were more sensitive to the changes in structures compared with stiffness changes. The damping matrix for the undamaged and the damaged cases were identified using an updated damping matrix identification iterative algorithm which was based on analytical mass and stiffness matrices and experimentally obtained natural frequencies, mode shapes, and damping ratios.

Zhong et al. (2008) proposed a damage detection method based on auxiliary mass spatial probing using the spectral center correction method. The method used the response time history of beam-like structures to get modal frequencies. Since this method requires accurate frequencies and the modal frequencies from the fast Fourier transform method are not accurate enough due to the leakage effect, the spectral center correction method is adopted and is able to provide more accurate frequencies. The auxiliary mass was used to enhance the effects of a crack and the changes of the modal parameters of a damaged beam. The method was validated using numerical examples.

Curadelli et al. (2008) presented a new damage detection scheme based on instantaneous damping coefficient identification using wavelet transform. Given the damage in the structure would cause more obvious changes in damping than in modal frequencies or mode shapes, the proposed method treated damping changes as damage indicators. The proposed method was validated by the application to a numerical simulation of 2D reinforced concrete frame, an experimental reinforced concrete beam, and an

experimental 3D frame model.

Gandomi et al. (2011) presented a new approach to detect and locate damage in plates based on mode shapes of the damaged and undamaged plates. This new approach used the governing differential equation on transverse deformation, the transverse shear force equation, and the invariant expression for the sum of transverse loading of an orthotropic plate. From the numerical study, it is concluded that the method is especially capable of detecting and locating damage in orthotropic plates.

Shinozuka et al. (2011) proposed a pipeline rupture detection method based on the measurement of pipe vibration. In this study, the acceleration data at the surface of the pipe were measured and analyzed in both time domain and frequency domain. In time domain, the sudden narrow increase of acceleration amplitude was treated as indication of damage. In the frequency domain, the damage were indicated by the frequency shifts which would be traced using a correlation function and the short time Fourier Transform technique.

### **1.2.2 Review of Time-Domain Methods**

Cattarius and Inman (1997) presented a time domain approach to detect both the mass and stiffness damage in the unknown structure. The proposed procedure relied on the comparison of the measured time responses from both the undamaged and damaged structures. By subtracting the two time responses from one another, the resulting beating phenomena could be acquired and used as an indication of the existence and extent of damage reflected in local mass and/or stiffness changes.

Lopez III and Zimmerman (2002) presented a damage detection method in time domain. The method used the modal minimum rank perturbation theory to compute the perturbation matrices estimating structural changes from a linear state to another linear state caused by damage. The method was validated using numerical examples. Although the method provides good indications of the locations of damage, the evaluation of damage severities in noise-polluted situation may need further studies.

Majumder and Manohar (2003) provided a time-domain method to detect changes in structural stiffness. The proposed method used acceleration, velocity, and displacements data from the vibration response of the detected structure. The source of excitation was induced by a moving vehicle. A finite element model was built to validate the proposed method.

Choi and Park (2003) presented a method to locate and evaluate damage in a truss structure. Based on the response data, the algorithm could size the damage by comparing the mean strain energy of an element from both undamaged and damaged case at a specified time period. Data from one complex numerical truss was used to validate the algorithm.

Ma et al. (2004) proposed a time domain structural health monitoring method. The method is mainly based on the proposed monitors that designed based on the residual generator technique. The main characteristic of these monitors is that they are only sensitive to the damage in the structural components that they are attached to. When there is damage in the structural component that the monitor is attached, the output will become nonzero. When there is no damage in the structural component, the output of the

monitor be closed to zero. In this way, the occurrence of the damage of one structural component can be detected. And because monitor will be attached to each key member of the structure, thus the damage will be located within the whole structure. With the input excitation signals and output structural reaction signals, the damage severities of the members can be computed using traditional time-domain system identification techniques.

The method required each structural component to be monitored by a structural health monitor designed using the residual generator technique. Each structural health monitor was only sensitive to the damage of the structural component connected to it. An obvious nonzero output from the monitor indicates the damage in the structural component under monitored. In this way, the proposed method could detect, locate and quantify structural damage.

Kang et al. (2005) presented a system identification method in time domain. The proposed method could be used to estimate the stiffness and damping parameters of structure using acceleration time history. The method required a priori knowledge of the mass and dealt with only linear structural behavior. The method was demonstrated on a numerical two-span truss bridge and an experimental three-story shear building model.

Frizzarin et al. (2010) presented a vibration based damage detection method in time domain. The proposed method used damping changes as an indication of damage. The method was validated using a large-scale concrete bridge model subjected to different levels of seismic damage simulated by shake table tests.

Gul and Catbas (2011) proposed a time-domain approach to detect, locate, and evaluate damage in given structure. The approach used statistic techniques to analyze the free response of the structure. An Auto-Regressive Model with exogenous input model (known as ARX model) was created for different sensor clusters by using the free response of the structure. Two different approaches are used for extracting damage features: 1. the coefficients of the ARX models were directly used as the damage features; 2. the ARX model fits ratios were used as the damage features.

Zhang et al. (2013) proposed a damage detection method in time domain. The method was generated based on the statistical moment-based damage detection in frequency domain. The method required the measurement of displacement responses and external excitations for both undamaged and damaged structures. The proposed method was validated using both numerical shear buildings models and shake table tests.

### **1.2.3 Review of Techniques That Simultaneously Evaluate Mass, Stiffness and Damping Damage**

Lindner and Kirby (1994) proposed a method to detect damage in a beam. The method assumed to know the model of the undamaged beam. The damaged beam model was updated from the undamaged model using the dynamic response data by an identification algorithm. By comparing the parameters in the undamaged and damaged beam models, the damage could be detected, located, and evaluated. The damage in stiffness and mass of an Euler-Bernoulli beam were detected.

Kiddy and Pines (1998) provide an approach to simultaneously update the stiffness and mass matrices. In the approach, the stiffness and mass matrix were updated

simultaneously by modal data after adding constrain in the damage detection problem. A numerical example was used to validate the approach.

Lin et al. (2005) applied the Hilbert-Huang transform (HHT) technique for damage identification to the phase I IASC-ASCE benchmark problem (Johnson et al 2004) for structural health monitoring. The approach can be used to identify the natural frequencies, damping ratios, mode shapes stiffness matrix, and damping matrix of a structure based on the measured noisy acceleration responses caused by ambient vibration.

Shin and Oh (2007) proposed a nonlinear time-domain system identification algorithm. The algorithm used the acceleration time history to synchronously evaluate the stiffness and damping parameters of the structure. The algorithm was validated using both numerical simulation and laboratory experiments.

Bighamian and Mirdamadi (2013) presented a new approach to simultaneously detect damage in mass and stiffness in aerospace structures. The presented procedure was only related to signals and was not related to modal parameters. The system digital pulse response data related to a selected number of collocated sensor-actuator DOFs to assess the extent of damage that occurred in the structure.

To find the current research background about the techniques which can simultaneously evaluate mass, stiffness, and damping damage, the author has searched several major journals, which are related to non-destructive damage detection techniques, during 2009-2013 period by using “damage” as the keyword in the title. Limited number of



papers was found. Although there are two or three techniques that may be able to provide information in mass, stiffness, and damping damage simultaneously but there wasn't one NDE technique that will provide detailed damage information in mass, stiffness, and damping as the one proposed in this proposal.

### **1.3 LIMITATIONS OF CURRENT NON-DESTRUCTIVE EVALUATION TECHNIQUES**

Vibration-Based Global nondestructive methods could be classified into two major categories: 1. Frequency-domain methods; 2. Time-domain methods.

The NDE methods in frequency domain are normally based on the modal parameters, such as modal frequencies, mode shapes or mode-shape curvatures. During the past two decades, a large number of NDE methods in frequency domain have been created and developed (e.g. Pandey et al. 1991, Stubbs et al. 1992, Pandey and Biswas 1994 and Zhang and Aktan 1995). However, the NDE methods in frequency domain have their own limitations:

#### **(1) Damage detection algorithm based on changes of frequency**

This type of algorithms has three major limitations: (i) the changes of the natural frequencies due to damage are not obvious (Farrar, et al., 1994, Doebling et al. 1996). Change of the environmental conditions, such as change of humidity and temperature, will cause the change of the material properties of the structural material such as mass, stiffness, and damping properties and finally result in the change of natural frequency. Thus it will be hard to decide whether the changes of natural frequencies are caused by damage in the structure or the change of environmental conditions. (ii) Different type

damage may result in same level changes of natural frequencies. That is same amount of damage at symmetric locations could cause the same change of frequencies and different amount of damage at different locations could cause the same changes of frequencies. Moreover, different combinations of damage in mass and stiffness could also result in same changes of frequencies.

#### (2) Damage detection algorithm based on changes of mode shapes

This type of damage detection algorithms is also not ideal. Mainly because mode shapes of a structure are not sensitive to damage (Huth et al. 2005). This could be demonstrated by the MAC and COMAC computation shown by Pandey et al. (1991), the nearly identical results can hardly be used as an indication of damage existence. Moreover, most of the algorithms based on changes of mode shapes are limited by locating damage and will not be able to provide detail damage information about each property of the material (Pandey et al. 1991, Lee et al. 2005).

#### (3) Damage detection algorithm based on the changes of mode shape curvatures

This type of algorithms might provide the false indications of damage locations when dealing with higher modes (Pandey et al. 1991), which might cause misjudge of damage locations. Since there is not a reasonable way to combine all the results from different mode shape curvatures, the damage detection algorithm will not be able to provide accurate damage severities estimations. Most of the algorithms in this group are limited by locating and evaluating general damage and will not be able to detect damage in mass, stiffness, and damping separately.

#### (4) Damage detection algorithm based on the changes of modal flexibility

That the modal flexibility provides a reasonable way to combine the damage information contained in the natural frequencies and the mode shapes of a structure. This type of methods may provide indication of damage existences and damage locations. However, since it's hard to relate the modal flexibility matrix to local stiffness, the accurate stiffness damage severities are hard to obtain (Pandey and Biswas 1994, Zhang and Aktan 1995). And obtaining the mass normalized modes could be an issue when the modes were obtained from ambient data (Farrar and Jauregui 1996). Moreover, the existing NDE techniques based on modal flexibility are mainly designed for static state, it is also difficult for this type of method to detect damage in mass and damping parameters.

#### (5) Damage detection algorithm based on the changes of modal strain energy

Since the modal strain energy is directly related to the mode shape curvatures. The algorithms based on modal strain energy may share the same drawbacks as the algorithms based on mode shape curvatures, such as the false indication of damage locations. Since there is currently not a reasonable way to combine all the damage information in each modes, the damage severities from each mode won't be exact (Stubbs et al. 1992). Also, because the existing NDE techniques based on modal strain energy are mainly designed for static state, it is difficult for this type of method to detect damage in mass and damping parameter.

In conclusion, one major drawback of the NDE methods in frequency domain is that most of the techniques, based on the literature review, are designed to detect stiffness damage only. Although some of the methods may be able to detect the damage resulting from mass changes, it is difficult for these methods to locate the mass damage, let alone

evaluate the mass damage accurately. This is because most of the current NDE methods in frequency domain are designed to work on static situation. Compared to the mass damage detection, it may be even harder for the NDE methods in frequency domain to detect damping damage. The reluctance of the modal parameters (i.e. modal frequencies, mode shapes and mode shape curvatures) towards damping changes (Hyung 2007) makes it even harder for the NDE methods in frequency domain to detect the damping damage. Thus, it is necessary to develop an NDE method in time domain which could evaluate the damage not only in stiffness but also in mass and damping.

On the other hand, the current existing NDE methods in time domain are not ideal either. Most of the existing techniques are limited by detecting the existence of damage (Cattarius and Inman 1997, Frizzarin et al. 2010, Shinozuka et al. 2011, Zimin and Zimmerman 2009) and locate damage (Trickey et al. 2002, Qu and Peng 2007, Gul and Catbas 2011,). Just a few methods could detect, locate and evaluate damage (Lopez III and Zimmerman 2002, Majumder and Manohar 2003, Ma et al. 2004,). It became even rarer that the NDE methods in time domain could detect and locate damage in mass and stiffness or in damping and stiffness at the same time (Kiddy and Pines 1998, Shin and Oh 2007, Bighamian and Mirdamadi 2013). Moreover, according to the current literature review, just a few methods (Lin et al. 2005), currently, can detect damage in mass, stiffness, and damping simultaneously.

#### **1.4 RESEARCH OBJECTIVES**

According to Rytter (1993), damage evaluation methods can be classified into four levels and the criterion for each level is defined as following:

Level I (Detection of Damage): A quantitative indication regarding the existence

- of damage in a structure;
- Level II (Localization of Damage): A quantitative indication specifying the location of damage;
- Level III (Assessment of the Severity of Damage): A quantitative indication regarding the severity of damage that was previously located; and
- Level IV (Performance Evaluation after Damage): A quantitative analysis regarding the impact of damage on the performance of structure. (Li 2013)

The objective of the present study is to develop a Level III non-destructive damage evaluation method in the time domain which can simultaneously detect damage in stiffness, mass, and damping. To achieve the goal of this study the following tasks are anticipated:

- Task 1 - Theoretical derivation of the nondestructive evaluation algorithm for discrete systems;
- Task 2 - Theoretical derivation of the nondestructive evaluation algorithm for continuous systems;
- Task 3 - Validation of the accuracy of the developed algorithm for discrete systems using structural deformational data generated from the dynamic analysis of the finite element models in SAP2000;
- Task 4 - Validation of the accuracy of the developed algorithm for continuous system using structural deformational data generated from the dynamic analysis of the finite element models in SAP2000; and
- Task 5 – Application of the methodology to an existing structure using real-world data.

In the current study, the state of damage will be evaluated by two parameters: namely, the Damage Index (DI) and the Damage Severity (DS). The damage is defined as the change of mass, stiffness, and/or damping.

### **1.5 SIGNIFICANCE OF THIS WORK**

Most NDE methods proposed to date are only classified as Level I or Level II methods, which means only the presences of the damage or at most, the locations of the damage can be detected. From the other side, most of these methods are limited in the detection of stiffness damage only and are not able to locate or evaluate mass damage and damping damage. The damage detection algorithm proposed here is a Level III method that has the following features:

- (1) It may detect damage in local stiffness, mass and damping;
- (2) It may provide a clear indicator to locate damage;
- (3) It may locate tiny and obscure damage;
- (4) It may provide accurate damage severities that are quantitative in value;
- (5) An analytical model of the structure is not required;
- (6) The data from the field experiment can be directly used to complete the analyses;
- (7) The method is applicable to many types of structures and as well as cases with multiple damage locations; and
- (8) The computation process is rather straight-forward.

According to the features listed above, this algorithm has the potential to be an excellent Level III non-destructive evaluation method. When fully developed, the method should

contribute to reduce property losses and maintenance cost of critical structures.

## **2 THEORY OF DAMAGE EVALUATION ON MASS, STIFFNESS, AND DAMPING FOR DISCRETE SYSTEMS**

### **2.1 INTRODUCTION**

In this section, five major sub tasks are addressed. In Section 2.2, the general form of the Power Method will be developed. In Section 2.3, the specific form of the Power Method for 1-DOF spring-mass-damper system will be developed; In Section 2.4, the specific form of the Power Method for 2-DOF spring-mass-damper system will be developed; In Section 2.5, the specific form of the Power Method for N-DOF (5-DOF) spring-mass-damper system will be developed; In Section 2.6, the specific form of the Power Method for an isolated spring-mass-damper system will be developed; In Section 2.7, the overall solution procedure will be provided.

### **2.2 DEVELOPMENT OF THE GENERAL POWER METHOD**

One of the most important concept used in this dissertation is concept of “power”. The power mentioned in this dissertation is different from the traditional definition of power in the classical mechanics. The word ”power” mentioned in this dissertation represents the dot product of an external force vector with any given combination velocity vector. Namely, since the pre-multiplied velocity vector can be arbitrarily selected and is not necessarily composed by the actual velocities at the force application locations, the computed power is different from the power defined in the more traditional physical senses.

For the undamaged and damaged discrete system, the equation of motion under the



external force can be written as,

$$[m]\{\ddot{x}\} + [c]\{\dot{x}\} + [k]\{x\} = \{p(t)\} \quad (2.1)$$

$$[m^*]\{\ddot{x}^*\} + [c^*]\{\dot{x}^*\} + [k^*]\{x^*\} = \{p^*(t)\} \quad (2.2)$$

Given any velocity vector,  $\{\dot{\Delta}\}$ , the power done by the external forces can be computed by pre-multiplying each term in Eq. 2.1 and Eq. 2.2. The resulting equations can be expressed as follows,

$$\{\dot{\Delta}\}^T [m]\{\ddot{x}\} + \{\dot{\Delta}\}^T [c]\{\dot{x}\} + \{\dot{\Delta}\}^T [k]\{x\} = \{\dot{\Delta}\}^T \{p(t)\} \quad (2.3)$$

$$\{\dot{\Delta}^*\}^T [m^*]\{\ddot{x}^*\} + \{\dot{\Delta}^*\}^T [c^*]\{\dot{x}^*\} + \{\dot{\Delta}^*\}^T [k^*]\{x^*\} = \{\dot{\Delta}^*\}^T \{p^*(t)\} \quad (2.4)$$

Where for discrete system, the external load vector can be expressed as,

$$\{p(t)\} = \begin{Bmatrix} p^1(t) \\ \vdots \\ p^i(t) \\ \vdots \\ p^n(t) \end{Bmatrix} \quad (2.5)$$

$$\{p^*(t)\} = \begin{Bmatrix} p^{*1}(t) \\ \vdots \\ p^{*i}(t) \\ \vdots \\ p^{*n}(t) \end{Bmatrix} \quad (2.6)$$

Note, the superscripts, in this dissertation, denote the properties of nodes/joints/lumped mass points and the subscripts denote the properties of elements/links (i.e. springs and dash pots). Thus, in the above expression, the superscript, 'i', denotes the  $i^{\text{th}}$  degree of

freedom (i.e. the  $i^{\text{th}}$  mass block) and  $p^i(t)$  represents the external force applied to the  $i^{\text{th}}$  degree of freedom.

Assume the applied external loads and velocities are the same for both the undamaged and damaged system,

$$\{p(t)\} = \{p^*(t)\} \quad (2.7)$$

$$\{\dot{\Delta}\} = \{\dot{\Delta}^*\} \quad (2.8)$$

Substituting Eq. 2.7 and Eq. 2.8 into Eq. 2.4 yields,

$$\{\dot{\Delta}\}^T [m^*] \{\ddot{x}^*\} + \{\dot{\Delta}\}^T [c^*] \{\dot{x}^*\} + \{\dot{\Delta}\}^T [k^*] \{x^*\} = \{\dot{\Delta}\}^T \{p(t)\} \quad (2.9)$$

Noticing the power done by the external load is the same for both the undamaged and damaged system. Substituting Eq. 2.9 into Eq. 2.3, yields,

$$\{\dot{\Delta}\}^T [m] \{\ddot{x}\} + \{\dot{\Delta}\}^T [c] \{\dot{x}\} + \{\dot{\Delta}\}^T [k] \{x\} = \{\dot{\Delta}\}^T [m^*] \{\ddot{x}^*\} + \{\dot{\Delta}\}^T [c^*] \{\dot{x}^*\} + \{\dot{\Delta}\}^T [k^*] \{x^*\} \quad (2.10)$$

The above equation is the connection between the undamaged and damaged system. The damage severities of mass, stiffness and damping can be estimated from the above equation using least square method.

To better indicate the location and extent of a damage, the damage index ( $\beta$ ) and damage severity ( $\alpha$ ) are used. The damage index ( $\beta$ ) is defined as the ratio of the property from the undamaged system and the counterpart property in the damaged system,

$$\beta_{\chi} = \frac{\chi}{\chi^*} \quad (2.11)$$

Where  $\chi$  is any physical property from the undamaged system;  $\chi^*$  is any physical property from the damaged system; and the asterisk (\*) indicates the parameters for damaged cases.

And the damage severity ( $\alpha$ ) is defined as the ratio of the difference between the stiffness of the damaged and undamaged structures and the stiffness of the undamaged structure,

$$\alpha_{\chi} = \frac{\chi^* - \chi}{\chi} \quad (2.12)$$

Where  $\chi$  is any physical property from the undamaged system;  $\chi^*$  is any physical property from the damaged system; and the asterisk (\*) indicates the parameters for damaged cases.

From the expression of Eq. 2.11 and Eq. 2.12, the relationship between damage index ( $\beta$ ) and damage severity ( $\alpha$ ) is found and is given as following

$$\alpha_{\chi} = \frac{\chi^* - \chi}{\chi} = \frac{\chi^*}{\chi} - 1 = \frac{1}{\beta_{\chi}} - 1 \quad (2.13)$$

### 2.3 THEORY FOR 1-DOF SPRING-MASS-DAMPER SYSTEMS

For a typical 1-DOF spring-mass-damper system, as shown in Figure 2.1, the system is composed of one lumped mass, one linear spring, and one linear dash pot.  $p(t)$  is the external dynamic force acting on the lumped mass at time point  $t$ .  $x(t)$  is the displacement of the lumped mass relative to the ground at time point  $t$ .  $\dot{x}(t)$  is the velocity of the lumped mass relative to the ground at time point  $t$ .  $\ddot{x}(t)$  is the acceleration

of the lumped mass relative to the ground at time point  $t$ .

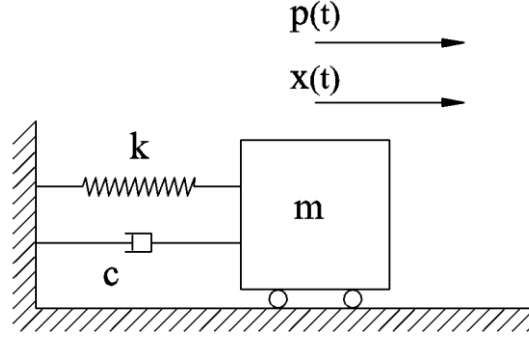


**Figure 2.1. 1-DOF Spring-Mass-Damper System**

For the 1-DOF spring-mass-damper system, Eq. 2.10 can be written as,

$$m\ddot{x}\dot{\Delta} + c\dot{x}\dot{\Delta} + kx\dot{\Delta} = m^* \ddot{x}^* \dot{\Delta} + c^* \dot{x}^* \dot{\Delta} + k^* x^* \dot{\Delta} \quad (2.14)$$

Dividing Eq. 2.14 by  $m^*$  yields,

$$\frac{m}{m^*} \ddot{x}\dot{\Delta} + \frac{c}{m^*} \dot{x}\dot{\Delta} + \frac{k}{m^*} x\dot{\Delta} = \ddot{x}^* \dot{\Delta} + \frac{c^*}{m^*} \dot{x}^* \dot{\Delta} + \frac{k^*}{m^*} x^* \dot{\Delta} \quad (2.15)$$

Rearranging the Eq. 2.15,

$$\frac{m}{m^*} \ddot{x}\dot{\Delta} + \frac{c}{m^*} \dot{x}\dot{\Delta} + \frac{k}{m^*} x\dot{\Delta} - \frac{c^*}{m^*} \dot{x}^* \dot{\Delta} - \frac{k^*}{m^*} x^* \dot{\Delta} = \ddot{x}^* \dot{\Delta} \quad (2.16)$$

Define the following coefficients,

$$\beta_1 = \frac{m}{m^*} \quad (2.17)$$

$$\beta_2 = \frac{c}{m^*} \quad (2.18)$$

$$\beta_3 = \frac{k}{m^*} \quad (2.19)$$

$$\beta_4 = \frac{c^*}{m} \quad (2.20)$$

$$\beta_5 = \frac{k^*}{m} \quad (2.21)$$

Substituting Eq. 2.17 through Eq. 2.21 to Eq. 2.16 yields,

$$\beta_1 \ddot{x}\dot{\Delta} + \beta_2 \dot{x}\dot{\Delta} + \beta_3 x\dot{\Delta} - \beta_4 \dot{x}^*\dot{\Delta} - \beta_5 x^*\dot{\Delta} = \ddot{x}^*\dot{\Delta} \quad (2.22)$$

Writing the Eq. 2.22 at different time point, yields the following groups of equations,

For  $t = t_0$ ,

$$\beta_1(\ddot{x}\dot{\Delta})|_{t_0} + \beta_2(\dot{x}\dot{\Delta})|_{t_0} + \beta_3(x\dot{\Delta})|_{t_0} - \beta_4(\dot{x}^*\dot{\Delta})|_{t_0} - \beta_5(x^*\dot{\Delta})|_{t_0} = (\ddot{x}^*\dot{\Delta})|_{t_0} \quad (2.23)$$

For  $t = t_i$ ,

$$\beta_1(\ddot{x}\dot{\Delta})|_{t_i} + \beta_2(\dot{x}\dot{\Delta})|_{t_i} + \beta_3(x\dot{\Delta})|_{t_i} - \beta_4(\dot{x}^*\dot{\Delta})|_{t_i} - \beta_5(x^*\dot{\Delta})|_{t_i} = (\ddot{x}^*\dot{\Delta})|_{t_i} \quad (2.24)$$

For  $t = t_N$ ,

$$\beta_1(\ddot{x}\dot{\Delta})|_{t_N} + \beta_2(\dot{x}\dot{\Delta})|_{t_N} + \beta_3(x\dot{\Delta})|_{t_N} - \beta_4(\dot{x}^*\dot{\Delta})|_{t_N} - \beta_5(x^*\dot{\Delta})|_{t_N} = (\ddot{x}^*\dot{\Delta})|_{t_N} \quad (2.25)$$

Arrange the above Equation group into matrix form,

$$\begin{bmatrix} (\ddot{x}\dot{\Delta})|_{t_0} & (\dot{x}\dot{\Delta})|_{t_0} & (x\dot{\Delta})|_{t_0} & -(\dot{x}^*\dot{\Delta})|_{t_0} & -(x^*\dot{\Delta})|_{t_0} \\ \vdots & \vdots & \vdots & \vdots & \vdots \\ (\ddot{x}\dot{\Delta})|_{t_i} & (\dot{x}\dot{\Delta})|_{t_i} & (x\dot{\Delta})|_{t_i} & -(\dot{x}^*\dot{\Delta})|_{t_i} & -(x^*\dot{\Delta})|_{t_i} \\ \vdots & \vdots & \vdots & \vdots & \vdots \\ (\ddot{x}\dot{\Delta})|_{t_N} & (\dot{x}\dot{\Delta})|_{t_N} & (x\dot{\Delta})|_{t_N} & -(\dot{x}^*\dot{\Delta})|_{t_N} & -(x^*\dot{\Delta})|_{t_N} \end{bmatrix}_{N \times 5} \begin{Bmatrix} \beta_1 \\ \beta_2 \\ \beta_3 \\ \beta_4 \\ \beta_5 \end{Bmatrix}_{5 \times 1} = \begin{Bmatrix} (\ddot{x}^*\dot{\Delta})|_{t_0} \\ \vdots \\ (\ddot{x}^*\dot{\Delta})|_{t_i} \\ \vdots \\ (\ddot{x}^*\dot{\Delta})|_{t_N} \end{Bmatrix}_{N \times 1} \quad (2.26)$$

Define

$$\mathbf{X} = \begin{bmatrix} (\ddot{x}\dot{\Delta})|_{t_0} & (\dot{x}\dot{\Delta})|_{t_0} & (x\dot{\Delta})|_{t_0} & -(\dot{x}^*\dot{\Delta})|_{t_0} & -(x^*\dot{\Delta})|_{t_0} \\ \vdots & \vdots & \vdots & \vdots & \vdots \\ (\ddot{x}\dot{\Delta})|_{t_i} & (\dot{x}\dot{\Delta})|_{t_i} & (x\dot{\Delta})|_{t_i} & -(\dot{x}^*\dot{\Delta})|_{t_i} & -(x^*\dot{\Delta})|_{t_i} \\ \vdots & \vdots & \vdots & \vdots & \vdots \\ (\ddot{x}\dot{\Delta})|_{t_N} & (\dot{x}\dot{\Delta})|_{t_N} & (x\dot{\Delta})|_{t_N} & -(\dot{x}^*\dot{\Delta})|_{t_N} & -(x^*\dot{\Delta})|_{t_N} \end{bmatrix} \quad (2.27)$$

$$\boldsymbol{\beta} = \begin{Bmatrix} \beta_1 \\ \beta_2 \\ \beta_3 \\ \beta_4 \\ \beta_5 \end{Bmatrix} \quad (2.28)$$

$$\mathbf{Y} = \begin{Bmatrix} (\ddot{x}^*\dot{\Delta})|_{t_0} \\ \vdots \\ (\ddot{x}^*\dot{\Delta})|_{t_i} \\ \vdots \\ (\ddot{x}^*\dot{\Delta})|_{t_N} \end{Bmatrix} \quad (2.29)$$

The above equation may be expressed as,

$$\mathbf{X}\boldsymbol{\beta} = \mathbf{Y} \quad (2.30)$$

Based on the Least Square Method, the  $\boldsymbol{\beta}$  can be computed from the following equation,

$$\boldsymbol{\beta} = (\mathbf{X}^T \mathbf{X})^{-1} (\mathbf{X}^T \mathbf{Y}) \quad (2.31)$$

According to the definition of the damage index in Eq. 2.11, the damage indices for stiffness, mass and damping can be computed as follows,

$$\beta_m = \frac{m}{m^*} = \beta_1 \quad (2.32)$$

$$\beta_c = \frac{c}{c^*} = \frac{\frac{c}{m^*}}{\frac{c^*}{m^*}} = \frac{\beta_2}{\beta_4} \quad (2.33)$$

$$\beta_k = \frac{k}{k^*} = \frac{\frac{k}{m^*}}{\frac{k^*}{m^*}} = \frac{\beta_3}{\beta_5} \quad (2.34)$$

According to the relationship between the damage severity and damage index of one element, shown in Eq. 2.13, the damage severities for stiffness, mass and damping can be computed as follows,

$$\alpha_m = \frac{1}{\beta_m} - 1 = \frac{1}{\beta_1} - 1 \quad (2.35)$$

$$\alpha_c = \frac{1}{\beta_c} - 1 = \frac{\beta_4}{\beta_2} - 1 \quad (2.36)$$

$$\alpha_k = \frac{1}{\beta_k} - 1 = \frac{\beta_5}{\beta_3} - 1 \quad (2.37)$$

## 2.4 THEORY FOR 2-DOF SPRING-MASS-DAMPER SYSTEMS

For a typical 2-DOF spring-mass-damper system, as shown in Figure 2.2, the system is composed of two lumped masses, three linear springs, and three linear dash pots.  $p^1(t)$

and  $p^2(t)$  are the external dynamic forces acting on lumped mass 1 and lumped mass 2 respectively.  $x^1(t)$  and  $x^2(t)$  are the displacements of mass block 1 and mass block 2 relative to the ground at time point  $t$ .  $\dot{x}^1(t)$  and  $\dot{x}^2(t)$  are the velocities of mass block 1 and mass block 2 relative to the ground at time point  $t$ .  $\ddot{x}^1(t)$  and  $\ddot{x}^2(t)$  are the accelerations of mass block 1 and mass block 2 relative to the ground at time point  $t$ .

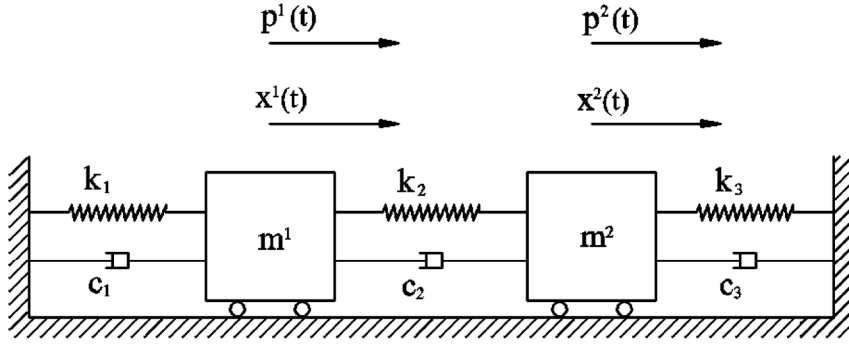


Figure 2.2. 2-DOF Spring-Mass-Damper System

For the 2-DOF spring-mass-damper system, Eq. 2.10 can be written as,

$$\begin{aligned}
 & \begin{Bmatrix} \dot{\Delta}^1 \\ \dot{\Delta}^2 \end{Bmatrix}^T \begin{bmatrix} m^1 & 0 \\ 0 & m^2 \end{bmatrix} \begin{Bmatrix} \ddot{x}^1 \\ \ddot{x}^2 \end{Bmatrix} + \begin{Bmatrix} \dot{\Delta}^1 \\ \dot{\Delta}^2 \end{Bmatrix}^T \begin{bmatrix} c_1 + c_2 & -c_2 \\ -c_2 & c_2 + c_3 \end{bmatrix} \begin{Bmatrix} \dot{x}^1 \\ \dot{x}^2 \end{Bmatrix} + \begin{Bmatrix} \dot{\Delta}^1 \\ \dot{\Delta}^2 \end{Bmatrix}^T \begin{bmatrix} k_1 + k_2 & -k_2 \\ -k_2 & k_2 + k_3 \end{bmatrix} \begin{Bmatrix} x^1 \\ x^2 \end{Bmatrix} \\
 &= \begin{Bmatrix} \dot{\Delta}^1 \\ \dot{\Delta}^2 \end{Bmatrix}^T \begin{bmatrix} m^{*1} & 0 \\ 0 & m^{*2} \end{bmatrix} \begin{Bmatrix} \ddot{x}^{*1} \\ \ddot{x}^{*2} \end{Bmatrix} + \begin{Bmatrix} \dot{\Delta}^1 \\ \dot{\Delta}^2 \end{Bmatrix}^T \begin{bmatrix} c_1^* + c_2^* & -c_2^* \\ -c_2^* & c_2^* + c_3^* \end{bmatrix} \begin{Bmatrix} \dot{x}^{*1} \\ \dot{x}^{*2} \end{Bmatrix} + \begin{Bmatrix} \dot{\Delta}^1 \\ \dot{\Delta}^2 \end{Bmatrix}^T \begin{bmatrix} k_1^* + k_2^* & -k_2^* \\ -k_2^* & k_2^* + k_3^* \end{bmatrix} \begin{Bmatrix} x^{*1} \\ x^{*2} \end{Bmatrix}
 \end{aligned}
 \tag{2.38}$$

Eq. 2.38 can be rewritten as,



$$\begin{aligned}
& m^1 \dot{x}^1 \dot{\Delta}^1 + m^2 \ddot{x}^2 \dot{\Delta}^2 + c_1 \dot{x}^1 \dot{\Delta}^1 + c_2 (\dot{x}^1 - \dot{x}^2)(\dot{\Delta}^1 - \dot{\Delta}^2) + c_3 \dot{x}^2 \dot{\Delta}^2 + k_1 x^1 \dot{\Delta}^1 \\
& + k_2 (x^1 - x^2)(\dot{\Delta}^1 - \dot{\Delta}^2) + k_3 x^2 \dot{\Delta}^2 \\
& = m^{*1} \dot{x}^{*1} \dot{\Delta}^1 + m^{*2} \ddot{x}^{*2} \dot{\Delta}^2 + c_1^* \dot{x}^{*1} \dot{\Delta}^1 + c_2^* (\dot{x}^{*1} - \dot{x}^{*2})(\dot{\Delta}^1 - \dot{\Delta}^2) + c_3^* \dot{x}^{*2} \dot{\Delta}^2 + k_1^* x^{*1} \dot{\Delta}^1 \\
& + k_2^* (x^{*1} - x^{*2})(\dot{\Delta}^1 - \dot{\Delta}^2) + k_3^* x^{*2} \dot{\Delta}^2
\end{aligned} \tag{2.39}$$

Dividing Eq. 2.39 by  $m^{*1}$  yields,

$$\begin{aligned}
& \frac{m^1}{m^{*1}} \dot{x}^1 \dot{\Delta}^1 + \frac{m^2}{m^{*1}} \ddot{x}^2 \dot{\Delta}^2 + \frac{c_1}{m^{*1}} \dot{x}^1 \dot{\Delta}^1 + \frac{c_2}{m^{*1}} (\dot{x}^1 - \dot{x}^2)(\dot{\Delta}^1 - \dot{\Delta}^2) + \frac{c_3}{m^{*1}} \dot{x}^2 \dot{\Delta}^2 + \frac{k_1}{m^{*1}} x^1 \dot{\Delta}^1 \\
& + \frac{k_2}{m^{*1}} (x^1 - x^2)(\dot{\Delta}^1 - \dot{\Delta}^2) + \frac{k_3}{m^{*1}} x^2 \dot{\Delta}^2 \\
& = \ddot{x}^{*1} \dot{\Delta}^1 + \frac{m^{*2}}{m^{*1}} \ddot{x}^{*2} \dot{\Delta}^2 + \frac{c_1^*}{m^{*1}} \dot{x}^{*1} \dot{\Delta}^1 + \frac{c_2^*}{m^{*1}} (\dot{x}^{*1} - \dot{x}^{*2})(\dot{\Delta}^1 - \dot{\Delta}^2) + \frac{c_3^*}{m^{*1}} \dot{x}^{*2} \dot{\Delta}^2 + \frac{k_1^*}{m^{*1}} x^{*1} \dot{\Delta}^1 \\
& + \frac{k_2^*}{m^{*1}} (x^{*1} - x^{*2})(\dot{\Delta}^1 - \dot{\Delta}^2) + \frac{k_3^*}{m^{*1}} x^{*2} \dot{\Delta}^2
\end{aligned} \tag{2.40}$$

Rearranging Eq. 2.40 yields

$$\begin{aligned}
& \frac{m^1}{m^{*1}} \dot{x}^1 \dot{\Delta}^1 + \frac{m^2}{m^{*1}} \ddot{x}^2 \dot{\Delta}^2 + \frac{c_1}{m^{*1}} \dot{x}^1 \dot{\Delta}^1 + \frac{c_2}{m^{*1}} (\dot{x}^1 - \dot{x}^2)(\dot{\Delta}^1 - \dot{\Delta}^2) + \frac{c_3}{m^{*1}} \dot{x}^2 \dot{\Delta}^2 + \frac{k_1}{m^{*1}} x^1 \dot{\Delta}^1 \\
& + \frac{k_2}{m^{*1}} (x^1 - x^2)(\dot{\Delta}^1 - \dot{\Delta}^2) + \frac{k_3}{m^{*1}} x^2 \dot{\Delta}^2 - \frac{m^{*2}}{m^{*1}} \ddot{x}^{*2} \dot{\Delta}^2 - \frac{c_1^*}{m^{*1}} \dot{x}^{*1} \dot{\Delta}^1 - \frac{c_2^*}{m^{*1}} (\dot{x}^{*1} - \dot{x}^{*2})(\dot{\Delta}^1 - \dot{\Delta}^2) \\
& - \frac{c_3^*}{m^{*1}} \dot{x}^{*2} \dot{\Delta}^2 - \frac{k_1^*}{m^{*1}} x^{*1} \dot{\Delta}^1 - \frac{k_2^*}{m^{*1}} (x^{*1} - x^{*2})(\dot{\Delta}^1 - \dot{\Delta}^2) - \frac{k_3^*}{m^{*1}} x^{*2} \dot{\Delta}^2 = \ddot{x}^{*1} \dot{\Delta}^1
\end{aligned} \tag{2.41}$$

Define,

$$\beta_1 = \frac{m^1}{m^{*1}} \tag{2.42}$$

$$\beta_2 = \frac{m^2}{m^{*1}} \quad (2.43)$$

$$\beta_3 = \frac{c_1}{m^{*1}} \quad (2.44)$$

$$\beta_4 = \frac{c_2}{m^{*1}} \quad (2.45)$$

$$\beta_5 = \frac{c_3}{m^{*1}} \quad (2.46)$$

$$\beta_6 = \frac{k_1}{m^{*1}} \quad (2.47)$$

$$\beta_7 = \frac{k_2}{m^{*1}} \quad (2.48)$$

$$\beta_8 = \frac{k_3}{m^{*1}} \quad (2.49)$$

$$\beta_9 = \frac{m^{*2}}{m^{*1}} \quad (2.50)$$

$$\beta_{10} = \frac{c_1^*}{m^{*1}} \quad (2.51)$$

$$\beta_{11} = \frac{c_2^*}{m^{*1}} \quad (2.52)$$

$$\beta_{12} = \frac{c_3^*}{m^{*1}} \quad (2.53)$$

$$\beta_{13} = \frac{k_1^*}{m^{*1}} \quad (2.54)$$

$$\beta_{14} = \frac{k_2^*}{m^{*1}} \quad (2.55)$$

$$\beta_{15} = \frac{k_3^*}{m^{*1}} \quad (2.56)$$

Substitute Eqs. 2.42 through 2.56 into Eq. 2.41, yields,

$$\begin{aligned}
& \beta_1 \ddot{x}^1 \dot{\Delta}^1 + \beta_2 \ddot{x}^2 \dot{\Delta}^2 + \beta_3 \dot{x}^1 \dot{\Delta}^1 + \beta_4 (\dot{x}^1 - \dot{x}^2)(\dot{\Delta}^1 - \dot{\Delta}^2) + \beta_5 \dot{x}^2 \dot{\Delta}^2 + \beta_6 x^1 \dot{\Delta}^1 \\
& + \beta_7 (x^1 - x^2)(\dot{\Delta}^1 - \dot{\Delta}^2) + \beta_8 x^2 \dot{\Delta}^2 - \beta_9 \ddot{x}^{*2} \dot{\Delta}^2 - \beta_{10} \dot{x}^{*1} \dot{\Delta}^1 - \beta_{11} (\dot{x}^{*1} - \dot{x}^{*2})(\dot{\Delta}^1 - \dot{\Delta}^2) \\
& - \beta_{12} \dot{x}^{*2} \dot{\Delta}^2 - \beta_{13} x^{*1} \dot{\Delta}^1 - \beta_{14} (x^{*1} - x^{*2})(\dot{\Delta}^1 - \dot{\Delta}^2) - \beta_{15} x^{*2} \dot{\Delta}^2 = \ddot{x}^{*1} \dot{\Delta}^1
\end{aligned} \tag{2.57}$$

Apply Eq. 2.57 at different time point,

For  $t = t_0$ ,

$$\begin{aligned}
& \beta_1 (\ddot{x}^1 \dot{\Delta}^1)|_{t_0} + \beta_2 (\ddot{x}^2 \dot{\Delta}^2)|_{t_0} + \beta_3 (\dot{x}^1 \dot{\Delta}^1)|_{t_0} + \beta_4 ((\dot{x}^1 - \dot{x}^2)(\dot{\Delta}^1 - \dot{\Delta}^2))|_{t_0} + \beta_5 (\dot{x}^2 \dot{\Delta}^2)|_{t_0} \\
& + \beta_6 (x^1 \dot{\Delta}^1)|_{t_0} + \beta_7 ((x^1 - x^2)(\dot{\Delta}^1 - \dot{\Delta}^2))|_{t_0} + \beta_8 (x^2 \dot{\Delta}^2)|_{t_0} - \beta_9 (\ddot{x}^{*2} \dot{\Delta}^2)|_{t_0} - \beta_{10} (\dot{x}^{*1} \dot{\Delta}^1)|_{t_0} \\
& - \beta_{11} ((\dot{x}^{*1} - \dot{x}^{*2})(\dot{\Delta}^1 - \dot{\Delta}^2))|_{t_0} - \beta_{12} (\dot{x}^{*2} \dot{\Delta}^2)|_{t_0} - \beta_{13} (x^{*1} \dot{\Delta}^1)|_{t_0} - \beta_{14} ((x^{*1} - x^{*2})(\dot{\Delta}^1 - \dot{\Delta}^2))|_{t_0} \\
& - \beta_{15} (x^{*2} \dot{\Delta}^2)|_{t_0} = (\ddot{x}^{*1} \dot{\Delta}^1)|_{t_0}
\end{aligned} \tag{2.58}$$

For  $t = t_i$ ,

$$\begin{aligned}
& \beta_1 (\ddot{x}^1 \dot{\Delta}^1)|_{t_i} + \beta_2 (\ddot{x}^2 \dot{\Delta}^2)|_{t_i} + \beta_3 (\dot{x}^1 \dot{\Delta}^1)|_{t_i} + \beta_4 ((\dot{x}^1 - \dot{x}^2)(\dot{\Delta}^1 - \dot{\Delta}^2))|_{t_i} + \beta_5 (\dot{x}^2 \dot{\Delta}^2)|_{t_i} \\
& + \beta_6 (x^1 \dot{\Delta}^1)|_{t_i} + \beta_7 ((x^1 - x^2)(\dot{\Delta}^1 - \dot{\Delta}^2))|_{t_i} + \beta_8 (x^2 \dot{\Delta}^2)|_{t_i} - \beta_9 (\ddot{x}^{*2} \dot{\Delta}^2)|_{t_i} - \beta_{10} (\dot{x}^{*1} \dot{\Delta}^1)|_{t_i} \\
& - \beta_{11} ((\dot{x}^{*1} - \dot{x}^{*2})(\dot{\Delta}^1 - \dot{\Delta}^2))|_{t_i} - \beta_{12} (\dot{x}^{*2} \dot{\Delta}^2)|_{t_i} - \beta_{13} (x^{*1} \dot{\Delta}^1)|_{t_i} - \beta_{14} ((x^{*1} - x^{*2})(\dot{\Delta}^1 - \dot{\Delta}^2))|_{t_i} \\
& - \beta_{15} (x^{*2} \dot{\Delta}^2)|_{t_i} = (\ddot{x}^{*1} \dot{\Delta}^1)|_{t_i}
\end{aligned} \tag{2.59}$$

For  $t = t_N$ ,

$$\begin{aligned}
& \beta_1 (\ddot{x}^1 \dot{\Delta}^1)|_{t_N} + \beta_2 (\ddot{x}^2 \dot{\Delta}^2)|_{t_N} + \beta_3 (\dot{x}^1 \dot{\Delta}^1)|_{t_N} + \beta_4 ((\dot{x}^1 - \dot{x}^2)(\dot{\Delta}^1 - \dot{\Delta}^2))|_{t_N} + \beta_5 (\dot{x}^2 \dot{\Delta}^2)|_{t_N} \\
& + \beta_6 (x^1 \dot{\Delta}^1)|_{t_N} + \beta_7 ((x^1 - x^2)(\dot{\Delta}^1 - \dot{\Delta}^2))|_{t_N} + \beta_8 (x^2 \dot{\Delta}^2)|_{t_N} - \beta_9 (\ddot{x}^{*2} \dot{\Delta}^2)|_{t_N} - \beta_{10} (\dot{x}^{*1} \dot{\Delta}^1)|_{t_N} \\
& - \beta_{11} ((\dot{x}^{*1} - \dot{x}^{*2})(\dot{\Delta}^1 - \dot{\Delta}^2))|_{t_N} - \beta_{12} (\dot{x}^{*2} \dot{\Delta}^2)|_{t_N} - \beta_{13} (x^{*1} \dot{\Delta}^1)|_{t_N} - \beta_{14} ((x^{*1} - x^{*2})(\dot{\Delta}^1 - \dot{\Delta}^2))|_{t_N} \\
& - \beta_{15} (x^{*2} \dot{\Delta}^2)|_{t_N} = (\ddot{x}^{*1} \dot{\Delta}^1)|_{t_N}
\end{aligned} \tag{2.60}$$

Put the above equation into matrix form, the coefficient matrix can be defined as,

$$\mathbf{X}^T = \begin{bmatrix} (\ddot{x}^1 \dot{\Delta}^1)|_{t_0} & \dots & (\ddot{x}^1 \dot{\Delta}^1)|_{t_i} & \dots & (\ddot{x}^1 \dot{\Delta}^1)|_{t_N} \\ (\ddot{x}^2 \dot{\Delta}^2)|_{t_0} & \dots & (\ddot{x}^2 \dot{\Delta}^2)|_{t_i} & \dots & (\ddot{x}^2 \dot{\Delta}^2)|_{t_N} \\ (\dot{x}^1 \dot{\Delta}^1)|_{t_0} & \dots & (\dot{x}^1 \dot{\Delta}^1)|_{t_i} & \dots & (\dot{x}^1 \dot{\Delta}^1)|_{t_N} \\ (\dot{x}^1 - \dot{x}^2)(\dot{\Delta}^1 - \dot{\Delta}^2)|_{t_0} & \dots & (\dot{x}^1 - \dot{x}^2)(\dot{\Delta}^1 - \dot{\Delta}^2)|_{t_i} & \dots & (\dot{x}^1 - \dot{x}^2)(\dot{\Delta}^1 - \dot{\Delta}^2)|_{t_N} \\ (\dot{x}^2 \dot{\Delta}^2)|_{t_0} & \dots & (\dot{x}^2 \dot{\Delta}^2)|_{t_i} & \dots & (\dot{x}^2 \dot{\Delta}^2)|_{t_N} \\ (x^1 \dot{\Delta}^1)|_{t_0} & \dots & (x^1 \dot{\Delta}^1)|_{t_i} & \dots & (x^1 \dot{\Delta}^1)|_{t_N} \\ ((x^1 - x^2)(\dot{\Delta}^1 - \dot{\Delta}^2))|_{t_0} & \dots & ((x^1 - x^2)(\dot{\Delta}^1 - \dot{\Delta}^2))|_{t_i} & \dots & ((x^1 - x^2)(\dot{\Delta}^1 - \dot{\Delta}^2))|_{t_N} \\ (x^2 \dot{\Delta}^2)|_{t_0} & \dots & (x^2 \dot{\Delta}^2)|_{t_i} & \dots & (x^2 \dot{\Delta}^2)|_{t_N} \\ (-\ddot{x}^{*2} \dot{\Delta}^2)|_{t_0} & \dots & (-\ddot{x}^{*2} \dot{\Delta}^2)|_{t_i} & \dots & (-\ddot{x}^{*2} \dot{\Delta}^2)|_{t_N} \\ (-\dot{x}^{*1} \dot{\Delta}^1)|_{t_0} & \dots & (-\dot{x}^{*1} \dot{\Delta}^1)|_{t_i} & \dots & (-\dot{x}^{*1} \dot{\Delta}^1)|_{t_N} \\ (-\dot{x}^{*1} - \dot{x}^{*2})(\dot{\Delta}^1 - \dot{\Delta}^2)|_{t_0} & \dots & (-\dot{x}^{*1} - \dot{x}^{*2})(\dot{\Delta}^1 - \dot{\Delta}^2)|_{t_i} & \dots & (-\dot{x}^{*1} - \dot{x}^{*2})(\dot{\Delta}^1 - \dot{\Delta}^2)|_{t_N} \\ (-\dot{x}^{*2} \dot{\Delta}^2)|_{t_0} & \dots & (-\dot{x}^{*2} \dot{\Delta}^2)|_{t_i} & \dots & (-\dot{x}^{*2} \dot{\Delta}^2)|_{t_N} \\ (-x^{*1} \dot{\Delta}^1)|_{t_0} & \dots & (-x^{*1} \dot{\Delta}^1)|_{t_i} & \dots & (-x^{*1} \dot{\Delta}^1)|_{t_N} \\ (-x^{*1} - x^{*2})(\dot{\Delta}^1 - \dot{\Delta}^2)|_{t_0} & \dots & (-x^{*1} - x^{*2})(\dot{\Delta}^1 - \dot{\Delta}^2)|_{t_i} & \dots & (-x^{*1} - x^{*2})(\dot{\Delta}^1 - \dot{\Delta}^2)|_{t_N} \\ (-x^{*2} \dot{\Delta}^2)|_{t_0} & \dots & (-x^{*2} \dot{\Delta}^2)|_{t_i} & \dots & (-x^{*2} \dot{\Delta}^2)|_{t_N} \end{bmatrix} \quad (2.61)$$

The vector of unknowns and the vector of known can be defined as,

$$\boldsymbol{\beta} = \begin{Bmatrix} \beta_1 \\ \beta_2 \\ \beta_3 \\ \beta_4 \\ \beta_5 \\ \beta_6 \\ \beta_7 \\ \beta_8 \\ \beta_9 \\ \beta_{10} \\ \beta_{11} \\ \beta_{12} \\ \beta_{13} \\ \beta_{14} \\ \beta_{15} \end{Bmatrix} \quad (2.62)$$

$$\mathbf{Y} = \begin{Bmatrix} (\ddot{\mathbf{x}}^{*1} \dot{\Delta}^1) |_{t_0} \\ \vdots \\ (\ddot{\mathbf{x}}^{*1} \dot{\Delta}^1) |_{t_i} \\ \vdots \\ (\ddot{\mathbf{x}}^{*1} \dot{\Delta}^1) |_{t_N} \end{Bmatrix} \quad (2.63)$$

The above equation may be expressed as,

$$\mathbf{X}\boldsymbol{\beta} = \mathbf{Y} \quad (2.64)$$

Based on the Least Square Method, the  $\boldsymbol{\beta}$  can be computed from the following equation,

$$\boldsymbol{\beta} = (\mathbf{X}^T \mathbf{X})^{-1} (\mathbf{X}^T \mathbf{Y}) \quad (2.65)$$

According to the definition of the damage index in Eq. 2.11, the damage indices for stiffness, mass and damping can be computed as follows,

$$\beta_{m^1} = \frac{m^1}{m^{*1}} = \beta_1 \quad (2.66)$$

$$\beta_{m^2} = \frac{m^2}{m^{*2}} = \frac{\frac{m^2}{m^{*1}}}{\frac{m^{*2}}{m^{*1}}} = \frac{\beta_2}{\beta_9} \quad (2.67)$$

$$\beta_{c_1} = \frac{c_1}{c_1^*} = \frac{\frac{c_1}{m^{*1}}}{\frac{c_1^*}{m^{*1}}} = \frac{\beta_3}{\beta_{10}} \quad (2.68)$$

$$\beta_{c_2} = \frac{c_2}{c_2^*} = \frac{\frac{c_2}{m^{*1}}}{\frac{c_2^*}{m^{*1}}} = \frac{\beta_4}{\beta_{11}} \quad (2.69)$$

$$\beta_{c_3} = \frac{c_3}{c_3^*} = \frac{\frac{c_3}{m^{*1}}}{\frac{c_3^*}{m^{*1}}} = \frac{\beta_5}{\beta_{12}} \quad (2.70)$$

$$\beta_{k_1} = \frac{k_1}{k_1^*} = \frac{\frac{k_1}{m^{*1}}}{\frac{k_1^*}{m^{*1}}} = \frac{\beta_6}{\beta_{13}} \quad (2.71)$$

$$\beta_{k_2} = \frac{k_2}{k_2^*} = \frac{\frac{k_2}{m^{*1}}}{\frac{k_2^*}{m^{*1}}} = \frac{\beta_7}{\beta_{14}} \quad (2.72)$$

$$\beta_{k_3} = \frac{k_3}{k_3^*} = \frac{\frac{k_3}{m^{*1}}}{\frac{k_3^*}{m^{*1}}} = \frac{\beta_8}{\beta_{15}} \quad (2.73)$$

According to the relationship between the damage severity and damage index of one element, shown in Eq. 2.13, the damage severities for stiffness, mass and damping can be

computed as follows,

$$\alpha_{m^1} = \frac{1}{\beta_{m^1}} - 1 = \frac{1}{\beta_1} - 1 \quad (2.74)$$

$$\alpha_{m^2} = \frac{1}{\beta_{m^2}} - 1 = \frac{\beta_9}{\beta_2} - 1 \quad (2.75)$$

$$\alpha_{c_1} = \frac{1}{\beta_{c_1}} - 1 = \frac{\beta_{10}}{\beta_3} - 1 \quad (2.76)$$

$$\alpha_{c_2} = \frac{1}{\beta_{c_2}} - 1 = \frac{\beta_{11}}{\beta_4} - 1 \quad (2.77)$$

$$\alpha_{c_3} = \frac{1}{\beta_{c_3}} - 1 = \frac{\beta_{12}}{\beta_5} - 1 \quad (2.78)$$

$$\alpha_{k_1} = \frac{1}{\beta_{k_1}} - 1 = \frac{\beta_{13}}{\beta_6} - 1 \quad (2.79)$$

$$\alpha_{k_2} = \frac{1}{\beta_{k_2}} - 1 = \frac{\beta_{14}}{\beta_7} - 1 \quad (2.80)$$

$$\alpha_{k_3} = \frac{1}{\beta_{k_3}} - 1 = \frac{\beta_{15}}{\beta_8} - 1 \quad (2.81)$$

## 2.5 THEORY FOR N-DOF SPRING-MASS-DAMPER SYSTEMS

For a typical 5-DOF spring-mass-damper system, as shown in Figure 2.3, the system is composed of five lumped masses, six linear springs, and six linear dash pots. The terms  $p^1(t)$  through  $p^5(t)$  are the external dynamic forces acting on lumped masses 1 through 5 separately at time point  $t$ . The terms  $x^1(t)$  through  $x^5(t)$  are the displacements of the five mass blocks relative to the ground at time point  $t$ . The terms  $\dot{x}^1(t)$  through  $\dot{x}^5(t)$

are the velocities of the five mass blocks relative to the ground at time point  $t$ . The terms  $\ddot{x}^1(t)$  through  $\ddot{x}^5(t)$  are the accelerations of the five mass blocks relative to the ground at time point  $t$ .

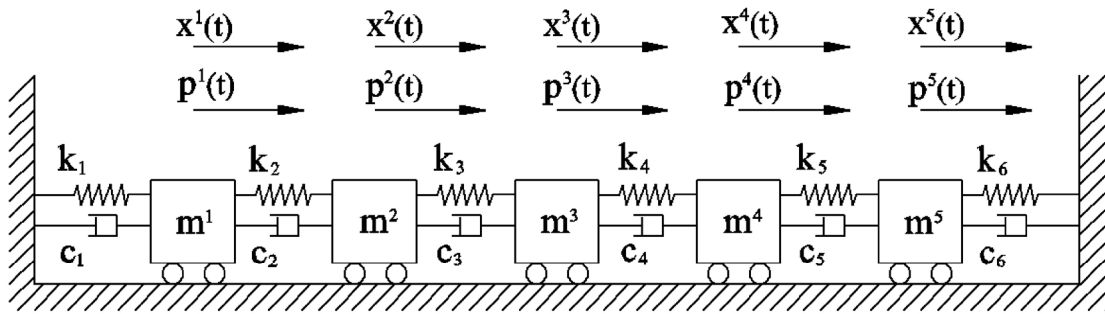


**Figure 2.3. 5-DOF Spring-Mass-Damper System**

For the 5-DOF spring-mass-damper system, Eq. 2.10 can be written as,



$$\begin{aligned}
& \begin{Bmatrix} \dot{\Delta}^1 \\ \dot{\Delta}^2 \\ \dot{\Delta}^3 \\ \dot{\Delta}^4 \\ \dot{\Delta}^5 \end{Bmatrix}^T \begin{bmatrix} m^1 & 0 & 0 & 0 & 0 \\ 0 & m^2 & 0 & 0 & 0 \\ 0 & 0 & m^3 & 0 & 0 \\ 0 & 0 & 0 & m^4 & 0 \\ 0 & 0 & 0 & 0 & m^5 \end{bmatrix} \begin{Bmatrix} \ddot{x}^1 \\ \ddot{x}^2 \\ \ddot{x}^3 \\ \ddot{x}^4 \\ \ddot{x}^5 \end{Bmatrix} \\
& + \begin{Bmatrix} \dot{\Delta}^1 \\ \dot{\Delta}^2 \\ \dot{\Delta}^3 \\ \dot{\Delta}^4 \\ \dot{\Delta}^5 \end{Bmatrix}^T \begin{bmatrix} c_1 + c_2 & -c_2 & 0 & 0 & 0 \\ -c_2 & c_2 + c_3 & -c_3 & 0 & 0 \\ 0 & -c_3 & c_3 + c_4 & -c_4 & 0 \\ 0 & 0 & -c_4 & c_4 + c_5 & -c_5 \\ 0 & 0 & 0 & -c_5 & c_5 + c_6 \end{bmatrix} \begin{Bmatrix} \dot{x}^1 \\ \dot{x}^2 \\ \dot{x}^3 \\ \dot{x}^4 \\ \dot{x}^5 \end{Bmatrix} \\
& + \begin{Bmatrix} \dot{\Delta}^1 \\ \dot{\Delta}^2 \\ \dot{\Delta}^3 \\ \dot{\Delta}^4 \\ \dot{\Delta}^5 \end{Bmatrix}^T \begin{bmatrix} k_1 + k_2 & -k_2 & 0 & 0 & 0 \\ -k_2 & k_2 + k_3 & -k_3 & 0 & 0 \\ 0 & -k_3 & k_3 + k_4 & -k_4 & 0 \\ 0 & 0 & -k_4 & k_4 + k_5 & -k_5 \\ 0 & 0 & 0 & -k_5 & k_5 + k_6 \end{bmatrix} \begin{Bmatrix} x^1 \\ x^2 \\ x^3 \\ x^4 \\ x^5 \end{Bmatrix}
\end{aligned}$$

(2.82)

$$\begin{aligned}
& = \begin{Bmatrix} \dot{\Delta}^1 \\ \dot{\Delta}^2 \\ \dot{\Delta}^3 \\ \dot{\Delta}^4 \\ \dot{\Delta}^5 \end{Bmatrix}^T \begin{bmatrix} m^{*1} & 0 & 0 & 0 & 0 \\ 0 & m^{*2} & 0 & 0 & 0 \\ 0 & 0 & m^{*3} & 0 & 0 \\ 0 & 0 & 0 & m^{*4} & 0 \\ 0 & 0 & 0 & 0 & m^{*5} \end{bmatrix} \begin{Bmatrix} \ddot{x}^{*1} \\ \ddot{x}^{*2} \\ \ddot{x}^{*3} \\ \ddot{x}^{*4} \\ \ddot{x}^{*5} \end{Bmatrix} \\
& + \begin{Bmatrix} \dot{\Delta}^1 \\ \dot{\Delta}^2 \\ \dot{\Delta}^3 \\ \dot{\Delta}^4 \\ \dot{\Delta}^5 \end{Bmatrix}^T \begin{bmatrix} c_1^* + c_2^* & -c_2^* & 0 & 0 & 0 \\ -c_2^* & c_2^* + c_3^* & -c_3^* & 0 & 0 \\ 0 & -c_3^* & c_3^* + c_4^* & -c_4^* & 0 \\ 0 & 0 & -c_4^* & c_4^* + c_5^* & -c_5^* \\ 0 & 0 & 0 & -c_5^* & c_5^* + c_6^* \end{bmatrix} \begin{Bmatrix} \dot{x}^{*1} \\ \dot{x}^{*2} \\ \dot{x}^{*3} \\ \dot{x}^{*4} \\ \dot{x}^{*5} \end{Bmatrix} \\
& + \begin{Bmatrix} \dot{\Delta}^1 \\ \dot{\Delta}^2 \\ \dot{\Delta}^3 \\ \dot{\Delta}^4 \\ \dot{\Delta}^5 \end{Bmatrix}^T \begin{bmatrix} k_1^* + k_2^* & -k_2^* & 0 & 0 & 0 \\ -k_2^* & k_2^* + k_3^* & -k_3^* & 0 & 0 \\ 0 & -k_3^* & k_3^* + k_4^* & -k_4^* & 0 \\ 0 & 0 & -k_4^* & k_4^* + k_5^* & -k_5^* \\ 0 & 0 & 0 & -k_5^* & k_5^* + k_6^* \end{bmatrix} \begin{Bmatrix} x^{*1} \\ x^{*2} \\ x^{*3} \\ x^{*4} \\ x^{*5} \end{Bmatrix}
\end{aligned}$$

Eq. 2.82 can be rewritten as,

$$\begin{aligned}
& m^1 \ddot{x}^1 \dot{\Delta}^1 + m^2 \ddot{x}^2 \dot{\Delta}^2 + m^3 \ddot{x}^3 \dot{\Delta}^3 + m^4 \ddot{x}^4 \dot{\Delta}^4 + m^5 \ddot{x}^5 \dot{\Delta}^5 \\
& + c_1 \dot{x}^1 \dot{\Delta}^1 + c_2 (\dot{x}^1 - \dot{x}^2)(\dot{\Delta}^1 - \dot{\Delta}^2) + c_3 (\dot{x}^2 - \dot{x}^3)(\dot{\Delta}^2 - \dot{\Delta}^3) + c_4 (\dot{x}^3 - \dot{x}^4)(\dot{\Delta}^3 - \dot{\Delta}^4) \\
& + c_5 (\dot{x}^4 - \dot{x}^5)(\dot{\Delta}^4 - \dot{\Delta}^5) + c_6 \dot{x}^5 \dot{\Delta}^5 \\
& + k_1 x^1 \dot{\Delta}^1 + k_2 (x^1 - x^2)(\dot{\Delta}^1 - \dot{\Delta}^2) + k_3 (x^2 - x^3)(\dot{\Delta}^2 - \dot{\Delta}^3) + k_4 (x^3 - x^4)(\dot{\Delta}^3 - \dot{\Delta}^4) \\
& + k_5 (x^4 - x^5)(\dot{\Delta}^4 - \dot{\Delta}^5) + k_6 x^5 \dot{\Delta}^5 \\
& = m^{*1} \ddot{x}^{*1} \dot{\Delta}^1 + m^{*2} \ddot{x}^{*2} \dot{\Delta}^2 + m^{*3} \ddot{x}^{*3} \dot{\Delta}^3 + m^{*4} \ddot{x}^{*4} \dot{\Delta}^4 + m^{*5} \ddot{x}^{*5} \dot{\Delta}^5 \\
& + c_1^* \dot{x}^{*1} \dot{\Delta}^1 + c_2^* (\dot{x}^{*1} - \dot{x}^{*2})(\dot{\Delta}^1 - \dot{\Delta}^2) + c_3^* (\dot{x}^{*2} - \dot{x}^{*3})(\dot{\Delta}^2 - \dot{\Delta}^3) + c_4^* (\dot{x}^{*3} - \dot{x}^{*4})(\dot{\Delta}^3 - \dot{\Delta}^4) \\
& + c_5^* (\dot{x}^{*4} - \dot{x}^{*5})(\dot{\Delta}^4 - \dot{\Delta}^5) + c_6^* \dot{x}^{*5} \dot{\Delta}^5 \\
& + k_1^* x^{*1} \dot{\Delta}^1 + k_2^* (x^{*1} - x^{*2})(\dot{\Delta}^1 - \dot{\Delta}^2) + k_3^* (x^{*2} - x^{*3})(\dot{\Delta}^2 - \dot{\Delta}^3) + k_4^* (x^{*3} - x^{*4})(\dot{\Delta}^3 - \dot{\Delta}^4) \\
& + k_5^* (x^{*4} - x^{*5})(\dot{\Delta}^4 - \dot{\Delta}^5) + k_6^* x^{*5} \dot{\Delta}^5
\end{aligned} \tag{2.83}$$

Rearranging Eq. 2.83 yields,

$$\begin{aligned}
& m^1 \ddot{x}^1 \dot{\Delta}^1 + m^2 \ddot{x}^2 \dot{\Delta}^2 + m^3 \ddot{x}^3 \dot{\Delta}^3 + m^4 \ddot{x}^4 \dot{\Delta}^4 + m^5 \ddot{x}^5 \dot{\Delta}^5 \\
& + c_1 \dot{x}^1 \dot{\Delta}^1 + c_2 (\dot{x}^1 - \dot{x}^2)(\dot{\Delta}^1 - \dot{\Delta}^2) + c_3 (\dot{x}^2 - \dot{x}^3)(\dot{\Delta}^2 - \dot{\Delta}^3) + c_4 (\dot{x}^3 - \dot{x}^4)(\dot{\Delta}^3 - \dot{\Delta}^4) \\
& + c_5 (\dot{x}^4 - \dot{x}^5)(\dot{\Delta}^4 - \dot{\Delta}^5) + c_6 \dot{x}^5 \dot{\Delta}^5 \\
& + k_1 x^1 \dot{\Delta}^1 + k_2 (x^1 - x^2)(\dot{\Delta}^1 - \dot{\Delta}^2) + k_3 (x^2 - x^3)(\dot{\Delta}^2 - \dot{\Delta}^3) + k_4 (x^3 - x^4)(\dot{\Delta}^3 - \dot{\Delta}^4) \\
& + k_5 (x^4 - x^5)(\dot{\Delta}^4 - \dot{\Delta}^5) + k_6 x^5 \dot{\Delta}^5 \\
& - m^{*2} \ddot{x}^{*2} \dot{\Delta}^2 - m^{*3} \ddot{x}^{*3} \dot{\Delta}^3 - m^{*4} \ddot{x}^{*4} \dot{\Delta}^4 - m^{*5} \ddot{x}^{*5} \dot{\Delta}^5 \\
& - c_1^* \dot{x}^{*1} \dot{\Delta}^1 - c_2^* (\dot{x}^{*1} - \dot{x}^{*2})(\dot{\Delta}^1 - \dot{\Delta}^2) - c_3^* (\dot{x}^{*2} - \dot{x}^{*3})(\dot{\Delta}^2 - \dot{\Delta}^3) - c_4^* (\dot{x}^{*3} - \dot{x}^{*4})(\dot{\Delta}^3 - \dot{\Delta}^4) \\
& - c_5^* (\dot{x}^{*4} - \dot{x}^{*5})(\dot{\Delta}^4 - \dot{\Delta}^5) - c_6^* \dot{x}^{*5} \dot{\Delta}^5 \\
& - k_1^* x^{*1} \dot{\Delta}^1 - k_2^* (x^{*1} - x^{*2})(\dot{\Delta}^1 - \dot{\Delta}^2) - k_3^* (x^{*2} - x^{*3})(\dot{\Delta}^2 - \dot{\Delta}^3) - k_4^* (x^{*3} - x^{*4})(\dot{\Delta}^3 - \dot{\Delta}^4) \\
& - k_5^* (x^{*4} - x^{*5})(\dot{\Delta}^4 - \dot{\Delta}^5) - k_6^* x^{*5} \dot{\Delta}^5 \\
& = m^{*1} \ddot{x}^{*1} \dot{\Delta}^1
\end{aligned} \tag{2.84}$$

Dividing each term in Eq. 2.84 by  $m^{*1}$  yields,

$$\begin{aligned}
& \frac{m^1}{m^{*1}} \ddot{x}^1 \dot{\Delta}^1 + \frac{m^2}{m^{*1}} \ddot{x}^2 \dot{\Delta}^2 + \frac{m^3}{m^{*1}} \ddot{x}^3 \dot{\Delta}^3 + \frac{m^4}{m^{*1}} \ddot{x}^4 \dot{\Delta}^4 + \frac{m^5}{m^{*1}} \ddot{x}^5 \dot{\Delta}^5 \\
& + \frac{c_1}{m^{*1}} \dot{x}^1 \dot{\Delta}^1 + \frac{c_2}{m^{*1}} (\dot{x}^1 - \dot{x}^2)(\dot{\Delta}^1 - \dot{\Delta}^2) + \frac{c_3}{m^{*1}} (\dot{x}^2 - \dot{x}^3)(\dot{\Delta}^2 - \dot{\Delta}^3) + \frac{c_4}{m^{*1}} (\dot{x}^3 - \dot{x}^4)(\dot{\Delta}^3 - \dot{\Delta}^4) \\
& + \frac{c_5}{m^{*1}} (\dot{x}^4 - \dot{x}^5)(\dot{\Delta}^4 - \dot{\Delta}^5) + \frac{c_6}{m^{*1}} \dot{x}^5 \dot{\Delta}^5 \\
& + \frac{k_1}{m^{*1}} x^1 \dot{\Delta}^1 + \frac{k_2}{m^{*1}} (x^1 - x^2)(\dot{\Delta}^1 - \dot{\Delta}^2) + \frac{k_3}{m^{*1}} (x^2 - x^3)(\dot{\Delta}^2 - \dot{\Delta}^3) + \frac{k_4}{m^{*1}} (x^3 - x^4)(\dot{\Delta}^3 - \dot{\Delta}^4) \\
& + \frac{k_5}{m^{*1}} (x^4 - x^5)(\dot{\Delta}^4 - \dot{\Delta}^5) + \frac{k_6}{m^{*1}} x^5 \dot{\Delta}^5 \\
& - \frac{m^{*2}}{m^{*1}} \ddot{x}^{*2} \dot{\Delta}^2 - \frac{m^{*3}}{m^{*1}} \ddot{x}^{*3} \dot{\Delta}^3 - \frac{m^{*4}}{m^{*1}} \ddot{x}^{*4} \dot{\Delta}^4 - \frac{m^{*5}}{m^{*1}} \ddot{x}^{*5} \dot{\Delta}^5 \\
& - \frac{c_1^*}{m^{*1}} \dot{x}^{*1} \dot{\Delta}^1 - \frac{c_2^*}{m^{*1}} (\dot{x}^{*1} - \dot{x}^{*2})(\dot{\Delta}^1 - \dot{\Delta}^2) - \frac{c_3^*}{m^{*1}} (\dot{x}^{*2} - \dot{x}^{*3})(\dot{\Delta}^2 - \dot{\Delta}^3) - \frac{c_4^*}{m^{*1}} (\dot{x}^{*3} - \dot{x}^{*4})(\dot{\Delta}^3 - \dot{\Delta}^4) \\
& - \frac{c_5^*}{m^{*1}} (\dot{x}^{*4} - \dot{x}^{*5})(\dot{\Delta}^4 - \dot{\Delta}^5) - \frac{c_6^*}{m^{*1}} \dot{x}^{*5} \dot{\Delta}^5 \\
& - \frac{k_1^*}{m^{*1}} x^{*1} \dot{\Delta}^1 - \frac{k_2^*}{m^{*1}} (x^{*1} - x^{*2})(\dot{\Delta}^1 - \dot{\Delta}^2) - \frac{k_3^*}{m^{*1}} (x^{*2} - x^{*3})(\dot{\Delta}^2 - \dot{\Delta}^3) - \frac{k_4^*}{m^{*1}} (x^{*3} - x^{*4})(\dot{\Delta}^3 - \dot{\Delta}^4) \\
& - \frac{k_5^*}{m^{*1}} (x^{*4} - x^{*5})(\dot{\Delta}^4 - \dot{\Delta}^5) - \frac{k_6^*}{m^{*1}} x^{*5} \dot{\Delta}^5 \\
& = \ddot{x}^{*1} \dot{\Delta}^1
\end{aligned} \tag{2.85}$$

Define,

$$\beta_1 = \frac{m^1}{m^{*1}} \tag{2.86}$$

$$\beta_2 = \frac{m^2}{m^{*1}} \tag{2.87}$$

$$\beta_3 = \frac{m^3}{m^{*1}} \tag{2.88}$$

$$\beta_4 = \frac{m^4}{m^{*1}} \tag{2.89}$$

$$\beta_5 = \frac{m^5}{m^{*1}} \tag{2.90}$$

$$\beta_6 = \frac{c_1}{m^{*1}} \quad (2.91)$$

$$\beta_7 = \frac{c_2}{m^{*1}} \quad (2.92)$$

$$\beta_8 = \frac{c_3}{m^{*1}} \quad (2.93)$$

$$\beta_9 = \frac{c_4}{m^{*1}} \quad (2.94)$$

$$\beta_{10} = \frac{c_5}{m^{*1}} \quad (2.95)$$

$$\beta_{11} = \frac{c_6}{m^{1*}} \quad (2.96)$$

$$\beta_{12} = \frac{k_1}{m^{*1}} \quad (2.97)$$

$$\beta_{13} = \frac{k_2}{m^{*1}} \quad (2.98)$$

$$\beta_{14} = \frac{k_3}{m^{*1}} \quad (2.99)$$

$$\beta_{15} = \frac{k_4}{m^{*1}} \quad (2.100)$$

$$\beta_{16} = \frac{k_5}{m^{*1}} \quad (2.101)$$

$$\beta_{17} = \frac{k_6}{m^{*1}} \quad (2.102)$$

$$\beta_{18} = \frac{m^{*2}}{m^{*1}} \quad (2.103)$$

$$\beta_{19} = \frac{m^{*3}}{m^{*1}} \quad (2.104)$$

$$\beta_{20} = \frac{m^{*4}}{m^{*1}} \quad (2.105)$$

$$\beta_{21} = \frac{m^{*5}}{m^{*1}} \quad (2.106)$$

$$\beta_{22} = \frac{c_1^*}{m^{*1}} \quad (2.107)$$

$$\beta_{23} = \frac{c_2^*}{m^{*1}} \quad (2.108)$$

$$\beta_{24} = \frac{c_3^*}{m^{*1}} \quad (2.109)$$

$$\beta_{25} = \frac{c_4^*}{m^{*1}} \quad (2.110)$$

$$\beta_{26} = \frac{c_5^*}{m^{*1}} \quad (2.111)$$

$$\beta_{27} = \frac{c_6^*}{m^{*1}} \quad (2.112)$$

$$\beta_{28} = \frac{k_1^*}{m^{*1}} \quad (2.113)$$

$$\beta_{29} = \frac{k_2^*}{m^{*1}} \quad (2.114)$$

$$\beta_{30} = \frac{k_3^*}{m^{*1}} \quad (2.115)$$

$$\beta_{31} = \frac{k_4^*}{m^{*1}} \quad (2.116)$$

$$\beta_{32} = \frac{k_5^*}{m^{*1}} \quad (2.117)$$

$$\beta_{33} = \frac{k_6^*}{m^{*1}} \quad (2.118)$$

Substitute Eqs. 2.86 through 2.118 into Eq. 2.85, yields,

$$\begin{aligned}
& \beta_1 \ddot{x}^1 \dot{\Delta}^1 + \beta_2 \ddot{x}^2 \dot{\Delta}^2 + \beta_3 \ddot{x}^3 \dot{\Delta}^3 + \beta_4 \ddot{x}^4 \dot{\Delta}^4 + \beta_5 \ddot{x}^5 \dot{\Delta}^5 \\
& + \beta_6 \dot{x}^1 \dot{\Delta}^1 + \beta_7 (\dot{x}^1 - \dot{x}^2)(\dot{\Delta}^1 - \dot{\Delta}^2) + \beta_8 (\dot{x}^2 - \dot{x}^3)(\dot{\Delta}^2 - \dot{\Delta}^3) + \beta_9 (\dot{x}^3 - \dot{x}^4)(\dot{\Delta}^3 - \dot{\Delta}^4) \\
& + \beta_{10} (\dot{x}^4 - \dot{x}^5)(\dot{\Delta}^4 - \dot{\Delta}^5) + \beta_{11} \dot{x}^5 \dot{\Delta}^5 \\
& + \beta_{12} x^1 \dot{\Delta}^1 + \beta_{13} (x^1 - x^2)(\dot{\Delta}^1 - \dot{\Delta}^2) + \beta_{14} (x^2 - x^3)(\dot{\Delta}^2 - \dot{\Delta}^3) + \beta_{15} (x^3 - x^4)(\dot{\Delta}^3 - \dot{\Delta}^4) \\
& + \beta_{16} (x^4 - x^5)(\dot{\Delta}^4 - \dot{\Delta}^5) + \beta_{17} x^5 \dot{\Delta}^5 \\
& - \beta_{18} \ddot{x}^{*2} \dot{\Delta}^2 - \beta_{19} \ddot{x}^{*3} \dot{\Delta}^3 - \beta_{20} \ddot{x}^{*4} \dot{\Delta}^4 - \beta_{21} \ddot{x}^{*5} \dot{\Delta}^5 \\
& - \beta_{22} \dot{x}^{*1} \dot{\Delta}^1 - \beta_{23} (\dot{x}^{*1} - \dot{x}^{*2})(\dot{\Delta}^1 - \dot{\Delta}^2) - \beta_{24} (\dot{x}^{*2} - \dot{x}^{*3})(\dot{\Delta}^2 - \dot{\Delta}^3) - \beta_{25} (\dot{x}^{*3} - \dot{x}^{*4})(\dot{\Delta}^3 - \dot{\Delta}^4) \\
& - \beta_{26} (\dot{x}^{*4} - \dot{x}^{*5})(\dot{\Delta}^4 - \dot{\Delta}^5) - \beta_{27} \dot{x}^{*5} \dot{\Delta}^5 \\
& - \beta_{28} x^{*1} \dot{\Delta}^1 - \beta_{29} (x^{*1} - x^{*2})(\dot{\Delta}^1 - \dot{\Delta}^2) - \beta_{30} (x^{*2} - x^{*3})(\dot{\Delta}^2 - \dot{\Delta}^3) - \beta_{31} (x^{*3} - x^{*4})(\dot{\Delta}^3 - \dot{\Delta}^4) \\
& - \beta_{32} (x^{*4} - x^{*5})(\dot{\Delta}^4 - \dot{\Delta}^5) - \beta_{33} x^{*5} \dot{\Delta}^5 \\
& = \ddot{x}^{*1} \dot{\Delta}^1
\end{aligned} \tag{2.119}$$

Apply Eq. 2.119 at different time point,

For  $t = t_0$ ,

$$\begin{aligned}
& \beta_1 (\ddot{x}^1 \dot{\Delta}^1)|_{t_0} + \beta_2 (\ddot{x}^2 \dot{\Delta}^2)|_{t_0} + \beta_3 (\ddot{x}^3 \dot{\Delta}^3)|_{t_0} + \beta_4 (\ddot{x}^4 \dot{\Delta}^4)|_{t_0} + \beta_5 (\ddot{x}^5 \dot{\Delta}^5)|_{t_0} \\
& + \beta_6 (\dot{x}^1 \dot{\Delta}^1)|_{t_0} + \beta_7 ((\dot{x}^1 - \dot{x}^2)(\dot{\Delta}^1 - \dot{\Delta}^2))|_{t_0} + \beta_8 ((\dot{x}^2 - \dot{x}^3)(\dot{\Delta}^2 - \dot{\Delta}^3))|_{t_0} \\
& + \beta_9 ((\dot{x}^3 - \dot{x}^4)(\dot{\Delta}^3 - \dot{\Delta}^4))|_{t_0} + \beta_{10} ((\dot{x}^4 - \dot{x}^5)(\dot{\Delta}^4 - \dot{\Delta}^5))|_{t_0} + \beta_{11} (\dot{x}^5 \dot{\Delta}^5)|_{t_0} \\
& + \beta_{12} (x^1 \dot{\Delta}^1)|_{t_0} + \beta_{13} ((x^1 - x^2)(\dot{\Delta}^1 - \dot{\Delta}^2))|_{t_0} + \beta_{14} ((x^2 - x^3)(\dot{\Delta}^2 - \dot{\Delta}^3))|_{t_0} \\
& + \beta_{15} ((x^3 - x^4)(\dot{\Delta}^3 - \dot{\Delta}^4))|_{t_0} + \beta_{16} ((x^4 - x^5)(\dot{\Delta}^4 - \dot{\Delta}^5))|_{t_0} + \beta_{17} (x^5 \dot{\Delta}^5)|_{t_0} \\
& - \beta_{18} (\ddot{x}^{*2} \dot{\Delta}^2)|_{t_0} - \beta_{19} (\ddot{x}^{*3} \dot{\Delta}^3)|_{t_0} - \beta_{20} (\ddot{x}^{*4} \dot{\Delta}^4)|_{t_0} - \beta_{21} (\ddot{x}^{*5} \dot{\Delta}^5)|_{t_0} \\
& - \beta_{22} (\dot{x}^{*1} \dot{\Delta}^1)|_{t_0} - \beta_{23} ((\dot{x}^{*1} - \dot{x}^{*2})(\dot{\Delta}^1 - \dot{\Delta}^2))|_{t_0} - \beta_{24} ((\dot{x}^{*2} - \dot{x}^{*3})(\dot{\Delta}^2 - \dot{\Delta}^3))|_{t_0} \\
& - \beta_{25} ((\dot{x}^{*3} - \dot{x}^{*4})(\dot{\Delta}^3 - \dot{\Delta}^4))|_{t_0} - \beta_{26} ((\dot{x}^{*4} - \dot{x}^{*5})(\dot{\Delta}^4 - \dot{\Delta}^5))|_{t_0} - \beta_{27} (\dot{x}^{*5} \dot{\Delta}^5)|_{t_0} \\
& - \beta_{28} (x^{*1} \dot{\Delta}^1)|_{t_0} - \beta_{29} ((x^{*1} - x^{*2})(\dot{\Delta}^1 - \dot{\Delta}^2))|_{t_0} - \beta_{30} ((x^{*2} - x^{*3})(\dot{\Delta}^2 - \dot{\Delta}^3))|_{t_0} \\
& - \beta_{31} ((x^{*3} - x^{*4})(\dot{\Delta}^3 - \dot{\Delta}^4))|_{t_0} - \beta_{32} ((x^{*4} - x^{*5})(\dot{\Delta}^4 - \dot{\Delta}^5))|_{t_0} - \beta_{33} (x^{*5} \dot{\Delta}^5)|_{t_0} \\
& = (\ddot{x}^{*1} \dot{\Delta}^1)|_{t_0}
\end{aligned} \tag{2.120}$$

For  $t = t_i$ ,

$$\begin{aligned}
& \beta_1 (\ddot{x}^1 \dot{\Delta}^1)|_{t_i} + \beta_2 (\ddot{x}^2 \dot{\Delta}^2)|_{t_i} + \beta_3 (\ddot{x}^3 \dot{\Delta}^3)|_{t_i} + \beta_4 (\ddot{x}^4 \dot{\Delta}^4)|_{t_i} + \beta_5 (\ddot{x}^5 \dot{\Delta}^5)|_{t_i} \\
& + \beta_6 (\dot{x}^1 \dot{\Delta}^1)|_{t_i} + \beta_7 ((\dot{x}^1 - \dot{x}^2)(\dot{\Delta}^1 - \dot{\Delta}^2))|_{t_i} + \beta_8 ((\dot{x}^2 - \dot{x}^3)(\dot{\Delta}^2 - \dot{\Delta}^3))|_{t_i} \\
& + \beta_9 ((\dot{x}^3 - \dot{x}^4)(\dot{\Delta}^3 - \dot{\Delta}^4))|_{t_i} + \beta_{10} ((\dot{x}^4 - \dot{x}^5)(\dot{\Delta}^4 - \dot{\Delta}^5))|_{t_i} + \beta_{11} (\dot{x}^5 \dot{\Delta}^5)|_{t_i} \\
& + \beta_{12} (x^1 \dot{\Delta}^1)|_{t_i} + \beta_{13} ((x^1 - x^2)(\dot{\Delta}^1 - \dot{\Delta}^2))|_{t_i} + \beta_{14} ((x^2 - x^3)(\dot{\Delta}^2 - \dot{\Delta}^3))|_{t_i} \\
& + \beta_{15} ((x^3 - x^4)(\dot{\Delta}^3 - \dot{\Delta}^4))|_{t_i} + \beta_{16} ((x^4 - x^5)(\dot{\Delta}^4 - \dot{\Delta}^5))|_{t_i} + \beta_{17} (x^5 \dot{\Delta}^5)|_{t_i} \\
& - \beta_{18} (\ddot{x}^{*2} \dot{\Delta}^2)|_{t_i} - \beta_{19} (\ddot{x}^{*3} \dot{\Delta}^3)|_{t_i} - \beta_{20} (\ddot{x}^{*4} \dot{\Delta}^4)|_{t_i} - \beta_{21} (\ddot{x}^{*5} \dot{\Delta}^5)|_{t_i} \\
& - \beta_{22} (\dot{x}^{*1} \dot{\Delta}^1)|_{t_i} - \beta_{23} ((\dot{x}^{*1} - \dot{x}^{*2})(\dot{\Delta}^1 - \dot{\Delta}^2))|_{t_i} - \beta_{24} ((\dot{x}^{*2} - \dot{x}^{*3})(\dot{\Delta}^2 - \dot{\Delta}^3))|_{t_i} \\
& - \beta_{25} ((\dot{x}^{*3} - \dot{x}^{*4})(\dot{\Delta}^3 - \dot{\Delta}^4))|_{t_i} - \beta_{26} ((\dot{x}^{*4} - \dot{x}^{*5})(\dot{\Delta}^4 - \dot{\Delta}^5))|_{t_i} - \beta_{27} (\dot{x}^{*5} \dot{\Delta}^5)|_{t_i} \\
& - \beta_{28} (x^{*1} \dot{\Delta}^1)|_{t_i} - \beta_{29} ((x^{*1} - x^{*2})(\dot{\Delta}^1 - \dot{\Delta}^2))|_{t_i} - \beta_{30} ((x^{*2} - x^{*3})(\dot{\Delta}^2 - \dot{\Delta}^3))|_{t_i} \\
& - \beta_{31} ((x^{*3} - x^{*4})(\dot{\Delta}^3 - \dot{\Delta}^4))|_{t_i} - \beta_{32} ((x^{*4} - x^{*5})(\dot{\Delta}^4 - \dot{\Delta}^5))|_{t_i} - \beta_{33} (x^{*5} \dot{\Delta}^5)|_{t_i} \\
& = (\ddot{x}^{*1} \dot{\Delta}^1)|_{t_i}
\end{aligned} \tag{2.121}$$

For  $t = t_N$ ,

$$\begin{aligned}
& \beta_1 (\ddot{x}^1 \dot{\Delta}^1)|_{t_N} + \beta_2 (\ddot{x}^2 \dot{\Delta}^2)|_{t_N} + \beta_3 (\ddot{x}^3 \dot{\Delta}^3)|_{t_N} + \beta_4 (\ddot{x}^4 \dot{\Delta}^4)|_{t_N} + \beta_5 (\ddot{x}^5 \dot{\Delta}^5)|_{t_N} \\
& + \beta_6 (\dot{x}^1 \dot{\Delta}^1)|_{t_N} + \beta_7 ((\dot{x}^1 - \dot{x}^2)(\dot{\Delta}^1 - \dot{\Delta}^2))|_{t_N} + \beta_8 ((\dot{x}^2 - \dot{x}^3)(\dot{\Delta}^2 - \dot{\Delta}^3))|_{t_N} \\
& + \beta_9 ((\dot{x}^3 - \dot{x}^4)(\dot{\Delta}^3 - \dot{\Delta}^4))|_{t_N} + \beta_{10} ((\dot{x}^4 - \dot{x}^5)(\dot{\Delta}^4 - \dot{\Delta}^5))|_{t_N} + \beta_{11} (\dot{x}^5 \dot{\Delta}^5)|_{t_N} \\
& + \beta_{12} (x^1 \dot{\Delta}^1)|_{t_N} + \beta_{13} ((x^1 - x^2)(\dot{\Delta}^1 - \dot{\Delta}^2))|_{t_N} + \beta_{14} ((x^2 - x^3)(\dot{\Delta}^2 - \dot{\Delta}^3))|_{t_N} \\
& + \beta_{15} ((x^3 - x^4)(\dot{\Delta}^3 - \dot{\Delta}^4))|_{t_N} + \beta_{16} ((x^4 - x^5)(\dot{\Delta}^4 - \dot{\Delta}^5))|_{t_N} + \beta_{17} (x^5 \dot{\Delta}^5)|_{t_N} \\
& - \beta_{18} (\ddot{x}^{*2} \dot{\Delta}^2)|_{t_N} - \beta_{19} (\ddot{x}^{*3} \dot{\Delta}^3)|_{t_N} - \beta_{20} (\ddot{x}^{*4} \dot{\Delta}^4)|_{t_N} - \beta_{21} (\ddot{x}^{*5} \dot{\Delta}^5)|_{t_N} \\
& - \beta_{22} (\dot{x}^{*1} \dot{\Delta}^1)|_{t_N} - \beta_{23} ((\dot{x}^{*1} - \dot{x}^{*2})(\dot{\Delta}^1 - \dot{\Delta}^2))|_{t_N} - \beta_{24} ((\dot{x}^{*2} - \dot{x}^{*3})(\dot{\Delta}^2 - \dot{\Delta}^3))|_{t_N} \\
& - \beta_{25} ((\dot{x}^{*3} - \dot{x}^{*4})(\dot{\Delta}^3 - \dot{\Delta}^4))|_{t_N} - \beta_{26} ((\dot{x}^{*4} - \dot{x}^{*5})(\dot{\Delta}^4 - \dot{\Delta}^5))|_{t_N} - \beta_{27} (\dot{x}^{*5} \dot{\Delta}^5)|_{t_N} \\
& - \beta_{28} (x^{*1} \dot{\Delta}^1)|_{t_N} - \beta_{29} ((x^{*1} - x^{*2})(\dot{\Delta}^1 - \dot{\Delta}^2))|_{t_N} - \beta_{30} ((x^{*2} - x^{*3})(\dot{\Delta}^2 - \dot{\Delta}^3))|_{t_N} \\
& - \beta_{31} ((x^{*3} - x^{*4})(\dot{\Delta}^3 - \dot{\Delta}^4))|_{t_N} - \beta_{32} ((x^{*4} - x^{*5})(\dot{\Delta}^4 - \dot{\Delta}^5))|_{t_N} - \beta_{33} (x^{*5} \dot{\Delta}^5)|_{t_N} \\
& = (\ddot{x}^{*1} \dot{\Delta}^1)|_{t_N}
\end{aligned} \tag{2.122}$$

Put the above equation into matrix form, yields the coefficient matrix

$$\mathbf{X}^T = \begin{bmatrix} (\ddot{x}^1 \dot{\Delta}^1)|_{t_0} & \cdots & (\ddot{x}^1 \dot{\Delta}^1)|_{t_i} & \cdots & (\ddot{x}^1 \dot{\Delta}^1)|_{t_N} \\ \vdots & \vdots & \vdots & \vdots & \vdots \\ (\ddot{x}^5 \dot{\Delta}^5)|_{t_0} & \cdots & (\ddot{x}^5 \dot{\Delta}^5)|_{t_i} & \cdots & (\ddot{x}^5 \dot{\Delta}^5)|_{t_N} \\ (\dot{x}^1 \dot{\Delta}^1)|_{t_0} & \cdots & (\dot{x}^1 \dot{\Delta}^1)|_{t_i} & \cdots & (\dot{x}^1 \dot{\Delta}^1)|_{t_N} \\ ((\dot{x}^1 - \dot{x}^2)(\dot{\Delta}^1 - \dot{\Delta}^2))|_{t_0} & \cdots & ((\dot{x}^1 - \dot{x}^2)(\dot{\Delta}^1 - \dot{\Delta}^2))|_{t_i} & \cdots & ((\dot{x}^1 - \dot{x}^2)(\dot{\Delta}^1 - \dot{\Delta}^2))|_{t_N} \\ \vdots & \vdots & \vdots & \vdots & \vdots \\ ((\dot{x}^4 - \dot{x}^5)(\dot{\Delta}^4 - \dot{\Delta}^5))|_{t_0} & \cdots & ((\dot{x}^4 - \dot{x}^5)(\dot{\Delta}^4 - \dot{\Delta}^5))|_{t_i} & \cdots & ((\dot{x}^4 - \dot{x}^5)(\dot{\Delta}^4 - \dot{\Delta}^5))|_{t_N} \\ (\dot{x}^5 \dot{\Delta}^5)|_{t_0} & \cdots & (\dot{x}^5 \dot{\Delta}^5)|_{t_i} & \cdots & (\dot{x}^5 \dot{\Delta}^5)|_{t_N} \\ (x^1 \dot{\Delta}^1)|_{t_0} & \cdots & (x^1 \dot{\Delta}^1)|_{t_i} & \cdots & (x^1 \dot{\Delta}^1)|_{t_N} \\ ((x^1 - x^2)(\dot{\Delta}^1 - \dot{\Delta}^2))|_{t_0} & \cdots & ((x^1 - x^2)(\dot{\Delta}^1 - \dot{\Delta}^2))|_{t_i} & \cdots & ((x^1 - x^2)(\dot{\Delta}^1 - \dot{\Delta}^2))|_{t_N} \\ \vdots & \vdots & \vdots & \vdots & \vdots \\ ((x^4 - x^5)(\dot{\Delta}^4 - \dot{\Delta}^5))|_{t_0} & \cdots & ((x^4 - x^5)(\dot{\Delta}^4 - \dot{\Delta}^5))|_{t_i} & \cdots & ((x^4 - x^5)(\dot{\Delta}^4 - \dot{\Delta}^5))|_{t_N} \\ (x^5 \dot{\Delta}^5)|_{t_0} & \cdots & (x^5 \dot{\Delta}^5)|_{t_i} & \cdots & (x^5 \dot{\Delta}^5)|_{t_N} \\ -(\dot{x}^{*2} \dot{\Delta}^2)|_{t_0} & \cdots & -(\dot{x}^{*2} \dot{\Delta}^2)|_{t_i} & \cdots & -(\dot{x}^{*2} \dot{\Delta}^2)|_{t_N} \\ \vdots & \vdots & \vdots & \vdots & \vdots \\ -(\dot{x}^{*5} \dot{\Delta}^5)|_{t_0} & \cdots & -(\dot{x}^{*5} \dot{\Delta}^5)|_{t_i} & \cdots & -(\dot{x}^{*5} \dot{\Delta}^5)|_{t_N} \\ -(\dot{x}^{*1} \dot{\Delta}^1)|_{t_0} & \cdots & -(\dot{x}^{*1} \dot{\Delta}^1)|_{t_i} & \cdots & -(\dot{x}^{*1} \dot{\Delta}^1)|_{t_N} \\ -((\dot{x}^{*1} - \dot{x}^{*2})(\dot{\Delta}^1 - \dot{\Delta}^2))|_{t_0} & \cdots & -((\dot{x}^{*1} - \dot{x}^{*2})(\dot{\Delta}^1 - \dot{\Delta}^2))|_{t_i} & \cdots & -((\dot{x}^{*1} - \dot{x}^{*2})(\dot{\Delta}^1 - \dot{\Delta}^2))|_{t_N} \\ \vdots & \vdots & \vdots & \vdots & \vdots \\ -((\dot{x}^{*4} - \dot{x}^{*5})(\dot{\Delta}^4 - \dot{\Delta}^5))|_{t_0} & \cdots & -((\dot{x}^{*4} - \dot{x}^{*5})(\dot{\Delta}^4 - \dot{\Delta}^5))|_{t_i} & \cdots & -((\dot{x}^{*4} - \dot{x}^{*5})(\dot{\Delta}^4 - \dot{\Delta}^5))|_{t_N} \\ -(\dot{x}^{*5} \dot{\Delta}^5)|_{t_0} & \cdots & -(\dot{x}^{*5} \dot{\Delta}^5)|_{t_i} & \cdots & -(\dot{x}^{*5} \dot{\Delta}^5)|_{t_N} \\ -(\dot{x}^{*1} \dot{\Delta}^1)|_{t_0} & \cdots & -(\dot{x}^{*1} \dot{\Delta}^1)|_{t_i} & \cdots & -(\dot{x}^{*1} \dot{\Delta}^1)|_{t_N} \\ -((x^{*1} - x^{*2})(\dot{\Delta}^1 - \dot{\Delta}^2))|_{t_0} & \cdots & -((x^{*1} - x^{*2})(\dot{\Delta}^1 - \dot{\Delta}^2))|_{t_i} & \cdots & -((x^{*1} - x^{*2})(\dot{\Delta}^1 - \dot{\Delta}^2))|_{t_N} \\ \vdots & \vdots & \vdots & \vdots & \vdots \\ -((x^{*4} - x^{*5})(\dot{\Delta}^4 - \dot{\Delta}^5))|_{t_0} & \cdots & -((x^{*4} - x^{*5})(\dot{\Delta}^4 - \dot{\Delta}^5))|_{t_i} & \cdots & -((x^{*4} - x^{*5})(\dot{\Delta}^4 - \dot{\Delta}^5))|_{t_N} \\ -(\dot{x}^{*5} \dot{\Delta}^5)|_{t_0} & \cdots & -(\dot{x}^{*5} \dot{\Delta}^5)|_{t_i} & \cdots & -(\dot{x}^{*5} \dot{\Delta}^5)|_{t_N} \end{bmatrix}, \quad (2.123)$$



Define

$$\boldsymbol{\beta} = \begin{Bmatrix} \beta_1 \\ \vdots \\ \beta_i \\ \vdots \\ \beta_{33} \end{Bmatrix} \quad (2.124)$$

$$\mathbf{Y} = \begin{Bmatrix} (\ddot{x}^{*1} \dot{\Delta}^1) |_{t_1} \\ \vdots \\ (\ddot{x}^{*1} \dot{\Delta}^1) |_{t_i} \\ \vdots \\ (\ddot{x}^{*1} \dot{\Delta}^1) |_{t_N} \end{Bmatrix} \quad (2.125)$$

The above equation may be expressed as,

$$\mathbf{X}\boldsymbol{\beta} = \mathbf{Y} \quad (2.126)$$

Based on the Least Square Method, the  $\beta$  can be computed from the following equation,

$$\boldsymbol{\beta} = (\mathbf{X}^T \mathbf{X})^{-1} (\mathbf{X}^T \mathbf{Y}) \quad (2.127)$$

According to the definition of the damage index in Eq. 2.11, the damage indices for stiffness, mass and damping can be computed as follows,

$$\beta_{m^1} = \frac{m^1}{m^{*1}} = \beta_1 \quad (2.128)$$

$$\beta_{m^2} = \frac{\frac{m^2}{m^{*1}}}{\frac{m^{*2}}{m^{*1}}} = \frac{\beta_2}{\beta_{18}} \quad (2.129)$$

$$\beta_{m^3} = \frac{\frac{m^3}{m^{*1}}}{\frac{m^{*3}}{m^{*1}}} = \frac{\beta_3}{\beta_{19}} \quad (2.130)$$

$$\beta_{m^4} = \frac{\frac{m^4}{m^{*1}}}{\frac{m^{*4}}{m^{*1}}} = \frac{\beta_4}{\beta_{20}} \quad (2.131)$$

$$\beta_{m^5} = \frac{\frac{m^5}{m^{*1}}}{\frac{m^{*5}}{m^{*1}}} = \frac{\beta_5}{\beta_{21}} \quad (2.132)$$

$$\beta_{c_1} = \frac{\frac{c_1}{m^{*1}}}{\frac{c_1^*}{m^{*1}}} = \frac{\beta_6}{\beta_{22}} \quad (2.133)$$

$$\beta_{c_2} = \frac{\frac{c_2}{m^{*1}}}{\frac{c_2^*}{m^{*1}}} = \frac{\beta_7}{\beta_{23}} \quad (2.134)$$

$$\beta_{c_3} = \frac{\frac{c_3}{m^{*1}}}{\frac{c_3^*}{m^{*1}}} = \frac{\beta_8}{\beta_{24}} \quad (2.135)$$

$$\beta_{c_4} = \frac{\frac{c_4}{m^{*1}}}{\frac{c_4^*}{m^{*1}}} = \frac{\beta_9}{\beta_{25}} \quad (2.136)$$

$$\beta_{c_5} = \frac{\frac{c_5}{m^{*1}}}{\frac{c_5^*}{m^{*1}}} = \frac{\beta_{10}}{\beta_{26}} \quad (2.137)$$

$$\beta_{c_6} = \frac{\frac{c_6}{m^{*1}}}{\frac{c_6^*}{m^{*1}}} = \frac{\beta_{11}}{\beta_{27}} \quad (2.138)$$

$$\beta_{k_1} = \frac{\frac{k_1}{m^{*1}}}{\frac{k_1^*}{m^{*1}}} = \frac{\beta_{12}}{\beta_{28}} \quad (2.139)$$

$$\beta_{k_2} = \frac{\frac{k_2}{m^{*1}}}{\frac{k_2^*}{m^{*1}}} = \frac{\beta_{13}}{\beta_{29}} \quad (2.140)$$

$$\beta_{k_3} = \frac{\frac{k_3}{m^{*1}}}{\frac{k_3^*}{m^{*1}}} = \frac{\beta_{14}}{\beta_{30}} \quad (2.141)$$

$$\beta_{k_4} = \frac{\frac{k_4}{m^{*1}}}{\frac{k_4^*}{m^{*1}}} = \frac{\beta_{15}}{\beta_{31}} \quad (2.142)$$

$$\beta_{k_5} = \frac{\frac{k_5}{m^{*1}}}{\frac{k_5^*}{m^{*1}}} = \frac{\beta_{16}}{\beta_{32}} \quad (2.143)$$

$$\beta_{k_6} = \frac{\frac{k_6}{m^{*1}}}{\frac{k_6^*}{m^{*1}}} = \frac{\beta_{17}}{\beta_{33}} \quad (2.144)$$

According to the relationship between the damage severity and damage index of one element, shown in Eq. 2.13, the damage severities for stiffness, mass and damping can be computed as follows,

$$\alpha_{m^1} = \frac{1}{\beta_{m^1}} - 1 = \frac{1}{\beta_1} - 1 \quad (2.145)$$

$$\alpha_{m^2} = \frac{1}{\beta_{m^2}} - 1 = \frac{\beta_{18}}{\beta_2} - 1 \quad (2.146)$$

$$\alpha_{m^3} = \frac{1}{\beta_{m^3}} - 1 = \frac{\beta_{19}}{\beta_3} - 1 \quad (2.147)$$

$$\alpha_{m^4} = \frac{1}{\beta_{m^4}} - 1 = \frac{\beta_{20}}{\beta_4} - 1 \quad (2.148)$$

$$\alpha_{m^5} = \frac{1}{\beta_{m^5}} - 1 = \frac{\beta_{21}}{\beta_5} - 1 \quad (2.149)$$

$$\alpha_{c_1} = \frac{1}{\beta_{c_1}} - 1 = \frac{\beta_{22}}{\beta_6} - 1 \quad (2.150)$$

$$\alpha_{c_2} = \frac{1}{\beta_{c_2}} - 1 = \frac{\beta_{23}}{\beta_7} - 1 \quad (2.151)$$

$$\alpha_{c_3} = \frac{1}{\beta_{c_3}} - 1 = \frac{\beta_{24}}{\beta_8} - 1 \quad (2.152)$$

$$\alpha_{c_4} = \frac{1}{\beta_{c_4}} - 1 = \frac{\beta_{25}}{\beta_9} - 1 \quad (2.153)$$

$$\alpha_{c_5} = \frac{1}{\beta_{c_5}} - 1 = \frac{\beta_{26}}{\beta_{10}} - 1 \quad (2.154)$$

$$\alpha_{c_6} = \frac{1}{\beta_{c_6}} - 1 = \frac{\beta_{27}}{\beta_{11}} - 1 \quad (2.155)$$

$$\alpha_{k_1} = \frac{1}{\beta_{k_1}} - 1 = \frac{\beta_{28}}{\beta_{12}} - 1 \quad (2.156)$$

$$\alpha_{k_2} = \frac{1}{\beta_{k_2}} - 1 = \frac{\beta_{29}}{\beta_{13}} - 1 \quad (2.157)$$

$$\alpha_{k_3} = \frac{1}{\beta_{k_3}} - 1 = \frac{\beta_{30}}{\beta_{14}} - 1 \quad (2.158)$$

$$\alpha_{k_4} = \frac{1}{\beta_{k_4}} - 1 = \frac{\beta_{31}}{\beta_{15}} - 1 \quad (2.159)$$

$$\alpha_{k_5} = \frac{1}{\beta_{k_5}} - 1 = \frac{\beta_{32}}{\beta_{16}} - 1 \quad (2.160)$$

$$\alpha_{k_6} = \frac{1}{\beta_{k_6}} - 1 = \frac{\beta_{33}}{\beta_{17}} - 1 \quad (2.161)$$

## 2.6 THEORY FOR ISOLATED SPRING-MASS-DAMPER SYSTEMS

An isolated spring-mass-damper system means a mass block along with the springs and dash pots attached to it are taken out from a discrete system and considered separately. A typical isolated spring-mass-damper system is shown schematically in Figure 2.4. The isolated spring-mass-damper system is composed of one lumped mass, two linear springs, and two linear dash pots.  $p^i(t)$  is the external dynamic force acting on lumped masses at time point  $t$ .  $x^i(t)$  is the displacement of the mass block relative to the ground at time point  $t$ .  $\dot{x}^i(t)$  is the velocity of the mass block relative to the ground at time point  $t$ .  $\ddot{x}^i(t)$  is the acceleration of the mass block relative to the ground at time point  $t$ .

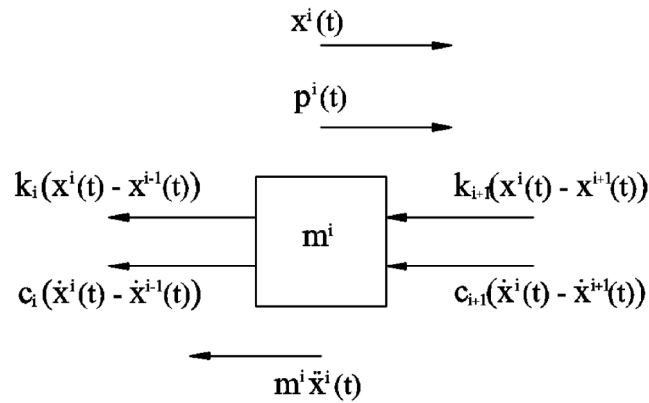


Figure 2.4. Isolated Spring-Mass-Damper System

For the isolated spring-mass-damper system, Eq. 2.10 can be written as,

$$\begin{aligned}
& \dot{\Delta}^i m^i \ddot{x}_i + \dot{\Delta}^i \begin{bmatrix} -c_i & c_i + c_{i+1} & -c_{i+1} \end{bmatrix} \begin{Bmatrix} \dot{x}_{i-1} \\ \dot{x}_i \\ \dot{x}_{i+1} \end{Bmatrix} + \dot{\Delta}^i \begin{bmatrix} -k_i & k_i + k_{i+1} & -k_{i+1} \end{bmatrix} \begin{Bmatrix} x_{i-1} \\ x_i \\ x_{i+1} \end{Bmatrix} \\
& = \dot{\Delta}^i m^{*i} \ddot{x}^{*i} + \dot{\Delta}^i \begin{bmatrix} -c_i^* & c_i^* + c_{i+1}^* & -c_{i+1}^* \end{bmatrix} \begin{Bmatrix} \dot{x}^{*i-1} \\ \dot{x}^{*i} \\ \dot{x}^{*i+1} \end{Bmatrix} + \dot{\Delta}^i \begin{bmatrix} -k_i^* & k_i^* + k_{i+1}^* & -k_{i+1}^* \end{bmatrix} \begin{Bmatrix} x^{*i-1} \\ x^{*i} \\ x^{*i+1} \end{Bmatrix} \quad (2.162)
\end{aligned}$$

Eq. 2.162 can be written as,

$$\begin{aligned}
& m^i \ddot{x}^i \dot{\Delta}^i + c_i (\dot{x}^i - \dot{x}^{i-1}) \dot{\Delta}^i + c_{i+1} (\dot{x}^i - \dot{x}^{i+1}) \dot{\Delta}^i + k_i (x^i - x^{i-1}) \dot{\Delta}^i + k_{i+1} (x^i - x^{i+1}) \dot{\Delta}^i \\
& = m^{*i} \ddot{x}^{*i} \dot{\Delta}^i + c_i^* (\dot{x}^{*i} - \dot{x}^{*i-1}) \dot{\Delta}^i + c_{i+1}^* (\dot{x}^{*i} - \dot{x}^{*i+1}) \dot{\Delta}^i + k_i^* (x^{*i} - x^{*i-1}) \dot{\Delta}^i + k_{i+1}^* (x^{*i} - x^{*i+1}) \dot{\Delta}^i \quad (2.163)
\end{aligned}$$

Dividing Eq. 2.163 by  $m_i^*$  yields,

$$\begin{aligned}
& \frac{m^i}{m^{*i}} \ddot{x}^i \dot{\Delta}^i + \frac{c_i}{m^{*i}} (\dot{x}^i - \dot{x}^{i-1}) \dot{\Delta}^i + \frac{c_{i+1}}{m^{*i}} (\dot{x}^i - \dot{x}^{i+1}) \dot{\Delta}^i + \frac{k_i}{m^{*i}} (x^i - x^{i-1}) \dot{\Delta}^i + \frac{k_{i+1}}{m^{*i}} (x^i - x^{i+1}) \dot{\Delta}^i \\
& = \ddot{x}^{*i} \dot{\Delta}^i + \frac{c_i^*}{m^{*i}} (\dot{x}^{*i} - \dot{x}^{*i-1}) \dot{\Delta}^i + \frac{c_{i+1}^*}{m^{*i}} (\dot{x}^{*i} - \dot{x}^{*i+1}) \dot{\Delta}^i + \frac{k_i^*}{m^{*i}} (x^{*i} - x^{*i-1}) \dot{\Delta}^i + \frac{k_{i+1}^*}{m^{*i}} (x^{*i} - x^{*i+1}) \dot{\Delta}^i \quad (2.164)
\end{aligned}$$

Rearranging Eq. 2.164, yields,

$$\begin{aligned}
& \frac{m^i}{m^{*i}} \ddot{x}^i \dot{\Delta}^i + \frac{c_i}{m^{*i}} (\dot{x}^i - \dot{x}^{i-1}) \dot{\Delta}^i + \frac{c_{i+1}}{m^{*i}} (\dot{x}^i - \dot{x}^{i+1}) \dot{\Delta}^i + \frac{k_i}{m^{*i}} (x^i - x^{i-1}) \dot{\Delta}^i + \frac{k_{i+1}}{m^{*i}} (x^i - x^{i+1}) \dot{\Delta}^i \\
& - \frac{c_i^*}{m^{*i}} (\dot{x}^{*i} - \dot{x}^{*i-1}) \dot{\Delta}^i - \frac{c_{i+1}^*}{m^{*i}} (\dot{x}^{*i} - \dot{x}^{*i+1}) \dot{\Delta}^i - \frac{k_i^*}{m^{*i}} (x^{*i} - x^{*i-1}) \dot{\Delta}^i - \frac{k_{i+1}^*}{m^{*i}} (x^{*i} - x^{*i+1}) \dot{\Delta}^i = \ddot{x}^{*i} \dot{\Delta}^i \quad (2.165)
\end{aligned}$$

Define the following coefficients,

$$\beta_1 = \frac{m_i}{m^{*i}} \quad (2.166)$$

$$\beta_2 = \frac{c_i}{m^{*i}} \quad (2.167)$$

$$\beta_3 = \frac{c_{i+1}}{m^{*i}} \quad (2.168)$$

$$\beta_4 = \frac{k_i}{m^{*i}} \quad (2.169)$$

$$\beta_5 = \frac{k_{i+1}}{m^{*i}} \quad (2.170)$$

$$\beta_6 = \frac{c_i^*}{m^{*i}} \quad (2.171)$$

$$\beta_7 = \frac{c_{i+1}^*}{m^{*i}} \quad (2.172)$$

$$\beta_8 = \frac{k_i^*}{m^{*i}} \quad (2.173)$$

$$\beta_9 = \frac{k_{i+1}^*}{m^{*i}} \quad (2.174)$$

Substituting Eq. 2.166 through Eq. 2.174 to Eq. 2.165 yields,

$$\begin{aligned} & \beta_1 \ddot{x}^i \dot{\Delta}^i + \beta_2 (\dot{x}^i - \dot{x}^{i-1}) \dot{\Delta}^i + \beta_3 (\dot{x}^i - \dot{x}^{i+1}) \dot{\Delta}^i + \beta_4 (x^i - x^{i-1}) \dot{\Delta}^i + \beta_5 (x^i - x^{i+1}) \dot{\Delta}^i \\ & - \beta_6 (\dot{x}^{*i} - \dot{x}^{*i-1}) \dot{\Delta}^i - \beta_7 (\dot{x}^{*i} - \dot{x}^{*i+1}) \dot{\Delta}^i - \beta_8 (x^{*i} - x^{*i-1}) \dot{\Delta}^i - \beta_9 (x^{*i} - x^{*i+1}) \dot{\Delta}^i = \ddot{x}^{*i} \dot{\Delta}^i \end{aligned} \quad (2.175)$$

Writing the Eq. 2.175 at different time point, yields the following groups of equations,

For  $t = t_0$ ,

$$\begin{aligned} & \beta_1 (\ddot{x}^i \dot{\Delta}^i)|_{t_0} + \beta_2 ((\dot{x}^i - \dot{x}^{i-1}) \dot{\Delta}^i)|_{t_0} + \beta_3 ((\dot{x}^i - \dot{x}^{i+1}) \dot{\Delta}^i)|_{t_0} + \beta_4 ((x^i - x^{i-1}) \dot{\Delta}^i)|_{t_0} \\ & + \beta_5 ((x^i - x^{i+1}) \dot{\Delta}^i)|_{t_0} - \beta_6 ((\dot{x}^{*i} - \dot{x}^{*i-1}) \dot{\Delta}^i)|_{t_0} - \beta_7 ((\dot{x}^{*i} - \dot{x}^{*i+1}) \dot{\Delta}^i)|_{t_0} - \beta_8 ((x^{*i} - x^{*i-1}) \dot{\Delta}^i)|_{t_0} \\ & - \beta_9 ((x^{*i} - x^{*i+1}) \dot{\Delta}^i)|_{t_0} = (\ddot{x}^{*i} \dot{\Delta}^i)|_{t_0} \end{aligned}$$

(2.176)

For  $t = t_i$ ,

$$\begin{aligned}
& \beta_1(\ddot{x}^i \dot{\Delta}^i)|_{t_i} + \beta_2((\dot{x}^i - \dot{x}^{i-1})\dot{\Delta}^i)|_{t_i} + \beta_3((\dot{x}^i - \dot{x}^{i+1})\dot{\Delta}^i)|_{t_i} + \beta_4((x^i - x^{i-1})\dot{\Delta}^i)|_{t_i} \\
& + \beta_5((x^i - x^{i+1})\dot{\Delta}^i)|_{t_i} - \beta_6((\dot{x}^{*i} - \dot{x}^{*i-1})\dot{\Delta}^i)|_{t_i} - \beta_7((\dot{x}^{*i} - \dot{x}^{*i+1})\dot{\Delta}^i)|_{t_i} - \beta_8((x^{*i} - x^{*i-1})\dot{\Delta}^i)|_{t_i} \\
& - \beta_9((x^{*i} - x^{*i+1})\dot{\Delta}^i)|_{t_i} = (\ddot{x}^{*i} \dot{\Delta}^i)|_{t_i}
\end{aligned}
\tag{2.177}$$

For  $t = t_N$ ,

$$\begin{aligned}
& \beta_1(\ddot{x}^i \dot{\Delta}^i)|_{t_N} + \beta_2((\dot{x}^i - \dot{x}^{i-1})\dot{\Delta}^i)|_{t_N} + \beta_3((\dot{x}^i - \dot{x}^{i+1})\dot{\Delta}^i)|_{t_N} + \beta_4((x^i - x^{i-1})\dot{\Delta}^i)|_{t_N} \\
& + \beta_5((x^i - x^{i+1})\dot{\Delta}^i)|_{t_N} - \beta_6((\dot{x}^{*i} - \dot{x}^{*i-1})\dot{\Delta}^i)|_{t_N} - \beta_7((\dot{x}^{*i} - \dot{x}^{*i+1})\dot{\Delta}^i)|_{t_N} - \beta_8((x^{*i} - x^{*i-1})\dot{\Delta}^i)|_{t_N} \\
& - \beta_9((x^{*i} - x^{*i+1})\dot{\Delta}^i)|_{t_N} = (\ddot{x}^{*i} \dot{\Delta}^i)|_{t_N}
\end{aligned}
\tag{2.178}$$

Arrange the above Equation group into matrix form,

$$\mathbf{X}^T = \begin{bmatrix}
(\ddot{x}^i \dot{\Delta}^i)|_{t_0} & \dots & (\ddot{x}^i \dot{\Delta}^i)|_{t_i} & \dots & (\ddot{x}^i \dot{\Delta}^i)|_{t_N} \\
((\dot{x}^i - \dot{x}^{i-1})\dot{\Delta}^i)|_{t_0} & \dots & ((\dot{x}^i - \dot{x}^{i-1})\dot{\Delta}^i)|_{t_i} & \dots & ((\dot{x}^i - \dot{x}^{i-1})\dot{\Delta}^i)|_{t_N} \\
((\dot{x}^i - \dot{x}^{i+1})\dot{\Delta}^i)|_{t_0} & \dots & ((\dot{x}^i - \dot{x}^{i+1})\dot{\Delta}^i)|_{t_i} & \dots & ((\dot{x}^i - \dot{x}^{i+1})\dot{\Delta}^i)|_{t_N} \\
((x^i - x^{i-1})\dot{\Delta}^i)|_{t_0} & \dots & ((x^i - x^{i-1})\dot{\Delta}^i)|_{t_i} & \dots & ((x^i - x^{i-1})\dot{\Delta}^i)|_{t_N} \\
((x^i - x^{i+1})\dot{\Delta}^i)|_{t_0} & \dots & ((x^i - x^{i+1})\dot{\Delta}^i)|_{t_i} & \dots & ((x^i - x^{i+1})\dot{\Delta}^i)|_{t_N} \\
-((\dot{x}^{*i} - \dot{x}^{*i-1})\dot{\Delta}^i)|_{t_0} & \dots & -((\dot{x}^{*i} - \dot{x}^{*i-1})\dot{\Delta}^i)|_{t_i} & \dots & -((\dot{x}^{*i} - \dot{x}^{*i-1})\dot{\Delta}^i)|_{t_N} \\
-((\dot{x}^{*i} - \dot{x}^{*i+1})\dot{\Delta}^i)|_{t_0} & \dots & -((\dot{x}^{*i} - \dot{x}^{*i+1})\dot{\Delta}^i)|_{t_i} & \dots & -((\dot{x}^{*i} - \dot{x}^{*i+1})\dot{\Delta}^i)|_{t_N} \\
-((x^{*i} - x^{*i-1})\dot{\Delta}^i)|_{t_0} & \dots & -((x^{*i} - x^{*i-1})\dot{\Delta}^i)|_{t_i} & \dots & -((x^{*i} - x^{*i-1})\dot{\Delta}^i)|_{t_N} \\
-((x^{*i} - x^{*i+1})\dot{\Delta}^i)|_{t_0} & \dots & -((x^{*i} - x^{*i+1})\dot{\Delta}^i)|_{t_i} & \dots & -((x^{*i} - x^{*i+1})\dot{\Delta}^i)|_{t_N}
\end{bmatrix}
\tag{2.179}$$

Define



$$\boldsymbol{\beta} = \begin{Bmatrix} \beta_1 \\ \beta_2 \\ \beta_3 \\ \beta_4 \\ \beta_5 \\ \beta_6 \\ \beta_7 \\ \beta_8 \\ \beta_9 \end{Bmatrix} \quad (2.180)$$

$$\mathbf{Y} = \begin{Bmatrix} (\ddot{x}^{*i} \dot{\Delta}^i)|_{t_0} \\ \vdots \\ (\ddot{x}^{*i} \dot{\Delta}^i)|_{t_i} \\ \vdots \\ (\ddot{x}^{*i} \dot{\Delta}^i)|_{t_N} \end{Bmatrix} \quad (2.181)$$

The above equation may be expressed as,

$$\mathbf{X}\boldsymbol{\beta} = \mathbf{Y} \quad (2.182)$$

Based on the Least Square Method, the  $\boldsymbol{\beta}$  can be computed from the following equation,

$$\boldsymbol{\beta} = (\mathbf{X}^T \mathbf{X})^{-1} (\mathbf{X}^T \mathbf{Y}) \quad (2.183)$$

According to the definition of the damage index in Eq. 2.11, the damage indices for stiffness, mass and damping can be computed as follows,

$$\beta_{m^i} = \frac{m^i}{m^{*i}} = \beta_1 \quad (2.184)$$

$$\beta_{c_i} = \frac{c_i}{c_i^*} = \frac{\frac{c_i}{m^{*i}}}{\frac{c_i^*}{m^{*i}}} = \frac{\beta_2}{\beta_6} \quad (2.185)$$

$$\beta_{c_{i+1}} = \frac{c_{i+1}}{c_{i+1}^*} = \frac{\frac{c_{i+1}}{m^{*i}}}{\frac{c_{i+1}^*}{m^{*i}}} = \frac{\beta_3}{\beta_7} \quad (2.186)$$

$$\beta_{k_i} = \frac{k_i}{k_i^*} = \frac{\frac{k_i}{m^{*i}}}{\frac{k_i^*}{m^{*i}}} = \frac{\beta_4}{\beta_8} \quad (2.187)$$

$$\beta_{k_{i+1}} = \frac{k_{i+1}}{k_{i+1}^*} = \frac{\frac{k_{i+1}}{m^{*i}}}{\frac{k_{i+1}^*}{m^{*i}}} = \frac{\beta_5}{\beta_9} \quad (2.188)$$

According to the relationship between the damage severity and damage index of one element, shown in Eq. 2.13, the damage severities for stiffness, mass, and damping can be computed as follows,

$$\alpha_{m^i} = \frac{1}{\beta_{m^i}} - 1 = \frac{1}{\beta_1} - 1 \quad (2.189)$$

$$\alpha_{c_i} = \frac{1}{\beta_{c_i}} - 1 = \frac{\beta_6}{\beta_2} - 1 \quad (2.190)$$

$$\alpha_{c_{i+1}} = \frac{1}{\beta_{c_{i+1}}} - 1 = \frac{\beta_7}{\beta_3} - 1 \quad (2.191)$$

$$\alpha_{k_i} = \frac{1}{\beta_{k_i}} - 1 = \frac{\beta_8}{\beta_4} - 1 \quad (2.192)$$

$$\alpha_{k_{i+1}} = \frac{1}{\beta_{k_{i+1}}} - 1 = \frac{\beta_9}{\beta_5} - 1 \quad (2.193)$$

## 2.7 OVERALL SOLUTION PROCEDURE

To perform the proposed damage detection method to discrete system, the following

steps should be followed:

- (1) Derive the linear equation group for the specific discrete system;
- (2) Collect the displacement, velocity, and acceleration records required by the coefficient matrix and the known vector of the linear equation group defined by step 1;
- (3) Use the least square method to solve for the unknown vector; and
- (4) Compute for the Damage Indices and Damage severities for each physical property in the discrete system.

The general process will be clearly demonstrated in Section 3.

## **2.8 SUMMARY**

In this Section, the algorithms of Power Method for 1-DOF, 2-DOF, N-DOF, and isolated spring-mass-damper system were derived. The damage index for each physical property in each discrete system was also provided. The derivation processes were demonstrated in Section 2.2 to Section 2.7. The general application process of the Power Method on one specific discrete system was provided in Section 2.8. Based on the analysis in Section 2, the Power Method can be applied to both simple and complex discrete systems. Moreover, the Power Method can be applied to the whole discrete system. When the Power Method is applied to the whole system, damage indices for all physical properties related to the system can be computed by one group of linear equations. The Power Method can also be applied to one isolated system, which is a part of the whole system. In this way, the damage indices of the physical properties related to the isolated system can be computed separately.

### **3 CASE STUDIES OF DAMAGE EVALUATION FOR DISCRETE SYSTEMS**

#### **3.1 INTRODUCTION**

The objective of this section is to validate the accuracy of the theory. To achieve this goal, the theory was validated using exact displacements, velocities, and accelerations of the undamaged and damaged discrete systems modeled within SAP2000 (version 15). The exact displacements, velocities, and accelerations are the linear direct integration results from SAP2000. The Hilber-Hughes-Taylor time integration method was used by SAP2000. The three parameters of the Hilber-Hughes-Taylor method: Gamma, Beta and Alpha were set to be 0.5, 0.25, and 0, respectively. Four numerical cases were studied in this section,

Case #1: the accuracy of the theory will be studied on a 1-DOF spring-mass-damper system. The algorithm of the Power Method for a 1-DOF spring-mass-damper system is provided in Section 2.3. The damage is simulated by the changes of mass, stiffness, and damping coefficient.

Case #2: the accuracy of the theory will be studied on a 2-DOF spring-mass-damper system. The algorithm of the Power Method for a 2-DOF spring-mass-damper system is provided in Section 2.4. The damage is simulated by the changes of masses, stiffness, and damping coefficients at multiple locations.

Case #3: the accuracy of the theory will be studied on a 5-DOF spring-mass-damper

system. The algorithm of the Power Method for a 5-DOF spring-mass-damper system is provided in Section 2.5. The damage is simulated by the changes of masses, stiffness, and damping coefficients at multiple locations.

Case #4: the accuracy of the theory will be studied on an isolated spring-mass-damper system. The algorithm of the Power Method for an isolated spring-mass-damper system is provided in Section 2.6. The damage is simulated by the changes of masses, stiffness, and damping coefficients at multiple locations.

### **3.2 DAMAGE EVALUATION FOR A 1-DOF SPRING-MASS-DAMPER SYSTEM**

In this section, a typical 1-DOF spring-mass-damper system will be developed and used to validate the accuracy of the Power Method. The numerical models for the damaged and undamaged 1-DOF mass-spring-damper system were generated using SAP2000. The 1-DOF spring-mass-damper system used in this case study is plotted in Figure 3.1. The physical properties in the undamaged and damaged systems are listed in Table 3.1. Both the undamaged and damaged systems are excited by the same external force. The applied external force is given at each 1E-4 seconds for 0.2 seconds and is plotted in Figure 3.2. In SAP2000, displacements, velocities, and accelerations of the mass block were computed every 1E-4 seconds (10,000 Hz) for 0.2 seconds. The displacements, velocities, and accelerations of the mass blocks in both the undamaged and damaged systems were plotted in Figure 3.3, Figure 3.4, and Figure 3.5, respectively.

In this case, the computed velocity ( $\dot{x}(t)$ ) of the mass block in the undamaged case was used as the velocity used to compute power ( $\dot{\Delta}$ ) for both undamaged and damaged cases. The coefficient matrices and known vector, X and Y, were constructed by substituting

the acceleration ( $\ddot{x}(t)$ ), velocity ( $\dot{x}(t)$ ), displacement ( $x(t)$ ), and velocity used to compute power ( $\dot{\Delta}$ ) into Eq. 2.27 and Eq. 2.29. The coefficient damage index vector,  $\beta$ , was computed using Eq. 2.31. Then the damage indices for mass, spring, and damper are computed using Eqs. 2.32 through 2.34. The damage severities for mass, spring and damper are computed using Eqs. 2.35 through 2.37. The estimated damage indices and the designed damage indices for each physical property are listed in Table 3.2 and are plotted in Figure 3.6. The estimated damage severities and the designed damage severities for each physical property are plotted in Figure 3.7. Comparing the estimated damage indices with the designed damage indices, the proposed method can accurately locate and size multiple damage in a typical 1-DOF spring-mass-damper system.

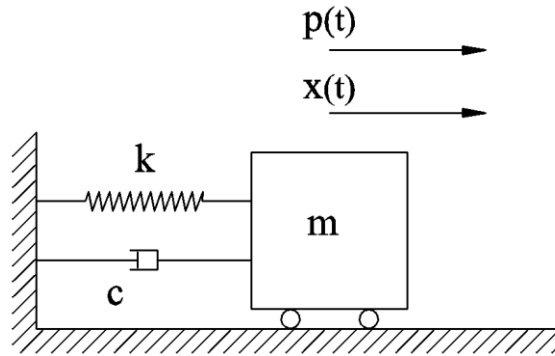


**Figure 3.1. Property Definition and Load Case of the 1-DOF Spring-Mass-Damper System**

**Table 3.1. Physical Properties of the 1-DOF Spring-Mass-Damper System**

Property	Undamaged System	Damaged System
$m$ (kip-s <sup>2</sup> /in.)	2	1.7
$c$ (kip-s/in.)	0.8	0.7
$k$ (kip/in.)	10	8

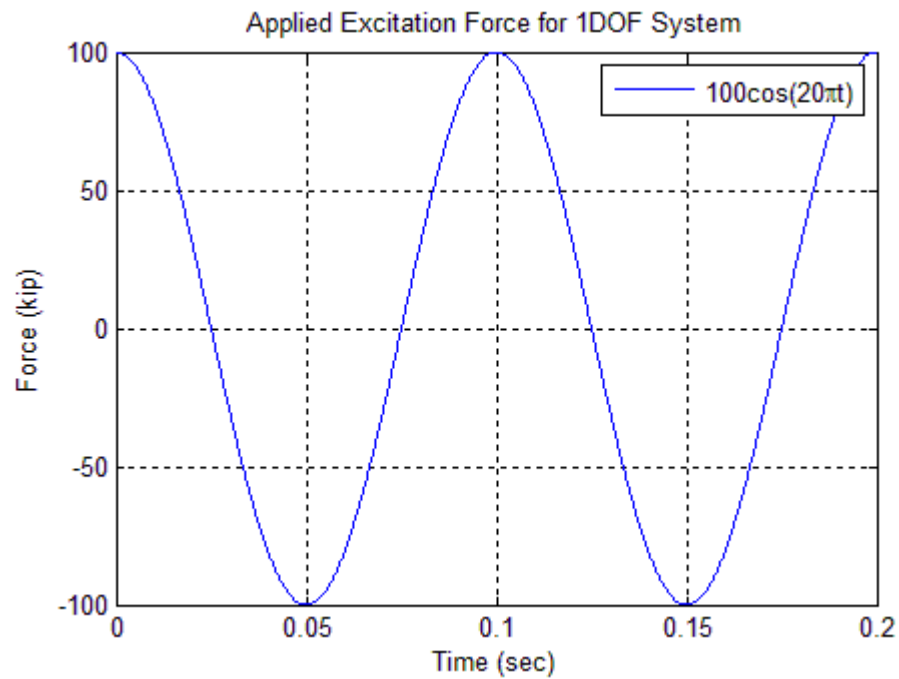


Figure 3.2. Applied External Load for Both the Undamaged and Damaged Cases

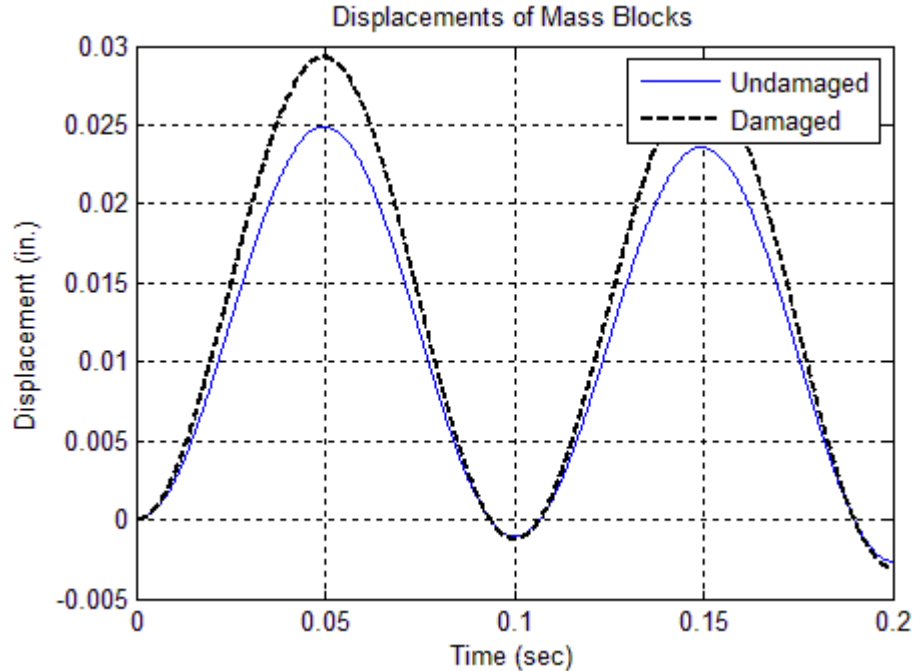


Figure 3.3. Displacements of the Mass Block under the Given External Load

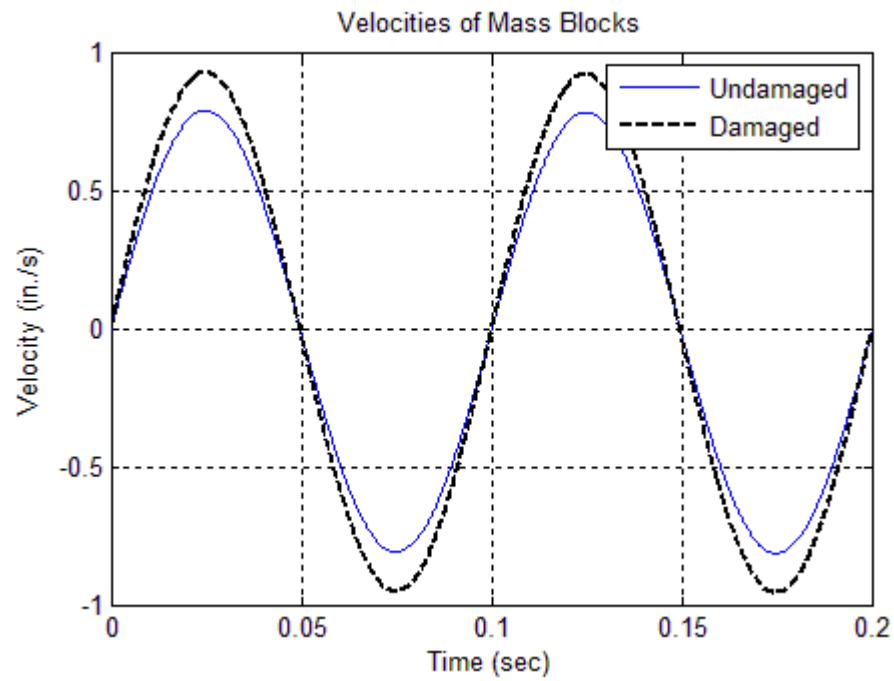


Figure 3.4. Velocities of the Mass Block under the Given External Load

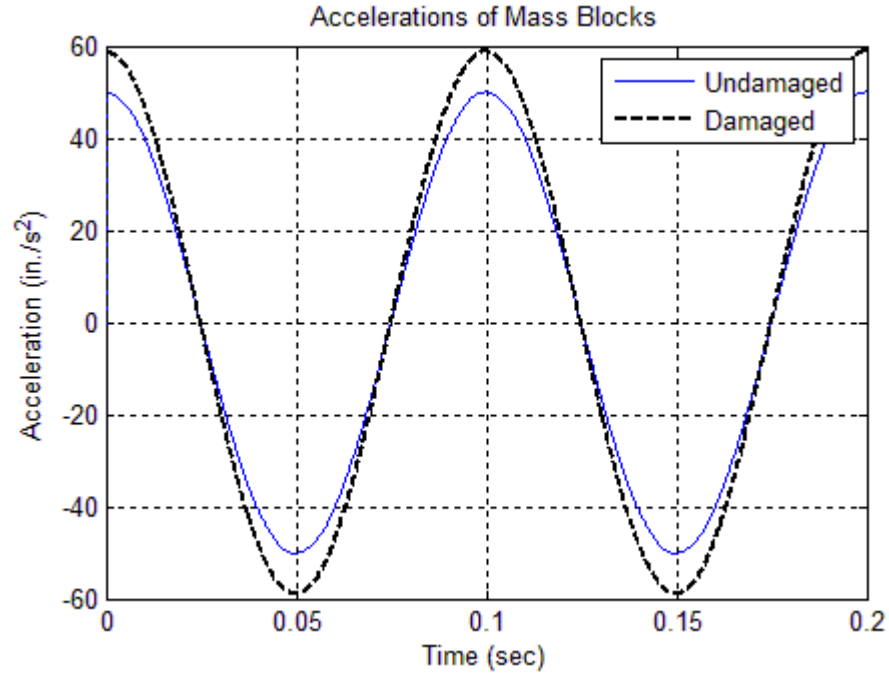
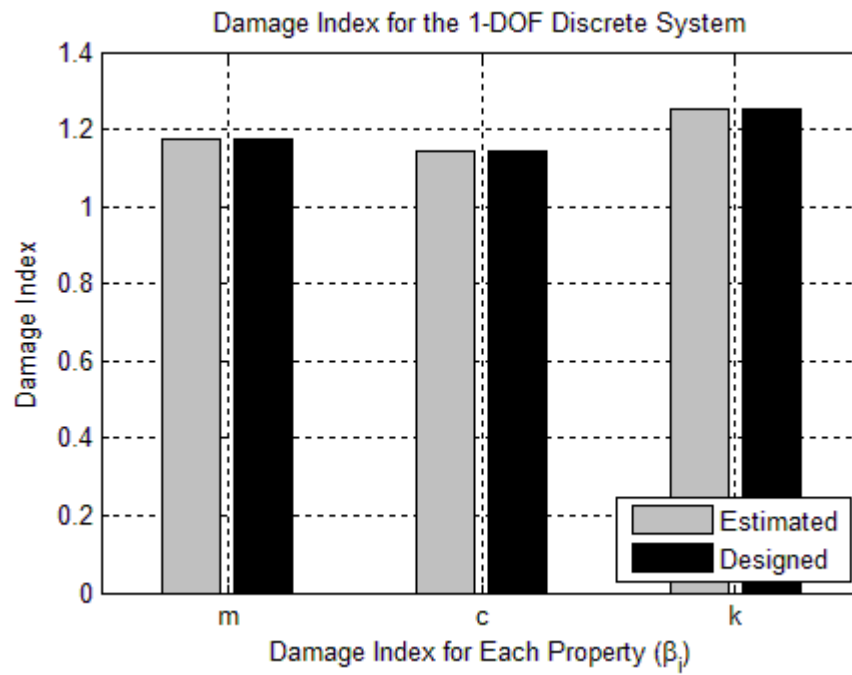


Figure 3.5. Accelerations of the Mass Block under the Given External Load



**Table 3.2. Damage Detection Results for the 1-DOF Spring-Mass-Damper System**

Property	Damage Index ( $\beta_i$ )	Damage Severity ( $\alpha_i$ , %)
m	1.18	-15.00
k	1.25	-20.00
c	1.14	-12.50



**Figure 3.6. Element Damage Indices ( $\beta_i$ ) for 1-DOF Spring-Mass-Damper System**

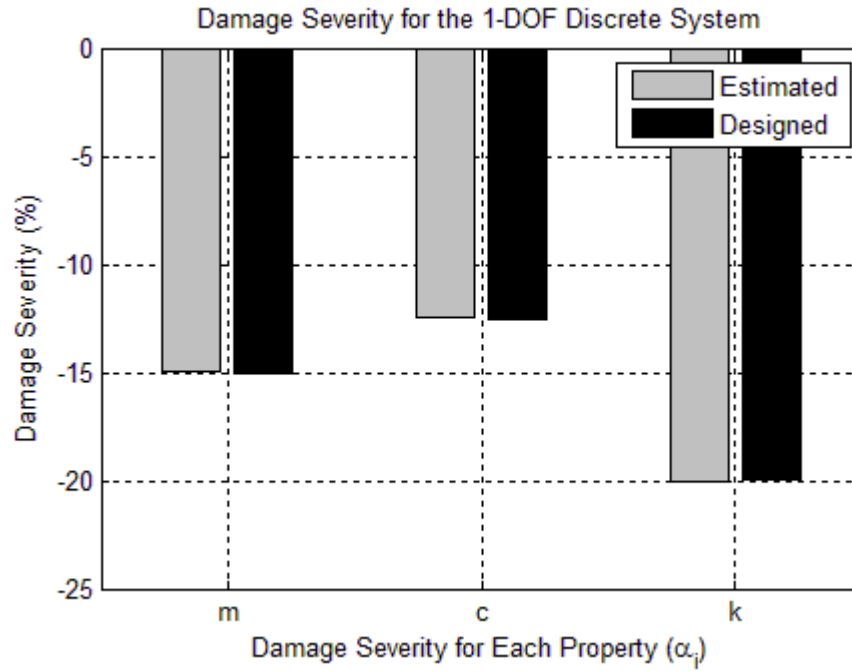


**Figure 3.7. Element Damage Severities ( $\alpha_i$ ) for 1-DOF Spring-Mass-Damper System**

### 3.3 DAMAGE EVALUATION FOR A 2-DOF SPRING-MASS-DAMPER SYSTEM

In this section, a typical 2-DOF spring-mass-damper system will be built and used to validate the accuracy of the Power Method. The numerical models for the damaged and undamaged 2-DOF mass-spring-damper systems were generated using SAP2000. The 2-DOF spring-mass-damper system used in this case study is plotted in Figure 3.8. The physical properties in the undamaged and damaged systems are listed in Table 3.3. Both the undamaged and damaged systems are excited by the same external force. The applied external force is given at each 1E-4 seconds for 0.2 seconds and is plotted in Figure 3.9. In SAP2000, displacements, velocities and accelerations of the mass blocks were computed every 1E-4 seconds (10,000 Hz) for 0.2 seconds. The displacements, velocities, and accelerations of the mass block 1 in both the undamaged and damaged

systems were plotted in Figure 3.10, Figure 3.11, and Figure 3.12, respectively.

In this case, the computed velocity ( $\dot{x}(t)$ ) of the mass block in the undamaged case was used as the velocity used to compute power ( $\dot{\Delta}$ ) for both undamaged and damaged cases. The coefficient matrices and known vector,  $X$  and  $Y$ , were constructed by substituting the acceleration ( $\ddot{x}(t)$ ), velocity ( $\dot{x}(t)$ ), displacement ( $x(t)$ ), and velocity used to compute power ( $\dot{\Delta}$ ) into Eq. 2.61 and Eq. 2.63. The coefficient damage index vector,  $\beta$ , was computed using Eq. 2.65. Then the damage indices for mass, spring and damper are computed using Eqs. 2.66 through 2.73. The damage severities for mass, spring and damper are computed using Eqs. 2.74 through 2.81. The estimated damage indices and the designed damage indices for each physical property are listed in Table 3.4 and are plotted in Figure 3.13. The estimated damage severities and the designed damage severities for each physical property are plotted in Figure 3.14. Comparing the estimated damage indices with the designed damage indices, the proposed method can accurately locate and size multiple damage in a typical 2-DOF spring-mass-damper system.

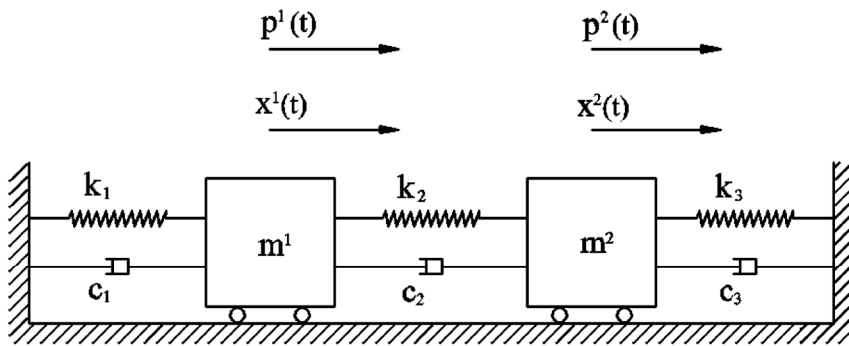
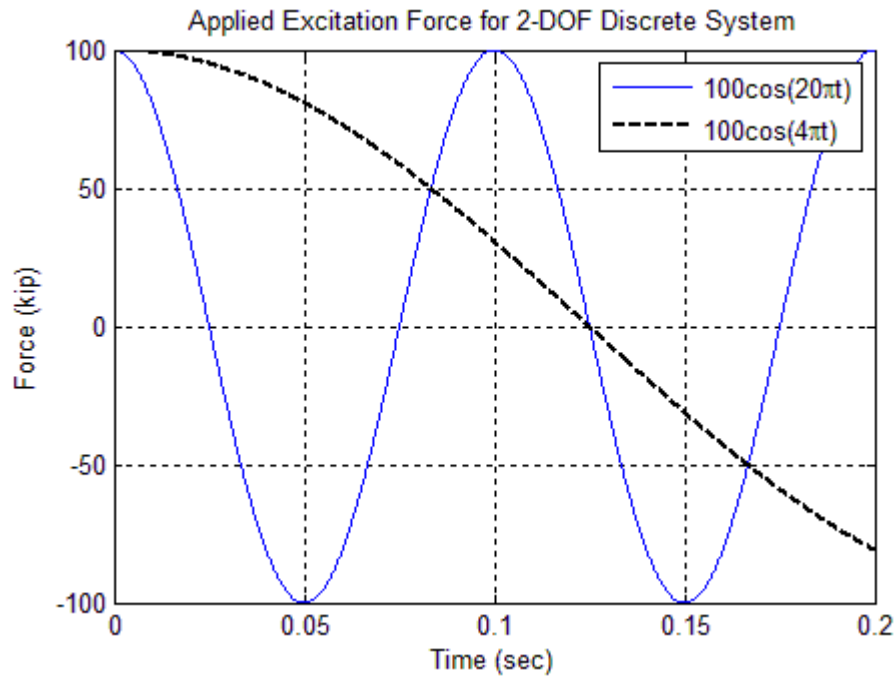


Figure 3.8. Property Definition and Load Case of the 2-DOF Spring-Mass-Damper System

**Table 3.3. Physical Properties of the 2-DOF System**

Property	Undamaged System	Damaged System
$m_1$ (kip-s <sup>2</sup> /in.)	2	1.7
$m_2$ (kip-s <sup>2</sup> /in.)	3	2.9
$c_1$ (kip-s/in.)	0.8	0.7
$c_2$ (kip-s/in.)	0.4	0.23
$c_3$ (kip-s/in.)	0.3	0.33
$k_1$ (kip/in.)	10	8
$k_2$ (kip/in.)	20	21
$k_3$ (kip/in.)	15	15.3



**Figure 3.9. Applied External Load for Both the Undamaged and Damaged Cases**

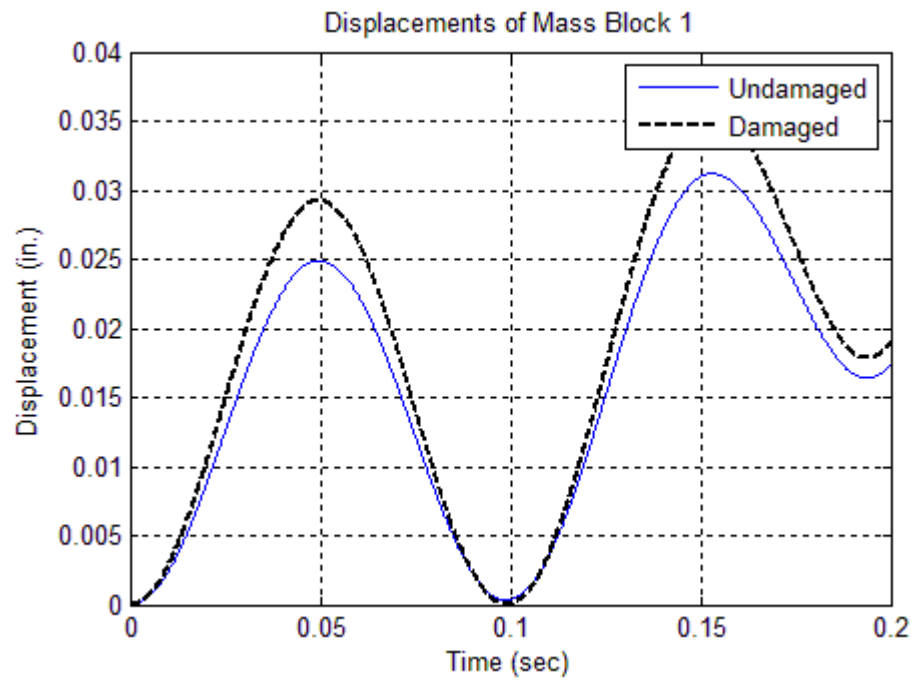


Figure 3.10. Displacements of the Mass Block 1 under the Given External Load

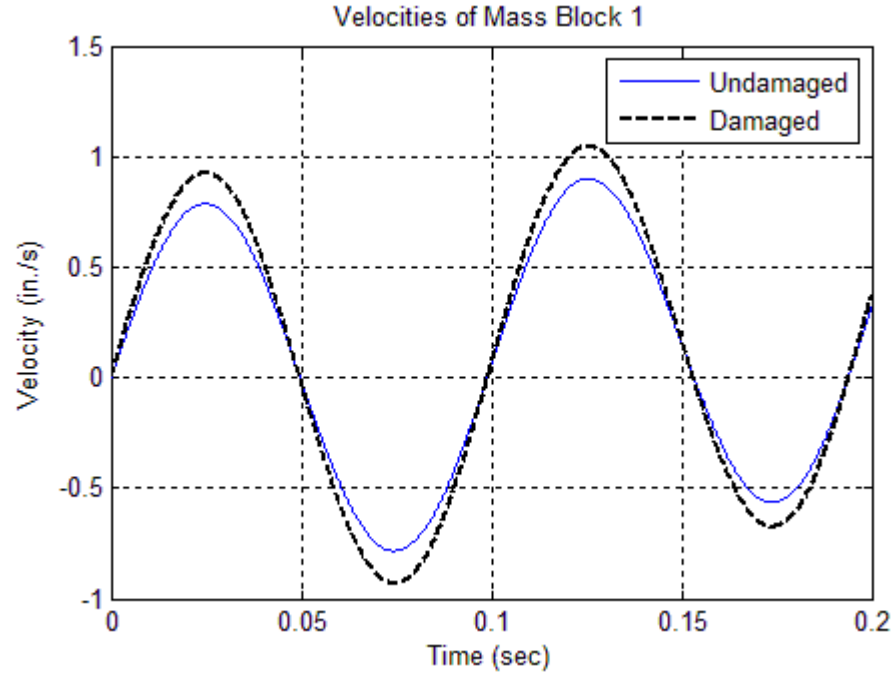


Figure 3.11. Velocities of the Mass Block 1 under the Given External Load

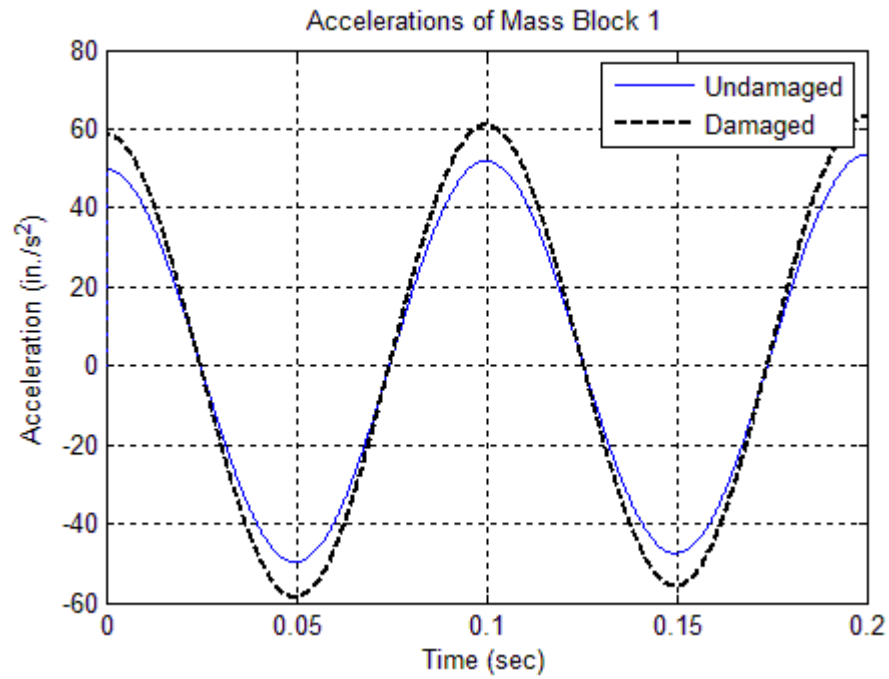


Figure 3.12. Accelerations of the Mass Block 1 under the Given External Load

Table 3.4. Damage Detection Results for the 2-DOF Spring-Mass-Damper System

Property	Damage Index ( $\beta_i$ , Esimated)	Damage Severity ( $\alpha_i$ , Esimated)	Damage Index ( $\beta_i$ , Designed)
$m_1$	1.18	-0.15	1.18
$m_2$	1.03	-0.03	1.03
$c_1$	1.14	-0.12	1.14
$c_2$	1.74	-0.43	1.74
$c_3$	0.91	0.10	0.91
$k_1$	1.25	-0.20	1.25
$k_2$	0.95	0.05	0.95
$k_3$	0.98	0.02	0.98

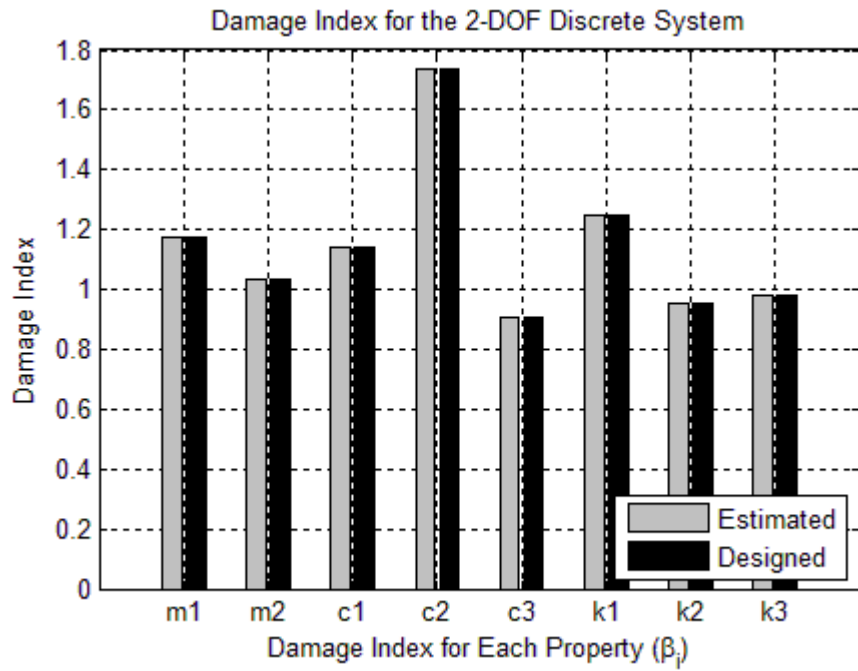


Figure 3.13. Element Damage Indices ( $\beta_i$ ) for 2-DOF Spring-Mass-Damper System

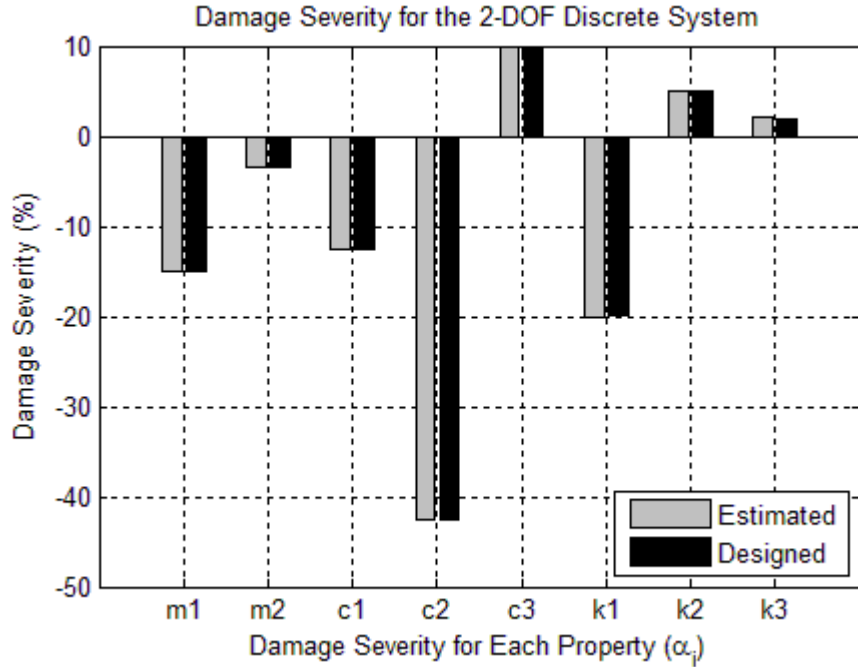


Figure 3.14. Element Damage Severities ( $\alpha_i$ ) for 2-DOF Spring-Mass-Damper System

### 3.4 DAMAGE EVALUATION FOR AN N-DOF SPRING-MASS-DAMPER SYSTEM

In this section, a typical 5-DOF spring-mass-damper system is used to simulate an N-DOF spring-mass-damper system and will be used to validate the accuracy of the Power Method. The numerical models for the damaged and undamaged 5-DOF mass-spring-damper systems were generated using SAP2000. The 5-DOF spring-mass-damper system used in this case study is plotted in Figure 3.15. The physical properties in the undamaged and damaged systems are listed in Table 3.5. Both the undamaged and damaged systems are excited by the same external force. The applied external force is given at each 1E-4 seconds for 0.2 seconds and is plotted in Figure 3.16. In SAP2000, displacements, velocities and accelerations of the mass blocks were computed every 1E-4 seconds (10,000 Hz) for 0.2 seconds. The displacements, velocities, and accelerations of the mass block 1 in both the undamaged and damaged systems were plotted in Figure 3.17, Figure 3.18, and Figure 3.19, respectively.

In this case, the computed velocity ( $\dot{x}(t)$ ) of the mass block in the undamaged case was used as the velocity used to compute power ( $\dot{\Delta}$ ) for both undamaged and damaged cases. The coefficient matrices and known vector, X and Y, were constructed by substituting the acceleration ( $\ddot{x}(t)$ ), velocity ( $\dot{x}(t)$ ), displacement ( $x(t)$ ), and velocity used to compute power ( $\dot{\Delta}$ ) into Eq. 2.123 and Eq. 2.125. The coefficient damage index vector,  $\beta$ , was computed using Eq. 2.127. Then the damage indices for mass, spring and damper are computed using Eqs. 2.128 through 2.144. The damage severities for mass, spring and damper are computed using Eqs. 2.145 through 2.161. The estimated damage indices and the designed damage indices for each physical property are listed in Table 3.6 and are plotted in Figure 3.20. The estimated damage severities and the designed damage



severities for each physical property are plotted in Figure 3.21. Comparing the estimated damage indices with the designed damage indices, the proposed method can accurately locate and size multiple damage in a typical 5-DOF spring-mass-damper system.

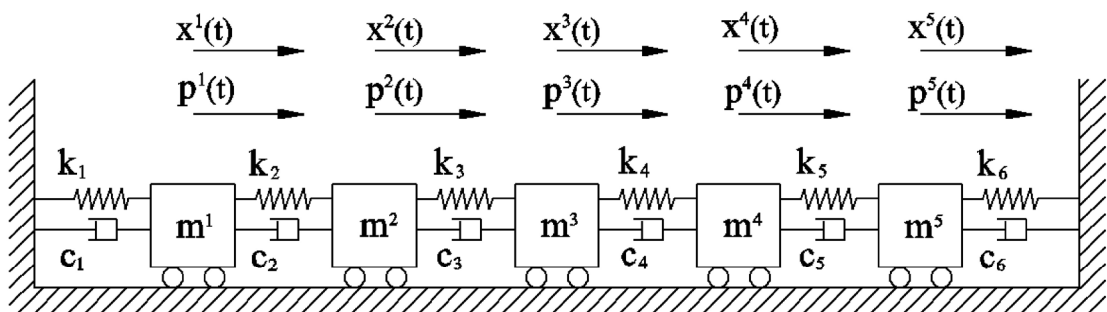


**Figure 3.15. Property Definition and Load Case of the 5-DOF Spring-Mass-Damper System**

**Table 3.5. Physical Properties of the 5-DOF System**

<b>Property</b>	<b>Undamaged System</b>	<b>Damaged System</b>
$m_1$ (kip-s <sup>2</sup> /in.)	2	1.7
$m_2$ (kip-s <sup>2</sup> /in.)	3	2.9
$m_3$ (kip-s <sup>2</sup> /in.)	5	4.7
$m_4$ (kip-s <sup>2</sup> /in.)	4	3.8
$m_5$ (kip-s <sup>2</sup> /in.)	1	0.6
$c_1$ (kip-s/in.)	0.8	0.7
$c_2$ (kip-s/in.)	0.4	0.23
$c_3$ (kip-s/in.)	0.3	0.33
$c_4$ (kip-s/in.)	0.7	0.66
$c_5$ (kip-s/in.)	0.55	0.5
$c_6$ (kip-s/in.)	0.6	0.4
$k_1$ (kip/in.)	10	8
$k_2$ (kip/in.)	20	21
$k_3$ (kip/in.)	15	15.3
$k_4$ (kip/in.)	30	26
$k_5$ (kip/in.)	18	16.8
$k_6$ (kip/in.)	13	12.3

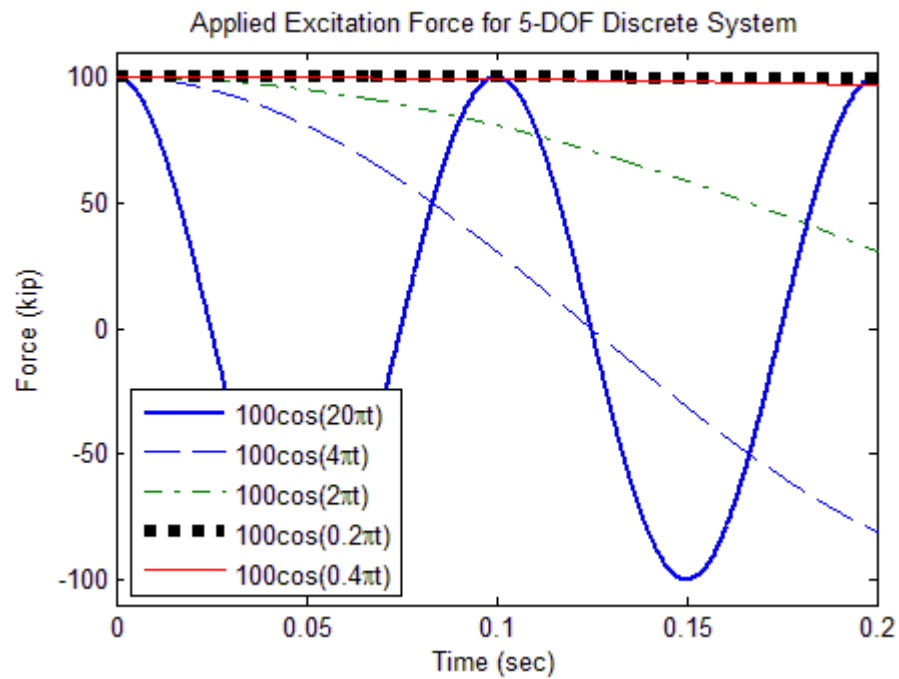


Figure 3.16. Applied External Load for Both the Undamaged and Damaged Cases

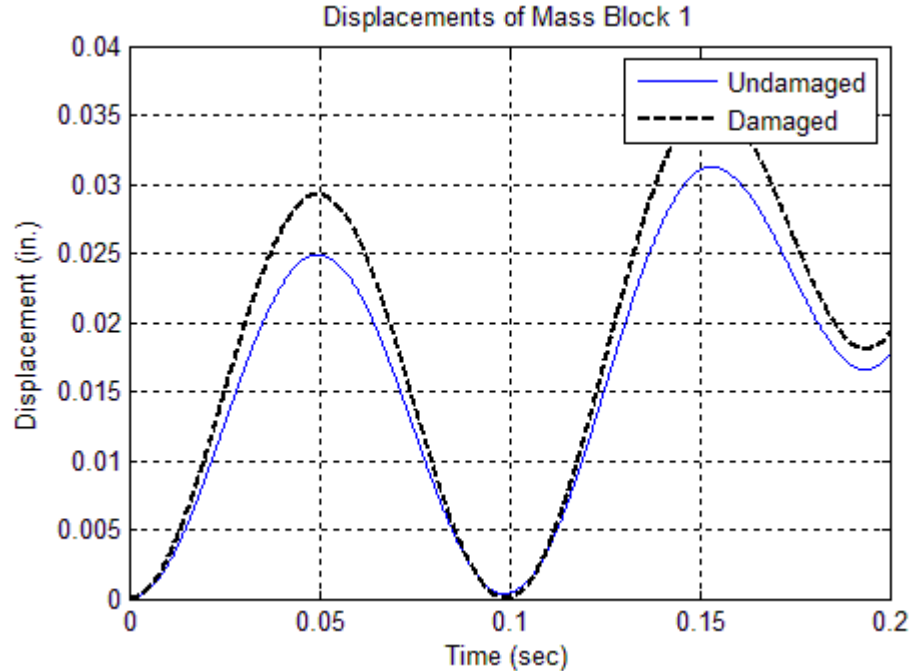


Figure 3.17. Displacements of the Mass Block 1 under the Given External Load

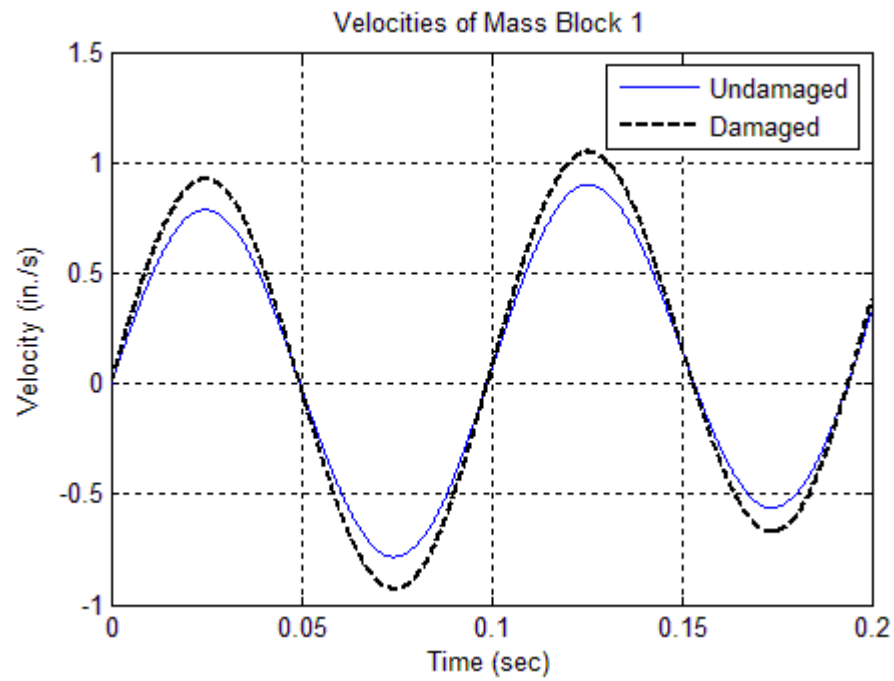


Figure 3.18. Velocities of the Mass Block 1 under the Given External Load

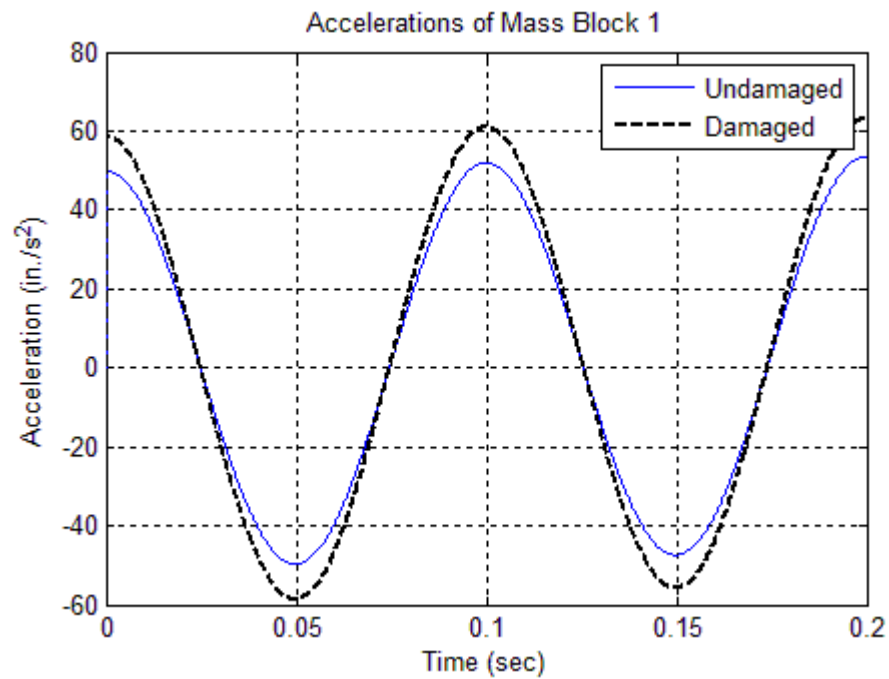


Figure 3.19. Accelerations of the Mass Block 1 under the Given External Load

**Table 3.6. Damage Detection Results for the 5-DOF Spring-Mass-Damper System**

<b>Property</b>	<b>Damage Index (<math>\beta_i</math>, Esimated)</b>	<b>Damage Severity (<math>\alpha_i</math>, Esimated)</b>	<b>Damage Index (<math>\beta_i</math>, Designed)</b>
$m_1$	1.18	-0.15	1.18
$m_2$	1.03	-0.03	1.03
$m_3$	1.06	-0.06	1.06
$m_4$	1.05	-0.05	1.05
$m_5$	1.67	-0.40	1.67
$c_1$	1.14	-0.12	1.14
$c_2$	1.74	-0.43	1.74
$c_3$	0.91	0.10	0.91
$c_4$	1.06	-0.06	1.06
$c_5$	1.10	-0.09	1.10
$c_6$	1.50	-0.33	1.50
$k_1$	1.25	-0.20	1.25
$k_2$	0.95	0.05	0.95
$k_3$	0.98	0.02	0.98
$k_4$	1.15	-0.13	1.15
$k_5$	1.07	-0.07	1.07
$k_6$	1.06	-0.05	1.06

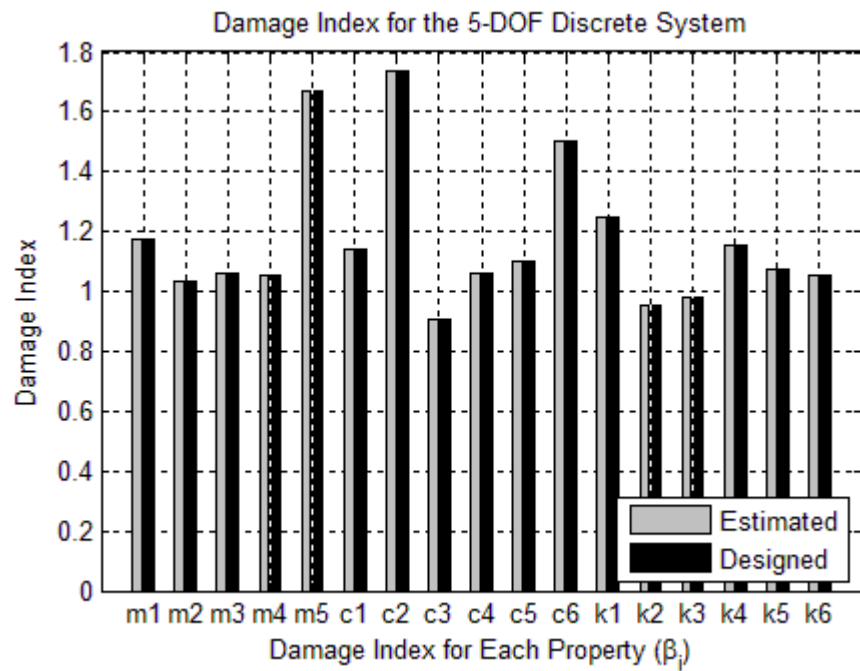


Figure 3.20. Element Damage Indices ( $\beta_i$ ) for 5-DOF Spring-Mass-Damper System

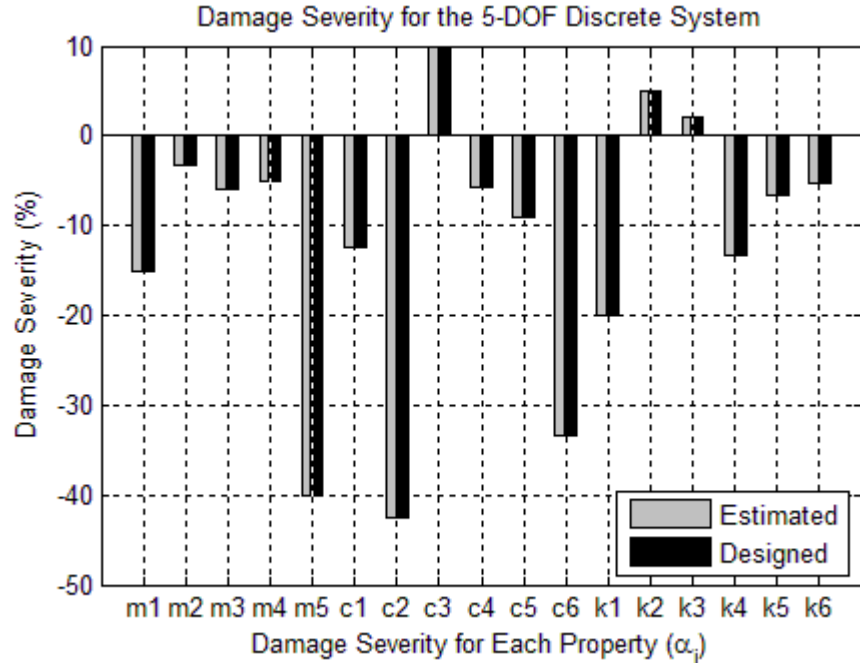


Figure 3.21. Element Damage Severities ( $\alpha_i$ ) for 5-DOF Spring-Mass-Damper System

### 3.5 DAMAGE EVALUATION FOR ISOLATED SPRING-MASS-DAMPER SYSTEMS

In this section, an isolated spring-mass-damper system is isolated from a 5-DOF system and is used to validate the accuracy of the Power Method. The numerical models for the damaged and undamaged 5-DOF mass-spring-damper systems were generated using SAP2000. The 5-DOF spring-mass-damper system used in this case study is plotted in Figure 3.15. The physical properties in the undamaged and damaged systems are listed in Table 3.7. Both the undamaged and damaged systems are excited by the same external force. The applied external force is given at each 1E-4 seconds for 0.2 seconds and is plotted in Figure 3.16. In SAP2000, displacements, velocities and accelerations of the mass blocks were computed every 1E-4 seconds (10,000 Hz) for 0.2 seconds. The displacements, velocities and accelerations of the mass block 1 in both the undamaged and damaged systems were plotted in Figure 3.17, Figure 3.18 and Figure 3.19, respectively.

In this case, the computed velocity ( $\dot{x}(t)$ ) of the mass block in the undamaged case was used as the velocity used to compute power ( $\dot{\Delta}$ ) for both undamaged and damaged cases. The coefficient matrices and known vector, X and Y, were constructed by substituting the acceleration ( $\ddot{x}(t)$ ), velocity ( $\dot{x}(t)$ ), displacement ( $x(t)$ ), and velocity used to compute power ( $\dot{\Delta}$ ) into Eq. 2.179 and Eq. 2.181. The coefficient damage index vector,  $\beta$ , was computed using Eq. 2.183. Then the damage indices for mass, spring and damper are computed using Eqs. 2.184 through 2.188. The damage severities for mass, spring and damper are computed using Eqs. 2.189 through 2.193. The estimated damage indices and the designed damage indices for each physical property are listed in Table 3.8 and are plotted in Figure 3.23. The estimated damage severities and the designed damage

severities for each physical property are plotted in Figure 3.24. Comparing the estimated damage indices with the designed damage indices, the proposed method can accurately locate and size multiple damage in an isolated spring-mass-damper system.

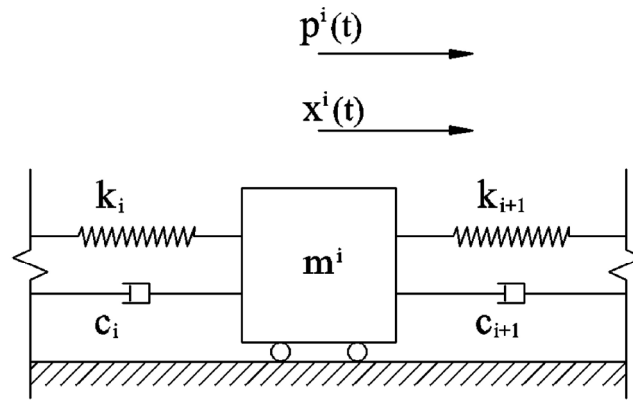


**Figure 3.22. Property Definition and Load Case of the Isolated Spring-Mass-Damper System**

**Table 3.7. Physical Properties of the Isolated Spring-Mass-Damper System**

Undamage Systems					
Property	System #1	System #2	System #3	System #4	System #5
$m_i$ (kip-s <sup>2</sup> /in.)	2.00	3.00	5.00	4.00	1.00
$c_i$ (kip-s/in.)	0.80	0.40	0.30	0.70	0.55
$c_{i+1}$ (kip-s/in.)	0.40	0.30	0.70	0.55	0.60
$k_i$ (kip/in.)	10.00	20.00	15.00	30.00	18.00
$k_{i+1}$ (kip/in.)	20.00	15.00	30.00	18.00	13.00
Damaged Systems					
Property	System #1	System #2	System #3	System #4	System #5
$m_i$ (kip-s <sup>2</sup> /in.)	1.70	2.90	4.70	3.80	0.60
$c_i$ (kip-s/in.)	0.70	0.23	0.33	0.66	0.50
$c_{i+1}$ (kip-s/in.)	0.23	0.33	0.66	0.50	0.40
$k_i$ (kip/in.)	8.00	21.00	15.40	26.00	16.80
$k_{i+1}$ (kip/in.)	21.00	15.30	26.00	16.80	12.30



**Table 3.8. Damage Detection Results for the Isolated Spring-Mass-Damper System**

Designed Damage Indices					
Property	System #1	System #2	System #3	System #4	System #5
$m_i$	1.18	1.03	1.06	1.05	1.67
$c_i$	1.14	1.74	0.91	1.06	1.10
$c_{i+1}$	1.74	0.91	1.06	1.10	1.50
$k_i$	1.25	0.95	0.98	1.15	1.07
$k_{i+1}$	0.95	0.98	1.15	1.07	1.06

Estimated Damage Indices					
Property	System #1	System #2	System #3	System #4	System #5
$m_i$	1.18	1.03	1.06	1.05	1.67
$c_i$	1.14	1.74	0.91	1.06	1.10
$c_{i+1}$	1.74	0.91	1.06	1.10	1.50
$k_i$	1.25	0.95	0.98	1.15	1.07
$k_{i+1}$	0.95	0.98	1.15	1.07	1.06

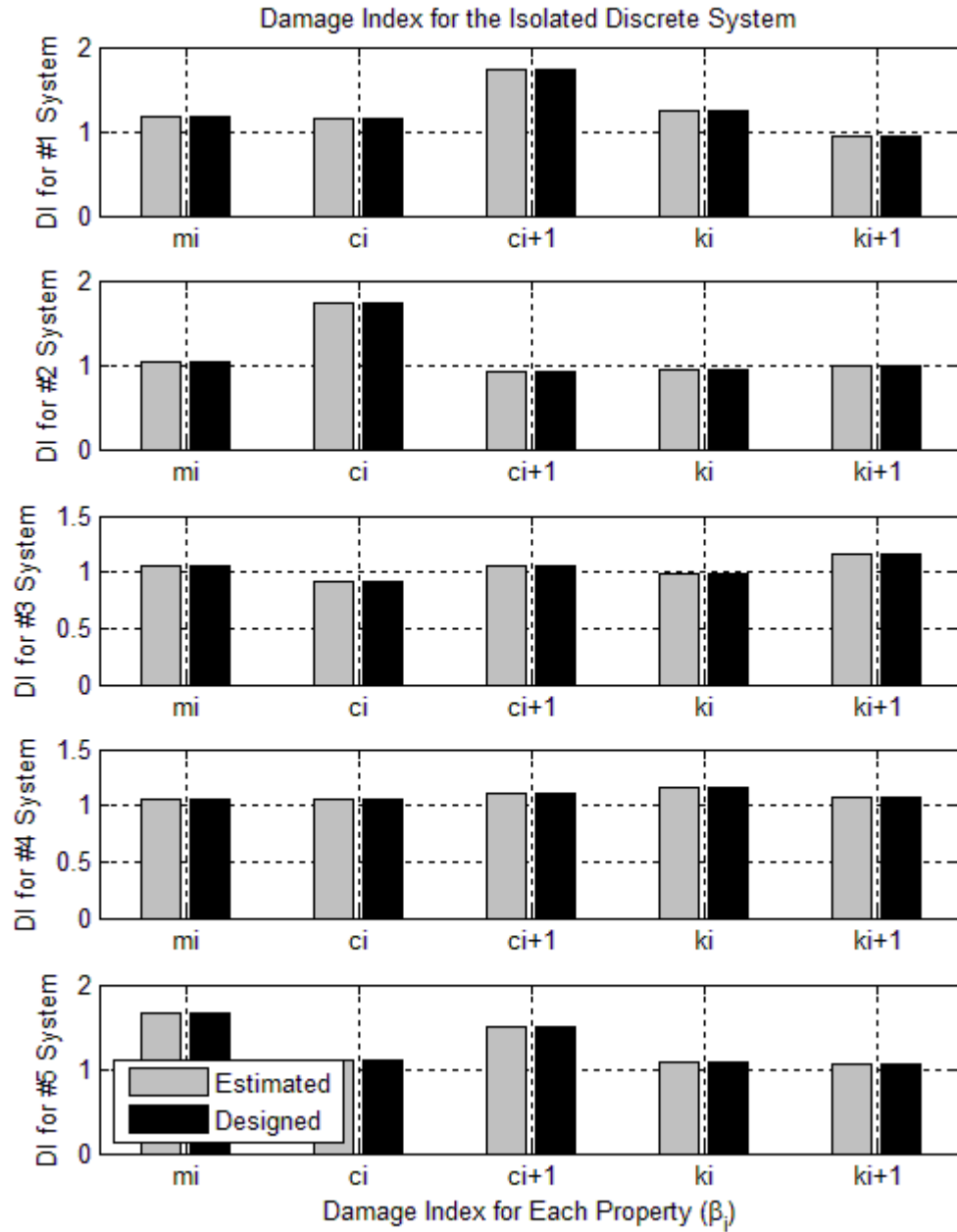
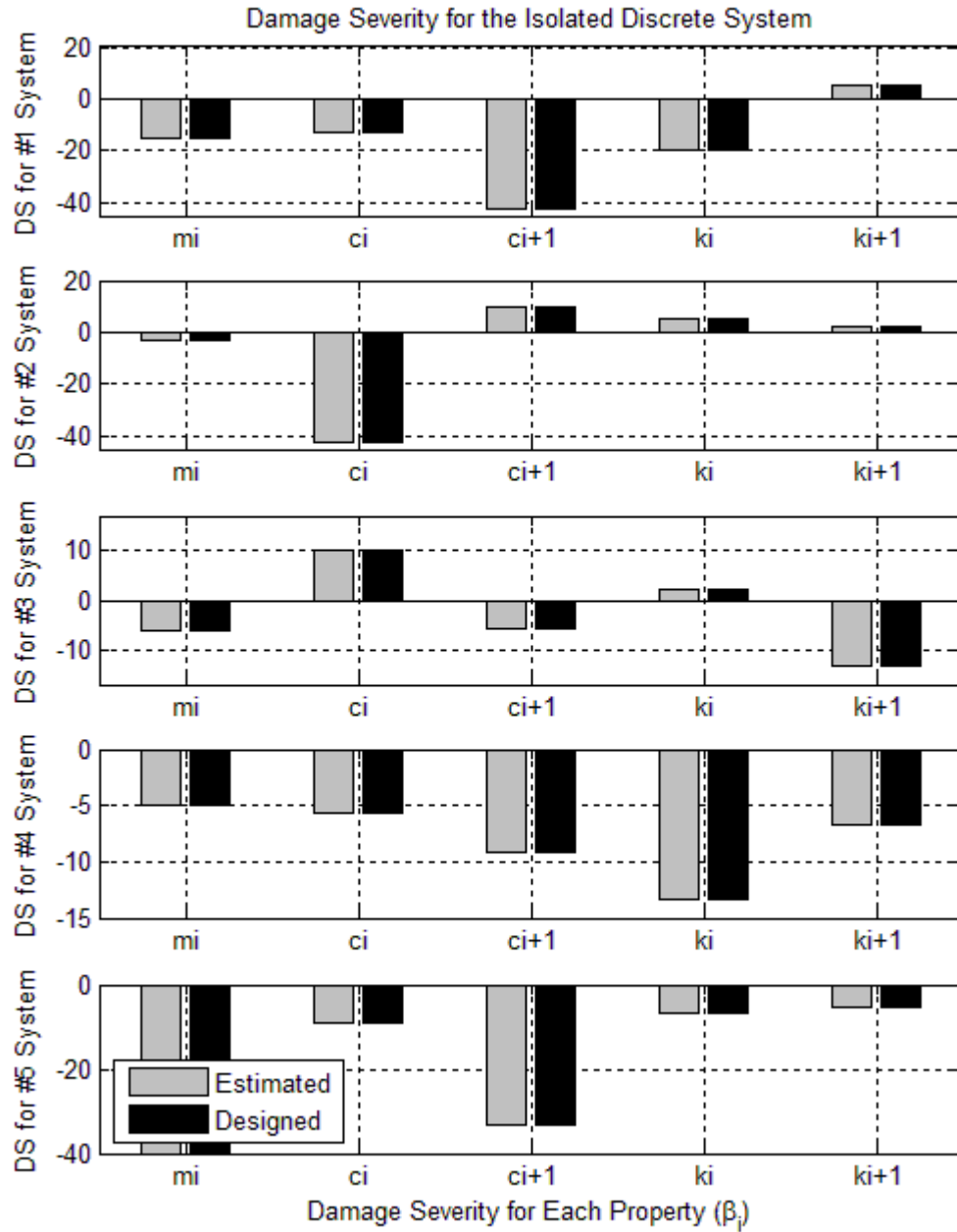


Figure 3.23. Element Damage Indices ( $\beta_i$ ) for Isolated Spring-Mass-Damper System



**Figure 3.24. Element Damage Severities ( $\alpha_i$ ) for Isolated Spring-Mass-Damper System**

### **3.6 SUMMARY**

In this section, 1-DOF, 2-DOF, 5-DOF and isolated spring-mass-damper systems were studied. In each numerical damage detection experiment, different levels of damage in mass, stiffness, and damping were simultaneously simulated in the related damaged system. For both the damaged and undamaged systems, the displacements, velocities and accelerations were exact values (i.e. free from signal noise pollution) and were computed using linear direct integration method in SAP2000. The algorithms given in the Section 2 were used to compute the damage indices and damage severities in each numerical experiment.

According to Table 3.2, Table 3.4, Table 3.6 and Table 3.8, all the designed damage in masses, springs, and dampers were located and evaluated accurately in each numerical experiment. Moreover, for all numerical experiments, neither false-positive damage index nor false-negative damage index was found. Namely, for the proposed damage detection method, if accurate displacement, velocity, and acceleration data are given, all type of damage will be located and evaluated without any error. In addition, the results from Section 3.4 and 3.5 indicate that the proposed method is applicable to both integral discrete system and isolated discrete system.

## 4 THEORY OF DAMAGE EVALUATION ON MASS AND STIFFNESS FOR CONTINUOUS SYSTEMS

### 4.1 INTRODUCTION

In this section, seven major subtasks are addressed. In Section 4.2, the specific form of the Power Method for rods is developed; In Section 4.3, the specific form of the Power Method for Euler-Bernoulli beams is developed; In Section 4.4, the specific form of the Power Method for plane frames is developed; In Section 4.5, the specific form of the Power Method for space trusses is developed; In Section 4.6, the overall solution procedures is provided. In Section 4.7, the summary for Section 4 is made.

### 4.2 THEORY FOR RODS

#### 4.2.1 Theory for Rods at Isolated Element Nodes

In this subsection, the proposed non-destructive evaluation theory is applied to the axial and torsional vibration of rods at a single node.

According to finite element method, one rod can be meshed into several elements. Isolating two nearby rod elements, as shown in Figure 4.1, the modulus of elasticity of the material for the Element  $i$  is denoted as  $E_i$ . The modulus of elasticity in shear of the material for the Element  $i$  is denoted as  $G_i$ . The length of the Element  $i$  is  $L_i$ . The area and the moment of inertia of the cross section of the Element  $i$  are denoted as  $A_i$  and  $I_i$ , respectively. The torsional constant of the cross section of the Element  $i$  is denoted  $J_i$ .

Let  $\{P^i\}$  be the force vector at Node  $i$ , where  $P_1^i$  denotes the axial force at Node  $i$ ,  $P_4^i$

denotes the torsional moment at Node  $i$ . As shown in the free body diagram of Node  $i$  in Figure 4.2, the external loads ( $\{P^i\}$ ), internal forces ( $\{F_i\}$  and  $\{F_{i+1}\}$ ) and inertial forces  $\{I^i\}$  form a dynamic equilibrium condition for Node  $i$ . The dynamic equilibrium condition can be written as,

$$\{I^i\} + \{F_i\} + \{F_{i+1}\} = \{P^i\} \quad (4.1)$$

For this subsection, only axial force and torsional moment will be considered. Thus, each force vector in Eq. 4.1 is composed by two force components: (1) axial force, (2) torsional moment. Namely, Eq. 4.1 can be developed into,

$$\begin{Bmatrix} I_1^i \\ I_4^i \end{Bmatrix} + \begin{Bmatrix} F_{i,1} \\ F_{i,4} \end{Bmatrix} + \begin{Bmatrix} F_{i+1,1} \\ F_{i+1,4} \end{Bmatrix} = \begin{Bmatrix} P_1^i \\ P_4^i \end{Bmatrix} \quad (4.2)$$

Where subscript one (“1”) indicates the force in axial direction of the rod and subscript four (“4”) indicates the force in torsional direction.

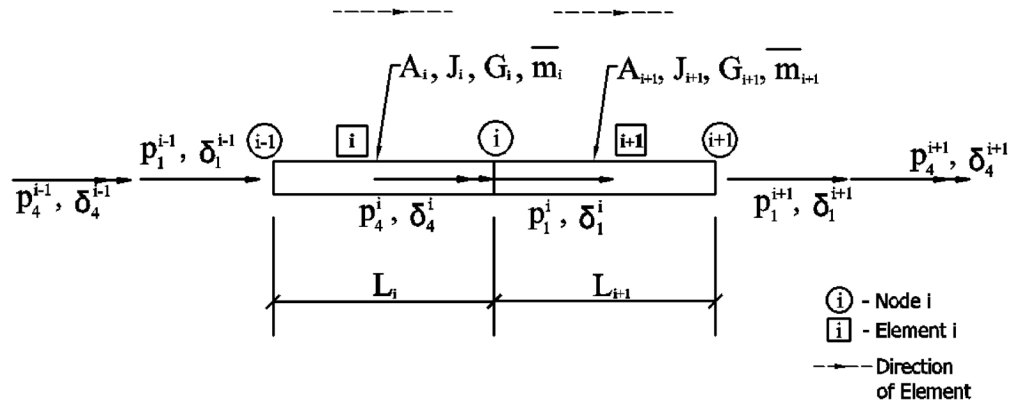
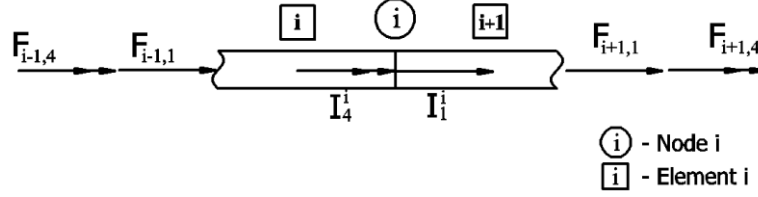


Figure 4.1. Two nearby Rod Elements



**Figure 4.2. Free Body Diagram of Node i under Axial and Torsional Effects**

Similarly, for the damaged case, the dynamic equilibrium condition can be expressed as,

$$\{I^{*i}\} + \{F_i^*\} + \{F_{i+1}^*\} = \{P^{*i}\} \quad (4.3)$$

Where the asterisk (“\*”) denotes the quantities from the damaged case.

Given any velocity vectors,  $\{\dot{\Delta}^i\}$  and  $\{\dot{\Delta}^{*i}\}$ , for the undamaged and damaged systems.

The power done by the external forces in the undamaged and damaged systems can be expressed as follows,

$$\{\dot{\Delta}^i\}^T \{I^i\} + \{\dot{\Delta}^i\}^T \{F_i\} + \{\dot{\Delta}^i\}^T \{F_{i+1}\} = \{\dot{\Delta}^i\}^T \{P^i\} \quad (4.4)$$

$$\{\dot{\Delta}^{*i}\}^T \{I^{*i}\} + \{\dot{\Delta}^{*i}\}^T \{F_i^*\} + \{\dot{\Delta}^{*i}\}^T \{F_{i+1}^*\} = \{\dot{\Delta}^{*i}\}^T \{P^{*i}\} \quad (4.5)$$

Assume that the applied external loads and velocities used to compute power at Node  $i$  are the same for both the undamaged and damaged systems,

$$\{\dot{\Delta}^i\} = \{\dot{\Delta}^{*i}\} \quad (4.6)$$

$$\{P^i\} = \{P^{*i}\} \quad (4.7)$$

Substituting Eq. 4.6 and Eq. 4.7 into Eq. 4.5 yields,

$$\{\dot{\Delta}^i\}^T \{I^{*i}\} + \{\dot{\Delta}^i\}^T \{F_i^*\} + \{\dot{\Delta}^i\}^T \{F_{i+1}^*\} = \{\dot{\Delta}^i\}^T \{P^i\} \quad (4.8)$$

Noticing the power performed by the external load is the same for both the undamaged and damaged systems, substituting Eq. 4.8 into Eq. 4.4 yields,

$$\{\dot{\Delta}^i\}^T \{I^i\} + \{\dot{\Delta}^i\}^T \{F_i\} + \{\dot{\Delta}^i\}^T \{F_{i+1}\} = \{\dot{\Delta}^i\}^T \{I^{*i}\} + \{\dot{\Delta}^i\}^T \{F_i^*\} + \{\dot{\Delta}^i\}^T \{F_{i+1}^*\} \quad (4.9)$$

Note Eq. 4.9 is equivalent to Eq. 2.10.

For the axial and torsional vibration, the inertial force,  $\{I^i\}$ , can be considered using lumped mass method. Namely,

For the axial vibration,

$$\{I_A^i\} = \left( \frac{\bar{m}_i L_i}{2} + \frac{\bar{m}_{i+1} L_{i+1}}{2} \right) \ddot{\delta}_1^i = m_A^i \ddot{\delta}_1^i \quad (4.10)$$

For the torsional vibration,

$$\{I_T^i\} = \left( \frac{\bar{m}_i I_{0,i} L_i}{2A_i} + \frac{\bar{m}_{i+1} I_{0,i+1} L_{i+1}}{2A_{i+1}} \right) \ddot{\delta}_4^i = m_T^i \ddot{\delta}_4^i \quad (4.11)$$

Where  $\bar{m}_i$  is the linear mass for Element  $i$ ;  $I_{0,i}$  is polar moment of inertia of the cross section of Element  $i$ .

In SAP2000, however, the torsional inertia force is equal to zero due to the zero mass in



the torsional direction. To make the theory application better match the later numerical example (i.e. in SAP2000, the inertial force of a bar element in torsional direction is neglected), the torsional inertia force will also be neglected. Namely, set

$$\{I_T^i\} = (0) \cdot \ddot{\delta}_4^i = \{0\} \quad (4.12)$$

Writing Eq. 4.12 and Eq. 4.10 into the matrix form, yields,

$$\{I^i\} = \begin{Bmatrix} I_A^i \\ I_T^i \end{Bmatrix} = \begin{bmatrix} \left( \frac{\bar{m}_i L_i}{2} + \frac{\bar{m}_{i+1} L_{i+1}}{2} \right) & 0 \\ 0 & 0 \end{bmatrix} \begin{Bmatrix} \ddot{\delta}_1^i \\ \ddot{\delta}_4^i \end{Bmatrix} \quad (4.13)$$

Extracting the physical properties from the above equation, yields,

$$\{I^i\} = \begin{Bmatrix} I_A^i \\ I_T^i \end{Bmatrix} = \left( \frac{\bar{m}_i L_i}{2} + \frac{\bar{m}_{i+1} L_{i+1}}{2} \right) \begin{bmatrix} 1 & 0 \\ 0 & 0 \end{bmatrix} \begin{Bmatrix} \ddot{\delta}_1^i \\ \ddot{\delta}_4^i \end{Bmatrix} = m^i [M_o^i] \{\ddot{\delta}^i\} \quad (4.14)$$

Where  $m_i$  is the lumped mass of the Node  $i$ ;  $[M_o^i]$  is commonly called the configuration matrix of the mass matrix.

Similarly, for the damaged system,

$$\{I^{*i}\} = \begin{Bmatrix} I_A^{*i} \\ I_T^{*i} \end{Bmatrix} = \left( \frac{\bar{m}_i L_i}{2} + \frac{\bar{m}_{i+1} L_{i+1}}{2} \right)^* \begin{bmatrix} 1 & 0 \\ 0 & 0 \end{bmatrix}^* \begin{Bmatrix} \ddot{\delta}_1^{*i} \\ \ddot{\delta}_4^{*i} \end{Bmatrix} = m^{*i} [M_o^{*i}] \{\ddot{\delta}^{*i}\} \quad (4.15)$$

The force vectors (i.e.  $\{F_i\}$ ,  $\{F_{i+1}\}$ ,  $\{F_i^*\}$ , and  $\{F_{i+1}^*\}$ ) in Eq. 4.19 can also be computed using stiffness matrices and node displacement vectors,

For axial motion,

$$\{F_{i,1}\} = \begin{bmatrix} -\frac{EA}{L} & \frac{EA}{L} \end{bmatrix}_i \begin{Bmatrix} \delta_1^{i-1} \\ \delta_1^i \end{Bmatrix} \quad (4.16)$$

$$\{F_{i+1,1}\} = \begin{bmatrix} \frac{EA}{L} & -\frac{EA}{L} \end{bmatrix}_{i+1} \begin{Bmatrix} \delta_1^i \\ \delta_1^{i+1} \end{Bmatrix} \quad (4.17)$$

For torsional load,

$$\{F_{i,4}\} = \begin{bmatrix} -\frac{JG}{L} & \frac{JG}{L} \end{bmatrix}_i \begin{Bmatrix} \delta_4^{i-1} \\ \delta_4^i \end{Bmatrix} \quad (4.18)$$

$$\{F_{i+1,4}\} = \begin{bmatrix} \frac{JG}{L} & -\frac{JG}{L} \end{bmatrix}_{i+1} \begin{Bmatrix} \delta_4^i \\ \delta_4^{i+1} \end{Bmatrix} \quad (4.19)$$

Similarly, for the damaged case, the force vectors can be computed as,

$$\{F_{i,1}^*\} = \begin{bmatrix} -\frac{EA}{L} & \frac{EA}{L} \end{bmatrix}_i^* \begin{Bmatrix} \delta_1^{*i-1} \\ \delta_1^{*i} \end{Bmatrix} \quad (4.20)$$

$$\{F_{i+1,1}^*\} = \begin{bmatrix} \frac{EA}{L} & -\frac{EA}{L} \end{bmatrix}_{i+1}^* \begin{Bmatrix} \delta_1^{*i} \\ \delta_1^{*i+1} \end{Bmatrix} \quad (4.21)$$

And

$$\{F_{i,4}^*\} = \begin{bmatrix} -\frac{JG}{L} & \frac{JG}{L} \end{bmatrix}_i^* \begin{Bmatrix} \delta_4^{*i-1} \\ \delta_4^{*i} \end{Bmatrix} \quad (4.22)$$

$$\{F_{i+1,4}^*\} = \begin{bmatrix} \frac{JG}{L} & -\frac{JG}{L} \end{bmatrix}_{i+1}^* \begin{Bmatrix} \delta_4^{*i} \\ \delta_4^{*i+1} \end{Bmatrix} \quad (4.23)$$

Combining Eq. 4.16 and Eq. 4.18 yields,

$$\{F_i\} = \begin{bmatrix} -\frac{EA}{L} & 0 & \frac{EA}{L} & 0 \\ 0 & -\frac{JG}{L} & 0 & \frac{JG}{L} \end{bmatrix}_i \begin{Bmatrix} \delta_1^{i-1} \\ \delta_4^{i-1} \\ \delta_1^i \\ \delta_4^i \end{Bmatrix} \quad (4.24)$$

Given the relationship between Young's modulus and shear modulus, the shear modulus can be expressed as,

$$G = \frac{E}{2(1+\nu)} \quad (4.25)$$

Substituting Eq. 4.25 into Eq. 4.24, yields,

$$\{F_i\} = \begin{bmatrix} -\frac{EA}{L} & 0 & \frac{EA}{L} & 0 \\ 0 & -\frac{JE}{2L(1+\nu)} & 0 & \frac{JE}{2L(1+\nu)} \end{bmatrix}_i \begin{Bmatrix} \delta_1^{i-1} \\ \delta_4^{i-1} \\ \delta_1^i \\ \delta_4^i \end{Bmatrix} \quad (4.26)$$

Extracting the common factor out, yields,

$$\{F_i\} = \left(\frac{E}{L}\right)_i \begin{bmatrix} -A & 0 & A & 0 \\ 0 & -\frac{J}{2(1+\nu)} & 0 & \frac{J}{2(1+\nu)} \end{bmatrix}_i \begin{Bmatrix} \delta_1^{i-1} \\ \delta_4^{i-1} \\ \delta_1^i \\ \delta_4^i \end{Bmatrix} = k_i [K_{o,i}] \{\delta_i\} \quad (4.27)$$

Similarly, other force vectors,  $\{F_{i+1}\}$ ,  $\{F_i^*\}$ , and  $\{F_{i+1}^*\}$ , can be computed as,

$$\{F_{i+1}\} = \left(\frac{E}{L}\right)_{i+1} \begin{bmatrix} A & 0 & -A & 0 \\ 0 & \frac{J}{2(1+\nu)} & 0 & -\frac{J}{2(1+\nu)} \end{bmatrix}_{i+1} \begin{Bmatrix} \delta_1^i \\ \delta_4^i \\ \delta_1^{i+1} \\ \delta_4^{i+1} \end{Bmatrix} = k_{i+1} [K_{o,i+1}] \{\delta_{i+1}\} \quad (4.28)$$

For damaged system,

$$\{F_i^*\} = \left(\frac{E}{L}\right)_i^* \begin{bmatrix} -A & 0 & A & 0 \\ 0 & -\frac{J}{2(1+\nu)} & 0 & \frac{J}{2(1+\nu)} \end{bmatrix}_i^* \begin{Bmatrix} \delta_1^{*i-1} \\ \delta_4^{*i-1} \\ \delta_1^{*i} \\ \delta_4^{*i} \end{Bmatrix} = k_i^* [K_{o,i}^*] \{\delta_i^*\} \quad (4.29)$$

$$\{F_{i+1}^*\} = \left(\frac{E}{L}\right)_{i+1}^* \begin{bmatrix} A & 0 & -A & 0 \\ 0 & \frac{J}{2(1+\nu)} & 0 & -\frac{J}{2(1+\nu)} \end{bmatrix}_{i+1}^* \begin{Bmatrix} \delta_1^{*i} \\ \delta_4^{*i} \\ \delta_1^{*i+1} \\ \delta_4^{*i+1} \end{Bmatrix} = k_{i+1}^* [K_{o,i+1}^*] \{\delta_{i+1}^*\} \quad (4.30)$$

Note as shown in the above equations (i.e. Eq. 4.14, Eq. 4.15, and Eqs. 4.27 through 4.30), the force vectors (i.e.  $\{I^i\}$ ,  $\{F_i\}$ ,  $\{F_{i+1}\}$ ,  $\{I^{*i}\}$ ,  $\{F_i^*\}$ , and  $\{F_{i+1}^*\}$ ) can be summarized as a combination of a property coefficient, a configuration matrix and a nodal deformation vector. Because the designed damage are simulated by the changes of Young's modulus ( $E$ ) and linear mass ( $\bar{m}$ ), other parameters, such as the length of the element ( $L$ ), the cross sectional area ( $A$ ), the torsional constant of element ( $J$ ) and the Poisson's ratio are not influenced by damage and remain the same for the undamaged and damaged elements. Consequently, the configuration matrices for the element stiffness and element mass are the same for both the damaged and undamaged elements, namely,

$$[K_{o,i}^*] = [K_{o,i}] \quad (4.31)$$

$$[K_{o,i+1}^*] = [K_{o,i+1}] \quad (4.32)$$

$$[M_o^{*i}] = [M_o^i] \quad (4.33)$$

Substitute Eqs. 4.31 through 4.33 into Eq. 4.15, Eq. 4.29 and Eq. 4.30, yields,

$$\{I^*\} = m^{*i} [M_o^i] \{\ddot{\delta}^{*i}\} \quad (4.34)$$

$$\{F_i^*\} = k_i^* [K_{o,i}] \{\delta_i^*\} \quad (4.35)$$

$$\{F_{i+1}^*\} = k_{i+1}^* [K_{o,i+1}] \{\delta_{i+1}^*\} \quad (4.36)$$

Substitute Eq. 4.14, Eq. 4.27, Eq. 4.28 and Eqs. 4.34 through 4.36 into Eq. 4.9, yields,

$$\begin{aligned} & \{\dot{\Delta}^i\}^T m^i [M_o^i] \{\ddot{\delta}^i\} + \{\dot{\Delta}^i\}^T k_i [K_{o,i}] \{\delta_i\} + \{\dot{\Delta}^i\}^T k_{i+1} [K_{o,i+1}] \{\delta_{i+1}\} \\ & = \{\dot{\Delta}^i\}^T m^{*i} [M_o^i] \{\ddot{\delta}^{*i}\} + \{\dot{\Delta}^i\}^T k_i^* [K_{o,i}] \{\delta_i^*\} + \{\dot{\Delta}^i\}^T k_{i+1}^* [K_{o,i+1}] \{\delta_{i+1}^*\} \end{aligned} \quad (4.37)$$

Rearranging Eq. 4.37,

$$\begin{aligned} & m^i \{\dot{\Delta}^i\}^T [M_o^i] \{\ddot{\delta}^i\} + k_i \{\dot{\Delta}^i\}^T [K_{o,i}] \{\delta_i\} + k_{i+1} \{\dot{\Delta}^i\}^T [K_{o,i+1}] \{\delta_{i+1}\} \\ & - k_i^* \{\dot{\Delta}^i\}^T [K_{o,i}] \{\delta_i^*\} - k_{i+1}^* \{\dot{\Delta}^i\}^T [K_{o,i+1}] \{\delta_{i+1}^*\} = m^{*i} \{\dot{\Delta}^i\}^T [M_o^i] \{\ddot{\delta}^{*i}\} \end{aligned} \quad (4.38)$$

Dividing Eq. 4.38 by  $m^{*i}$ ,

$$\begin{aligned} & \frac{m^i}{m^{*i}} \{\dot{\Delta}^i\}^T [M_o^i] \{\ddot{\delta}^i\} + \frac{k_i}{m^{*i}} \{\dot{\Delta}^i\}^T [K_{o,i}] \{\delta_i\} + \frac{k_{i+1}}{m^{*i}} \{\dot{\Delta}^i\}^T [K_{o,i+1}] \{\delta_{i+1}\} \\ & - \frac{k_i^*}{m^{*i}} \{\dot{\Delta}^i\}^T [K_{o,i}] \{\delta_i^*\} - \frac{k_{i+1}^*}{m^{*i}} \{\dot{\Delta}^i\}^T [K_{o,i+1}] \{\delta_{i+1}^*\} = \{\dot{\Delta}^i\}^T [M_o^i] \{\ddot{\delta}^{*i}\} \end{aligned} \quad (4.39)$$

Define the following coefficients,

$$\beta_1 = \frac{m^i}{m^{*i}} \quad (4.40)$$

$$\beta_2 = \frac{k_i}{m^{*i}} \quad (4.41)$$

$$\beta_3 = \frac{k_{i+1}}{m^{*i}} \quad (4.42)$$

$$\beta_4 = \frac{k_i^*}{m^{*i}} \quad (4.43)$$

$$\beta_5 = \frac{k_{i+1}^*}{m^{*i}} \quad (4.44)$$

Substituting Eq. 4.40 through Eq. 4.44 into Eq. 4.39, yields,

$$\begin{aligned} & \beta_1 \{\dot{\Delta}^i\}^T [M_o^i] \{\ddot{\delta}^i\} + \beta_2 \{\dot{\Delta}^i\}^T [K_{o,i}] \{\delta_i\} + \beta_3 \{\dot{\Delta}^i\}^T [K_{o,i+1}] \{\delta_{i+1}\} \\ & - \beta_4 \{\dot{\Delta}^i\}^T [K_{o,i}] \{\delta_i^*\} - \beta_5 \{\dot{\Delta}^i\}^T [K_{o,i+1}] \{\delta_{i+1}^*\} = \{\dot{\Delta}^i\}^T [M_o^i] \{\ddot{\delta}^{*i}\} \end{aligned} \quad (4.45)$$

Writing the Eq. 4.45 at different time point, yields the following groups of equations,

For  $t = t_0$ ,

$$\begin{aligned} & \beta_1 (\{\dot{\Delta}^i\}^T [M_o^i] \{\ddot{\delta}^i\})|_{t_0} + \beta_2 (\{\dot{\Delta}^i\}^T [K_{o,i}] \{\delta_i\})|_{t_0} + \beta_3 (\{\dot{\Delta}^i\}^T [K_{o,i+1}] \{\delta_{i+1}\})|_{t_0} \\ & - \beta_4 (\{\dot{\Delta}^i\}^T [K_{o,i}] \{\delta_i^*\})|_{t_0} - \beta_5 (\{\dot{\Delta}^i\}^T [K_{o,i+1}] \{\delta_{i+1}^*\})|_{t_0} = (\{\dot{\Delta}^i\}^T [M_o^i] \{\ddot{\delta}^{*i}\})|_{t_0} \end{aligned} \quad (4.46)$$

For  $t = t_j$ ,

$$\begin{aligned} & \beta_1 (\{\dot{\Delta}^i\}^T [M_o^i] \{\ddot{\delta}^i\})|_{t_j} + \beta_2 (\{\dot{\Delta}^i\}^T [K_{o,i}] \{\delta_i\})|_{t_j} + \beta_3 (\{\dot{\Delta}^i\}^T [K_{o,i+1}] \{\delta_{i+1}\})|_{t_j} \\ & - \beta_4 (\{\dot{\Delta}^i\}^T [K_{o,i}] \{\delta_i^*\})|_{t_j} - \beta_5 (\{\dot{\Delta}^i\}^T [K_{o,i+1}] \{\delta_{i+1}^*\})|_{t_j} = (\{\dot{\Delta}^i\}^T [M_o^i] \{\ddot{\delta}^{*i}\})|_{t_j} \end{aligned} \quad (4.47)$$

For  $t = t_N$ ,

$$\begin{aligned} & \beta_1 (\{\dot{\Delta}^i\}^T [M_o^i] \{\ddot{\delta}^i\})|_{t_N} + \beta_2 (\{\dot{\Delta}^i\}^T [K_{o,i}] \{\delta_i\})|_{t_N} + \beta_3 (\{\dot{\Delta}^i\}^T [K_{o,i+1}] \{\delta_{i+1}\})|_{t_N} \\ & - \beta_4 (\{\dot{\Delta}^i\}^T [K_{o,i}] \{\delta_i^*\})|_{t_N} - \beta_5 (\{\dot{\Delta}^i\}^T [K_{o,i+1}] \{\delta_{i+1}^*\})|_{t_N} = (\{\dot{\Delta}^i\}^T [M_o^i] \{\ddot{\delta}^{*i}\})|_{t_N} \end{aligned} \quad (4.48)$$

Arrange the above Equation group into matrix form, yields,

$$\mathbf{X}\boldsymbol{\beta} = \mathbf{Y} \quad (4.49)$$

Where the coefficient matrix of the linear equation group is given as following (note, due to the limitation of the page size, the transposed form of the matrix is provided),

$$\mathbf{X}^T = \begin{bmatrix} (\{\dot{\Delta}^i\}^T [M_{o,i}] \{\ddot{\delta}^i\})|_{t_0} & \dots & (\{\dot{\Delta}^i\}^T [M_{o,i}] \{\ddot{\delta}^i\})|_{t_j} & \dots & (\{\dot{\Delta}^i\}^T [M_{o,i}] \{\ddot{\delta}^i\})|_{t_N} \\ (\{\dot{\Delta}^i\}^T [K_{o,i}] \{\delta_i\})|_{t_0} & \dots & (\{\dot{\Delta}^i\}^T [K_{o,i}] \{\delta_i\})|_{t_j} & \dots & (\{\dot{\Delta}^i\}^T [K_{o,i}] \{\delta_i\})|_{t_N} \\ (\{\dot{\Delta}^i\}^T [K_{o,i+1}] \{\delta_{i+1}\})|_{t_0} & \dots & (\{\dot{\Delta}^i\}^T [K_{o,i+1}] \{\delta_{i+1}\})|_{t_j} & \dots & (\{\dot{\Delta}^i\}^T [K_{o,i+1}] \{\delta_{i+1}\})|_{t_N} \\ -(\{\dot{\Delta}^i\}^T [K_{o,i}] \{\delta_i^*\})|_{t_0} & \dots & -(\{\dot{\Delta}^i\}^T [K_{o,i}] \{\delta_i^*\})|_{t_j} & \dots & -(\{\dot{\Delta}^i\}^T [K_{o,i}] \{\delta_i^*\})|_{t_N} \\ -(\{\dot{\Delta}^i\}^T [K_{o,i+1}] \{\delta_{i+1}^*\})|_{t_0} & \dots & -(\{\dot{\Delta}^i\}^T [K_{o,i+1}] \{\delta_{i+1}^*\})|_{t_j} & \dots & -(\{\dot{\Delta}^i\}^T [K_{o,i+1}] \{\delta_{i+1}^*\})|_{t_N} \end{bmatrix} \quad (4.50)$$

The vector of unknowns and the vector of known are given as,

$$\boldsymbol{\beta} = \begin{Bmatrix} \beta_1 \\ \beta_2 \\ \beta_3 \\ \beta_4 \\ \beta_5 \end{Bmatrix} \quad (4.51)$$

$$\mathbf{Y} = \begin{Bmatrix} (\{\dot{\Delta}^i\}^T [M_o^i] \{\ddot{\delta}^{*i}\})|_{t_0} \\ \vdots \\ (\{\dot{\Delta}^i\}^T [M_o^i] \{\ddot{\delta}^{*i}\})|_{t_j} \\ \vdots \\ (\{\dot{\Delta}^i\}^T [M_o^i] \{\ddot{\delta}^{*i}\})|_{t_N} \end{Bmatrix} \quad (4.52)$$

Based on the Least Square Method, the  $\boldsymbol{\beta}$  can be computed from the following equation,

$$\boldsymbol{\beta} = (\mathbf{X}^T \mathbf{X})^{-1} (\mathbf{X}^T \mathbf{Y}) \quad (4.53)$$

The damage indices for stiffness, mass and damping can be computed as follows,

$$\beta_{m^i} = \frac{m^i}{m^{*i}} = \frac{\left( \frac{\bar{m}_i L_i}{2} + \frac{\bar{m}_{i+1} L_{i+1}}{2} \right)}{\left( \frac{\bar{m}_i^* L_i}{2} + \frac{\bar{m}_{i+1}^* L_{i+1}}{2} \right)} = \beta_1 \quad (4.54)$$

$$\beta_{k_i} = \frac{k_i}{k_i^*} = \frac{\frac{k_i}{m^{*i}}}{\frac{k_i^*}{m^{*i}}} = \frac{\beta_2}{\beta_4} \quad (4.55)$$

$$\beta_{k_{i+1}} = \frac{k_{i+1}}{k_{i+1}^*} = \frac{\frac{k_{i+1}}{m^{*i}}}{\frac{k_{i+1}^*}{m^{*i}}} = \frac{\beta_3}{\beta_5} \quad (4.56)$$

#### 4.2.2 Theory for Rods among Multiple Nodes

In this subsection, the proposed non-destructive evaluation theory will be applied to multiple nodes on a rod. The damage detection to the physical properties (i.e. mass, stiffness, damping, etc.) related to these nodes will be completed simultaneously. Since the idea of combining the axial and torsional vibrations has already been demonstrated in the above sub-section, for simplicity purposes, the torsional vibration will not be considered in this subsection.

Given two nearby rod elements, as shown in Figure 4.3, the modulus of elasticity of the material for Element  $i$  is denoted as  $E_i$ . The length of Element  $i$  is  $L_i$ . The cross sectional area of Element  $i$  is denoted as  $A_i$ . Let  $P_1^i$  denotes the external axial force applied at



Node  $i$ . As shown in the free body diagram of Node  $i$  in Figure 4.4, the external axial load ( $P_1^i$ ), internal axial forces ( $F_{i,1}$  and  $F_{i+1,1}$ ) and inertial axial forces  $I_1^i$  form a dynamic equilibrium condition for Node  $i$ . The dynamic equilibrium condition can be written as,

$$I_1^i + F_{i,1} + F_{i+1,1} = P_1^i \quad (4.57)$$

Where the subscript ' $i$ ' denotes Node  $i$  and the '1' denotes the component in axial direction.

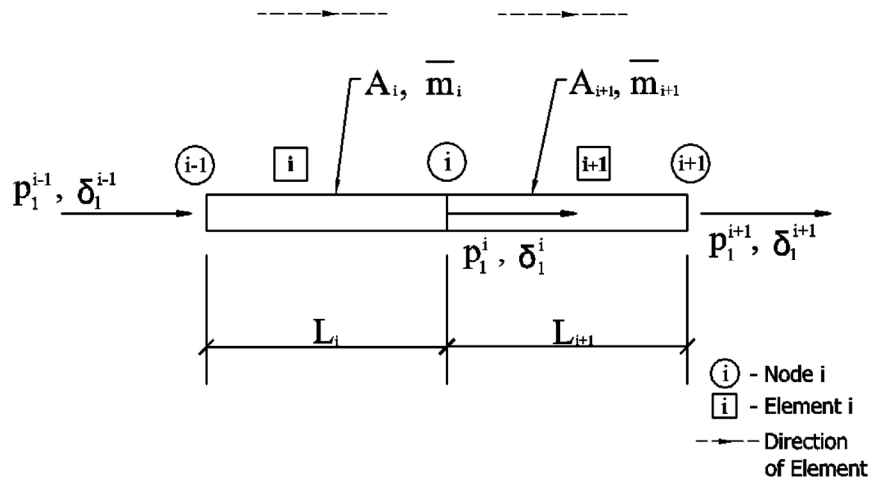


Figure 4.3. Two nearby Rod Elements

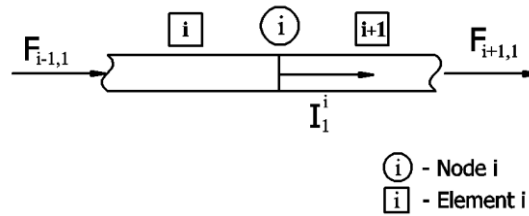


Figure 4.4. Free Body Diagram of Node  $i$  under Axial Effects

For the damaged case, the dynamic equilibrium condition is,

$$I_1^{*i} + F_{i,1}^* + F_{i+1,1}^* = P_1^{*i} \quad (4.58)$$

Where the asterisk (“\*”) denotes the quantities from the damaged case.

Given any node axial velocity,  $\dot{\Delta}_1^i$ , the power done by the external axial loads in the undamaged and damaged system can be computed as follows,

$$\dot{\Delta}_1^i I_1^i + \dot{\Delta}_1^i F_{i,1} + \dot{\Delta}_1^i F_{i+1,1} = \dot{\Delta}_1^i P_1^i \quad (4.59)$$

$$\dot{\Delta}_1^{*i} I_1^{*i} + \dot{\Delta}_1^{*i} F_{i,1}^* + \dot{\Delta}_1^{*i} F_{i+1,1}^* = \dot{\Delta}_1^{*i} P_1^{*i} \quad (4.60)$$

For N nodes in the structure, the axial force vector can be written as,

$$\{P_1\} = \begin{Bmatrix} P_1^1 \\ \vdots \\ P_1^i \\ \vdots \\ P_1^N \end{Bmatrix} \quad (4.61)$$

Given any node axial velocity vector,  $\{\dot{\Delta}_1\}$ , the power done by the external axial loads in the undamaged system can be computed as following,

$$\{\dot{\Delta}_1\} \{P_1\} = \begin{Bmatrix} \dot{\Delta}_1^1 \\ \vdots \\ \dot{\Delta}_1^i \\ \vdots \\ \dot{\Delta}_1^N \end{Bmatrix}^T \begin{Bmatrix} P_1^1 \\ \vdots \\ P_1^i \\ \vdots \\ P_1^N \end{Bmatrix} = \begin{Bmatrix} \dot{\Delta}_1^1 \\ \vdots \\ \dot{\Delta}_1^i \\ \vdots \\ \dot{\Delta}_1^N \end{Bmatrix}^T \begin{Bmatrix} I_1^1 + F_{1,1} + F_{2,1} \\ \vdots \\ I_1^i + F_{i,1} + F_{i+1,1} \\ \vdots \\ I_1^N + F_{N,1} + F_{N+1,1} \end{Bmatrix} \quad (4.62)$$

Similarly, for the damaged system, the power done by the external axial loads can be

computed as follows,

$$\{\dot{\Delta}_1^*\} \{P_1^*\} = \begin{Bmatrix} \dot{\Delta}_1^{*1} \\ \vdots \\ \dot{\Delta}_1^{*i} \\ \vdots \\ \dot{\Delta}_1^{*N} \end{Bmatrix}^T \begin{Bmatrix} P_1^{*1} \\ \vdots \\ P_1^{*i} \\ \vdots \\ P_1^{*N} \end{Bmatrix} = \begin{Bmatrix} \dot{\Delta}_1^{*1} \\ \vdots \\ \dot{\Delta}_1^{*i} \\ \vdots \\ \dot{\Delta}_1^{*N} \end{Bmatrix}^T \begin{Bmatrix} I_1^{*1} + F_{1,1}^* + F_{2,1}^* \\ \vdots \\ I_1^{*i} + F_{i,1}^* + F_{i+1,1}^* \\ \vdots \\ I_1^{*N} + F_{N,1}^* + F_{N+1,1}^* \end{Bmatrix} \quad (4.63)$$

Assuming the applied external loads and velocities used to compute power are the same for both the undamaged and damaged system. Namely

$$\{\dot{\Delta}_1\} = \{\dot{\Delta}_1^*\} \quad (4.64)$$

$$\{P_1\} = \{P_1^*\} \quad (4.65)$$

Substituting Eq. 4.64 and Eq. 4.65 into Eq. 4.63 yields,

$$\{\dot{\Delta}_1^*\} \{P_1^*\} = \{\dot{\Delta}_1\} \{P_1\} = \begin{Bmatrix} \dot{\Delta}_1^1 \\ \vdots \\ \dot{\Delta}_1^i \\ \vdots \\ \dot{\Delta}_1^N \end{Bmatrix}^T \begin{Bmatrix} P_1^1 \\ \vdots \\ P_1^i \\ \vdots \\ P_1^N \end{Bmatrix} = \begin{Bmatrix} \dot{\Delta}_1^1 \\ \vdots \\ \dot{\Delta}_1^i \\ \vdots \\ \dot{\Delta}_1^N \end{Bmatrix}^T \begin{Bmatrix} I_1^{*1} + F_{1,1}^* + F_{2,1}^* \\ \vdots \\ I_1^{*i} + F_{i,1}^* + F_{i+1,1}^* \\ \vdots \\ I_1^{*N} + F_{N,1}^* + F_{N+1,1}^* \end{Bmatrix} \quad (4.66)$$

Noticing the power performed by the external load is the same for both the undamaged and damaged system. Substituting Eq. 4.66 into Eq. 4.62, yields,

$$\begin{Bmatrix} \dot{\Delta}_1^1 \\ \vdots \\ \dot{\Delta}_1^i \\ \vdots \\ \dot{\Delta}_1^N \end{Bmatrix}^T \begin{Bmatrix} I_1^1 + F_{1,1} + F_{2,1} \\ \vdots \\ I_1^i + F_{i,1} + F_{i+1,1} \\ \vdots \\ I_1^N + F_{N,1} + F_{N+1,1} \end{Bmatrix} = \begin{Bmatrix} \dot{\Delta}_1^1 \\ \vdots \\ \dot{\Delta}_1^i \\ \vdots \\ \dot{\Delta}_1^N \end{Bmatrix}^T \begin{Bmatrix} I_1^{*1} + F_{1,1}^* + F_{2,1}^* \\ \vdots \\ I_1^{*i} + F_{i,1}^* + F_{i+1,1}^* \\ \vdots \\ I_1^{*N} + F_{N,1}^* + F_{N+1,1}^* \end{Bmatrix} \quad (4.67)$$

Note, Eq. 4.67 is equivalent to Eq. 2.10.

Eq. 4.67 can be developed into the following equation,

$$\begin{aligned} & \dot{\Delta}_1(I_1^1 + F_1^1 + F_1^2) + \dots + \dot{\Delta}_1(I_1^i + F_{i,1} + F_{i+1,1}) + \dots + \dot{\Delta}_1(I_1^N + F_{N,1} + F_{N+1,1}) \\ & = \dot{\Delta}_1(I_1^{*1} + F_{1,1}^* + F_{2,1}^*) + \dots + \dot{\Delta}_1(I_1^{*i} + F_{i,1}^* + F_{i+1,1}^*) + \dots + \dot{\Delta}_1(I_1^{*N} + F_{N,1}^* + F_{N+1,1}^*) \end{aligned} \quad (4.68)$$

Rearranging Eq. 4.68 yields,

$$\begin{aligned} & \dot{\Delta}_1(I_1^1 + F_1^1 + F_1^2) + \dots + \dot{\Delta}_1(I_1^i + F_{i,1} + F_{i+1,1}) + \dots + \dot{\Delta}_1(I_1^N + F_{N,1} + F_{N+1,1}) \\ & - \dot{\Delta}_1(I_1^{*1} + F_{1,1}^* + F_{2,1}^*) - \dots - \dot{\Delta}_1(I_1^{*i} + F_{i,1}^* + F_{i+1,1}^*) - \dots - \dot{\Delta}_1(I_1^{*N} + F_{N,1}^* + F_{N+1,1}^*) = \dot{\Delta}_1 I_1^{*N} \end{aligned} \quad (4.69)$$

However, since two nearby nodes will share the same rod element, the same force vector will appear twice in the above equation, which means rows in the coefficient matrix are linearly depend. This will create singularity problem in the later least square analysis. To avoid the singularity problem, the common terms in the above equation will be extracted and merged together. This is process is demonstrated by the following derivations,

A more detailed expression for Eq. 4.69 is given as,

$$\begin{aligned} & \dot{\Delta}_1(I_1^1 + F_{1,1} + F_{2,1}) + \dot{\Delta}_1(I_1^2 + F_{2,1} + F_{3,1}) + \dots + \dot{\Delta}_1(I_1^i + F_{i,1} + F_{i+1,1}) \\ & + \dot{\Delta}_1(I_1^{i+1} + F_{i+1,1} + F_{i+2,1}) + \dots + \dot{\Delta}_1(I_1^{N-1} + F_{N-1,1} + F_{N,1}) + \dot{\Delta}_1(I_1^N + F_{N,1} + F_{N+1,1}) \\ & - \dot{\Delta}_1(I_1^{*1} + F_{1,1}^* + F_{2,1}^*) - \dot{\Delta}_1(I_1^{*2} + F_{2,1}^* + F_{3,1}^*) - \dots - \dot{\Delta}_1(I_1^{*i} + F_{i,1}^* + F_{i+1,1}^*) \\ & - \dot{\Delta}_1(I_1^{*i+1} + F_{i+1,1}^* + F_{i+2,1}^*) - \dots - \dot{\Delta}_1(I_1^{*N-1} + F_{N-1,1}^* + F_{N,1}^*) - \dot{\Delta}_1(I_1^{*N} + F_{N,1}^* + F_{N+1,1}^*) \\ & = \dot{\Delta}_1 I_1^{*N} \end{aligned} \quad (4.70)$$

According to Eq. 4.10, Eq. 4.16, Eq. 4.17, Eq. 4.20, and Eq. 4.21,

$$\{I_A^i\} = \left( \frac{\bar{m}_i L_i}{2} + \frac{\bar{m}_{i+1} L_{i+1}}{2} \right) \ddot{\delta}_1^i = m^i \ddot{\delta}_1^i \quad (4.10)$$

$$\{I_A^{*i}\} = \left( \frac{\bar{m}_i^* L_i^*}{2} + \frac{\bar{m}_{i+1}^* L_{i+1}^*}{2} \right) \ddot{\delta}_1^{*i} = m^{*i} \ddot{\delta}_1^{*i} \quad (4.71)$$

$$\{F_{i,1}\} = \left( \frac{EA}{L} \right)_i (-\delta_1^{i-1} + \delta_1^i) = k_i (-\delta_1^{i-1} + \delta_1^i) \quad (4.72)$$

$$\{F_{i+1,1}\} = \left( \frac{EA}{L} \right)_{i+1} (\delta_1^i - \delta_1^{i+1}) = k_{i+1} (\delta_1^i - \delta_1^{i+1}) \quad (4.73)$$

$$\{F_{i,1}^*\} = \left( \frac{EA}{L} \right)_i^* (-\delta_1^{*i-1} + \delta_1^{*i}) = k_i^* (-\delta_1^{*i-1} + \delta_1^{*i}) \quad (4.74)$$

$$\{F_{i+1,1}^*\} = \left( \frac{EA}{L} \right)_{i+1}^* (\delta_1^{*i} - \delta_1^{*i+1}) = k_{i+1}^* (\delta_1^{*i} - \delta_1^{*i+1}) \quad (4.75)$$

Substituting Eq. 4.10 and Eqs. 4.71 through 4.75 into the Eq. 4.70, yields,

$$\begin{aligned} & \dot{\Delta}_1^1 (m^1 \ddot{\delta}_1^1 + k_1 (-\delta_1^0 + \delta_1^1) + k_2 (\delta_1^1 - \delta_1^2)) \\ & + \dot{\Delta}_1^2 (m^2 \ddot{\delta}_1^2 + k_2 (-\delta_1^1 + \delta_1^2) + k_3 (\delta_1^2 - \delta_1^3)) + \dots \\ & + \dot{\Delta}_1^i (m^i \ddot{\delta}_1^i + k_i (-\delta_1^{i-1} + \delta_1^i) + k_{i+1} (\delta_1^i - \delta_1^{i+1})) \\ & + \dot{\Delta}_1^{i+1} (m^{i+1} \ddot{\delta}_1^{i+1} + k_{i+1} (-\delta_1^i + \delta_1^{i+1}) + k_{i+2} (\delta_1^{i+1} - \delta_1^{i+2})) + \dots \\ & + \dot{\Delta}_1^N (m^N \ddot{\delta}_1^N + k_N (-\delta_1^{N-1} + \delta_1^N) + k_{N+1} (\delta_1^N - \delta_1^{N+1})) \\ & - \dot{\Delta}_1^1 (m_1^{*1} \ddot{\delta}_1^{*1} + k_1^* (-\delta_1^{*0} + \delta_1^{*1}) + k_2^* (\delta_1^{*1} - \delta_1^{*2})) \\ & - \dot{\Delta}_1^2 (m^{*2} \ddot{\delta}_1^{*2} + k_2^* (-\delta_1^{*1} + \delta_1^{*2}) + k_3^* (\delta_1^{*2} - \delta_1^{*3})) - \dots \\ & - \dot{\Delta}_1^i (m^{*i} \ddot{\delta}_1^{*i} + k_i^* (-\delta_1^{*i-1} + \delta_1^{*i}) + k_{i+1}^* (\delta_1^{*i} - \delta_1^{*i+1})) \\ & - \dot{\Delta}_1^{i+1} (m^{*i+1} \ddot{\delta}_1^{*i+1} + k_{i+1}^* (-\delta_1^{*i} + \delta_1^{*i+1}) + k_{i+2}^* (\delta_1^{*i+1} - \delta_1^{*i+2})) - \dots \\ & - \dot{\Delta}_1^N k_N^* (-\delta_1^{*N-1} + \delta_1^{*N}) - \dot{\Delta}_1^N k_{N+1}^* (\delta_1^{*N} - \delta_1^{*N+1}) = \dot{\Delta}_1^N m^{*N} \ddot{\delta}_1^{*N} \end{aligned} \quad (4.76)$$

Extracting and merging the common term in the above equation, yields,

$$\begin{aligned}
& \dot{\Delta}_1^1 m^1 \ddot{\delta}_1^1 + \dots + \dot{\Delta}_1^i m^i \ddot{\delta}_1^i + \dots + \dot{\Delta}_1^N m^N \ddot{\delta}_1^N \\
& + \dot{\Delta}_1^1 k_1 (-\delta_1^0 + \delta_1^1) + (\dot{\Delta}_1^1 - \dot{\Delta}_1^2) k_2 (\delta_1^1 - \delta_1^2) + \dots + (\dot{\Delta}_1^{i-1} - \dot{\Delta}_1^i) k_i (\delta_1^{i-1} - \delta_1^i) \\
& + \dots + (\dot{\Delta}_1^{N-1} - \dot{\Delta}_1^N) k_N (\delta_1^{N-1} - \delta_1^N) + \dot{\Delta}_1^N k_{N+1} (\delta_1^N - \delta_1^{N+1}) \\
& - \dot{\Delta}_1^1 m^{*1} \ddot{\delta}_1^{*1} - \dots - \dot{\Delta}_1^i m^{*i} \ddot{\delta}_1^{*i} - \dots - \dot{\Delta}_1^{N-1} m^{*N-1} \ddot{\delta}_1^{*N-1} \\
& - \dot{\Delta}_1^1 k_1^* (-\delta_1^{*0} + \delta_1^{*1}) - (\dot{\Delta}_1^1 - \dot{\Delta}_1^2) k_2^* (\delta_1^{*1} - \delta_1^{*2}) - \dots - (\dot{\Delta}_1^{i-1} - \dot{\Delta}_1^i) k_i^* (\delta_1^{*i-1} - \delta_1^{*i}) \\
& - \dots - (\dot{\Delta}_1^{N-1} - \dot{\Delta}_1^N) k_N^* (\delta_1^{*N-1} - \delta_1^{*N}) - \dot{\Delta}_1^N k_{N+1}^* (\delta_1^{*N} - \delta_1^{*N+1}) \\
& = \dot{\Delta}_1^N m^{*N} \ddot{\delta}_1^{*N}
\end{aligned} \tag{4.77}$$

Moving the physical property to the front of each term yields,

$$\begin{aligned}
& m^1 \dot{\Delta}_1^1 \ddot{\delta}_1^1 + \dots + m^i \dot{\Delta}_1^i \ddot{\delta}_1^i + \dots + m^N \dot{\Delta}_1^N \ddot{\delta}_1^N \\
& + k_1 \dot{\Delta}_1^1 (-\delta_1^0 + \delta_1^1) + k_2 (\dot{\Delta}_1^1 - \dot{\Delta}_1^2) (\delta_1^1 - \delta_1^2) + \dots + k_i (\dot{\Delta}_1^{i-1} - \dot{\Delta}_1^i) (\delta_1^{i-1} - \delta_1^i) \\
& + \dots + k_N (\dot{\Delta}_1^{N-1} - \dot{\Delta}_1^N) (\delta_1^{N-1} - \delta_1^N) + k_{N+1} \dot{\Delta}_1^N (\delta_1^N - \delta_1^{N+1}) \\
& - m^{*1} \dot{\Delta}_1^1 \ddot{\delta}_1^{*1} - \dots - m^{*i} \dot{\Delta}_1^i \ddot{\delta}_1^{*i} - \dots - m^{*N-1} \dot{\Delta}_1^{N-1} \ddot{\delta}_1^{*N-1} \\
& - k_1^* \dot{\Delta}_1^1 (-\delta_1^{*0} + \delta_1^{*1}) - k_2^* (\dot{\Delta}_1^1 - \dot{\Delta}_1^2) (\delta_1^{*1} - \delta_1^{*2}) - \dots - k_i^* (\dot{\Delta}_1^{i-1} - \dot{\Delta}_1^i) (\delta_1^{*i-1} - \delta_1^{*i}) \\
& - \dots - k_N^* (\dot{\Delta}_1^{N-1} - \dot{\Delta}_1^N) (\delta_1^{*N-1} - \delta_1^{*N}) - k_{N+1}^* \dot{\Delta}_1^N (\delta_1^{*N} - \delta_1^{*N+1}) \\
& = m^{*N} \dot{\Delta}_1^N \ddot{\delta}_1^{*N}
\end{aligned} \tag{4.78}$$

Dividing Eq. 4.78 by  $m^{*N}$  yields,

$$\begin{aligned}
& \frac{m^1}{m^{*N}} \dot{\Delta}_1 \ddot{\delta}_1^1 + \dots + \frac{m^i}{m^{*N}} \dot{\Delta}_1 \ddot{\delta}_1^i + \dots + \frac{m^N}{m^{*N}} \dot{\Delta}_1 \ddot{\delta}_1^N \\
& + \frac{k_1}{m^{*N}} \dot{\Delta}_1 (-\delta_1^0 + \delta_1^1) + \frac{k_2}{m^{*N}} (\dot{\Delta}_1 - \dot{\Delta}_1^2) (\delta_1^1 - \delta_1^2) + \dots + \frac{k_i}{m^{*N}} (\dot{\Delta}_1^{i-1} - \dot{\Delta}_1^i) (\delta_1^{i-1} - \delta_1^i) \\
& + \dots + \frac{k_N}{m^{*N}} (\dot{\Delta}_1^{N-1} - \dot{\Delta}_1^N) (\delta_1^{N-1} - \delta_1^N) + \frac{k_{N+1}}{m^{*N}} \dot{\Delta}_1^N (\delta_1^N - \delta_1^{N+1}) \\
& - \frac{m^{*1}}{m^{*N}} \dot{\Delta}_1 \ddot{\delta}_1^{*1} - \dots - \frac{m^{*i}}{m^{*N}} \dot{\Delta}_1 \ddot{\delta}_1^{*i} - \dots - \frac{m^{*N-1}}{m^{*N}} \dot{\Delta}_1^{N-1} \ddot{\delta}_1^{*N-1} \\
& - \frac{k_1^*}{m^{*N}} \dot{\Delta}_1 (-\delta_1^{*0} + \delta_1^{*1}) - \frac{k_2^*}{m^{*N}} (\dot{\Delta}_1 - \dot{\Delta}_1^2) (\delta_1^{*1} - \delta_1^{*2}) - \dots - \frac{k_i^*}{m^{*N}} (\dot{\Delta}_1^{i-1} - \dot{\Delta}_1^i) (\delta_1^{*i-1} - \delta_1^{*i}) \\
& - \dots - \frac{k_N^*}{m^{*N}} (\dot{\Delta}_1^{N-1} - \dot{\Delta}_1^N) (\delta_1^{*N-1} - \delta_1^{*N}) - \frac{k_{N+1}^*}{m^{*N}} \dot{\Delta}_1^N (\delta_1^{*N} - \delta_1^{*N+1}) \\
& = \dot{\Delta}_1^N \ddot{\delta}_1^{*N}
\end{aligned} \tag{4.79}$$

Define the following  $(4N+1)$  coefficients,

$$\beta_1 = \frac{m^1}{m^{*N}} \tag{4.80}$$

...

$$\beta_i = \frac{m^i}{m^{*N}} \tag{4.81}$$

...

$$\beta_N = \frac{m^N}{m^{*N}} \tag{4.82}$$

$$\beta_{N+1} = \frac{k_1}{m_N^*} \tag{4.83}$$

...

$$\beta_{N+i} = \frac{k_i}{m^{*N}} \quad (4.84)$$

...

$$\beta_{2N+1} = \frac{k_{N+1}}{m^{*N}} \quad (4.85)$$

$$\beta_{2N+2} = \frac{m^{*1}}{m^{*N}} \quad (4.86)$$

...

$$\beta_{2N+1+i} = \frac{m^{*i}}{m^{*N}} \quad (4.87)$$

...

$$\beta_{3N} = \frac{m^{*N-1}}{m^{*N}} \quad (4.88)$$

$$\beta_{3N+1} = \frac{k_1^*}{m^{*N}} \quad (4.89)$$

...

$$\beta_{4N+1} = \frac{k_{N+1}^*}{m^{*N}} \quad (4.90)$$

Substituting Eq. 4.80 through Eq. 4.90 to Eq. 4.79 yields,



$$\begin{aligned}
& \beta_1 \dot{\Delta}_1 \ddot{\delta}_1^1 + \cdots + \beta_i \dot{\Delta}_1 \ddot{\delta}_1^i + \cdots + \beta_N \dot{\Delta}_1 \ddot{\delta}_1^N \\
& + \beta_{N+1} \dot{\Delta}_1 (-\delta_1^0 + \delta_1^1) + \beta_{N+2} (\dot{\Delta}_1^1 - \dot{\Delta}_1^2) (\delta_1^1 - \delta_1^2) + \cdots + \beta_{N+i} (\dot{\Delta}_1^{i-1} - \dot{\Delta}_1^i) (\delta_1^{i-1} - \delta_1^i) \\
& + \cdots + \beta_{2N} (\dot{\Delta}_1^{N-1} - \dot{\Delta}_1^N) (\delta_1^{N-1} - \delta_1^N) + \beta_{2N+1} \dot{\Delta}_1^N (\delta_1^N - \delta_1^{N+1}) \\
& - \beta_{2N+2} \dot{\Delta}_1^1 \ddot{\delta}_1^{*1} - \cdots - \beta_{2N+1+i} \dot{\Delta}_1^i \ddot{\delta}_1^{*i} - \cdots - \beta_{3N} \dot{\Delta}_1^{N-1} \ddot{\delta}_1^{*N-1} \\
& - \beta_{3N+1} \dot{\Delta}_1^1 (-\delta_1^{*0} + \delta_1^{*1}) - \beta_{3N+2} (\dot{\Delta}_1^1 - \dot{\Delta}_1^2) (\delta_1^{*1} - \delta_1^{*2}) - \cdots - \beta_{3N+i} (\dot{\Delta}_1^{i-1} - \dot{\Delta}_1^i) (\delta_1^{*i-1} - \delta_1^{*i}) \\
& - \cdots - \beta_{4N} (\dot{\Delta}_1^{N-1} - \dot{\Delta}_1^N) (\delta_1^{*N-1} - \delta_1^{*N}) - \beta_{4N+1} \dot{\Delta}_1^N (\delta_1^{*N} - \delta_1^{*N+1}) \\
& = \dot{\Delta}_1^N \ddot{\delta}_1^{*N}
\end{aligned} \tag{4.91}$$

Writing the Eq. 4.91 at different time point, yields the following groups of equations,

For  $t = t_0$ ,

$$\begin{aligned}
& \beta_1 (\dot{\Delta}_1 \ddot{\delta}_1^1)|_{t_0} + \cdots + \beta_i (\dot{\Delta}_1 \ddot{\delta}_1^i)|_{t_0} + \cdots + \beta_N (\dot{\Delta}_1 \ddot{\delta}_1^N)|_{t_0} + \beta_{N+1} (\dot{\Delta}_1 (-\delta_1^0 + \delta_1^1))|_{t_0} \\
& + \beta_{N+2} ((\dot{\Delta}_1^1 - \dot{\Delta}_1^2) (\delta_1^1 - \delta_1^2))|_{t_0} + \cdots + \beta_{N+i} ((\dot{\Delta}_1^{i-1} - \dot{\Delta}_1^i) (\delta_1^{i-1} - \delta_1^i))|_{t_0} \\
& + \cdots + \beta_{2N} ((\dot{\Delta}_1^{N-1} - \dot{\Delta}_1^N) (\delta_1^{N-1} - \delta_1^N))|_{t_0} + \beta_{2N+1} (\dot{\Delta}_1^N (\delta_1^N - \delta_1^{N+1}))|_{t_0} - \beta_{2N+2} (\dot{\Delta}_1^1 \ddot{\delta}_1^{*1})|_{t_0} \\
& - \cdots - \beta_{2N+1+i} (\dot{\Delta}_1^i \ddot{\delta}_1^{*i})|_{t_0} - \cdots - \beta_{3N} (\dot{\Delta}_1^{N-1} \ddot{\delta}_1^{*N-1})|_{t_0} - \beta_{3N+1} (\dot{\Delta}_1^1 (-\delta_1^{*0} + \delta_1^{*1}))|_{t_0} \\
& - \beta_{3N+2} ((\dot{\Delta}_1^1 - \dot{\Delta}_1^2) (\delta_1^{*1} - \delta_1^{*2}))|_{t_0} - \cdots - \beta_{3N+i} ((\dot{\Delta}_1^{i-1} - \dot{\Delta}_1^i) (\delta_1^{*i-1} - \delta_1^{*i}))|_{t_0} \\
& - \cdots - \beta_{4N} ((\dot{\Delta}_1^{N-1} - \dot{\Delta}_1^N) (\delta_1^{*N-1} - \delta_1^{*N}))|_{t_0} - \beta_{4N+1} (\dot{\Delta}_1^N (\delta_1^{*N} - \delta_1^{*N+1}))|_{t_0} \\
& = (\dot{\Delta}_1^N \ddot{\delta}_1^{*N})|_{t_0}
\end{aligned} \tag{4.92}$$

For  $t = t_j$ ,

$$\begin{aligned}
& \beta_1(\dot{\Delta}_1^1 \ddot{\delta}_1^1)|_{t_j} + \dots + \beta_i(\dot{\Delta}_1^i \ddot{\delta}_1^i)|_{t_j} + \dots + \beta_N(\dot{\Delta}_1^N \ddot{\delta}_1^N)|_{t_j} + \beta_{N+1}(\dot{\Delta}_1^1(-\delta_1^0 + \delta_1^1))|_{t_j} \\
& + \beta_{N+2}((\dot{\Delta}_1^1 - \dot{\Delta}_1^2)(\delta_1^1 - \delta_1^2))|_{t_j} + \dots + \beta_{N+i}((\dot{\Delta}_1^{i-1} - \dot{\Delta}_1^i)(\delta_1^{i-1} - \delta_1^i))|_{t_j} \\
& + \dots + \beta_{2N}((\dot{\Delta}_1^{N-1} - \dot{\Delta}_1^N)(\delta_1^{N-1} - \delta_1^N))|_{t_j} + \beta_{2N+1}(\dot{\Delta}_1^N(\delta_1^N - \delta_1^{N+1}))|_{t_j} - \beta_{2N+2}(\dot{\Delta}_1^1 \ddot{\delta}_1^{*1})|_{t_j} \\
& - \dots - \beta_{2N+1+i}(\dot{\Delta}_1^i \ddot{\delta}_1^{*i})|_{t_j} - \dots - \beta_{3N}(\dot{\Delta}_1^{N-1} \ddot{\delta}_1^{*N-1})|_{t_j} - \beta_{3N+1}(\dot{\Delta}_1^1(-\delta_1^{*0} + \delta_1^{*1}))|_{t_j} \\
& - \beta_{3N+2}((\dot{\Delta}_1^1 - \dot{\Delta}_1^2)(\delta_1^{*1} - \delta_1^{*2}))|_{t_j} - \dots - \beta_{3N+i}((\dot{\Delta}_1^{i-1} - \dot{\Delta}_1^i)(\delta_1^{*i-1} - \delta_1^{*i}))|_{t_j} \\
& - \dots - \beta_{4N}((\dot{\Delta}_1^{N-1} - \dot{\Delta}_1^N)(\delta_1^{*N-1} - \delta_1^{*N}))|_{t_j} - \beta_{4N+1}(\dot{\Delta}_1^N(\delta_1^{*N} - \delta_1^{*N+1}))|_{t_j} \\
& = (\dot{\Delta}_1^N \ddot{\delta}_1^{*N})|_{t_j}
\end{aligned} \tag{4.93}$$

For  $t = t_N$ ,

$$\begin{aligned}
& \beta_1(\dot{\Delta}_1^1 \ddot{\delta}_1^1)|_{t_N} + \dots + \beta_i(\dot{\Delta}_1^i \ddot{\delta}_1^i)|_{t_N} + \dots + \beta_N(\dot{\Delta}_1^N \ddot{\delta}_1^N)|_{t_N} + \beta_{N+1}(\dot{\Delta}_1^1(-\delta_1^0 + \delta_1^1))|_{t_N} \\
& + \beta_{N+2}((\dot{\Delta}_1^1 - \dot{\Delta}_1^2)(\delta_1^1 - \delta_1^2))|_{t_N} + \dots + \beta_{N+i}((\dot{\Delta}_1^{i-1} - \dot{\Delta}_1^i)(\delta_1^{i-1} - \delta_1^i))|_{t_N} \\
& + \dots + \beta_{2N}((\dot{\Delta}_1^{N-1} - \dot{\Delta}_1^N)(\delta_1^{N-1} - \delta_1^N))|_{t_N} + \beta_{2N+1}(\dot{\Delta}_1^N(\delta_1^N - \delta_1^{N+1}))|_{t_N} - \beta_{2N+2}(\dot{\Delta}_1^1 \ddot{\delta}_1^{*1})|_{t_N} \\
& - \dots - \beta_{2N+1+i}(\dot{\Delta}_1^i \ddot{\delta}_1^{*i})|_{t_N} - \dots - \beta_{3N}(\dot{\Delta}_1^{N-1} \ddot{\delta}_1^{*N-1})|_{t_N} - \beta_{3N+1}(\dot{\Delta}_1^1(-\delta_1^{*0} + \delta_1^{*1}))|_{t_N} \\
& - \beta_{3N+2}((\dot{\Delta}_1^1 - \dot{\Delta}_1^2)(\delta_1^{*1} - \delta_1^{*2}))|_{t_N} - \dots - \beta_{3N+i}((\dot{\Delta}_1^{i-1} - \dot{\Delta}_1^i)(\delta_1^{*i-1} - \delta_1^{*i}))|_{t_N} \\
& - \dots - \beta_{4N}((\dot{\Delta}_1^{N-1} - \dot{\Delta}_1^N)(\delta_1^{*N-1} - \delta_1^{*N}))|_{t_N} - \beta_{4N+1}(\dot{\Delta}_1^N(\delta_1^{*N} - \delta_1^{*N+1}))|_{t_N} \\
& = (\dot{\Delta}_1^N \ddot{\delta}_1^{*N})|_{t_N}
\end{aligned} \tag{4.94}$$

Arrange the above Equation group into matrix form, yields,

$$\mathbf{X}\boldsymbol{\beta} = \mathbf{Y} \tag{4.95}$$

Where the coefficient matrix of the linear equation group is given as following (note, due to the limitation of the page size, the transposed form of the matrix is provided),

$$\mathbf{X}^T = \begin{bmatrix}
(\dot{\Delta}_1^1 \ddot{\delta}_1^1)|_{t_0} & \cdots & (\dot{\Delta}_1^1 \ddot{\delta}_1^1)|_{t_j} & \cdots & (\dot{\Delta}_1^1 \ddot{\delta}_1^1)|_{t_N} \\
\vdots & \cdots & \vdots & \cdots & \vdots \\
(\dot{\Delta}_1^i \ddot{\delta}_1^i)|_{t_0} & \cdots & (\dot{\Delta}_1^i \ddot{\delta}_1^i)|_{t_j} & \cdots & (\dot{\Delta}_1^i \ddot{\delta}_1^i)|_{t_N} \\
\vdots & \cdots & \vdots & \cdots & \vdots \\
(\dot{\Delta}_1^N \ddot{\delta}_1^N)|_{t_0} & \cdots & (\dot{\Delta}_1^N \ddot{\delta}_1^N)|_{t_j} & \cdots & (\dot{\Delta}_1^N \ddot{\delta}_1^N)|_{t_N} \\
(\dot{\Delta}_1^1(-\delta_1^0 + \delta_1^1))|_{t_0} & \cdots & (\dot{\Delta}_1^1(-\delta_1^0 + \delta_1^1))|_{t_j} & \cdots & (\dot{\Delta}_1^1(-\delta_1^0 + \delta_1^1))|_{t_N} \\
((\dot{\Delta}_1^1 - \dot{\Delta}_1^2)(\delta_1^1 - \delta_1^2))|_{t_0} & \cdots & ((\dot{\Delta}_1^1 - \dot{\Delta}_1^2)(\delta_1^1 - \delta_1^2))|_{t_j} & \cdots & ((\dot{\Delta}_1^1 - \dot{\Delta}_1^2)(\delta_1^1 - \delta_1^2))|_{t_N} \\
\vdots & \cdots & \vdots & \cdots & \vdots \\
((\dot{\Delta}_1^{i-1} - \dot{\Delta}_1^i)(\delta_1^{i-1} - \delta_1^i))|_{t_0} & \cdots & ((\dot{\Delta}_1^{i-1} - \dot{\Delta}_1^i)(\delta_1^{i-1} - \delta_1^i))|_{t_j} & \cdots & ((\dot{\Delta}_1^{i-1} - \dot{\Delta}_1^i)(\delta_1^{i-1} - \delta_1^i))|_{t_N} \\
\vdots & \cdots & \vdots & \cdots & \vdots \\
((\dot{\Delta}_1^{N-1} - \dot{\Delta}_1^N)(\delta_1^{N-1} - \delta_1^N))|_{t_0} & \cdots & ((\dot{\Delta}_1^{N-1} - \dot{\Delta}_1^N)(\delta_1^{N-1} - \delta_1^N))|_{t_j} & \cdots & ((\dot{\Delta}_1^{N-1} - \dot{\Delta}_1^N)(\delta_1^{N-1} - \delta_1^N))|_{t_N} \\
(\dot{\Delta}_1^N(\delta_1^N - \delta_1^{N+1}))|_{t_0} & \cdots & (\dot{\Delta}_1^N(\delta_1^N - \delta_1^{N+1}))|_{t_j} & \cdots & (\dot{\Delta}_1^N(\delta_1^N - \delta_1^{N+1}))|_{t_N} \\
-(\dot{\Delta}_1^1 \ddot{\delta}_1^{*1})|_{t_0} & \cdots & -(\dot{\Delta}_1^1 \ddot{\delta}_1^{*1})|_{t_j} & \cdots & -(\dot{\Delta}_1^1 \ddot{\delta}_1^{*1})|_{t_N} \\
\vdots & \cdots & \vdots & \cdots & \vdots \\
-(\dot{\Delta}_1^i \ddot{\delta}_1^{*i})|_{t_0} & \cdots & -(\dot{\Delta}_1^i \ddot{\delta}_1^{*i})|_{t_j} & \cdots & -(\dot{\Delta}_1^i \ddot{\delta}_1^{*i})|_{t_N} \\
\vdots & \cdots & \vdots & \cdots & \vdots \\
-(\dot{\Delta}_1^{N-1} \ddot{\delta}_1^{*N-1})|_{t_0} & \cdots & -(\dot{\Delta}_1^{N-1} \ddot{\delta}_1^{*N-1})|_{t_j} & \cdots & -(\dot{\Delta}_1^{N-1} \ddot{\delta}_1^{*N-1})|_{t_N} \\
-(\dot{\Delta}_1^1(-\delta_1^{*0} + \delta_1^{*1}))|_{t_0} & \cdots & -(\dot{\Delta}_1^1(-\delta_1^{*0} + \delta_1^{*1}))|_{t_j} & \cdots & -(\dot{\Delta}_1^1(-\delta_1^{*0} + \delta_1^{*1}))|_{t_N} \\
-((\dot{\Delta}_1^1 - \dot{\Delta}_1^2)(\delta_1^{*1} - \delta_1^{*2}))|_{t_0} & \cdots & -((\dot{\Delta}_1^1 - \dot{\Delta}_1^2)(\delta_1^{*1} - \delta_1^{*2}))|_{t_j} & \cdots & -((\dot{\Delta}_1^1 - \dot{\Delta}_1^2)(\delta_1^{*1} - \delta_1^{*2}))|_{t_N} \\
\vdots & \cdots & \vdots & \cdots & \vdots \\
-((\dot{\Delta}_1^{i-1} - \dot{\Delta}_1^i)(\delta_1^{*i-1} - \delta_1^{*i}))|_{t_0} & \cdots & -((\dot{\Delta}_1^{i-1} - \dot{\Delta}_1^i)(\delta_1^{*i-1} - \delta_1^{*i}))|_{t_j} & \cdots & -((\dot{\Delta}_1^{i-1} - \dot{\Delta}_1^i)(\delta_1^{*i-1} - \delta_1^{*i}))|_{t_N} \\
\vdots & \cdots & \vdots & \cdots & \vdots \\
-((\dot{\Delta}_1^{N-1} - \dot{\Delta}_1^N)(\delta_1^{*N-1} - \delta_1^{*N}))|_{t_0} & \cdots & -((\dot{\Delta}_1^{N-1} - \dot{\Delta}_1^N)(\delta_1^{*N-1} - \delta_1^{*N}))|_{t_j} & \cdots & -((\dot{\Delta}_1^{N-1} - \dot{\Delta}_1^N)(\delta_1^{*N-1} - \delta_1^{*N}))|_{t_N} \\
-(\dot{\Delta}_1^N(\delta_1^{*N} - \delta_1^{*N+1}))|_{t_0} & \cdots & -(\dot{\Delta}_1^N(\delta_1^{*N} - \delta_1^{*N+1}))|_{t_j} & \cdots & -(\dot{\Delta}_1^N(\delta_1^{*N} - \delta_1^{*N+1}))|_{t_N}
\end{bmatrix} \quad (4.96)$$

The vector of unknown and the vector of known are given as,

$$\boldsymbol{\beta} = \begin{Bmatrix} \beta_1 \\ \vdots \\ \beta_i \\ \vdots \\ \beta_N \\ \beta_{N+1} \\ \vdots \\ \beta_{N+i} \\ \vdots \\ \beta_{2N+1} \\ \beta_{2N+2} \\ \vdots \\ \beta_{2N+1+i} \\ \vdots \\ \beta_{3N} \\ \beta_{3N+1} \\ \vdots \\ \beta_{4N+1} \end{Bmatrix} \quad (4.97)$$

$$\mathbf{Y} = \begin{Bmatrix} (\dot{\Delta}_1^N \ddot{\delta}_1^{*N})|_{t_0} \\ \vdots \\ (\dot{\Delta}_1^N \ddot{\delta}_1^{*N})|_{t_j} \\ \vdots \\ (\dot{\Delta}_1^N \ddot{\delta}_1^{*N})|_{t_N} \end{Bmatrix} \quad (4.98)$$

Based on the Least Square Method, the  $\boldsymbol{\beta}$  can be computed from the following equation,

$$\boldsymbol{\beta} = (\mathbf{X}^T \mathbf{X})^{-1} (\mathbf{X}^T \mathbf{Y}) \quad (4.99)$$

Then the damage indices for stiffness, mass and damping can be computed as follows,

$$\beta_{m^1} = \frac{\left(\frac{\bar{m}_1 L_1}{2} + \frac{\bar{m}_2 L_2}{2}\right)}{\left(\frac{\bar{m}_1^* L_1}{2} + \frac{\bar{m}_2^* L_2}{2}\right)} = \frac{m^1}{m^{*1}} = \frac{\frac{m^1}{m^{*N}}}{\frac{m^{*1}}{m^{*N}}} = \frac{\beta_1}{\beta_{2N+2}} \quad (4.100)$$

...

$$\beta_{m^i} = \frac{\left(\frac{\bar{m}_i L_i}{2} + \frac{\bar{m}_{i+1} L_{i+1}}{2}\right)}{\left(\frac{\bar{m}_i^* L_i}{2} + \frac{\bar{m}_{i+1}^* L_{i+1}}{2}\right)} = \frac{m^i}{m^{*i}} = \frac{\frac{m^i}{m^{*N}}}{\frac{m^{*i}}{m^{*N}}} = \frac{\beta_i}{\beta_{2N+1+i}} \quad (4.101)$$

...

$$\beta_{m^{N-1}} = \frac{\left(\frac{\bar{m}_{N-1} L_{N-1}}{2} + \frac{\bar{m}_N L_N}{2}\right)}{\left(\frac{\bar{m}_{N-1}^* L_{N-1}}{2} + \frac{\bar{m}_N^* L_N}{2}\right)} = \frac{m^{N-1}}{m^{*N-1}} = \frac{\frac{m^{N-1}}{m^{*N}}}{\frac{m^{*N-1}}{m^{*N}}} = \frac{\beta_{N-1}}{\beta_{3N}} \quad (4.102)$$

$$\beta_{m^N} = \frac{\left(\frac{\bar{m}_N L_N}{2} + \frac{\bar{m}_{N+1} L_{N+1}}{2}\right)}{\left(\frac{\bar{m}_N^* L_N}{2} + \frac{\bar{m}_{N+1}^* L_{N+1}}{2}\right)} = \frac{m^N}{m^{*N}} = \beta_N \quad (4.103)$$

...

$$\beta_{k_1} = \frac{\left(\frac{EA}{L}\right)_1}{\left(\frac{EA}{L}\right)^*_1} = \frac{k_1}{k_1^*} = \frac{\frac{k_1}{m^{*N}}}{\frac{k_1^*}{m^{*N}}} = \frac{\beta_{N+1}}{\beta_{3N+1}} \quad (4.104)$$

...

$$\beta_{k_i} = \frac{\left(\frac{EA}{L}\right)_i}{\left(\frac{EA}{L}\right)^*_i} = \frac{k_i}{k_i^*} = \frac{\frac{k_i}{m^{*N}}}{\frac{k_i^*}{m^{*N}}} = \frac{\beta_{N+i}}{\beta_{3N+i}} \quad (4.105)$$

...

$$\beta_{k_{N+1}} = \frac{\left(\frac{EA}{L}\right)_{N+1}}{\left(\frac{EA}{L}\right)^*_{N+1}} = \frac{k_{N+1}}{k^*_{N+1}} = \frac{\frac{k_{N+1}}{m^{*N}}}{\frac{k^*_{N+1}}{m^{*N}}} = \frac{\beta_{2N+1}}{\beta_{4N+1}} \quad (4.106)$$

### 4.3 THEORY FOR EULER-BERNOULLI BEAMS

In this subsection, the proposed non-destructive evaluation theory will be applied to the bending vibration of Euler-Bernoulli beam.

According to the finite element method, one beam can be meshed into several elements. Isolating two nearby beam elements, as shown in Figure 4.5, the modulus of elasticity of the material for Element  $i$  is denoted as  $E_i$ . The length of Element  $i$  is  $L_i$ . The area and the moment of inertia of the cross section of Element  $i$  are denoted as  $A_i$  and  $I_i$ , respectively. Let  $\{P^i\}$  be the force vector at Node  $i$ , where  $P_2^i$  denotes the shear force at Node  $i$ ,  $P_3^i$  denotes the bending moment at Node  $i$ . As shown in the free body diagram of Node  $i$  in Figure 4.6, the external loads ( $\{P^i\}$ ), internal forces ( $\{F_i\}$  and  $\{F_{i+1}\}$ ) and inertial forces  $\{I^i\}$  form a dynamic equilibrium condition for Node  $i$ . The dynamic equilibrium condition can be written as,

$$\{I^i\} + \{F_i\} + \{F_{i+1}\} = \{P^i\} \quad (4.107)$$

The beam element will only consider shear and moment in two directions. Each force vector in Eq. 4.107 is composed by two force components: (1) shear force, (2) bending moment. Namely, Eq. 4.107 can be developed into,

$$\begin{Bmatrix} I_2^i \\ I_3^i \end{Bmatrix} + \begin{Bmatrix} F_{i,2} \\ F_{i,3} \end{Bmatrix} + \begin{Bmatrix} F_{i+1,2} \\ F_{i+1,3} \end{Bmatrix} = \begin{Bmatrix} P_2^i \\ P_3^i \end{Bmatrix} \quad (4.108)$$

Where subscript two (“2”) indicates shear force and subscript three (“3”) indicates bending moment.

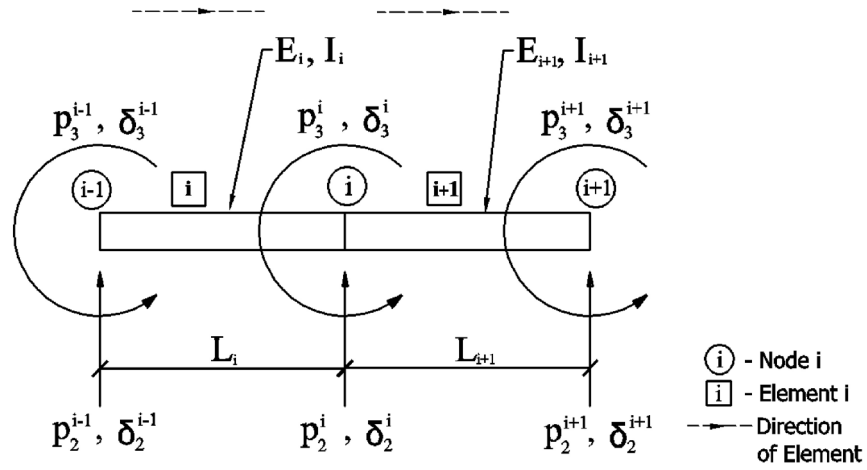


**Figure 4.5. Two nearby Euler-Bernoulli Beam Elements Considering Shear Force and Bending Moment**

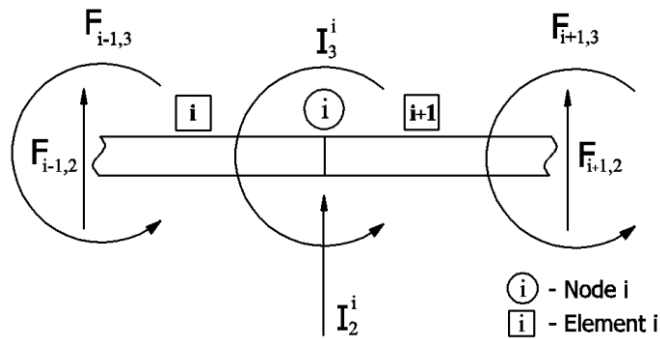


**Figure 4.6. Free Body Diagram of Node i Considering Shear Force and Bending Moment**

Similarly, for the damaged case, the dynamic equilibrium condition is,

$$\{I^{*i}\} + \{F_i^*\} + \{F_{i+1}^*\} = \{P^{*i}\} \quad (4.109)$$

Where the asterisk (“\*”) denotes the quantities from the damaged case.

Given any velocity vectors,  $\{\dot{\Delta}^i\}$  and  $\{\dot{\Delta}^{*i}\}$ , for the undamaged and damaged systems.

The power done by the external forces in the undamaged and damaged systems can be expressed as follows,

$$\{\dot{\Delta}^i\}^T \{I^i\} + \{\dot{\Delta}^i\}^T \{F_i\} + \{\dot{\Delta}^i\}^T \{F_{i+1}\} = \{\dot{\Delta}^i\}^T \{P^i\} \quad (4.110)$$

$$\{\dot{\Delta}^{*i}\}^T \{I^{*i}\} + \{\dot{\Delta}^{*i}\}^T \{F_i^*\} + \{\dot{\Delta}^{*i}\}^T \{F_{i+1}^*\} = \{\dot{\Delta}^{*i}\}^T \{P^{*i}\} \quad (4.111)$$

Assume that the applied external loads and velocities used to compute power at Node  $i$  are the same for both the undamaged and damaged systems,

$$\{\dot{\Delta}^i\} = \{\dot{\Delta}^{*i}\} \quad (4.112)$$

$$\{P^i\} = \{P^{*i}\} \quad (4.113)$$

Substituting Eq. 4.112 and Eq. 4.113 into Eq. 4.111 yields,

$$\{\dot{\Delta}^i\}^T \{I^{*i}\} + \{\dot{\Delta}^i\}^T \{F_i^*\} + \{\dot{\Delta}^i\}^T \{F_{i+1}^*\} = \{\dot{\Delta}^i\}^T \{P^i\} \quad (4.114)$$

Noticing the power done by the external load are the same for both the undamaged and damaged system. Substituting Eq. 4.114 into Eq. 4.110 yields,



$$\{\dot{\Delta}^i\}^T \{I^i\} + \{\dot{\Delta}^i\}^T \{F_i\} + \{\dot{\Delta}^i\}^T \{F_{i+1}\} = \{\dot{\Delta}^i\}^T \{I^{*i}\} + \{\dot{\Delta}^i\}^T \{F_i^*\} + \{\dot{\Delta}^i\}^T \{F_{i+1}^*\} \quad (4.115)$$

Note, Eq. 4.115 is equivalent to Eq. 2.10.

The inertia force vectors in this case can be written as following, (note that the inertial effect associated with any rotational degree of freedom is neglected)

$$\{I^i\} = \left[ \left( \frac{\bar{m}_i L_i}{2} \right) + \left( \frac{\bar{m}_{i+1} L_{i+1}}{2} \right) \right] \begin{bmatrix} 1 & 0 \\ 0 & 0 \end{bmatrix} \begin{Bmatrix} \ddot{\delta}_2^i \\ \ddot{\delta}_3^i \end{Bmatrix} = m^i [M_o^i] \{\ddot{\delta}^i\} \quad (4.116)$$

Where  $\bar{m}_i$  is the linear mass of Element  $i$ ;  $\ddot{\delta}_2^i$  is the acceleration in transverse direction at Node  $i$  and  $\ddot{\delta}_3^i$  is acceleration in bending rotation direction at Node  $i$  within the plain.  $m^i$  is the lumped mass at Node  $i$ ;  $[M_o^i]$  is the configuration matrix for the nodal mass.

Similarly, for the damaged system, the inertia force vector can be computed as,

$$\{I^{*i}\} = \left[ \left( \frac{\bar{m}_i^* L_i^*}{2} \right) + \left( \frac{\bar{m}_{i+1}^* L_{i+1}^*}{2} \right) \right] \begin{bmatrix} 1 & 0 \\ 0 & 0 \end{bmatrix} \begin{Bmatrix} \ddot{\delta}_2^{*i} \\ \ddot{\delta}_3^{*i} \end{Bmatrix} = m^{*i} [M_o^{*i}] \{\ddot{\delta}^{*i}\} \quad (4.117)$$

According to the finite element method, the force vectors (i.e.  $\{F_i\}$ ,  $\{F_{i+1}\}$ ,  $\{F_i^*\}$ , and  $\{F_{i+1}^*\}$ ) in Eq. 4.115 can be computed using stiffness matrices and nodal deformation vectors,

$$\{F_i\} = \left(\frac{EI}{L^3}\right)_i \begin{bmatrix} -12 & -6L & 12 & -6L \\ 6L & 2L^2 & -6L & 4L^2 \end{bmatrix}_i \begin{Bmatrix} \delta_2^{i-1} \\ \delta_3^{i-1} \\ \delta_2^i \\ \delta_3^i \end{Bmatrix} = k_i [K_{o,i}] \{\delta_i\} \quad (4.118)$$

$$\{F_{i+1}\} = \left(\frac{EI}{L^3}\right)_{i+1} \begin{bmatrix} 12 & 6L & -12 & 6L \\ 6L & 4L^2 & -6L & 2L^2 \end{bmatrix}_{i+1} \begin{Bmatrix} \delta_2^i \\ \delta_3^i \\ \delta_2^{i+1} \\ \delta_3^{i+1} \end{Bmatrix} = k_{i+1} [K_{o,i+1}] \{\delta_{i+1}\} \quad (4.119)$$

Similarly, for the damaged case,

$$\{F_i^*\} = \left(\frac{EI}{L^3}\right)_i^* \begin{bmatrix} -12 & -6L & 12 & -6L \\ 6L & 2L^2 & -6L & 4L^2 \end{bmatrix}_i^* \begin{Bmatrix} \delta_2^{*i-1} \\ \delta_3^{*i-1} \\ \delta_2^{*i} \\ \delta_3^{*i} \end{Bmatrix} = k_i^* [K_{o,i}^*] \{\delta_i^*\} \quad (4.119)$$

$$\{F_{i+1}^*\} = \left(\frac{EI}{L^3}\right)_{i+1}^* \begin{bmatrix} 12 & 6L & -12 & 6L \\ 6L & 4L^2 & -6L & 2L^2 \end{bmatrix}_{i+1}^* \begin{Bmatrix} \delta_2^{*i} \\ \delta_3^{*i} \\ \delta_2^{*i+1} \\ \delta_3^{*i+1} \end{Bmatrix} = k_{i+1}^* [K_{o,i+1}^*] \{\delta_{i+1}^*\} \quad (4.120)$$

Where  $\delta_2^i$  is the displacement in vertical direction at Node  $i$ ;  $\delta_3^i$  is the nodal rotation within the plain at Node  $i$ .

Substitute Eqs. 4.116 through 4.120 into Eq. 4.115 yields,

$$\begin{aligned} & \{\dot{\Delta}^i\}^T m^i [M_o^i] \{\ddot{\delta}^i\} + \{\dot{\Delta}^i\}^T k_i [K_{o,i}] \{\delta_i\} + \{\dot{\Delta}^i\}^T k_{i+1} [K_{o,i+1}] \{\delta_{i+1}\} \\ & = \{\dot{\Delta}^i\}^T m^{*i} [M_o^{*i}] \{\ddot{\delta}^{*i}\} + \{\dot{\Delta}^i\}^T k_i^* [K_{o,i}^*] \{\delta_i^*\} + \{\dot{\Delta}^i\}^T k_{i+1}^* [K_{o,i+1}^*] \{\delta_{i+1}^*\} \end{aligned} \quad (4.121)$$

Note the force vectors (i.e.  $\{I^i\}$ ,  $\{F_i\}$ ,  $\{F_{i+1}\}$ ,  $\{I^{*i}\}$ ,  $\{F_i^*\}$  and  $\{F_{i+1}^*\}$ ) can be

summarized as the multiplication of a property coefficient, a configuration matrix and a node displacement vector. Because the designed damage are simulated by the changes of Young's modulus (  $E$  ) and linear mass (  $\bar{m}$  ), the length of element (  $L$  ) is not influenced by damage and remain the same for the undamaged and damaged elements. Consequently, the configuration matrices for the element stiffness and element mass are the same for both the damaged and undamaged elements. Namely,

$$[K_{o,i}^*] = [K_{o,i}] \quad (4.122)$$

$$[K_{o,i+1}^*] = [K_{o,i+1}] \quad (4.123)$$

$$[M_o^{*i}] = [M_o^i] \quad (4.124)$$

Substituting Eqs. 4.122 through 4.124 into Eq. 4.121 yields,

$$\begin{aligned} & \{\dot{\Delta}^i\}^T m^i [M_o^i] \{\ddot{\delta}^i\} + \{\dot{\Delta}^i\}^T k_i [K_{o,i}] \{\delta_i\} + \{\dot{\Delta}^i\}^T k_{i+1} [K_{o,i+1}] \{\delta_{i+1}\} \\ &= \{\dot{\Delta}^i\}^T m^{*i} [M_o^i] \{\ddot{\delta}^{*i}\} + \{\dot{\Delta}^i\}^T k_i^* [K_{o,i}] \{\delta_i^*\} + \{\dot{\Delta}^i\}^T k_{i+1}^* [K_{o,i+1}] \{\delta_{i+1}^*\} \end{aligned} \quad (4.125)$$

Moving forward the property constant from each term in Eq. 16 yields,

$$\begin{aligned} & m^i \{\dot{\Delta}^i\}^T [M_o^i] \{\ddot{\delta}^i\} + k_i \{\dot{\Delta}^i\}^T [K_{o,i}] \{\delta_i\} + k_{i+1} \{\dot{\Delta}^i\}^T [K_{o,i+1}] \{\delta_{i+1}\} \\ & - k_i^* \{\dot{\Delta}^i\}^T [K_{o,i}] \{\delta_i^*\} - k_{i+1}^* \{\dot{\Delta}^i\}^T [K_{o,i+1}] \{\delta_{i+1}^*\} = m^{*i} \{\dot{\Delta}^i\}^T [M_o^i] \{\ddot{\delta}^{*i}\} \end{aligned} \quad (4.126)$$

Dividing Eq. 4.126 by  $m^{*i}$  yields,

$$\begin{aligned} & \frac{m^i}{m^{*i}} \{\dot{\Delta}^i\}^T [M_o^i] \{\ddot{\delta}^i\} + \frac{k_i}{m^{*i}} \{\dot{\Delta}^i\}^T [K_{o,i}] \{\delta_i\} + \frac{k_{i+1}}{m^{*i}} \{\dot{\Delta}^i\}^T [K_{o,i+1}] \{\delta_{i+1}\} \\ & - \frac{k_i^*}{m^{*i}} \{\dot{\Delta}^i\}^T [K_{o,i}] \{\delta_i^*\} - \frac{k_{i+1}^*}{m^{*i}} \{\dot{\Delta}^i\}^T [K_{o,i+1}] \{\delta_{i+1}^*\} = \{\dot{\Delta}^i\}^T [M_o^i] \{\ddot{\delta}^{*i}\} \end{aligned} \quad (4.127)$$

Define the following coefficients,

$$\beta_1 = \frac{m^i}{m^{*i}} \quad (4.128)$$

$$\beta_2 = \frac{k_i}{m^{*i}} \quad (4.129)$$

$$\beta_3 = \frac{k_{i+1}}{m^{*i}} \quad (4.130)$$

$$\beta_4 = \frac{k_i^*}{m^{*i}} \quad (4.131)$$

$$\beta_5 = \frac{k_{i+1}^*}{m^{*i}} \quad (4.132)$$

Substituting Eq. 4.128 through Eq. 4.132 into Eq. 4.127 yields,

$$\begin{aligned} & \beta_1 \{\dot{\Delta}^i\}^T [M_o^i] \{\ddot{\delta}^i\} + \beta_2 \{\dot{\Delta}^i\}^T [K_{o,i}] \{\delta_i\} + \beta_3 \{\dot{\Delta}^i\}^T [K_{o,i+1}] \{\delta_{i+1}\} \\ & - \beta_4 \{\dot{\Delta}^i\}^T [K_{o,i}] \{\delta_i^*\} - \beta_5 \{\dot{\Delta}^i\}^T [K_{o,i+1}] \{\delta_{i+1}^*\} = \{\dot{\Delta}^i\}^T [M_o^i] \{\ddot{\delta}^{*i}\} \end{aligned} \quad (4.133)$$

Writing the Eq. 4.133 at different time point, yields the following groups of equations,

For  $t = t_0$ ,

$$\begin{aligned} & \beta_1 (\{\dot{\Delta}^i\}^T [M_o^i] \{\ddot{\delta}^i\})|_{t_0} + \beta_2 (\{\dot{\Delta}^i\}^T [K_{o,i}] \{\delta_i\})|_{t_0} + \beta_3 (\{\dot{\Delta}^i\}^T [K_{o,i+1}] \{\delta_{i+1}\})|_{t_0} \\ & - \beta_4 (\{\dot{\Delta}^i\}^T [K_{o,i}] \{\delta_i^*\})|_{t_0} - \beta_5 (\{\dot{\Delta}^i\}^T [K_{o,i+1}] \{\delta_{i+1}^*\})|_{t_0} = (\{\dot{\Delta}^i\}^T [M_o^i] \{\ddot{\delta}^{*i}\})|_{t_0} \end{aligned} \quad (4.134)$$

For  $t = t_j$ ,

$$\begin{aligned} & \beta_1 (\{\dot{\Delta}^i\}^T [M_o^i] \{\ddot{\delta}^i\})|_{t_j} + \beta_2 (\{\dot{\Delta}^i\}^T [K_{o,i}] \{\delta_i\})|_{t_j} + \beta_3 (\{\dot{\Delta}^i\}^T [K_{o,i+1}] \{\delta_{i+1}\})|_{t_j} \\ & - \beta_4 (\{\dot{\Delta}^i\}^T [K_{o,i}] \{\delta_i^*\})|_{t_j} - \beta_5 (\{\dot{\Delta}^i\}^T [K_{o,i+1}] \{\delta_{i+1}^*\})|_{t_j} = (\{\dot{\Delta}^i\}^T [M_o^i] \{\ddot{\delta}^{*i}\})|_{t_j} \end{aligned} \quad (4.135)$$

For  $t = t_N$ ,

$$\begin{aligned} & \beta_1(\{\dot{\Delta}^i\}^T[M_o^i]\{\ddot{\delta}^i\})|_{t_N} + \beta_2(\{\dot{\Delta}^i\}^T[K_{o,i}]\{\delta_i\})|_{t_N} + \beta_3(\{\dot{\Delta}^i\}^T[K_{o,i+1}]\{\delta_{i+1}\})|_{t_N} \\ & - \beta_4(\{\dot{\Delta}^i\}^T[K_{o,i}]\{\delta_i^*\})|_{t_N} - \beta_5(\{\dot{\Delta}^i\}^T[K_{o,i+1}]\{\delta_{i+1}^*\})|_{t_N} = (\{\dot{\Delta}^i\}^T[M_o^i]\{\ddot{\delta}^i\})|_{t_N} \end{aligned} \quad (4.136)$$

Arranging the above linear equation group into matrix form, yields,

$$\mathbf{X}\boldsymbol{\beta} = \mathbf{Y} \quad (4.137)$$

Where the coefficient matrix of the linear equation group is given as following (note, due to the limitation of the page size, the transposed form of the matrix is provided),

$$\begin{aligned} \mathbf{X}^T = & \begin{bmatrix} (\{\dot{\Delta}^i\}^T[M_o^i]\{\ddot{\delta}^i\})|_{t_0} & \dots & (\{\dot{\Delta}^i\}^T[M_o^i]\{\ddot{\delta}^i\})|_{t_j} & \dots & (\{\dot{\Delta}^i\}^T[M_o^i]\{\ddot{\delta}^i\})|_{t_N} \\ (\{\dot{\Delta}^i\}^T[K_{o,i}]\{\delta_i\})|_{t_0} & \dots & (\{\dot{\Delta}^i\}^T[K_{o,i}]\{\delta_i\})|_{t_j} & \dots & (\{\dot{\Delta}^i\}^T[K_{o,i}]\{\delta_i\})|_{t_N} \\ (\{\dot{\Delta}^i\}^T[K_{o,i+1}]\{\delta_{i+1}\})|_{t_0} & \dots & (\{\dot{\Delta}^i\}^T[K_{o,i+1}]\{\delta_{i+1}\})|_{t_j} & \dots & (\{\dot{\Delta}^i\}^T[K_{o,i+1}]\{\delta_{i+1}\})|_{t_N} \\ -(\{\dot{\Delta}^i\}^T[K_{o,i}]\{\delta_i^*\})|_{t_0} & \dots & -(\{\dot{\Delta}^i\}^T[K_{o,i}]\{\delta_i^*\})|_{t_j} & \dots & -(\{\dot{\Delta}^i\}^T[K_{o,i}]\{\delta_i^*\})|_{t_N} \\ -(\{\dot{\Delta}^i\}^T[K_{o,i+1}]\{\delta_{i+1}^*\})|_{t_0} & \dots & -(\{\dot{\Delta}^i\}^T[K_{o,i+1}]\{\delta_{i+1}^*\})|_{t_j} & \dots & -(\{\dot{\Delta}^i\}^T[K_{o,i+1}]\{\delta_{i+1}^*\})|_{t_N} \end{bmatrix} \end{aligned} \quad (4.138)$$

The vector of unknown and the vector of known are given as,

$$\boldsymbol{\beta} = \begin{Bmatrix} \beta_1 \\ \beta_2 \\ \beta_3 \\ \beta_4 \\ \beta_5 \end{Bmatrix} \quad (4.139)$$

$$\mathbf{Y} = \begin{Bmatrix} (\{\dot{\Delta}^i\}^T [M_o^i] \{\ddot{\delta}^{*i}\})|_{t_0} \\ \vdots \\ (\{\dot{\Delta}^i\}^T [M_o^i] \{\ddot{\delta}^{*i}\})|_{t_j} \\ \vdots \\ (\{\dot{\Delta}^i\}^T [M_o^i] \{\ddot{\delta}^{*i}\})|_{t_N} \end{Bmatrix} \quad (4.140)$$

Using the Least Square Method, the vector of unknown, ‘ $\boldsymbol{\beta}$ ’, can be computed from the following equation,

$$\boldsymbol{\beta} = (\mathbf{X}^T \mathbf{X})^{-1} (\mathbf{X}^T \mathbf{Y}) \quad (4.141)$$

With the vector of unknown computed, the damage indices for stiffness, mass, and damping can be computed as follows,

$$\beta_{m^i} = \frac{m^i}{m^{*i}} = \frac{\left( \frac{\bar{m}_i L_i}{2} + \frac{\bar{m}_{i+1} L_{i+1}}{2} \right)}{\left( \frac{\bar{m}_i^* L_i}{2} + \frac{\bar{m}_{i+1}^* L_{i+1}}{2} \right)} = \beta_1 \quad (4.142)$$

$$\beta_{k_i} = \frac{\frac{k_i}{m^{*i}}}{\frac{k_i^*}{m^{*i}}} = \frac{k_i}{k_i^*} = \frac{\left( \frac{EI}{L^3} \right)_i}{\left( \frac{EI}{L^3} \right)^*} = \frac{\beta_2}{\beta_4} \quad (4.143)$$

$$\beta_{k_{i+1}} = \frac{\frac{k_{i+1}}{m^{*i}}}{\frac{k_{i+1}^*}{m^{*i}}} = \frac{k_{i+1}}{k_{i+1}^*} = \frac{\left( \frac{EI}{L^3} \right)_{i+1}}{\left( \frac{EI}{L^3} \right)^*} = \frac{\beta_3}{\beta_5} \quad (4.144)$$

Note, because the proposed damage detection algorithm used no information on the

boundary conditions of the beam, the damage detection algorithm can be applied to beams with any support conditions.

#### 4.4 THEORY FOR PLANE FRAMES

In this subsection, the proposed non-destructive evaluation theory will be applied to the axial and bending vibration of plane frame.

According to the finite element method, one frame structure can be meshed into several elements. Isolating two nearby plain frame elements, as shown in Figure 4.7, the modulus of elasticity of the material for Element  $i$  is denoted as  $E_i$ . The length of Element  $i$  is  $L_i$ . The area and the moment of inertia of the cross section of Element  $i$  are denoted as  $A_i$  and  $I_i$ , respectively. Let  $\{P^i\}$  be the force vector at Node  $i$ , in which  $P_1^i$  denotes the axial force at Node  $i$ ,  $P_2^i$  denotes the shear force at Node  $i$ ,  $P_3^i$  denotes the nodal moment at Node  $i$ . As shown in the free body diagram of Node  $i$  in Figure 4.8, the external loads ( $\{P^i\}$ ), internal forces ( $\{F_i\}$  and  $\{F_{i+1}\}$ ) and inertial forces  $\{I^i\}$  form a dynamic equilibrium condition for Node  $i$ . The dynamic equilibrium condition can be written as,

$$\{I^i\} + \{F_i\} + \{F_{i+1}\} = \{P^i\} \quad (4.145)$$

In this case, degrees of freedom in axial, transversal, and rotational directions will be taken into consideration. Thus each force vector in Eq. 4.145 is composed by three force components: (1) Axial force; (2) shear force; (3) bending moment.

$$\begin{Bmatrix} I_1^i \\ I_2^i \\ I_3^i \end{Bmatrix} + \begin{Bmatrix} F_{i,1} \\ F_{i,2} \\ F_{i,3} \end{Bmatrix} + \begin{Bmatrix} F_{i+1,1} \\ F_{i+1,2} \\ F_{i+1,3} \end{Bmatrix} = \begin{Bmatrix} P_1^i \\ P_2^i \\ P_3^i \end{Bmatrix} \quad (4.146)$$

Where subscript one (“1”) indicates axial force, subscript two (“2”) indicates shear force and subscript three (“3”) indicates bending moment.

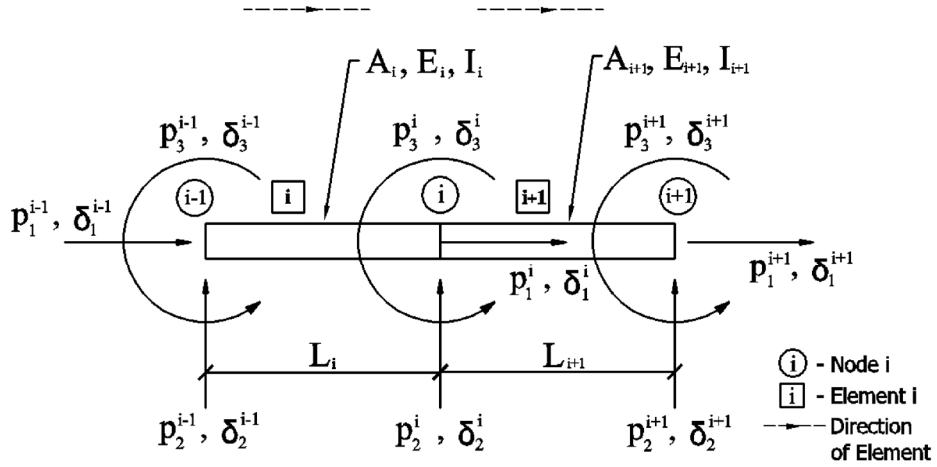


Figure 4.7. Two nearby Plane Frame Elements

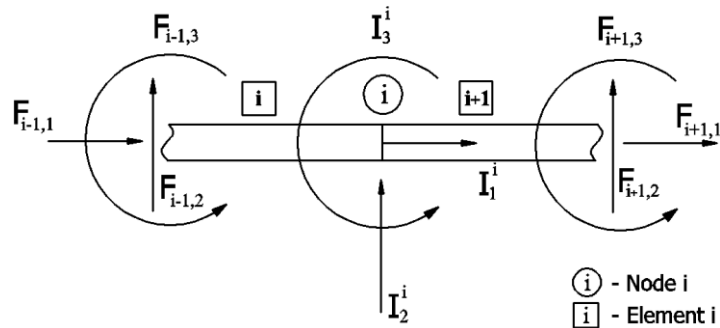


Figure 4.8. Free Body Diagram of Node i Considering Axial, Shear Forces, and Bending Moment



Similarly, for the damaged case, the dynamic equilibrium condition is,

$$\{I^{*i}\} + \{F_i^*\} + \{F_{i+1}^*\} = \{P^{*i}\} \quad (4.147)$$

Where the asterisk (“\*”) denotes the quantities from the damaged case.

Given any velocity vectors,  $\{\dot{\Delta}^i\}$  and  $\{\dot{\Delta}^{*i}\}$ , for the undamaged and damaged systems, the power performed by the external forces in the undamaged and damaged systems can be expressed as follows,

$$\{\dot{\Delta}^i\}^T \{I^i\} + \{\dot{\Delta}^i\}^T \{F_i\} + \{\dot{\Delta}^i\}^T \{F_{i+1}\} = \{\dot{\Delta}^i\}^T \{P^i\} \quad (4.148)$$

$$\{\dot{\Delta}^{*i}\}^T \{I^{*i}\} + \{\dot{\Delta}^{*i}\}^T \{F_i^*\} + \{\dot{\Delta}^{*i}\}^T \{F_{i+1}^*\} = \{\dot{\Delta}^{*i}\}^T \{P^{*i}\} \quad (4.149)$$

Assume that the applied external loads and velocities used to compute power at Node  $i$  are the same for both the undamaged and damaged systems,

$$\{\dot{\Delta}^i\} = \{\dot{\Delta}^{*i}\} \quad (4.150)$$

$$\{P^i\} = \{P^{*i}\} \quad (4.151)$$

Substituting Eq. 4.150 and Eq. 4.151 into Eq. 4.149 yields,

$$\{\dot{\Delta}^i\}^T \{I^{*i}\} + \{\dot{\Delta}^i\}^T \{F_i^*\} + \{\dot{\Delta}^i\}^T \{F_{i+1}^*\} = \{\dot{\Delta}^i\}^T \{P^i\} \quad (4.152)$$

Noticing the power performed by the external load is the same for both the undamaged and damaged system. Substituting Eq. 4.152 into Eq. 4.148 yields,

$$\{\dot{\Delta}^i\}^T \{I^i\} + \{\dot{\Delta}^i\}^T \{F_i\} + \{\dot{\Delta}^i\}^T \{F_{i+1}\} = \{\dot{\Delta}^i\}^T \{I^{*i}\} + \{\dot{\Delta}^i\}^T \{F_i^*\} + \{\dot{\Delta}^i\}^T \{F_{i+1}^*\} \quad (4.153)$$

Note, Eq. 153 is equivalent to Eq. 10.

In this case, the inertial forces for the undamaged system can be expressed using the following lumped mass matrix. Note that the inertial effect associated with any rotational degree of freedom is neglected.

$$\{I^i\} = \left[ \left( \frac{\bar{m}_i L_i}{2} \right) + \left( \frac{\bar{m}_{i+1} L_{i+1}}{2} \right) \right] \begin{bmatrix} 1 & & \\ & 1 & \\ & & 0 \end{bmatrix}_i \begin{Bmatrix} \ddot{\delta}_1^i \\ \ddot{\delta}_2^i \\ \ddot{\delta}_3^i \end{Bmatrix} = m^i [M_o^i] \{\ddot{\delta}^i\} \quad (4.154)$$

where  $\bar{m}_i$  is the linear mass of Element  $i$ ;  $\ddot{\delta}_1^i$  is the acceleration in axial direction at Node  $i$ ;  $\ddot{\delta}_2^i$  is the acceleration in transverse direction at Node  $i$  and  $\ddot{\delta}_3^i$  is the rotational acceleration in bending direction within the plain at Node  $i$ .

Similarly, for the damaged system,

$$\{I^{*i}\} = \left[ \left( \frac{\bar{m}_i^* L_i^*}{2} \right) + \left( \frac{\bar{m}_{i+1}^* L_{i+1}^*}{2} \right) \right] \begin{bmatrix} 1 & & \\ & 1 & \\ & & 0 \end{bmatrix}_i \begin{Bmatrix} \ddot{\delta}_1^{*i} \\ \ddot{\delta}_2^{*i} \\ \ddot{\delta}_3^{*i} \end{Bmatrix} = m^{*i} [M_o^{*i}] \{\ddot{\delta}^{*i}\} \quad (4.155)$$

The force vectors (i.e.  $\{F_i\}$ ,  $\{F_{i+1}\}$ ,  $\{F_i^*\}$ , and  $\{F_{i+1}^*\}$ ) in Eq. 4.153 can be computed using stiffness matrices and node displacement vectors,

$$\{F_i\} = \left(\frac{EI}{L^3}\right)_i \begin{bmatrix} -\frac{AL^2}{I} & 0 & 0 & \frac{AL^2}{I} & 0 & 0 \\ 0 & -12 & -6L & 0 & 12 & -6L \\ 0 & 6L & 2L^2 & 0 & -6L & 4L^2 \end{bmatrix}_i \begin{Bmatrix} \delta_1^{i-1} \\ \delta_2^{i-1} \\ \delta_3^{i-1} \\ \delta_1^i \\ \delta_2^i \\ \delta_3^i \end{Bmatrix} = k_i [K_{o,i}] \{\delta_i\} \quad (4.156)$$

$$\{F_{i+1}\} = \left(\frac{EI}{L^3}\right)_{i+1} \begin{bmatrix} \frac{AL^2}{I} & 0 & 0 & -\frac{AL^2}{I} & 0 & 0 \\ 0 & 12 & 6L & 0 & -12 & 6L \\ 0 & 6L & 4L^2 & 0 & -6L & 2L^2 \end{bmatrix}_{i+1} \begin{Bmatrix} \delta_1^i \\ \delta_2^i \\ \delta_3^i \\ \delta_1^{i+1} \\ \delta_2^{i+1} \\ \delta_3^{i+1} \end{Bmatrix} = k_{i+1} [K_{o,i+1}] \{\delta_{i+1}\} \quad (4.157)$$

For the damaged case,

$$\{F_i^*\} = \left(\frac{EI}{L^3}\right)_i^* \begin{bmatrix} -\frac{AL^2}{I} & 0 & 0 & \frac{AL^2}{I} & 0 & 0 \\ 0 & -12 & -6L & 0 & 12 & -6L \\ 0 & 6L & 2L^2 & 0 & -6L & 4L^2 \end{bmatrix}_i^* \begin{Bmatrix} \delta_1^{*i-1} \\ \delta_2^{*i-1} \\ \delta_3^{*i-1} \\ \delta_1^{*i} \\ \delta_2^{*i} \\ \delta_3^{*i} \end{Bmatrix} = k_i^* [K_{o,i}^*] \{\delta_i^*\} \quad (4.158)$$

$$\{F_{i+1}^*\} = \left(\frac{EI}{L^3}\right)_{i+1}^* \begin{bmatrix} \frac{AL^2}{I} & 0 & 0 & -\frac{AL^2}{I} & 0 & 0 \\ 0 & 12 & 6L & 0 & -12 & 6L \\ 0 & 6L & 4L^2 & 0 & -6L & 2L^2 \end{bmatrix}_{i+1}^* \begin{Bmatrix} \delta_1^{*i} \\ \delta_2^{*i} \\ \delta_3^{*i} \\ \delta_1^{*i+1} \\ \delta_2^{*i+1} \\ \delta_3^{*i+1} \end{Bmatrix} = k_{i+1}^* [K_{o,i+1}^*] \{\delta_{i+1}^*\} \quad (4.159)$$

Where  $\delta_1^i$  is the displacement in axial direction at Node  $i$ ;  $\delta_2^i$  is displacement in transverse direction at Node  $i$ ;  $\delta_3^i$  is the nodal rotation in bending rotation direction within the plain at Node  $i$ .

Substitute Eqs. 4.154 through 4.159 into Eq. 4.153 yields,

$$\begin{aligned} & \{\dot{\Delta}^i\}^T m^i [M_o^i] \{\ddot{\delta}^i\} + \{\dot{\Delta}^i\}^T k_i [K_{o,i}] \{\delta_i\} + \{\dot{\Delta}^i\}^T k_{i+1} [K_{o,i+1}] \{\delta_{i+1}\} \\ & = \{\dot{\Delta}^i\}^T m^{*i} [M_o^{*i}] \{\ddot{\delta}^{*i}\} + \{\dot{\Delta}^i\}^T k_i^* [K_{o,i}^*] \{\delta_i^*\} + \{\dot{\Delta}^i\}^T k_{i+1}^* [K_{o,i+1}^*] \{\delta_{i+1}^*\} \end{aligned} \quad (4.160)$$

Note that the force vectors (i.e.  $\{I^i\}$ ,  $\{F_i\}$ ,  $\{F_{i+1}\}$ ,  $\{I^{*i}\}$ ,  $\{F_i^*\}$ , and  $\{F_{i+1}^*\}$ ) can be summarized as the multiplication of a property coefficient, a configuration matrix and a node displacement vector. Because the designed damage are simulated by the changes of Young's modulus ( $E$ ) and linear mass ( $\bar{m}$ ), other parameters, the length of element ( $L$ ), the cross sectional area ( $A$ ) and the moment inertia of the cross section ( $I$ ), are not influenced by damage and remain the same for the undamaged and damaged elements. Consequently, the configuration matrices for the element stiffness and element mass are the same for both the damaged and undamaged elements. Namely,

$$[K_{o,i}^*] = [K_{o,i}] \quad (4.161)$$

$$[K_{o,i+1}^*] = [K_{o,i+1}] \quad (4.162)$$

$$[M_o^{*i}] = [M_o^i] \quad (4.163)$$

Substituting Eqs. 4.161 through 4.163 into Eq. 4.160 yields,

$$\begin{aligned}
& \{\dot{\Delta}^i\}^T m^i [M_o^i] \{\ddot{\delta}^i\} + \{\dot{\Delta}^i\}^T k_i [K_{o,i}] \{\delta_i\} + \{\dot{\Delta}^i\}^T k_{i+1} [K_{o,i+1}] \{\delta_{i+1}\} \\
& = \{\dot{\Delta}^i\}^T m^{*i} [M_o^{*i}] \{\ddot{\delta}^{*i}\} + \{\dot{\Delta}^i\}^T k_i^* [K_{o,i}^*] \{\delta_i^*\} + \{\dot{\Delta}^i\}^T k_{i+1}^* [K_{o,i+1}^*] \{\delta_{i+1}^*\}
\end{aligned} \tag{4.164}$$

Moving forward the property constant from each term in Eq. 4.164 yields,

$$\begin{aligned}
& m^i \{\dot{\Delta}^i\}^T [M_o^i] \{\ddot{\delta}^i\} + k_i \{\dot{\Delta}^i\}^T [K_{o,i}] \{\delta_i\} + k_{i+1} \{\dot{\Delta}^i\}^T [K_{o,i+1}] \{\delta_{i+1}\} \\
& - k_i^* \{\dot{\Delta}^i\}^T [K_{o,i}^*] \{\delta_i^*\} - k_{i+1}^* \{\dot{\Delta}^i\}^T [K_{o,i+1}^*] \{\delta_{i+1}^*\} = m^{*i} \{\dot{\Delta}^i\}^T [M_o^{*i}] \{\ddot{\delta}^{*i}\}
\end{aligned} \tag{4.165}$$

Dividing Eq. 4.165 by  $m^{*i}$  yields,

$$\begin{aligned}
& \frac{m^i}{m^{*i}} \{\dot{\Delta}^i\}^T [M_o^i] \{\ddot{\delta}^i\} + \frac{k_i}{m^{*i}} \{\dot{\Delta}^i\}^T [K_{o,i}] \{\delta_i\} + \frac{k_{i+1}}{m^{*i}} \{\dot{\Delta}^i\}^T [K_{o,i+1}] \{\delta_{i+1}\} \\
& - \frac{k_i^*}{m^{*i}} \{\dot{\Delta}^i\}^T [K_{o,i}^*] \{\delta_i^*\} - \frac{k_{i+1}^*}{m^{*i}} \{\dot{\Delta}^i\}^T [K_{o,i+1}^*] \{\delta_{i+1}^*\} = \{\dot{\Delta}^i\}^T [M_o^{*i}] \{\ddot{\delta}^{*i}\}
\end{aligned} \tag{4.166}$$

Define the following coefficients,

$$\beta_1 = \frac{m^i}{m^{*i}} \tag{4.167}$$

$$\beta_2 = \frac{k_i}{m^{*i}} \tag{4.168}$$

$$\beta_3 = \frac{k_{i+1}}{m^{*i}} \tag{4.169}$$

$$\beta_4 = \frac{k_i^*}{m^{*i}} \tag{4.170}$$

$$\beta_5 = \frac{k_{i+1}^*}{m^{*i}} \tag{4.171}$$

Substituting Eq. 4.167 through Eq. 4.171 to Eq. 4.166 yields,

$$\begin{aligned} & \beta_1 \{\dot{\Delta}^i\}^T [M_o^i] \{\ddot{\delta}^i\} + \beta_2 \{\dot{\Delta}^i\}^T [K_{o,i}] \{\delta_i\} + \beta_3 \{\dot{\Delta}^i\}^T [K_{o,i+1}] \{\delta_{i+1}\} \\ & - \beta_4 \{\dot{\Delta}^i\}^T [K_{o,i}^*] \{\delta_i^*\} - \beta_5 \{\dot{\Delta}^i\}^T [K_{o,i+1}^*] \{\delta_{i+1}^*\} = \{\dot{\Delta}^i\}^T [M_o^{*i}] \{\ddot{\delta}^{*i}\} \end{aligned} \quad (4.172)$$

Writing the Eq. 4.172 at different time point, yields the following groups of equations,

For  $t = t_0$ ,

$$\begin{aligned} & \beta_1 (\{\dot{\Delta}^i\}^T [M_o^i] \{\ddot{\delta}^i\})|_{t_0} + \beta_2 (\{\dot{\Delta}^i\}^T [K_{o,i}] \{\delta_i\})|_{t_0} + \beta_3 (\{\dot{\Delta}^i\}^T [K_{o,i+1}] \{\delta_{i+1}\})|_{t_0} \\ & - \beta_4 (\{\dot{\Delta}^i\}^T [K_{o,i}^*] \{\delta_i^*\})|_{t_0} - \beta_5 (\{\dot{\Delta}^i\}^T [K_{o,i+1}^*] \{\delta_{i+1}^*\})|_{t_0} = (\{\dot{\Delta}^i\}^T [M_o^{*i}] \{\ddot{\delta}^{*i}\})|_{t_0} \end{aligned} \quad (4.173)$$

For  $t = t_j$ ,

$$\begin{aligned} & \beta_1 (\{\dot{\Delta}^i\}^T [M_o^i] \{\ddot{\delta}^i\})|_{t_j} + \beta_2 (\{\dot{\Delta}^i\}^T [K_{o,i}] \{\delta_i\})|_{t_j} + \beta_3 (\{\dot{\Delta}^i\}^T [K_{o,i+1}] \{\delta_{i+1}\})|_{t_j} \\ & - \beta_4 (\{\dot{\Delta}^i\}^T [K_{o,i}^*] \{\delta_i^*\})|_{t_j} - \beta_5 (\{\dot{\Delta}^i\}^T [K_{o,i+1}^*] \{\delta_{i+1}^*\})|_{t_j} = (\{\dot{\Delta}^i\}^T [M_o^{*i}] \{\ddot{\delta}^{*i}\})|_{t_j} \end{aligned} \quad (4.174)$$

For  $t = t_N$ ,

$$\begin{aligned} & \beta_1 (\{\dot{\Delta}^i\}^T [M_o^i] \{\ddot{\delta}^i\})|_{t_N} + \beta_2 (\{\dot{\Delta}^i\}^T [K_{o,i}] \{\delta_i\})|_{t_N} + \beta_3 (\{\dot{\Delta}^i\}^T [K_{o,i+1}] \{\delta_{i+1}\})|_{t_N} \\ & - \beta_4 (\{\dot{\Delta}^i\}^T [K_{o,i}^*] \{\delta_i^*\})|_{t_N} - \beta_5 (\{\dot{\Delta}^i\}^T [K_{o,i+1}^*] \{\delta_{i+1}^*\})|_{t_N} = (\{\dot{\Delta}^i\}^T [M_o^{*i}] \{\ddot{\delta}^{*i}\})|_{t_N} \end{aligned} \quad (4.175)$$

Arranging the above linear equation group into matrix form, yields,

$$\mathbf{X}\boldsymbol{\beta} = \mathbf{Y} \quad (4.176)$$

Where the coefficient matrix of the linear equation group is given as following, (note, due to the limitation of the page size, the transposed form of the matrix is provided)

$$\mathbf{X}^T = \begin{bmatrix} (\{\dot{\Delta}^i\}^T [M_o^i] \{\ddot{\delta}^i\})|_{t_0} & \dots & (\{\dot{\Delta}^i\}^T [M_o^i] \{\ddot{\delta}^i\})|_{t_j} & \dots & (\{\dot{\Delta}^i\}^T [M_o^i] \{\ddot{\delta}^i\})|_{t_N} \\ (\{\dot{\Delta}^i\}^T [K_{o,i}] \{\delta_i\})|_{t_0} & \dots & (\{\dot{\Delta}^i\}^T [K_{o,i}] \{\delta_i\})|_{t_j} & \dots & (\{\dot{\Delta}^i\}^T [K_{o,i}] \{\delta_i\})|_{t_N} \\ (\{\dot{\Delta}^i\}^T [K_{o,i+1}] \{\delta_{i+1}\})|_{t_0} & \dots & (\{\dot{\Delta}^i\}^T [K_{o,i+1}] \{\delta_{i+1}\})|_{t_j} & \dots & (\{\dot{\Delta}^i\}^T [K_{o,i+1}] \{\delta_{i+1}\})|_{t_N} \\ -(\{\dot{\Delta}^i\}^T [K_{o,i}] \{\delta_i^*\})|_{t_0} & \dots & -(\{\dot{\Delta}^i\}^T [K_{o,i}] \{\delta_i^*\})|_{t_j} & \dots & -(\{\dot{\Delta}^i\}^T [K_{o,i}] \{\delta_i^*\})|_{t_N} \\ -(\{\dot{\Delta}^i\}^T [K_{o,i+1}] \{\delta_{i+1}^*\})|_{t_0} & \dots & -(\{\dot{\Delta}^i\}^T [K_{o,i+1}] \{\delta_{i+1}^*\})|_{t_j} & \dots & -(\{\dot{\Delta}^i\}^T [K_{o,i+1}] \{\delta_{i+1}^*\})|_{t_N} \end{bmatrix} \quad (4.177)$$

The vector of unknown and the vector of known are given as,

$$\boldsymbol{\beta} = \begin{Bmatrix} \beta_1 \\ \beta_2 \\ \beta_3 \\ \beta_4 \\ \beta_5 \end{Bmatrix} \quad (4.178)$$

$$\mathbf{Y} = \begin{Bmatrix} (\{\dot{\Delta}^i\}^T [M_o^i] \{\ddot{\delta}^{*i}\})|_{t_0} \\ \vdots \\ (\{\dot{\Delta}^i\}^T [M_o^i] \{\ddot{\delta}^{*i}\})|_{t_j} \\ \vdots \\ (\{\dot{\Delta}^i\}^T [M_o^i] \{\ddot{\delta}^{*i}\})|_{t_N} \end{Bmatrix} \quad (4.179)$$

Using the Least Square Method, the vector of unknown, ' $\boldsymbol{\beta}$ ', can be computed from the following equation,

$$\boldsymbol{\beta} = (\mathbf{X}^T \mathbf{X})^{-1} (\mathbf{X}^T \mathbf{Y}) \quad (4.180)$$

With the vector of unknown computed, the damage indices for stiffness, mass, and damping can be computed as follows,

$$\beta_{m^i} = \frac{m^i}{m^{*i}} = \frac{\left( \frac{\bar{m}_i L_i}{2} + \frac{\bar{m}_{i+1} L_{i+1}}{2} \right)}{\left( \frac{\bar{m}_i^* L_i}{2} + \frac{\bar{m}_{i+1}^* L_{i+1}}{2} \right)} = \beta_1 \quad (4.181)$$

$$\beta_{k_i} = \frac{\frac{k_i}{m^{*i}}}{\frac{k_i^*}{m^{*i}}} = \frac{k_i}{k_i^*} = \frac{\left( \frac{EI}{L^3} \right)_i}{\left( \frac{EI}{L^3} \right)_i^*} = \frac{\beta_2}{\beta_4} \quad (4.182)$$

$$\beta_{k_{i+1}} = \frac{\frac{k_{i+1}}{m^{*i}}}{\frac{k_{i+1}^*}{m^{*i}}} = \frac{k_{i+1}}{k_{i+1}^*} = \frac{\left( \frac{EI}{L^3} \right)_{i+1}}{\left( \frac{EI}{L^3} \right)_{i+1}^*} = \frac{\beta_3}{\beta_5} \quad (4.183)$$

#### 4.5 THEORY FOR SPACE TRUSSES

In this subsection, the proposed non-destructive evaluation theory will be applied to space truss at each joint considering vibrations in the global X, Y, and Z directions simultaneously.

For a joint in space, as shown in Figure 4.9, assume that there are  $n$  bars jointed to the Joint  $\gamma$  and each bar has a defined direction from negative end towards positive end. The modulus of elasticity of the material for Bar  $i$  is denoted as  $E_i$ . The length of Bar  $i$  is  $L_i$ . The cross sectional area of Bar  $i$  is denoted as  $A_i$ . The axial force of Bar  $i$  is denoted as  $F_{i,1}$ . The unit vector in the direction of Bar  $i$  is denoted as  $n_i$ . According to the free body diagram at Joint  $\gamma$  shown in Figure 4.10, the dynamic equilibrium condition for the undamaged system at Joint  $\gamma$  can be expressed as,



$$\{I^\gamma\} + F_{1,1}\{n_1\} + \dots + F_{i,1}\{n_i\} + \dots + F_{n,1}\{n_n\} = \{P^\gamma\} \quad (4.184)$$

Similarly, for the damaged case, the dynamic equilibrium condition at Joint  $i$  can be expressed as,

$$\{I^{*\gamma}\} + F_{1,1}^*\{n_1^*\} + \dots + F_{i,1}^*\{n_i^*\} + \dots + F_{n,1}^*\{n_n^*\} = \{P^{*\gamma}\} \quad (4.185)$$

Where the asterisk (“\*”) denotes the quantities from the damaged case.

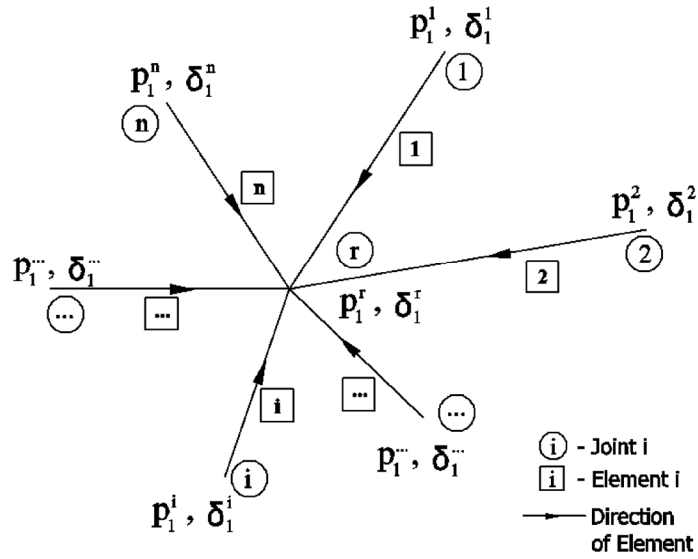
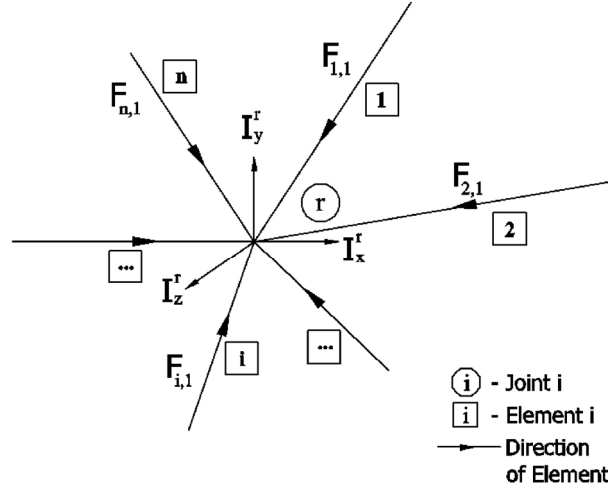


Figure 4.9. One Joint from a Space Truss with All Bars Joined to the Joint  $\gamma$



**Figure 4.10. Free Body Diagram of Joint  $\gamma$  in Space**

Given any velocity vectors,  $\{\dot{\Delta}^\gamma\}$  and  $\{\dot{\Delta}^{*\gamma}\}$ , for the undamaged and damaged systems, the power performed by the external forces in the undamaged and damaged systems can be expressed as following,

$$\{\dot{\Delta}^\gamma\}^T \{I^\gamma\} + \{\dot{\Delta}^\gamma\}^T F_{1,1} \{n_1\} + \dots + \{\dot{\Delta}^\gamma\}^T F_{i,1} \{n_i\} + \dots + \{\dot{\Delta}^\gamma\}^T F_{n,1} \{n_n\} = \{\dot{\Delta}^\gamma\}^T \{P^\gamma\} \quad (4.186)$$

Similarly, for the damaged case,

$$\{\dot{\Delta}^{*\gamma}\}^T \{I^{*\gamma}\} + \{\dot{\Delta}^{*\gamma}\}^T F_{1,1}^* \{n_1^*\} + \dots + \{\dot{\Delta}^{*\gamma}\}^T F_{i,1}^* \{n_i^*\} + \dots + \{\dot{\Delta}^{*\gamma}\}^T F_{n,1}^* \{n_n^*\} = \{\dot{\Delta}^{*\gamma}\}^T \{P^{*\gamma}\} \quad (4.187)$$

Assume that the applied external loads and velocities used to compute power at Joint  $\gamma$  are the same for both the undamaged and damaged systems,

$$\{\dot{\Delta}^\gamma\} = \{\dot{\Delta}^{*\gamma}\} \quad (4.188)$$

$$\{P^\gamma\} = \{P^{*\gamma}\} \quad (4.189)$$

Substituting Eq. 4.188 and Eq. 4.189 into Eq. 4.187 yields,

$$\{\dot{\Delta}^\gamma\}^T \{I^{*\gamma}\} + \{\dot{\Delta}^\gamma\}^T F_{1,1}^* \{n_1^*\} + \dots + \{\dot{\Delta}^\gamma\}^T F_{i,1}^* \{n_i^*\} + \dots + \{\dot{\Delta}^\gamma\}^T F_{n,1}^* \{n_n^*\} = \{\dot{\Delta}^\gamma\}^T \{P^\gamma\} \quad (4.190)$$

Noticing the power performed by the external load are the same for both the undamaged and damaged system. Substituting Eq. 4.190 into Eq. 4.186 yields,

$$\begin{aligned} & \{\dot{\Delta}^\gamma\}^T \{I^\gamma\} + \{\dot{\Delta}^\gamma\}^T F_{1,1} \{n_1\} + \dots + \{\dot{\Delta}^\gamma\}^T F_{i,1} \{n_i\} + \dots + \{\dot{\Delta}^\gamma\}^T F_{n,1} \{n_n\} \\ &= \{\dot{\Delta}^\gamma\}^T \{I^{*\gamma}\} + \{\dot{\Delta}^\gamma\}^T F_{1,1}^* \{n_1^*\} + \dots + \{\dot{\Delta}^\gamma\}^T F_{i,1}^* \{n_i^*\} + \dots + \{\dot{\Delta}^\gamma\}^T F_{n,1}^* \{n_n^*\} \end{aligned} \quad (4.191)$$

Note, Eq. 4.191 is equivalent to Eq. 2.10.

In this case, the inertial forces can be expressed using the following lumped mass matrix.

Namely,

$$\{I^\gamma\} = \left[ \left( \frac{\bar{m}_1 L_1}{2} \right) + \dots + \left( \frac{\bar{m}_i L_i}{2} \right) + \dots + \left( \frac{\bar{m}_n L_n}{2} \right) \right] \begin{bmatrix} 1 & & \\ & 1 & \\ & & 1 \end{bmatrix}_\gamma \begin{Bmatrix} \ddot{\delta}_x^\gamma \\ \ddot{\delta}_y^\gamma \\ \ddot{\delta}_z^\gamma \end{Bmatrix} = m^\gamma [M_o^\gamma] \{\ddot{\delta}^\gamma\} \quad (4.192)$$

Where  $\bar{m}_i$  is the linear mass of Bar  $i$ ;  $\ddot{\delta}_x^\gamma$  is the acceleration of Joint  $\gamma$  in x-direction in the global coordinate system;  $\ddot{\delta}_y^\gamma$  is the acceleration of Joint  $\gamma$  in y-direction in the global coordinate system and  $\ddot{\delta}_z^\gamma$  is the acceleration of Joint  $\gamma$  in z-direction in the global coordinate system;  $m^\gamma$  is the lumped mass of the Joint  $\gamma$ ; and  $[M_o^\gamma]$  is the

configuration matrix of the mass matrix.

Similarly, for the damaged system,

$$\{I^{*\gamma}\} = \left[ \left( \frac{\bar{m}_1^* L_1^*}{2} \right) + \dots + \left( \frac{\bar{m}_i^* L_i^*}{2} \right) + \dots + \left( \frac{\bar{m}_n^* L_n^*}{2} \right) \right] \begin{bmatrix} 1 & & \\ & 1 & \\ & & 1 \end{bmatrix}_\gamma \begin{Bmatrix} \ddot{\delta}_x^{*\gamma} \\ \ddot{\delta}_y^{*\gamma} \\ \ddot{\delta}_z^{*\gamma} \end{Bmatrix} = m^{*\gamma} [M_o^{*\gamma}] \{\ddot{\delta}^{*\gamma}\} \quad (4.193)$$

Note, in this case, the  $[M_o^\gamma]$  and  $[M_o^{*\gamma}]$  are both  $3 \times 3$  identity matrices, thus,

$$[M_o^{*\gamma}] = [M_o^\gamma] \quad (4.194)$$

Substituting Eq. 4.194 into Eq. 4.193 yields,

$$\{I^{*\gamma}\} = m^{*\gamma} [M_o^\gamma] \{\ddot{\delta}^{*\gamma}\} \quad (4.195)$$

The axial force of the  $i^{\text{th}}$  bar connected the Joint  $\gamma$  can be computed as,

$$F_{i,1} = \left( \frac{EA}{L} \right)_i \begin{bmatrix} 1 & -1 \end{bmatrix}_i \begin{Bmatrix} \hat{\delta}_{i,1}^+ \\ \hat{\delta}_{i,1}^- \end{Bmatrix} = \left( \frac{EA}{L} \right)_i (\hat{\delta}_{i,1}^+ - \hat{\delta}_{i,1}^-) \quad (4.196)$$

where,  $\hat{\delta}_{i,1}^+$  is the axial direction movement of the positive end of the Bar  $i$  connected to Joint  $\gamma$  in local coordinate system;  $\hat{\delta}_{i,1}^-$  is the axial direction movement of the negative end of Bar  $i$  connected with Joint  $\gamma$  in the local coordinate system. The upward arrow (' $\wedge$ ') means the value in the local coordinate.

According to vector projection, the axial direction movement of the positive end of the  $i^{\text{th}}$  bar can be computed as,

$$\hat{\delta}_{i,1}^+ = \{n_i\}^T \{\delta_i^+\} \quad (4.197)$$

The axial direction movement of the negative end of the  $i^{\text{th}}$  bar can be computed as,

$$\hat{\delta}_{i,1}^- = \{n_i\}^T \{\delta_i^-\} \quad (4.198)$$

Substituting Eq. 4.197 and Eq. 4.198 into Eq. 4.196, yields,

$$F_{i,1} = \left( \frac{EA}{L} \right)_i \{n_i\}^T (\{\delta_i^+\} - \{\delta_i^-\}) \quad (4.199)$$

Which can be also written as,

$$F_{i,1} = k_i \{n_i\}^T (\{\delta_i^+\} - \{\delta_i^-\}) \quad (4.200)$$

For the damaged system,

$$F_{i,1}^* = k_i^* \{n_i^*\}^T (\{\delta_i^{*+}\} - \{\delta_i^{*-}\}) \quad (4.201)$$

Substituting Eq. 4.192, Eq. 4.195, Eq. 4.200, Eq. 4.201 into Eq. 4.191

$$\begin{aligned} & \{\dot{\Delta}^\gamma\}^T m^\gamma [M_o^\gamma] \{\ddot{\delta}^\gamma\} + \{\dot{\Delta}^\gamma\}^T k_1 \{n_1\}^T (\{\delta_1^+\} - \{\delta_1^-\}) \{n_1\} + \dots \\ & + \{\dot{\Delta}^\gamma\}^T k_i \{n_i\}^T (\{\delta_i^+\} - \{\delta_i^-\}) \{n_i\} + \dots + \{\dot{\Delta}^\gamma\}^T k_n \{n_n\}^T (\{\delta_n^+\} - \{\delta_n^-\}) \{n_n\} \\ & = \{\dot{\Delta}^\gamma\}^T m^{*\gamma} [M_o^\gamma] \{\ddot{\delta}^{*\gamma}\} + \{\dot{\Delta}^\gamma\}^T k_1^* \{n_1^*\}^T (\{\delta_1^{*+}\} - \{\delta_1^{*-}\}) \{n_1^*\} + \dots \\ & + \{\dot{\Delta}^\gamma\}^T k_i^* \{n_i^*\}^T (\{\delta_i^{*+}\} - \{\delta_i^{*-}\}) \{n_i^*\} + \dots + \{\dot{\Delta}^\gamma\}^T k_n^* \{n_n^*\}^T (\{\delta_n^{*+}\} - \{\delta_n^{*-}\}) \{n_n^*\} \end{aligned} \quad (4.202)$$

Rearranging Eq. 4.202 yields,

$$\begin{aligned}
& m^\gamma \{\dot{\Delta}^\gamma\}^T [M_o^\gamma] \{\ddot{\delta}^\gamma\} + k_1 \{\dot{\Delta}^\gamma\}^T \{n_1\}^T (\{\delta_1^+\} - \{\delta_1^-\}) \{n_1\} + \dots \\
& + k_i \{\dot{\Delta}^\gamma\}^T \{n_i\}^T (\{\delta_i^+\} - \{\delta_i^-\}) \{n_i\} + \dots + k_n \{\dot{\Delta}^\gamma\}^T \{n_n\}^T (\{\delta_n^+\} - \{\delta_n^-\}) \{n_n\} \\
& - k_1^* \{\dot{\Delta}^\gamma\}^T \{n_1^*\}^T (\{\delta_1^{*+}\} - \{\delta_1^{*-}\}) \{n_1^*\} - \dots - k_i^* \{\dot{\Delta}^\gamma\}^T \{n_i^*\}^T (\{\delta_i^{*+}\} - \{\delta_i^{*-}\}) \{n_i^*\} \\
& - \dots - k_n^* \{\dot{\Delta}^\gamma\}^T \{n_n^*\}^T (\{\delta_n^{*+}\} - \{\delta_n^{*-}\}) \{n_n^*\} = m^{*\gamma} \{\dot{\Delta}^\gamma\}^T [M_o^\gamma] \{\ddot{\delta}^{*\gamma}\}
\end{aligned} \tag{4.203}$$

Dividing Eq. 4.203 by  $m^{*\gamma}$  yields,

$$\begin{aligned}
& \frac{m^\gamma}{m^{*\gamma}} \{\dot{\Delta}^\gamma\}^T [M_o^\gamma] \{\ddot{\delta}^\gamma\} + \frac{k_1}{m^{*\gamma}} \{\dot{\Delta}^\gamma\}^T \{n_1\}^T (\{\delta_1^+\} - \{\delta_1^-\}) \{n_1\} + \dots \\
& + \frac{k_i}{m^{*\gamma}} \{\dot{\Delta}^\gamma\}^T \{n_i\}^T (\{\delta_i^+\} - \{\delta_i^-\}) \{n_i\} + \dots + \frac{k_n}{m^{*\gamma}} \{\dot{\Delta}^\gamma\}^T \{n_n\}^T (\{\delta_n^+\} - \{\delta_n^-\}) \{n_n\} \\
& - \frac{k_1^*}{m^{*\gamma}} \{\dot{\Delta}^\gamma\}^T \{n_1^*\}^T (\{\delta_1^{*+}\} - \{\delta_1^{*-}\}) \{n_1^*\} - \dots - \frac{k_i^*}{m^{*\gamma}} \{\dot{\Delta}^\gamma\}^T \{n_i^*\}^T (\{\delta_i^{*+}\} - \{\delta_i^{*-}\}) \{n_i^*\} \\
& - \dots - \frac{k_n^*}{m^{*\gamma}} \{\dot{\Delta}^\gamma\}^T \{n_n^*\}^T (\{\delta_n^{*+}\} - \{\delta_n^{*-}\}) \{n_n^*\} = \{\dot{\Delta}^\gamma\}^T [M_o^\gamma] \{\ddot{\delta}^{*\gamma}\}
\end{aligned} \tag{4.204}$$

Define the following coefficients,

$$\beta_1 = \frac{m^\gamma}{m^{*\gamma}} \tag{4.205}$$

$$\beta_2 = \frac{k_1}{m^{*\gamma}} \tag{4.206}$$

...

$$\beta_{i+1} = \frac{k_i}{m^{*\gamma}} \tag{4.207}$$

...

$$\beta_{n+1} = \frac{k_n}{m^{*\gamma}} \quad (4.208)$$

$$\beta_{n+2} = \frac{k_1^*}{m^{*\gamma}} \quad (4.209)$$

...

$$\beta_{i+n+1} = \frac{k_i^*}{m^{*\gamma}} \quad (4.210)$$

...

$$\beta_{2n+1} = \frac{k_n^*}{m^{*\gamma}} \quad (4.211)$$

Substituting Eq. 4.205 through Eq. 4.211 to Eq. 4.204 yields,

$$\begin{aligned} & \beta_1 \{\dot{\Delta}^\gamma\}^T [M_o^\gamma] \{\ddot{\delta}^\gamma\} + \beta_2 \{\dot{\Delta}^\gamma\}^T \{n_1\}^T (\{\delta_1^+\} - \{\delta_1^-\}) \{n_1\} + \dots \\ & + \beta_{i+1} \{\dot{\Delta}^\gamma\}^T \{n_i\}^T (\{\delta_i^+\} - \{\delta_i^-\}) \{n_i\} + \dots + \beta_{n+1} \{\dot{\Delta}^\gamma\}^T \{n_n\}^T (\{\delta_n^+\} - \{\delta_n^-\}) \{n_n\} \\ & - \beta_{n+2} \{\dot{\Delta}^\gamma\}^T \{n_1^*\}^T (\{\delta_1^{*+}\} - \{\delta_1^{*-}\}) \{n_1^*\} - \dots - \beta_{i+n+1} \{\dot{\Delta}^\gamma\}^T \{n_i^*\}^T (\{\delta_i^{*+}\} - \{\delta_i^{*-}\}) \{n_i^*\} \\ & - \dots - \beta_{2n+1} \{\dot{\Delta}^\gamma\}^T \{n_n^*\}^T (\{\delta_n^{*+}\} - \{\delta_n^{*-}\}) \{n_n^*\} = \{\dot{\Delta}^\gamma\}^T [M_o^\gamma] \{\ddot{\delta}^{*\gamma}\} \end{aligned} \quad (4.212)$$

Writing the Eq. 4.212 at different time point, yields the following groups of equations,

For  $t = t_0$ ,

$$\begin{aligned} & \beta_1 (\{\dot{\Delta}^\gamma\}^T [M_o^\gamma] \{\ddot{\delta}^\gamma\})|_{t_0} + \beta_2 (\{\dot{\Delta}^\gamma\}^T \{n_1\}^T (\{\delta_1^+\} - \{\delta_1^-\}) \{n_1\})|_{t_0} + \dots \\ & + \beta_{i+1} (\{\dot{\Delta}^\gamma\}^T \{n_i\}^T (\{\delta_i^+\} - \{\delta_i^-\}) \{n_i\})|_{t_0} + \dots + \beta_{n+1} (\{\dot{\Delta}^\gamma\}^T \{n_n\}^T (\{\delta_n^+\} - \{\delta_n^-\}) \{n_n\})|_{t_0} \\ & - \beta_{n+2} (\{\dot{\Delta}^\gamma\}^T \{n_1^*\}^T (\{\delta_1^{*+}\} - \{\delta_1^{*-}\}) \{n_1^*\})|_{t_0} - \dots - \beta_{i+n+1} (\{\dot{\Delta}^\gamma\}^T \{n_i^*\}^T (\{\delta_i^{*+}\} - \{\delta_i^{*-}\}) \{n_i^*\})|_{t_0} \\ & - \dots - \beta_{2n+1} (\{\dot{\Delta}^\gamma\}^T \{n_n^*\}^T (\{\delta_n^{*+}\} - \{\delta_n^{*-}\}) \{n_n^*\})|_{t_0} = (\{\dot{\Delta}^\gamma\}^T [M_o^\gamma] \{\ddot{\delta}^{*\gamma}\})|_{t_0} \end{aligned} \quad (4.213)$$

For  $t = t_j$ ,

$$\begin{aligned}
& \beta_1(\{\dot{\Delta}^\gamma\}^T [M_o^\gamma] \{\ddot{\delta}^\gamma\})|_{t_j} + \beta_2(\{\dot{\Delta}^\gamma\}^T \{n_1\}^T (\{\delta_1^+\} - \{\delta_1^-\}) \{n_1\})|_{t_j} + \dots \\
& + \beta_{i+1}(\{\dot{\Delta}^\gamma\}^T \{n_i\}^T (\{\delta_i^+\} - \{\delta_i^-\}) \{n_i\})|_{t_j} + \dots + \beta_{n+1}(\{\dot{\Delta}^\gamma\}^T \{n_n\}^T (\{\delta_n^+\} - \{\delta_n^-\}) \{n_n\})|_{t_j} \\
& - \beta_{n+2}(\{\dot{\Delta}^\gamma\}^T \{n_1^*\}^T (\{\delta_1^{*+}\} - \{\delta_1^{*-}\}) \{n_1^*\})|_{t_j} - \dots - \beta_{i+n+1}(\{\dot{\Delta}^\gamma\}^T \{n_i^*\}^T (\{\delta_i^{*+}\} - \{\delta_i^{*-}\}) \{n_i^*\})|_{t_j} \\
& - \dots - \beta_{2n+1}(\{\dot{\Delta}^\gamma\}^T \{n_n^*\}^T (\{\delta_n^{*+}\} - \{\delta_n^{*-}\}) \{n_n^*\})|_{t_j} = (\{\dot{\Delta}^\gamma\}^T [M_o^\gamma] \{\ddot{\delta}^{*\gamma}\})|_{t_j}
\end{aligned} \tag{4.214}$$

For  $t = t_N$ ,

$$\begin{aligned}
& \beta_1(\{\dot{\Delta}^\gamma\}^T [M_o^\gamma] \{\ddot{\delta}^\gamma\})|_{t_N} + \beta_2(\{\dot{\Delta}^\gamma\}^T \{n_1\}^T (\{\delta_1^+\} - \{\delta_1^-\}) \{n_1\})|_{t_N} + \dots \\
& + \beta_{i+1}(\{\dot{\Delta}^\gamma\}^T \{n_i\}^T (\{\delta_i^+\} - \{\delta_i^-\}) \{n_i\})|_{t_N} + \dots + \beta_{n+1}(\{\dot{\Delta}^\gamma\}^T \{n_n\}^T (\{\delta_n^+\} - \{\delta_n^-\}) \{n_n\})|_{t_N} \\
& - \beta_{n+2}(\{\dot{\Delta}^\gamma\}^T \{n_1^*\}^T (\{\delta_1^{*+}\} - \{\delta_1^{*-}\}) \{n_1^*\})|_{t_N} - \dots - \beta_{i+n+1}(\{\dot{\Delta}^\gamma\}^T \{n_i^*\}^T (\{\delta_i^{*+}\} - \{\delta_i^{*-}\}) \{n_i^*\})|_{t_N} \\
& - \dots - \beta_{2n+1}(\{\dot{\Delta}^\gamma\}^T \{n_n^*\}^T (\{\delta_n^{*+}\} - \{\delta_n^{*-}\}) \{n_n^*\})|_{t_N} = (\{\dot{\Delta}^\gamma\}^T [M_o^\gamma] \{\ddot{\delta}^{*\gamma}\})|_{t_N}
\end{aligned} \tag{4.215}$$

Arranging the above linear equation group into matrix form, yields,

$$\mathbf{X}\boldsymbol{\beta} = \mathbf{Y} \tag{4.216}$$

Where the coefficient matrix of the linear equation group is given as following, (note, due to the limitation of the page size, the transposed form of the matrix is provided),



$$\begin{aligned}
\mathbf{X}^T = & \left[ \begin{array}{ccc}
(\{\dot{\Delta}^\gamma\}^T [M_o^\gamma] \{\ddot{\mathcal{S}}^\gamma\})|_{t_0} & \cdots & (\{\dot{\Delta}^\gamma\}^T [M_o^\gamma] \{\ddot{\mathcal{S}}^\gamma\})|_{t_j} & \cdots & (\{\dot{\Delta}^\gamma\}^T [M_o^\gamma] \{\ddot{\mathcal{S}}^\gamma\})|_{t_N} \\
(\{\dot{\Delta}^\gamma\}^T \{n_1\}^T (\{\delta_1^+\} - \{\delta_1^-\}) \{n_1\})|_{t_0} & \cdots & (\{\dot{\Delta}^\gamma\}^T \{n_1\}^T (\{\delta_1^+\} - \{\delta_1^-\}) \{n_1\})|_{t_j} & \cdots & (\{\dot{\Delta}^\gamma\}^T \{n_1\}^T (\{\delta_1^+\} - \{\delta_1^-\}) \{n_1\})|_{t_N} \\
\vdots & \vdots & \vdots & \vdots & \vdots \\
(\{\dot{\Delta}^\gamma\}^T \{n_i\}^T (\{\delta_i^+\} - \{\delta_i^-\}) \{n_i\})|_{t_0} & \cdots & (\{\dot{\Delta}^\gamma\}^T \{n_i\}^T (\{\delta_i^+\} - \{\delta_i^-\}) \{n_i\})|_{t_j} & \cdots & (\{\dot{\Delta}^\gamma\}^T \{n_i\}^T (\{\delta_i^+\} - \{\delta_i^-\}) \{n_i\})|_{t_N} \\
\vdots & \vdots & \vdots & \vdots & \vdots \\
(\{\dot{\Delta}^\gamma\}^T \{n_n\}^T (\{\delta_n^+\} - \{\delta_n^-\}) \{n_n\})|_{t_0} & \cdots & (\{\dot{\Delta}^\gamma\}^T \{n_n\}^T (\{\delta_n^+\} - \{\delta_n^-\}) \{n_n\})|_{t_j} & \cdots & (\{\dot{\Delta}^\gamma\}^T \{n_n\}^T (\{\delta_n^+\} - \{\delta_n^-\}) \{n_n\})|_{t_N} \\
(\{\dot{\Delta}^\gamma\}^T \{n_1^*\}^T (\{\delta_1^{*+}\} - \{\delta_1^{*-}\}) \{n_1^*\})|_{t_0} & \cdots & (\{\dot{\Delta}^\gamma\}^T \{n_1^*\}^T (\{\delta_1^{*+}\} - \{\delta_1^{*-}\}) \{n_1^*\})|_{t_j} & \cdots & (\{\dot{\Delta}^\gamma\}^T \{n_1^*\}^T (\{\delta_1^{*+}\} - \{\delta_1^{*-}\}) \{n_1^*\})|_{t_N} \\
\vdots & \vdots & \vdots & \vdots & \vdots \\
(\{\dot{\Delta}^\gamma\}^T \{n_i^*\}^T (\{\delta_i^{*+}\} - \{\delta_i^{*-}\}) \{n_i^*\})|_{t_0} & \cdots & (\{\dot{\Delta}^\gamma\}^T \{n_i^*\}^T (\{\delta_i^{*+}\} - \{\delta_i^{*-}\}) \{n_i^*\})|_{t_j} & \cdots & (\{\dot{\Delta}^\gamma\}^T \{n_i^*\}^T (\{\delta_i^{*+}\} - \{\delta_i^{*-}\}) \{n_i^*\})|_{t_N} \\
\vdots & \vdots & \vdots & \vdots & \vdots \\
(\{\dot{\Delta}^\gamma\}^T \{n_n^*\}^T (\{\delta_n^{*+}\} - \{\delta_n^{*-}\}) \{n_n^*\})|_{t_0} & \cdots & (\{\dot{\Delta}^\gamma\}^T \{n_n^*\}^T (\{\delta_n^{*+}\} - \{\delta_n^{*-}\}) \{n_n^*\})|_{t_j} & \cdots & (\{\dot{\Delta}^\gamma\}^T \{n_n^*\}^T (\{\delta_n^{*+}\} - \{\delta_n^{*-}\}) \{n_n^*\})|_{t_N}
\end{array} \right]
\end{aligned}
\tag{4.217}$$

The vector of unknown and the vector of known are given as,

$$\mathbf{\beta} = \left\{ \begin{array}{c} \beta_1 \\ \beta_2 \\ \vdots \\ \beta_{i+1} \\ \vdots \\ \beta_{n+1} \\ \beta_{n+2} \\ \vdots \\ \beta_{i+n+1} \\ \vdots \\ \beta_{2n+1} \end{array} \right\} \quad (4.218)$$

$$\mathbf{Y} = \left\{ \begin{array}{c} ((\dot{\Delta}^\gamma)^T [M_o^\gamma] \{\ddot{\delta}^{*\gamma}\})|_{t_0} \\ \vdots \\ ((\dot{\Delta}^\gamma)^T [M_o^\gamma] \{\ddot{\delta}^{*\gamma}\})|_{t_j} \\ \vdots \\ ((\dot{\Delta}^\gamma)^T [M_o^\gamma] \{\ddot{\delta}^{*\gamma}\})|_{t_N} \end{array} \right\} \quad (4.219)$$

Using the Least Square Method, the vector of unknown, ' $\mathbf{\beta}$ ', can be computed from the following equation,

$$\mathbf{\beta} = (\mathbf{X}^T \mathbf{X})^{-1} (\mathbf{X}^T \mathbf{Y}) \quad (4.220)$$

With the vector of unknown computed, the damage indices for stiffness, mass and damping can be computed as follows,

$$\beta_{m^\gamma} = \frac{m^\gamma}{m^{*\gamma}} = \frac{\left(\frac{\overline{m}_1 L_1}{2}\right) + \dots + \left(\frac{\overline{m}_i L_i}{2}\right) + \dots + \left(\frac{\overline{m}_n L_n}{2}\right)}{\left(\frac{\overline{m}_1^* L_1^*}{2}\right) + \dots + \left(\frac{\overline{m}_i^* L_i^*}{2}\right) + \dots + \left(\frac{\overline{m}_n^* L_n^*}{2}\right)} = \beta_1 \quad (4.221)$$

$$\beta_{k_1} = \frac{\left(\frac{EA}{L}\right)_1}{\left(\frac{EA}{L}\right)_1^*} = \frac{k_1}{k_1^*} = \frac{\frac{k_1}{m^{*\gamma}}}{\frac{k_1^*}{m^{*\gamma}}} = \frac{\beta_2}{\beta_{n+2}} \quad (4.222)$$

...

$$\beta_{k_i} = \frac{\left(\frac{EA}{L}\right)_i}{\left(\frac{EA}{L}\right)_i^*} = \frac{k_i}{k_i^*} = \frac{\frac{k_i}{m^{*\gamma}}}{\frac{k_i^*}{m^{*\gamma}}} = \frac{\beta_{i+1}}{\beta_{i+n+1}} \quad (4.223)$$

...

$$\beta_{k_n} = \frac{\left(\frac{EA}{L}\right)_n}{\left(\frac{EA}{L}\right)_n^*} = \frac{k_n}{k_n^*} = \frac{\frac{k_n}{m^{*\gamma}}}{\frac{k_n^*}{m^{*\gamma}}} = \frac{\beta_{n+1}}{\beta_{2n+1}} \quad (4.224)$$

#### 4.6 OVERALL SOLUTION PROCEDURE

To perform the proposed damage detection method to continuous system, the following steps should be followed:

- (1) Derive the linear equation group for the specific continuous system based on the power equilibrium at a single joint or among multiple joints;
- (2) Collect the displacement, velocity, and acceleration records required by the coefficient matrix and the vector of knowns of the linear equation group defined by step 1;
- (3) Use the least square method to solve the linear equation group for the vector of unknown; and
- (4) Compute for the Damage Indices and Damage severities for each physical property based on the vector of unknown computed from Step 3.

The general process will be clearly demonstrated in Section 5.

#### **4.7 SUMMARY**

In this Section, the Power Method for a rod, Euler-Bernoulli beam, plane frame, and space truss were studied. The derivation processes were provided in Section 4.2 to Section 4.5 and the overall solution procedure was provided in Section 4.6. In section 4.2.1, the specific form of the proposed method was derived to detect and evaluate damage in rod elements based on the power equilibrium at each joint. In Section 4.2.2, the specific form of the proposed method was derived to detect and evaluate damage in rod elements based on the power equilibrium at multiple joints. In Section 4.3, the specific form of the proposed method was derived to detect and evaluate damage in beam elements based on the power equilibrium at each joint. In Section 4.4, the specific form of the proposed method was derived to detect and evaluate damage in plane frame elements based on the power equilibrium at each joint. In Section 4.5, the specific form of the proposed method was derived to detect and evaluate damage in space truss elements (bars) based on the power equilibrium at each joint.

The advantage of the Power Method is that the method was able to simultaneously detect damage in physical properties of multiple structural members related to multiple types of vibrations. In other words,

- (1) In real experiment, the vibration is not limited in one direction and one type.

By using the dynamic data from vibration of all related directions, the Power Method will provide more reliable damage evaluation results; and

- (2) The Power Method provides the option of detecting damage in the whole

structure or at multiple locations of the structure, besides at single location.

This advantage can be used to increase the computation efficiency.

## **5 CASE STUDIES OF DAMAGE EVALUATION FOR CONTINUOUS SYSTEMS**

### **5.1 INTRODUCTION**

The objective of this section is to validate the proposed theory for continuous systems using numerical examples. To achieve this goal, the theory is validated using exact displacements, velocities, and accelerations of the undamaged and damaged continuous systems modeled within SAP2000 (Version 15). The exact displacements, velocities, and accelerations are computed from the linear direct integration in SAP2000. The Hilber-Hughes-Taylor time integration method was used by SAP2000. The three parameters of the Hilber-Hughes-Taylor method: Gamma, Beta and Alpha were set to be 0.5, 0.25 and 0, respectively. Five linearly elastic numerical cases are studied in this section,

Case #1: the accuracy of the theory will be studied on a rod under axial and torsional vibrations. The rod is fixed at its left end. The damage detection algorithm of the Power Method for a rod under axial and torsional vibration is derived and is provided in Section 4.2.1. The damage is simulated by the changes of masses and stiffness of specific rod elements.

Case #2: the accuracy of the theory will be studied on the same rod under axial vibration. The algorithm of the Power Method for the whole rod under axial vibration is derived and is provided in Section 4.2.2. The damage is simulated by the changes of masses and stiffness of specific rod elements.

Case #3: the accuracy of the theory will be studied on a propped cantilever beam under bending vibration. The algorithm of the Power Method for an Euler-Bernoulli beam under bending vibration is derived and is provided in Section 4.3. The damage is simulated by the changes of masses and stiffness of specific beam elements.

Case #4: the accuracy of the theory will be studied on a two-bay frame. The algorithm of the Power Method for a plane frame under axial and bending vibration is derived and is provided in Section 4.4. The damage is simulated by the changes of masses and stiffness of specific frame elements.

Case #5: the accuracy of the theory will be studied on a simple space truss. The algorithm of the Power Method for a space truss is derived and is provided in Section 4.5. The damage is simulated by the changes of masses and stiffness of specific truss elements.

## **5.2 DAMAGE EVALUATION FOR A ROD**

In Case #1, a rod fixed at its left end is used to evaluate the proposed theory. Figure 5.1 indicates the geometry, and damage scenario under consideration. The geometry of the cross-section of the rod is shown in Figure 5.2. The modulus of elasticity ( $E$ ) of the material is 29,000 ksi. The modulus of elasticity in shear ( $G$ ) of the material is 11,154 ksi. The Poisson's ratio of the material ( $\nu$ ) is 0.3. The torsional constant of the cross section of ( $J$ ) is 7.9522. The mass density of the material is  $7.345 \times 10^{-7}$  kip·sec<sup>2</sup>/in<sup>4</sup>. In this case, four elements with damaged mass and stiffness are studied.

The rod is meshed into 12 elements and has 13 equally spaced nodes. The length of each element is 1.0 inches. For illustrative purposes, typical elements are indicated in Figure 5.1. The damage is simulated by a ten percent (10%) reduction of the modulus of elasticity and twenty percent (20%) reduction of the mass of Elements 5, 6, 9, and 10.

For each node in the rod model, a dynamic force,  $100\cos(2\pi t)$ , is applied in both axial ( $x_1$ ) and torsional ( $\theta_1$ ) direction. Given the applied load case, the displacement, velocity, and acceleration time histories in both axial and torsional direction are directly generated from SAP2000 using linear direct integration method. The computation step is  $1E-4$  seconds (10,000 Hz) for total 0.2 seconds. For both the undamaged and damaged Rods, the displacements, velocities and accelerations of the Node 13 in axial direction were plotted in Figure 5.3, Figure 5.4, and Figure 5.5.

In this case, the computed velocity ( $\dot{x}(t)$ ) of each node in the undamaged case was used as the velocity used to compute power ( $\dot{\Delta}$ ) for both the undamaged and damaged cases. For every two nearby elements, the coefficient matrices ('X') and known vector ('Y') were constructed by substituting the acceleration ( $\ddot{x}(t)$ ), velocity ( $\dot{x}(t)$ ), displacement ( $x(t)$ ), and velocity used to compute power ( $\dot{\Delta}$ ) into Eq. 4.50 and Eq. 4.52. The coefficient damage index vector,  $\beta$ , related to the two nearby elements, is computed using Eq. 4.53. Then the damage indices for mass and stiffness are computed using Eqs. 4.54 through 4.56. The damage severities for mass and stiffness are computed using Eq. 2.13. For each two nearby elements, the above process is performed. For simplicity purposes, no overlap element is used. Thus, the proposed theory is only applied to six pairs of elements. The estimated damage indices and the designed damage indices for



each physical property are listed in Table 5.1 and are plotted in Figure 5.6 for nodal mass and Figure 5.8 for element stiffness. The estimated damage severities and the designed damage severities for each physical property are plotted in Figure 5.7 for nodal mass and Figure 5.9 for element stiffness. Because the proposed method is applied at the center node of two nearby elements, only six nodes were taken into consideration (i.e. Nodes 2, 4, 6, 8, 10, and 12). Comparing the estimated damage indices with the designed damage indices, the proposed method can accurately locate and size multiple damage in a rod with axial and torsional vibrations.

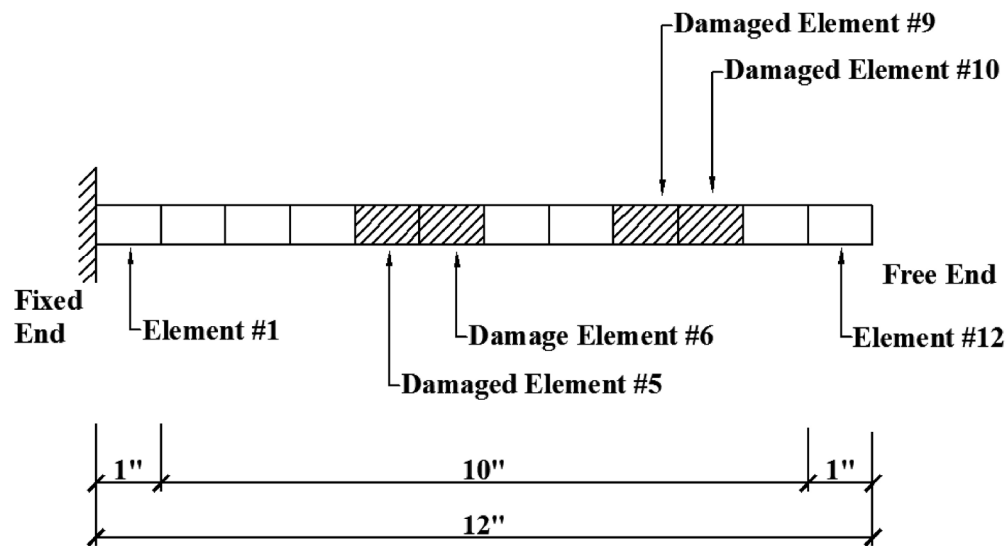


**Figure 5.1. Geometry, Damage Scenario, and Finite Element Discretization of the Rod**

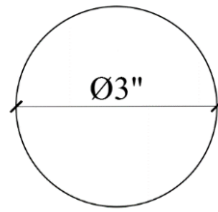


**Figure 5.2. Geometry of the Cross-Section of the Rod**

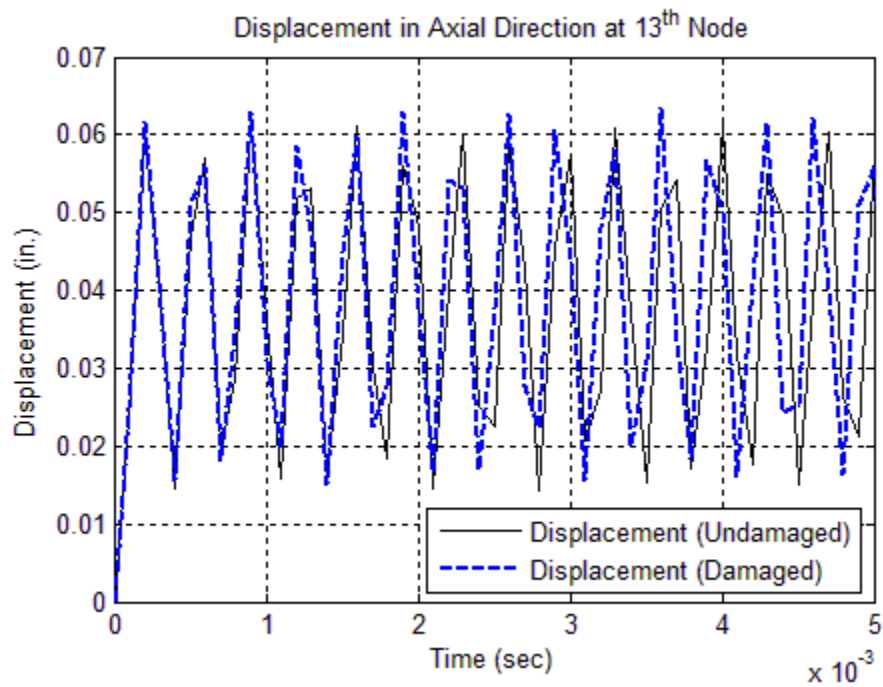


**Figure 5.3. Displacements in Axial Direction of the Node 13 of the Undamaged and Damaged Rods under the Given External Load**

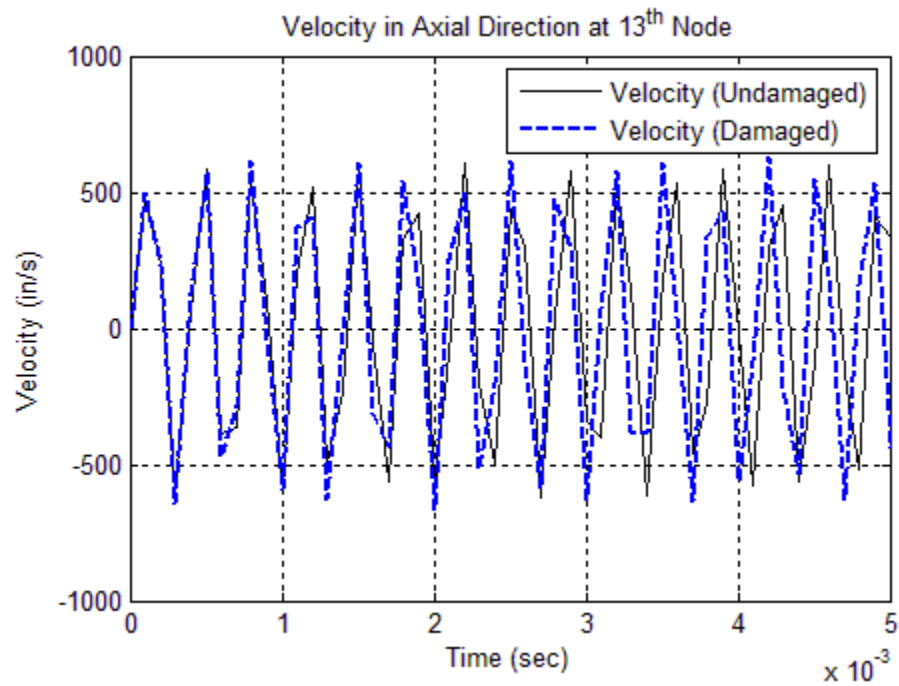


**Figure 5.4. Velocities of the Node 13 in Axial Direction of the Undamaged and Damaged Rods under the Given External Load**

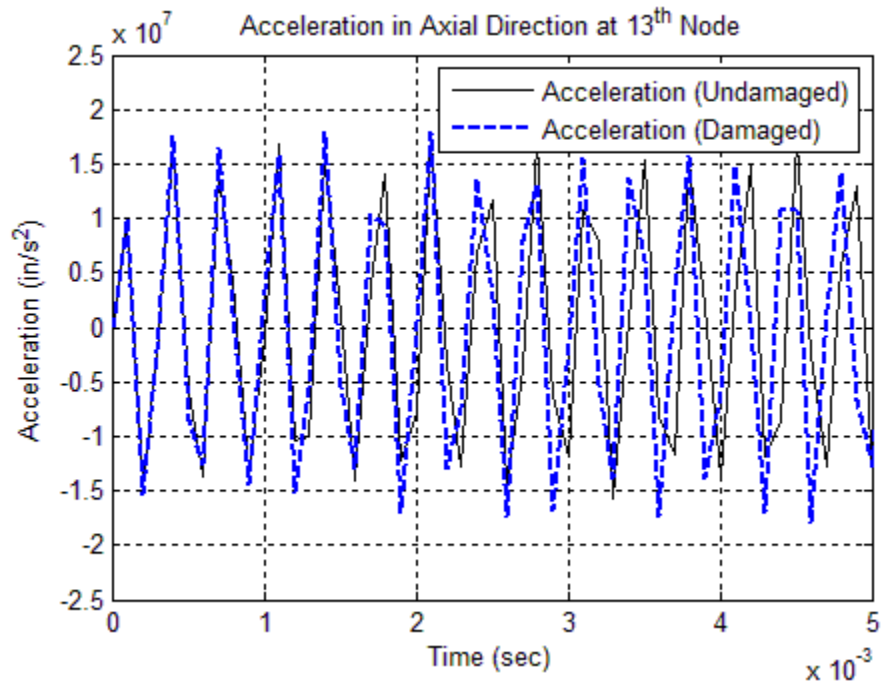


**Figure 5.5. Accelerations of the Node 13 in Axial Direction of the Undamaged and Damaged Rods under the Given External Load**

**Table 5.1. Damage Detection Results for the Rod under Axial and Torsional Vibrations**

Property	Damage Index ( $\beta_i$ , Estimated)	Damage Severity ( $\alpha_i$ , Estimated) (%)	Damage Index ( $\beta_i$ , Designed)
$m_2$	1.00	0.00	1.00
$m_4$	1.00	0.00	1.00
$m_6$	1.25	-20.00	1.25
$m_8$	1.00	0.00	1.00
$m_{10}$	1.25	-20.00	1.25
$m_{12}$	1.00	0.00	1.00
$k_1$	1.00	0.00	1.00
$k_2$	1.00	0.00	1.00
$k_3$	1.00	0.00	1.00
$k_4$	1.00	0.00	1.00
$k_5$	1.11	-10.00	1.11
$k_6$	1.11	-10.00	1.11
$k_7$	1.00	0.00	1.00
$k_8$	1.00	0.00	1.00
$k_9$	1.11	-10.00	1.11
$k_{10}$	1.11	-10.00	1.11
$k_{11}$	1.00	0.00	1.00
$k_{12}$	1.00	0.00	1.00

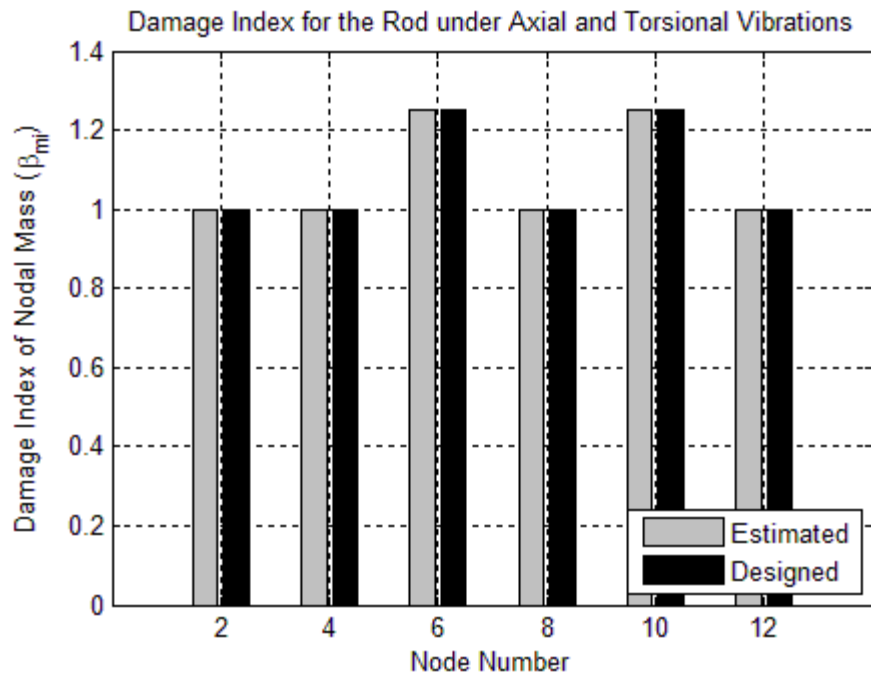


Figure 5.6. Damage Indices of Nodal Mass ( $\beta_m$ ) for the Rod under Axial and Torsional Vibrations

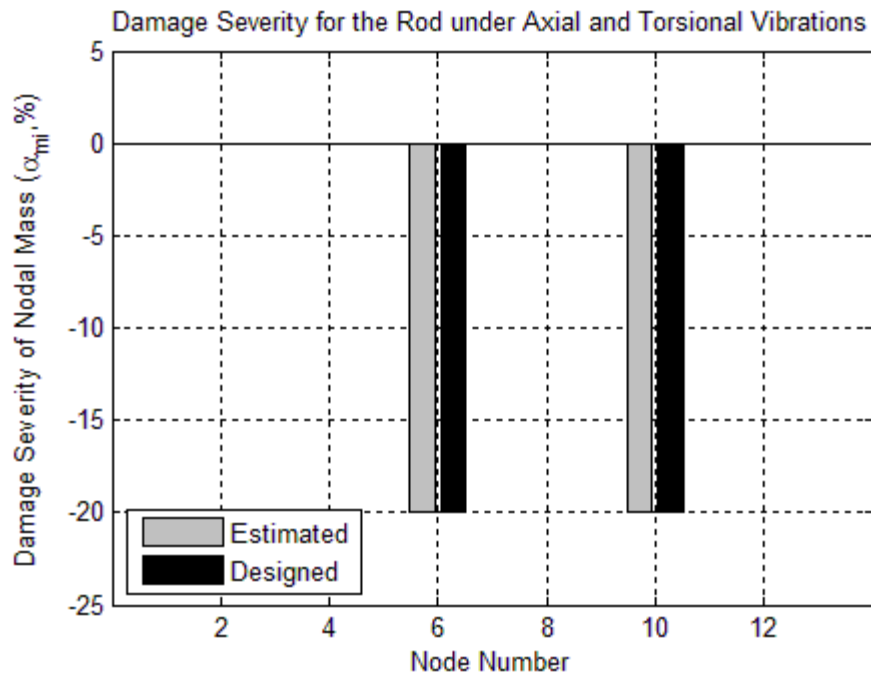


Figure 5.7. Damage Severities of Nodal Mass ( $\alpha_m$ ) for the Rod under Axial and Torsional Vibrations

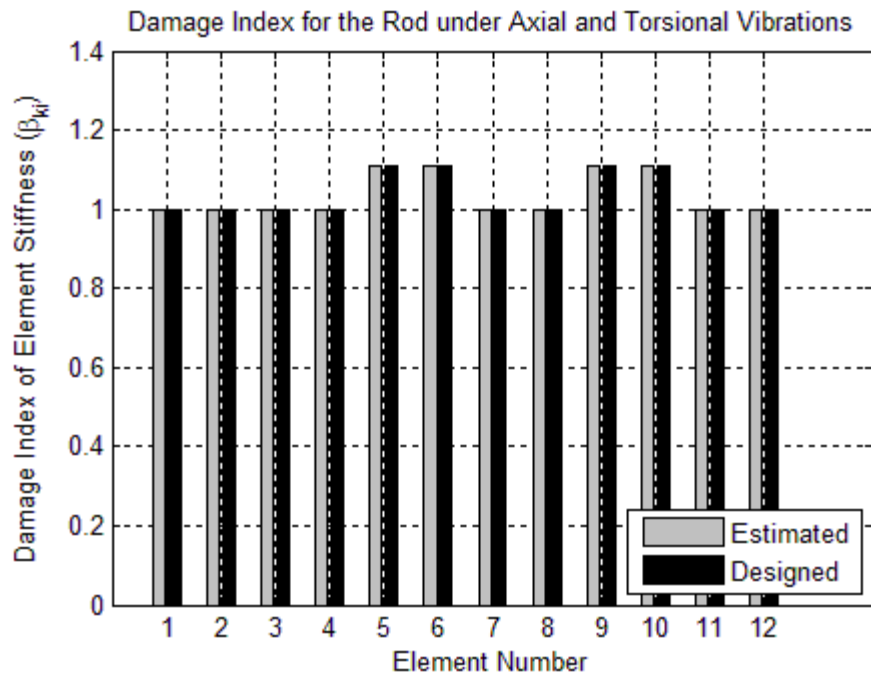


Figure 5.8. Damage Indices of Element Stiffness ( $\beta_{ki}$ ) for the Rod under Axial and Torsional Vibrations

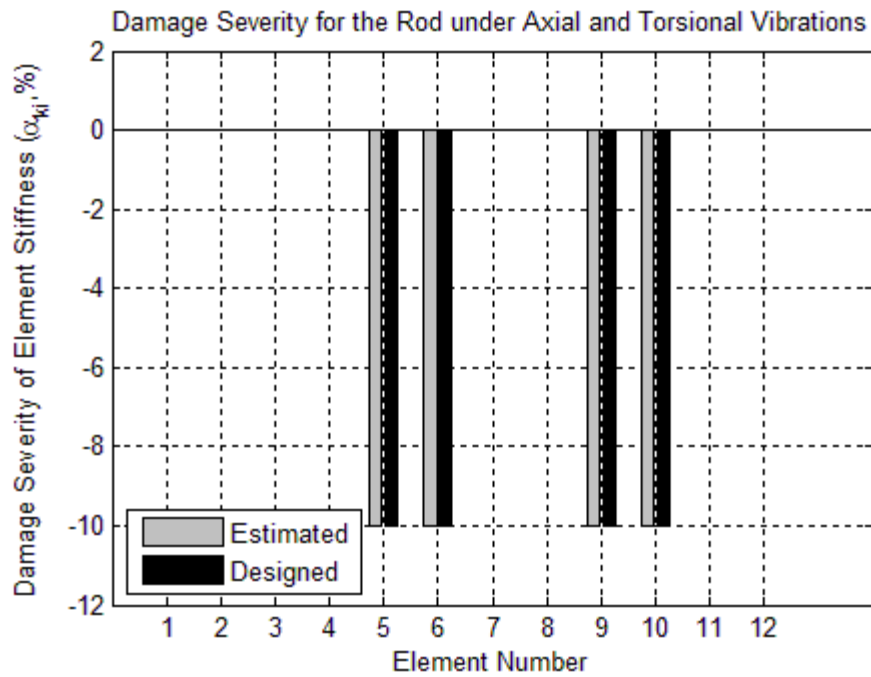


Figure 5.9. Damage Severities of Element Stiffness ( $\alpha_{ki}$ ) for the Rod under Axial and Torsional Vibrations

### 5.3 DAMAGE EVALUATION FOR A ROD AS A WHOLE SYSTEM

In Case #2, the same rod is used to evaluate the proposed theory. The geometry, damage scenario and finite element discretization under consideration are indicated in Figure 5.10. The geometry of the cross-section of the rod is shown in Figure 5.2. The modulus of elasticity ( $E$ ) of the material is 29,000 ksi. The modulus of elasticity in shear ( $G$ ) of the material is 11154 ksi. The Poisson's ratio of the material ( $\nu$ ) is 0.3. The torsional constant of the cross section of ( $J$ ) is 7.9522. The mass density of the material is  $7.345 \times 10^{-7}$  kip·sec<sup>2</sup>/in<sup>4</sup>. In this case, four elements with damaged mass and stiffness are studied.

The rod is meshed into 12 elements and has 13 equally spaced nodes. The length of each element is 1.0 inches. For illustrative purposes, typical elements are indicated in Figure 5.10. The damage is simulated by a ten percent (10%) reduction of the modulus of elasticity and twenty percent (20%) reduction of the mass of Elements 5, 6, 9, and 10.

For each node in the rod model, a dynamic force,  $100\cos(2\pi t)$ , is applied in only axial ( $x_1$ ) direction. Given the external load case, the displacement, velocity, and acceleration time histories are directly generated from SAP2000 using linear direct integration method. The computation step is 1E-4 seconds (10,000Hz) for total 0.2 seconds. The displacements, velocities and accelerations of Node 13 in both the undamaged and damaged rods were plotted in Figure 5.11, Figure 5.12, and Figure 5.13.

In this case, the computed velocity ( $\dot{x}(t)$ ) of each node in the undamaged case was used as the velocity used to compute power ( $\dot{\Delta}$ ) for both the undamaged and damaged cases. For all the nodes in the rod, the coefficient matrices ( $\mathbf{X}$ ) and known vector ( $\mathbf{Y}$ ) were constructed at one time by substituting the acceleration ( $\ddot{x}(t)$ ), velocity ( $\dot{x}(t)$ ),

displacement ( $x(t)$ ), and velocity used to compute power ( $\dot{\Delta}$ ) into Eq. 4.96 and Eq. 4.98. The coefficient damage index vector,  $\beta$ , related to the each element in the rod was computed using Eq. 4.99. Then the damage indices for mass and stiffness are computed using Eqs. 4.100 through 4.106. The damage severities for mass and stiffness are computed using Eq. 2.13. For the whole rod, the above process is performed only once. The estimated damage indices and the designed damage indices for each physical property are listed in Table 5.2 and are plotted in Figure 5.14 for nodal mass and Figure 5.16 for element stiffness. The estimated damage severities and the designed damage severities for each physical property are plotted in Figure 5.15 for nodal mass and Figure 5.17 for element stiffness. Because the proposed method is applied at the each node of the whole rod, thus all nodes, except for the fixed node, were taken into consideration (i.e. Nodes 1 through 12). Comparing the estimated damage indices with the designed damage indices, the proposed method can accurately locate and size multiple damage in a rod with axial and torsional vibrations.



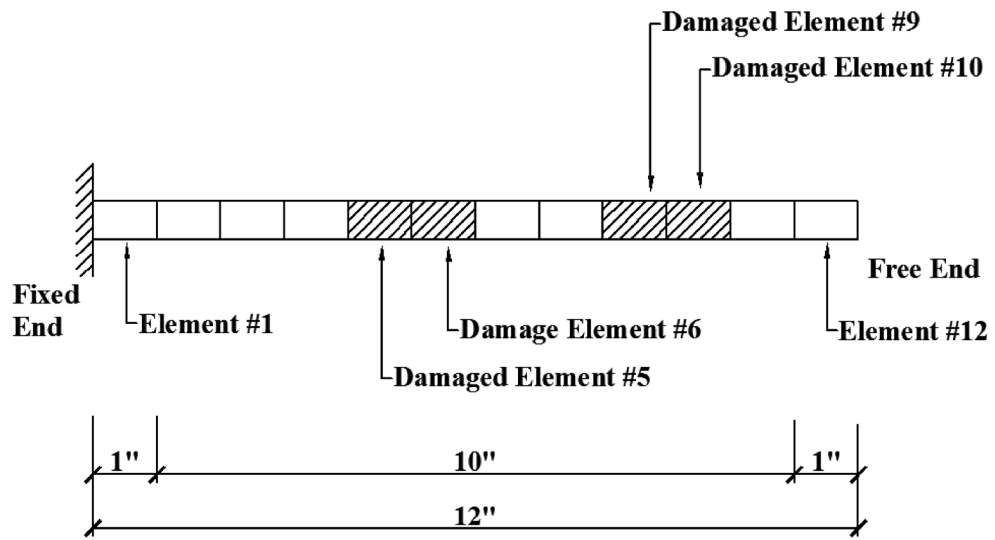


Figure 5.10. Geometry, Damage Scenario, and Finite Element Discretization of the Rod

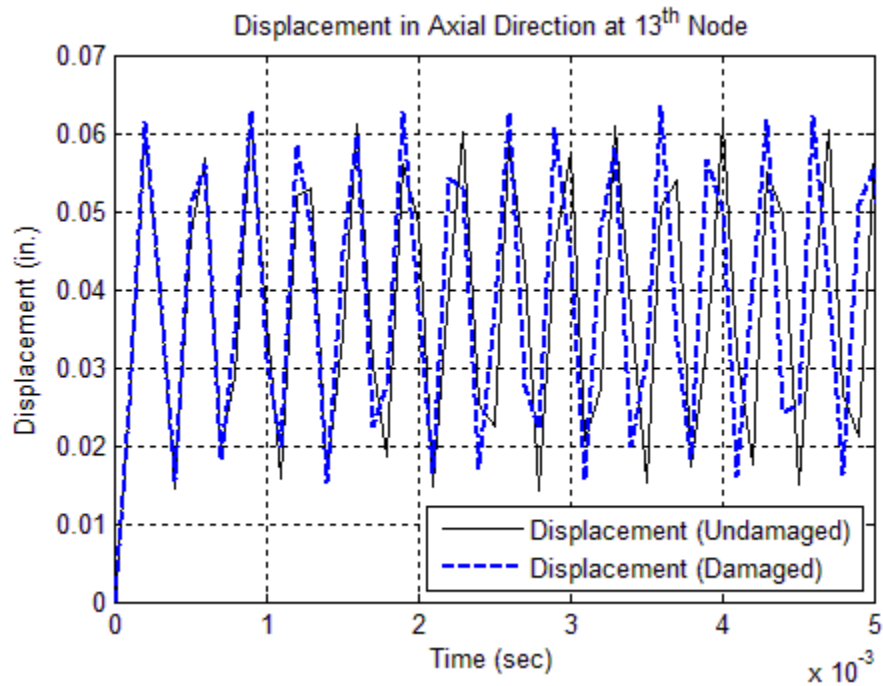
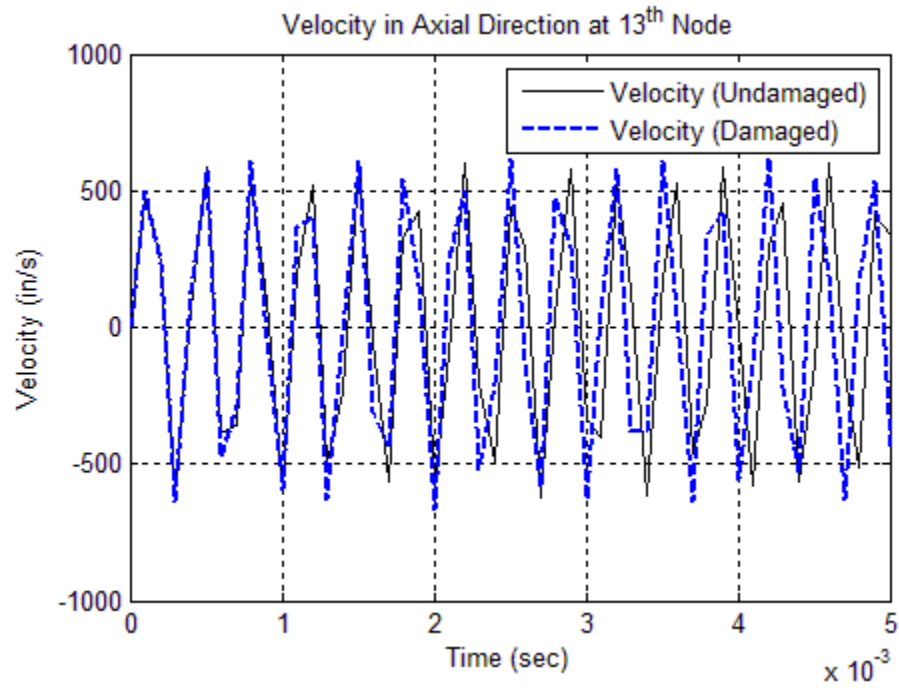
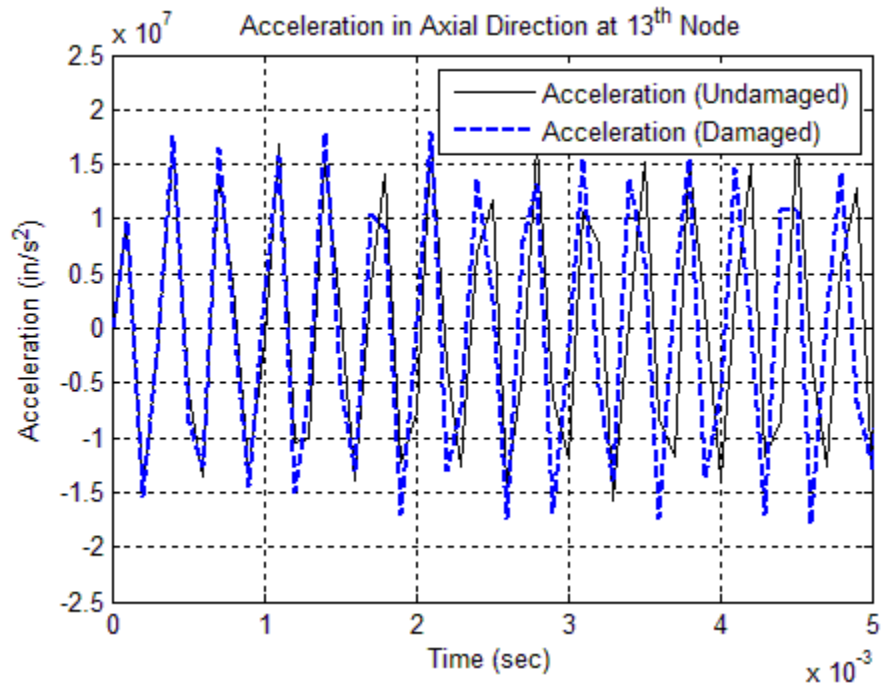


Figure 5.11. Displacements in Axial Direction of Node 13 of the Undamaged and Damaged Rods under the Given External Load



**Figure 5.12. Velocities of Node 13 in Axial Direction of the Undamaged and Damaged Rods under the Given External Load**



**Figure 5.13. Accelerations of Node 13 in Axial Direction of the Undamaged and Damaged Rods under the Given External Load**

**Table 5.2. Damage Detection Results for the Analysis of Rod under Axial As a Whole**

<b>Property</b>	<b>Damage Index (<math>\beta_i</math>, Estimated)</b>	<b>Damage Severity (<math>\alpha_i</math>, Estimated) (%)</b>	<b>Damage Index (<math>\beta_i</math>, Designed)</b>
$m_1$	1.00	0.00	1.00
$m_2$	1.00	0.00	1.00
$m_3$	1.00	0.00	1.00
$m_4$	1.11	-10.00	1.11
$m_5$	1.25	-20.00	1.25
$m_6$	1.11	-10.00	1.11
$m_7$	1.00	0.00	1.00
$m_8$	1.11	-10.00	1.11
$m_9$	1.25	-20.00	1.25
$m_{10}$	1.11	-10.00	1.11
$m_{11}$	1.00	0.00	1.00
$m_{12}$	1.00	0.00	1.00
$k_1$	1.00	0.00	1.00
$k_2$	1.00	0.00	1.00
$k_3$	1.00	0.00	1.00
$k_4$	1.00	0.00	1.00
$k_5$	1.11	-10.00	1.11
$k_6$	1.11	-10.00	1.11
$k_7$	1.00	0.00	1.00
$k_8$	1.00	0.00	1.00
$k_9$	1.11	-10.00	1.11
$k_{10}$	1.11	-10.00	1.11
$k_{11}$	1.00	0.00	1.00
$k_{12}$	1.00	0.00	1.00

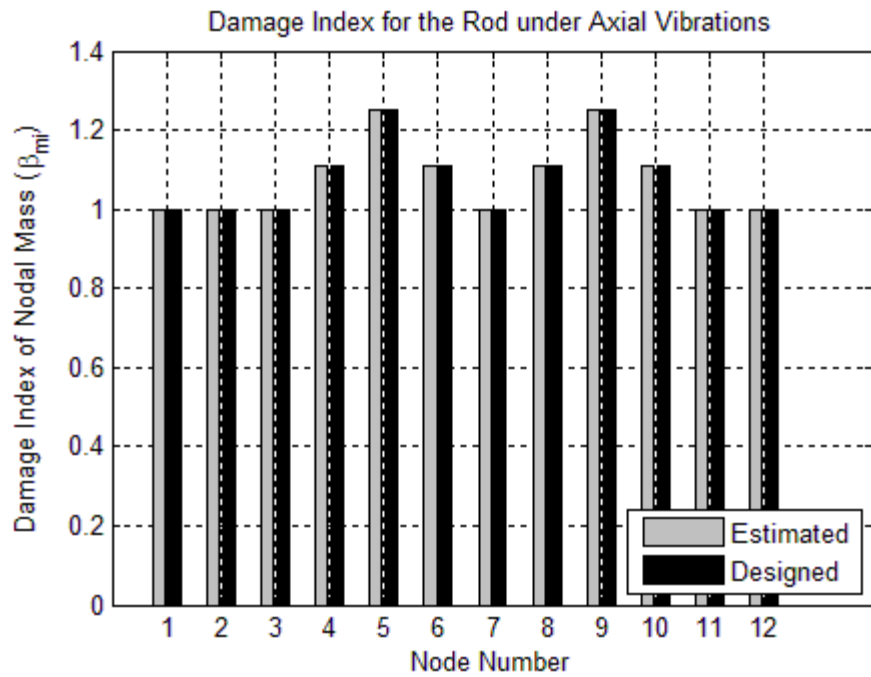


Figure 5.14. Damage Indices of Nodal Mass ( $\beta_{mi}$ ) for the Rod under Axial and Torsional Vibrations

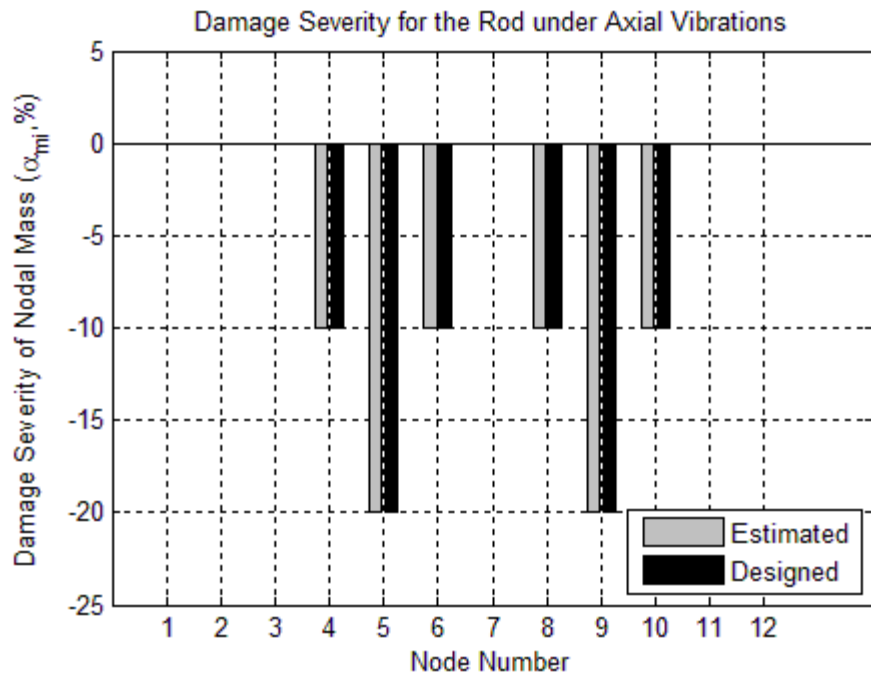


Figure 5.15. Damage Severities of Nodal Mass ( $\alpha_{mi}$ ) for the Rod under Axial and Torsional Vibrations

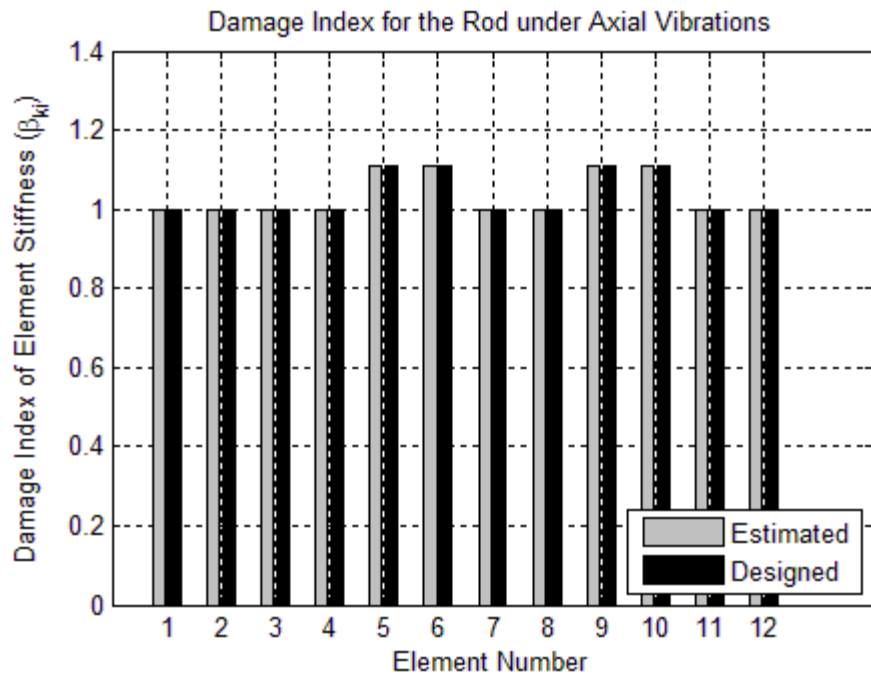


Figure 5.16. Damage Indices of Element Stiffness ( $\beta_{ki}$ ) for the Rod under Axial and Torsional Vibrations

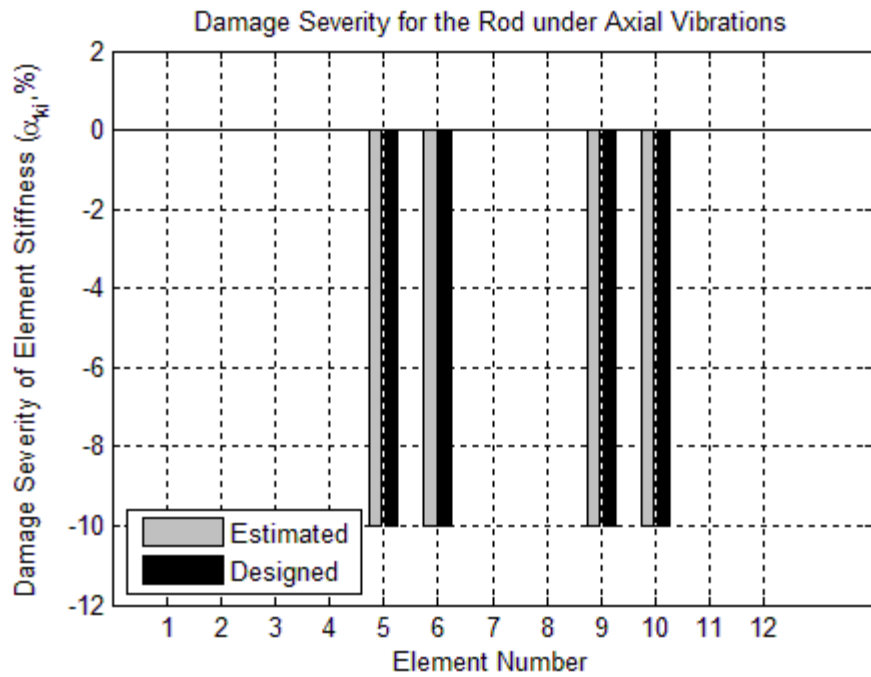


Figure 5.17. Damage Severities of Element Stiffness ( $\alpha_{ki}$ ) for the Rod under Axial and Torsional Vibrations

#### 5.4 DAMAGE EVALUATION FOR AN EULER-BERNOULLI BEAM

In Case #3, a propped cantilever is used to evaluate the proposed theory. The geometry, damage scenario, and load case under consideration are indicated in Figure 5.18. The geometry of the cross-section of the cantilever is shown in Figure 5.19. The modulus of elasticity ( $E$ ) of the material is 29,000 ksi. The mass density of the material is  $7.345 \times 10^{-7}$  kip·sec<sup>2</sup>/in<sup>4</sup>.

The propped cantilever is meshed into 12 elements and has 13 equally spaced nodes. The length of each element is 1.0 inches. For illustrative purposes, typical elements are indicated in Figure 5.18. Four elements with damaged mass and stiffness are studied. The damage is simulated by a ten percent (10%) reduction of the modulus of elasticity and twenty percent (20%) reduction of the mass of Element 5 and Element 6 and a five percent (5%) reduction of the modulus of elasticity and ten percent (10%) reduction of the mass of Element 11 and Element 12 of the beam.

For each node of the propped cantilever beam, a dynamic point load,  $10\cos(2\pi t)$ , is applied in transverse direction at each node. Given the external load case, the displacement, velocity, and acceleration time histories are directly generated from SAP2000 using linear direct integration method. The computation step is 1E-4 seconds (10,000 Hz) for total 0.2 seconds. The deflections, velocities in transverse direction and accelerations in transverse direction of Node 7 in both the undamaged and damaged propped cantilever were plotted in Figure 5.20, Figure 5.21, and Figure 5.22.

In this case, the computed velocity ( $\dot{x}(t)$ ) of each node in the undamaged case was used as the velocity used to compute power ( $\dot{\Delta}$ ) for both the undamaged and damaged cases.

For every two nearby elements, the coefficient matrices (' $\mathbf{X}$ ') and known vector (' $\mathbf{Y}$ ') were constructed by substituting the acceleration ( $\ddot{x}(t)$ ), velocity ( $\dot{x}(t)$ ), displacement ( $x(t)$ ), and velocity used to compute power ( $\dot{\Delta}$ ) into Eq. 4.138 and Eq. 4.140. The coefficient damage index vector,  $\beta$ , related to the two nearby elements was computed using Eq. 4.141. Then the damage indices for mass and stiffness are computed using Eqs. 4.142 through 4.144. The damage severities for mass and stiffness are computed using Eq. 2.13. For each two nearby elements, the above process is performed. For simplicity purposes, no overlap element is used. Thus, the proposed theory is only applied to six pairs of elements. The estimated damage indices and the designed damage indices for each physical property are listed in Table 5.3 and are plotted in Figure 5.23 for nodal mass and Figure 5.25 for element stiffness. The estimated damage severities and the designed damage severities for each physical property are plotted in Figure 5.24 for nodal mass and Figure 5.26 for element stiffness. Comparing the estimated damage indices with the designed damage indices, the proposed method can accurately locate and size multiple damage in a beam with bending vibrations.

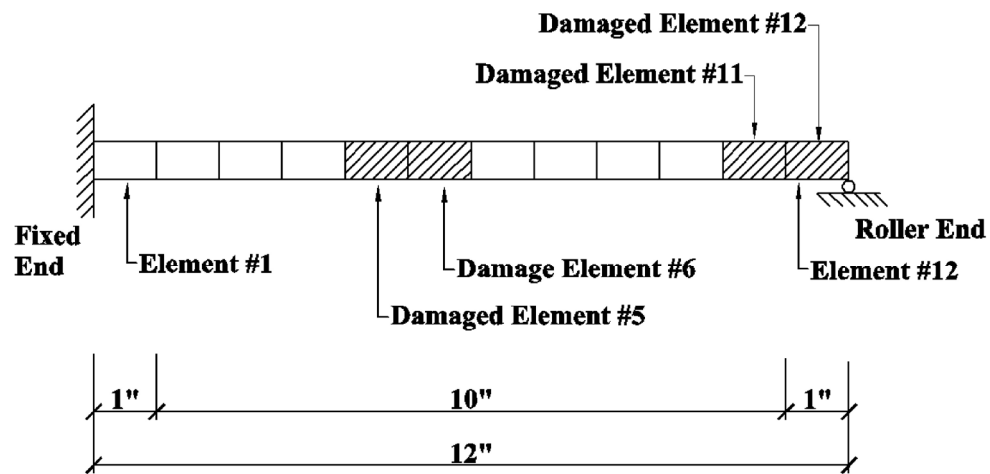


Figure 5.18. Geometry, Damage Scenario, and Load Case for the Propped Cantilever

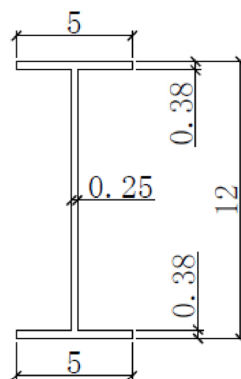
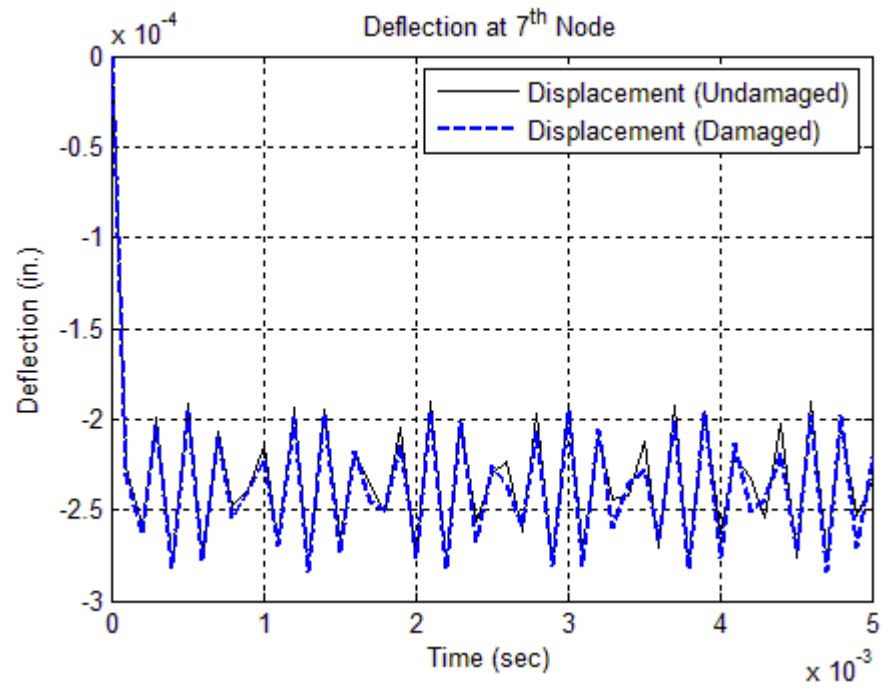
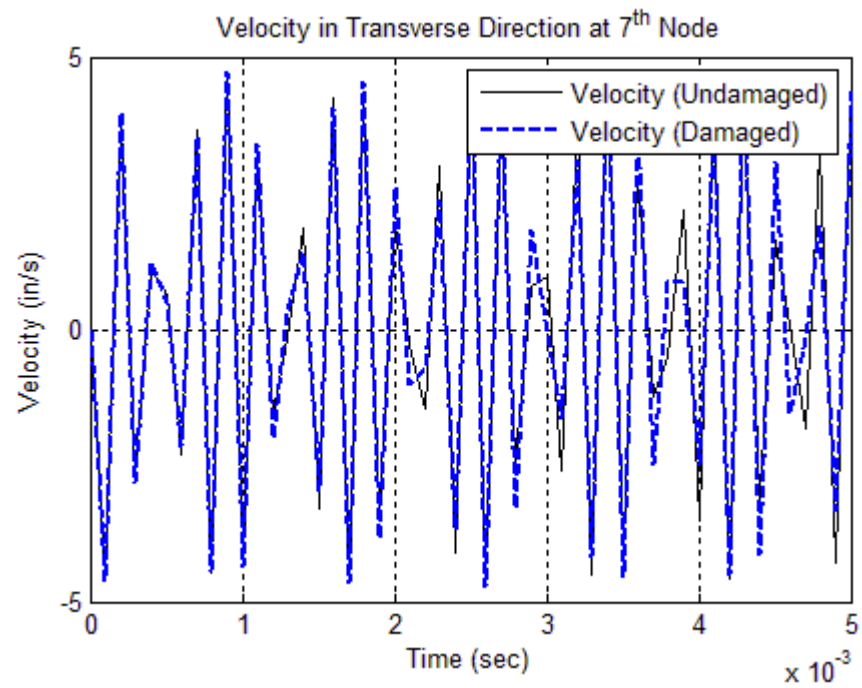


Figure 5.19. Geometry of the Cross-Section of the I Beam





**Figure 5.20. Deflection of the Node 7 of the Undamaged and Damaged Cases under the Given External Load**



**Figure 5.21. Velocities in Transverse Direction of the Node 7 of the Undamaged and Damaged Cases under the Given External Load**

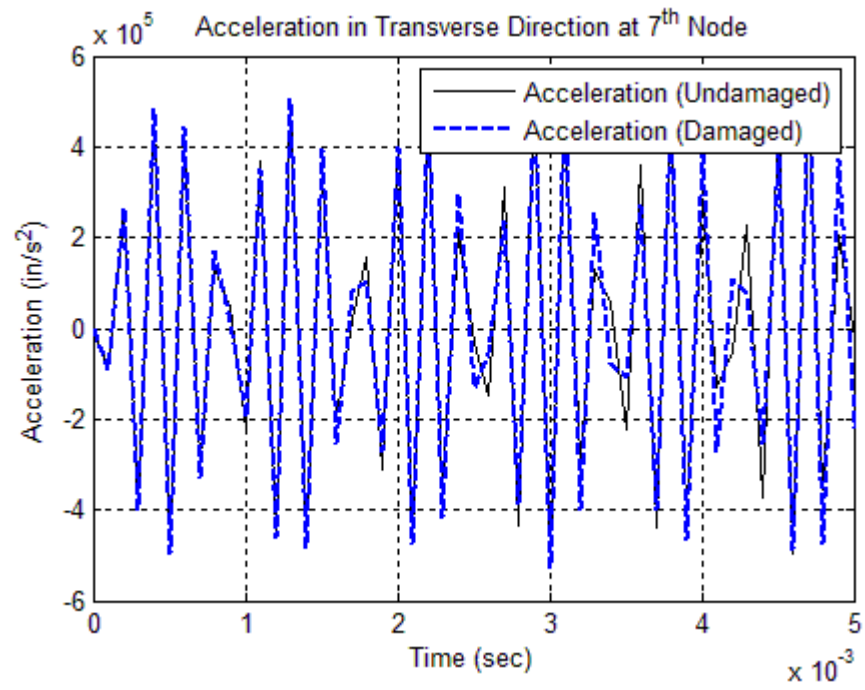


**Figure 5.22. Accelerations in Transverse Direction of the Node 7 of the Undamaged and Damaged Cases under the Given External Load**

**Table 5.3. Damage Detection Results for the Propped Cantilever**

<b>Property</b>	<b>Damage Index (<math>\beta_i</math>, Estimated)</b>	<b>Damage Severity (<math>\alpha_i</math>, Estimated) (%)</b>	<b>Damage Index (<math>\beta_i</math>, Designed)</b>
$m_2$	1.000	0.000	1.000
$m_4$	1.000	0.000	1.000
$m_6$	1.250	-20.000	1.250
$m_8$	1.000	0.000	1.000
$m_{10}$	1.000	0.000	1.000
$m_{12}$	1.111	-10.000	1.111
$k_1$	1.000	0.000	1.000
$k_2$	1.000	0.000	1.000
$k_3$	1.000	0.000	1.000
$k_4$	1.000	0.000	1.000
$k_5$	1.111	-10.000	1.111
$k_6$	1.111	-10.000	1.111
$k_7$	1.000	0.000	1.000
$k_8$	1.000	0.000	1.000
$k_9$	1.000	0.000	1.000
$k_{10}$	1.000	0.000	1.000
$k_{11}$	1.053	-5.000	1.053
$k_{12}$	1.053	-5.000	1.053

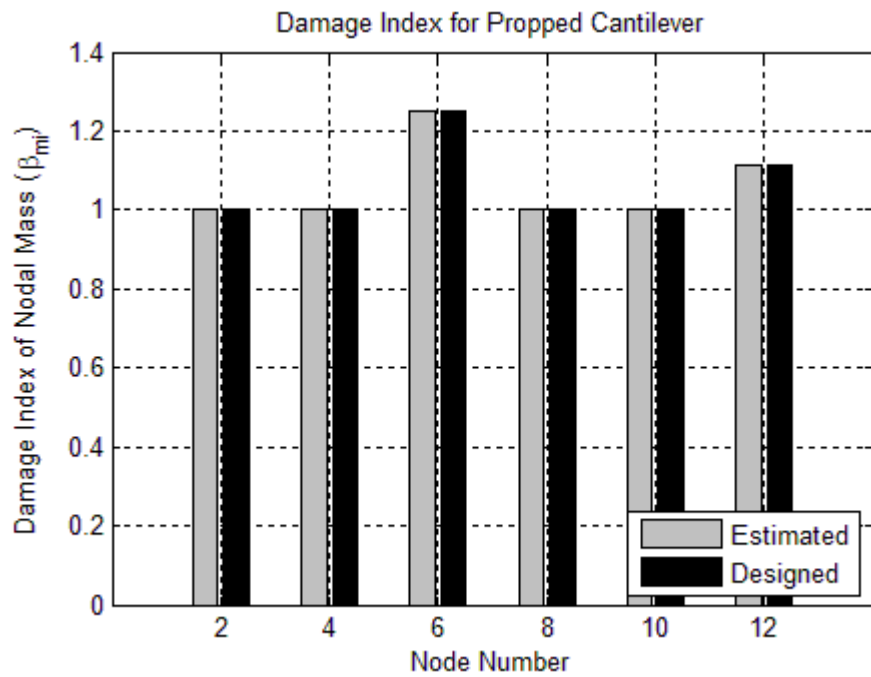


Figure 5.23. Damage Indices of Nodal Mass ( $\beta_{mi}$ ) for the Propped Cantilever

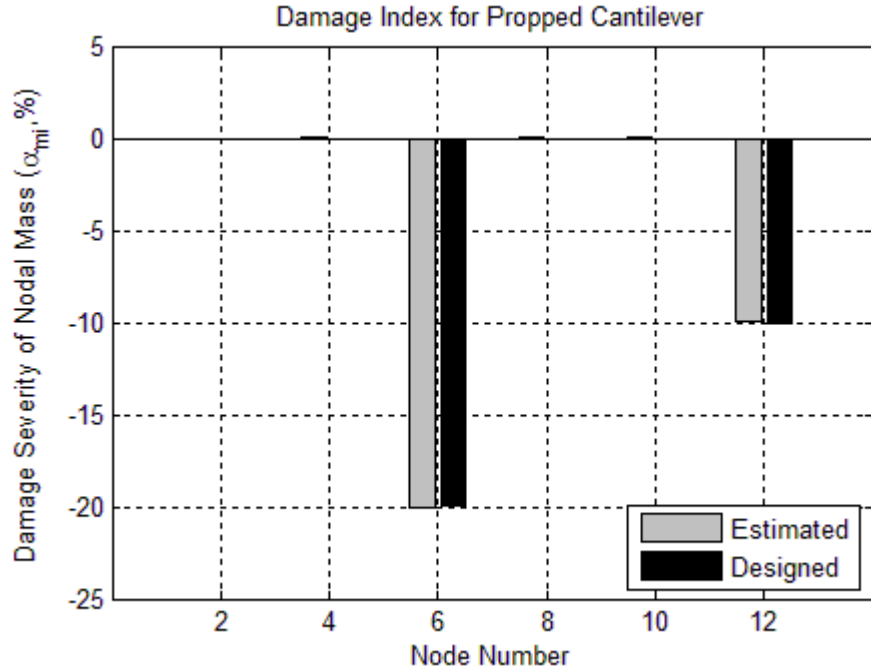


Figure 5.24. Damage Severities of Nodal Mass ( $\alpha_{mi}$ ) for the Propped Cantilever

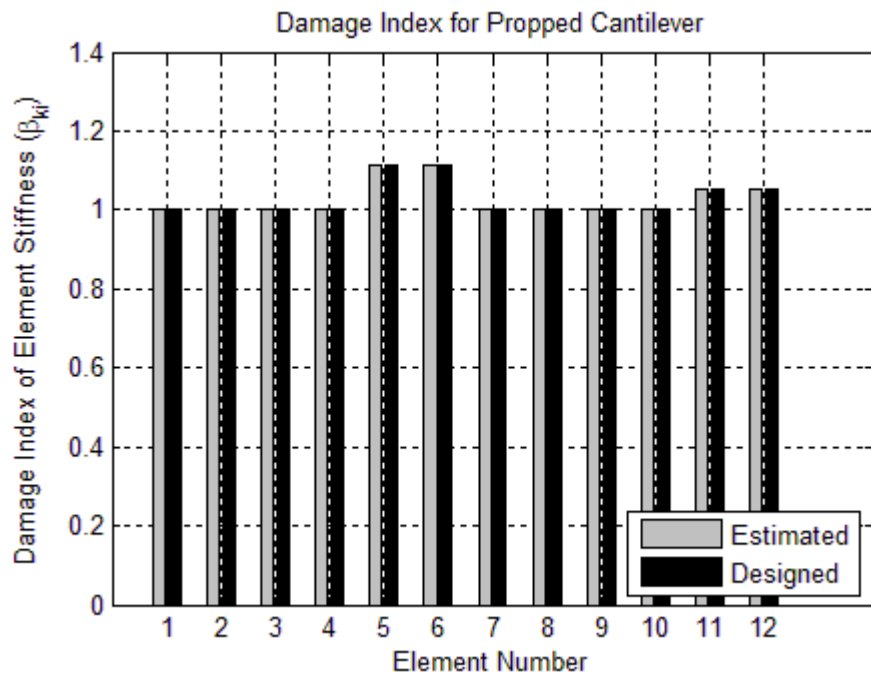


Figure 5.25. Damage Indices of Element Stiffness ( $\beta_{ki}$ ) for the Propped Cantilever

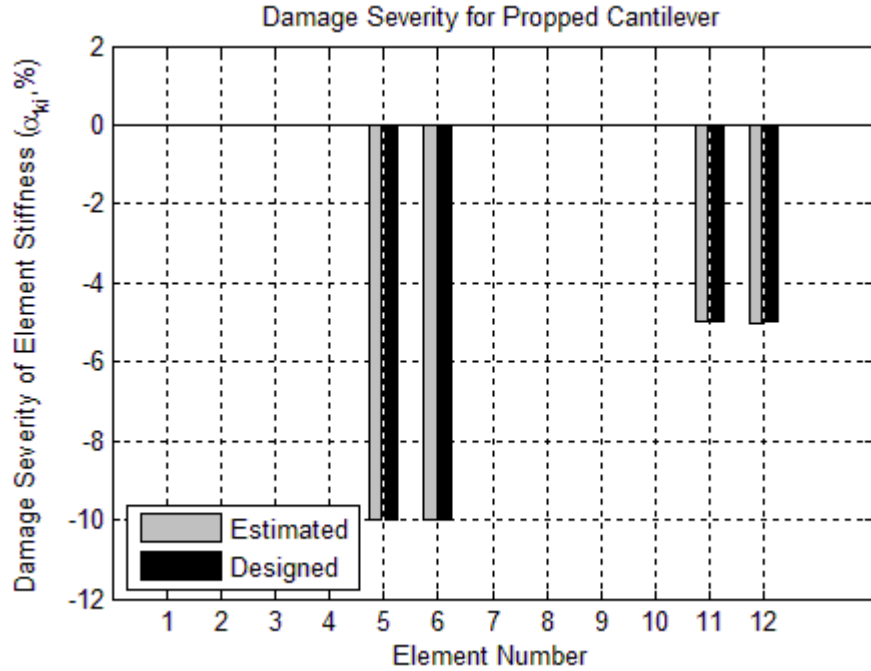


Figure 5.26. Damage Severities of Element Stiffness ( $\alpha_{ki}$ ) for the Propped Cantilever

## 5.5 DAMAGE EVALUATION FOR A PLAIN FRAME

In Case #4, a two-bay frame is used to evaluate the proposed theory. The structure includes three types of members: a continuous beam, three columns, and elastic isolators in between. Three elastic isolators are fixed to the beam and each column is fixed to the end of each isolator. The elastic isolators are simulated by beam elements with smaller cross section, shown in Figure 5.28. The cross sections for the continuous beam and the columns are the same and the geometry of the cross section is shown in Figure 5.19. The material properties for the all three types of members are the same. The modulus of elasticity ( $E$ ) of the material is 29,000 ksi. The mass density of the material is  $7.345 \times 10^{-7}$  kip·sec<sup>2</sup>/in<sup>4</sup>. A cosine external point load,  $10\cos(2\pi t)$  kips, is applied on each node of the frame. The geometry of the structure and the damage scenario are shown in Figure 5.27.

The damage scenario for this case is as follows: (1) both of the two spans of the continuous beam are damaged; (2) the two left isolators are damaged; and (3) the two left columns are damaged. The right isolator and right column are intact. The damage are simulated by a ten percent (10%) reduction of the modulus of elasticity and twenty percent (20%) reduction of the mass of the damaged elements. The damaged elements in the damaged two-bay frame include: (1) Element 43, Element 44, Element 103 and Element 104 on the continuous beam; (2) all elements in the left and middle isolators (i.e. six elements for each isolator); (3) Element 43 and Element 44 in each of the left two columns. The damaged isolators are denoted by “Damaged Isolator A” and “Damaged Isolator B” and the damaged elements on both the beam (43<sup>rd</sup>, 44<sup>th</sup>, 103<sup>rd</sup> and 104<sup>th</sup>) and the two columns (43<sup>rd</sup> and 44<sup>th</sup>) are indicated as a solid black in Figure 5.27.

The beam is meshed into 120 elements and has 121 equally spaced nodes. Each of the

elastic isolators is meshed into 6 elements and has 7 equally spaced nodes. Each column is meshed into 60 elements and has 61 equally spaced nodes. The length of each element in the three types of members is 2.0 inches. For illustrative purposes, several typical elements are indicated in Figure 5.27.

Given the external load case, the displacement, velocity, and acceleration time histories are directly generated from SAP2000 using linear direct integration method. The computation step is  $1\text{E-}4$  seconds (10,000 Hz) for total 0.01 seconds. The deflections, velocities in transverse direction and accelerations in transverse direction of Node 61 in both the undamaged and damaged propped cantilever were plotted in Figure 5.29, Figure 5.30, and Figure 5.31. (Note, the two-bay frame is a linearly elastic frame)

In this case, the computed velocity ( $\dot{x}(t)$ ) of each node in the undamaged case was used as the velocity used to compute power ( $\dot{\Delta}$ ) for both the undamaged and damaged cases. For every two nearby elements, the coefficient matrices ('X') and known vector ('Y') were constructed by substituting the acceleration ( $\ddot{x}(t)$ ), velocity ( $\dot{x}(t)$ ), displacement ( $x(t)$ ), and velocity used to compute power ( $\dot{\Delta}$ ) into Eq. 4.177 and Eq. 4.179. The coefficient damage index vector,  $\beta$ , related to the two nearby elements was computed using Eq. 4.180. Then the damage indices for mass and stiffness are computed using Eqs. 4.181 through 4.183. The damage severities for mass and stiffness are computed using Eq. 2.13. For each two nearby elements, the above process is performed. The estimated damage indices for nodal mass and element stiffness for the continuous beam are plotted in Figure 5.32 and Figure 5.34, respectively. The estimated damage severities for nodal mass and element stiffness for the continuous beam are plotted in Figure 5.33 and Figure

5.35, respectively.

The estimated damage indices for nodal mass and element stiffness for the Isolator and Column A are plotted in Figure 5.36 and Figure 5.38, respectively. The estimated damage severities for nodal mass and element stiffness for the Isolator and Column A are plotted in Figure 5.37 and Figure 5.39, respectively.

The estimated damage indices for nodal mass and element stiffness for the Isolator and Column B are plotted in Figure 5.40 and Figure 5.42, respectively. The estimated damage severities for nodal mass and element stiffness for the Isolator and Column B are plotted in Figure 5.41 and Figure 5.43, respectively.

The estimated damage indices for nodal mass and element stiffness for the Isolator and Column C are plotted in Figure 5.44 and Figure 5.46, respectively. The estimated damage severities for nodal mass and element stiffness for the Isolator and Column C are plotted in Figure 5.45 and Figure 5.47, respectively.

Comparing the estimated damage indices with the designed damage indices, the proposed method can accurately locate and size multiple damage in a two-bay frame.



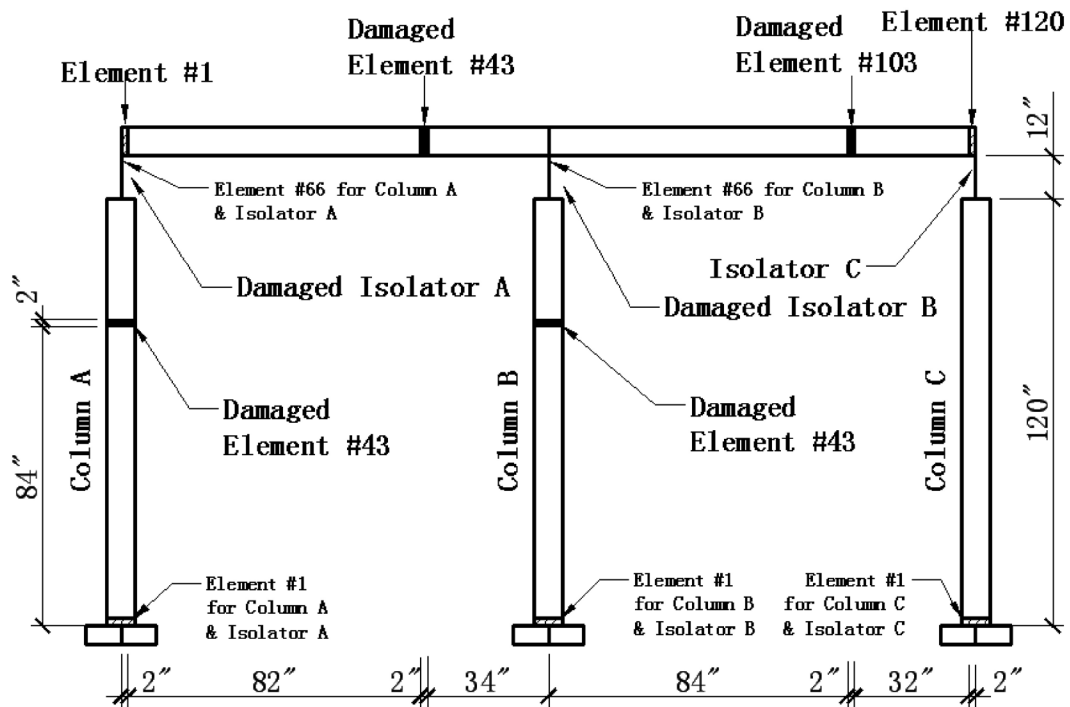


Figure 5.27. Geometry, Damage Scenario, and Finite Element Discretization for the Two-Bay Frame

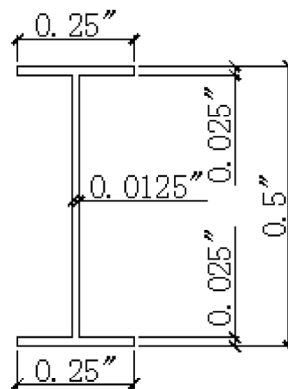
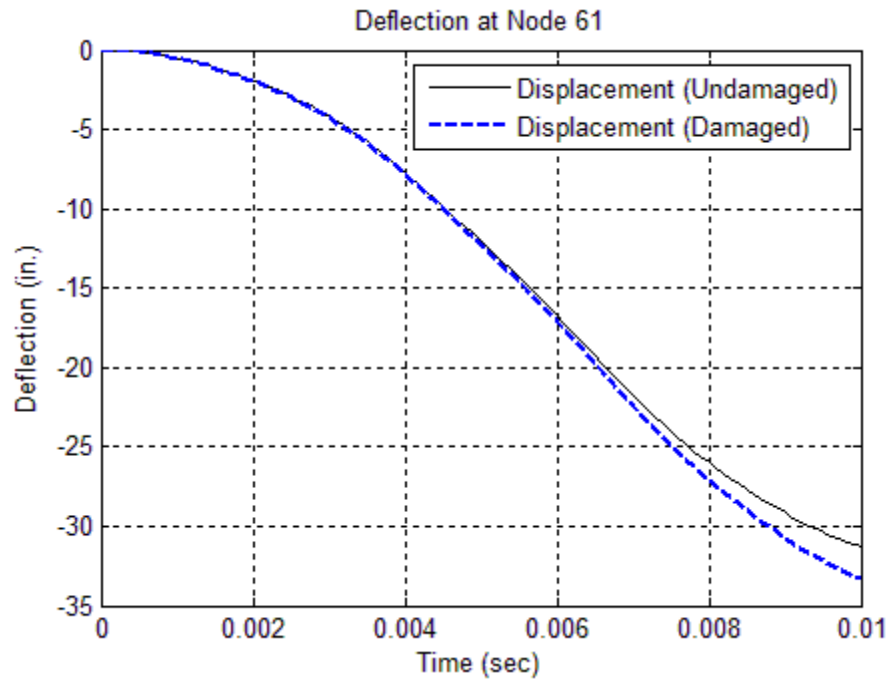
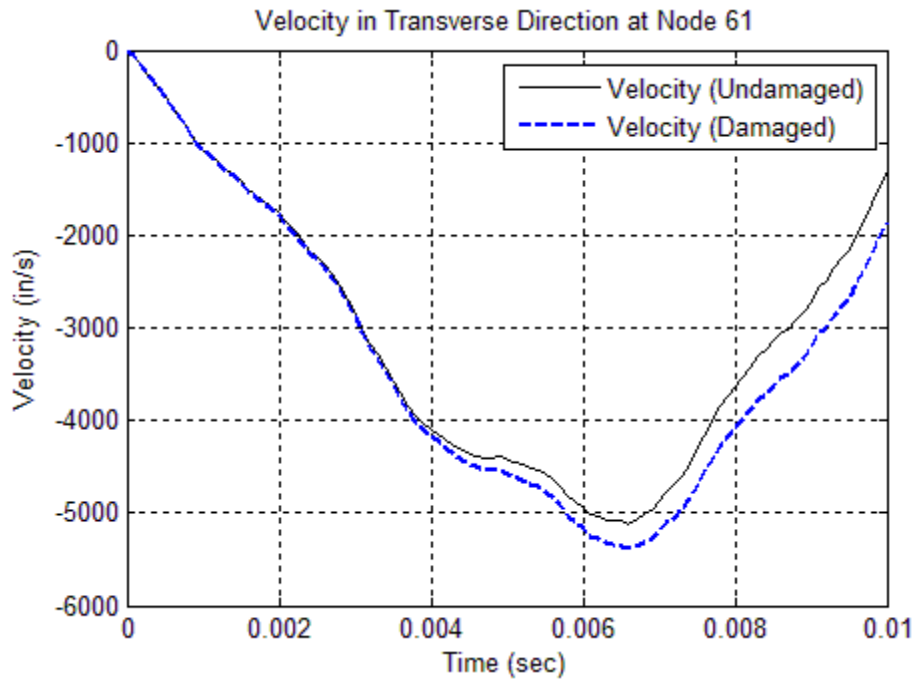


Figure 5.28. Cross Sectional Geometries of the Three Elastic Isolators



**Figure 5.29. Displacements of the Node 61 on the Continuous Beam for Both the Undamaged and Damaged Cases under the Given External Load**



**Figure 5.30. Velocities of the Node 61 on the Continuous Beam for Both the Undamaged and Damaged Cases under the Given External Load**

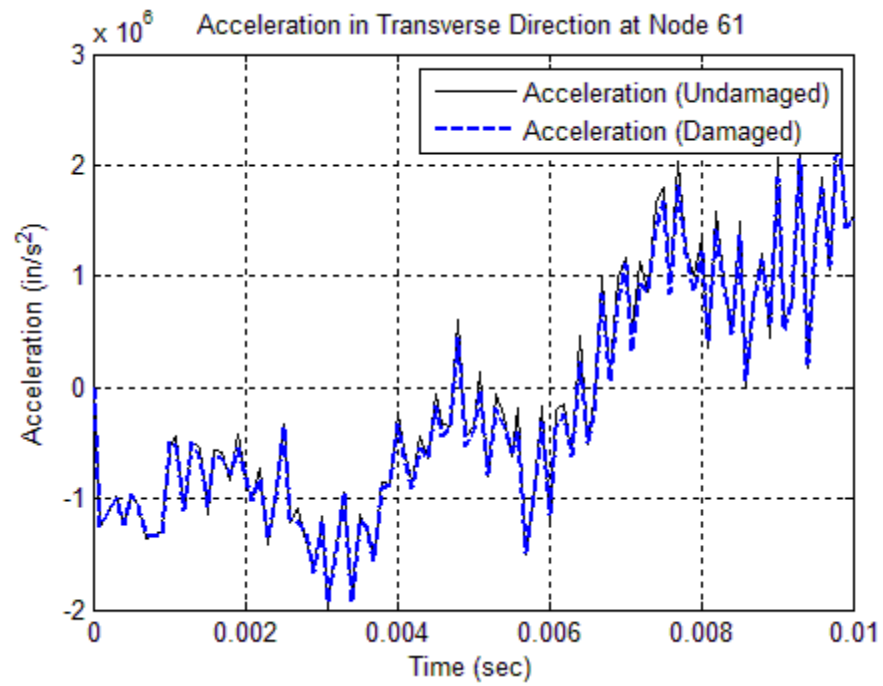


Figure 5.31. Accelerations of the Node 61 on the Continuous Beam for Both the Undamaged and Damaged Cases under the Given External Load

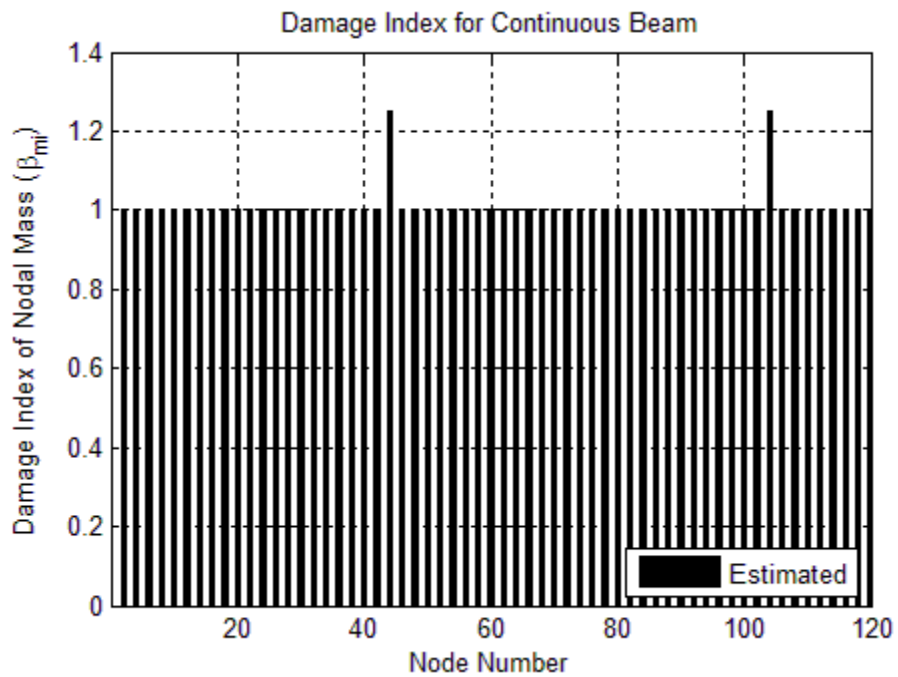


Figure 5.32. Damage Indices of Nodal Mass ( $\beta_{mi}$ ) for the Continuous Beam from the Two-Bay Frame

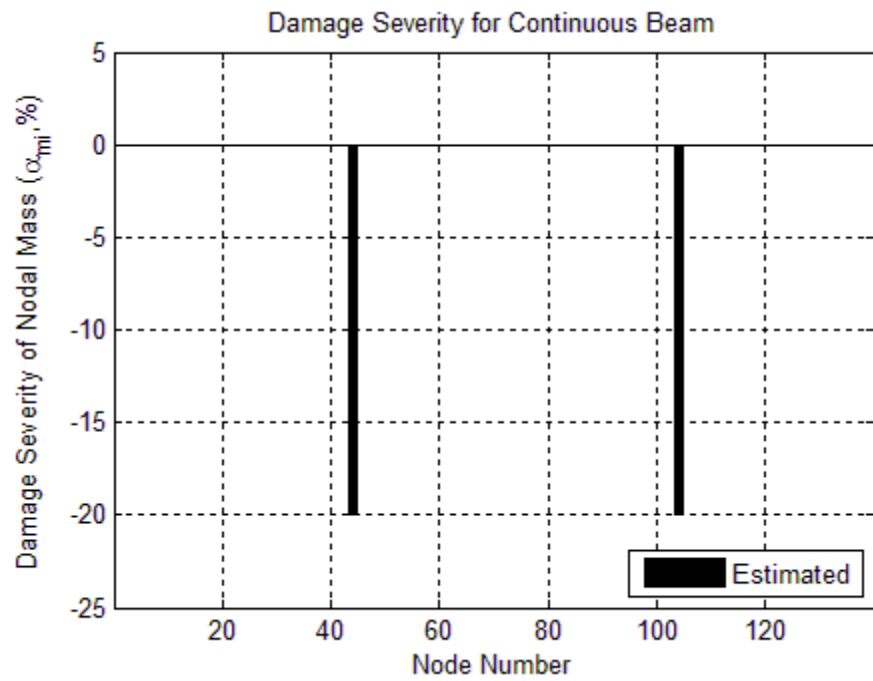


Figure 5.33. Damage Severities of Nodal Mass ( $\alpha_{mi}$ ) for the Continuous Beam from the Two-Bay Frame

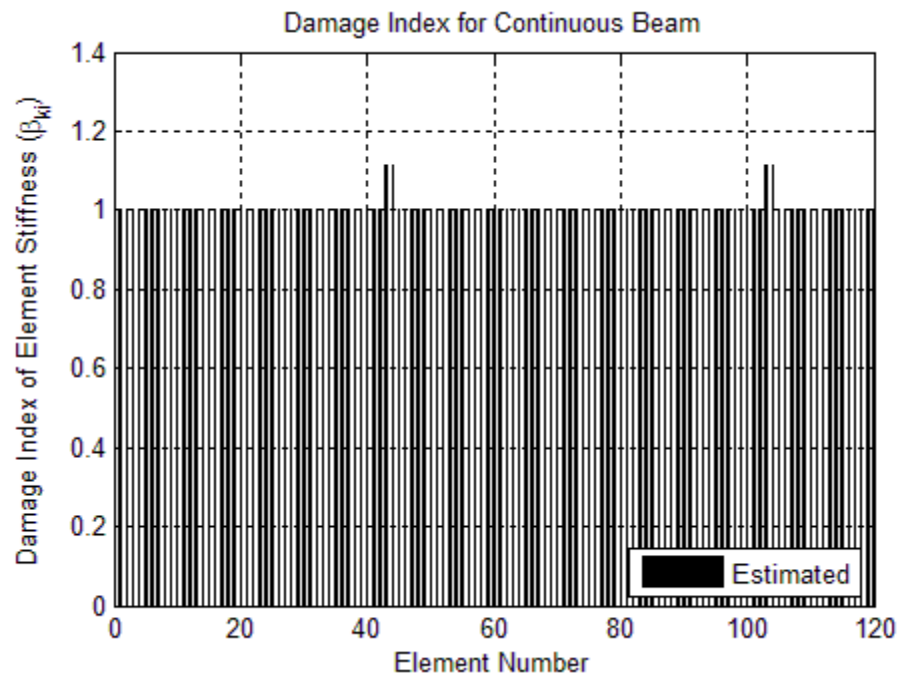


Figure 5.34. Damage Indices of Element Stiffness ( $\beta_{ki}$ ) for the Continuous Beam from the Two-Bay Frame

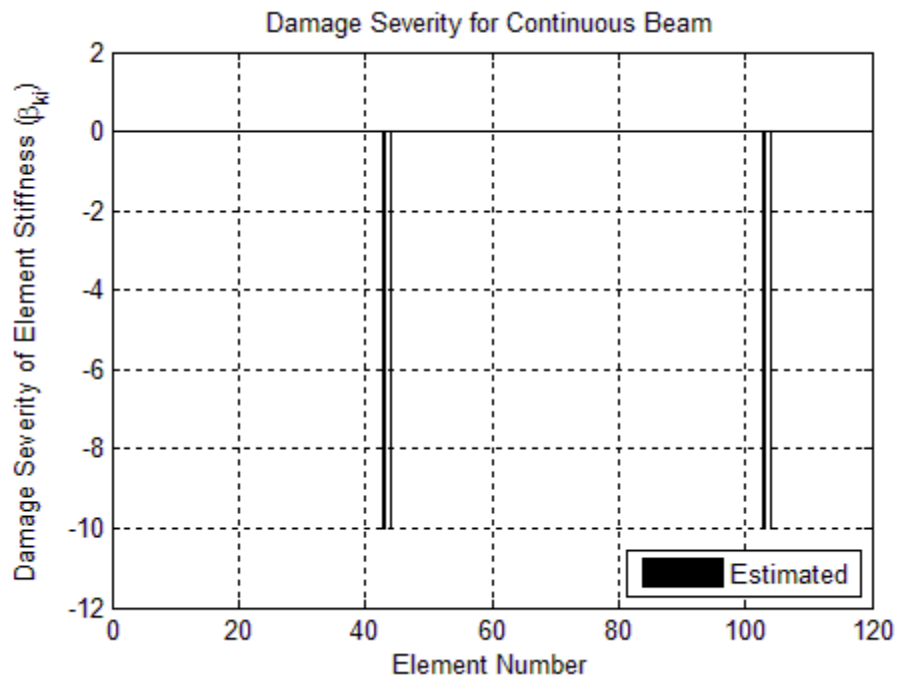


Figure 5.35. Damage Severities of Element Stiffness ( $\beta_{ki}$ ) for the Continuous Beam from the Two-Bay Frame

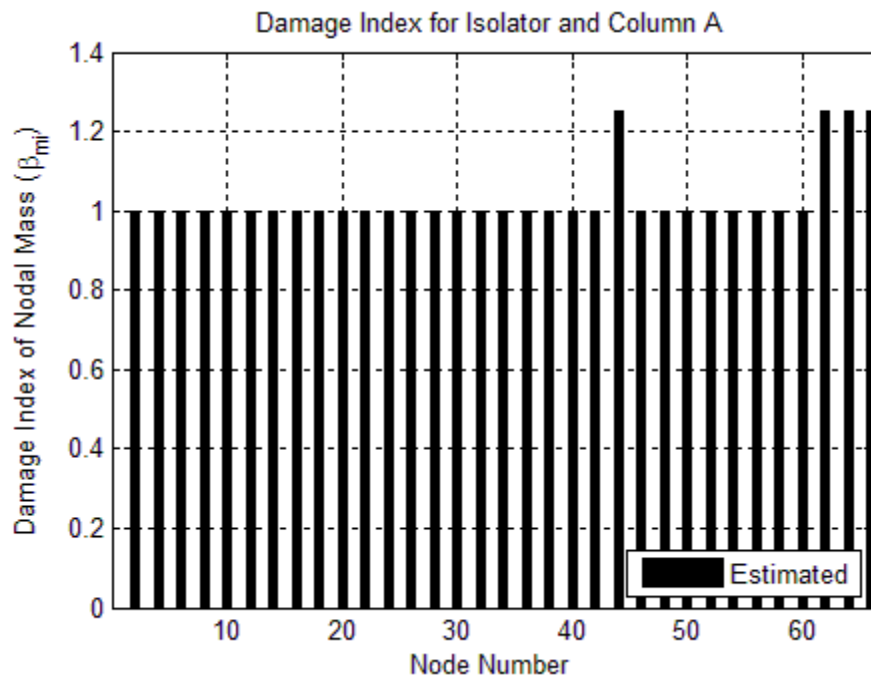


Figure 5.36. Damage Indices of Nodal Mass ( $\beta_{mi}$ ) for the Isolator and Column A from the Two-Bay Frame

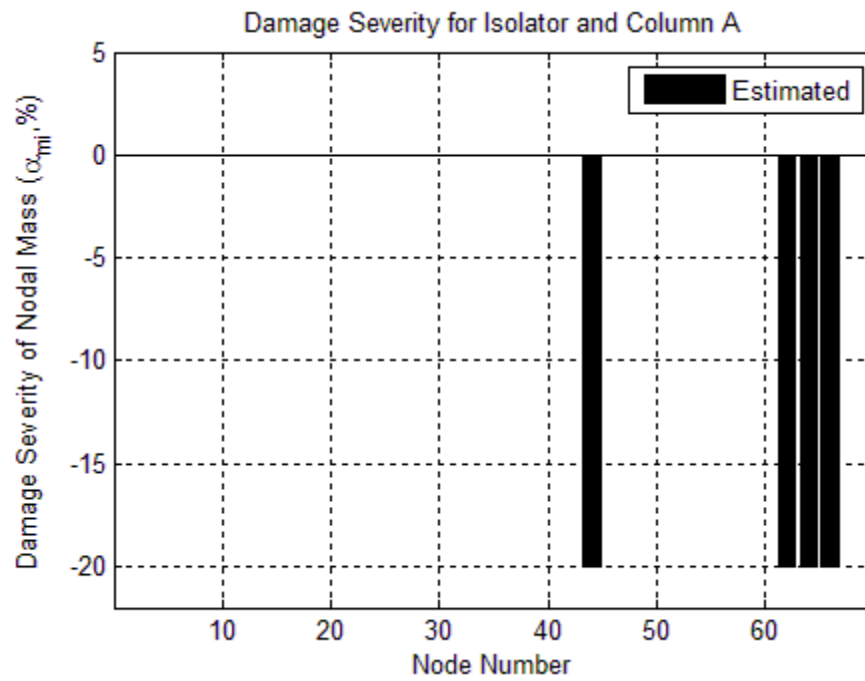


Figure 5.37. Damage Severities of Nodal Mass ( $\alpha_{mi}$ ) for the Isolator and Column A from the Two-Bay Frame

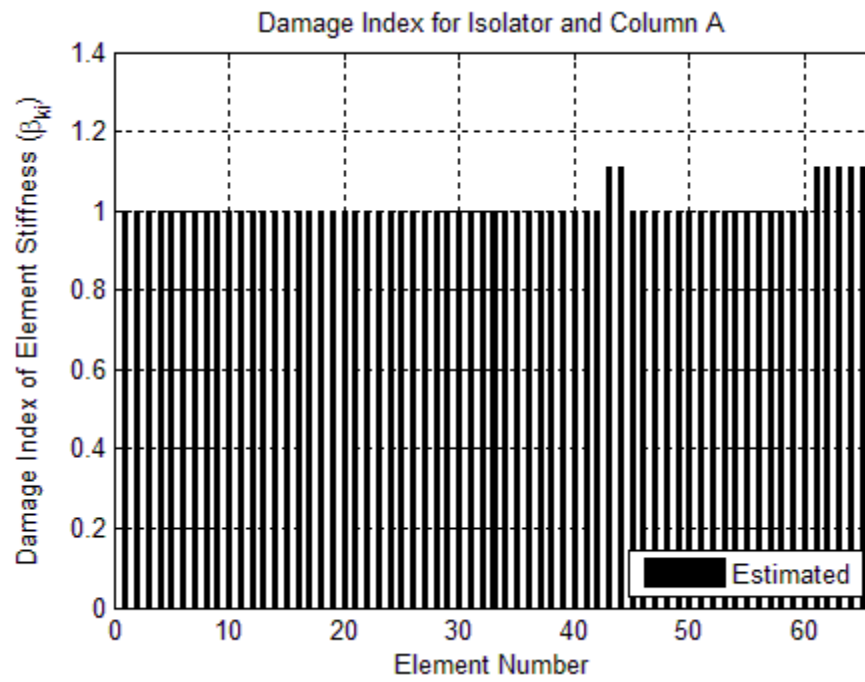


Figure 5.38. Damage Indices of Element Stiffness ( $\beta_{ki}$ ) for the Isolator and Column A from the Two-Bay Frame

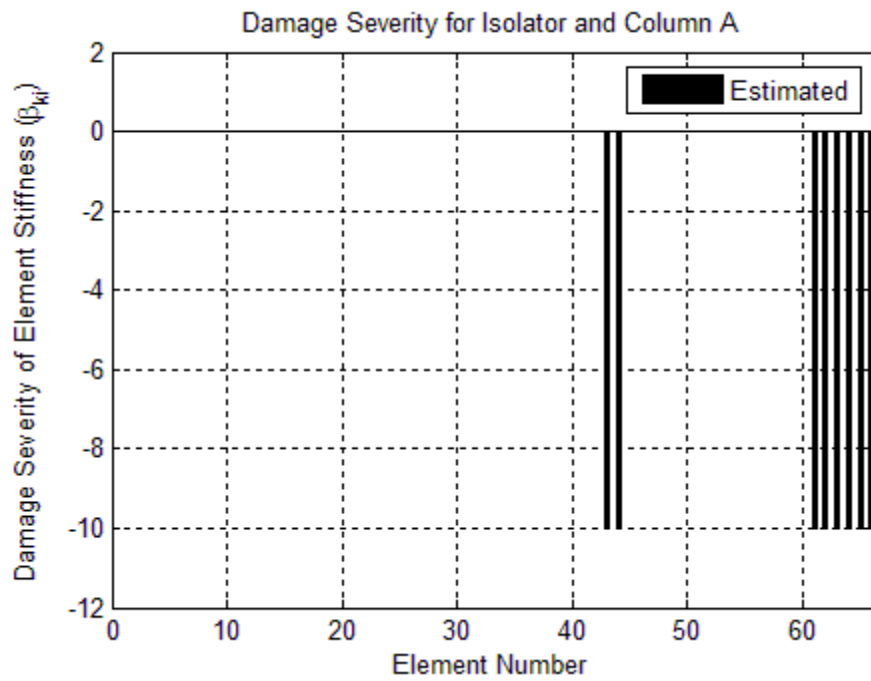


Figure 5.39. Damage Severities of Element Stiffness ( $\beta_{ki}$ ) for the Isolator and Column A from the Two-Bay Frame

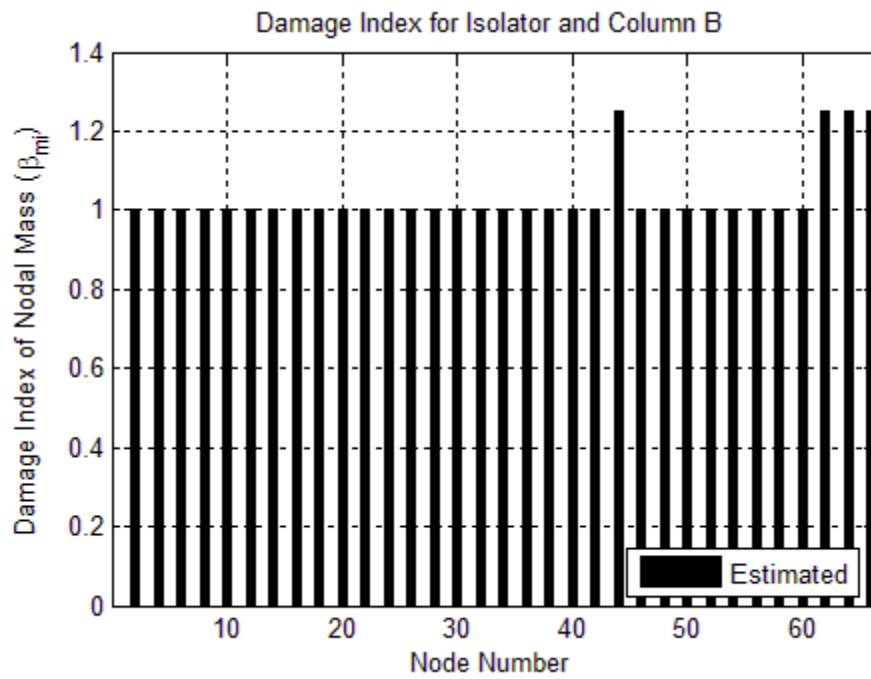


Figure 5.40. Damage Indices of Nodal Mass ( $\beta_{mi}$ ) for the Isolator and Column B from the Two-Bay Frame

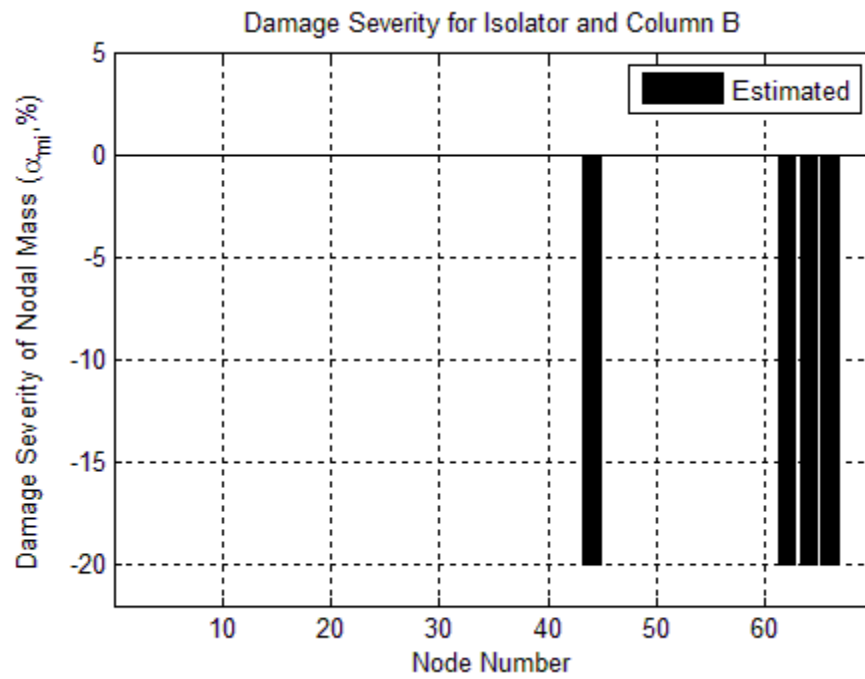


Figure 5.41. Damage Severities of Nodal Mass ( $\alpha_{mi}$ ) for the Isolator and Column B from the Two-Bay Frame

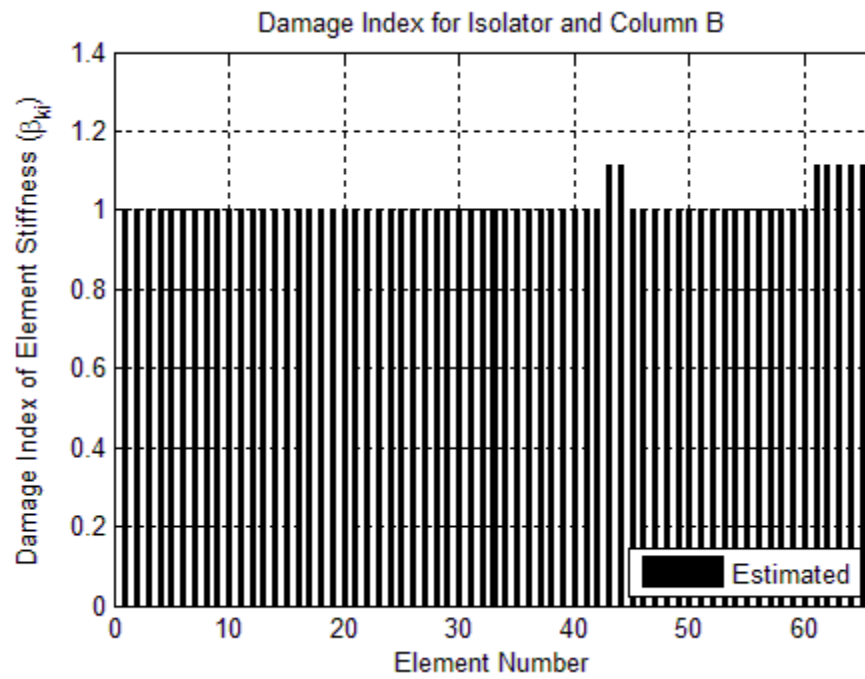


Figure 5.42. Damage Indices of Element Stiffness ( $\beta_{ki}$ ) for the Isolator and Column B from the Two-Bay Frame



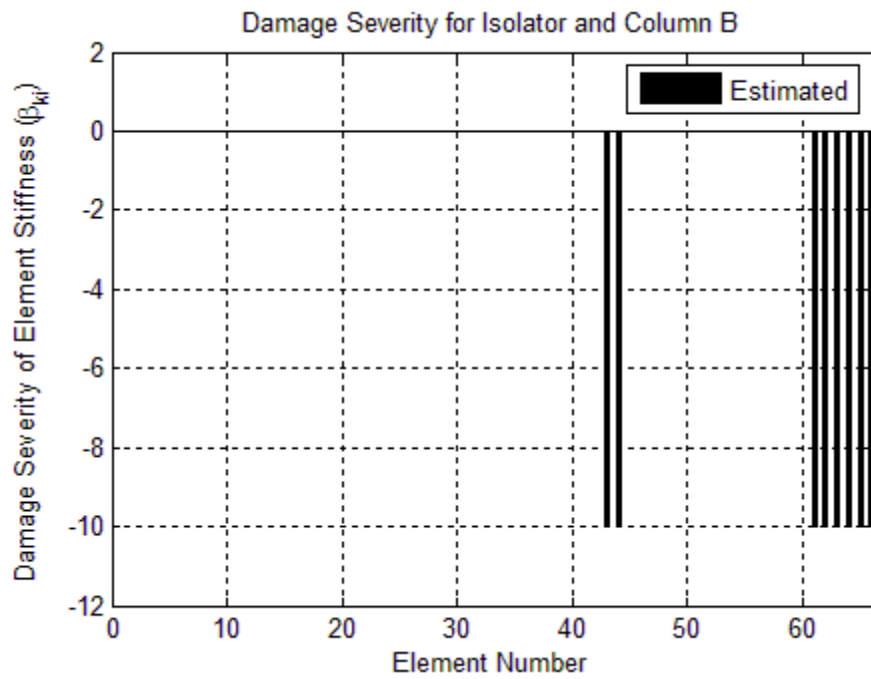


Figure 5.43. Damage Severities of Element Stiffness ( $\beta_{ki}$ ) for the Isolator and Column B from the Two-Bay Frame

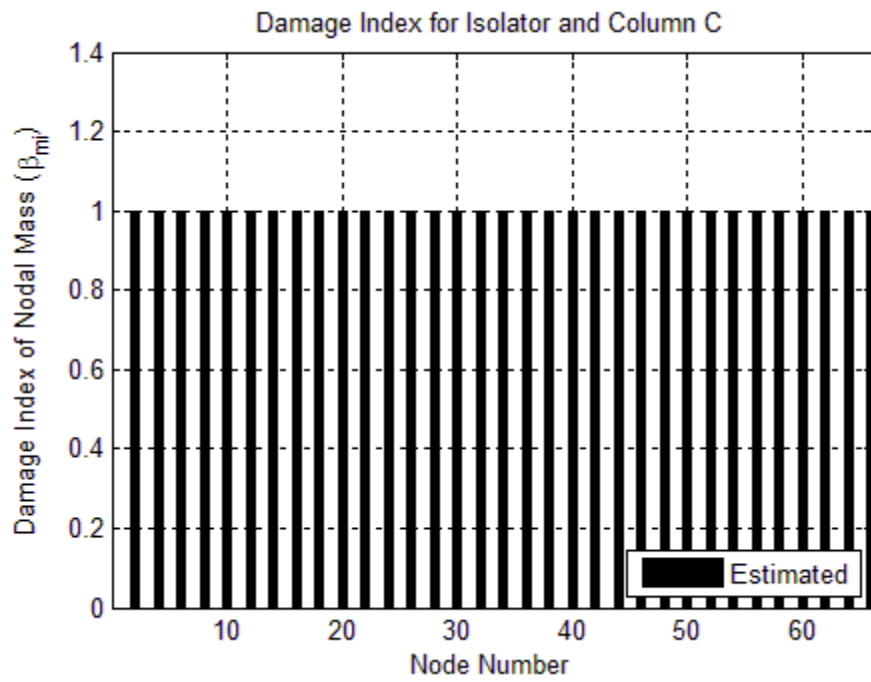


Figure 5.44. Damage Indices of Nodal Mass ( $\beta_{mi}$ ) for the Isolator and Column C from the Two-Bay Frame

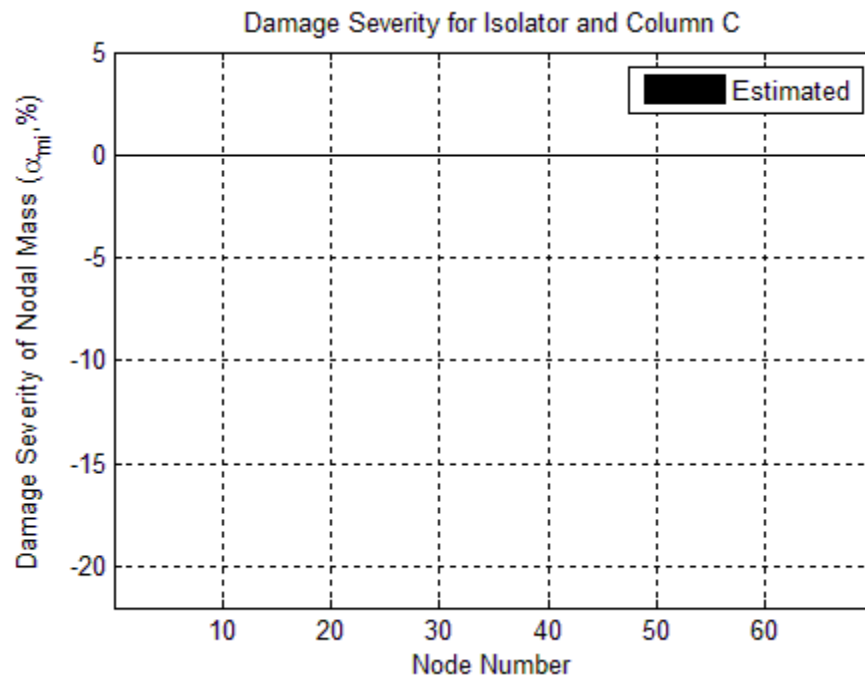


Figure 5.45. Damage Severities of Nodal Mass ( $\alpha_{mi}$ ) for the Isolator and Column C from the Two-Bay Frame (note: all values are close to zeros, no damage)

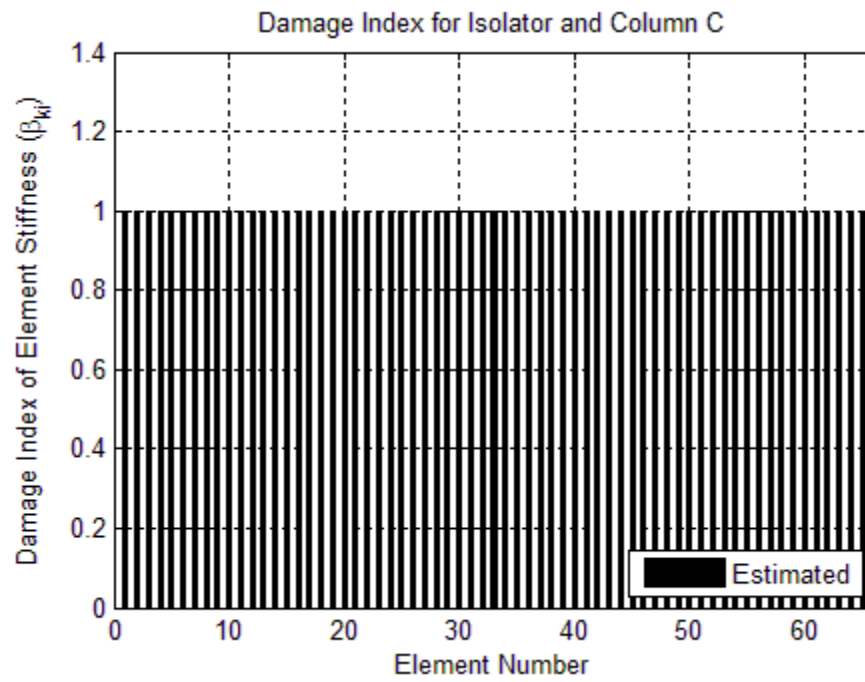
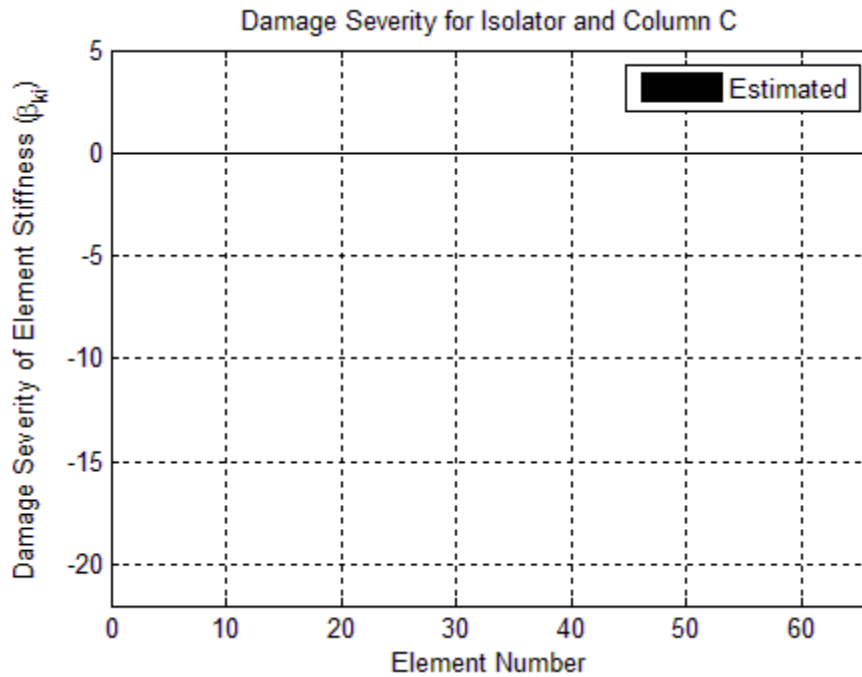


Figure 5.46. Damage Indices of Element Stiffness ( $\beta_{ki}$ ) for the Isolator and Column C from the Two-Bay Frame



**Figure 5.47. Damage Severities of Element Stiffness ( $\alpha_{ki}$ ) for the Isolator and Column C from the Two-Bay Frame** (note: all values are close to zeros, no damage)

## 5.6 DAMAGE EVALUATION FOR A SPACE TRUSS

In Case #5, a space truss is used to validate the proposed theory. The geometry, damage scenario, and finite element discretization under consideration are indicated in Figure 5.48. There are 18 truss members and eight (8) joints in the space truss. The lower four (4) joints are pin connected to the ground. Each of the above four (4) joints has three (3) transitional degrees of freedom (i.e. global X, Y, Z directions). The numbering systems of joints and of truss members are given in Figure 5.48. To better describe the geometry of the space truss, the coordinate of each joint in the space truss is also given in Figure 5.48.

The geometry of the cross-section of the truss member is shown in Figure 5.19. The

modulus of elasticity ( $E$ ) of the material is 29,000 ksi. The mass density of the material is  $7.345 \times 10^{-7}$  kip·sec<sup>2</sup>/in<sup>4</sup>. In this case, four elements with damaged mass and stiffness are studied. The damage is simulated by a ten percent (10%) reduction of the modulus of elasticity and twenty percent (20%) reduction of the mass of both Member 26 and Member 25, and fifteen percent (15%) reduction of the modulus of elasticity and thirty percent (30%) reduction of the mass of Member 68.

The load case is simulated by applying four cosine forces in the global X direction at each of the free joints. For Joint 5, a cosine force,  $400\cos(2\pi t)$ , in the global X direction is applied. For Joint 6, a cosine force,  $100\cos(2\pi t)$ , in the global X direction is applied. For Joint 7, a cosine force,  $200\cos(2\pi t)$ , in the global X direction is applied. For Joint 8, a cosine force,  $300\cos(2\pi t)$ , in the global X direction is applied. Given the external load case, the displacement, velocity, and acceleration time histories of the movable joints are directly generated from SAP2000 using linear direct integration method. The computation step is 1E-4 seconds (10,000 Hz) for total 0.2 seconds. The displacement, velocity, and acceleration of Joint 6 in global x direction for both the undamaged and damaged systems were plotted in Figure 5.49, Figure 5.50, and Figure 5.51.

In this case, the computed velocity ( $\dot{x}(t)$ ) of each joint in the undamaged case was used as the velocity used to compute power ( $\dot{\Delta}$ ) for both the undamaged and damaged cases. For each joint, the coefficient matrices (' $\mathbf{X}$ ') and known vector (' $\mathbf{Y}$ ') were constructed by substituting the acceleration ( $\ddot{x}(t)$ ), velocity ( $\dot{x}(t)$ ), displacement ( $x(t)$ ), and velocity used to compute power ( $\dot{\Delta}$ ) into Eq. 4.217 and Eq. 4.219. The coefficient damage index vector,  $\beta$ , related to the two nearby elements was computed using Eq. 4.220. Then the damage indices for mass and stiffness are computed using Eqs. 4.221

through 4.224. The damage severities for mass and stiffness are computed using Eq. 2.13. For each joint, the above process is performed. The estimated damage indices and the designed damage indices for each physical property are listed in Table 5.4 and are plotted in Figure 5.52 for joint mass and Figure 5.54 for element stiffness. The estimated damage severities and the designed damage severities for each physical property are plotted in Figure 5.53 for joint mass and Figure 5.55 for element stiffness. Comparing the estimated damage indices with the designed damage indices, the proposed method can accurately locate and size multiple damage in a space truss.

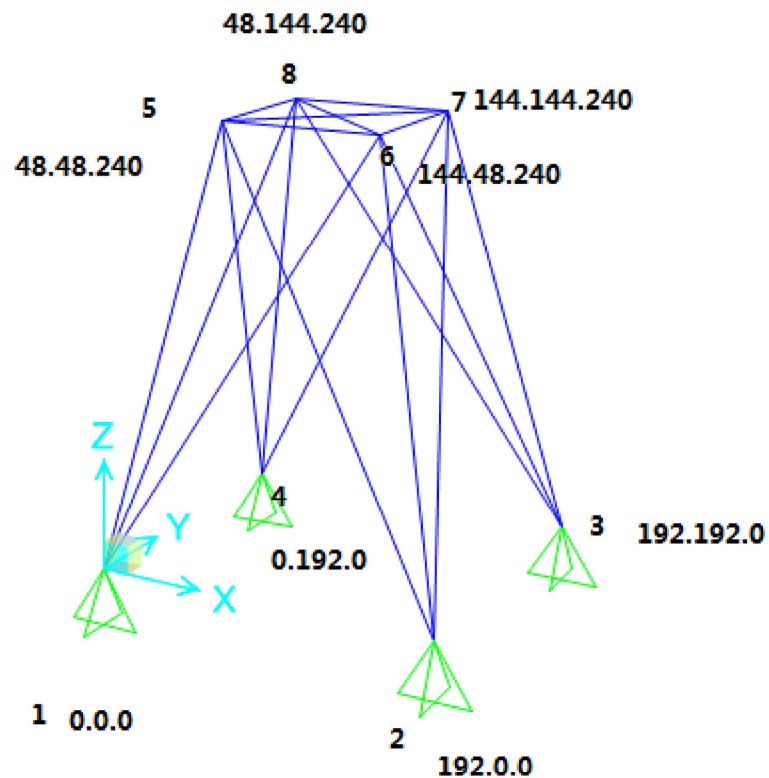


**Figure 5.48. Geometry, Damage Scenario, and Finite Element Discretization for the Space Truss**

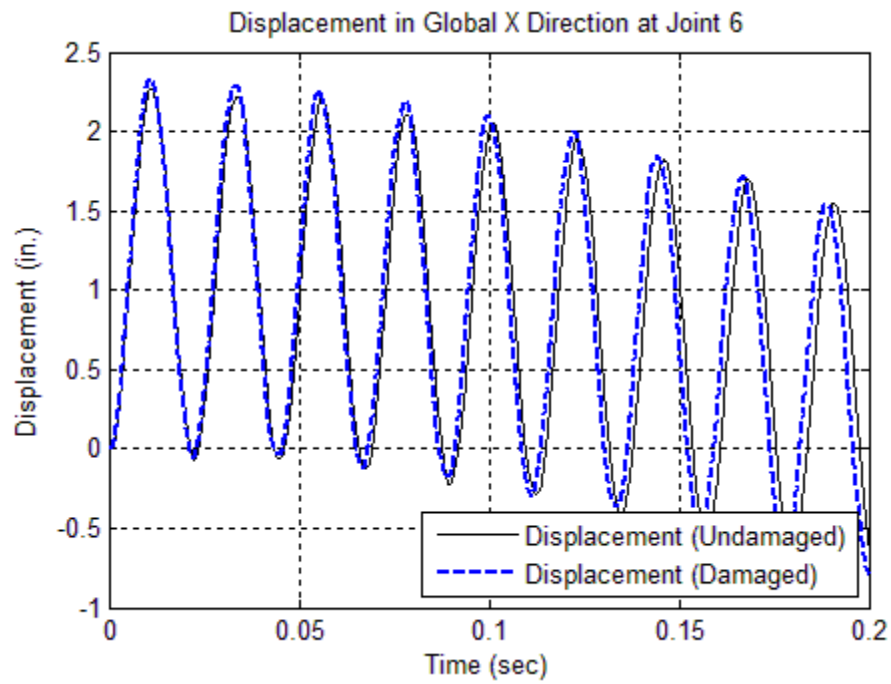


**Figure 5.49. Displacements of the Joint 6 in Global X Direction for Both the Undamaged and Damaged Systems under the Given External Load**

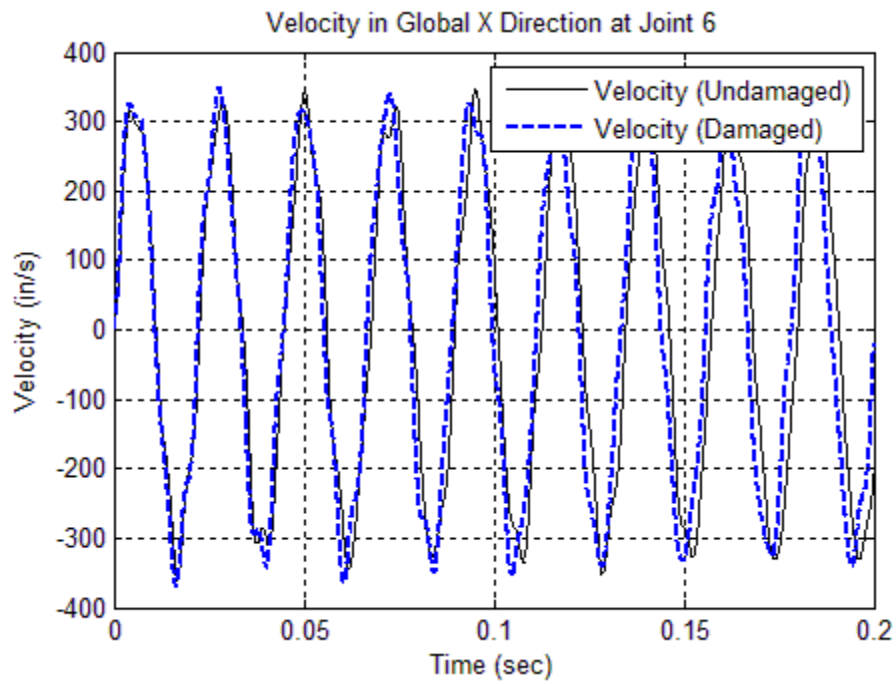


**Figure 5.50. Velocities of the Joint 6 in Global X Direction for Both the Undamaged and Damaged Systems under the Given External Load**

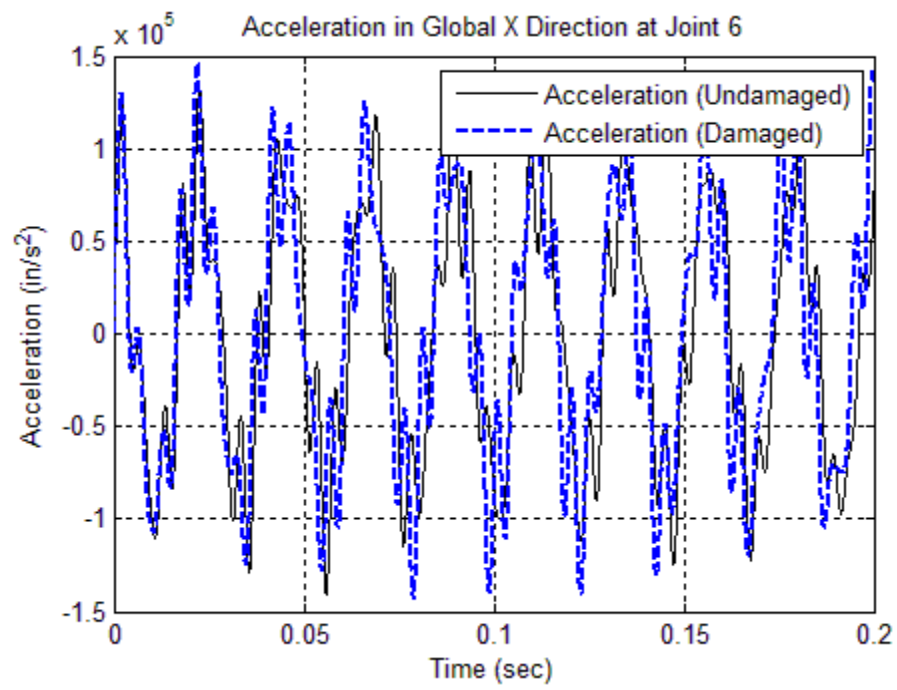


**Figure 5.51. Accelerations of the Joint 6 in Global X Direction for Both the Undamaged and Damaged Systems under the Given External Load**

**Table 5.4. Damage Detection Results for the Space Truss**

<b>Property</b>	<b>Damage Index (<math>\beta_i</math>, Estimated)</b>	<b>Damage Severity (<math>\alpha_i</math>, Estimated) (%)</b>	<b>Damage Index (<math>\beta_i</math>, Designed)</b>
$m_5$	1.052	-4.960	1.052
$m_6$	1.086	-7.919	1.086
$m_7$	1.000	-0.003	1.000
$m_8$	1.037	-3.553	1.037
$k_{15}$	1.000	-0.018	1.000
$k_{16}$	1.000	-0.012	1.000
$k_{18}$	0.999	0.081	1.000
$k_{25}$	1.111	-9.980	1.111
$k_{26}$	1.111	-10.001	1.111
$k_{27}$	0.997	0.256	1.000
$k_{36}$	1.000	-0.007	1.000
$k_{37}$	1.001	-0.127	1.000
$k_{38}$	1.000	-0.006	1.000
$k_{45}$	1.000	0.003	1.000
$k_{47}$	1.000	-0.005	1.000
$k_{48}$	1.001	-0.052	1.000
$k_{56}$	1.000	-0.002	1.000
$k_{57}$	0.999	0.097	1.000
$k_{58}$	1.000	0.039	1.000
$k_{67}$	0.999	0.084	1.000
$k_{68}$	1.175	-14.907	1.176
$k_{78}$	1.002	-0.151	1.000



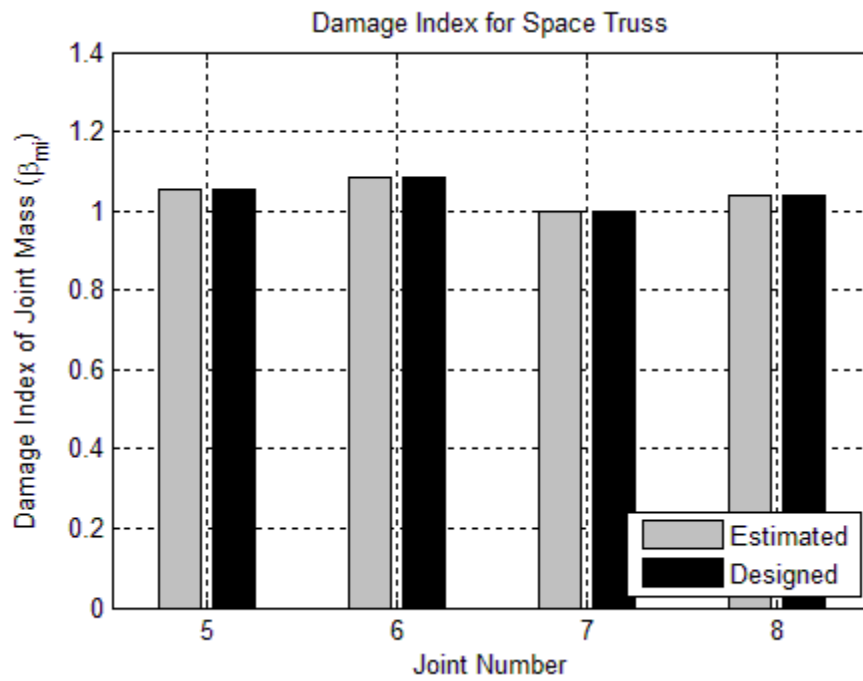


Figure 5.52. Damage Indices of Joint Mass ( $\beta_{mi}$ ) for the Space Truss

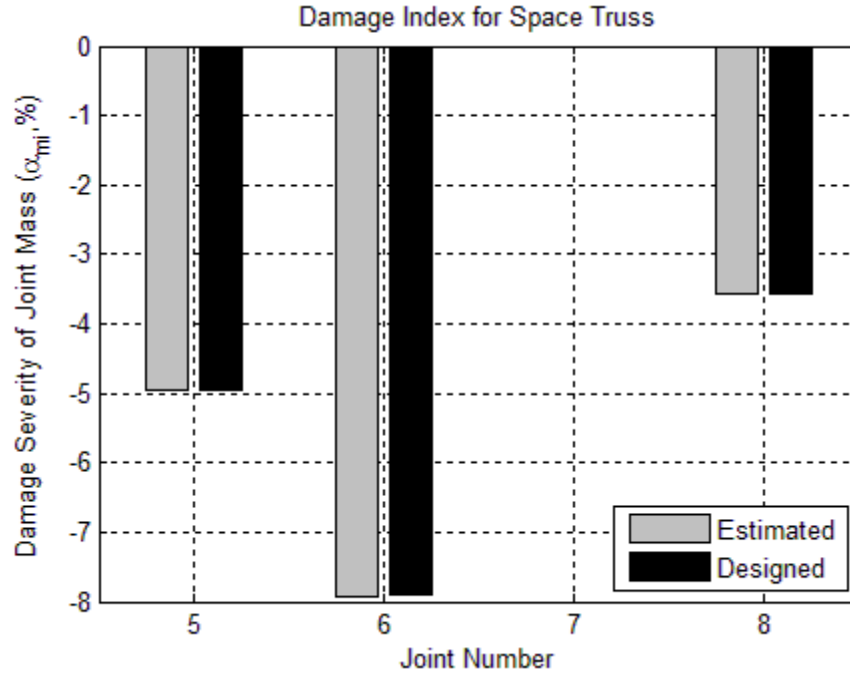


Figure 5.53. Damage Severities of Joint Mass ( $\alpha_{mi}$ ) for the Space Truss

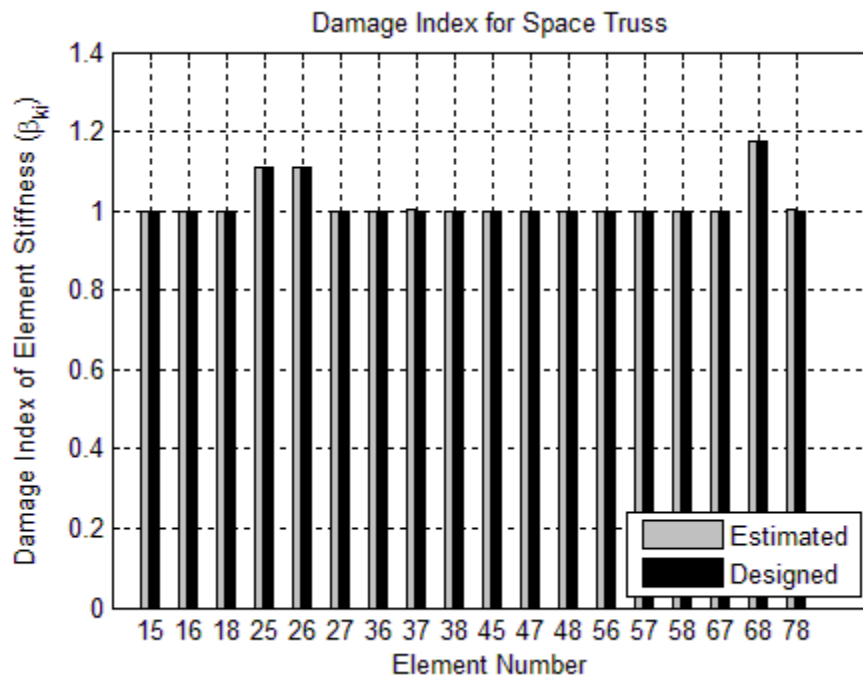


Figure 5.54. Damage Indices of Member Stiffness ( $\beta_{ki}$ ) for the Space Truss

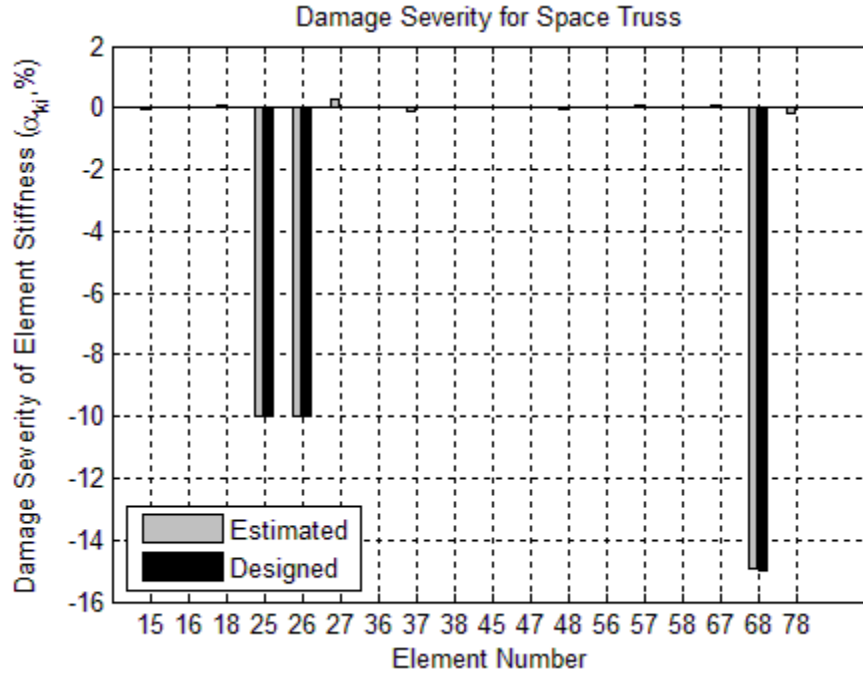


Figure 5.55. Damage Severities of Member Stiffness ( $\alpha_{ki}$ ) for the Space Truss

## 5.7 SUMMARY

In this section, numerical models of rod under axial and torsional vibration, rod under axial vibration only, beam under bending vibration, plane frame under axial and bending vibration, and space truss under axial vibration were simulated and studied. In each numerical damage detection experiment, damage in mass, stiffness were simultaneously simulated in each damaged system. For both the damaged and undamaged systems, the displacements, velocities and accelerations were computed using linear direct integration method in SAP2000. The displacements, velocities and accelerations used in the Section 5 are exact data without noise. The algorithms given in the Section 4 were used to compute the damage indices and damage severities in each numerical case.

For each numerical case, all the designed damage in masses and stiffness were located and evaluated accurately. Moreover, for all numerical experiments, neither false-positive damage index nor false-negative damage index was found. Namely, for the proposed damage detection method, if accurate displacement, velocity, and acceleration data are given, all type of damage will be accurately located and evaluated. In addition, according to the results from Section 5.2 and Section 5.3, the proposed method was proved to be applicable to both the integral continuous system and isolated continuous system. The proposed method was also proved to be able to detect and evaluation damage by using measured data from different types of vibrations

## **6 STUDIES OF NOISE INFLUENCE TO THE PERFORMANCE OF THE POWER METHOD**

### **6.1 INTRODUCTION**

The objective of this section is to evaluate the accuracy of the theory when the inputs are noise-polluted. To simulate the noise-polluted inputs, exact accelerations contaminated by white noise are used as the input acceleration; the input velocities and input displacements are estimated based on the noise-polluted accelerations. Eight numerical cases including two noise levels are taken into consideration and general description of each numerical cases are given as follows,

Case #6.1: The Power Method for  $n$ -DOF discrete system was applied on a 5-DOF spring-mass-damper system. The noise-polluted accelerations were simulated by the superposition of 1% of white noise and the exact accelerations outputted from the discrete system. The algorithm of the Power Method for a 5-DOF spring-mass-damper system is provided in Section 2.5.

Case #6.2: The Power Method for  $n$ -DOF discrete system was applied on a 5-DOF spring-mass-damper system. The noise-polluted accelerations were simulated by the superposition of 5% of white noise and the exact accelerations outputted from the discrete system. The algorithm of the Power Method for a 5-DOF spring-mass-damper system is provided in Section 2.5.

Case #6.3: The Power Method for Isolated discrete system was applied on a 5-DOF

spring-mass-damper system. The noise-polluted accelerations were simulated by the superposition of 1% of white noise and the exact accelerations outputted from the discrete system. The algorithm of the Power Method for a 5-DOF spring-mass-damper system is provided in Section 2.6.

Case #6.4: The Power Method for Isolated discrete system was applied on a 5-DOF spring-mass-damper system. The noise-polluted accelerations were simulated by the superposition of 5% of white noise and the exact accelerations outputted from the discrete system. The algorithm of the Power Method for a 5-DOF spring-mass-damper system is provided in Section 2.6.

Case #6.5: The Power Method for whole rod analysis was applied on a fixed-fixed beam. The noise-polluted accelerations were simulated by the superposition of 1% of white noise and the exact accelerations outputted from the discrete system. The algorithm of the Power Method for whole rod analysis is provided in Section 4.2.2.

Case #6.6: The Power Method for whole rod analysis was applied on a fixed-fixed beam. The noise-polluted accelerations were simulated by the superposition of 5% of white noise and the exact accelerations outputted from the discrete system. The algorithm of the Power Method for whole rod analysis is provided in Section 4.2.2.

Case #6.7: The Power Method for isolated rod element analysis was applied on a fixed-fixed beam. The noise-polluted accelerations were simulated by the superposition of 1% of white noise and the exact accelerations outputted from the discrete system. The algorithm of the Power Method for whole rod analysis is provided in Section 4.2.1.

Case #6.8: The Power Method for isolated rod element analysis was applied on a fixed-fixed beam. The noise-polluted accelerations were simulated by the superposition of 5% of white noise and the exact accelerations outputted from the discrete system. The algorithm of the Power Method for whole rod analysis is provided in Section 4.2.1.

### 6.1.1 Generation of Noise-Polluted Accelerations

The noise-polluted accelerations are computed using the following equation,

$$a_{noise}(t_i) = a_{pure}(t_i) + w(t_i) \cdot \rho \cdot \frac{std(a_{pure})}{std(w)} \quad (6.1)$$

Where  $a_{noise}(t_i)$  is the noise-polluted acceleration at time  $t_i$ ;  $a_{pure}(t_i)$  is the exact acceleration at time  $t_i$ ;  $w(t_i)$  is the random white noise at time  $t_i$ ;  $\rho$  is the percent of noise selected to add into the pure acceleration data;  $std(x)$  indicates the standard deviation of Vector  $x$ .

### 6.1.2 Estimation of Velocity and Displacement

The velocity time histories are estimated based on the filtered noise-polluted acceleration time histories, using,

$$v(t_1) = v(t_0) + \frac{a(t_1) + a(t_0)}{2} (t_1 - t_0) \quad (6.2)$$

Where, the initial velocity and initial acceleration are zeros. Namely,  $v(0) = 0$ ,  $a(0) = 0$ ,  $(t_1 - t_0) = dt = 0.0001$  seconds.

The displacement time histories are estimated based on the velocity time histories from Eq.

6.2, using,

$$s(t_1) = s(t_0) + \frac{v(t_1) + v(t_0)}{2}(t_1 - t_0) \quad (6.3)$$

Where, the initial displacement and initial velocity are zeros for the shake table test.

Namely,  $s(0) = 0$ ,  $v(0) = 0$ ,  $(t_1 - t_0) = dt = 0.0001$  seconds.

### 6.1.3 Normalized Damage Index and Damage Possibility Index

According to the later study, the damage indices for undamaged and damaged elements can be less than the expected values due to the noise and applied digital band-pass filter. For these cases, the normalized damage indices might be more illustrative. Given the normalized damage index, the damage possibility index can be computed based on standard normal distribution.

The expression of the normalized damage index,

$$\beta_{n,i} = \frac{\beta_i - \mu}{\sigma} \quad (6.4)$$

Where  $\mu$  is the average value of the  $\beta_i$  series, and  $\sigma$  is the standard deviation of the  $\beta_i$  series.

The standard normal probability density function used to generate damage possibility index is given as following,

$$f(\beta_{n,i} | \mu = 0, \sigma = 1) = \frac{1}{\sigma\sqrt{2\pi}} e^{-\frac{(\beta_{n,i} - \mu)^2}{2\sigma^2}} \quad (6.5)$$

## 6.2 STUDIES OF NOISE INFLUENCE TO A DISCRETE SYSTEM USING INTEGRAL METHOD

In this subsection, noise influence to the performance of integrated system method for discrete systems will be studied. The proposed damage detection algorithm is performed on a 5-DOF spring-mass-damper system. The numerical models for the damaged and undamaged 5-DOF mass-spring-damper systems were generated within SAP2000. The 5-DOF spring-mass-damper system used in this case study is plotted in Figure 6.1. The physical properties in the undamaged and damaged systems are listed in Table 6.1. Both the undamaged and damaged systems are excited by the same external force. The applied external forces are given at each 1E-4 seconds for 0.2 seconds and are plotted in Figure 6.2. In SAP2000, exact accelerations of the five mass blocks were computed every 1E-4 seconds (10,000 Hz) for 0.2 seconds. Then the accelerations of the five mass blocks were contaminated by 1% and 5% white noise. To reduce the influence from the noise in the input signals, a band-pass digital filter was used to filter the noise-polluted accelerations. The velocities of the mass blocks are estimated using Eq. 6.2 based on the filtered noise-polluted accelerations and the displacements of the mass blocks are estimated using Eq. 6.3 based on the filtered estimated velocities.

In this case, the computed velocity ( $\dot{x}(t)$ ) of the mass block in the undamaged case was used as the velocity used to compute power ( $\dot{\Delta}$ ) for both undamaged and damaged cases. The coefficient matrices and known vector, X and Y, were constructed by substituting the acceleration ( $\ddot{x}(t)$ ), velocity ( $\dot{x}(t)$ ), displacement ( $x(t)$ ), and velocity used to compute power ( $\dot{\Delta}$ ) into Eq. 2.123 and Eq. 2.125. The coefficient damage index vector,  $\beta$ , was computed using Eq. 2.127. Then the damage indices for mass, spring and damper are computed using Eqs. 2.128 through 2.144. The damage severities for mass, spring and



dampers are computed using Eqs. 2.145 through 2.161.

### 6.2.1 Case #6.1: Discrete System with 1% Noise Pollution Using Integral Method

In this case, the exact accelerations of the mass blocks outputted directly from SAP2000 were contaminated by 1% of white noise. The noise-polluted accelerations of Mass Block #2 in both the undamaged and damaged cases are plotted in Figure 6.3. The filtered accelerations, estimated velocities, and estimated displacements of mass Block #2 are plotted in Figure 6.4, Figure 6.5, and Figure 6.6, respectively.

The estimated damage indices and the designed damage indices for each physical property are listed in Table 6.2 and are plotted in Figure 6.7. The estimated damage severities and the designed damage severities for each physical property are also listed in Table 6.2 and are plotted in Figure 6.8. The normalized damage indices are computed using Eq. 6.4 and are plotted in Figure 6.9. The damage possibility indices are plotted in Figure 6.10. Comparing the estimated damage indices with the designed damage indices, the integrated system analysis method can accurately locate and size multiple damage with 1% noise-polluted input data from a typical 5-DOF spring-mass-damper system.

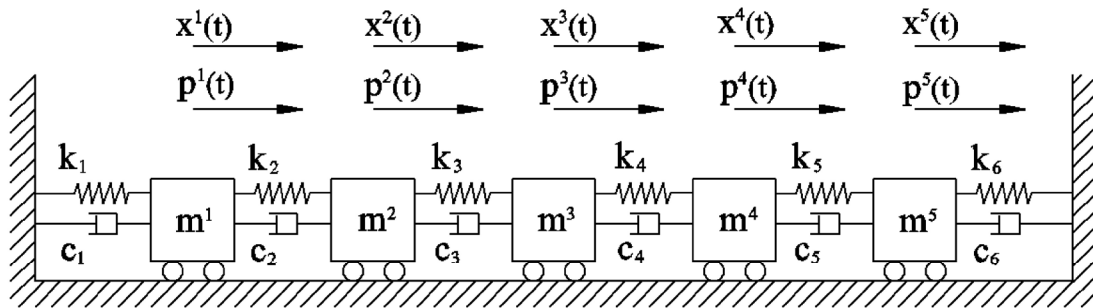
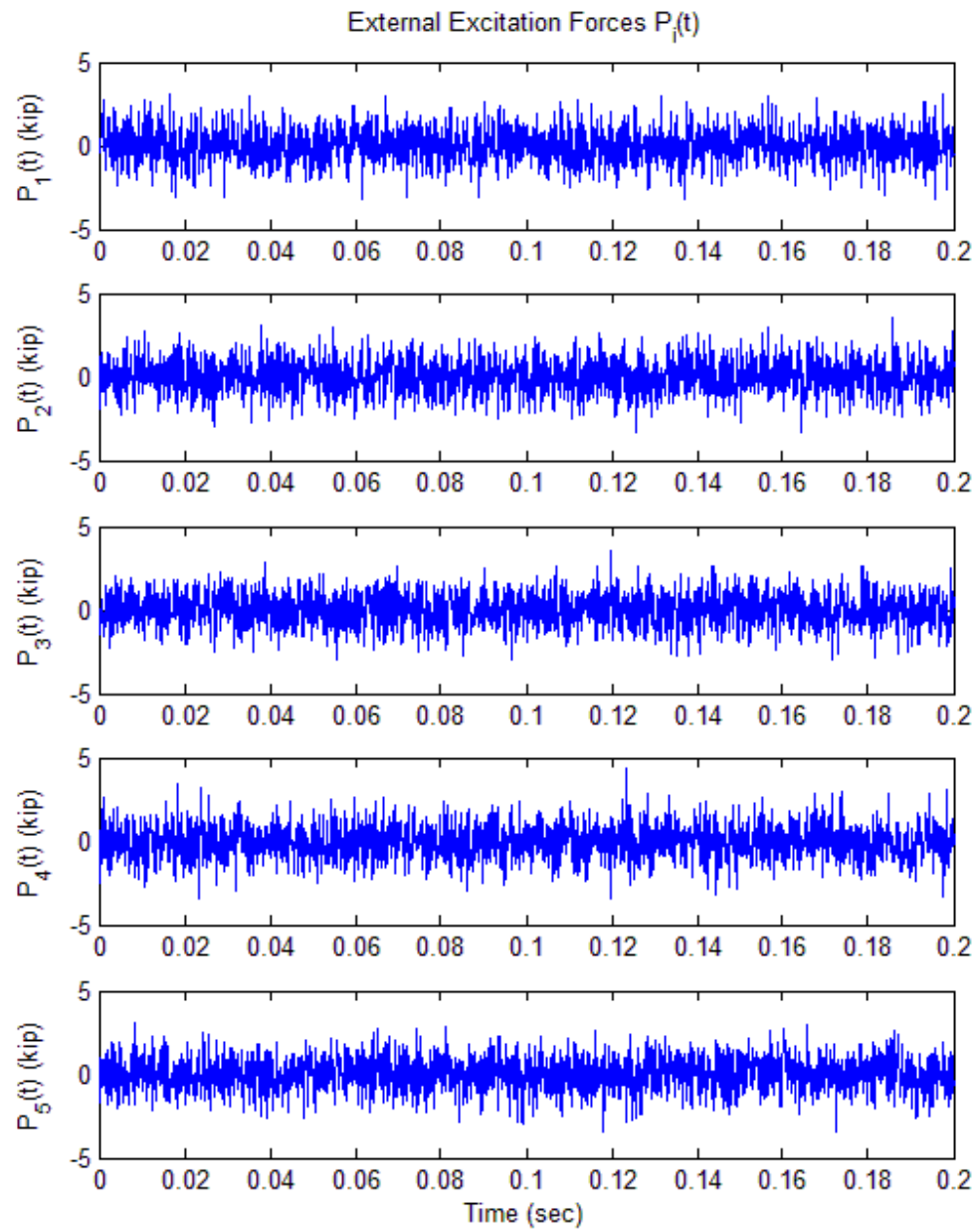


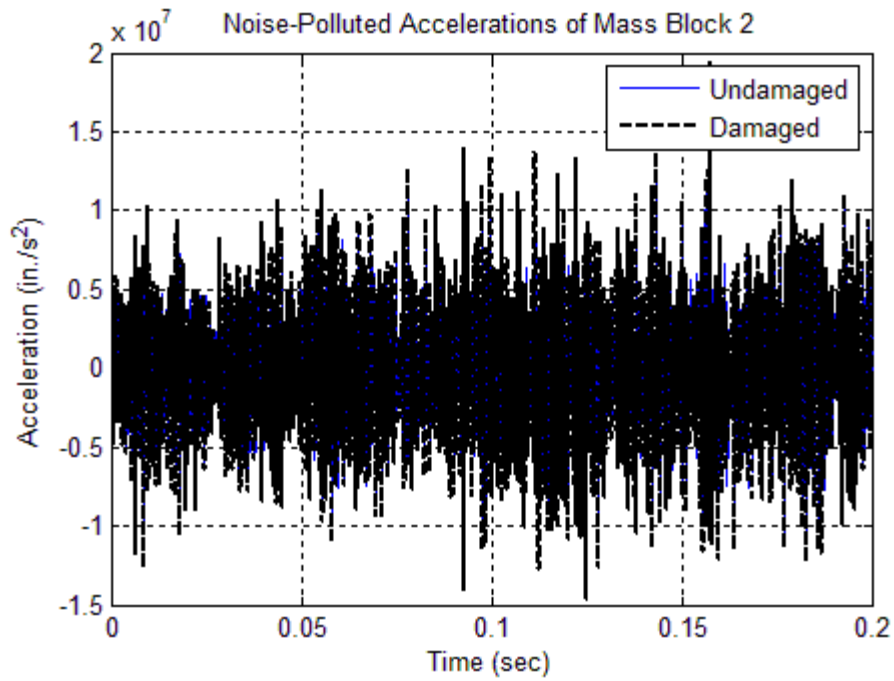
Figure 6.1. Property Definition and Load Case of the 5-DOF Spring-Mass-Damper System

**Table 6.1. Physical Properties of the 5-DOF System for Noise Study**

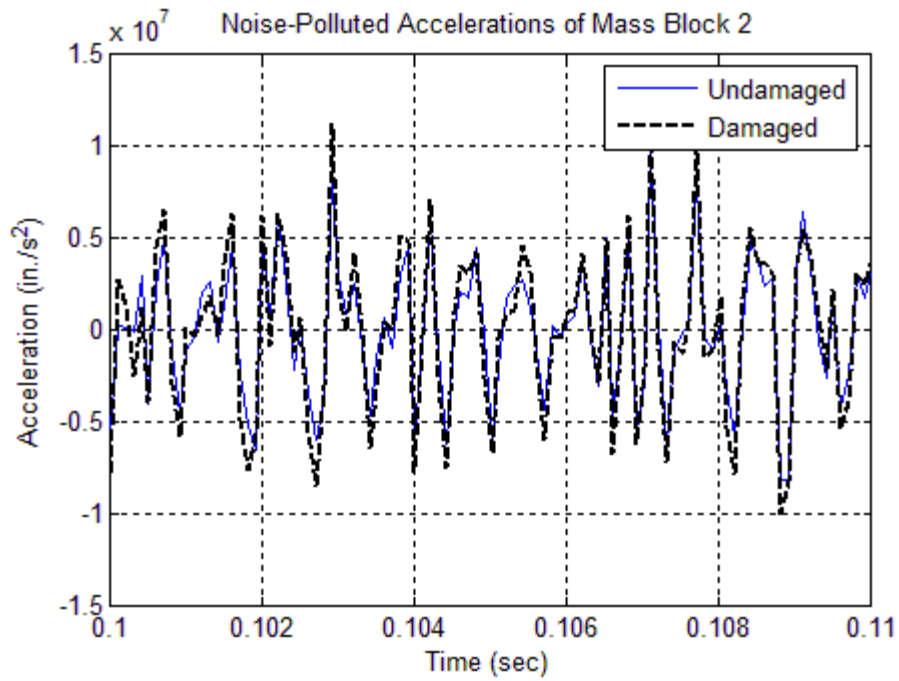
Property	Undamaged System	Damaged System
$m_1$ (kip-s <sup>2</sup> /in.)	5.8257E-05	4.66E-05
$m_2$ (kip-s <sup>2</sup> /in.)	5.8257E-05	5.24E-05
$m_3$ (kip-s <sup>2</sup> /in.)	5.8257E-05	5.83E-05
$m_4$ (kip-s <sup>2</sup> /in.)	5.8257E-05	5.83E-05
$m_5$ (kip-s <sup>2</sup> /in.)	5.8257E-05	5.83E-05
$c_1$ (kip-s/in.)	0.1	0.05
$c_2$ (kip-s/in.)	0.1	0.05
$c_3$ (kip-s/in.)	0.1	0.1
$c_4$ (kip-s/in.)	0.1	0.1
$c_5$ (kip-s/in.)	0.1	0.1
$c_6$ (kip-s/in.)	0.1	0.1
$k_1$ (kip/in.)	15974.167	14376.750
$k_2$ (kip/in.)	15974.167	14376.750
$k_3$ (kip/in.)	15974.167	14376.750
$k_4$ (kip/in.)	15974.167	14376.750
$k_5$ (kip/in.)	15974.167	14376.750
$k_6$ (kip/in.)	15974.167	14376.750



**Figure 6.2. Applied External Excitation Forces at Each Mass Block**

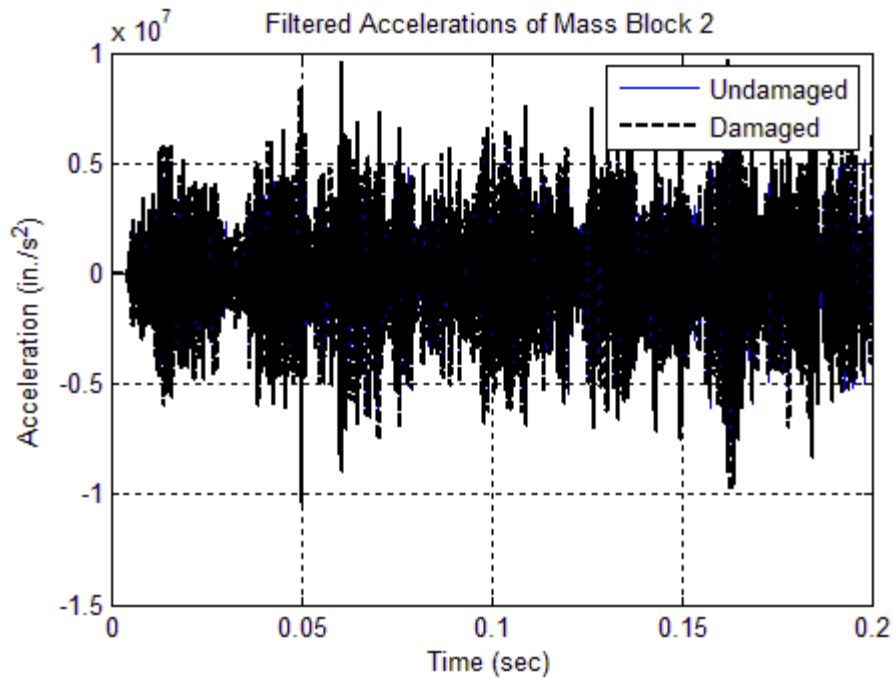


(a)

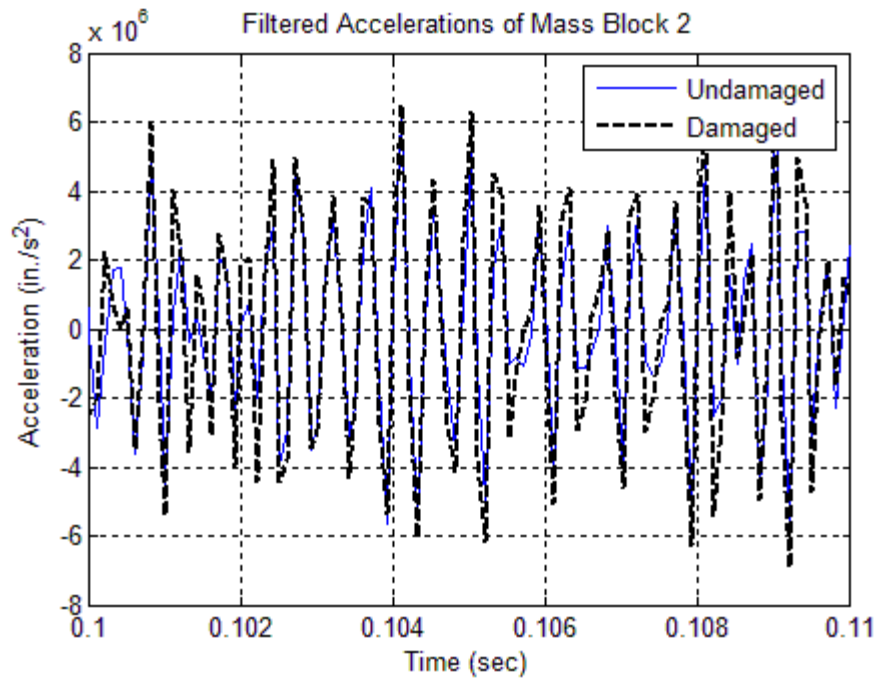


(b)

**Figure 6.3. Noise-Polluted Accelerations of Mass Block 2 for the Undamaged and Damaged Models of Case #6.1 (1% Noise): (a) Full Plot and (b) Zoomed in Plot**

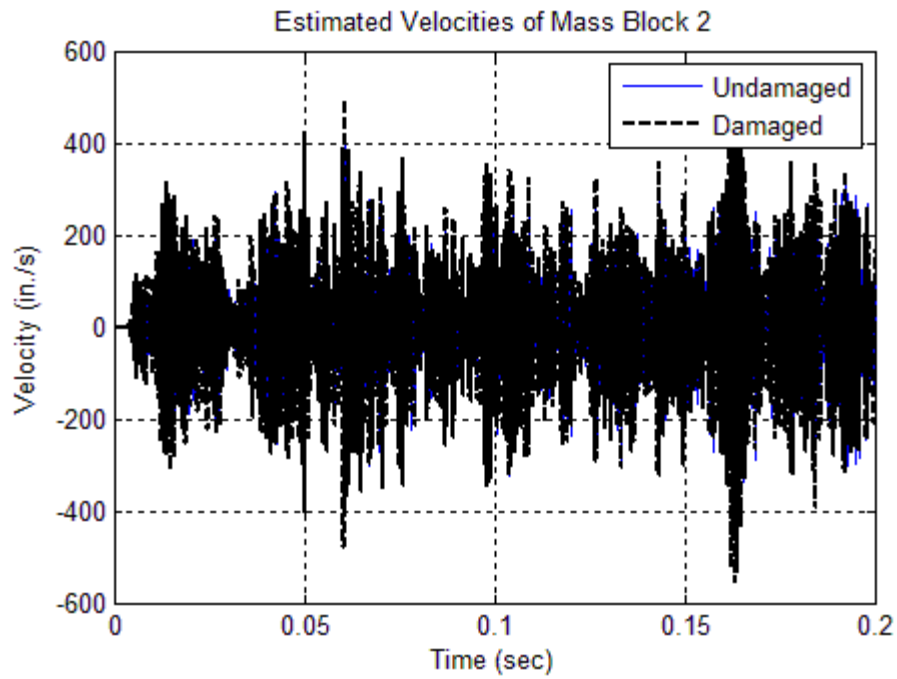


(a)

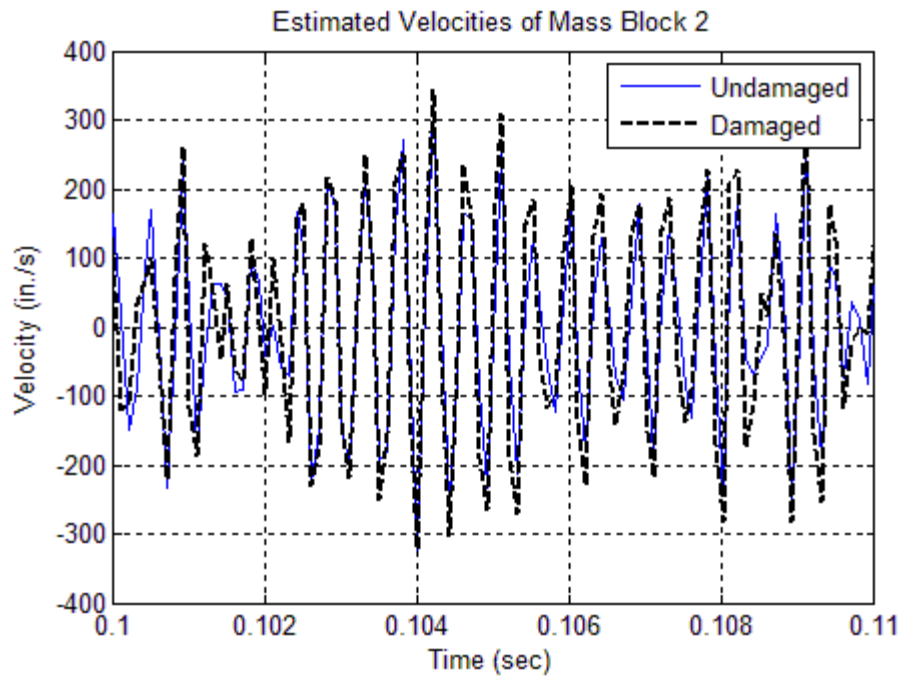


(b)

**Figure 6.4. Filtered Noise-Polluted Accelerations of Mass Block 2 for the Undamaged and Damaged Models of Case #6.1 (1% Noise): (a) Full Plot and (b) Zoomed in Plot**

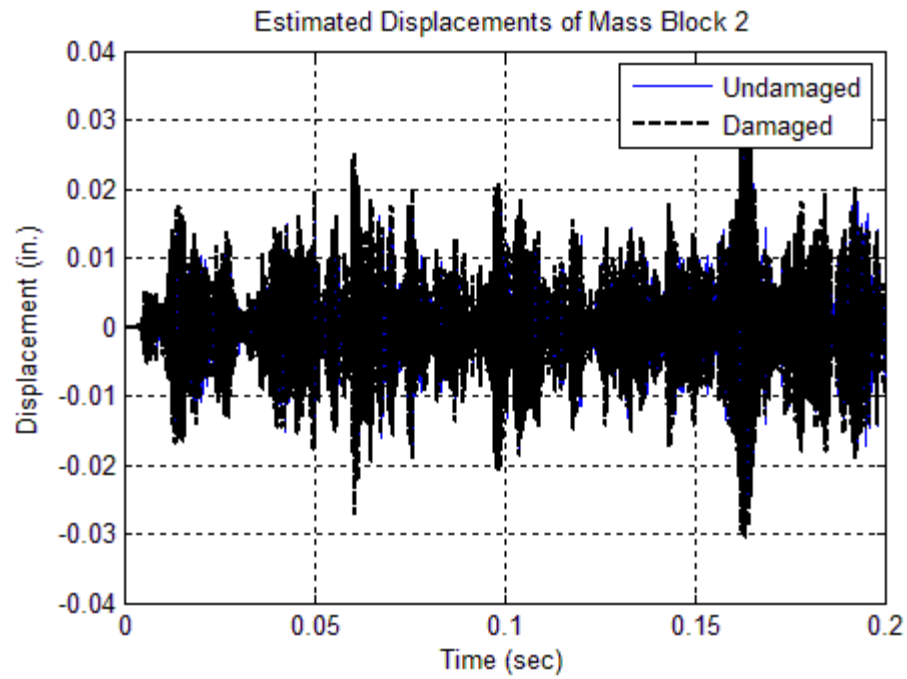


(a)

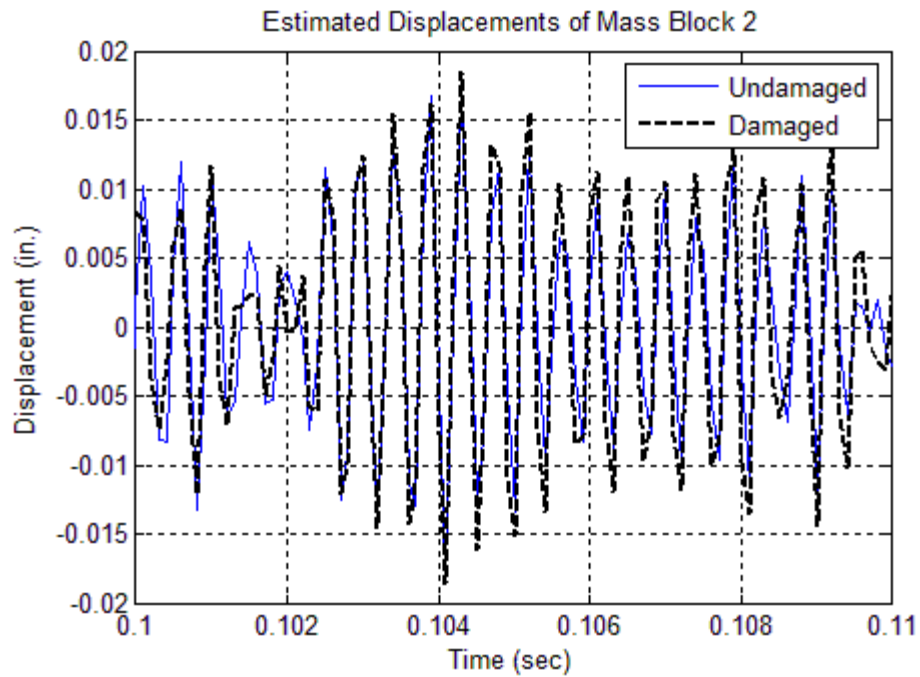


(b)

**Figure 6.5. Estimated Velocities of Mass Block 2 for the Undamaged and Damaged Models of Case #6.1 (1% Noise): (a) Full Plot and (b) Zoomed in Plot**



(a)



(b)

**Figure 6.6. Estimated Displacements of Mass Block 2 for the Undamaged and Damaged Models of Case #6.1 (1% Noise): (a) Full Plot and (b) Zoomed in Plot**

**Table 6.2. Damage Detection Results for the 5-DOF Spring-Mass-Damper System (1% Noise Pollution)**

<b>Property</b>	<b>Damage Index (<math>\beta_i</math>, Esimated)</b>	<b>Damage Severity (<math>\alpha_i</math>, Esimated)</b>	<b>Damage Index (<math>\beta_i</math>, Designed)</b>
$m_1$	1.25	-0.20	1.25
$m_2$	1.10	-0.09	1.11
$m_3$	0.99	0.01	1.00
$m_4$	1.00	0.00	1.00
$m_5$	1.00	0.00	1.00
$c_1$	1.99	-0.50	2.00
$c_2$	1.92	-0.48	2.00
$c_3$	0.99	0.01	1.00
$c_4$	1.00	0.00	1.00
$c_5$	1.01	-0.01	1.00
$c_6$	1.00	0.00	1.00
$k_1$	1.12	-0.11	1.11
$k_2$	1.11	-0.10	1.11
$k_3$	1.00	0.00	1.00
$k_4$	1.00	0.00	1.00
$k_5$	1.00	0.00	1.00
$k_6$	1.01	-0.01	1.00



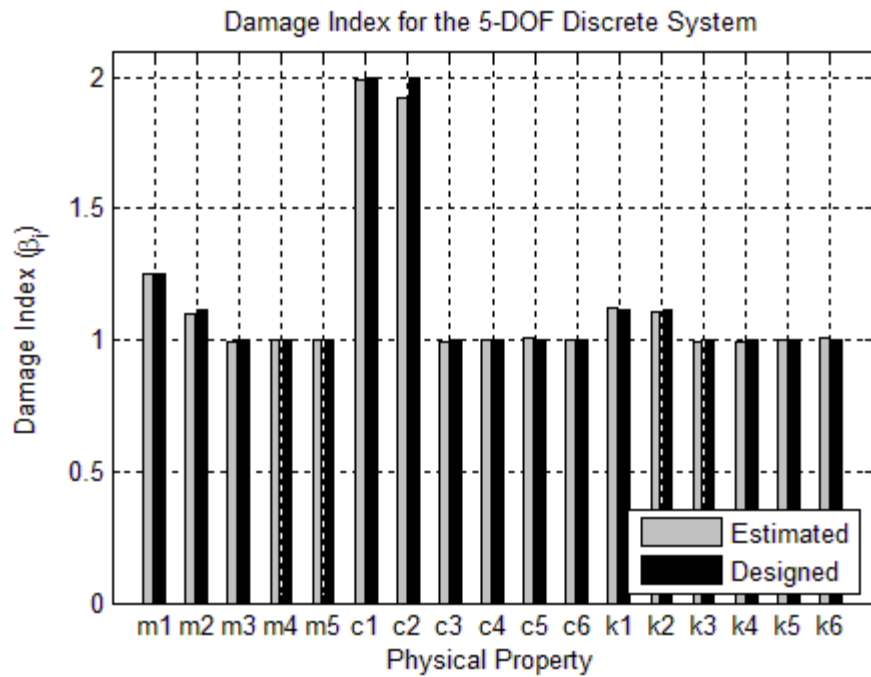


Figure 6.7. Damage Indices ( $\beta_i$ ) for 5-DOF Spring-Mass-Damper System with Noise-Polluted Accelerations (1% Noise)

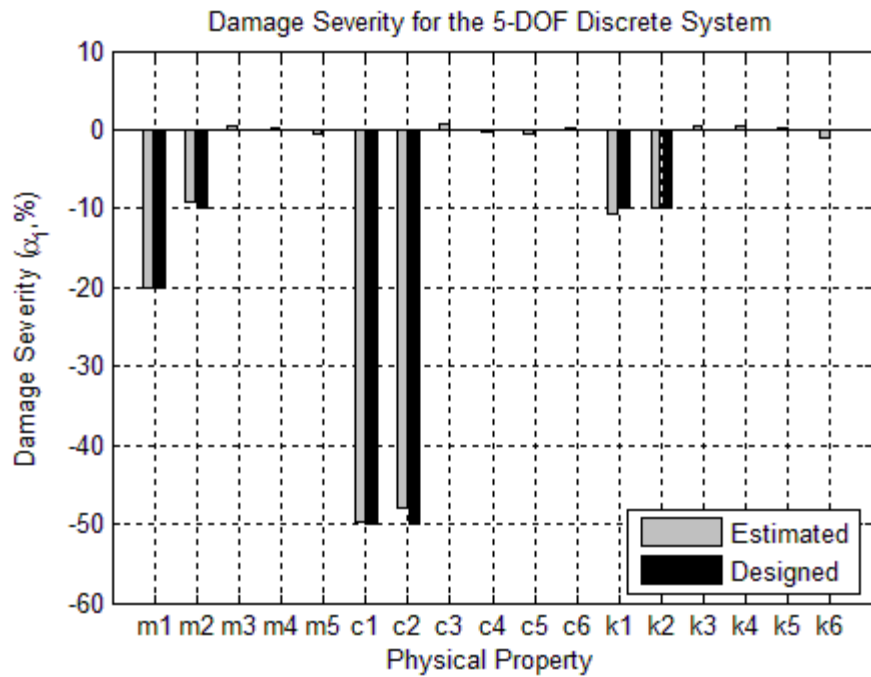


Figure 6.8. Damage Severities ( $\alpha_i$ ) for 5-DOF Spring-Mass-Damper System with Noise-Polluted Accelerations (1% Noise)

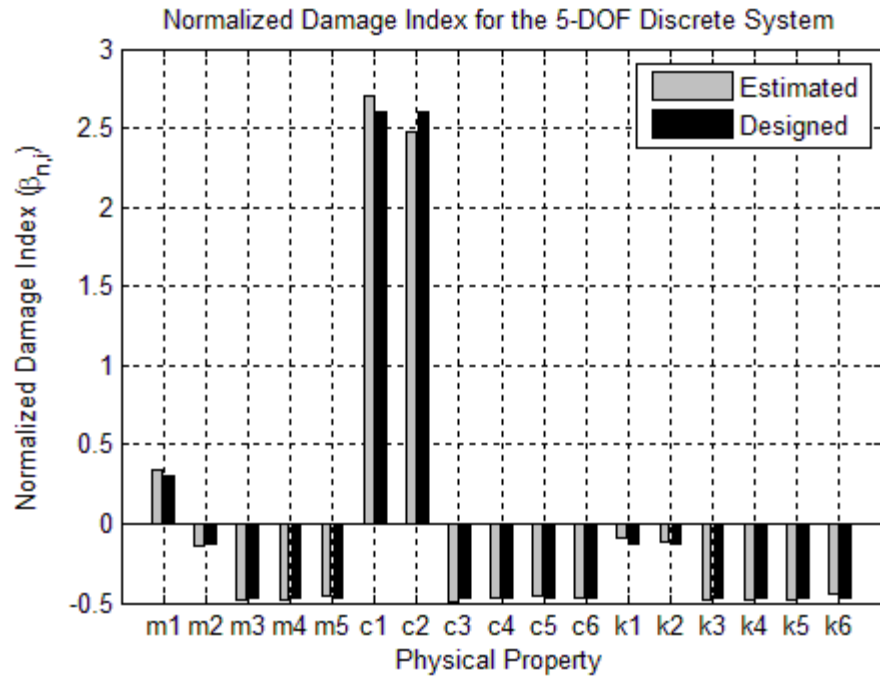


Figure 6.9. Normalized Damage Indices ( $\beta_{n,i}$ ) for 5-DOF Spring-Mass-Damper System with Noise-Polluted Accelerations (1% Noise)

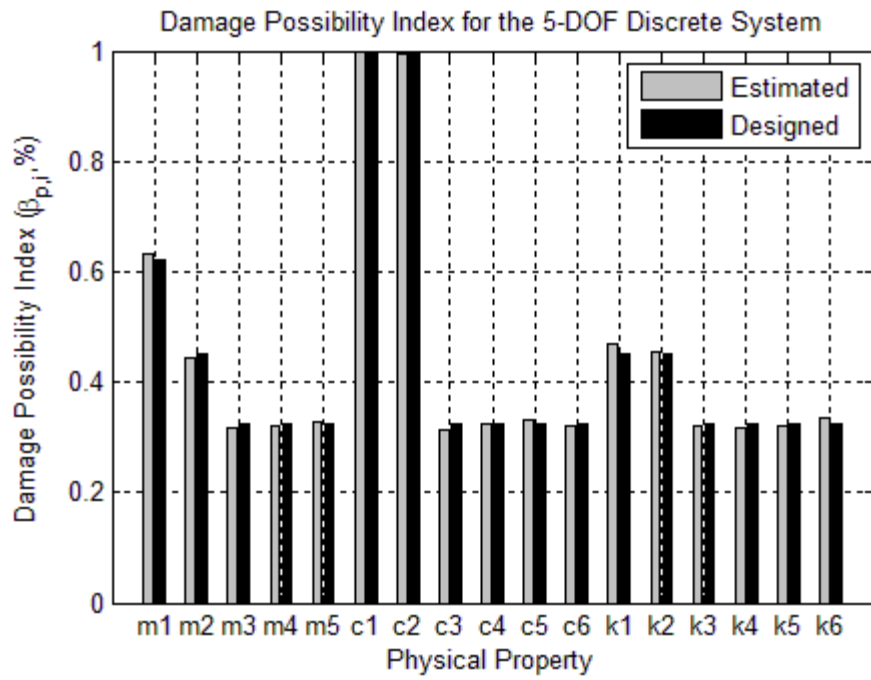
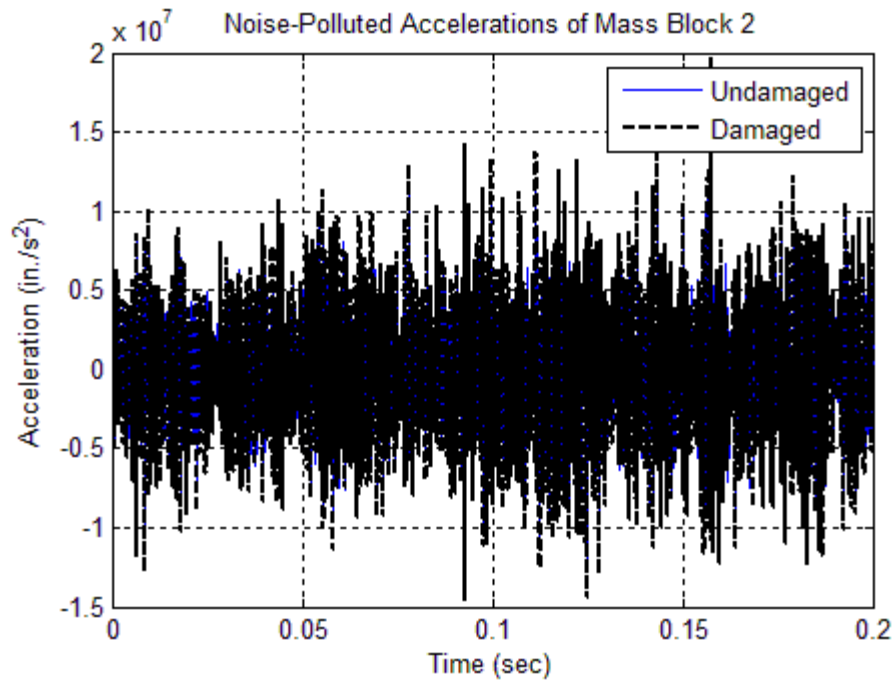


Figure 6.10. Probability Damage Indices ( $\beta_{p,i}$ ) for 5-DOF Spring-Mass-Damper System with Noise-Polluted Accelerations (1% Noise)

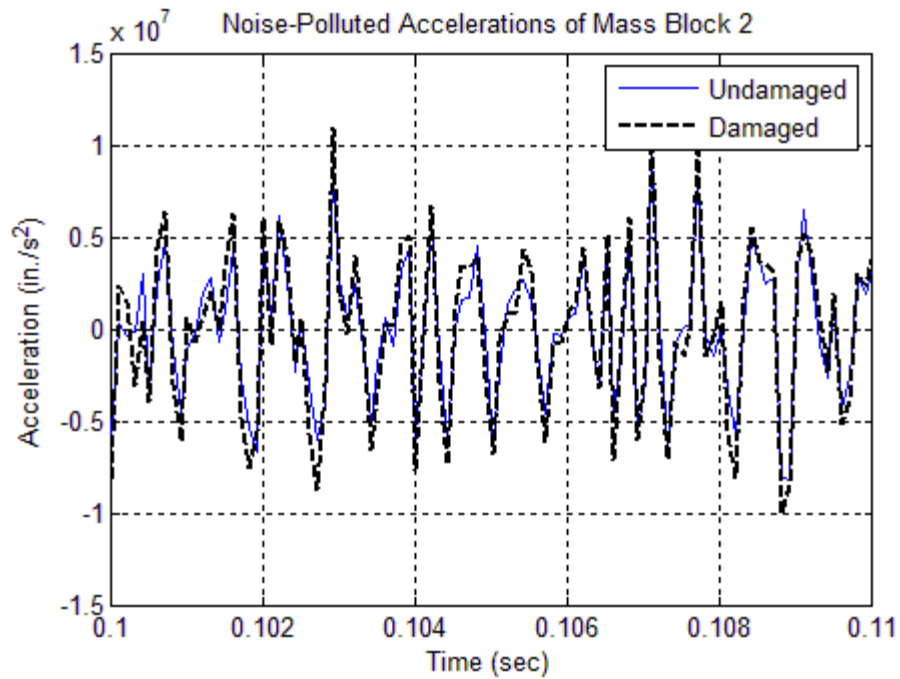
### **6.2.2 Case #6.2: Discrete System with 5% Noise Pollution Using Integral Method**

In this case, the exact accelerations of the mass blocks outputted directly from SAP2000 were contaminated by 5% of white noise. The noise-polluted accelerations of Mass Block #2 in both the undamaged and damaged cases are plotted in Figure 6.11. The filtered accelerations, estimated velocities and estimated displacements of Mass Block #2 are plotted in Figure 6.12, Figure 6.13, and Figure 6.14, respectively.

The estimated damage indices and the designed damage indices for each physical property are listed in Table 6.3 and are plotted in Figure 6.15. The estimated damage severities and the designed damage severities for each physical property are also listed in Table 6.3 and are plotted in Figure 6.16. The normalized damage indices are computed using Eq. 6.4 and are plotted in Figure 6.17. The damage possibility indices are plotted in Figure 6.18. Comparing the estimated damage indices with the designed damage indices, the integrated system analysis method can accurately locate and size multiple damage with 5% noise-polluted input data from a typical 5-DOF spring-mass-damper system.

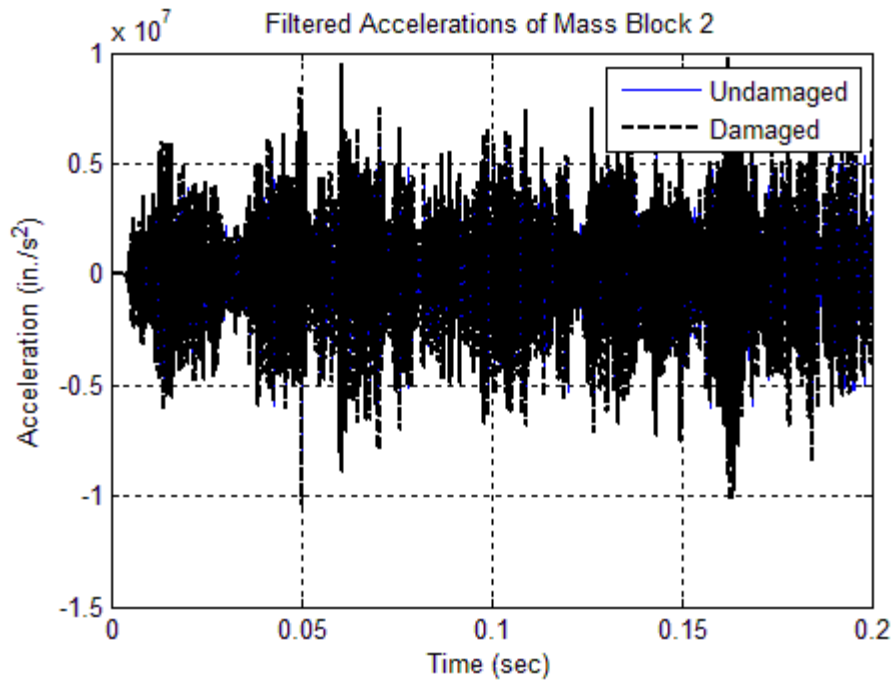


(a)

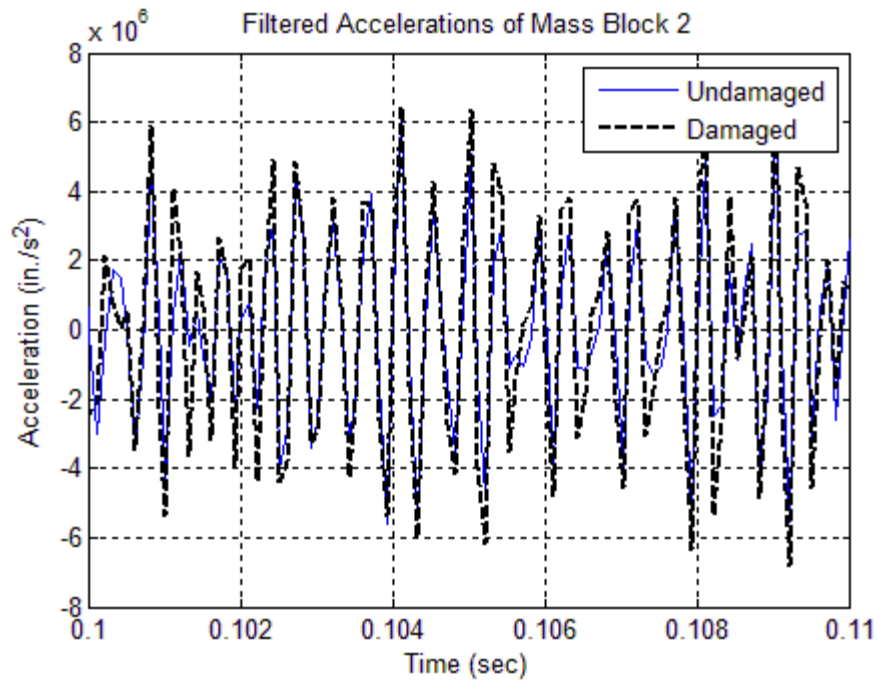


(b)

**Figure 6.11. Noise-Polluted Accelerations of Mass Block 2 for the Undamaged and Damaged Models of Case #6.2 (5% Noise): (a) Full Plot and (b) Zoomed in Plot**

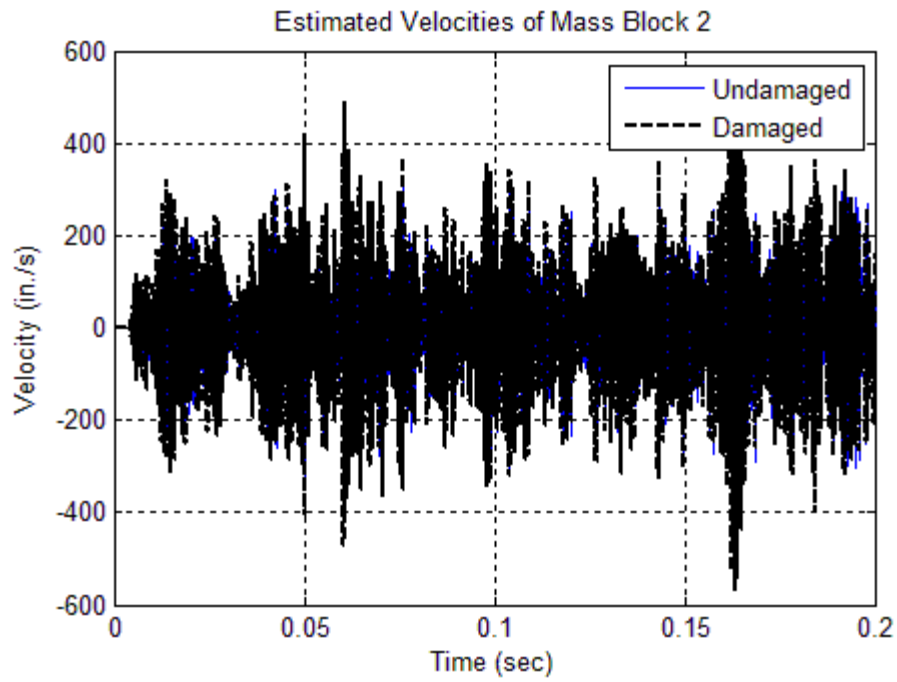


(a)

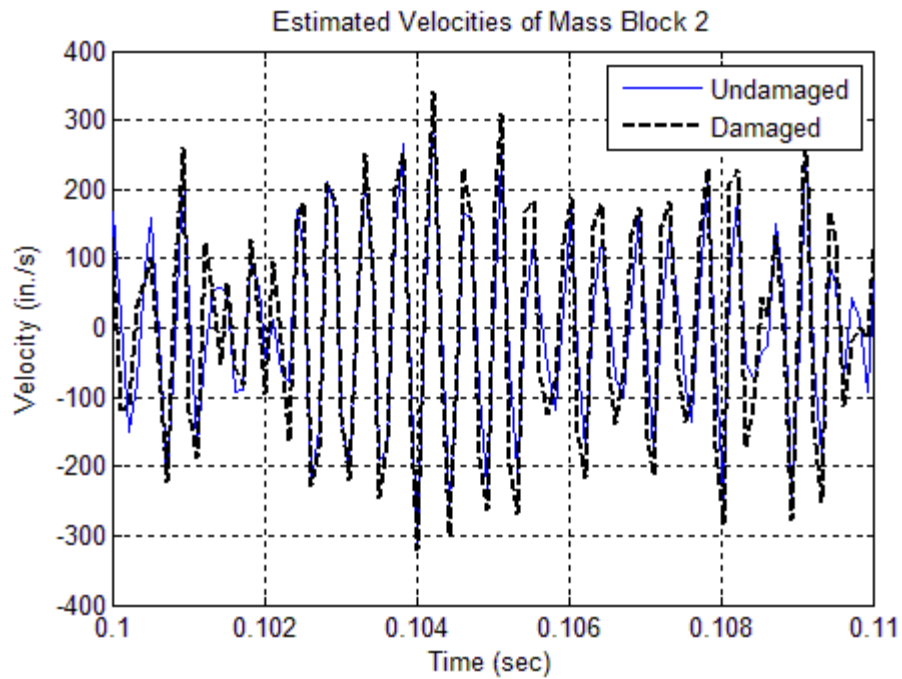


(b)

**Figure 6.12. Filtered Noise-Polluted Accelerations of Mass Block 2 for the Undamaged and Damaged Models of Case #6.2 (5% Noise): (a) Full Plot and (b) Zoomed in Plot**

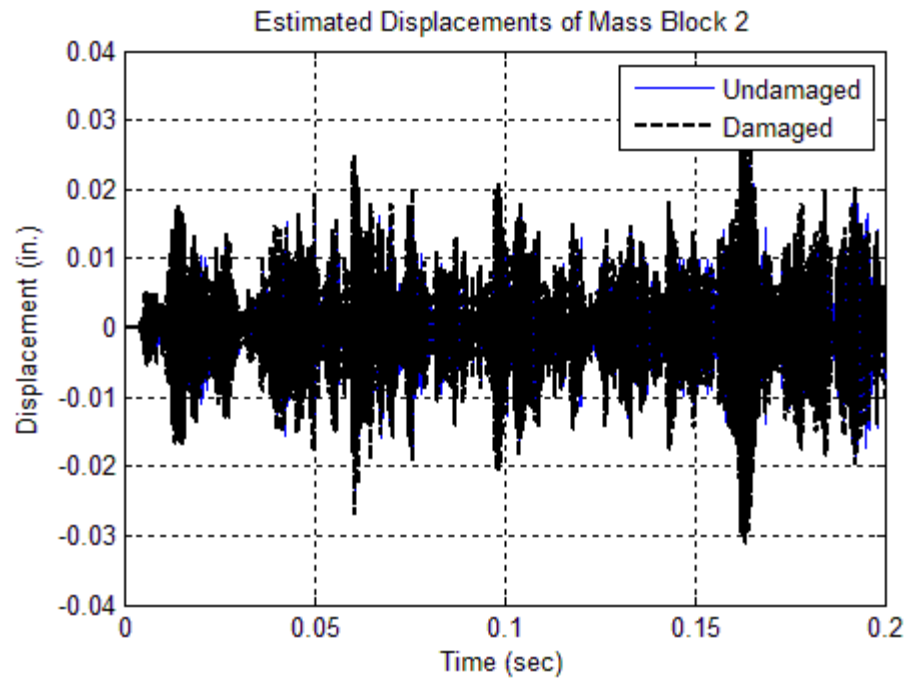


(a)

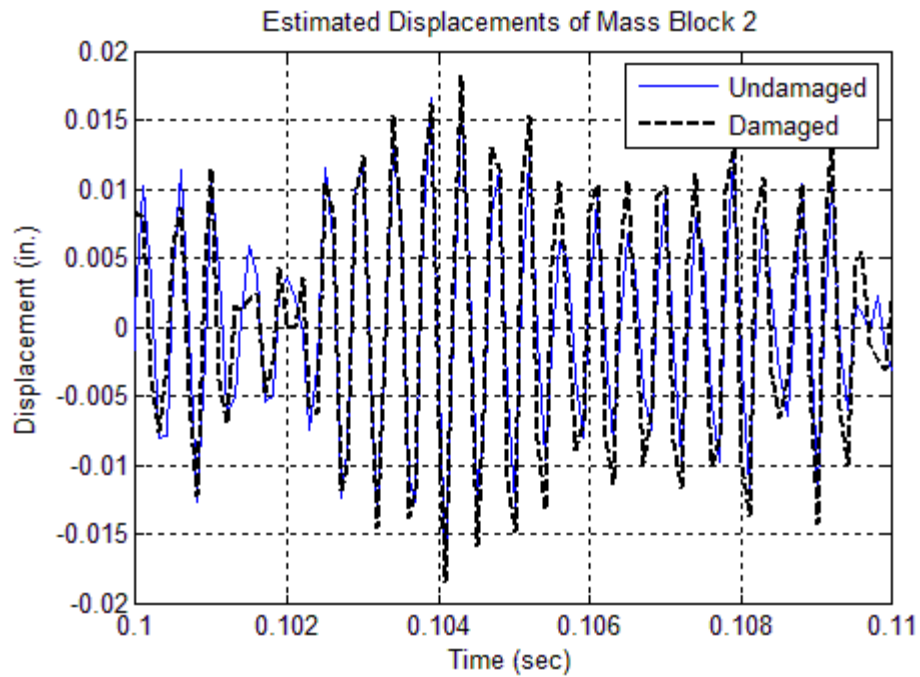


(b)

**Figure 6.13. Estimated Velocities of Mass Block 2 for the Undamaged and Damaged Models of Case #6.2 (5% Noise): (a) Full Plot and (b) Zoomed in Plot**



(a)



(b)

**Figure 6.14. Estimated Displacements of Mass Block 2 for the Undamaged and Damaged Models of Case #6.2 (5% Noise): (a) Full Plot and (b) Zoomed in Plot**

**Table 6.3. Damage Detection Results for the 5-DOF Spring-Mass-Damper System (5% Noise Pollution)**

<b>Property</b>	<b>Damage Index (<math>\beta_i</math>, Esimated)</b>	<b>Damage Severity (<math>\alpha_i</math>, Esimated)</b>	<b>Damage Index (<math>\beta_i</math>, Designed)</b>
$m_1$	1.28	-0.22	1.25
$m_2$	1.08	-0.07	1.11
$m_3$	1.00	0.00	1.00
$m_4$	1.02	-0.02	1.00
$m_5$	1.00	0.00	1.00
$c_1$	1.37	-0.27	2.00
$c_2$	1.64	-0.39	2.00
$c_3$	0.88	0.14	1.00
$c_4$	0.89	0.12	1.00
$c_5$	0.86	0.17	1.00
$c_6$	1.19	-0.16	1.00
$k_1$	1.14	-0.13	1.11
$k_2$	1.09	-0.09	1.11
$k_3$	1.01	-0.01	1.00
$k_4$	1.01	-0.01	1.00
$k_5$	0.99	0.01	1.00
$k_6$	1.00	0.00	1.00



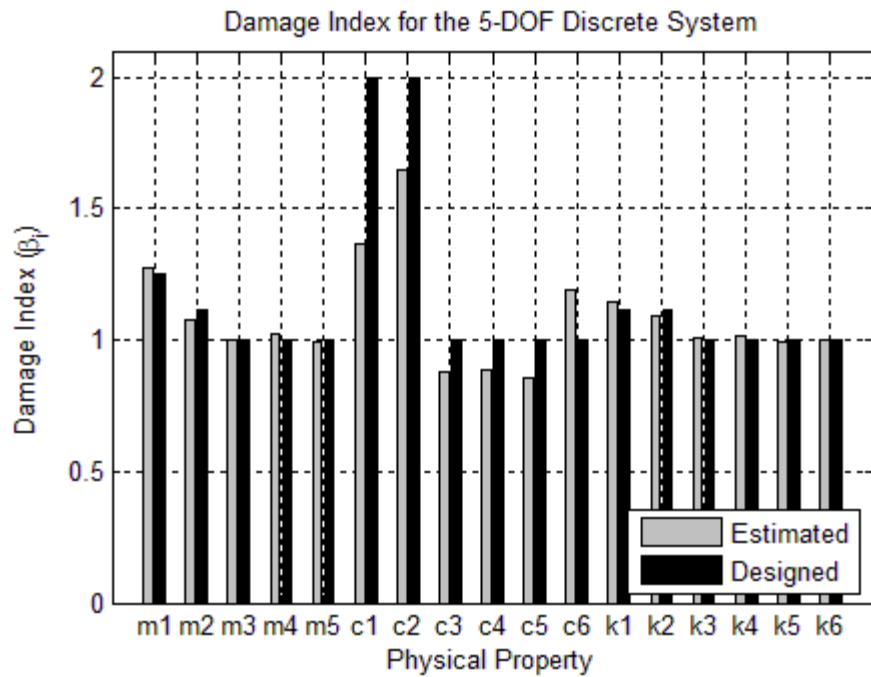


Figure 6.15. Damage Indices ( $\beta_i$ ) for 5-DOF Spring-Mass-Damper System with Noise-Polluted Accelerations (5% Noise)

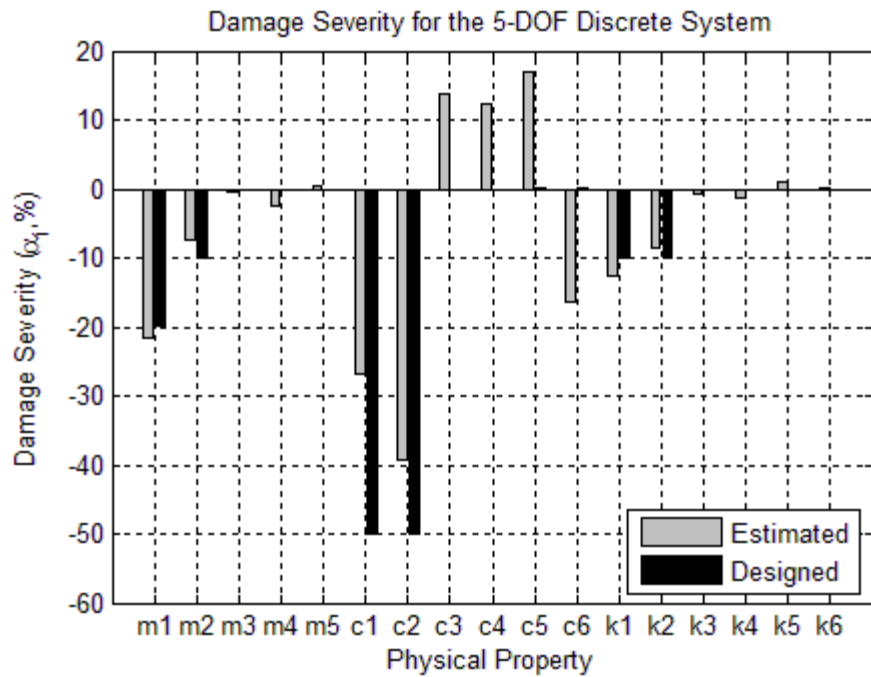


Figure 6.16. Damage Severities ( $\alpha_i$ ) for 5-DOF Spring-Mass-Damper System with Noise-Polluted Accelerations (5% Noise)

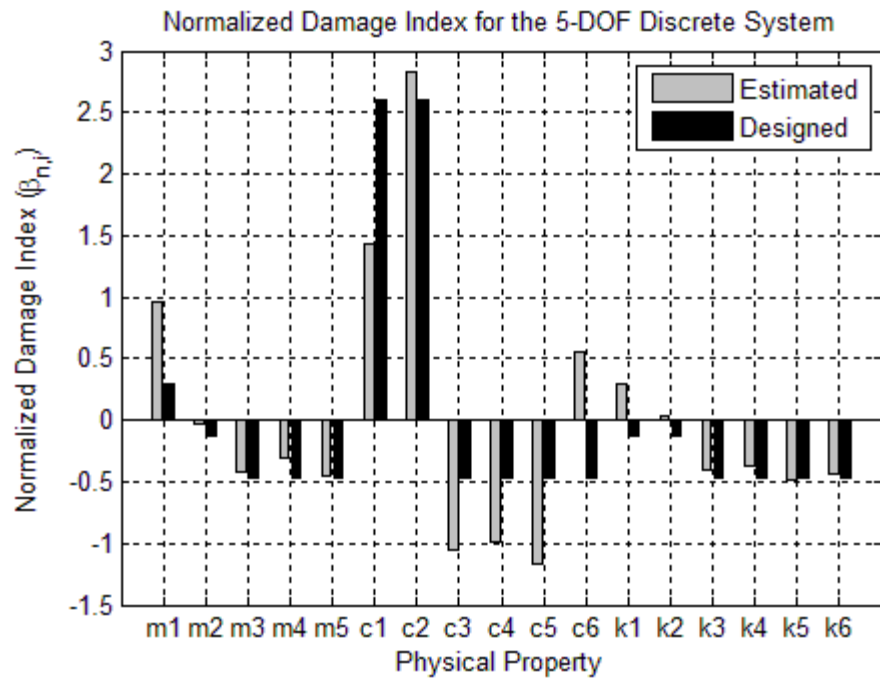


Figure 6.17. Normalized Damage Indices ( $\beta_{n,i}$ ) for 5-DOF Spring-Mass-Damper System with Noise-Polluted Accelerations (5% Noise)

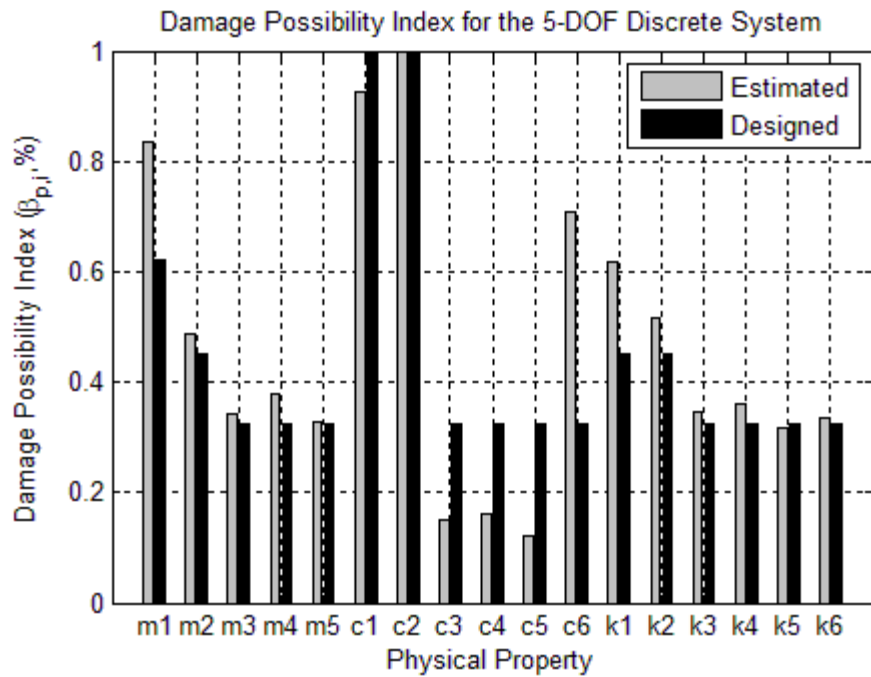


Figure 6.18. Probability Damage Indices ( $\beta_{p,i}$ ) for 5-DOF Spring-Mass-Damper System with Noise-Polluted Accelerations (5% Noise)

### 6.3 STUDIES OF NOISE INFLUENCE TO A DISCRETE SYSTEM USING ISOLATION METHOD

In this subsection, noise influence to the performance of isolated system method for discrete systems will be studied. Isolated spring-mass-damper systems from a 5-DOF system were used to study the accuracy of the Power Method. The numerical models for the damaged and undamaged 5-DOF mass-spring-damper systems were generated using SAP2000. The 5-DOF spring-mass-damper system used in this case study is plotted in Figure 6.1. The physical properties in the undamaged and damaged systems are listed in Table 6.4. Both the undamaged and damaged systems are excited by the same external force. The applied external forces are given at each 1E-4 seconds for 0.2 seconds and are plotted in Figure 6.2. In SAP2000, exact accelerations of the five mass blocks were computed every 1E-4 seconds (10,000 Hz) for 0.2 seconds. Then the accelerations of the five mass blocks were contaminated by 1% and 5% white noise. To reduce the influence from the noise in the input signals, a bandpass digital filter was used to filter the noise-polluted accelerations. The velocities of the mass blocks are estimated using Eq. 6.2 based on the filtered noise-polluted accelerations and the displacements of the mass blocks are estimated using Eq. 6.3 based on the filtered estimated velocities.

In this case, the computed velocity ( $\dot{x}(t)$ ) of the mass block in the undamaged case was used as the velocity used to compute power ( $\dot{\Delta}$ ) for both undamaged and damaged cases. The coefficient matrices and known vector, X and Y, were constructed by substituting the acceleration ( $\ddot{x}(t)$ ), velocity ( $\dot{x}(t)$ ), displacement ( $x(t)$ ), and velocity used to compute power ( $\dot{\Delta}$ ) into Eq. 2.179 and Eq. 2.181. The coefficient damage index vector,  $\beta$ , was computed using Eq. 2.183. Then the damage indices for mass, spring and damper are computed using Eqs. 2.184 through 2.188. The damage severities for mass, spring and

damper are computed using Eqs. 2.189 through 2.193.

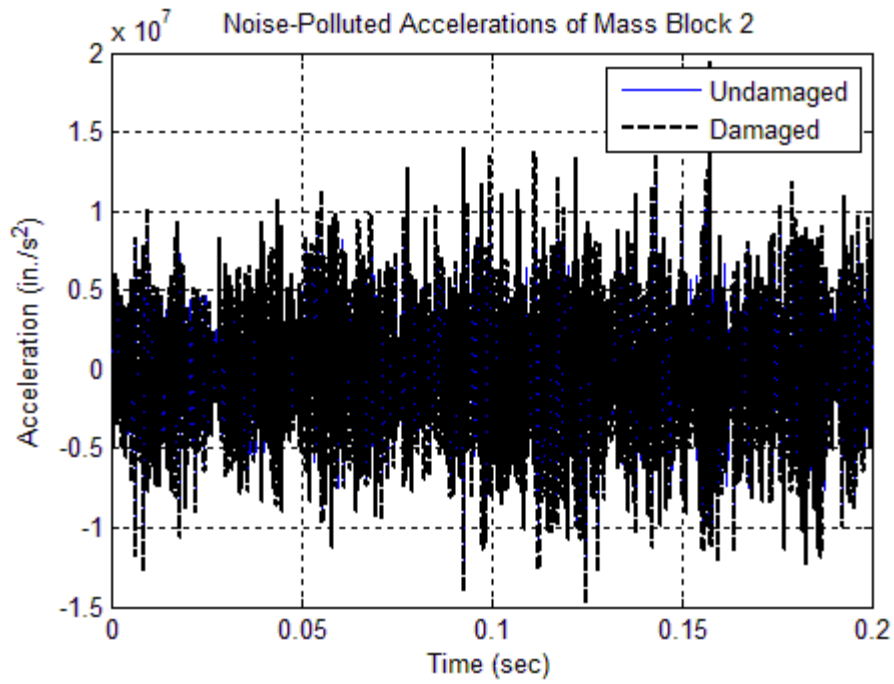
### **6.3.1 Case #6.3: Discrete System with 1% Noise Pollution Using Isolation Method**

In this case, the exact accelerations of the mass blocks outputted directly from SAP2000 were contaminated by 1% of white noise. The noise-polluted accelerations of Mass Block #2 in both the undamaged and damaged cases are plotted in Figure 6.19. The filtered accelerations, estimated velocities and estimated displacements of Mass Block #2 are plotted in Figure 6.20, Figure 6.21, and Figure 6.22, respectively.

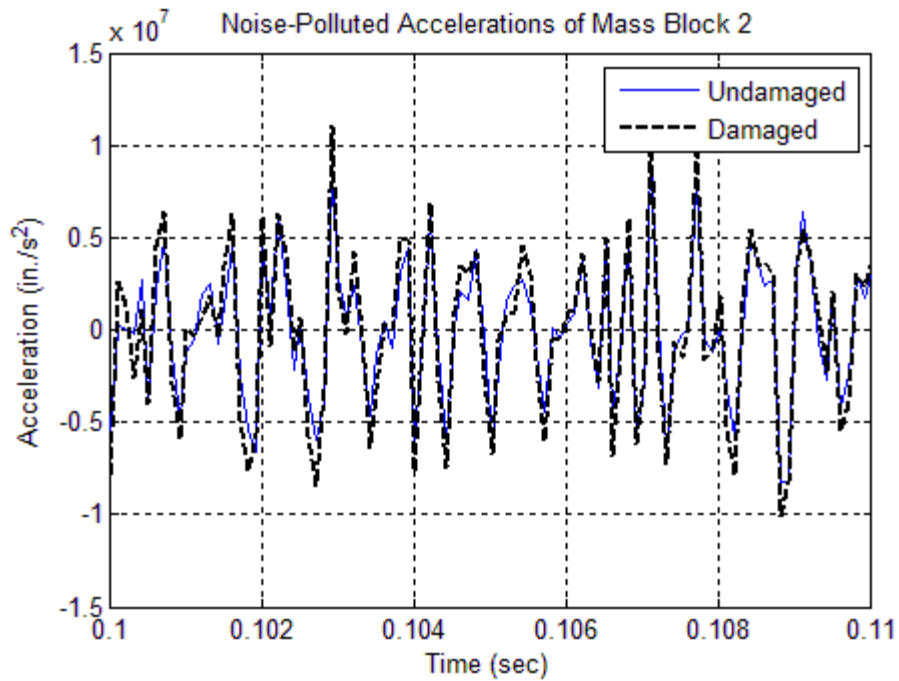
The estimated damage indices and the designed damage indices for each physical property are listed in Table 6.5 and are plotted in Figure 6.23. The estimated damage severities and the designed damage severities for each physical property are also listed in Table 6.5 and are plotted in Figure 6.24. The normalized damage indices are computed using Eq. 6.4 and are plotted in Figure 6.25. The damage possibility indices are plotted in Figure 6.26. Comparing the estimated damage indices with the designed damage indices, the isolated system analysis method can accurately locate and size multiple damage with 1% noise-polluted input data from a typical 5-DOF spring-mass-damper system.

**Table 6.4. Physical Properties of the 5 Isolated Spring-Mass-Damper Systems for Noise Study**

<b>Undamage Systems</b>					
<b>Property</b>	<b>System #1</b>	<b>System #2</b>	<b>System #3</b>	<b>System #4</b>	<b>System #5</b>
$m_i$ (kip-s <sup>2</sup> /in.)	5.826E-05	5.826E-05	5.826E-05	5.826E-05	5.826E-05
$c_i$ (kip-s/in.)	0.10	0.10	0.10	0.10	0.10
$c_{i+1}$ (kip-s/in.)	0.10	0.10	0.10	0.10	0.10
$k_i$ (kip/in.)	15974.17	15974.17	15974.17	15974.17	15974.17
$k_{i+1}$ (kip/in.)	15974.17	15974.17	15974.17	15974.17	15974.17
<b>Damaged Systems</b>					
<b>Property</b>	<b>System #1</b>	<b>System #2</b>	<b>System #3</b>	<b>System #4</b>	<b>System #5</b>
$m_i$ (kip-s <sup>2</sup> /in.)	4.661E-05	5.243E-05	5.826E-05	5.826E-05	5.826E-05
$c_i$ (kip-s/in.)	0.05	0.05	0.10	0.10	0.10
$c_{i+1}$ (kip-s/in.)	0.05	0.10	0.10	0.10	0.10
$k_i$ (kip/in.)	14376.75	14376.75	15974.17	15974.17	15974.17
$k_{i+1}$ (kip/in.)	14376.75	15974.17	15974.17	15974.17	15974.17

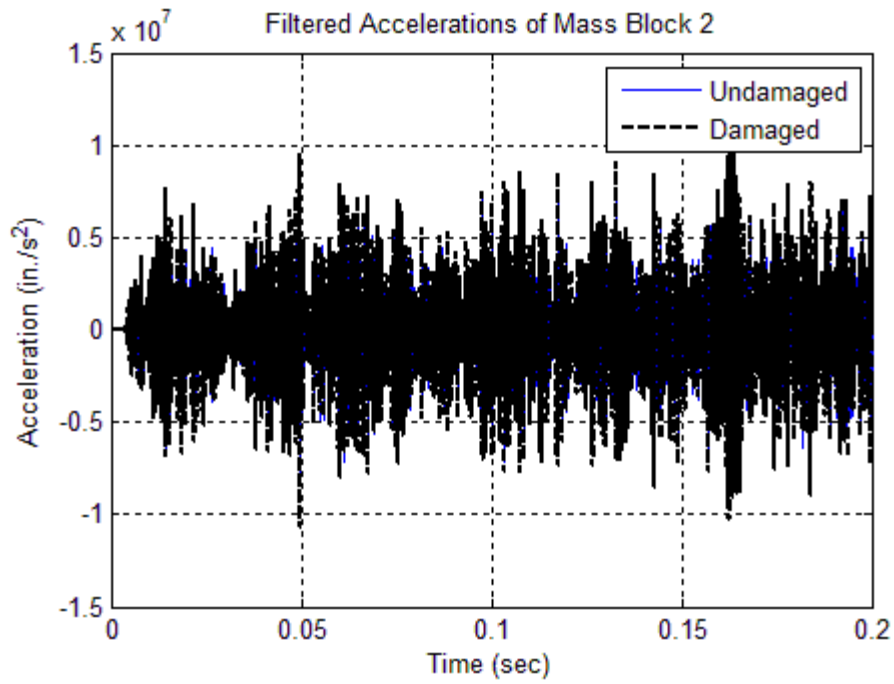


(a)

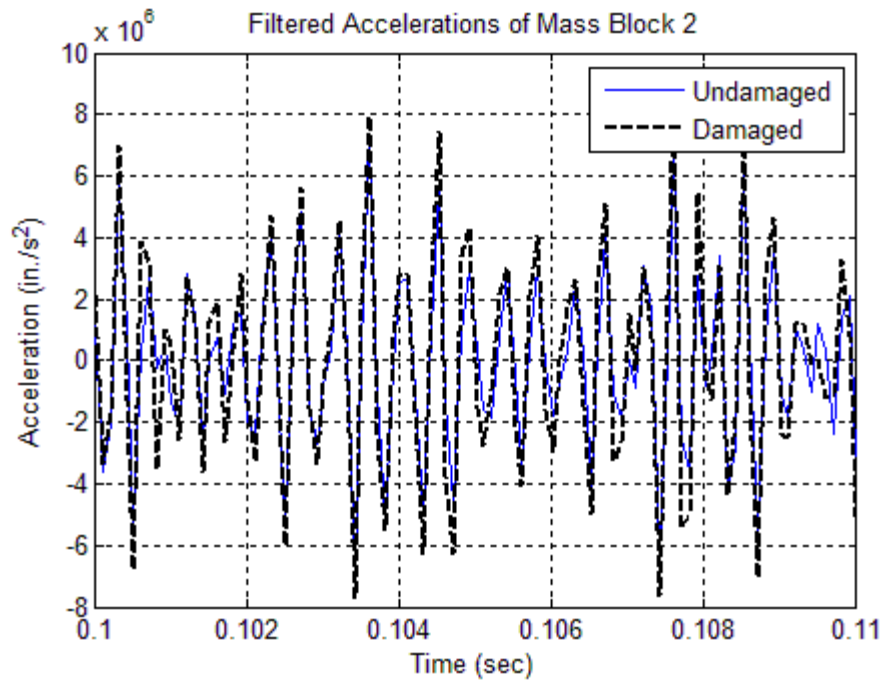


(b)

**Figure 6.19. Noise-Polluted Accelerations of Mass Block 2 for the Undamaged and Damaged Models of Case #6.3 (1% Noise): (a) Full Plot and (b) Zoomed in Plot**

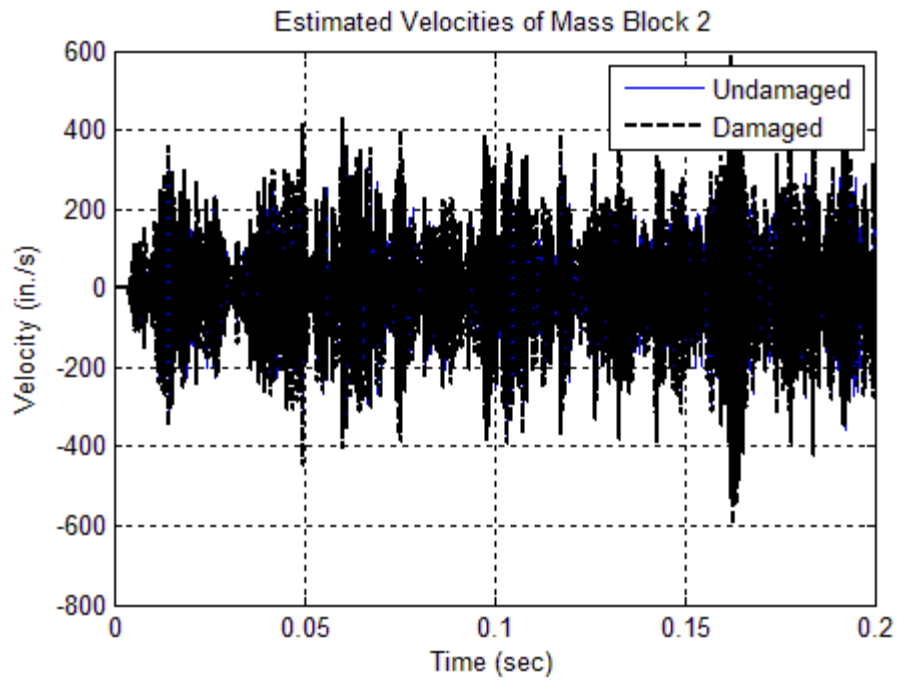


(a)

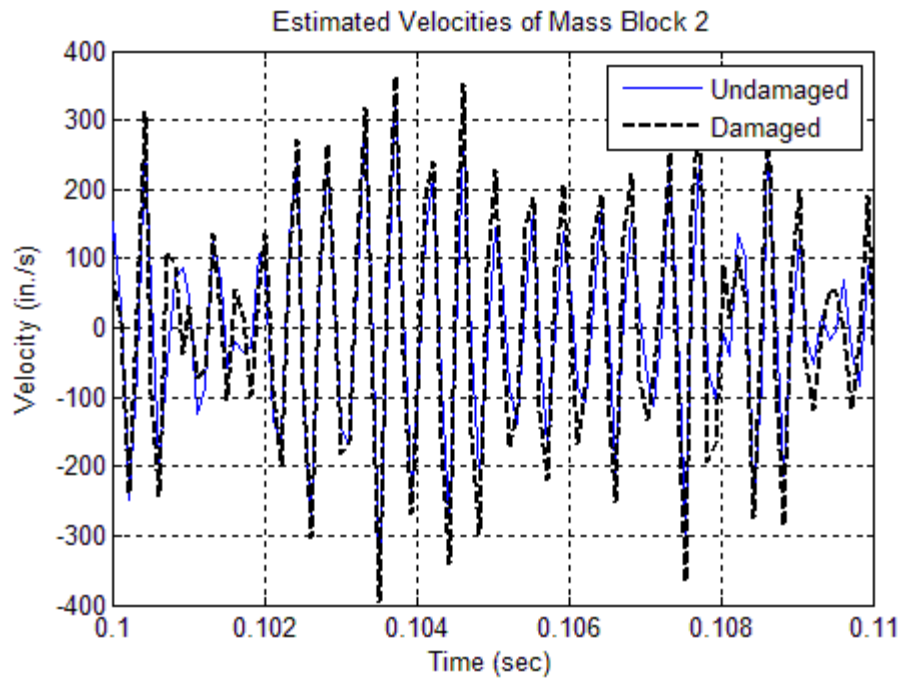


(b)

**Figure 6.20. Filtered Noise-Polluted Accelerations of Mass Block 2 for the Undamaged and Damaged Models of Case #6.3 (1% Noise): (a) Full Plot and (b) Zoomed in Plot**



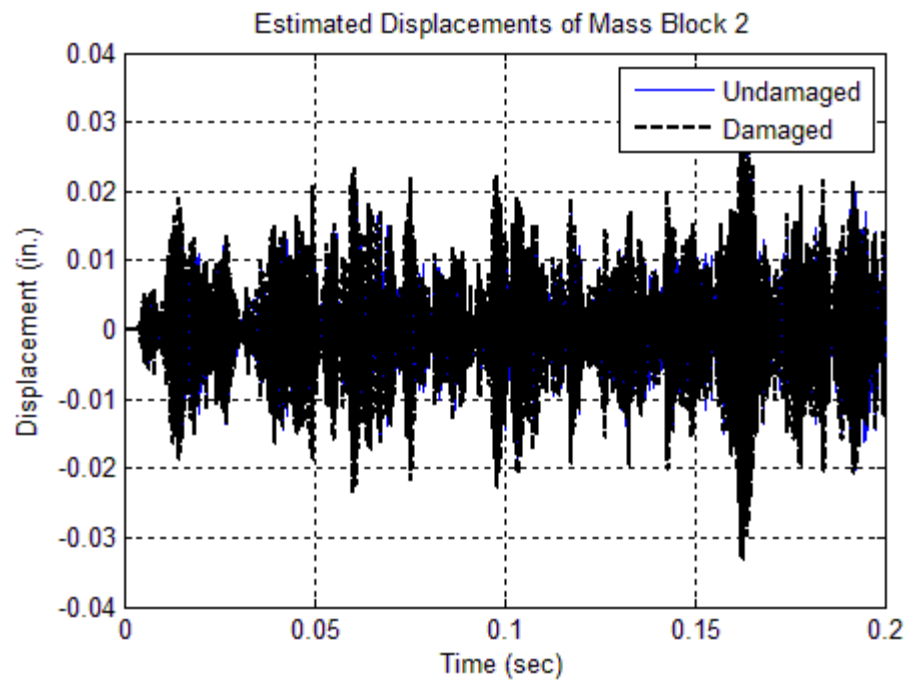
(a)



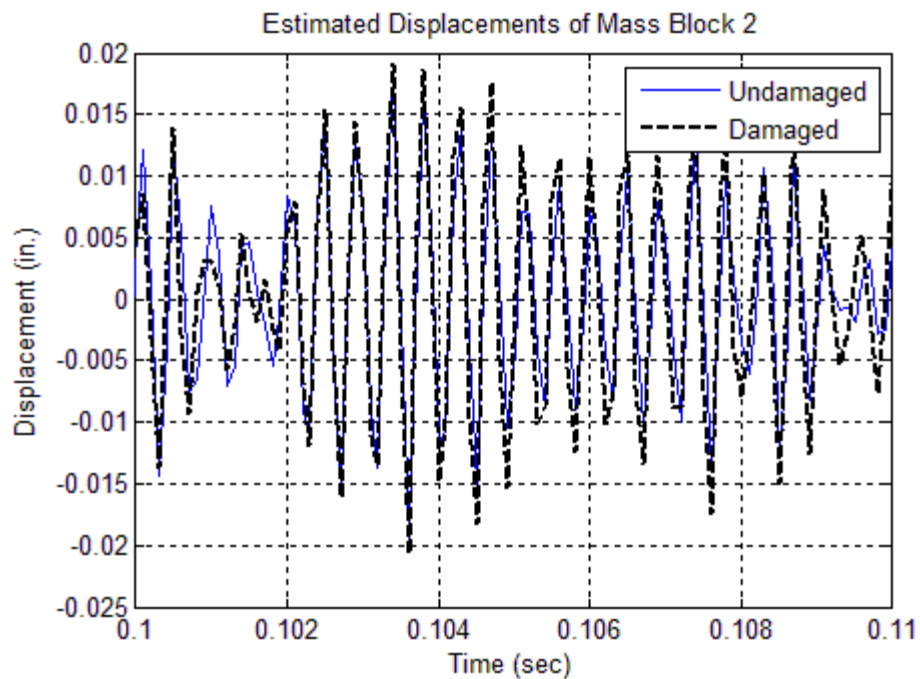
(b)

**Figure 6.21. Estimated Velocities of Mass Block 2 for the Undamaged and Damaged Models of Case #6.3 (1% Noise): (a) Full Plot and (b) Zoomed in Plot**





(a)



(b)

**Figure 6.22. Estimated Displacements of Mass Block 2 for the Undamaged and Damaged Models of Case #6.3 (1% Noise): (a) Full Plot and (b) Zoomed in Plot**

**Table 6.5. Damage Detection Results for the 5 Isolated Spring-Mass-Damper System (1% Noise Pollution)**

<b>Designed Damage Indices</b>					
<b>Property</b>	<b>System #1</b>	<b>System #2</b>	<b>System #3</b>	<b>System #4</b>	<b>System #5</b>
$m_i$	1.25	1.11	1.00	1.00	1.00
$c_i$	2.00	2.00	1.00	1.00	1.00
$c_{i+1}$	2.00	1.00	1.00	1.00	1.00
$k_i$	1.11	1.11	1.00	1.00	1.00
$k_{i+1}$	1.11	1.00	1.00	1.00	1.00
<b>Estimated Damage Indices</b>					
<b>Property</b>	<b>System #1</b>	<b>System #2</b>	<b>System #3</b>	<b>System #4</b>	<b>System #5</b>
$m_i$	1.25	1.11	1.00	0.99	1.00
$c_i$	1.91	2.04	0.99	1.00	0.98
$c_{i+1}$	1.98	1.00	0.99	0.97	1.02
$k_i$	1.11	1.11	1.00	0.99	1.00
$k_{i+1}$	1.11	0.99	1.00	0.99	1.00

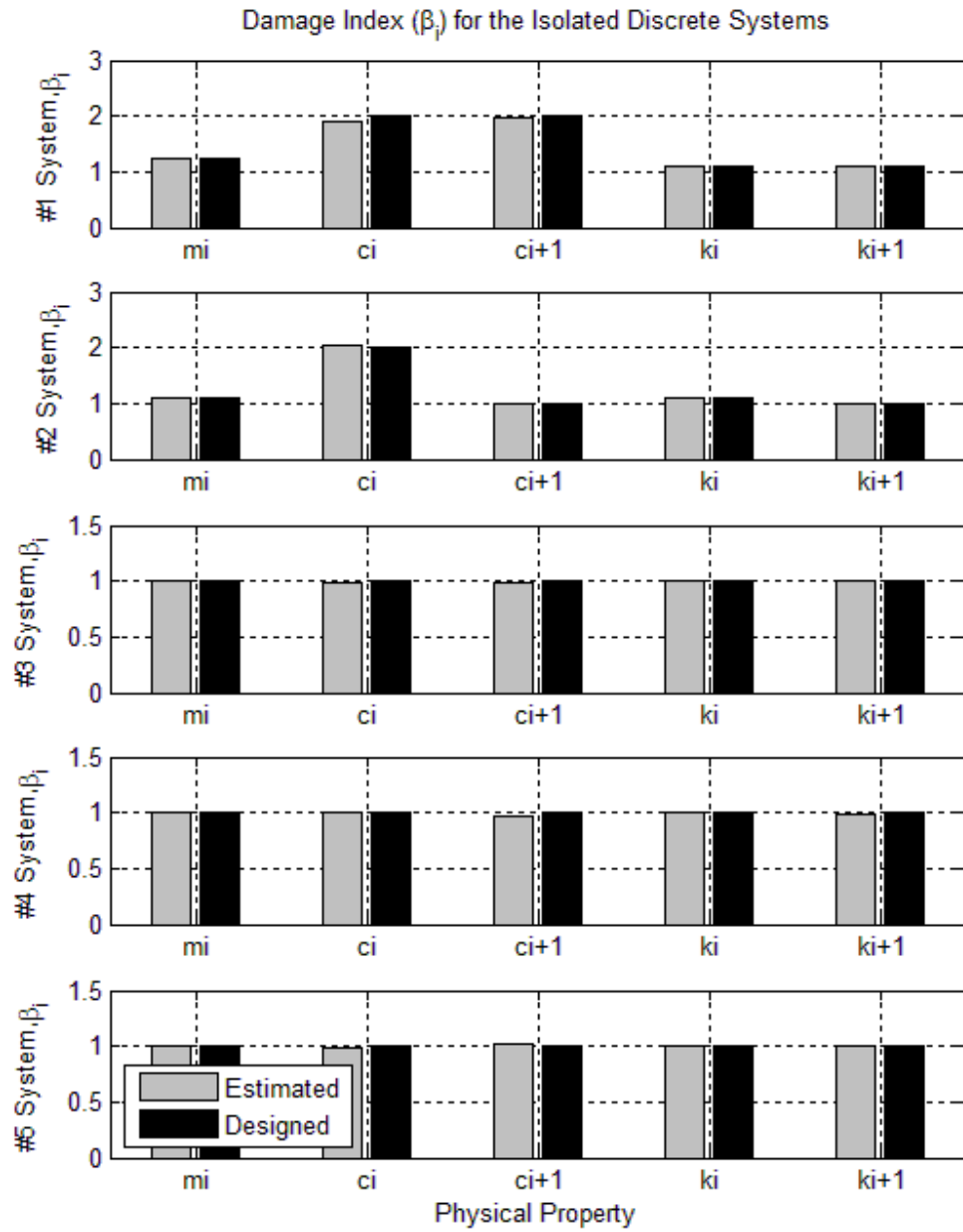


Figure 6.23. Damage Indices ( $\beta_i$ ) for the 5 Isolated Spring-Mass-Damper System with Noise-Polluted Accelerations (1% Noise)

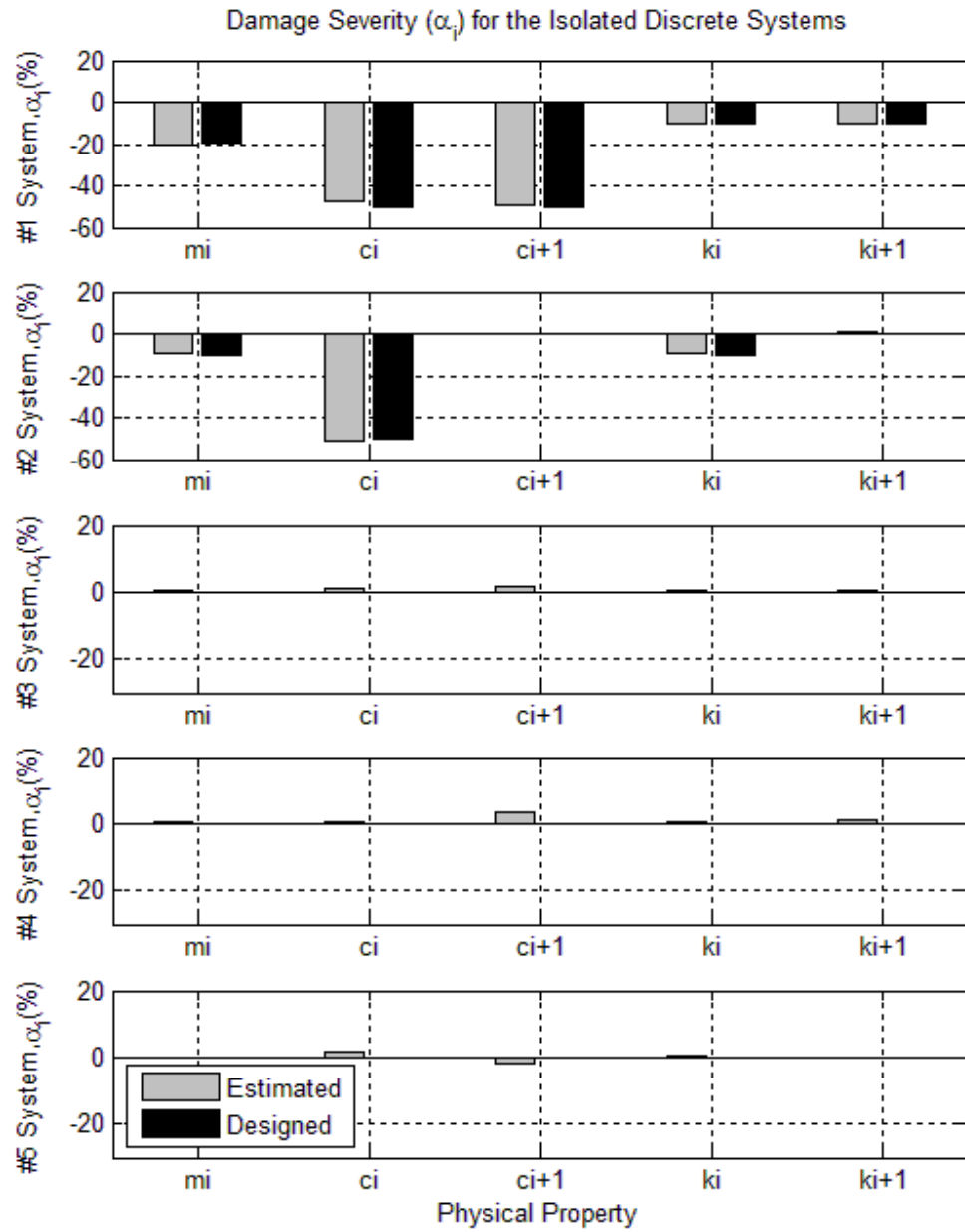


Figure 6.24. Damage Severities ( $\alpha_i$ ) for 5-DOF Spring-Mass-Damper System with Noise-Polluted Accelerations (1% Noise)

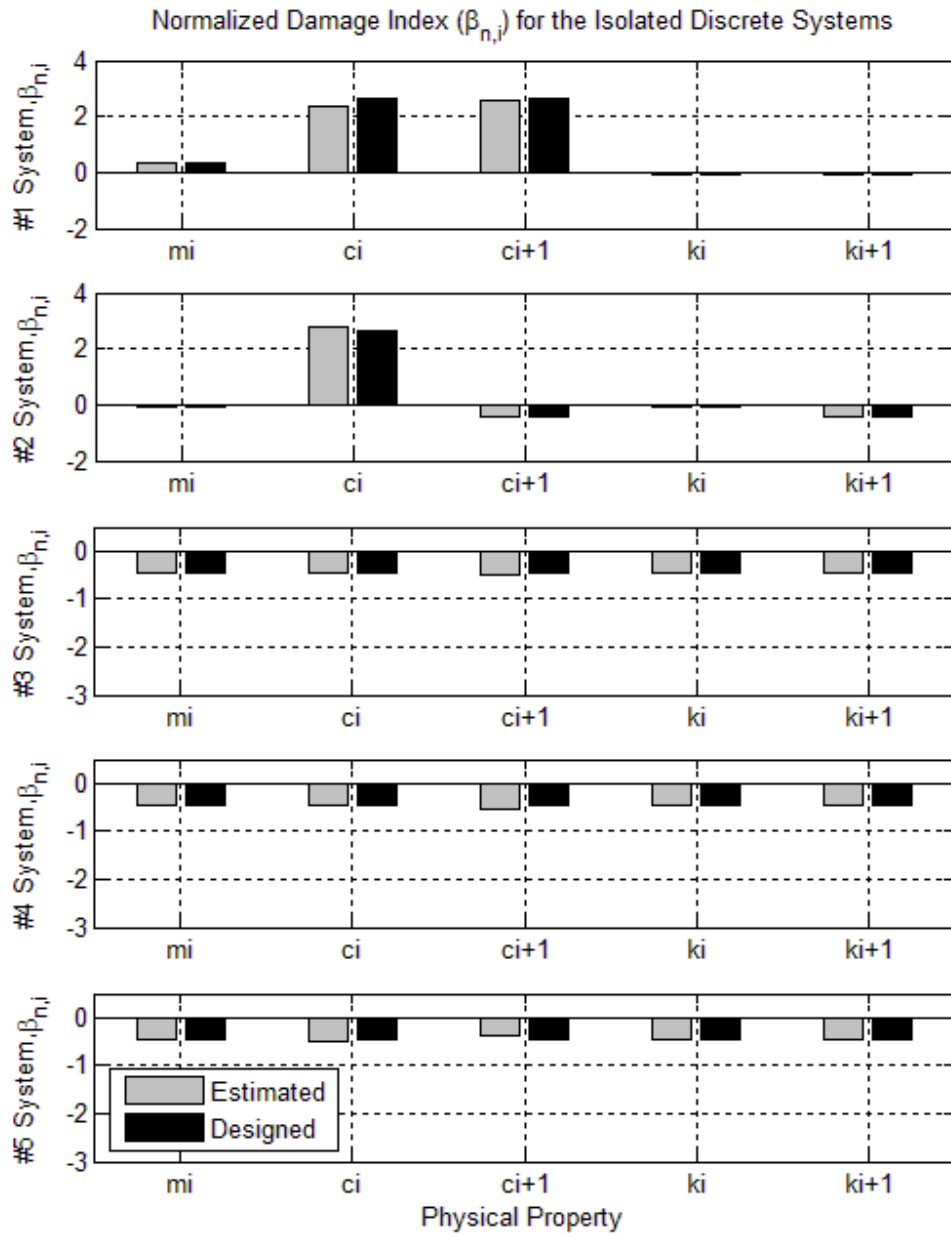


Figure 6.25. Normalized Damage Indices ( $\beta_{n,i}$ ) for 5-DOF Spring-Mass-Damper System with Noise-Polluted Accelerations (1% Noise)

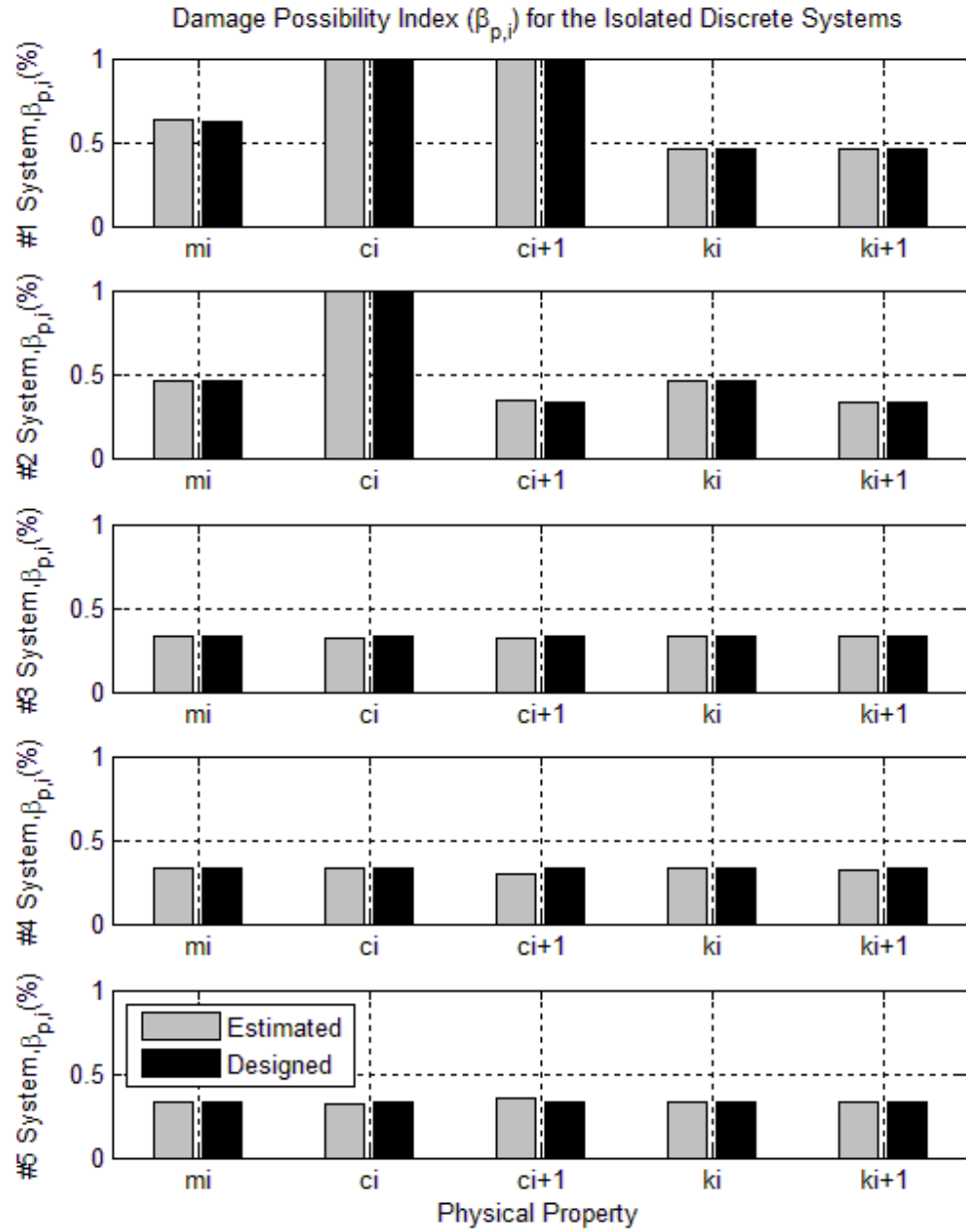
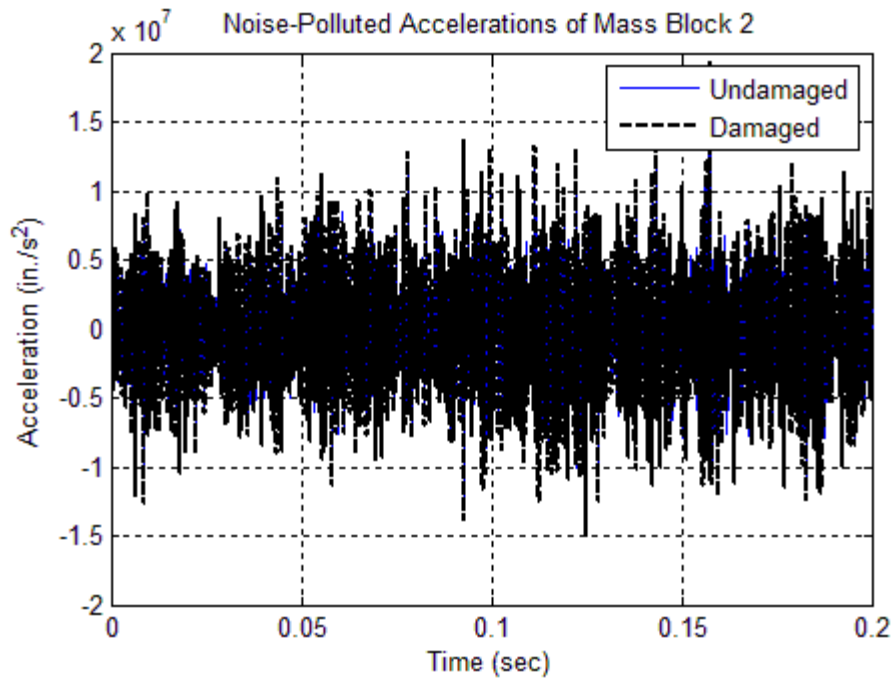


Figure 6.26. Damage Possibility Indices ( $\beta_{p,i}$ ) for 5-DOF Spring-Mass-Damper System with Noise-Polluted Accelerations (1% Noise)

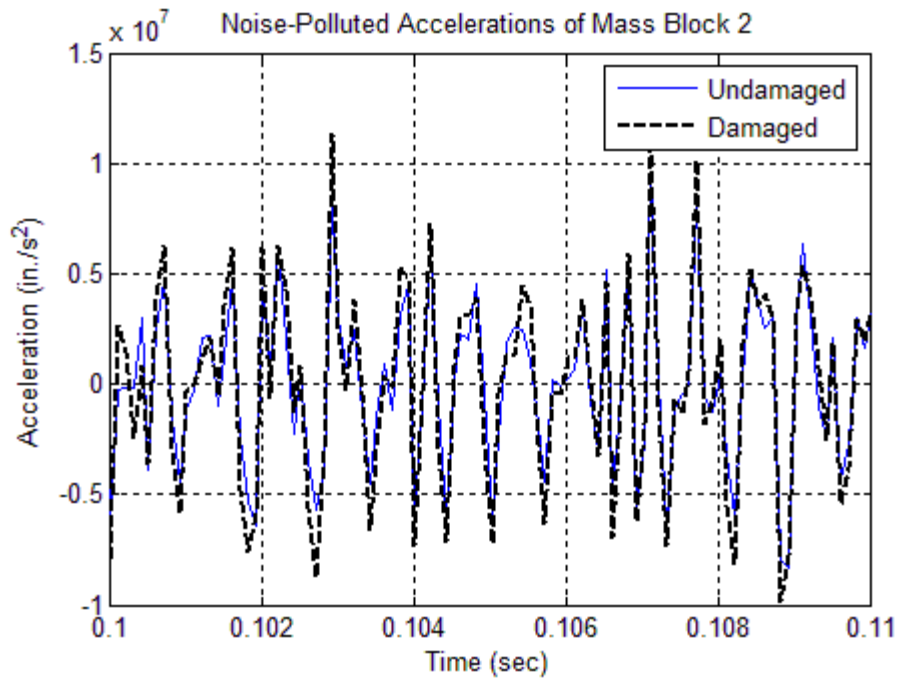
### **6.3.2 Case #6.4: Discrete System with 5% Noise Pollution Using Isolation Method**

In this case, the exact accelerations of the mass blocks outputted directly from SAP2000 were contaminated by 5% of white noise. The noise-polluted accelerations of Mass Block #2 in both the undamaged and damaged cases are plotted in Figure 6.27. The filtered accelerations, estimated velocities and estimated displacements of Mass Block #2 are plotted in Figure 6.28, Figure 6.29, and Figure 6.30, respectively.

The estimated damage indices and the designed damage indices for each physical property are listed in Table 6.6 and are plotted in Figure 6.31. The estimated damage severities and the designed damage severities for each physical property are also listed in Table 6.6 and are plotted in Figure 6.32. The normalized damage indices are computed using Eq. 6.4 and are plotted in Figure 6.33. The damage possibility indices are plotted in Figure 6.34. Comparing the estimated damage indices with the designed damage indices, the integrated system analysis method can accurately locate and size multiple damage with 5% noise-polluted input data from a typical 5-DOF spring-mass-damper system.



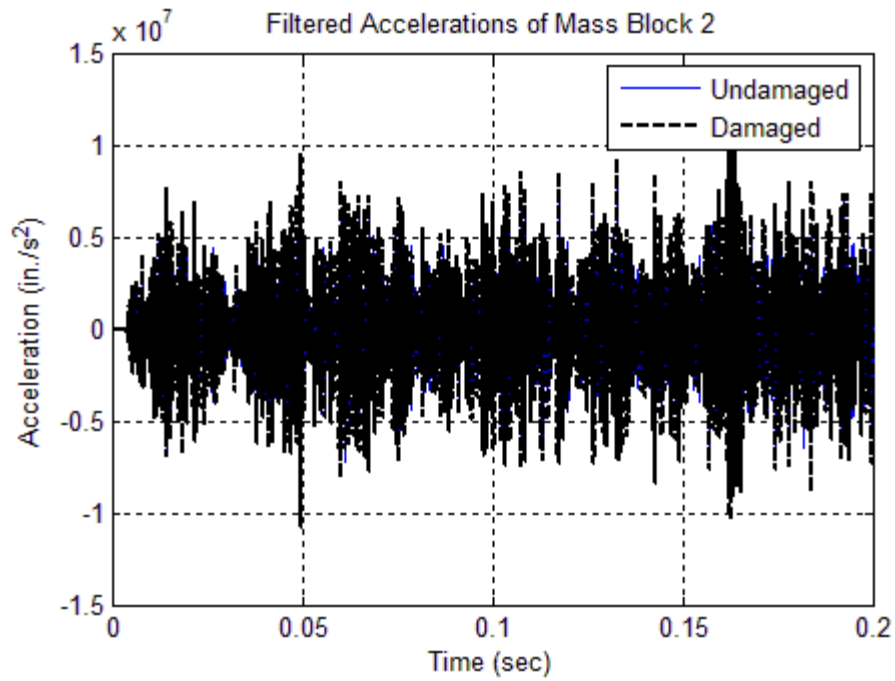
(a)



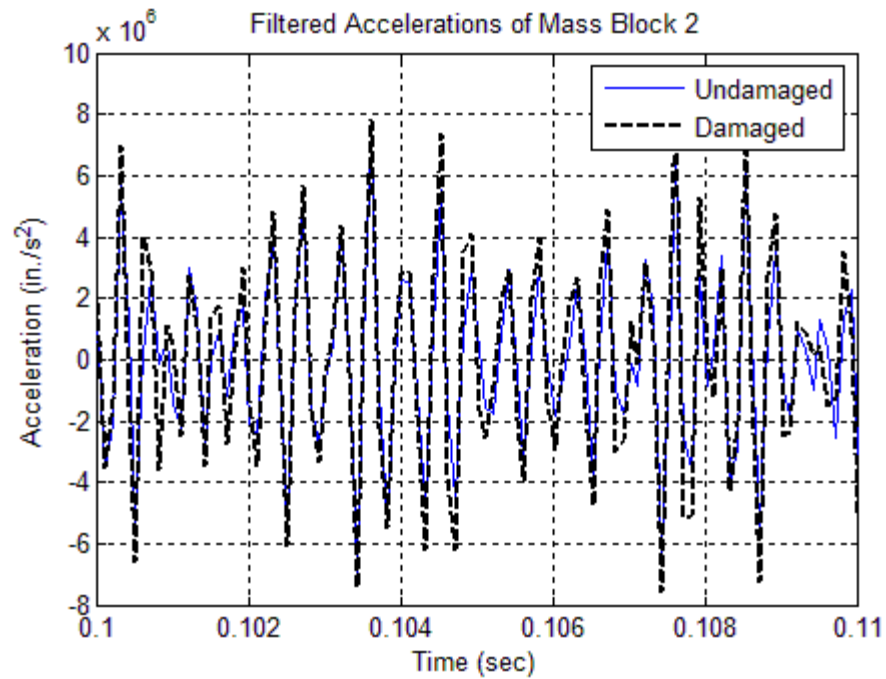
(b)

**Figure 6.27. Noise-Polluted Accelerations of Mass Block 2 for the Undamaged and Damaged Models of Case #6.4 (5% Noise): (a) Full Plot and (b) Zoomed in Plot**



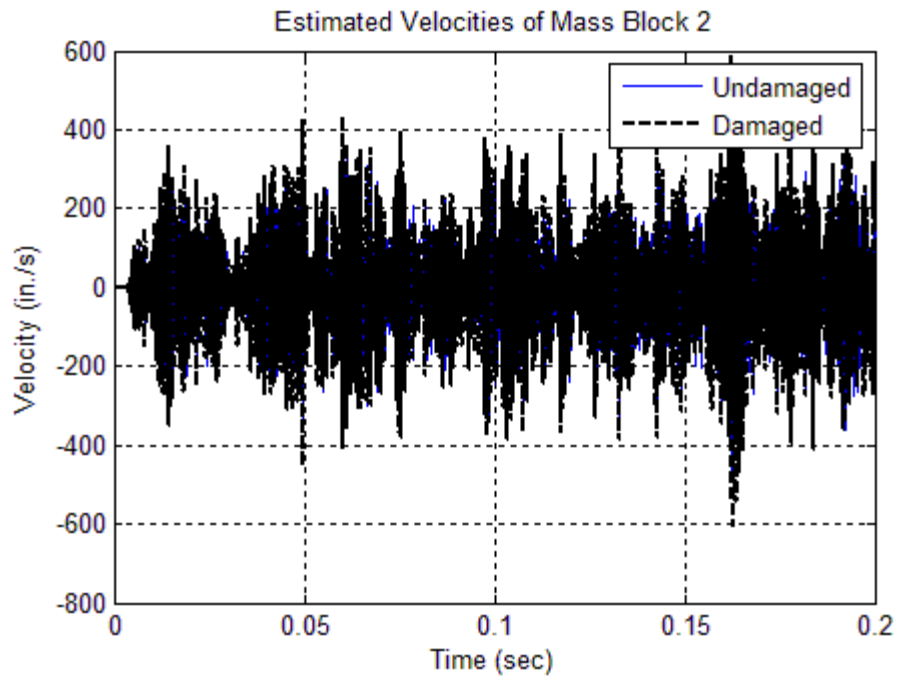


(a)

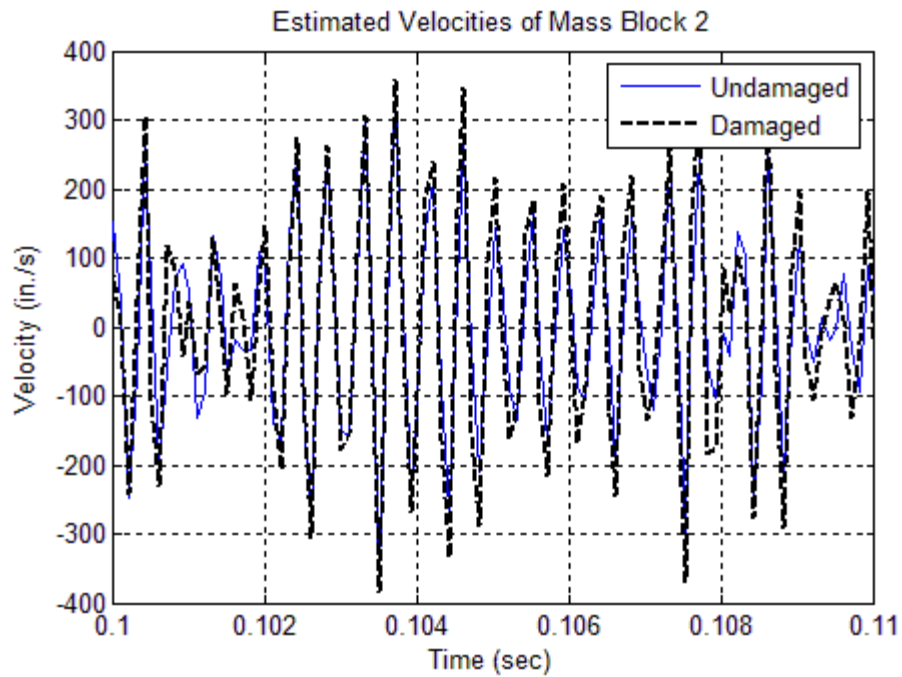


(b)

**Figure 6.28. Filtered Noise-Polluted Accelerations of Mass Block 2 for the Undamaged and Damaged Models of Case #6.4 (5% Noise): (a) Full Plot and (b) Zoomed in Plot**

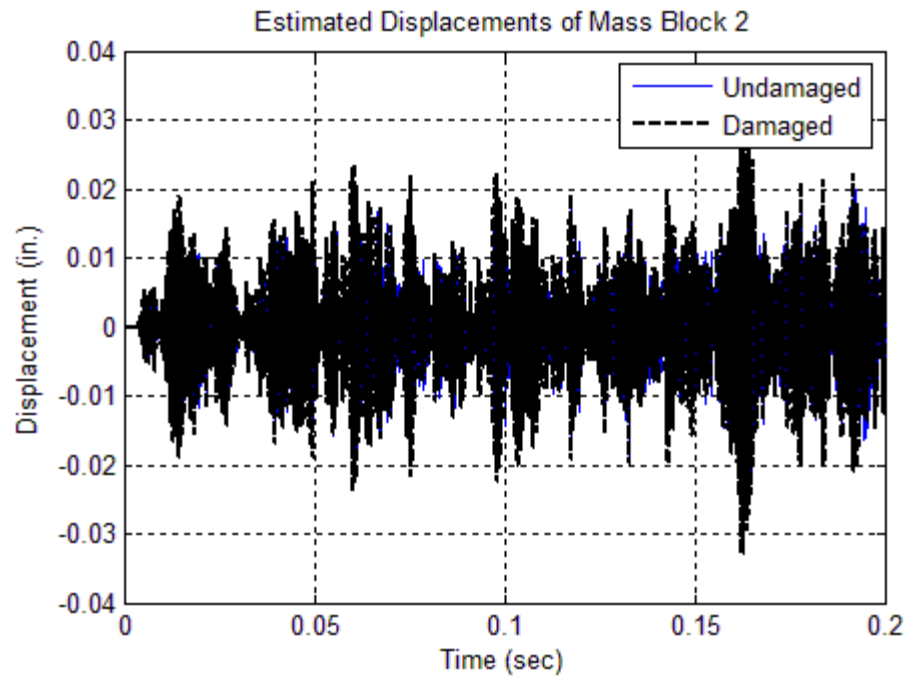


(a)

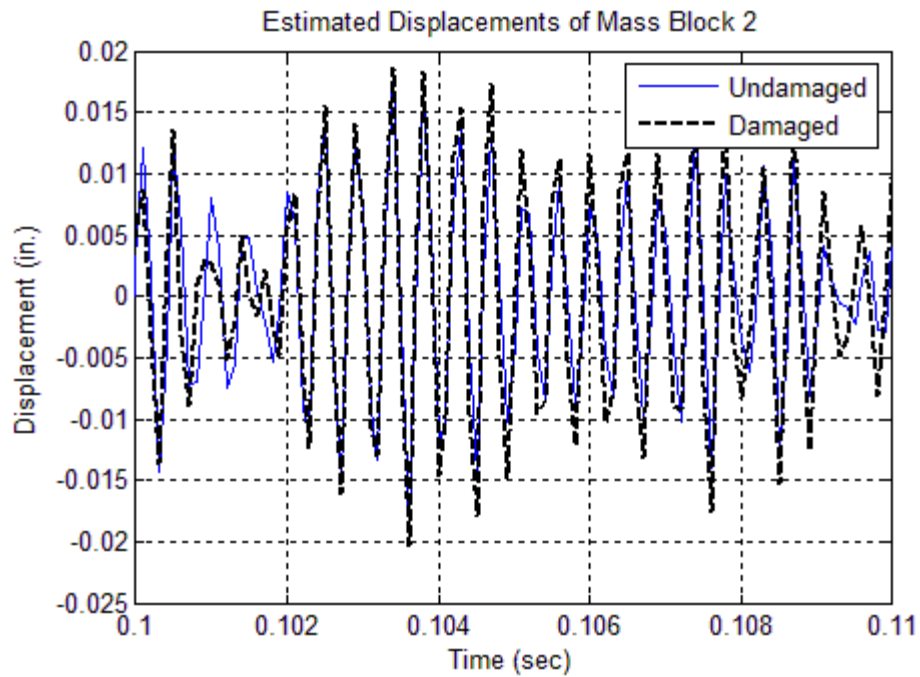


(b)

**Figure 6.29. Estimated Velocities of Mass Block 2 for the Undamaged and Damaged Models of Case #6.4 (5% Noise): (a) Full Plot and (b) Zoomed in Plot**



(a)



(b)

**Figure 6.30. Estimated Displacements of Mass Block 2 for the Undamaged and Damaged Models of Case #6.4 (5% Noise): (a) Full Plot and (b) Zoomed in Plot**

**Table 6.6. Damage Detection Results for the 5 Isolated Spring-Mass-Damper System (5% Noise Pollution)**

<b>Designed Damage Indices</b>					
<b>Property</b>	<b>System #1</b>	<b>System #2</b>	<b>System #3</b>	<b>System #4</b>	<b>System #5</b>
$m_i$	1.25	1.11	1.00	1.00	1.00
$c_i$	2.00	2.00	1.00	1.00	1.00
$c_{i+1}$	2.00	1.00	1.00	1.00	1.00
$k_i$	1.11	1.11	1.00	1.00	1.00
$k_{i+1}$	1.11	1.00	1.00	1.00	1.00
<b>Estimated Damage Indices</b>					
<b>Property</b>	<b>System #1</b>	<b>System #2</b>	<b>System #3</b>	<b>System #4</b>	<b>System #5</b>
$m_i$	1.25	1.10	1.01	0.97	0.99
$c_i$	1.96	1.60	0.87	1.01	0.58
$c_{i+1}$	1.68	0.95	0.95	0.52	0.99
$k_i$	1.13	1.09	1.00	0.97	1.00
$k_{i+1}$	1.10	0.99	1.01	0.93	0.97

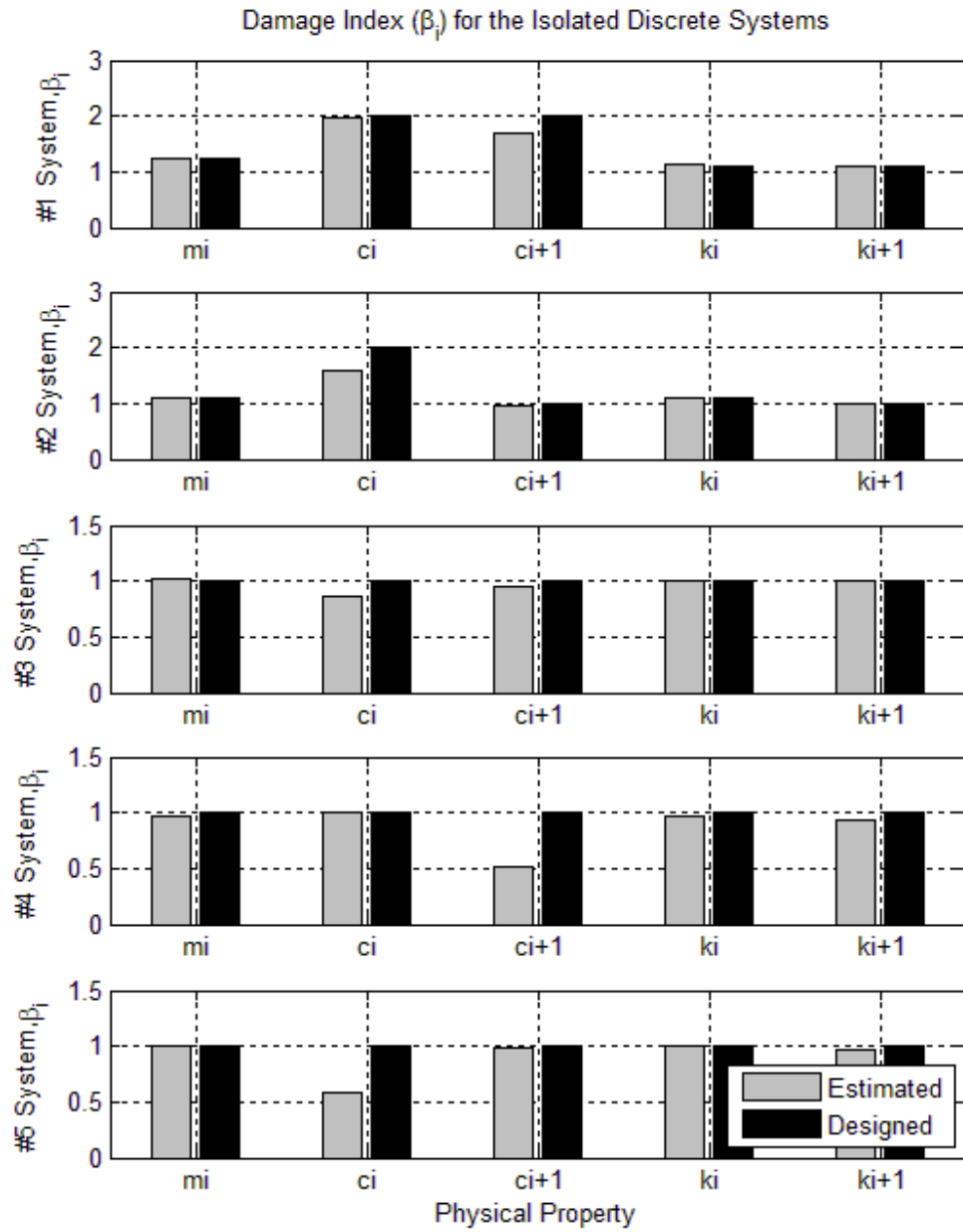


**Figure 6.31. Damage Indices ( $\beta_i$ ) for the 5 Isolated Spring-Mass-Damper System with Noise-Polluted Accelerations (5% Noise)**

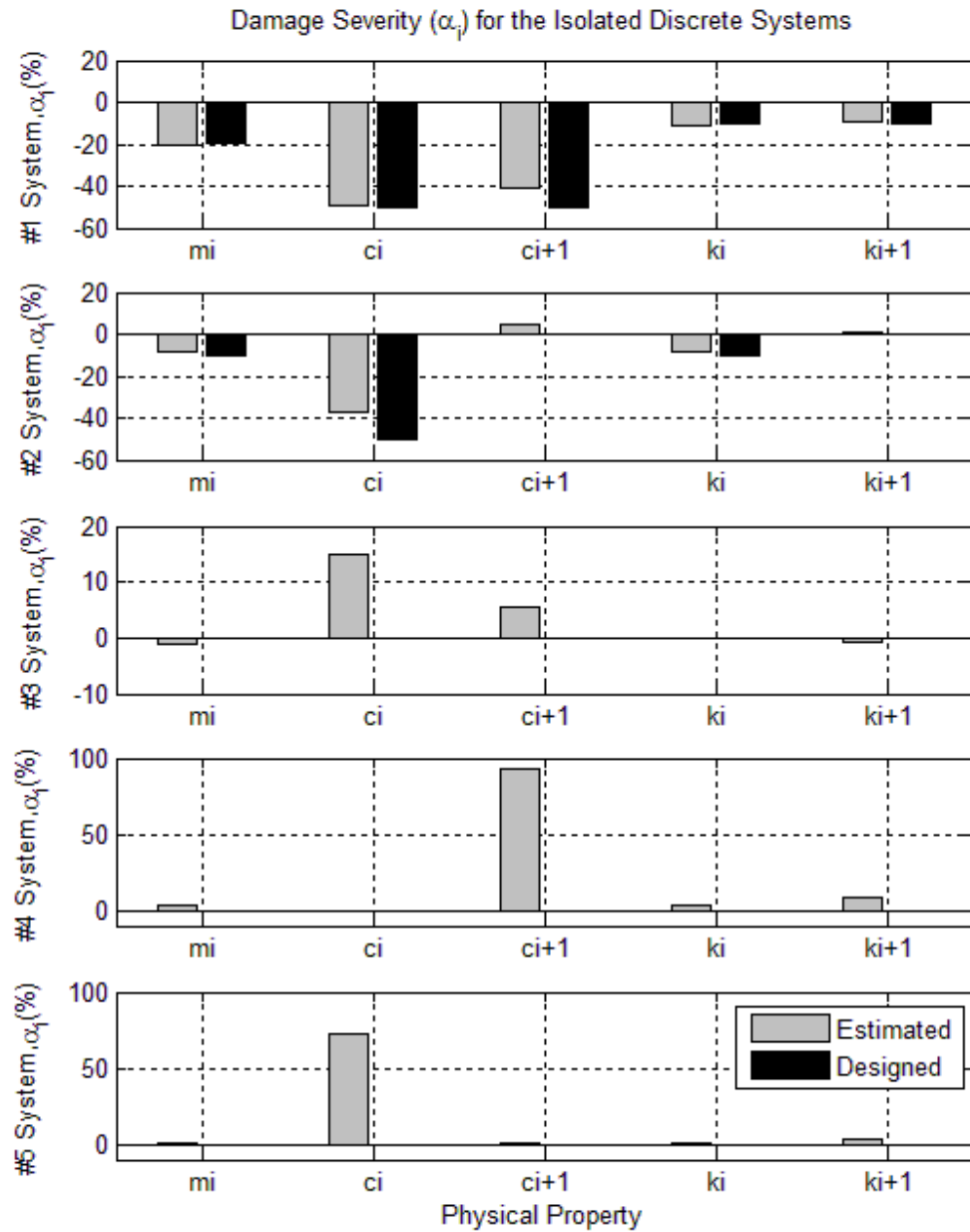


Figure 6.32. Damage Severities ( $\alpha_i$ ) for 5-DOF Spring-Mass-Damper System with Noise-Polluted Accelerations (5% Noise)

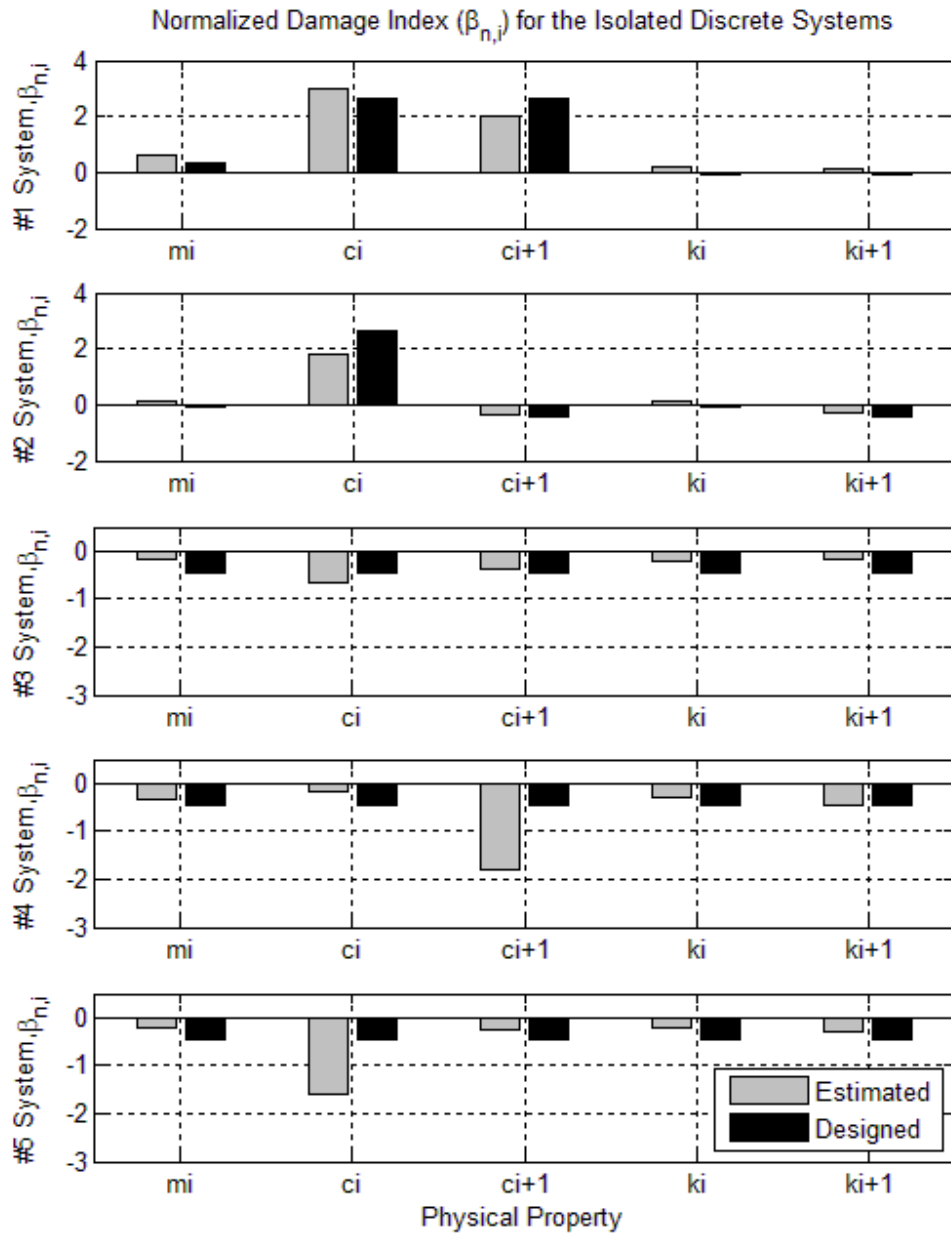


Figure 6.33. Normalized Damage Indices ( $\beta_{n,i}$ ) for 5-DOF Spring-Mass-Damper System with Noise-Polluted Accelerations (5% Noise)

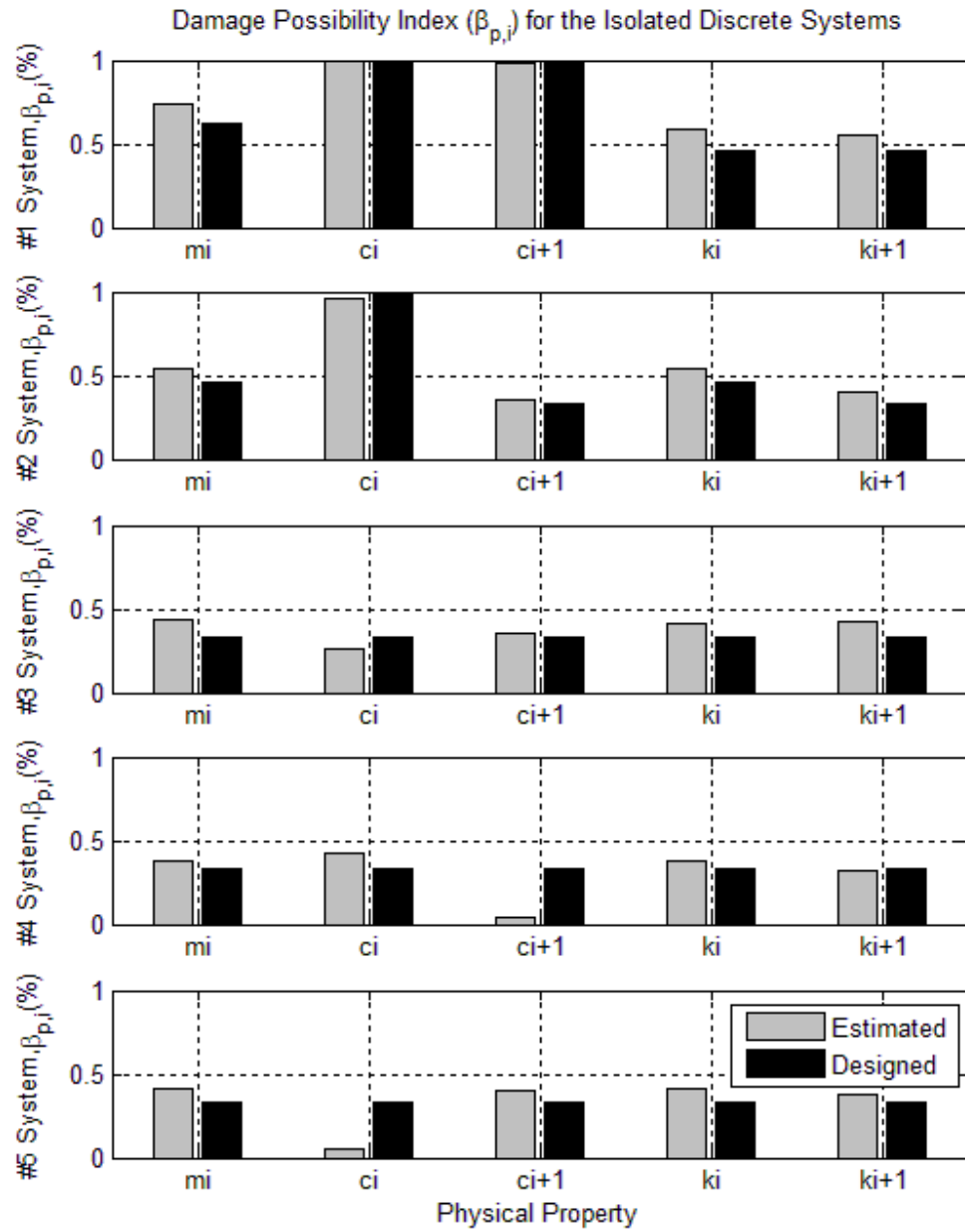


Figure 6.34. Damage Possibility Indices ( $\beta_{p,i}$ ) for 5-DOF Spring-Mass-Damper System with Noise-Polluted Accelerations (5% Noise)



## 6.4 STUDIES OF NOISE INFLUENCE TO A CONTINUOUS SYSTEM USING INTEGRAL METHOD

In this subsection, a fixed-fixed beam is used to evaluate the performance of the proposed theory in dealing with noise-polluted data. The geometry and damage scenario under consideration are indicated in Figure 6.35. The geometry of the cross-section of the beam is shown in Figure 5.19. The modulus of elasticity ( $E$ ) of the material is 29,000 ksi. The mass density of the material is  $7.345 \times 10^{-7}$  kip·sec<sup>2</sup>/in<sup>4</sup>.

The fixed-fixed beam is meshed into 6 elements and has 7 equally spaced nodes. The length of each element is 12.0 inches. For illustrative purposes, typical elements are indicated in Figure 6.35. Two elements with damaged mass and stiffness are studied. The damage is simulated by a ten percent (10%) reduction of the modulus of elasticity and twenty percent (20%) reduction of the mass of the first (1<sup>st</sup>) and second (2<sup>nd</sup>) elements on the beam.

For each node on the beam, a white noise,  $100 \times \text{random}(-1,1)$ , is used as node force and is applied in axial direction. The five white-noise forces are the same as the one applied in the above four cases and are plotted in Figure 6.2. Given the external load case, exact accelerations of the five nodes were computed at every  $1\text{E-}4$  seconds (10,000 Hz) for 0.2 seconds. Then the accelerations of the five nodes were contaminated by 1% and 5% white noise. To reduce the influence from the noise in the input signals, a bandpass digital filter was used to filter the noise-polluted accelerations. The velocities of the mass blocks are estimated using Eq. 6.2 based on the filtered noise-polluted accelerations and the displacements of the mass blocks are estimated using Eq. 6.3 based on the filtered estimated velocities.

In this case, the computed velocity ( $\dot{x}(t)$ ) of each node in the undamaged case was used as the velocity used to compute power ( $\dot{\Delta}$ ) for both the undamaged and damaged cases. For every two nearby elements, the coefficient matrices ('**X**') and known vector ('**Y**') were constructed by substituting the acceleration ( $\ddot{x}(t)$ ), velocity ( $\dot{x}(t)$ ), displacement ( $x(t)$ ), and velocity used to compute power ( $\dot{\Delta}$ ) into Eq. 4.96 and Eq. 4.98. The coefficient damage index vector,  $\beta$ , related to the two nearby elements was computed using Eq. 4.95. Then the damage indices for mass and stiffness are computed using Eqs. 4.100 through 4.106. The damage severities for mass and stiffness are computed using Eq. 2.13.

#### **6.4.1 Case #6.5: Continuous System with 1% Noise Pollution Using Integral**

##### **Method**

In this case, the exact accelerations of the mass blocks outputted directly from SAP2000 were contaminated by 1% of white noise. The noise-polluted accelerations of Node 2 in both the undamaged and damaged cases are plotted in Figure 6.36. The filtered accelerations, estimated velocities and estimated displacements of Node 2 are plotted in Figure 6.37, Figure 6.38, and Figure 6.39, respectively.

The estimated damage indices and the designed damage indices for each physical property are listed in Table 6.7 and are plotted in Figure 6.40. The estimated damage severities and the designed damage severities for each physical property are also listed in Table 6.7 and are plotted in Figure 6.41. The normalized damage indices are computed using Eq. 6.4 and are plotted in Figure 6.42. The damage possibility indices are plotted in Figure 6.43. Comparing the estimated damage indices with the designed damage indices, the integrated system analysis method can accurately locate and size multiple damage with 1%

noise-polluted input data from a typical fixed-fixed beam.

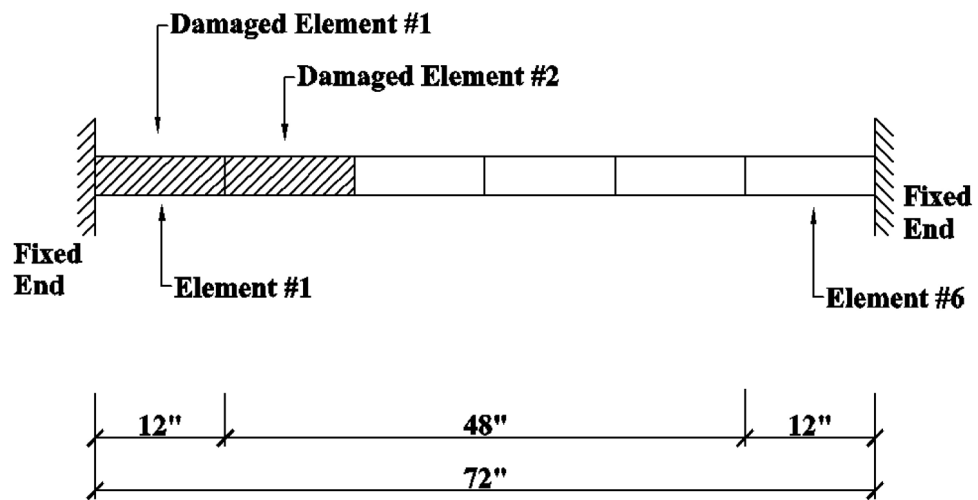
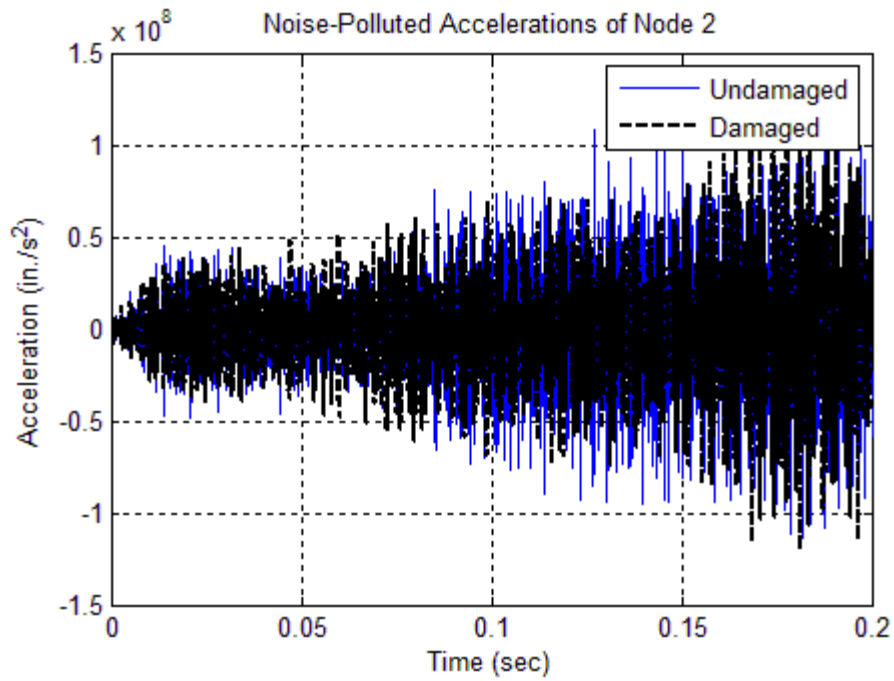
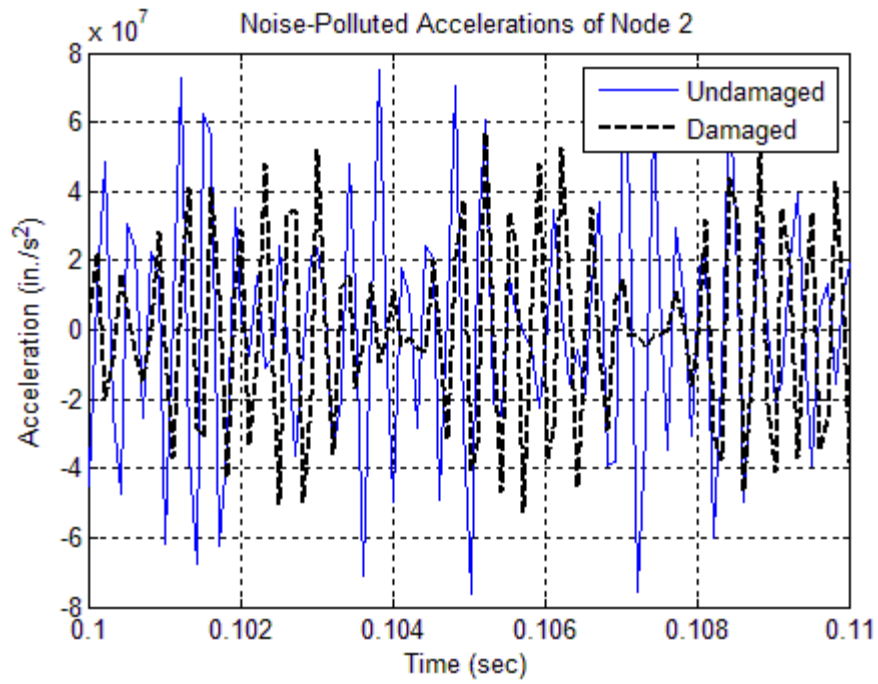


Figure 6.35. Geometry and Damage Scenario for the Fixed-Fixed Beam

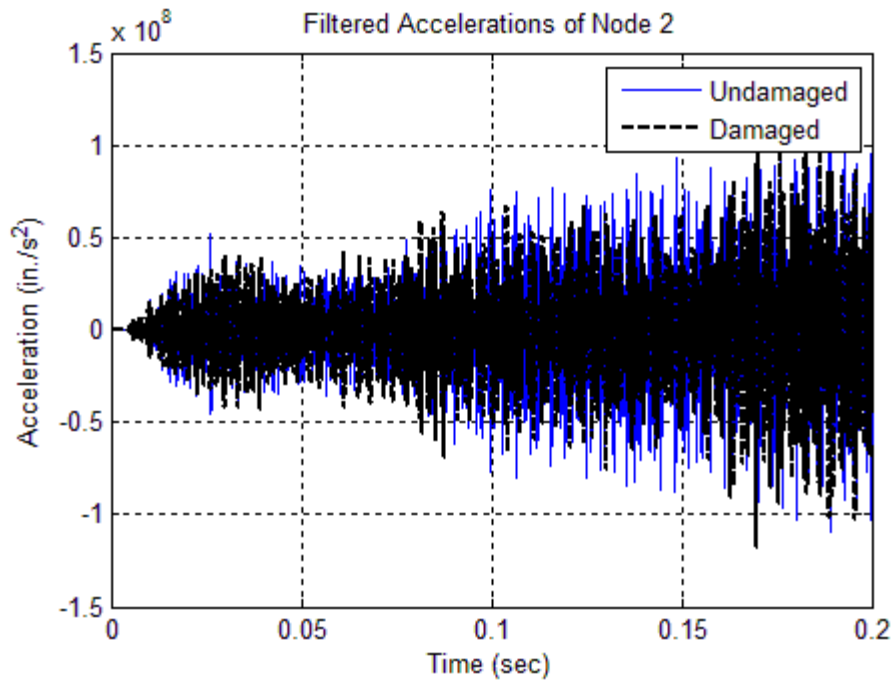


(a)

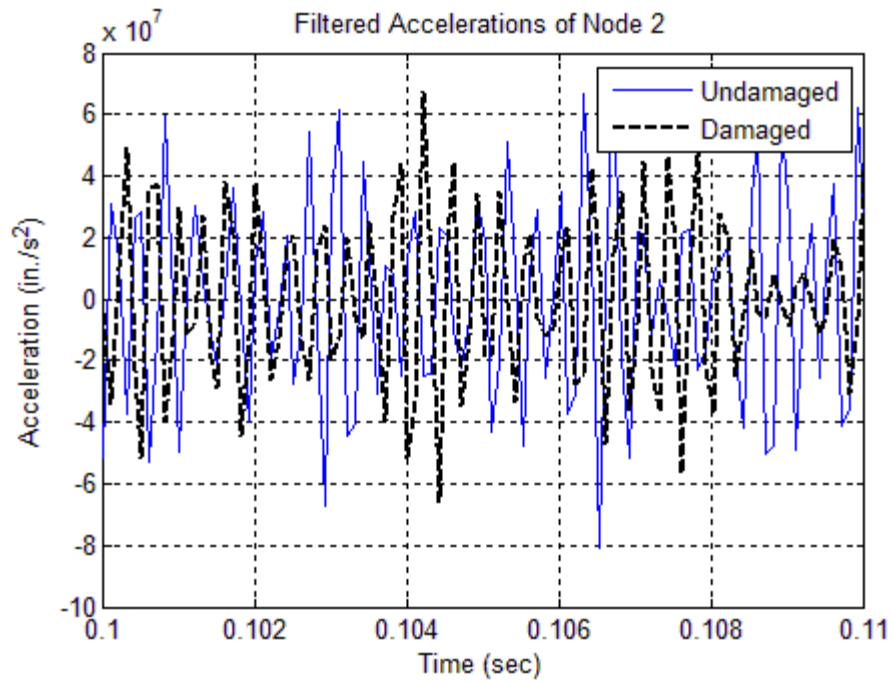


(b)

Figure 6.36. Noise-Polluted Accelerations of Node 2 for the Undamaged and Damaged Models of Case #6.5 (1% Noise): (a) Full Plot and (b) Zoomed in Plot

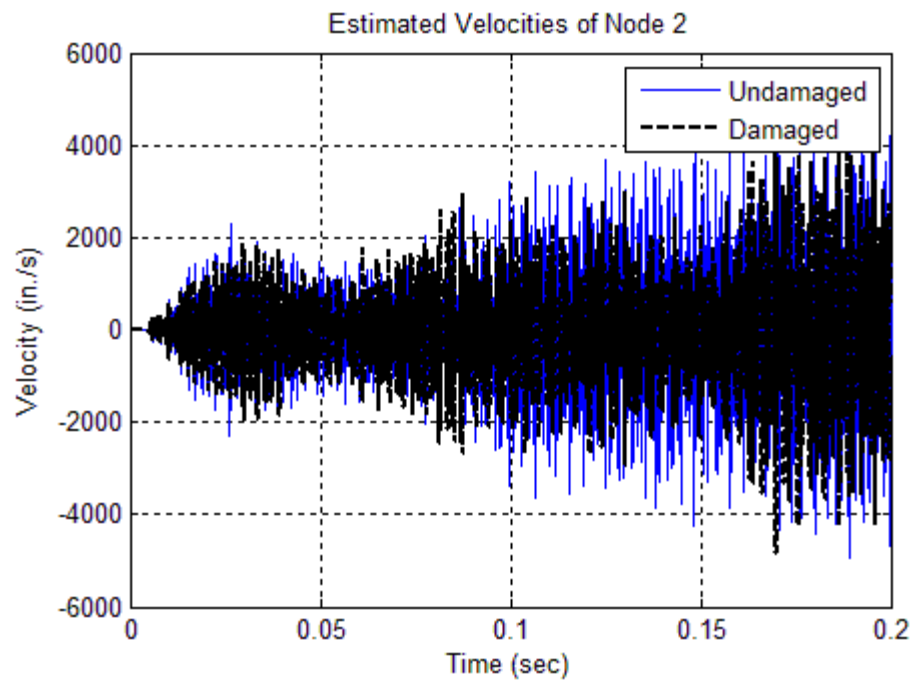


(a)

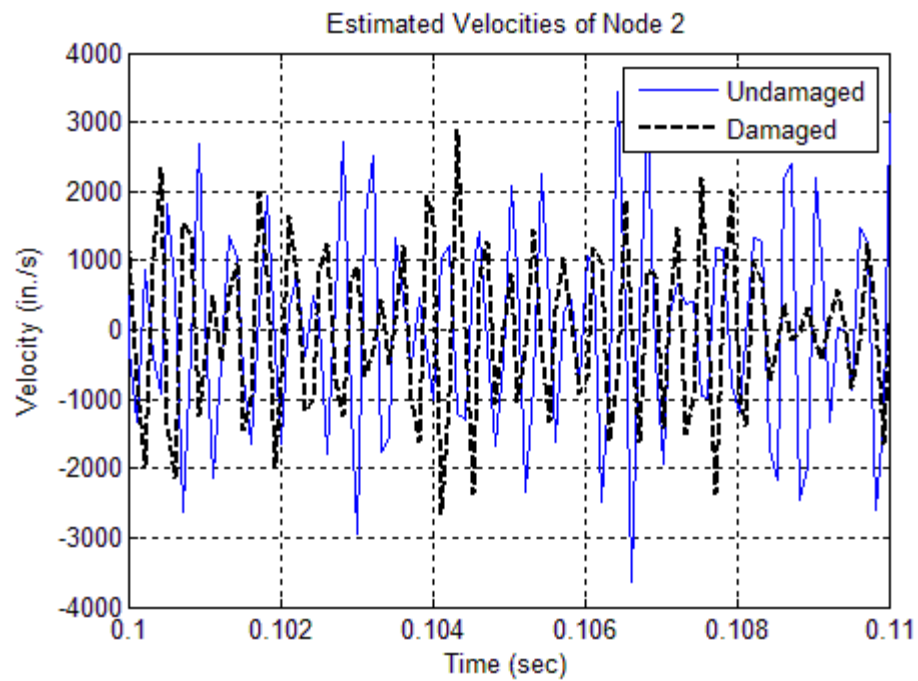


(b)

**Figure 6.37. Filtered Noise-Polluted Accelerations of Node 2 for the Undamaged and Damaged Models of Case #6.5 (1% Noise): (a) Full Plot and (b) Zoomed in Plot**

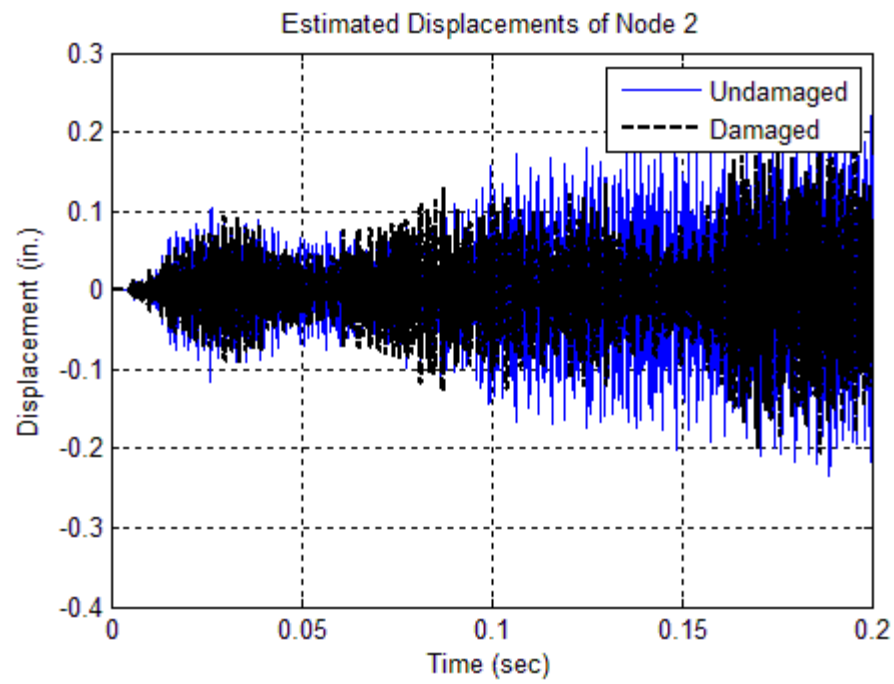


(a)

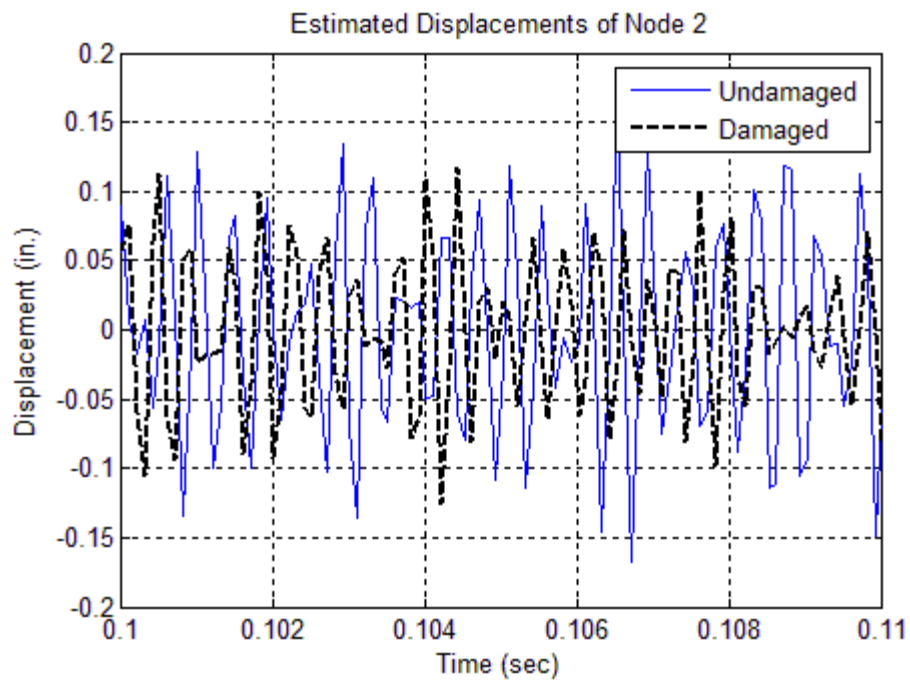


(b)

Figure 6.38. Estimated Velocities of Node 2 for the Undamaged and Damaged Models of Case #6.5 (1% Noise): (a) Full Plot and (b) Zoomed in Plot



(a)



(b)

**Figure 6.39. Estimated Displacements of Node 2 for the Undamaged and Damaged Models of Case #6.5 (1% Noise): (a) Full Plot and (b) Zoomed in Plot**

**Table 6.7. Damage Detection Results for the Fixed-Fixed Beam (1% Noise Pollution)**

Property	Damage Index ( $\beta_i$ , Esimated)	Damage Severity ( $\alpha_i$ , Esimated)	Damage Index ( $\beta_i$ , Designed)
$m_1$	1.15	-0.13	1.25
$m_2$	1.03	-0.03	1.11
$m_3$	0.93	0.08	1.00
$m_4$	0.93	0.08	1.00
$m_5$	0.93	0.08	1.00
$k_1$	1.02	-0.02	1.11
$k_2$	1.02	-0.02	1.11
$k_3$	0.93	0.07	1.00
$k_4$	0.93	0.08	1.00
$k_5$	0.92	0.08	1.00
$k_6$	0.94	0.07	1.00

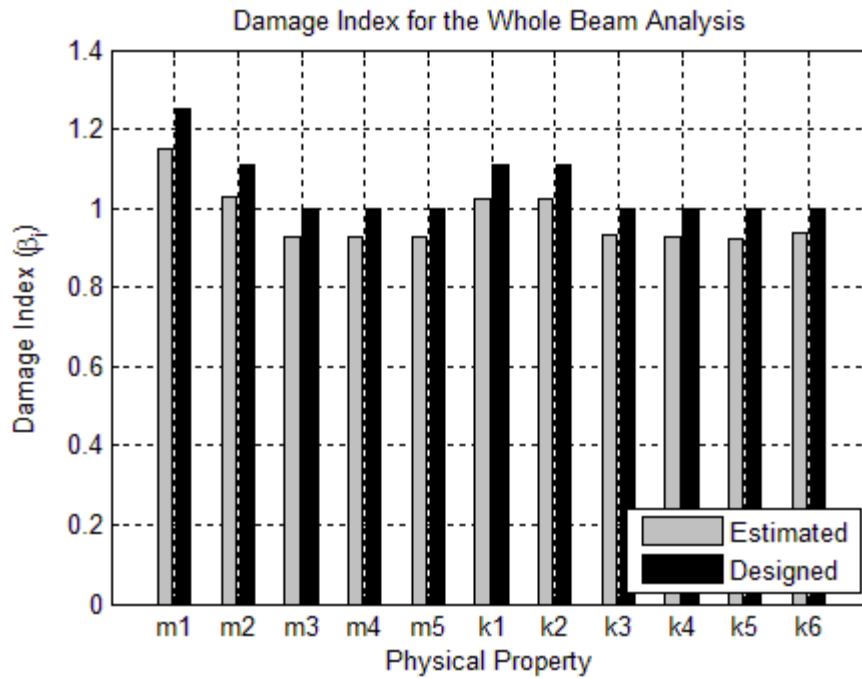


**Figure 6.40. Damage Indices ( $\beta_i$ ) for the Fixed-Fixed Beam with Noise-Polluted Accelerations (1% Noise)**



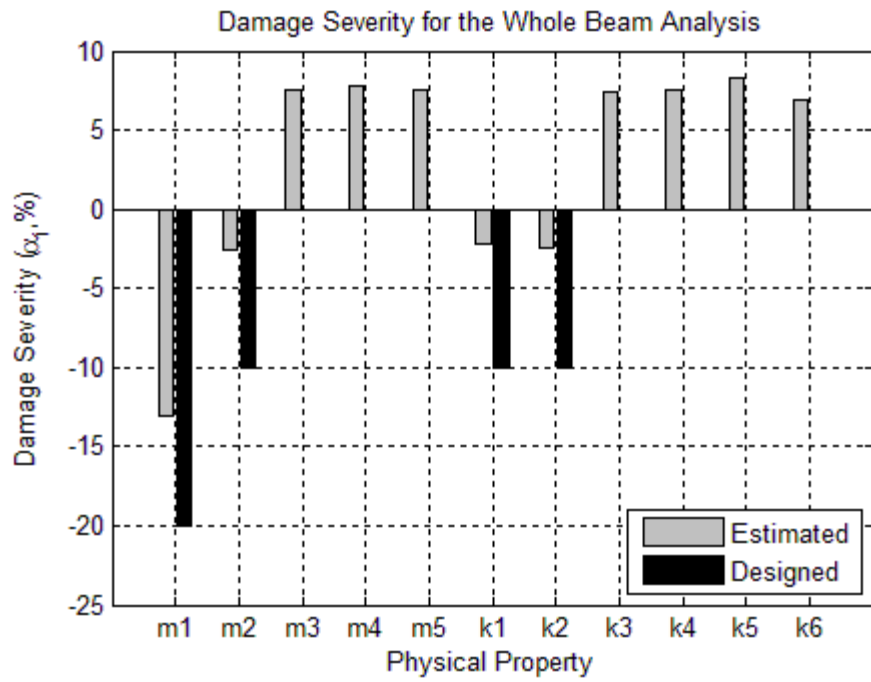


Figure 6.41. Damage Severities (a) for the Fixed-Fixed Beam with Noise-Polluted Accelerations (1% Noise)

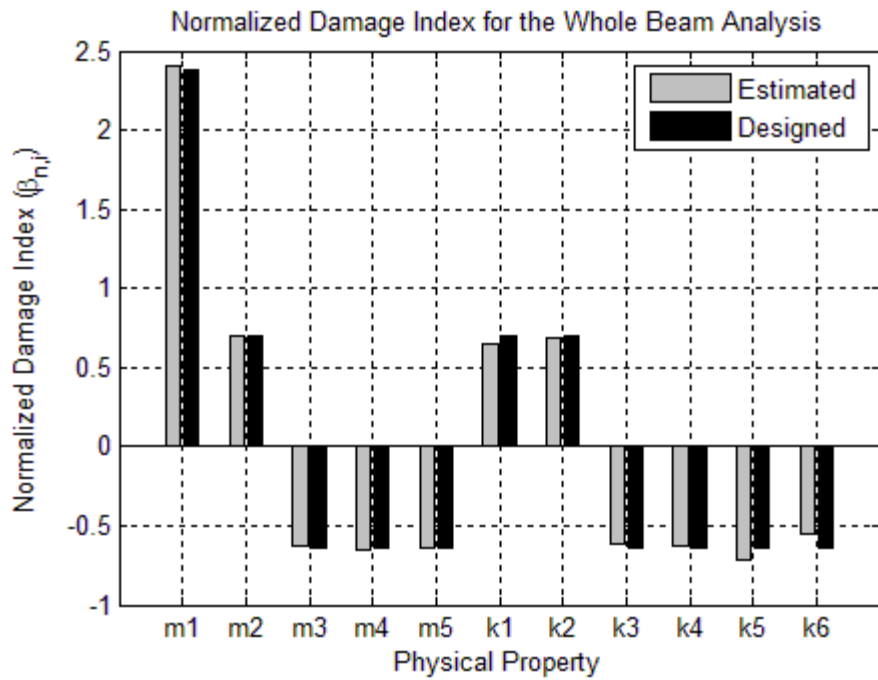
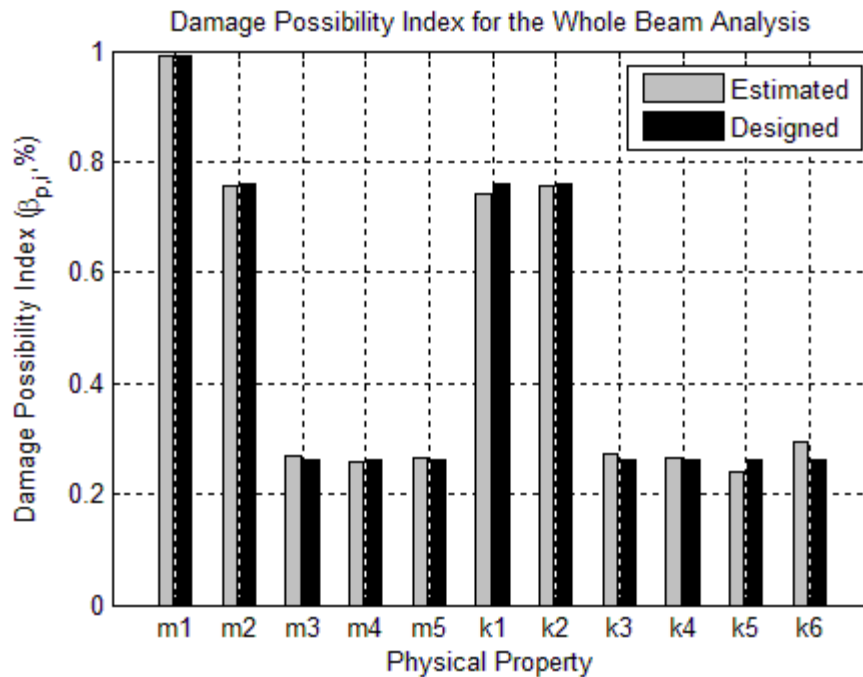


Figure 6.42. Normalized Damage Indices (β<sub>n,i</sub>) for the Fixed-Fixed Beam with Noise-Polluted Accelerations (1% Noise)



**Figure 6.43. Probability Damage Indices ( $\beta_{p,i}$ ) for the Fixed-Fixed Beam with Noise-Polluted Accelerations (1% Noise)**

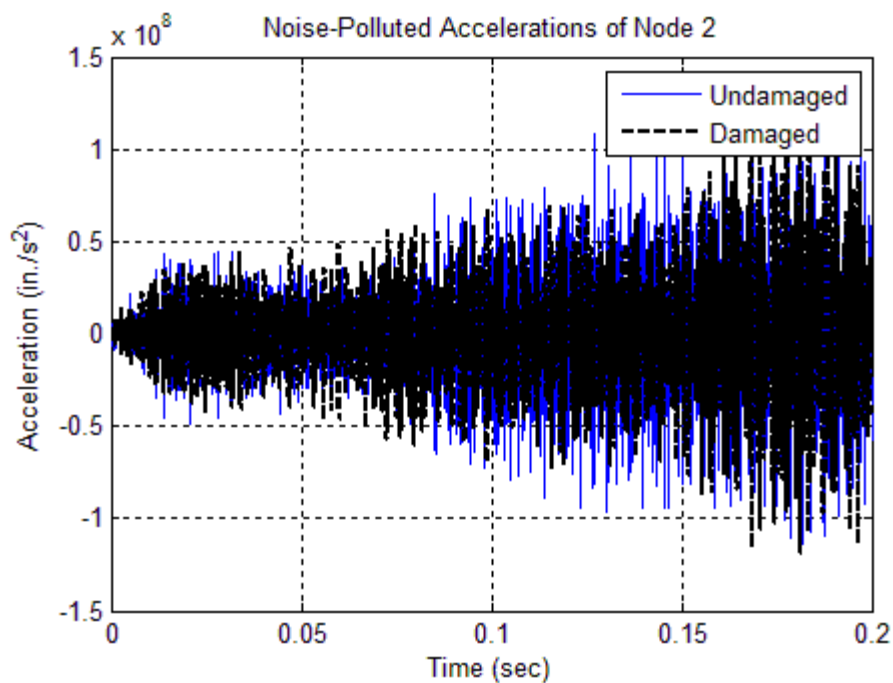
#### 6.4.2 Case #6.6: Continuous System with 5% Noise Pollution Using Integral

##### Method

In this case, the exact accelerations of the mass blocks outputted directly from SAP2000 were contaminated by 5% of white noise. The noise-polluted accelerations of Node 2 in both the undamaged and damaged cases are plotted in Figure 6.44. The filtered accelerations, estimated velocities and estimated displacements of Node 2 are plotted in Figure 6.45, Figure 6.46, and Figure 6.47, respectively.

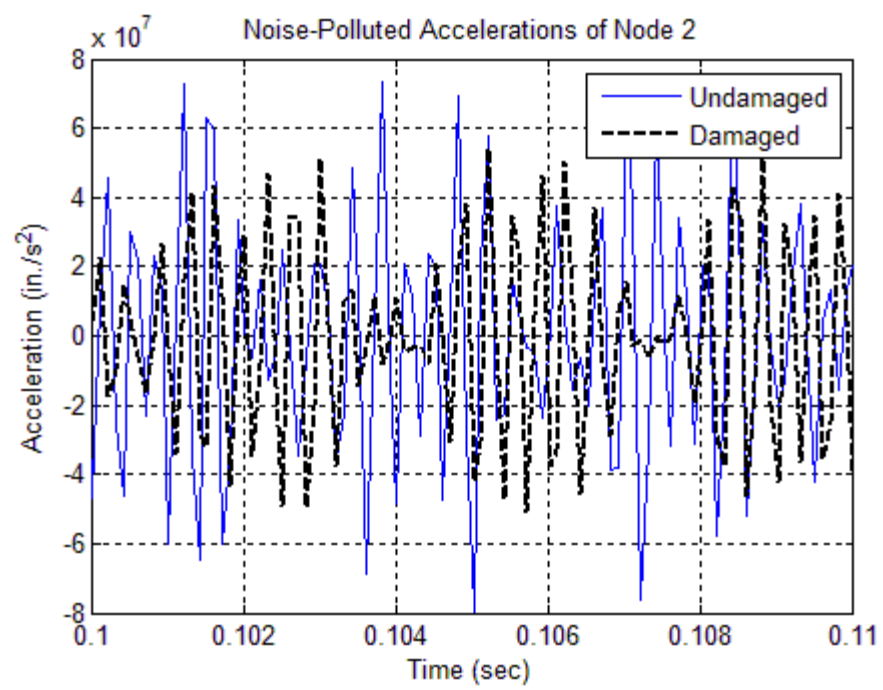
The estimated damage indices and the designed damage indices for each physical property are listed in Table 6.7 and are plotted in Figure 6.48. The estimated damage severities and the designed damage severities for each physical property are also listed in Table 6.7 and

are plotted in Figure 6.49. The normalized damage indices are computed using Eq. 6.4 and are plotted in Figure 6.50. The damage possibility indices are plotted in Figure 6.51. Comparing the estimated damage indices with the designed damage indices, the integrated system analysis method can accurately locate and size multiple damage with 5% noise-polluted input data from a typical fixed-fixed beam.



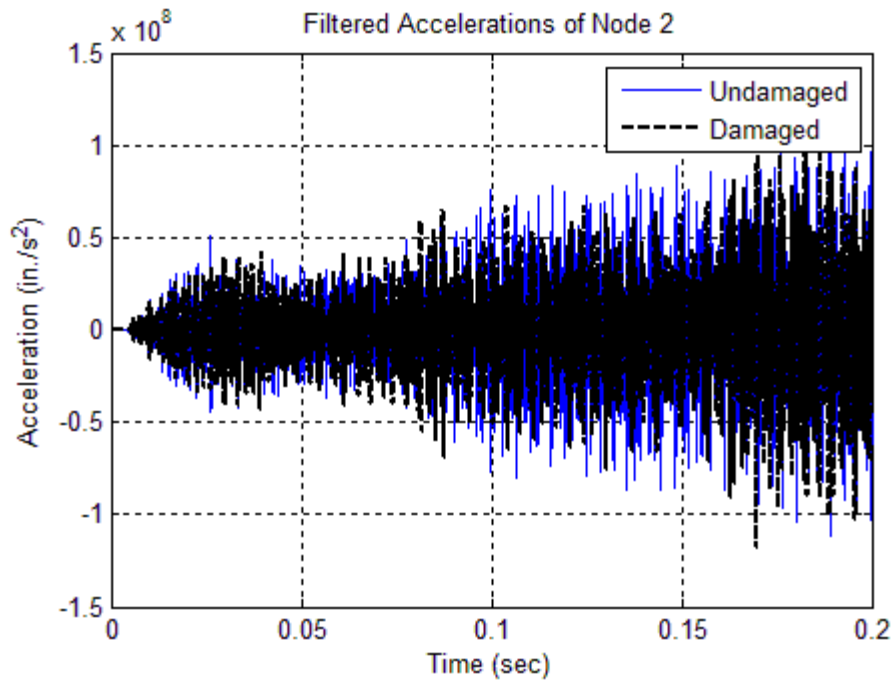
(a)

**Figure 6.44. Noise-Polluted Accelerations of Node 2 for the Undamaged and Damaged Models of Case #6.6 (5% Noise): (a) Full Plot and (b) Zoomed in Plot**

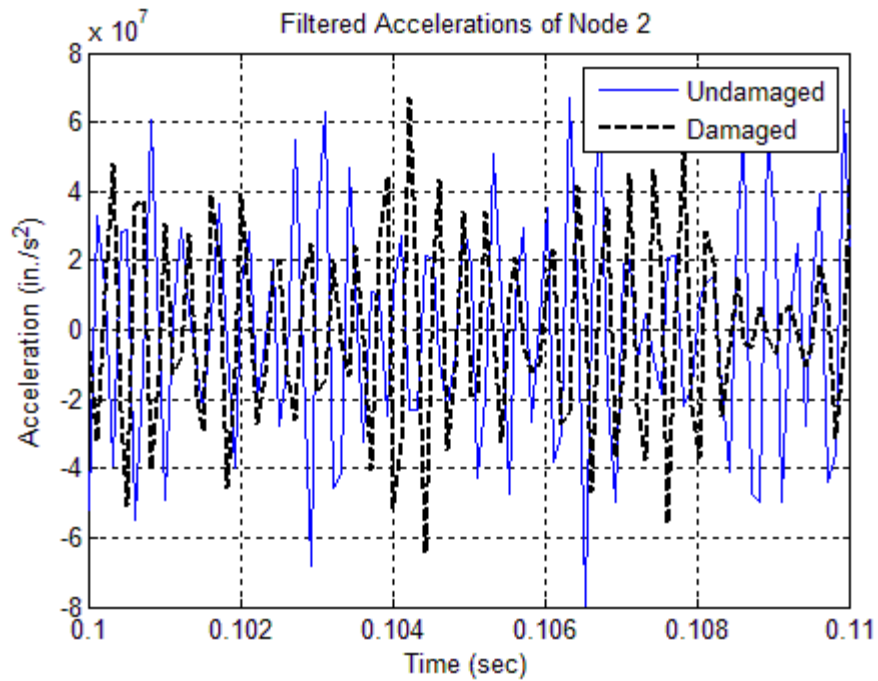


(b)

Figure 6.44. Continued

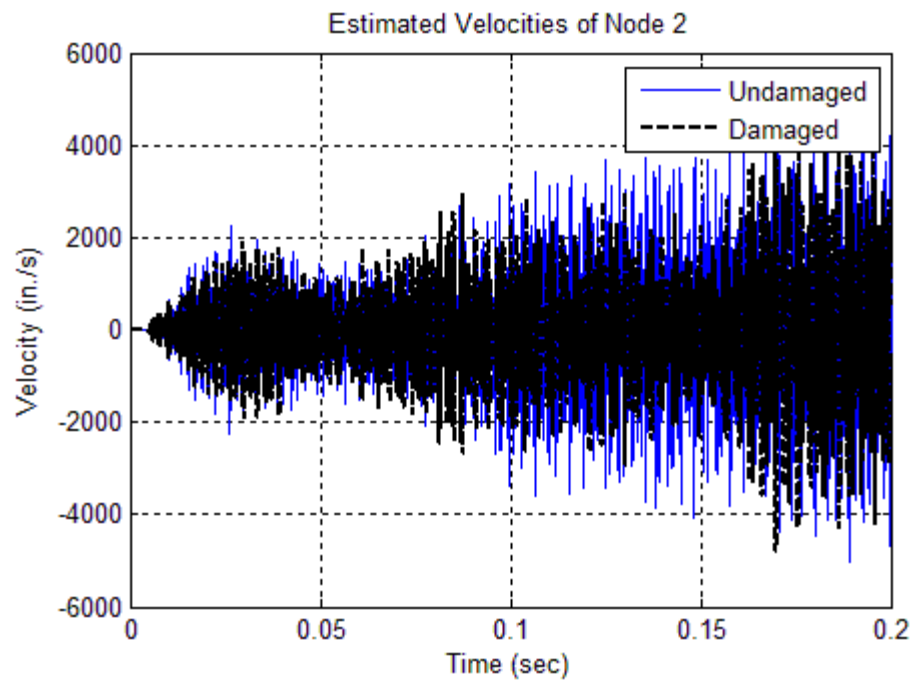


(a)

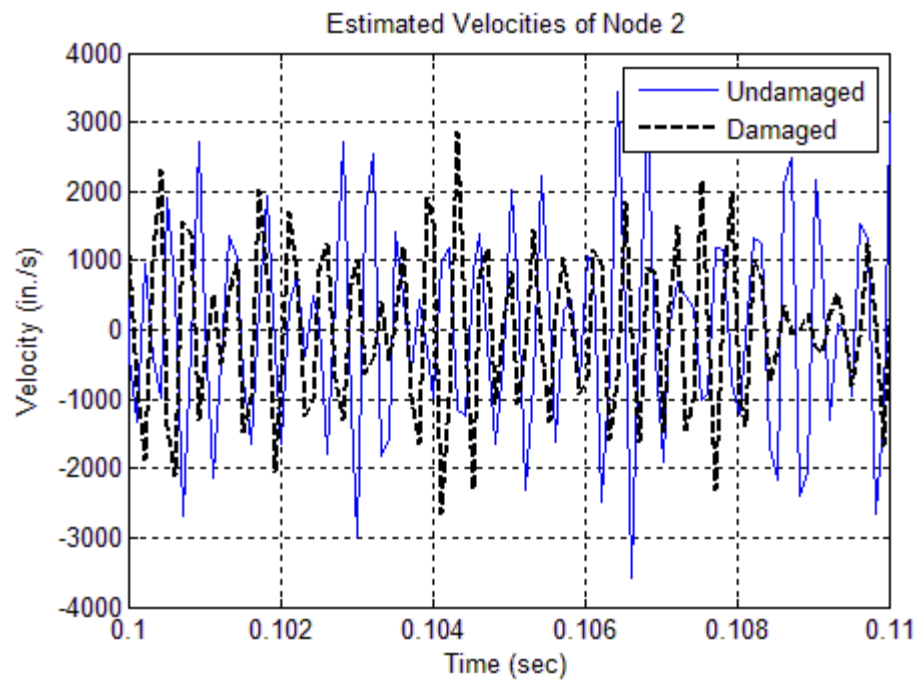


(b)

**Figure 6.45. Filtered Noise-Polluted Accelerations of Node 2 for the Undamaged and Damaged Models of Case #6.6 (5% Noise): (a) Full Plot and (b) Zoomed in Plot**

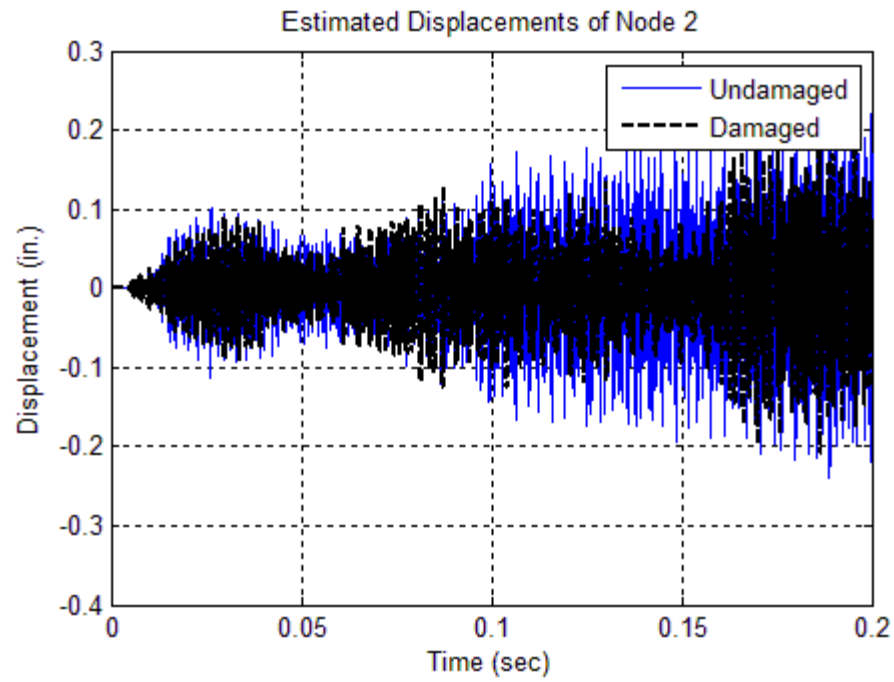


(a)

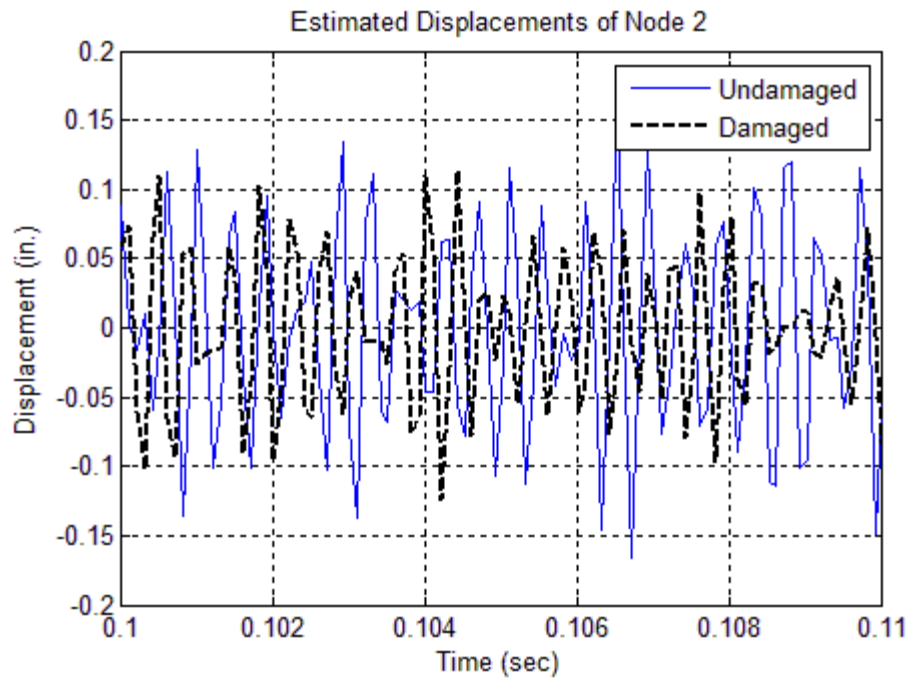


(b)

Figure 6.46. Estimated Velocities of Node 2 for the Undamaged and Damaged Models of Case #6.6 (5% Noise): (a) Full Plot and (b) Zoomed in Plot



(a)



(b)

**Figure 6.47. Estimated Displacements of Node 2 for the Undamaged and Damaged Models of Case #6.6 (5% Noise): (a) Full Plot and (b) Zoomed in Plot**

**Table 6.8. Damage Detection Results for the Fixed-Fixed Beam (5% Noise Pollution)**

Property	Damage Index ( $\beta_i$ , Esimated)	Damage Severity ( $\alpha_i$ , Esimated)	Damage Index ( $\beta_i$ , Designed)
$m_1$	0.76	0.31	1.25
$m_2$	0.69	0.45	1.11
$m_3$	0.63	0.59	1.00
$m_4$	0.61	0.63	1.00
$m_5$	0.62	0.61	1.00
$k_1$	0.68	0.48	1.11
$k_2$	0.68	0.46	1.11
$k_3$	0.62	0.60	1.00
$k_4$	0.62	0.61	1.00
$k_5$	0.61	0.64	1.00
$k_6$	0.63	0.58	1.00

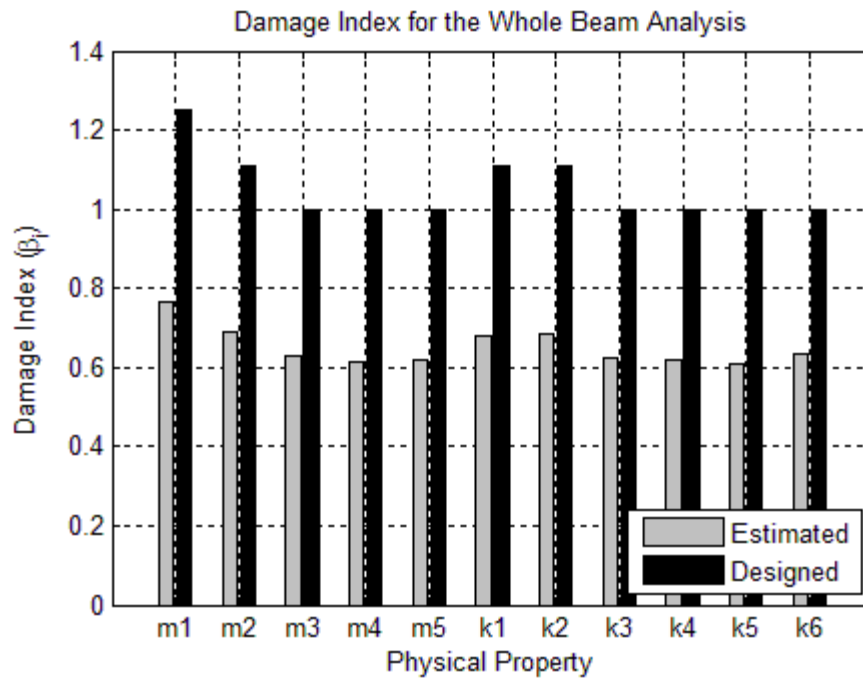


**Figure 6.48. Damage Indices ( $\beta_i$ ) for the Fixed-Fixed Beam with Noise-Polluted Accelerations (5% Noise)**



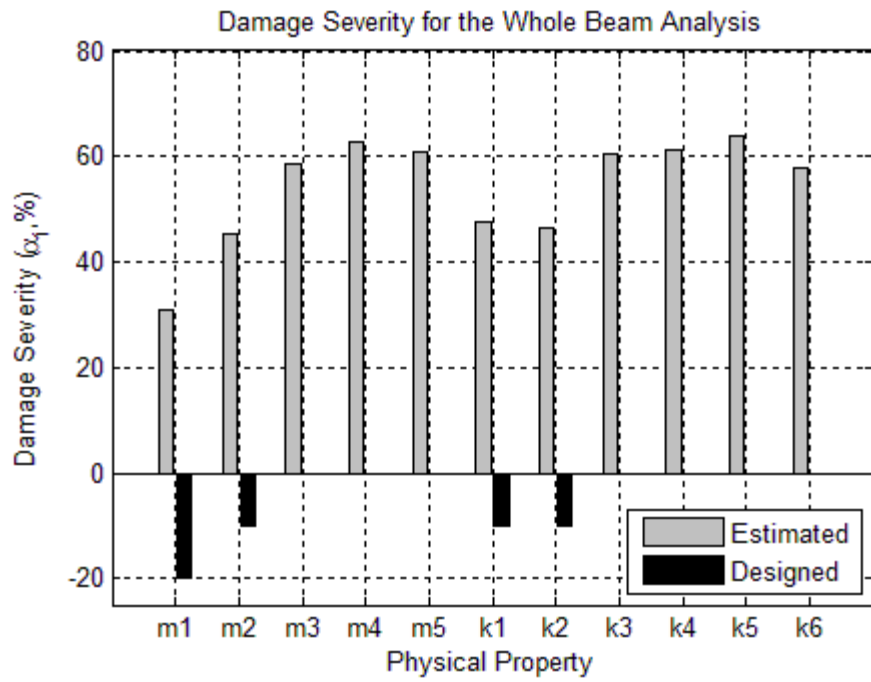


Figure 6.49. Damage Severities (a<sub>i</sub>) for the Fixed-Fixed Beam with Noise-Polluted Accelerations (5% Noise)

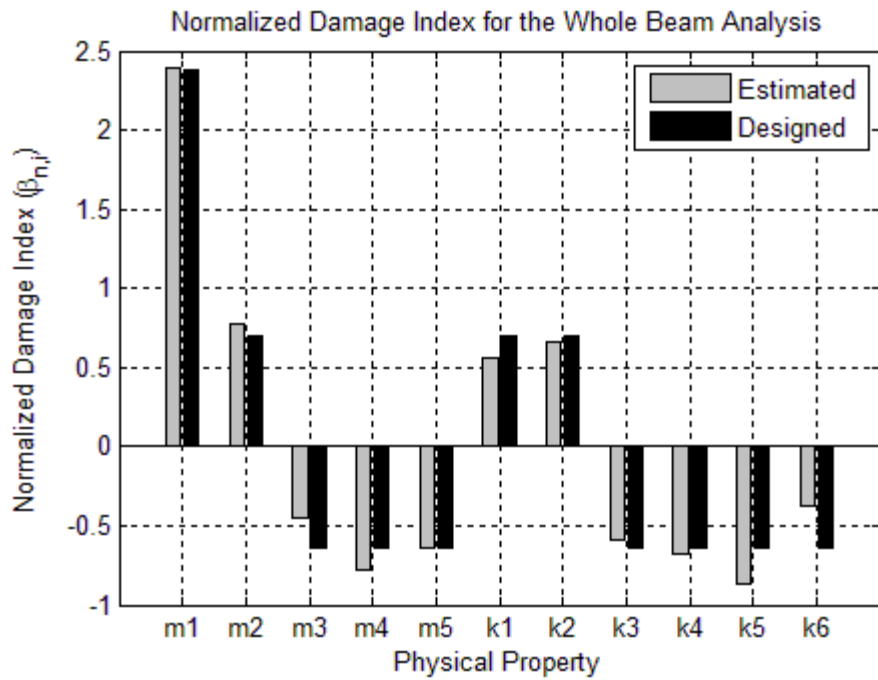
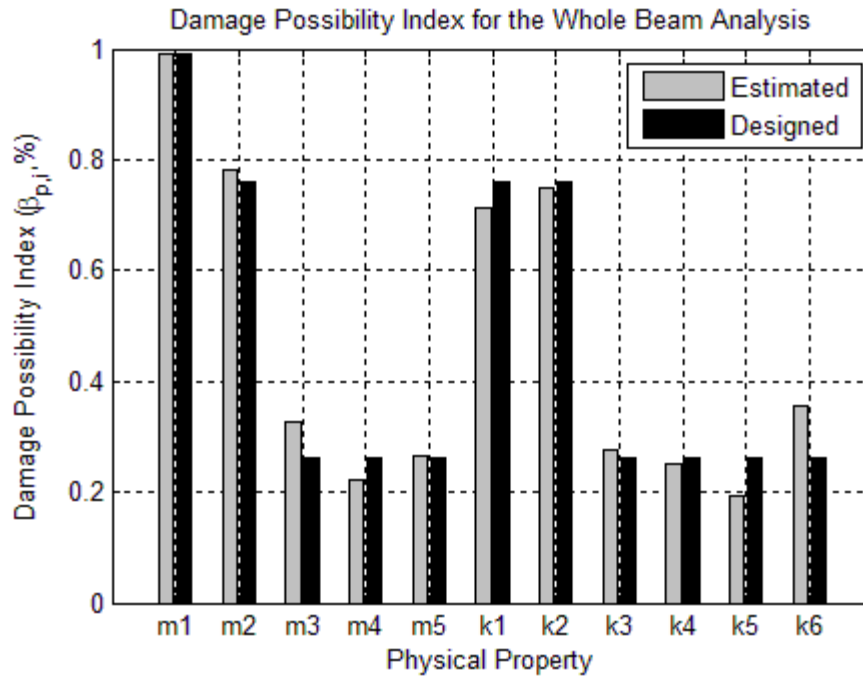


Figure 6.50. Normalized Damage Indices (β<sub>n,i</sub>) for the Fixed-Fixed Beam with Noise-Polluted Accelerations (5% Noise)



**Figure 6.51. Probability Damage Indices ( $\beta_{p,i}$ ) for the Fixed-Fixed Beam with Noise-Polluted Accelerations (5% Noise)**

## 6.5 STUDIES OF NOISE INFLUENCE TO A CONTINUOUS SYSTEM USING ISOLATION METHOD

In this subsection, noise influence to the performance of isolated system method for continuous systems will be studied. The proposed damage detection algorithm is performed on the same fixed-fixed beam as used in the above subsection. The geometry and damage scenario under consideration are indicated in Figure 6.35. The geometry of the cross-section of the beam is shown in Figure 5.19. The modulus of elasticity ( $E$ ) of the material is 29,000 ksi. The mass density of the material is  $7.345 \times 10^{-7}$  kip·sec<sup>2</sup>/in<sup>4</sup>.

The fixed-fixed beam is meshed into 6 elements and has 7 equally spaced nodes. The length of each element is 12.0 inches. For illustrative purposes, typical elements are

indicated in Figure 6.35. Two elements with damaged mass and stiffness are studied. The damage is simulated by a ten percent (10%) reduction of the modulus of elasticity and twenty percent (20%) reduction of the mass of the first (1<sup>st</sup>) and second (2<sup>nd</sup>) elements on the beam.

For each node on the beam, a white noise,  $100 \times \text{random}(-1,1)$ , is used as node force and is applied in axial direction. The five white-noise forces are the same as the one applied in the above four cases and are plotted in Figure 6.2. Given the external load case, exact accelerations of the five nodes were computed at every  $1\text{E-}4$  seconds (10,000 Hz) for 0.2 seconds. Then the accelerations of the five nodes were contaminated by 1% and 5% white noise. To reduce the influence from the noise in the input signals, a bandpass digital filter was used to filter the noise-polluted accelerations. The velocities of the mass blocks are estimated using Eq. 6.2 based on the filtered noise-polluted accelerations and the displacements of the mass blocks are estimated using Eq. 6.3 based on the filtered estimated velocities.

In this case, the computed velocity ( $\dot{x}(t)$ ) of each node in the undamaged case was used as the velocity used to compute power ( $\dot{\Delta}$ ) for both the undamaged and damaged cases. For every two nearby elements, the coefficient matrices ('X') and known vector ('Y') were constructed by substituting the acceleration ( $\ddot{x}(t)$ ), velocity ( $\dot{x}(t)$ ), displacement ( $x(t)$ ), and velocity used to compute power ( $\dot{\Delta}$ ) into Eq. 4.50 and Eq. 4.52. The coefficient damage index vector,  $\beta$ , related to the two nearby elements was computed using Eq. 4.49. Then the damage indices for mass and stiffness are computed using Eqs. 4.54 through 4.56. The damage severities for mass and stiffness are computed using Eq. 2.13. For each two nearby elements, the above process is performed. Thus, the proposed theory is applied to

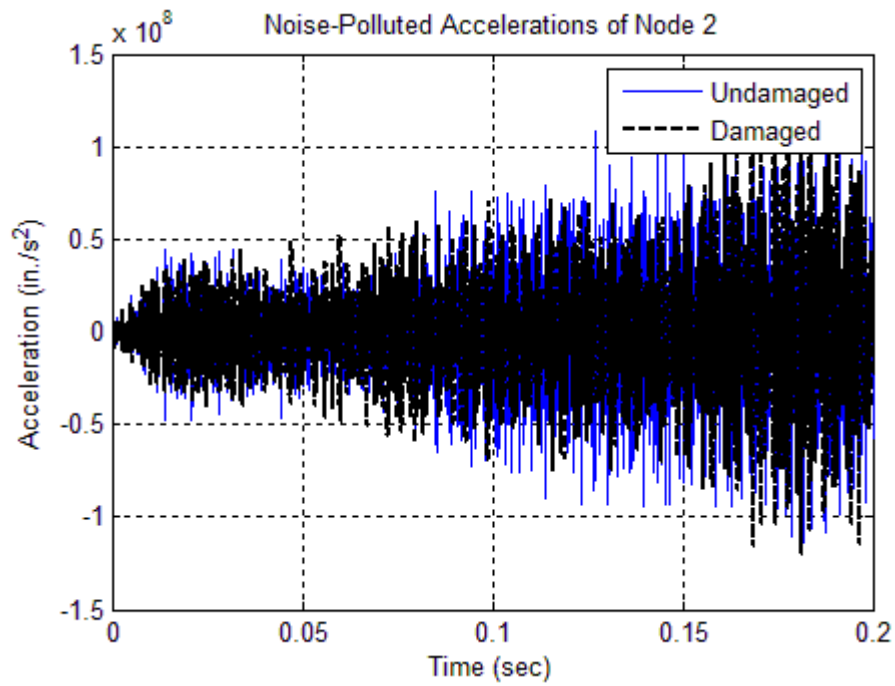
five pairs of elements.

### **6.5.1 Case #6.7: Continuous System with 1% Noise Pollution Using Isolation**

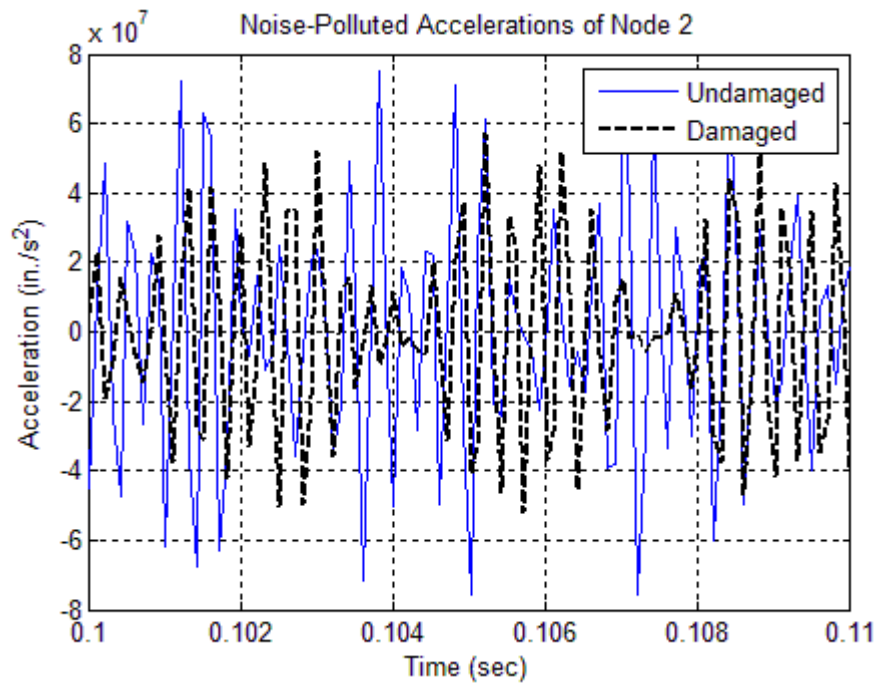
#### **Method**

In this case, the exact accelerations of the mass blocks outputted directly from SAP2000 were contaminated by 1% of white noise. The noise-polluted accelerations of Node 2 in both the undamaged and damaged cases are plotted in Figure 6.52. The filtered accelerations, estimated velocities, and estimated displacements of Node 2 are plotted in Figure 6.53, Figure 6.54, and Figure 6.55, respectively.

The estimated damage indices and the designed damage indices for each physical property are listed in Table 6.9 and are plotted in Figure 6.56. The estimated damage severities and the designed damage severities for each physical property are also listed in Table 6.9 and are plotted in Figure 6.57. The normalized damage indices are computed using Eq. 6.4 and are plotted in Figure 6.58. The damage possibility indices are plotted in Figure 6.59. Comparing the estimated damage indices with the designed damage indices, the isolated system analysis method can accurately locate and size multiple damage with 1% noise-polluted input data from a typical fixed-fixed beam.

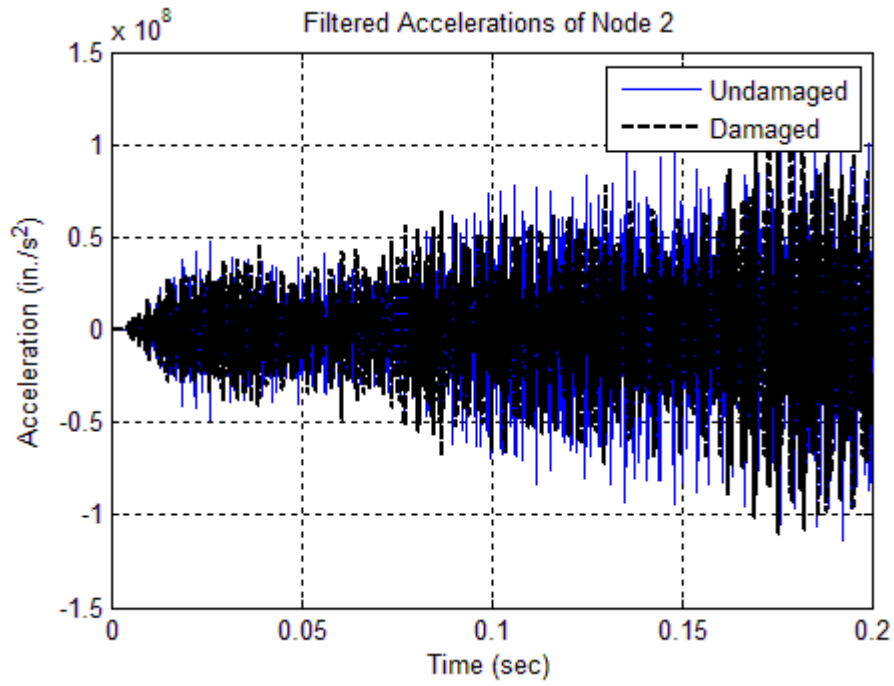


(a)

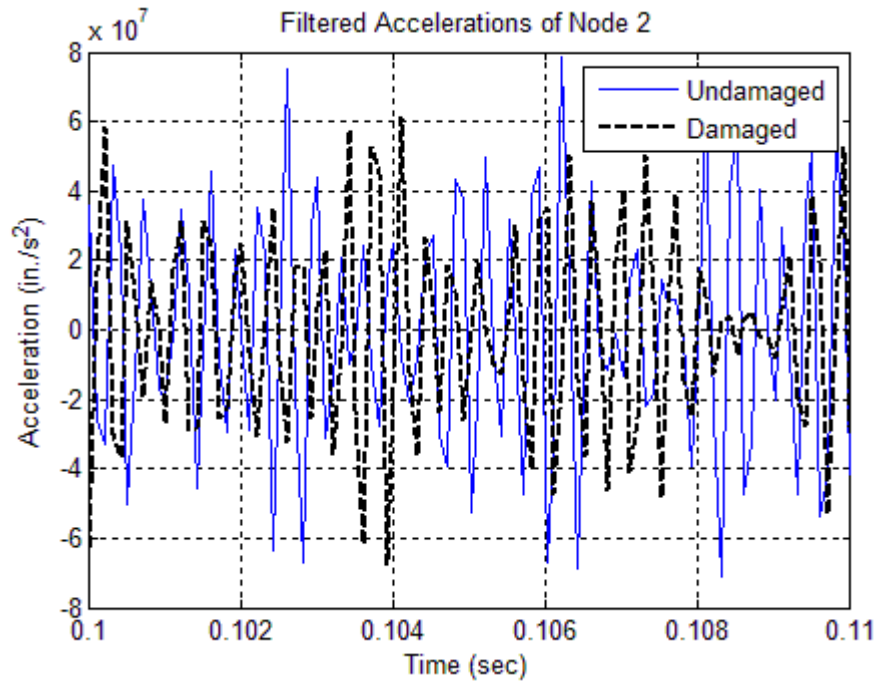


(b)

**Figure 6.52. Noise-Polluted Accelerations of Node 2 for the Undamaged and Damaged Models of Case #6.7 (5% Noise): (a) Full Plot and (b) Zoomed in Plot**

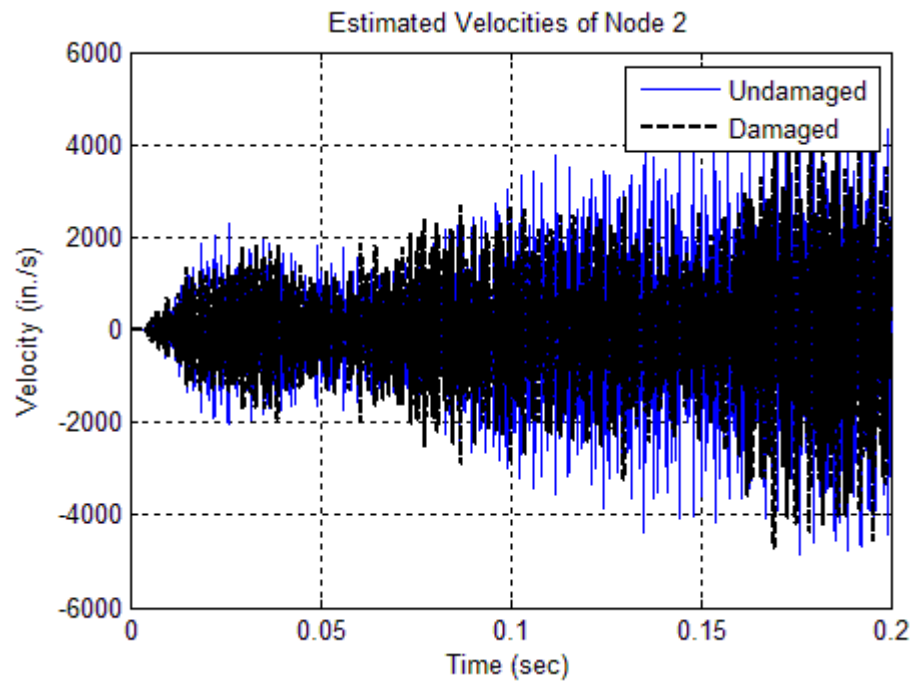


(a)

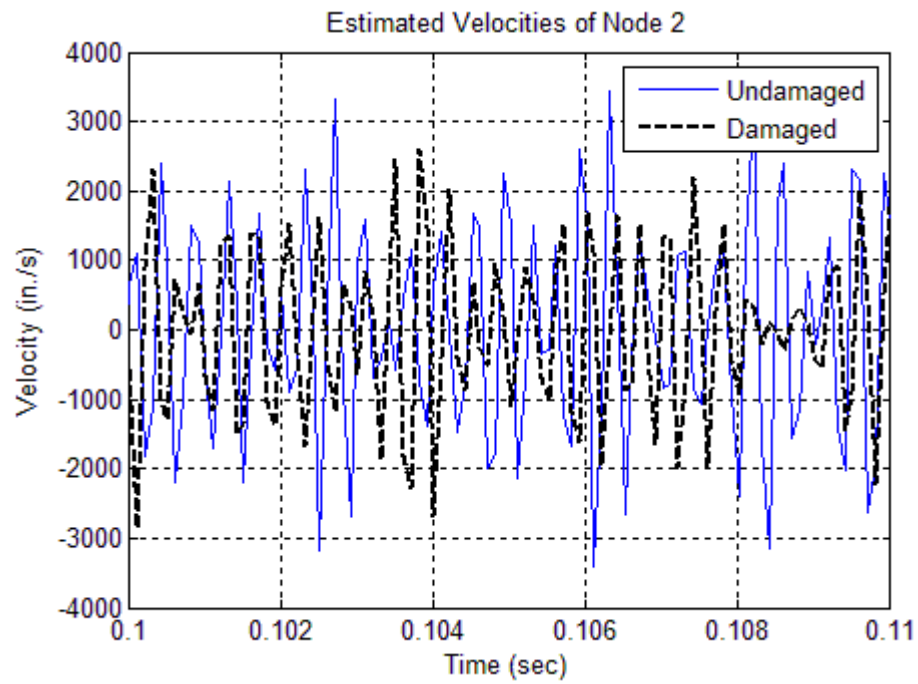


(b)

**Figure 6.53. Filtered Noise-Polluted Accelerations of Node 2 for the Undamaged and Damaged Models of Case #6.7 (5% Noise): (a) Full Plot and (b) Zoomed in Plot**

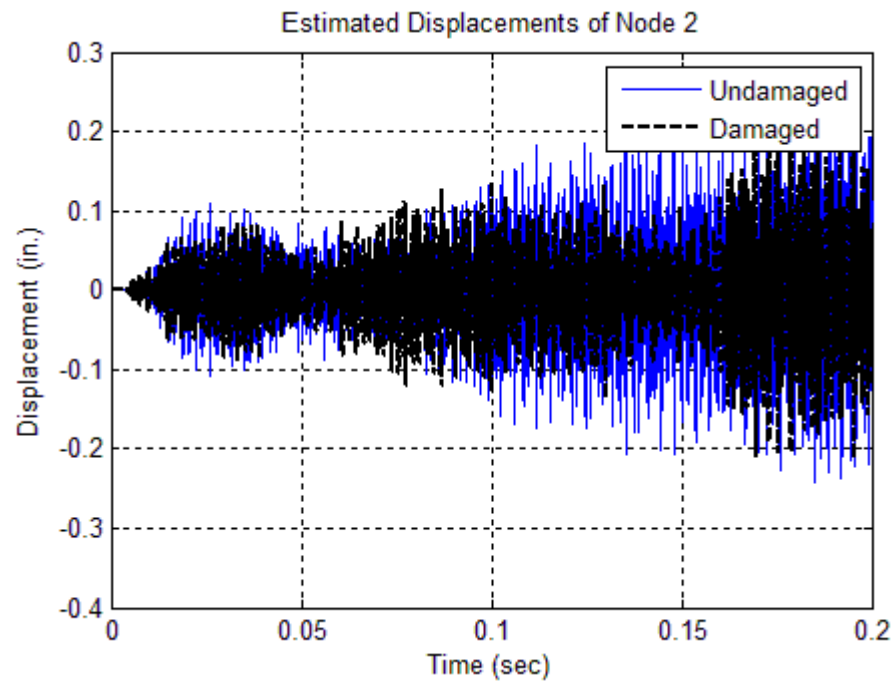


(a)

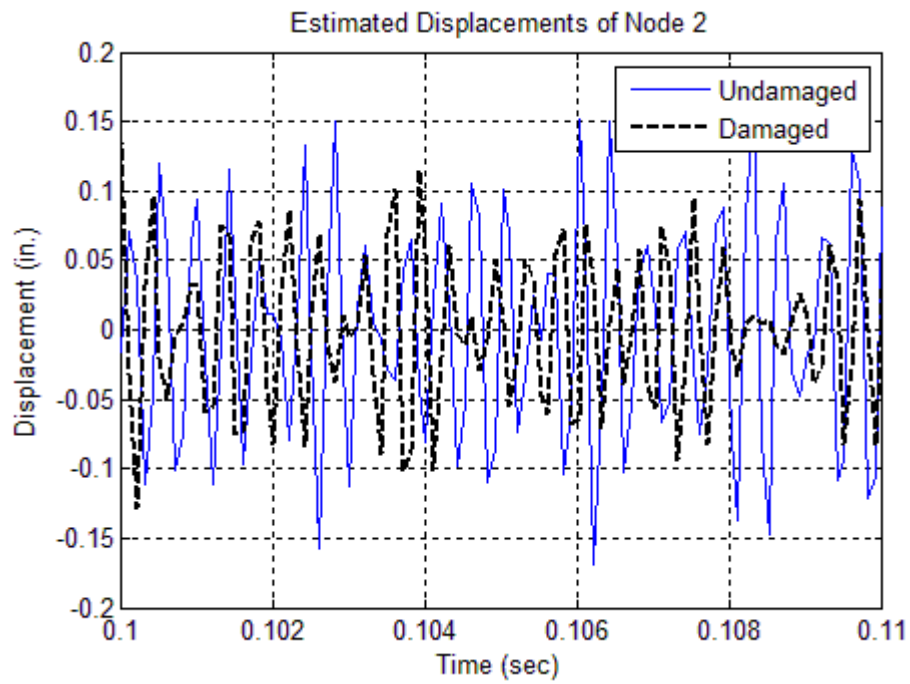


(b)

**Figure 6.54. Estimated Velocities of Node 2 for the Undamaged and Damaged Models of Case #6.7 (5% Noise): (a) Full Plot and (b) Zoomed in Plot**



(a)



(b)

**Figure 6.55. Estimated Displacements of Node 2 for the Undamaged and Damaged Models of Case #6.7 (5% Noise): (a) Full Plot and (b) Zoomed in Plot**



**Table 6.9. Damage Detection Results for the Fixed-Fixed Beam Using Isolated Method (1% Noise Pollution)**

<b>Designed Damage Indices</b>					
<b>Property</b>	<b>System #1</b>	<b>System #2</b>	<b>System #3</b>	<b>System #4</b>	<b>System #5</b>
$m_i$	1.25	1.11	1.00	1.00	1.00
$k_i$	1.11	1.11	1.00	1.00	1.00
$k_{i+1}$	1.11	1.00	1.00	1.00	1.00
<b>Estimated Damage Indices</b>					
<b>Property</b>	<b>System #1</b>	<b>System #2</b>	<b>System #3</b>	<b>System #4</b>	<b>System #5</b>
$m_i$	1.13	1.00	0.95	0.98	0.89
$k_i$	1.00	1.00	0.95	0.98	0.88
$k_{i+1}$	1.00	0.91	0.95	0.98	0.89

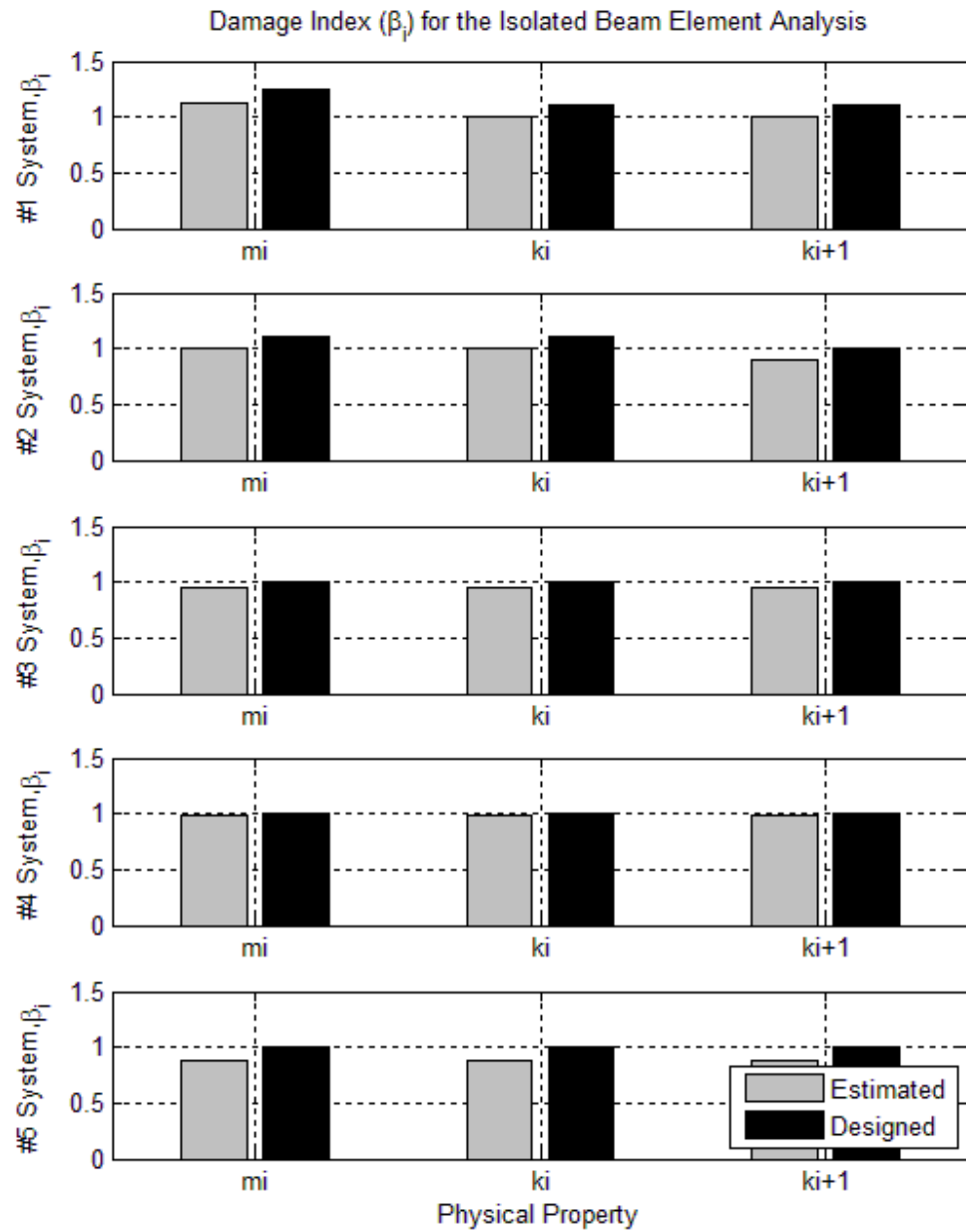


**Figure 6.56. Damage Indices ( $\beta_i$ ) for the Fixed-Fixed Beam with Noise-Polluted Accelerations Using Isolated Beam Element Analysis Method (1% Noise)**

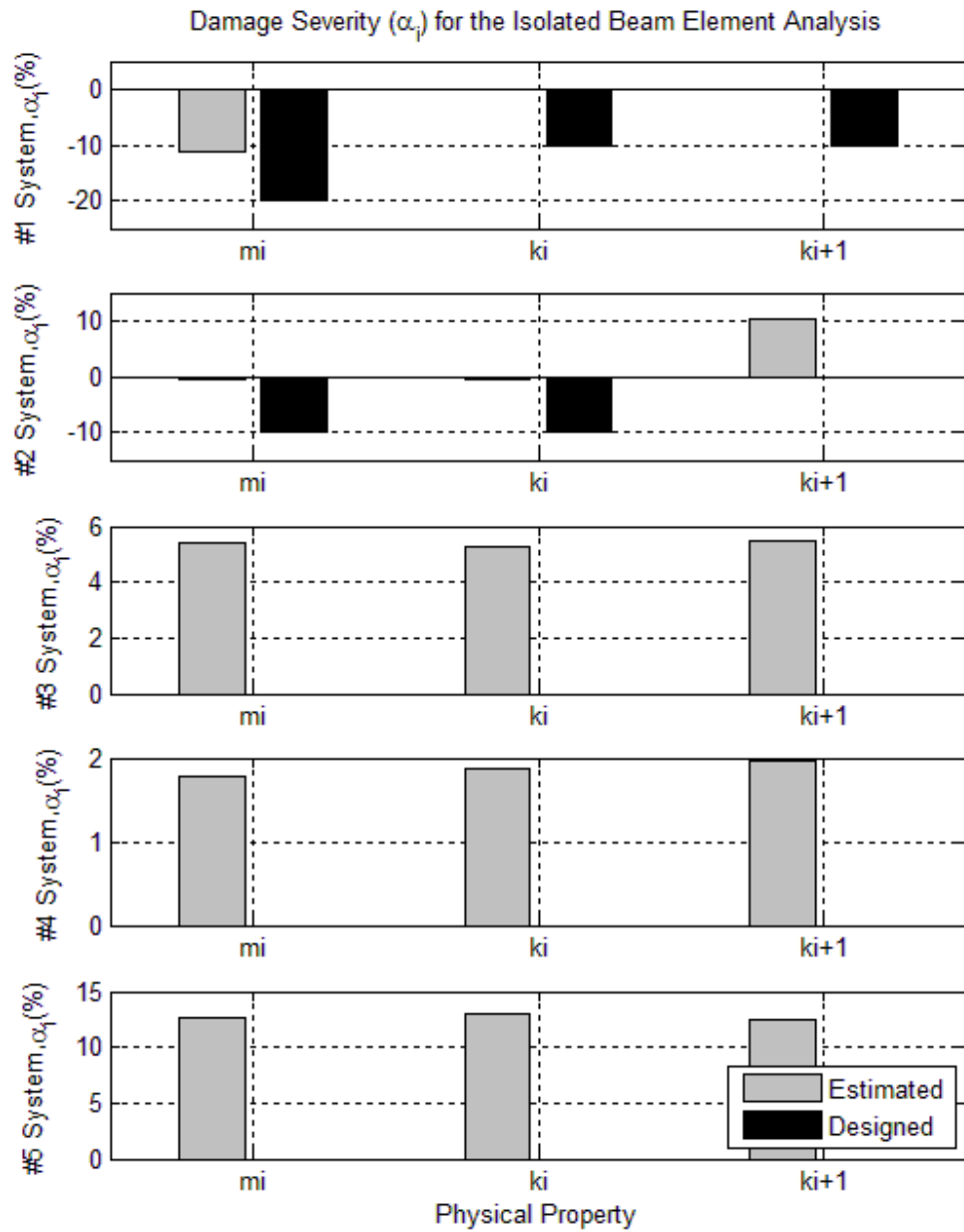


**Figure 6.57. Damage Severities (a) for the Fixed-Fixed Beam with Noise-Polluted Accelerations Using Isolated Beam Element Analysis Method (1% Noise)**

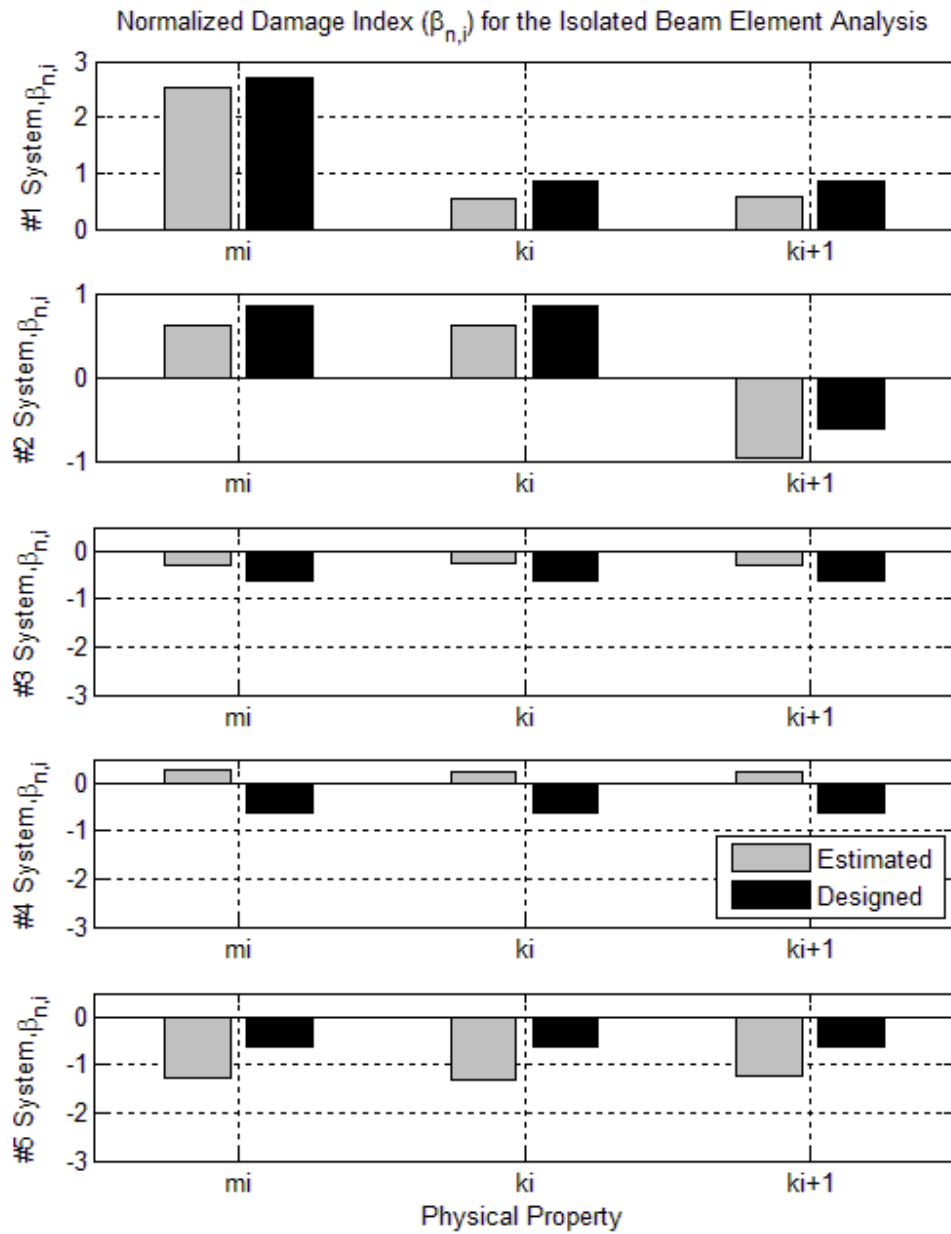
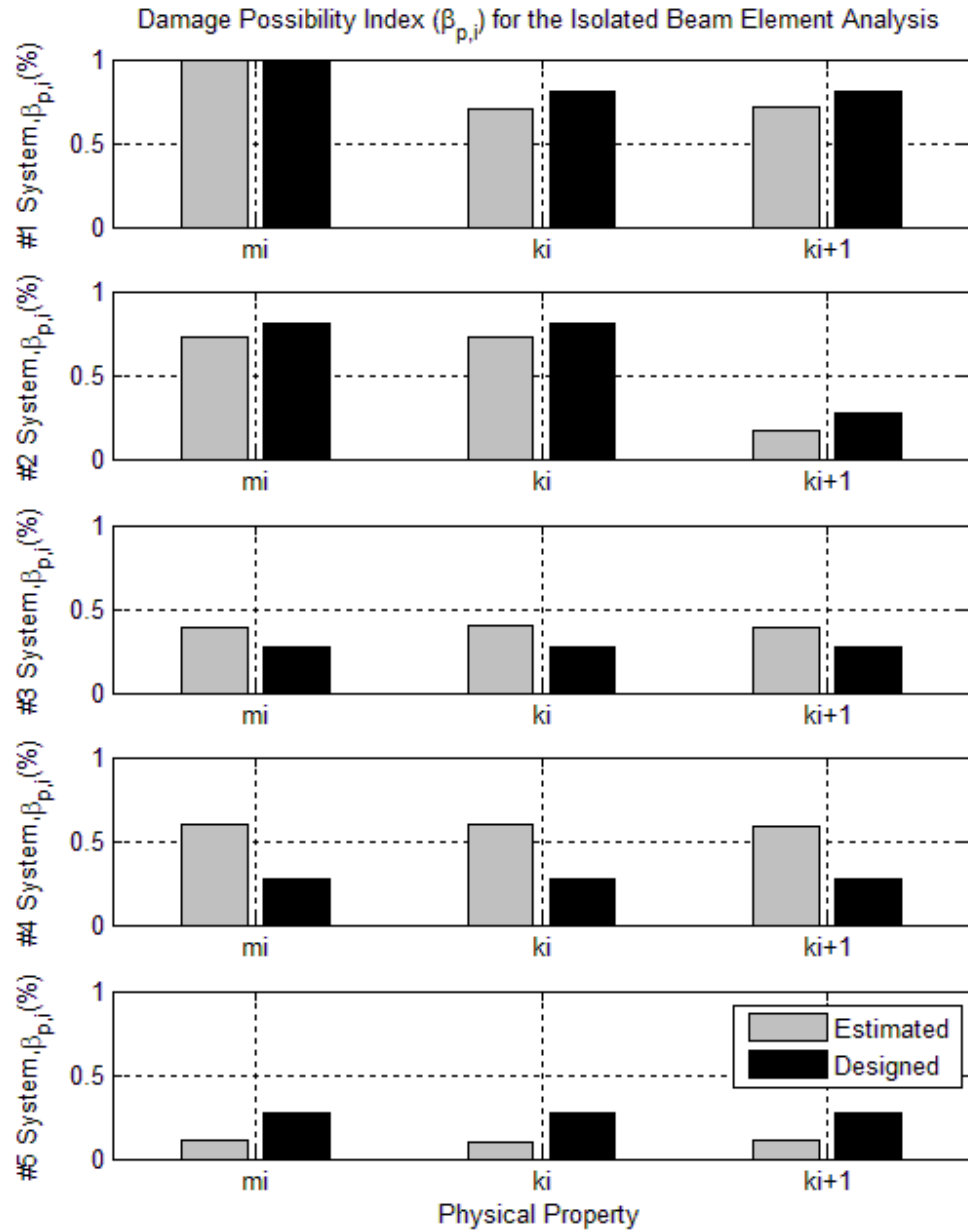


Figure 6.58. Normalized Damage Indices ( $\beta_{n,i}$ ) for the Fixed-Fixed Beam with Noise-Polluted Accelerations Using Isolated Beam Element Analysis Method (1% Noise)



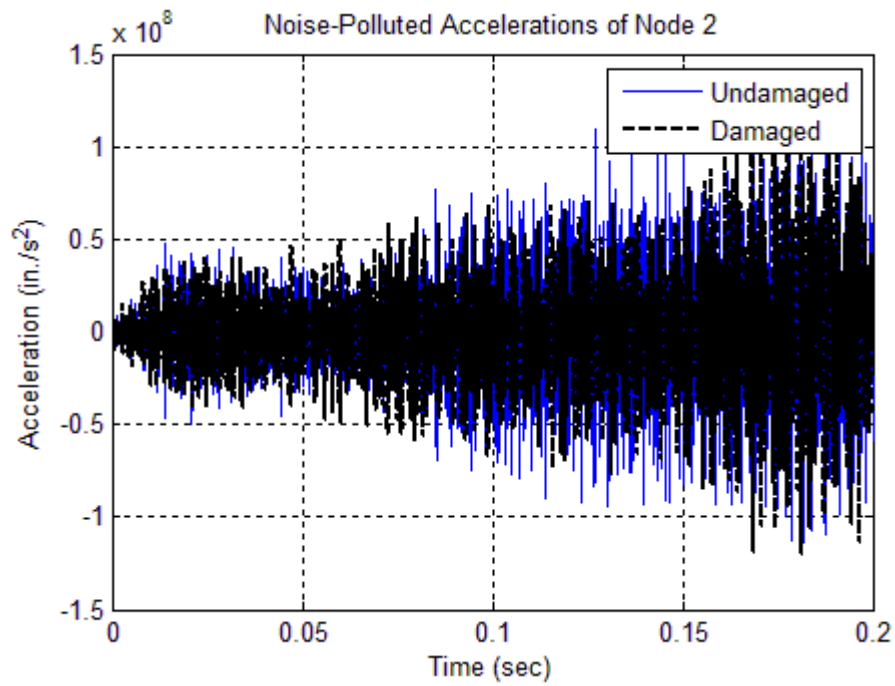
**Figure 6.59. Probability Damage Indices ( $\beta_{p,i}$ ) for the Fixed-Fixed Beam with Noise-Polluted Accelerations Using Isolated Beam Element Analysis Method (1% Noise)**

### **6.5.2 Case #6.8: Continuous System with 5% Noise Pollution Using Isolation**

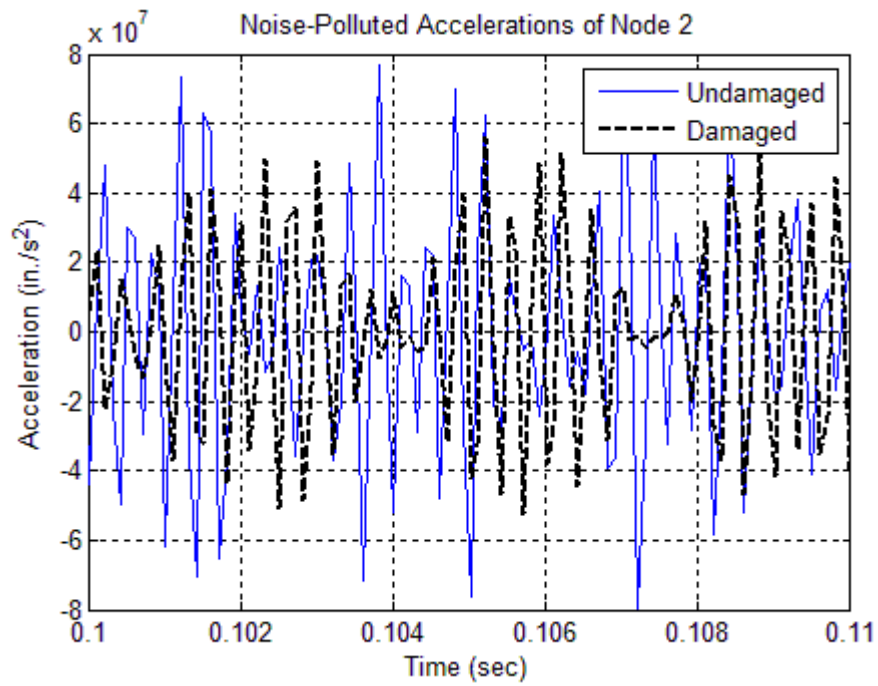
#### **Method**

In this case, the exact accelerations of the mass blocks outputted directly from SAP2000 were contaminated by 5% of white noise. The noise-polluted accelerations of Node 2 in both the undamaged and damaged cases are plotted in Figure 6.60. The filtered accelerations, estimated velocities, and estimated displacements of Node 2 are plotted in Figure 6.61, Figure 6.62, and Figure 6.63, respectively.

The estimated damage indices and the designed damage indices for each physical property are listed in Table 6.10 and are plotted in Figure 6.64. The estimated damage severities and the designed damage severities for each physical property are also listed in Table 6.10 and are plotted in Figure 6.65. The normalized damage indices are computed using Eq. 6.4 and are plotted in Figure 6.66. The damage possibility indices are plotted in Figure 6.67. Comparing the estimated damage indices with the designed damage indices, the integrated system analysis method can accurately locate and size multiple damage with 5% noise-polluted input data from a typical fixed-fixed beam.

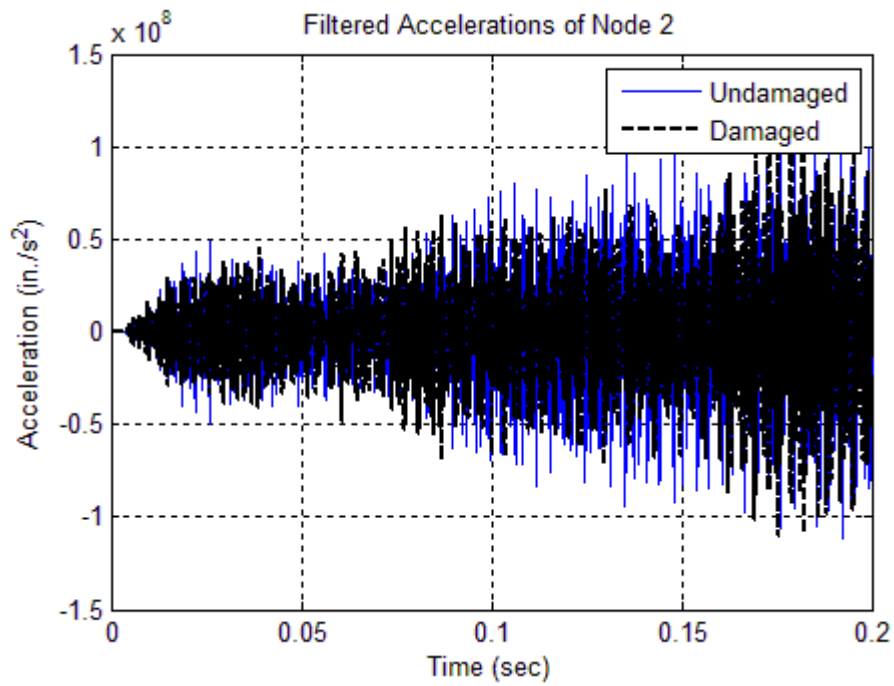


(a)

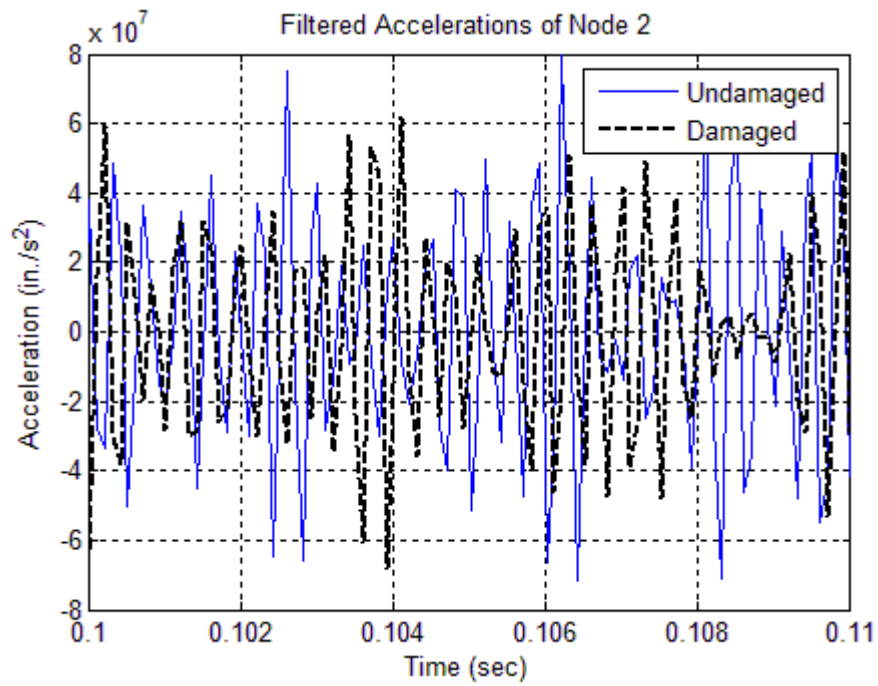


(b)

Figure 6.60. Noise-Polluted Accelerations of Node 2 for the Undamaged and Damaged Models of Case #6.8 (5% Noise): (a) Full Plot and (b) Zoomed in Plot



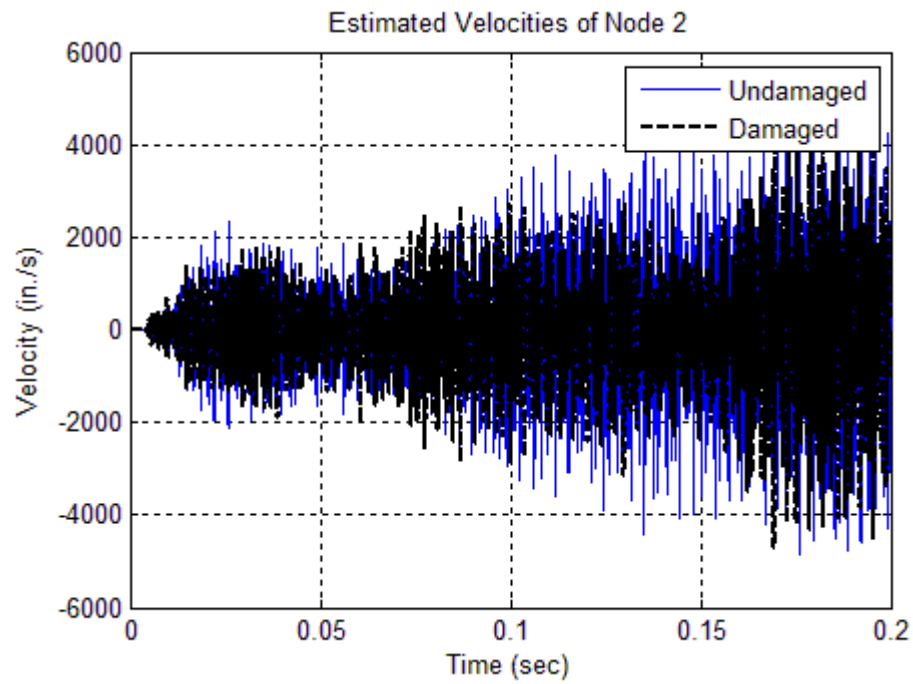
(a)



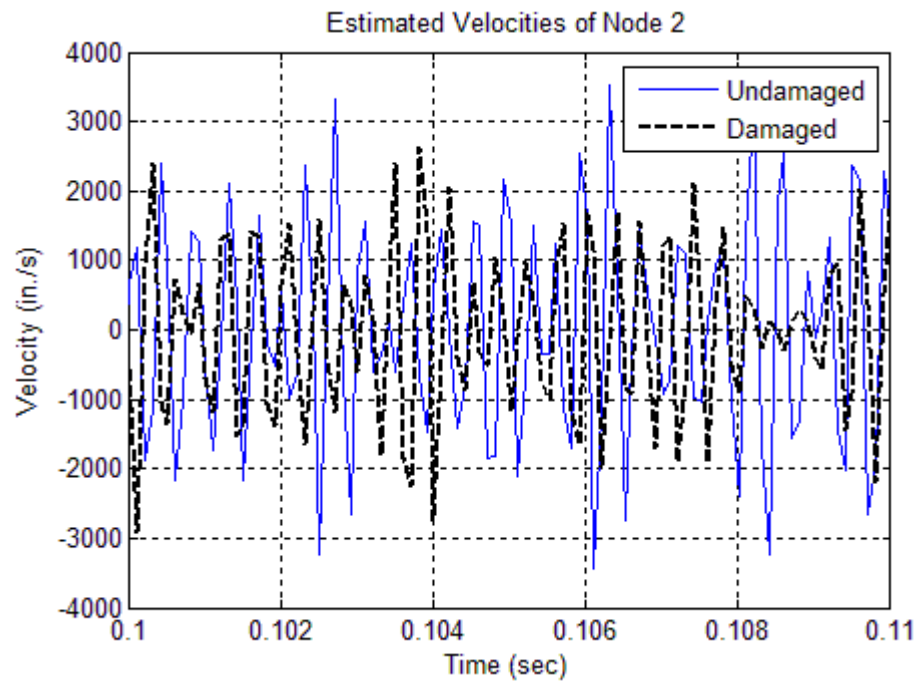
(b)

**Figure 6.61. Filtered Noise-Polluted Accelerations of Node 2 for the Undamaged and Damaged Models of Case #6.8 (5% Noise): (a) Full Plot and (b) Zoomed in Plot**



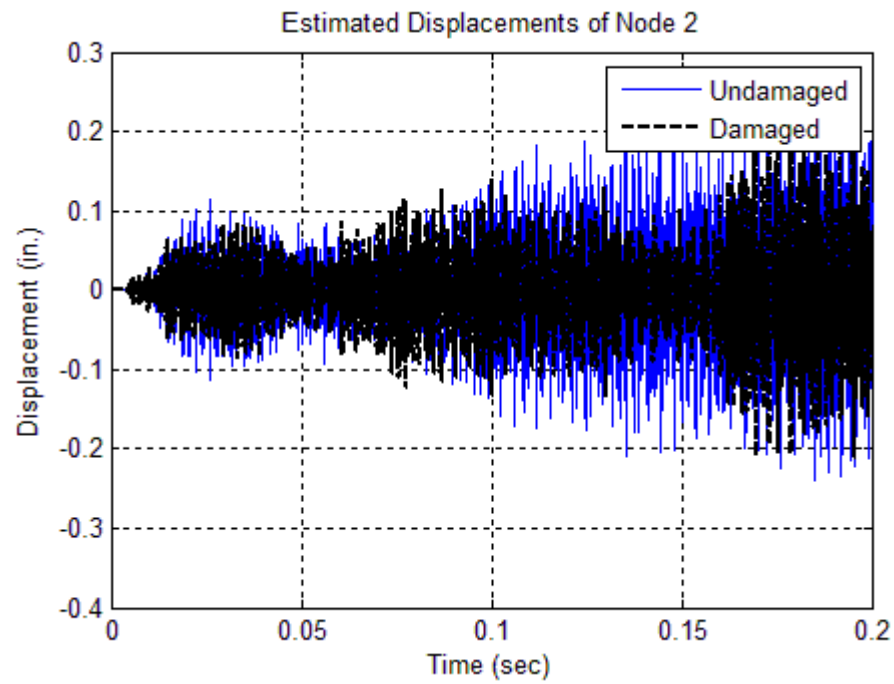


(a)

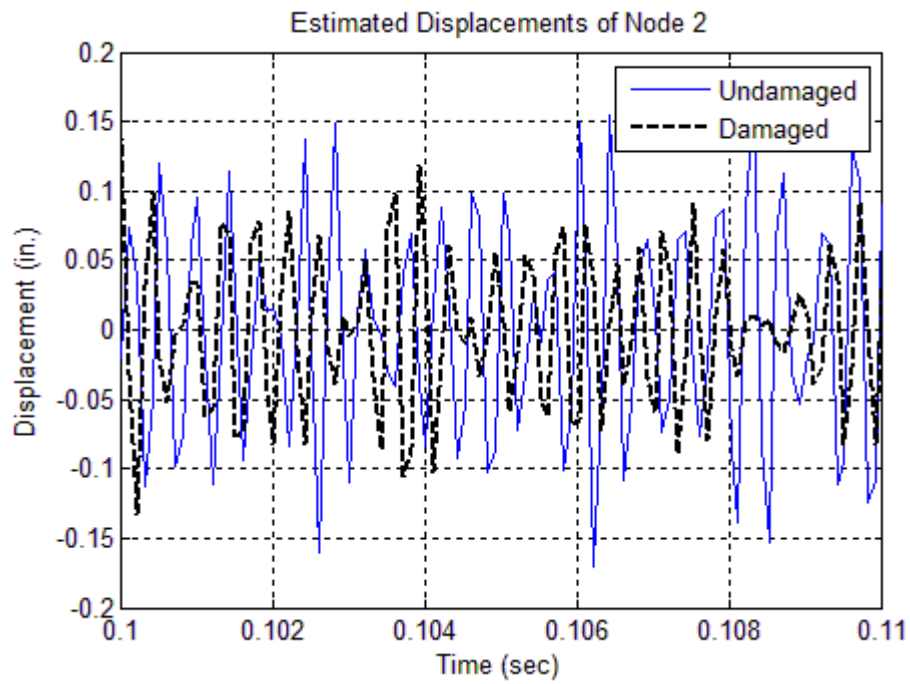


(b)

**Figure 6.62. Estimated Velocities of Node 2 for the Undamaged and Damaged Models of Case #6.8 (5% Noise): (a) Full Plot and (b) Zoomed in Plot**



(a)



(b)

**Figure 6.63. Estimated Displacements of Node 2 for the Undamaged and Damaged Models of Case #6.8 (5% Noise): (a) Full Plot and (b) Zoomed in Plot**

**Table 6.10. Damage Detection Results for the Fixed-Fixed Beam Using Isolated Method (1% Noise Pollution)**

<b>Designed Damage Indices</b>					
<b>Property</b>	<b>System #1</b>	<b>System #2</b>	<b>System #3</b>	<b>System #4</b>	<b>System #5</b>
$m_i$	1.25	1.11	1.00	1.00	1.00
$k_i$	1.11	1.11	1.00	1.00	1.00
$k_{i+1}$	1.11	1.00	1.00	1.00	1.00
<b>Estimated Damage Indices</b>					
<b>Property</b>	<b>System #1</b>	<b>System #2</b>	<b>System #3</b>	<b>System #4</b>	<b>System #5</b>
$m_i$	0.75	0.66	0.51	0.46	0.55
$k_i$	0.67	0.66	0.51	0.46	0.56
$k_{i+1}$	0.67	0.60	0.51	0.46	0.55

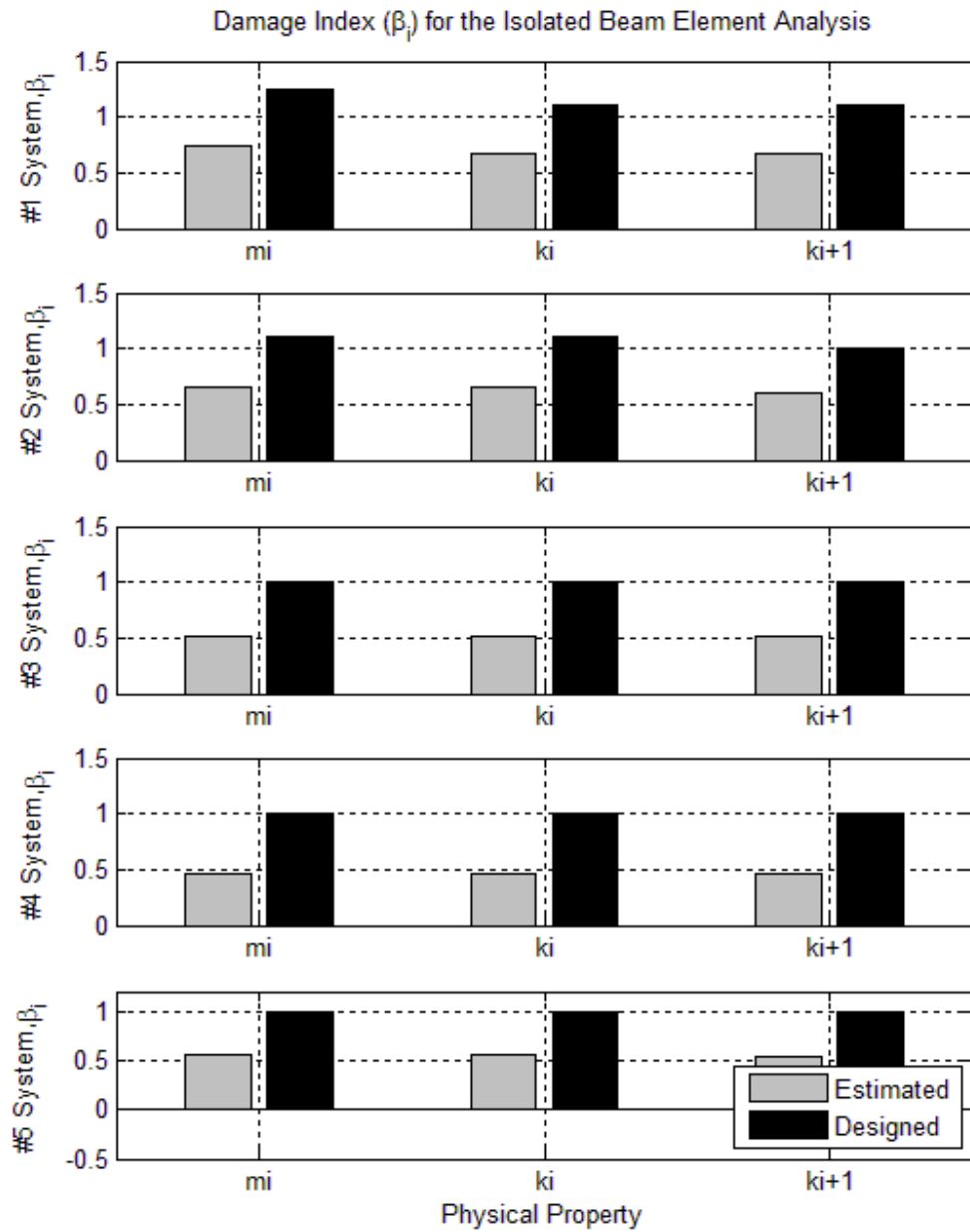


**Figure 6.64. Damage Indices ( $\beta_i$ ) for the Fixed-Fixed Beam with Noise-Polluted Accelerations  
Using Isolated Beam Element Analysis Method (5% Noise)**

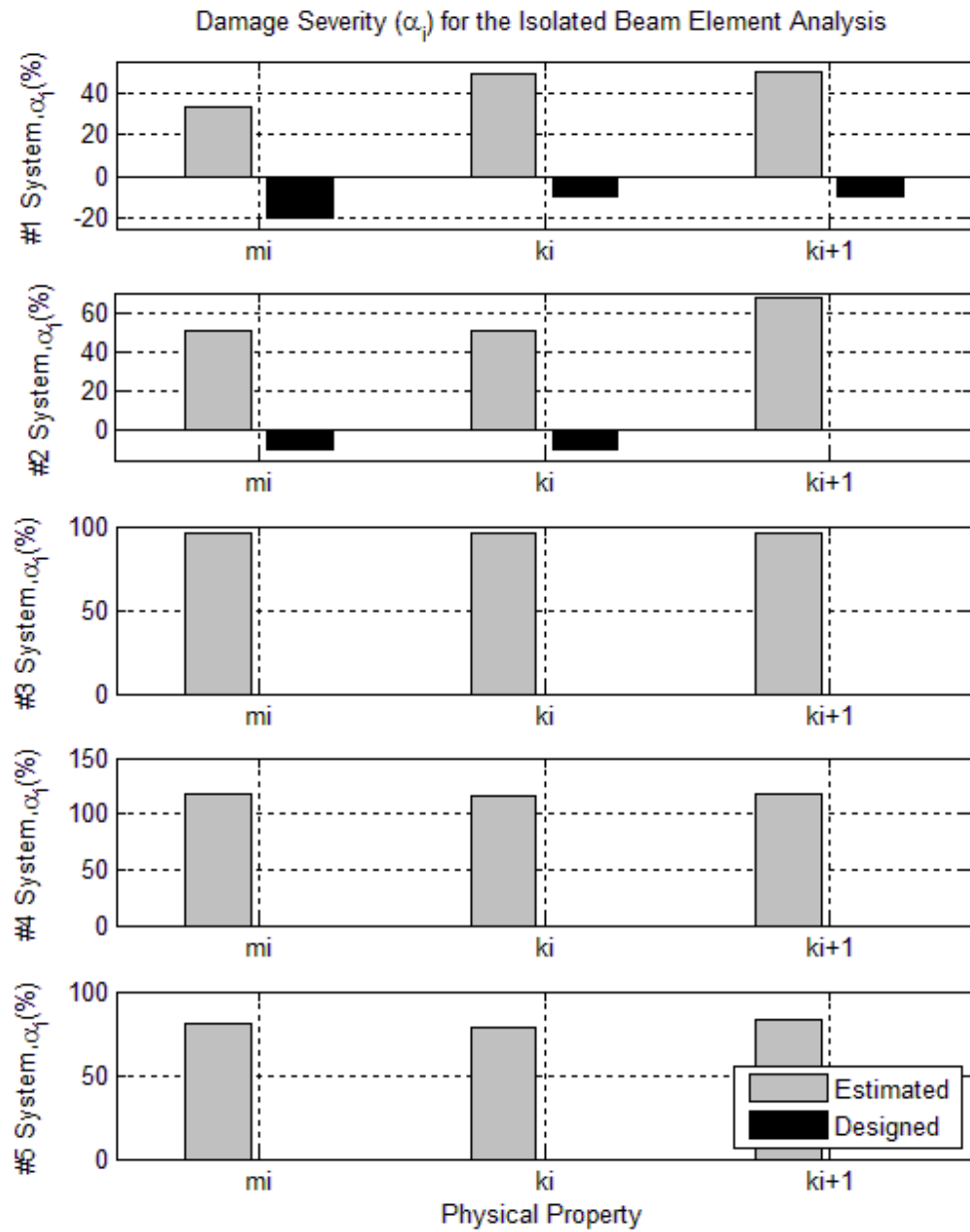


**Figure 6.65. Damage Severities (a) for the Fixed-Fixed Beam with Noise-Polluted Accelerations Using Isolated Beam Element Analysis Method (5% Noise)**

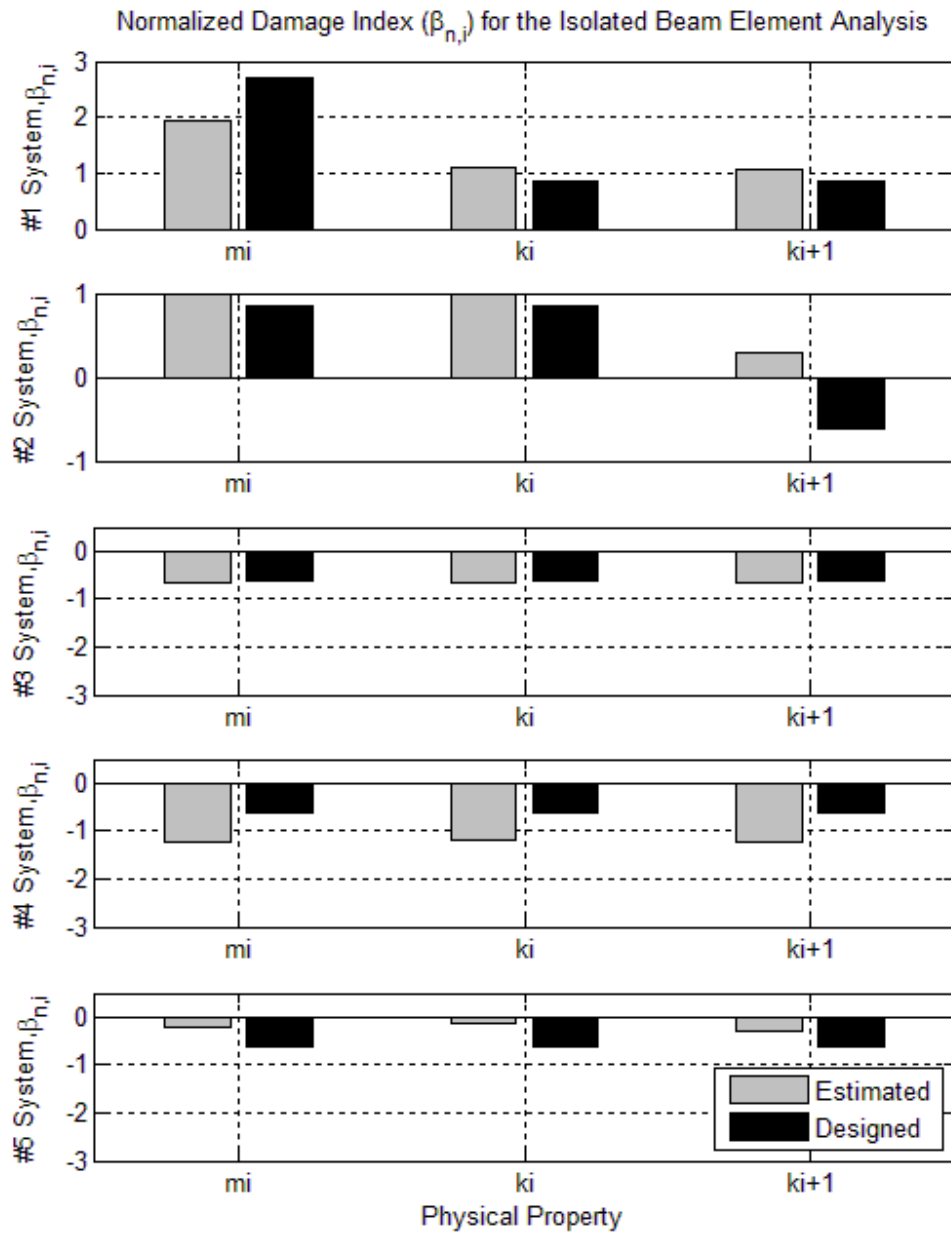
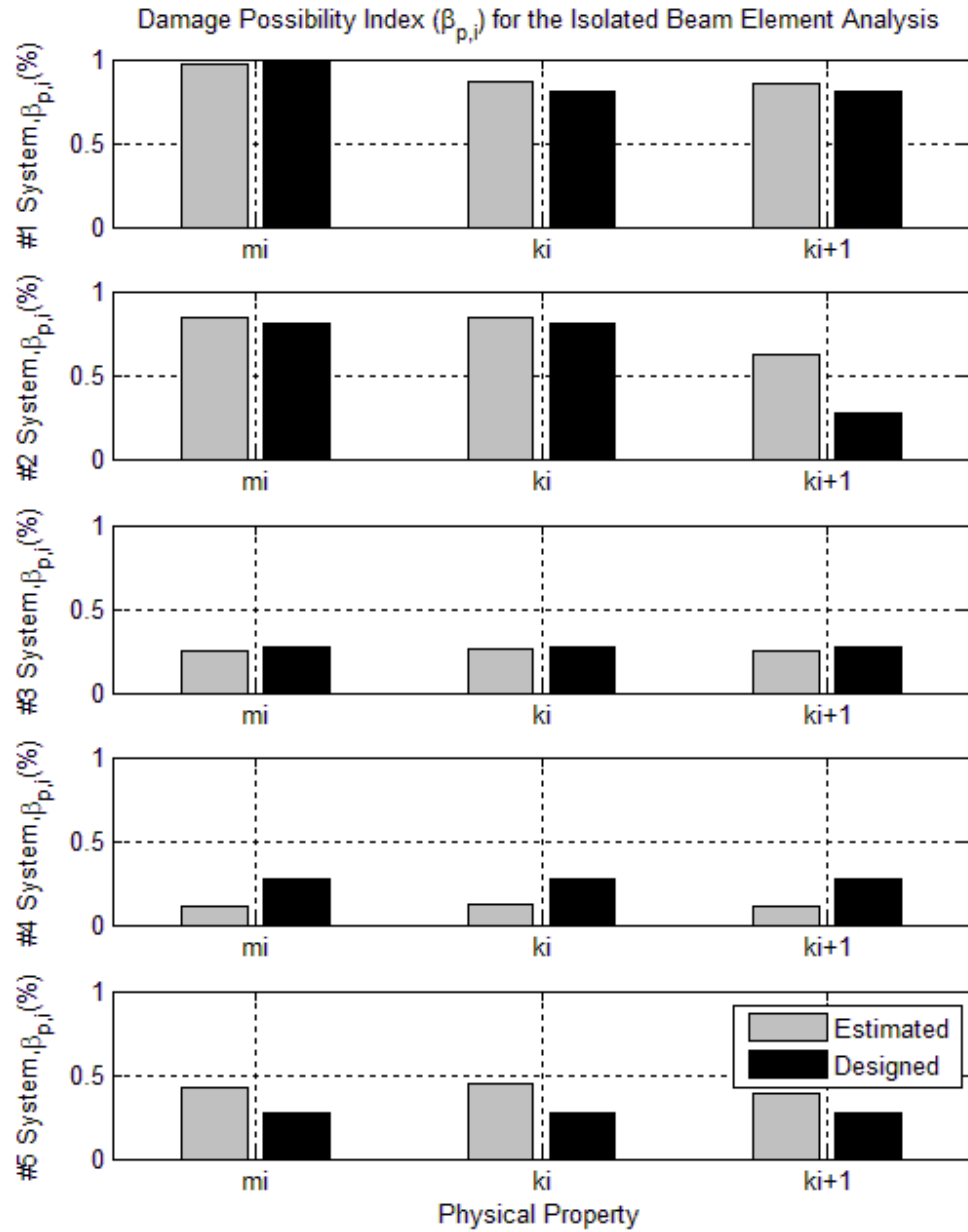


Figure 6.66. Normalized Damage Indices ( $\beta_{n,i}$ ) for the Fixed-Fixed Beam with Noise-Polluted Accelerations Using Isolated Beam Element Analysis Method (5% Noise)



**Figure 6.67. Damage Possibility Indices ( $\beta_{p,i}$ ) for the Fixed-Fixed Beam with Noise-Polluted Accelerations Using Isolated Beam Element Analysis Method (5% Noise)**

## **6.6 EVALUATION OF RESULTS**

In this subsection, all the results from the previous subsection of Section 6 will be summarized and evaluated. Because for some cases, the traditional damage index will be influenced severely by the existence of noise and the application of band-pass filters, the results evaluations will be mainly based on the damage possibility indices.

To distinguish the damaged elements from the undamaged elements, the damage judgement criterion for the Damage Possibility Index is subjectively set as 50%. Namely, if the Damage Possibility Index is greater than 50%, the element property is considered to be damaged.

### **6.6.1 Evaluation of Results for Case #6.1**

From Figure 6.7 through Figure 6.10, the damage detection results using the data contaminated by 1% noise are very close to the designed damage detection results. Only small discrepancies can be found. The percentage error between the Designed Damage Possibility Indices and Estimated Damage Possibility Indices are displayed in Table 6.11. The false negatives reported in Table 6.11 are due to the damage criteria set in the beginning of the section, not due to noise influence. For this case, since the Damage Indices and Damage Severities, shown in Figure 6.7 and Figure 6.8 are not severely influenced by the noise, the damage locations and damage extents can still be well estimated by using Damage Indices and Damage Severities.



**Table 6.11. Results Evaluation for Discrete System with 1% Noise Pollution Using Integral Method**

<b>Physical Properties</b>	<b>Measured Damage Possibility Indices, <math>\beta_{p,i}</math></b>	<b>Designed Damage Possibility Indices, <math>\beta_{p,i}</math></b>	<b>Percentage Error (%)</b>	<b>False Positive</b>	<b>False Negative</b>
$m_1$	0.6331	0.6217	1.83	0	0
$m_2$	0.4443	0.4522	1.75	0	1
$m_3$	0.3156	0.3228	2.21	0	0
$m_4$	0.3192	0.3228	1.11	0	0
$m_5$	0.3264	0.3228	1.11	0	0
$c_1$	0.9966	0.9953	0.13	0	0
$c_2$	0.9934	0.9953	0.19	0	0
$c_3$	0.3121	0.3228	3.31	0	0
$c_4$	0.3228	0.3228	0.00	0	0
$c_5$	0.3300	0.3228	2.23	0	0
$c_6$	0.3192	0.3228	1.11	0	0
$k_1$	0.4681	0.4522	3.51	0	1
$k_2$	0.4562	0.4522	0.88	0	1
$k_3$	0.3192	0.3228	1.11	0	0
$k_4$	0.3156	0.3228	2.21	0	0
$k_5$	0.3192	0.3228	1.11	0	0
$k_6$	0.3336	0.3228	3.36	0	0

### 6.6.2 Evaluation of Results for Case #6.2

From Figure 6.15 and Figure 6.16, the Damage Indices and Damage Severities are influenced by the noise. However, the damage designed in  $m_1$ ,  $m_2$ ,  $c_1$ ,  $c_2$ ,  $k_1$ , and  $k_2$  can still be detected and well estimated and only one false positive is found at  $c_6$ . The percentage error between the Designed Damage Possibility Indices and Estimated

Damage Possibility Indices are displayed in Table 6.12. The false negatives reported in Table 6.12 are due to the damage criteria set in the beginning of the section, not due to noise influence. The false positive shown in Table 6.12 is resulted from noise influence. However, the results displayed in Figure 6.15 through Figure 6.18 are the results from only one experiment. Better results can be acquired if the experiments can be repeated.

**Table 6.12. Results Evaluation for Discrete System with 5% Noise Pollution Using Integral Method**

<b>Physical Properties</b>	<b>Measured Damage Possibility Indices, <math>\beta_{p,i}</math></b>	<b>Designed Damage Possibility Indices, <math>\beta_{p,i}</math></b>	<b>Percentage Error (%)</b>	<b>False Positive</b>	<b>False Negative</b>
$m_1$	0.8340	0.6217	34.14	0	0
$m_2$	0.4880	0.4522	7.91	0	1
$m_3$	0.3409	0.3228	5.62	0	0
$m_4$	0.3783	0.3228	17.20	0	0
$m_5$	0.3264	0.3228	1.11	0	0
$c_1$	0.9251	0.9953	7.06	0	0
$c_2$	0.9977	0.9953	0.23	0	0
$c_3$	0.1492	0.3228	53.78	0	0
$c_4$	0.1611	0.3228	50.09	0	0
$c_5$	0.1230	0.3228	61.88	0	0
$c_6$	0.7088	0.3228	119.62	1	0
$k_1$	0.6179	0.4522	36.63	0	0
$k_2$	0.5160	0.4522	14.09	0	0
$k_3$	0.3446	0.3228	6.76	0	0
$k_4$	0.3594	0.3228	11.36	0	0
$k_5$	0.3156	0.3228	2.21	0	0
$k_6$	0.3336	0.3228	3.36	0	0

### **6.6.3 Evaluation of Results for Case #6.3**

From Figure 6.23 through Figure 6.26, the damage detection results using the data contaminated by 1% noise are very close to the designed damage detection results. Only small discrepancies can be found. The percentage error between the Designed Damage Possibility Indices and Estimated Damage Possibility Indices are displayed in Table 6.13. The false negatives reported in Table 6.13 are due to the damage criteria set in the beginning of the section, not due to noise influence. For this case, since the Damage Indices and Damage Severities, shown in Figure 6.23 and Figure 6.24 are not severely influenced by the noise, the damage locations and damage extents can still be well estimated by using Damage Indices and Damage Severities.

**Table 6.13. Results Evaluation for Discrete System with 1% Noise Pollution Using Isolated Method**

System Number	Physical Properties	Measured Damage Possibility Indices, $\beta_{p,i}$	Designed Damage Possibility Indices, $\beta_{p,i}$	Percentage Error (%)	False Positive	False Negative
Isolated System #1	$m_i$	0.6368	0.6255	1.81	0	0
	$c_i$	0.9918	0.9955	0.37	0	0
	$c_{i+1}$	0.9953	0.9955	0.01	0	0
	$k_i$	0.4641	0.4562	1.74	0	1
	$k_{i+1}$	0.4641	0.4562	1.74	0	1
Isolated System #2	$m_i$	0.4562	0.4562	0.00	0	1
	$c_i$	0.9974	0.9955	0.20	0	0
	$c_{i+1}$	0.3372	0.3264	3.34	0	0
	$k_i$	0.4602	0.4562	0.87	0	1
	$k_{i+1}$	0.3264	0.3264	0.00	0	0
Isolated System #3	$m_i$	0.3300	0.3264	1.11	0	0
	$c_i$	0.3192	0.3264	2.20	0	0
	$c_{i+1}$	0.3156	0.3264	3.29	0	0
	$k_i$	0.3300	0.3264	1.11	0	0
	$k_{i+1}$	0.3264	0.3264	0.00	0	0
Isolated System #4	$m_i$	0.3264	0.3264	0.00	0	0
	$c_i$	0.3300	0.3264	1.11	0	0
	$c_{i+1}$	0.2981	0.3264	8.67	0	0
	$k_i$	0.3264	0.3264	0.00	0	0
	$k_{i+1}$	0.3228	0.3264	1.10	0	0
Isolated System #5	$m_i$	0.3300	0.3264	1.11	0	0
	$c_i$	0.3156	0.3264	3.29	0	0
	$c_{i+1}$	0.3520	0.3264	7.85	0	0
	$k_i$	0.3300	0.3264	1.11	0	0
	$k_{i+1}$	0.3336	0.3264	2.22	0	0

#### **6.6.4 Evaluation of Results for Case #6.4**

From Figure 6.31 and Figure 6.32, the Damage Indices and Damage Severities are influenced by the noise. However, the damage designed in  $m_i$ ,  $c_i$ ,  $c_{i+1}$ ,  $k_i$ , and  $k_{i+1}$  in System #1 and  $m_i$ ,  $c_i$ , and  $k_i$  in System #2 can still be detected and well estimated. Neither obvious false positives nor false negative was reported in Figure 6.31 and Figure 6.32. The percentage error between the Designed Damage Possibility Indices and Estimated Damage Possibility Indices are displayed in Table 6.14. Moreover, neither false negative nor false negative was reported in Table 6.14, either. The current results displayed in Figure 6.31 through Figure 6.34 are the results from only one experiment. Better results can be acquired if the experiments can be repeated.

**Table 6.14. Results Evaluation for Discrete System with 5% Noise Pollution Using Isolated Method**

System Number	Physical Properties	Measured Damage Possibility Indices, $\beta_{p,i}$	Designed Damage Possibility Indices, $\beta_{p,i}$	Percentage Error (%)	False Positive	False Negative
Isolated System #1	$m_i$	0.7357	0.6255	17.61	0	0
	$c_i$	0.9985	0.9955	0.31	0	0
	$c_{i+1}$	0.9798	0.9955	1.57	0	0
	$k_i$	0.5910	0.4562	29.54	0	0
	$k_{i+1}$	0.5478	0.4562	20.07	0	0
Isolated System #2	$m_i$	0.5438	0.4562	19.20	0	0
	$c_i$	0.9616	0.9955	3.40	0	0
	$c_{i+1}$	0.3594	0.3264	10.13	0	0
	$k_i$	0.5398	0.4562	18.33	0	0
	$k_{i+1}$	0.4013	0.3264	22.96	0	0
Isolated System #3	$m_i$	0.4325	0.3264	32.53	0	0
	$c_i$	0.2611	0.3264	20.00	0	0
	$c_{i+1}$	0.3520	0.3264	7.85	0	0
	$k_i$	0.4168	0.3264	27.72	0	0
	$k_{i+1}$	0.4286	0.3264	31.32	0	0
Isolated System #4	$m_i$	0.3745	0.3264	14.75	0	0
	$c_i$	0.4286	0.3264	31.32	0	0
	$c_{i+1}$	0.0359	0.3264	88.99	0	0
	$k_i$	0.3821	0.3264	17.08	0	0
	$k_{i+1}$	0.3228	0.3264	1.10	0	0
Isolated System #5	$m_i$	0.4090	0.3264	25.34	0	0
	$c_i$	0.0548	0.3264	83.21	0	0
	$c_{i+1}$	0.4052	0.3264	24.15	0	0
	$k_i$	0.4129	0.3264	26.53	0	0
	$k_{i+1}$	0.3821	0.3264	17.08	0	0

### **6.6.5 Evaluation of Results for Case #6.5**

From Figure 6.40 and Figure 6.41, all the Damage Indices are reduced by certain levels and all Damage Severities are shifted upward to the positive side. This is resulted from the application of band-pass filter and the noise influence. Although the damage in  $m_1$ ,  $m_2$ ,  $k_1$ , and  $k_2$  can still be located, the differences between the estimated damage severities and designed damage severities are obvious. However, this problem can be solved by using the Normalized Damage Index and Damage Possibility Index. From Figure 6.42 and Figure 6.43, the estimated results matches well with the designed results. Because the designed Damage Indices for the damage properties are closed to each other, all the damage possibility indices for the damaged properties are greater than 50%. Consequently, no false negative is reported in Table 6.15. In addition, no false positive is found using the Damage Possibility Index.

**Table 6.15. Results Evaluation for Continuous System with 1% Noise Pollution Using Integral Method**

<b>Physical Properties</b>	<b>Measured Damage Possibility Indices, <math>\beta_{p,i}</math></b>	<b>Designed Damage Possibility Indices, <math>\beta_{p,i}</math></b>	<b>Percentage Error (%)</b>	<b>False Positive</b>	<b>False Negative</b>
$m_1$	0.9922	0.9913	0.09	0	0
$m_2$	0.7580	0.7611	0.41	0	0
$m_3$	0.2676	0.2611	2.51	0	0
$m_4$	0.2578	0.2611	1.24	0	0
$m_5$	0.2643	0.2611	1.25	0	0
$k_1$	0.7422	0.7611	2.50	0	0
$k_2$	0.7549	0.7611	0.82	0	0
$k_3$	0.2709	0.2611	3.77	0	0
$k_4$	0.2643	0.2611	1.25	0	0
$k_5$	0.2389	0.2611	8.52	0	0
$k_6$	0.2946	0.2611	12.84	0	0

#### 6.6.6 Evaluation of Results for Case #6.6

From Figure 6.48 and Figure 6.49, all the Damage Indices are reduced by certain level and all Damage Severities are shifted upward to the positive side. This is resulted from the application of band-pass filter and the noise influence. With the 5% white noise mixed in the acceleration data, the damage in  $m_1$ ,  $m_2$ ,  $k_1$ , and  $k_2$  cannot be located, the differences between the estimated damage severities and designed damage severities are obvious. However, this problem can be solved by using the Normalized Damage Index and Damage Possibility Index. From Figure 6.50 and Figure 6.51, the estimated results matches well with the designed results. Because the designed Damage Indices for the damage properties are closed to each other, all the damage possibility indices for the damaged properties are



greater than 50%. Consequently, no false negatives are reported in Table 6.16. In addition, no false positives are found using the Damage Possibility Index.

**Table 6.16. Results Evaluation for Continuous System with 5% Noise Pollution Using Integral Method**

<b>Physical Properties</b>	<b>Measured Damage Possibility Indices, <math>\beta_{p,i}</math></b>	<b>Designed Damage Possibility Indices, <math>\beta_{p,i}</math></b>	<b>Percentage Error (%)</b>	<b>False Positive</b>	<b>False Negative</b>
$m_1$	0.9918	0.9913	0.05	0	0
$m_2$	0.7823	0.7611	2.78	0	0
$m_3$	0.3264	0.2611	25.00	0	0
$m_4$	0.2207	0.2611	15.49	0	0
$m_5$	0.2643	0.2611	1.25	0	0
$k_1$	0.7123	0.7611	6.42	0	0
$k_2$	0.7486	0.7611	1.65	0	0
$k_3$	0.2776	0.2611	6.32	0	0
$k_4$	0.2514	0.2611	3.70	0	0
$k_5$	0.1949	0.2611	25.35	0	0
$k_6$	0.3557	0.2611	36.23	0	0

#### **6.6.7 Evaluation of Results for Case #6.7**

From Figure 6.56, only the damage in  $m_1$  in System #1 was located. From Figure 6.57, the damage severities are found to be shifted upward to the positive side. This can be seen from the values of other damage severities. Because no properties are designed to be strengthened in this case, thus the positive damage severities of other elements indicate the shift of the damage severities. Consequently, the damage indices in Figure 6.56 are, in fact,

shifted downward and thus, not all damage were detected. However, this problem can be solved by using the Normalized Damage Index and Damage Possibility Index. From Figure 6.58 and Figure 6.59, the designed damage in  $m_i$ ,  $k_i$ , and  $k_{i+1}$  in System #1 and  $m_i$  and  $k_i$  in System #2 were successfully detected. However, according to Table 6.17, false positives were found in System #4. The false positives in System #4 are due to the differences of amplitudes of shift for each isolated system. This can be seen from Table 6.9: for System #3, the average value is 0.95; for System #4, the average value is 0.98; for System #5, the average value is 0.89. Consequently, after normalization, the average value for System #4 will be bigger than the average values of System #3 and System #5 after normalization. The differences of amplitudes of shift for each isolated system are natural because each isolated system is analyzed separately.

**Table 6.17. Results Evaluation for Continuous System with 1% Noise Pollution Using Isolated Method**

System Number	Physical Properties	Measured Damage Possibility Indices, $\beta_{p,i}$	Designed Damage Possibility Indices, $\beta_{p,i}$	Percentage Error (%)	False Positive	False Negative
Isolated System #1	$m_i$	0.9946	0.9965	0.19	0	0
	$k_i$	0.7088	0.8051	11.96	0	0
	$k_{i+1}$	0.7157	0.8051	11.11	0	0
Isolated System #2	$m_i$	0.7324	0.8051	9.03	0	0
	$k_i$	0.7324	0.8051	9.03	0	0
	$k_{i+1}$	0.1685	0.2709	37.80	0	0
Isolated System #3	$m_i$	0.3897	0.2709	43.85	0	0
	$k_i$	0.3974	0.2709	46.69	0	0
	$k_{i+1}$	0.3859	0.2709	42.44	0	0
Isolated System #4	$m_i$	0.6026	0.2709	122.40	1	0
	$k_i$	0.5987	0.2709	120.98	1	0
	$k_{i+1}$	0.5910	0.2709	118.12	1	0
Isolated System #5	$m_i$	0.1057	0.2709	61.00	0	0
	$k_i$	0.0968	0.2709	64.27	0	0
	$k_{i+1}$	0.1112	0.2709	58.94	0	0

### 6.6.8 Evaluation of Results for Case #6.8

From Figure 6.64 and Figure 6.65, all the Damage Indices are reduced by certain level and all Damage Severities are shifted upward to the positive side. This is resulted from the application of band-pass filter and the noise influence. However, this problem can be solved by using the Normalized Damage Index and Damage Possibility Index. According to Table 6.18, the designed damage in  $m_i$ ,  $k_i$  and  $k_{i+1}$  in System #1 and  $m_i$  and  $k_i$  in System #2 were successfully detected. One false positive was found in Table 6.18 in  $k_{i+1}$  in System #2. This false positive is resulted from the noise influence. Comparing to the previous case,

with increased noise influence, no false positives were found in other isolated systems. These indicate the certain instability of the isolated method, which might be resolved by taking the average values from repeating the experiments and the analysis processes.

**Table 6.18. Results Evaluation for Continuous System with 5% Noise Pollution Using Isolated Method**

System Number	Physical Properties	Measured Damage Possibility Indices, $\beta_{p,i}$	Designed Damage Possibility Indices, $\beta_{p,i}$	Percentage Error (%)	False Positive	False Negative
Isolated System #1	$m_i$	0.9732	0.9965	2.34	0	0
	$k_i$	0.8643	0.8051	7.36	0	0
	$k_{i+1}$	0.8554	0.8051	6.25	0	0
Isolated System #2	$m_i$	0.8389	0.8051	4.20	0	0
	$k_i$	0.8389	0.8051	4.20	0	0
	$k_{i+1}$	0.6179	0.2709	128.07	1	0
Isolated System #3	$m_i$	0.2514	0.2709	7.20	0	0
	$k_i$	0.2578	0.2709	4.83	0	0
	$k_{i+1}$	0.2546	0.2709	6.02	0	0
Isolated System #4	$m_i$	0.1075	0.2709	60.33	0	0
	$k_i$	0.1170	0.2709	56.81	0	0
	$k_{i+1}$	0.1094	0.2709	59.64	0	0
Isolated System #5	$m_i$	0.4207	0.2709	55.29	0	0
	$k_i$	0.4443	0.2709	64.00	0	0
	$k_{i+1}$	0.3897	0.2709	43.85	0	0

## **7 REANALYSIS**

### **7.1 INTRODUCTION**

In this section, three problems that are either arose in the previous numerical examples or anticipated in the further applications will be demonstrated and the solutions are provided.

The problems will be analyzed in the following subsections are,

- (1) Case #7.1: Nodes without external loads;
- (2) Case #7.2: Efficiency of noise-influence reduction by repeating experiment;
- (3) Case #7.3: Damage detection in Continuous structure with proportional damping;

### **7.2 STUDY OF NODES WITHOUT EXTERNAL LOADS (CASE #7.1)**

#### **7.2.1 Introduction**

In this subsection, the problem caused by nodes without external loads will be studied and solved. For all the numerical cases that are studied in the previous sections, external loads had been applied at each node that was analyzed. This is not a problem for the integral system method of the Power Method, because the power equilibrium of the integral method can be applied if there is one node with external loads. However, for the isolated system method, the algorithm given in the previous section will only be applicable to the node with external load. For the node without external load, the previous algorithm for isolated system won't work due to the rank deficiency of the coefficient matrix for the final linear equation groups. Under this situation, a new algorithm is proposed in Subsection 7.2.2.

### 7.2.2 Theory for Node without External Loads

In this subsection, the theory for node without external load will be provided. For simplicity purposes, only the theory for node without external loads for plain frame will be provided and the theory for node without external loads for other structural components can be easily completed following the same idea and process.

According to the finite element method, one plain frame can be meshed into several elements. Isolating two nearby plain frame elements, as shown in Figure 7.1, the modulus of elasticity of the material for Element  $i$  is denoted as  $E_i$ . The length of Element  $i$  is  $L_i$ . The area and the moment of inertia of the cross section of Element  $i$  are denoted as  $A_i$  and  $I_i$ , respectively. Let  $\{P^i\}$  be the force vector at Node  $i$ , where  $P_1^i$  denotes the axial force at Node  $i$ ,  $P_2^i$  denotes the shear force at Node  $i$ ,  $P_3^i$  denotes the bending moment at Node  $i$ . As shown in the free body diagram of Node  $i$  in Figure 7.2, the external loads ( $\{P^i\}$ ), internal forces ( $\{F_i\}$  and  $\{F_{i+1}\}$ ), and inertial forces ( $\{I^i\}$ ) form a dynamic equilibrium condition at Node  $i$ . The dynamic equilibrium condition can be written as,

$$\{I^i\} + \{F_i\} + \{F_{i+1}\} = \{P^i\} \quad (7.1)$$

In this case, degrees of freedom in axial, transversal and rotational directions will be taken into consideration. Thus each force vector in Eq. 7.1 is composed by three force components: (1) Axial force; (2) shear force; (3) bending moment.

$$\begin{Bmatrix} I_1^i \\ I_2^i \\ I_3^i \end{Bmatrix} + \begin{Bmatrix} F_{i,1} \\ F_{i,2} \\ F_{i,3} \end{Bmatrix} + \begin{Bmatrix} F_{i+1,1} \\ F_{i+1,2} \\ F_{i+1,3} \end{Bmatrix} = \begin{Bmatrix} P_1^i \\ P_2^i \\ P_3^i \end{Bmatrix} \quad (7.2)$$

Where subscript one (“1”) indicates axial force; subscript two (“2”) indicates shear force and subscript three (“3”) indicates bending moment.

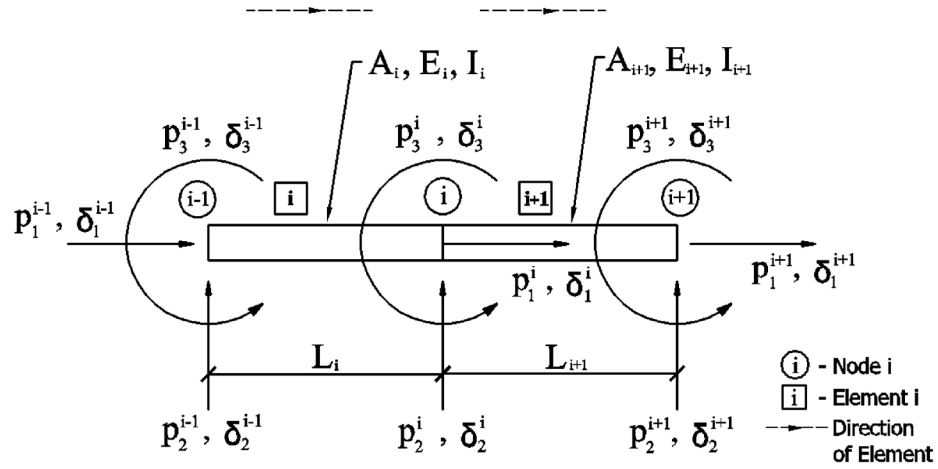


Figure 7.1. Two nearby Plane Frame Elements

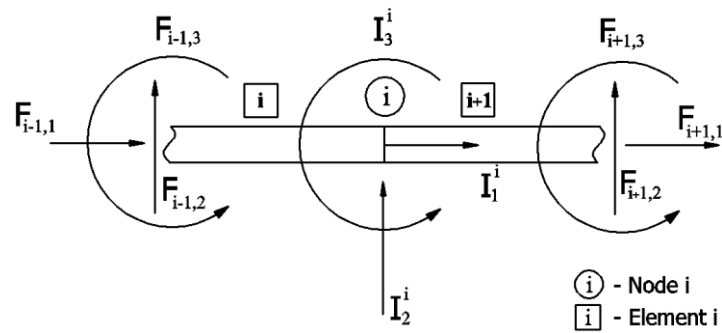


Figure 7.2. Free Body Diagram of Node  $i$  Considering Axial, Shear Forces, and Bending Moment

For this case, the external applied loads are all zeros, thus Eq. 7.1 can be written as,

$$\{I^i\} + \{F_i\} + \{F_{i+1}\} = \{0\} \quad (7.3)$$

Given any velocity vectors,  $\{\dot{\Delta}^i\}$ , the power done by the external forces can be expressed as following,

$$\{\dot{\Delta}^i\}^T \{I^i\} + \{\dot{\Delta}^i\}^T \{F_i\} + \{\dot{\Delta}^i\}^T \{F_{i+1}\} = \{\dot{\Delta}^i\}^T \{P^i\} = \{0\} \quad (7.4)$$

Rearrange Eq. 7.4 yields,

$$\{\dot{\Delta}^i\}^T \{F_i\} + \{\dot{\Delta}^i\}^T \{F_{i+1}\} = -\{\dot{\Delta}^i\}^T \{I^i\} \quad (7.5)$$

In this case, the inertial forces for the undamaged system can be expressed using the following lumped mass matrix, (note that the inertial effect associated with any rotational degree of freedom is neglected)

$$\{I^i\} = \left[ \left( \frac{\bar{m}_i L_i}{2} \right) + \left( \frac{\bar{m}_{i+1} L_{i+1}}{2} \right) \right] \begin{bmatrix} 1 & & \\ & 1 & \\ & & 0 \end{bmatrix}_i \begin{Bmatrix} \ddot{\delta}_1^i \\ \ddot{\delta}_2^i \\ \ddot{\delta}_3^i \end{Bmatrix} = m^i [M_o^i] \{\ddot{\delta}^i\} \quad (7.6)$$

Where  $\bar{m}_i$  is the linear mass of Element  $i$ ;  $\ddot{\delta}_1^i$  is the acceleration in axial direction at Node  $i$ ;  $\ddot{\delta}_2^i$  is the acceleration in transverse direction at Node  $i$  and  $\ddot{\delta}_3^i$  is the acceleration in bending rotation direction within the plain at Node  $i$ .

The force vectors (i.e.  $\{F_i\}$  and  $\{F_{i+1}\}$ ) in Eq. 7.5 can be computed using stiffness matrices and node deformation vectors,



$$\{F_i\} = [K_i] \{\delta_i\} = \left( \frac{EI}{L^3} \right)_i \begin{bmatrix} -\frac{AL^2}{I} & 0 & 0 & \frac{AL^2}{I} & 0 & 0 \\ 0 & -12 & -6L & 0 & 12 & -6L \\ 0 & 6L & 2L^2 & 0 & -6L & 4L^2 \end{bmatrix}_i \begin{Bmatrix} \delta_{i,1}^- \\ \delta_{i,2}^- \\ \delta_{i,3}^- \\ \delta_{i,1}^+ \\ \delta_{i,2}^+ \\ \delta_{i,3}^+ \end{Bmatrix} \quad (7.7)$$

$$= k_i [K_{o,i}] \{\delta_i\}$$

$$\{F_{i+1}\} = [K_{i+1}] \{\delta_{i+1}\} = \left( \frac{EI}{L^3} \right)_{i+1} \begin{bmatrix} \frac{AL^2}{I} & 0 & 0 & -\frac{AL^2}{I} & 0 & 0 \\ 0 & 12 & 6L & 0 & -12 & 6L \\ 0 & 6L & 4L^2 & 0 & -6L & 2L^2 \end{bmatrix}_{i+1} \begin{Bmatrix} \delta_{i+1,1}^- \\ \delta_{i+1,2}^- \\ \delta_{i+1,3}^- \\ \delta_{i+1,1}^+ \\ \delta_{i+1,2}^+ \\ \delta_{i+1,3}^+ \end{Bmatrix}$$

$$= k_{i+1} [K_{o,i+1}] \{\delta_{i+1}\}$$

(7.8)

Where  $\delta_{i,1}^+$  and  $\delta_{i,1}^-$  are the displacement in axial direction at the positive and negative ends of Element  $i$ , respectively;  $\delta_{i,2}^+$  and  $\delta_{i,2}^-$  are the displacement in transverse direction at the positive and negative ends of Element  $i$ , respectively;  $\delta_{i,3}^+$  and  $\delta_{i,3}^-$  are the node rotations in bending rotation direction at the positive and negative ends of Element  $i$ , respectively.

Substitute Eqs. 7.6 through 7.8 into Eq. 7.5 yields,

$$\{\dot{\Delta}^i\}^T k_i [K_{o,i}] \{\delta_i\} + \{\dot{\Delta}^i\}^T k_{i+1} [K_{o,i+1}] \{\delta_{i+1}\} = -\{\dot{\Delta}^i\}^T m^i [M_o^i] \{\ddot{\delta}^i\} \quad (7.9)$$

Moving forward the property constant from each term in Eq. 7.9 yields,

$$k_i \{\dot{\Delta}^i\}^T [K_{o,i}] \{\delta_i\} + k_{i+1} \{\dot{\Delta}^i\}^T [K_{o,i+1}] \{\delta_{i+1}\} = -m^i \{\dot{\Delta}^i\}^T [M_o^i] \{\ddot{\delta}^i\} \quad (7.10)$$

Dividing each term in Eq. 7.10 by  $m^i$  yields,

$$\frac{k_i}{m^i} \{\dot{\Delta}^i\}^T [K_{o,i}] \{\delta_i\} + \frac{k_{i+1}}{m^i} \{\dot{\Delta}^i\}^T [K_{o,i+1}] \{\delta_{i+1}\} = -\{\dot{\Delta}^i\}^T [M_o^i] \{\ddot{\delta}^i\} \quad (7.11)$$

Define the following coefficients,

$$\beta_1 = \frac{k_i}{m^i} \quad (7.12)$$

$$\beta_2 = \frac{k_{i+1}}{m^i} \quad (7.13)$$

Substituting Eq. 7.12 and Eq. 7.13 to Eq. 7.11 yields,

$$\beta_1 \{\dot{\Delta}^i\}^T [K_{o,i}] \{\delta_i\} + \beta_2 \{\dot{\Delta}^i\}^T [K_{o,i+1}] \{\delta_{i+1}\} = -\{\dot{\Delta}^i\}^T [M_o^i] \{\ddot{\delta}^i\} \quad (7.14)$$

Writing the Eq. 7.14 at different time point, yields the following groups of equations,

For  $t = t_0$ ,

$$\beta_1 (\{\dot{\Delta}^i\}^T [K_{o,i}] \{\delta_i\})|_{t_0} + \beta_2 (\{\dot{\Delta}^i\}^T [K_{o,i+1}] \{\delta_{i+1}\})|_{t_0} = -(\{\dot{\Delta}^i\}^T [M_o^i] \{\ddot{\delta}^i\})|_{t_0} \quad (7.15)$$

For  $t = t_j$ ,

$$\beta_1 (\{\dot{\Delta}^i\}^T [K_{o,i}] \{\delta_i\})|_{t_j} + \beta_2 (\{\dot{\Delta}^i\}^T [K_{o,i+1}] \{\delta_{i+1}\})|_{t_j} = -(\{\dot{\Delta}^i\}^T [M_o^i] \{\ddot{\delta}^i\})|_{t_j} \quad (7.16)$$

For  $t = t_N$ ,

$$\beta_1(\{\dot{\Delta}^i\}^T[K_{o,i}]\{\delta_i\})|_{t_N} + \beta_2(\{\dot{\Delta}^i\}^T[K_{o,i+1}]\{\delta_{i+1}\})|_{t_N} = -(\{\dot{\Delta}^i\}^T[M_o^i]\{\ddot{\delta}^i\})|_{t_N} \quad (7.17)$$

Arranging the above linear equation group into matrix form, yields,

$$\mathbf{X}\boldsymbol{\beta} = \mathbf{Y} \quad (7.18)$$

Where the coefficient matrix of the linear equation group is given as following (note, due to the limitation of the page size, the transposed form of the matrix is provided),

$$\mathbf{X} = \begin{bmatrix} (\{\dot{\Delta}^i\}^T[K_{o,i}]\{\delta_i\})|_{t_0} & (\{\dot{\Delta}^i\}^T[K_{o,i+1}]\{\delta_{i+1}\})|_{t_0} \\ \vdots & \vdots \\ (\{\dot{\Delta}^i\}^T[K_{o,i}]\{\delta_i\})|_{t_j} & (\{\dot{\Delta}^i\}^T[K_{o,i+1}]\{\delta_{i+1}\})|_{t_j} \\ \vdots & \vdots \\ (\{\dot{\Delta}^i\}^T[K_{o,i}]\{\delta_i\})|_{t_N} & (\{\dot{\Delta}^i\}^T[K_{o,i+1}]\{\delta_{i+1}\})|_{t_N} \end{bmatrix} \quad (7.19)$$

The vector of unknown and the vector of known are given as,

$$\boldsymbol{\beta} = \begin{Bmatrix} \beta_1 \\ \beta_2 \end{Bmatrix} \quad (7.20)$$

$$\mathbf{Y} = \begin{Bmatrix} -(\{\dot{\Delta}^i\}^T[M_o^i]\{\ddot{\delta}^i\})|_{t_0} \\ \vdots \\ -(\{\dot{\Delta}^i\}^T[M_o^i]\{\ddot{\delta}^i\})|_{t_j} \\ \vdots \\ -(\{\dot{\Delta}^i\}^T[M_o^i]\{\ddot{\delta}^i\})|_{t_N} \end{Bmatrix} \quad (7.21)$$

Using the Least Square Method, the vector of unknown, ' $\boldsymbol{\beta}$ ', can be computed from the following equation,

$$\boldsymbol{\beta} = (\mathbf{X}^T \mathbf{X})^{-1} (\mathbf{X}^T \mathbf{Y}) \quad (7.22)$$

With the vector of unknown computed, the damage indices for stiffness can be computed as follows,

$$\beta_k = \frac{\frac{k_i}{m^i}}{\frac{k_{i+1}}{m^i}} = \frac{k_i}{k_{i+1}} = \frac{\left(\frac{EI}{L^3}\right)_i}{\left(\frac{EI}{L^3}\right)_{i+1}} = \frac{\beta_{1,system i}}{\beta_{2,system i}} \quad (7.23)$$

$$\beta_m = \frac{\frac{m^i}{m^{i+1}}}{\frac{k_{i+1}}{m^i}} = \frac{\frac{k_{i+1}}{m^{i+1}}}{\frac{k_{i+1}}{m^i}} = \frac{\beta_{1,system i+1}}{\beta_{2,system i}} \quad (7.24)$$

### 7.2.3 Damage Evaluation for Cantilever with External Load at Free End Only

In this subsection, a cantilever beam is used to evaluate the performance of the proposed theory in dealing with nodes without external loads. The geometry of the cantilever and damage scenario under consideration are indicated Figure 7.3. The geometry of the cross-section of the beam is shown in Figure 5.19. The modulus of elasticity ( $E$ ) of the material is 29,000 ksi. The mass density of the material is  $7.345 \times 10^{-7}$  kip·sec<sup>2</sup>/in<sup>4</sup>.

The cantilever beam is meshed into 6 elements and has 7 equally spaced nodes. The length of each element is 12.0 inches. For illustrative purposes, typical elements are indicated in Figure 7.3. Two elements with damaged mass and stiffness are studied. The damage is simulated by a ten percent (10%) reduction of the modulus of elasticity and twenty percent (20%) reduction of the mass of the second (2<sup>nd</sup>) and fifth (5<sup>th</sup>) elements on the beam.

Only the node at the free end of the cantilever is excited by external nodal load, which is

simulated using a white noise,  $100 \times \text{random}(-1,1)$  and is applied in axial direction. This external nodal load is plotted in Figure 7.4. Given the external load case, exact accelerations, velocities and displacements of the six nodes were computed at every  $1\text{E-}4$  seconds (10,000 Hz) for 0.2 seconds.

In this case, the computed velocity ( $\dot{x}(t)$ ) of each node in the undamaged case was used as the velocity used to compute power ( $\dot{\Delta}$ ) for both the undamaged and damaged cases. For every two nearby elements, the coefficient matrices ('X') and known vector ('Y') were constructed by substituting the acceleration ( $\ddot{x}(t)$ ), velocity ( $\dot{x}(t)$ ), displacement ( $x(t)$ ), and velocity used to compute power ( $\dot{\Delta}$ ) into Eq. 7.19 and Eq. 7.21. The coefficient damage index vector,  $\beta$ , related to the two nearby elements was computed using Eq. 7.22. Then the damage indices for Element stiffness and Nodal mass are computed using Eq. 7.23 and Eq. 7.24, respectively. The damage severities for stiffness are computed using Eq. 2.13.

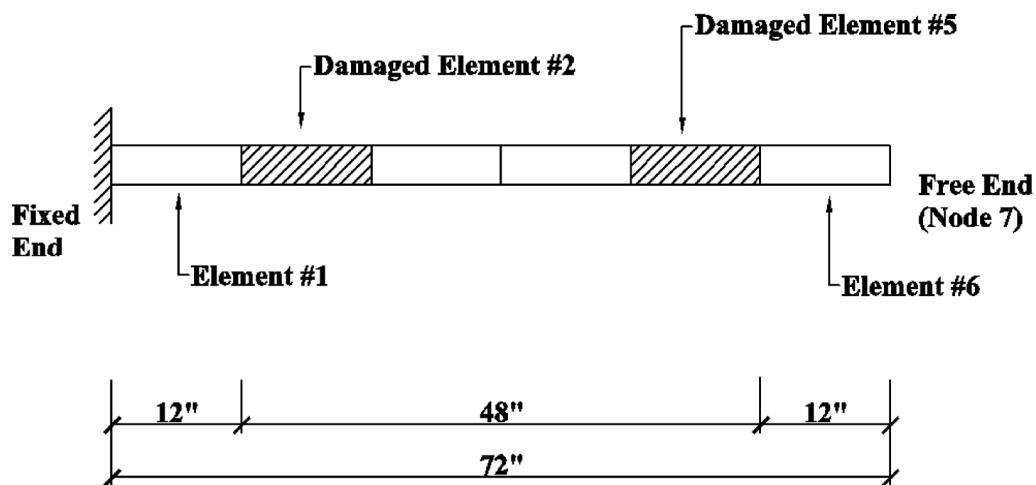
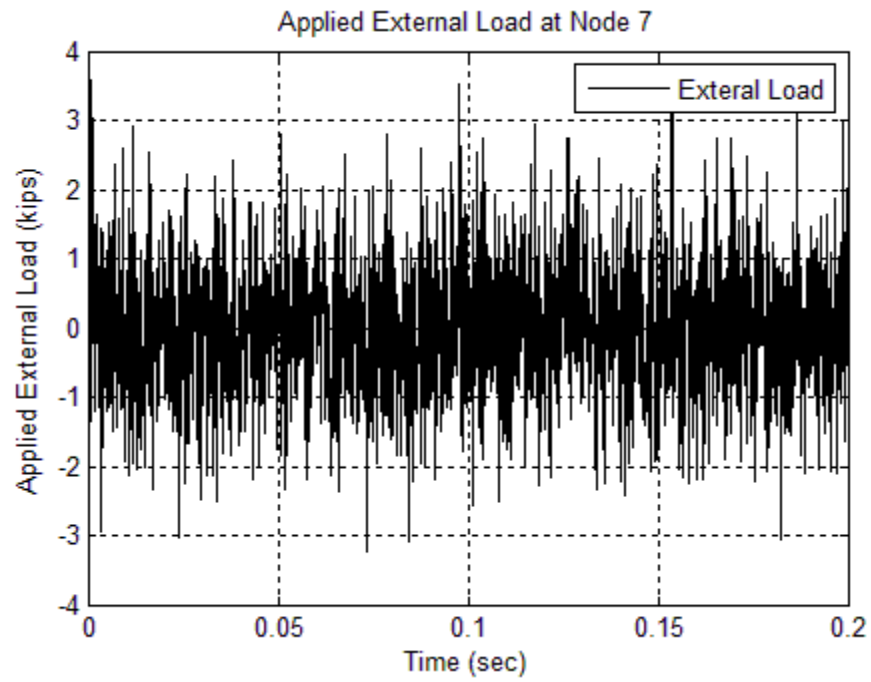
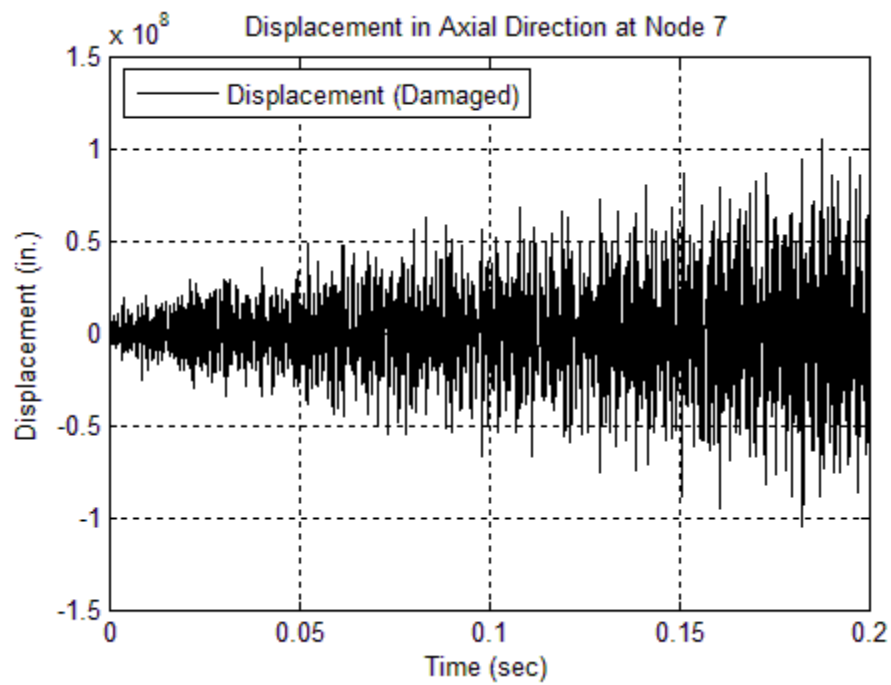


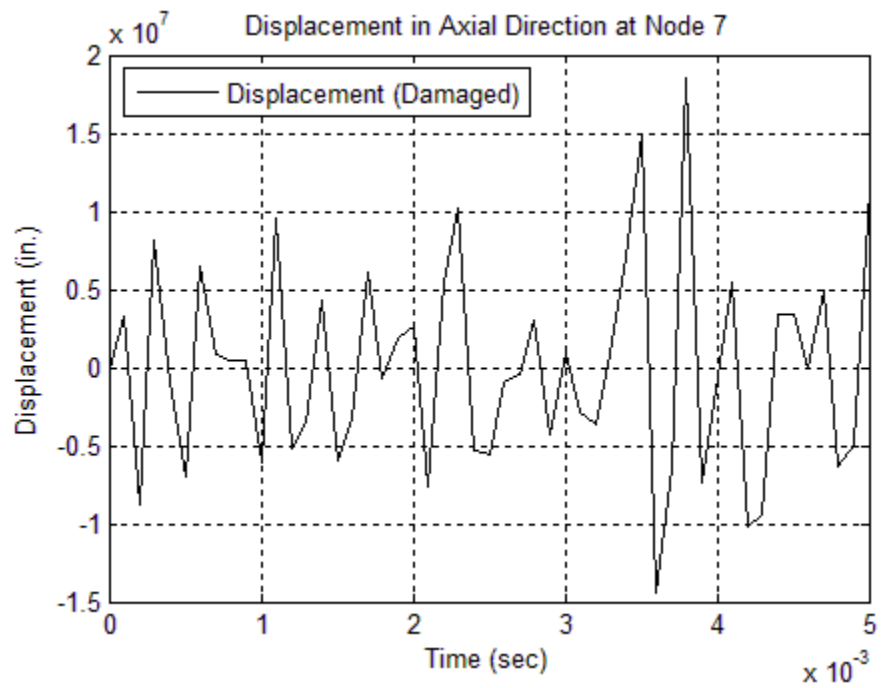
Figure 7.3. Geometry and Damage Scenario for the Cantilever Beam



**Figure 7.4. Applied External Load at the Free End of the Cantilever**

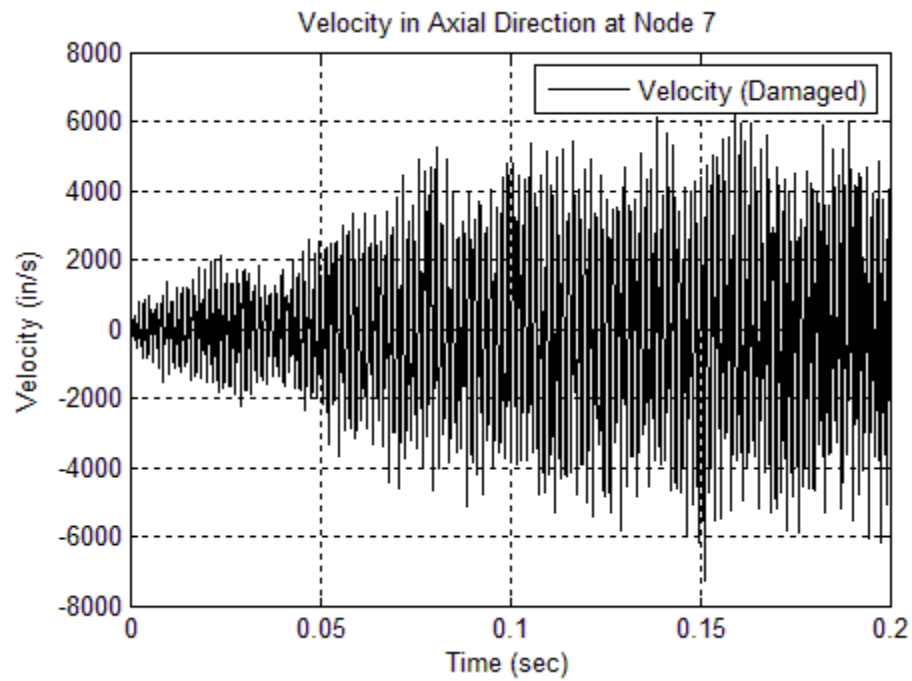


(a)

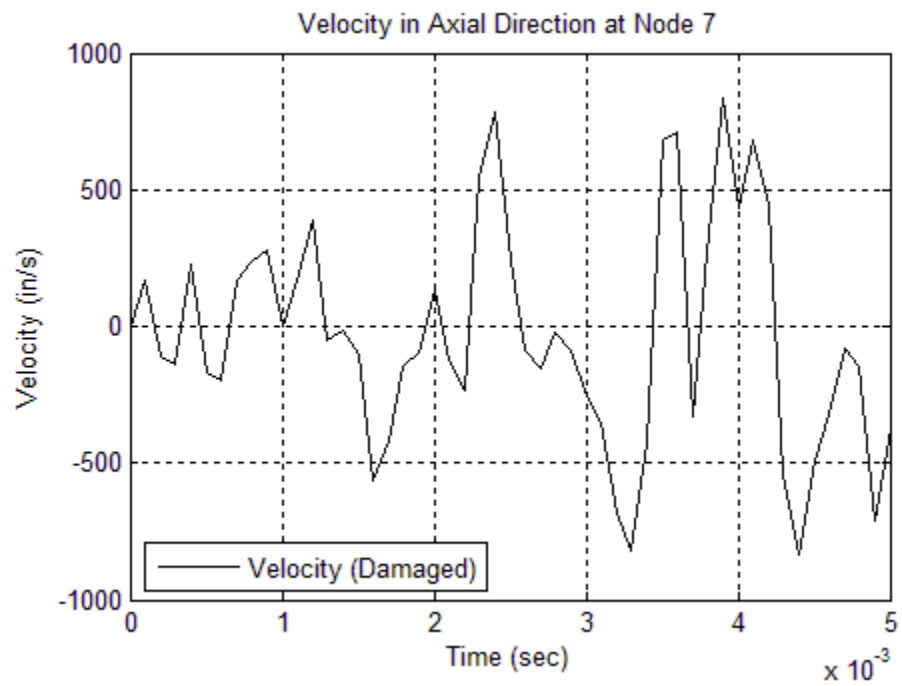


(b)

**Figure 7.5. Displacements in Axial Direction of Node 7 of the Cantilever under the Given External Load: (a) Full Plot and (b) Zoomed in Plot**



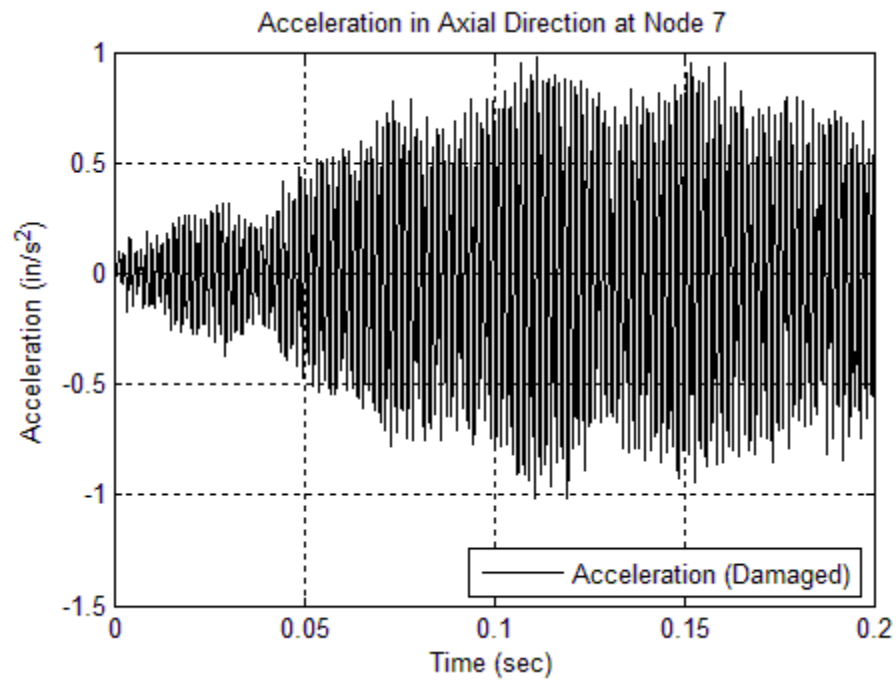
(a)



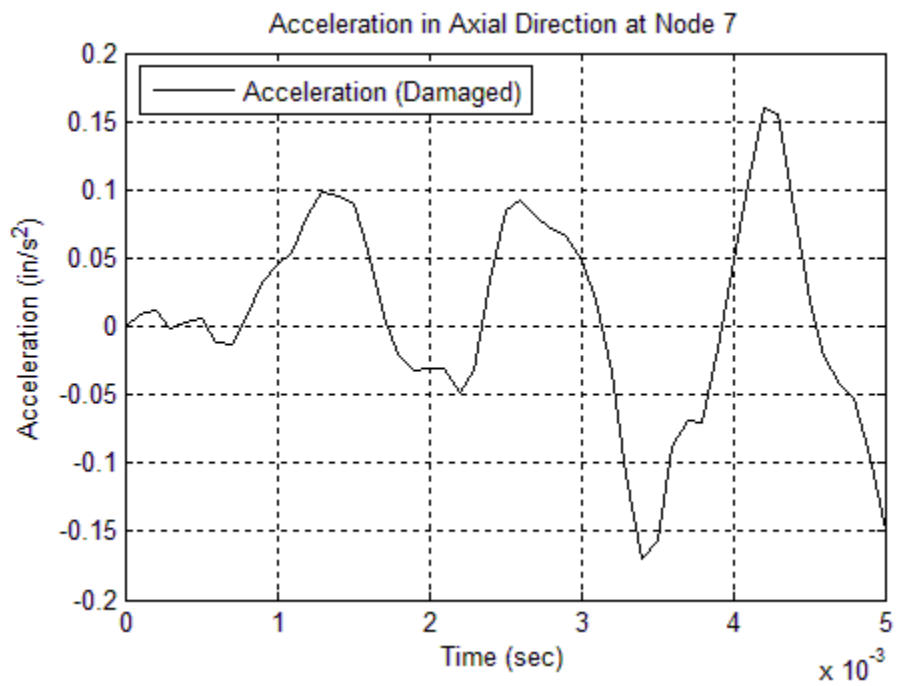
(b)

**Figure 7.6. Velocities in Axial Direction of the Node 7 of the Cantilever under the Given External Load: (a) Full Plot and (b) Zoomed in Plot**





(a)



(b)

**Figure 7.7. Accelerations in Axial Direction of Node 7 of the Cantilever under the Given External Load: (a) Full Plot and (b) Zoomed in Plot**

**Table 7.1. Damage Detection Results for the Cantilever under Axial Vibrations**

Property Comparison	Damage Index ( $\beta_i$ , Estimated)	Damage Severity ( $\alpha_i$ , Estimated)	Damage Index ( $\beta_i$ , Designed)
$k_1 \backslash k_2$	1.11	-0.10	1.11
$k_2 \backslash k_3$	0.90	0.11	0.90
$k_3 \backslash k_4$	1.00	0.00	1.00
$k_4 \backslash k_5$	1.11	-0.10	1.11
$k_5 \backslash k_6$	0.90	0.11	0.90
$m_1 \backslash m_2$	1.00	0.00	1.00
$m_2 \backslash m_3$	0.90	0.11	0.90
$m_3 \backslash m_4$	1.11	-0.10	1.11
$m_4 \backslash m_5$	1.00	0.00	1.00

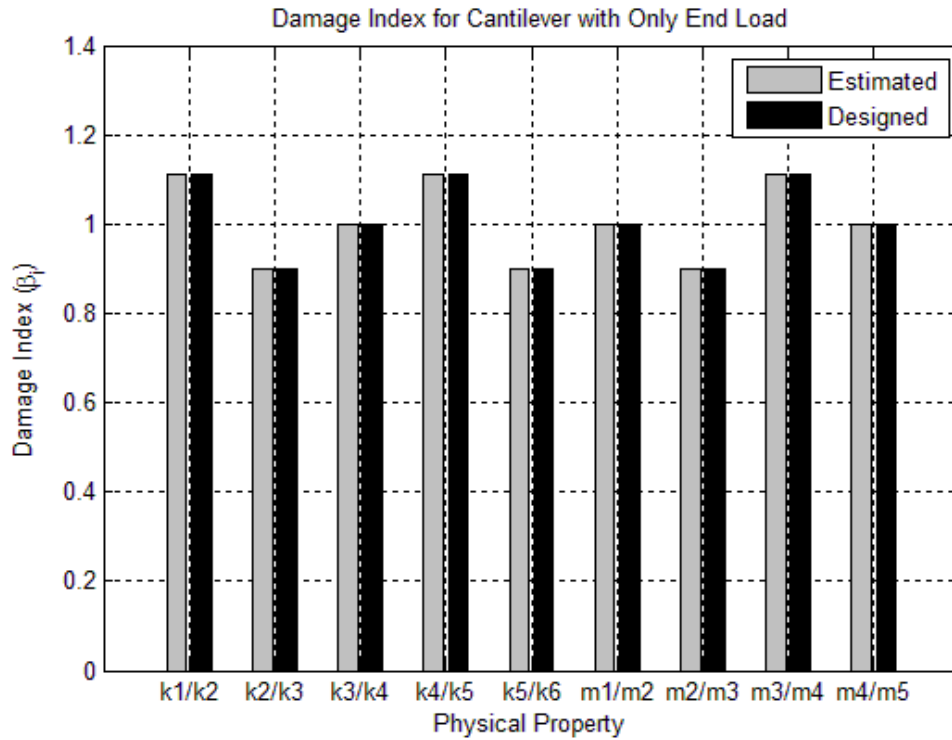


**Figure 7.8. Damage Indices ( $\beta_i$ ) for the Fixed-Fixed Beam with Proportional Damping Using Isolated Beam Element Analysis Method**

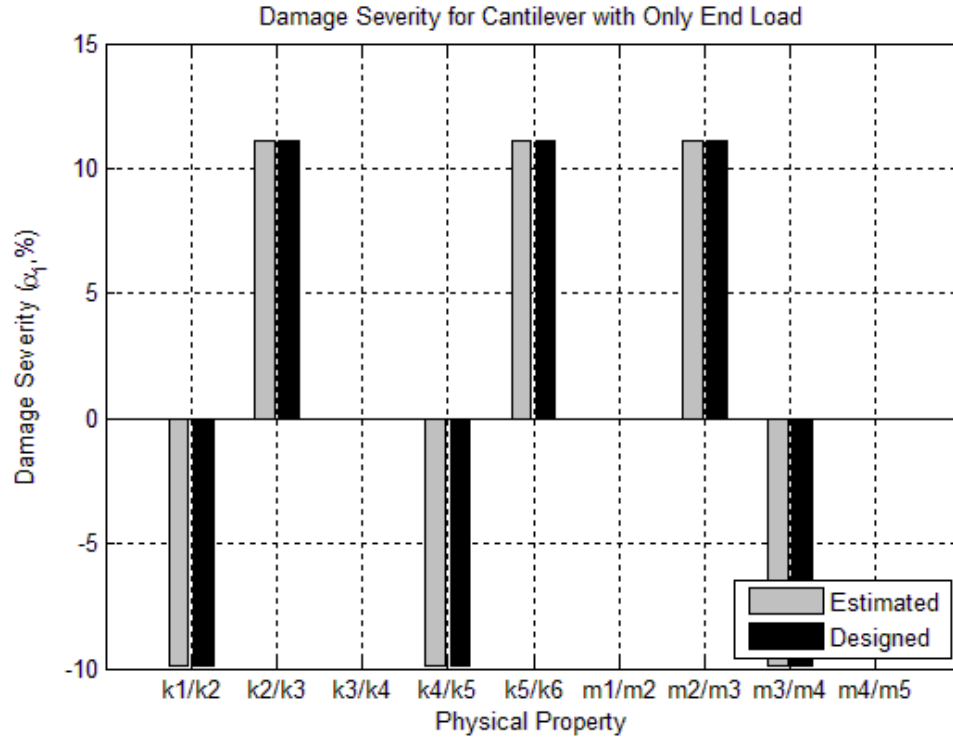


**Figure 7.9. Damage Severities ( $\alpha_i$ ) for the Fixed-Fixed Beam with Proportional Damping Using Isolated Beam Element Analysis Method**

#### 7.2.4 Summary

In Subsection 7.2, the Power Method for nodes without external loads is derived and numerically validated. The displacements, velocities and accelerations used in the Section 7 are the exact data without noise. From the damage detection results, shown in Table 7.1, Figure 7.8, and Figure 7.9, the designed damage in masses and stiffness were located and evaluated accurately. Moreover, for all numerical experiments, neither false-positive damage index nor false-negative damage index were found.

## **7.3 STUDY OF EFFICIENCY OF NOISE-INFLUENCE REDUCTION BY REPEATING THE EXPERIMENT (CASE #7.2)**

### **7.3.1 Introduction**

In this subsection, the efficiency of noise-influence reduction will be studied. According to the damage detection results in Section 6, when the acceleration inputs are contaminated by noise signals, the estimations of the damage severities will become less reliable, which, for example, can be seen in Figure 6.15 and Figure 6.18. For repeatable experiments, the noise influence can be reduced by repeating experiments and the white noise signals can be reduced by averaging white noises.

There are mainly two ways to reduce white noise influence:

- (1) Compute damage indices based on each experimental measurement and then compute the average of the damage indices; and
- (2) Compute the average inputs from the combination of all the measurements and compute the damage indices based on the average inputs.

### **7.3.2 Efficiency Study of Noise-Influence Reduction Based on Averaged Damage Detection Results**

In this subsection, the efficiency of noise-influence reduction based on averaged damage detection results will be studied using the 5-DOF spring-mass-damper system introduced in Case #6.2 in Section 6.2.2.

The inputs will be simulated by the exact accelerations of the mass blocks directly outputted from SAP2000 were contaminated by 5% of white noise. For illustration purposes, the noise-polluted accelerations of Mass Block #2 in both the undamaged and

damaged cases can be seen in Figure 6.11. The filtered accelerations, estimated velocities and estimated displacements of Mass Block #2 are can be seen from Figure 6.12, Figure 6.13, and Figure 6.14, respectively.

For illustration purposes, the vibration test for the 5-DOF spring-mass-damper system was assumed to be conducted ten times. The computed damage indices based on each vibration test, the averaged damage indices and the designed damage indices are listed in Table 7.2. The averaged damage indices and the designed damage indices are plotted in Figure 7.10. The related damage severities are plotted in Figure 7.11. The normalized damage indices are computed using Eq. 6.4 and are plotted in Figure 7.12. The damage possibility indices are plotted in Figure 7.13. Comparing the averaged damage indices with the designed damage indices, the accuracy of the damage indices are not obviously improved.

**Table 7.2. Summary of Damage Detection Results for the 5-DOF Spring-Mass-Damper System (5% Noise Pollution, Ten Tests)**

Property	Damage Index ( $\beta_i$ , Estimated)											Damage Index ( $\beta_i$ , Designed)
	Test #1	Test #2	Test #3	Test #4	Test #5	Test #6	Test #7	Test #8	Test #9	Test #10	Averaged	
$m_1$	1.27	1.27	1.27	1.29	1.29	1.27	1.27	1.28	1.29	1.28	1.28	1.25
$m_2$	1.09	1.05	1.08	1.07	1.10	1.05	1.09	1.08	1.09	1.08	1.08	1.11
$m_3$	0.99	0.94	1.00	0.97	0.99	0.95	0.97	1.00	0.99	0.98	0.98	1.00
$m_4$	0.99	0.97	1.00	0.99	1.00	0.99	1.01	1.00	0.99	0.99	0.99	1.00
$m_5$	1.00	0.99	1.00	1.00	1.01	0.98	0.99	0.98	1.00	0.97	0.99	1.00
$c_1$	1.32	1.24	1.40	1.35	1.28	1.57	1.56	1.27	1.35	1.36	1.37	2.00
$c_2$	1.63	1.67	1.62	1.64	1.58	1.49	1.54	1.72	1.66	1.64	1.62	2.00
$c_3$	0.97	0.97	0.94	0.88	0.98	0.94	0.94	0.87	0.97	0.91	0.94	1.00
$c_4$	0.94	0.80	0.62	0.85	0.95	0.99	0.90	1.05	0.61	0.91	0.86	1.00
$c_5$	0.87	0.34	0.77	0.27	0.95	0.75	0.89	0.94	0.68	0.93	0.74	1.00
$c_6$	1.05	1.14	1.19	1.13	0.88	1.29	1.13	1.03	1.15	1.25	1.12	1.00
$k_1$	1.14	1.15	1.15	1.16	1.17	1.16	1.16	1.15	1.17	1.16	1.16	1.11
$k_2$	1.11	1.06	1.09	1.10	1.10	1.07	1.09	1.10	1.11	1.10	1.09	1.11
$k_3$	1.01	0.96	1.00	0.99	0.99	0.96	0.98	1.00	1.00	1.00	0.99	1.00
$k_4$	1.01	0.98	1.01	1.01	1.02	0.98	1.02	1.01	1.04	0.98	1.00	1.00
$k_5$	1.04	1.01	1.03	1.05	1.04	0.97	0.99	0.98	1.04	0.96	1.01	1.00
$k_6$	0.99	0.98	0.98	0.99	1.00	0.98	0.98	0.96	0.96	0.99	0.98	1.00

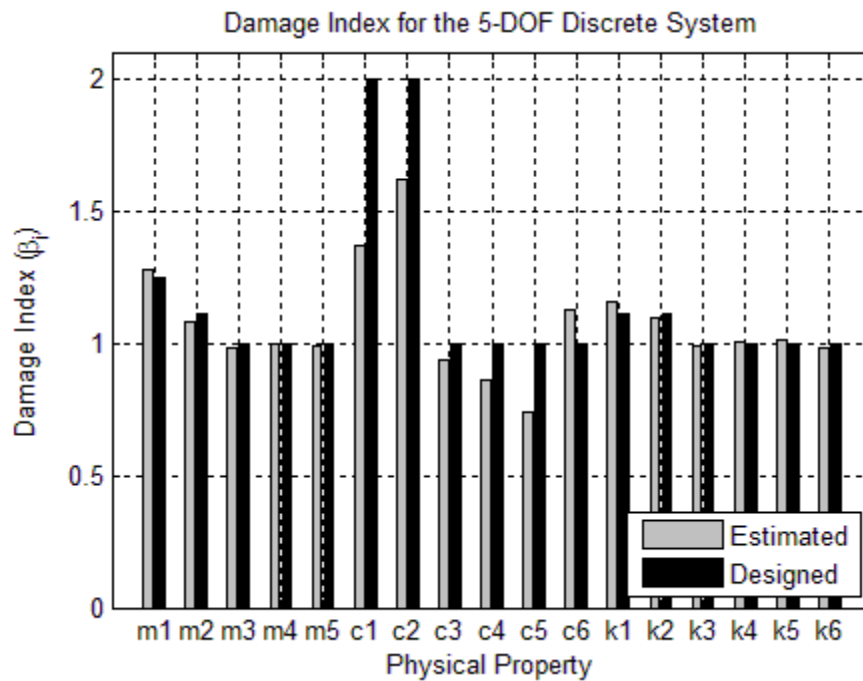


Figure 7.10. Averaged Damage Indices ( $\beta_i$ ) for 5-DOF Spring-Mass-Damper System with Noise-Polluted Accelerations (5% Noise, Ten Tests)

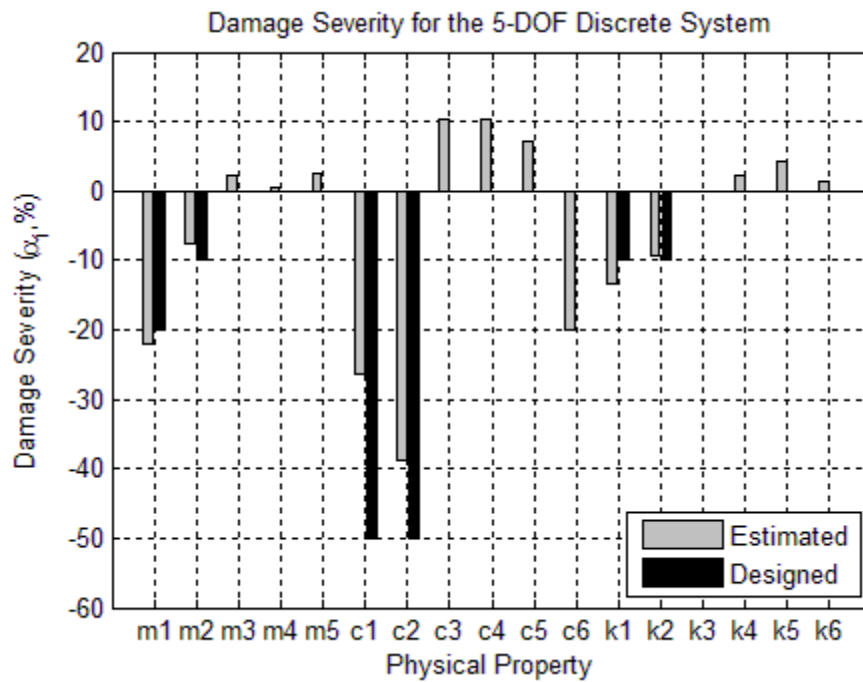


Figure 7.11. Averaged Damage Severities ( $\alpha_i$ ) for 5-DOF Spring-Mass-Damper System with Noise-Polluted Accelerations (5% Noise, Ten Tests)

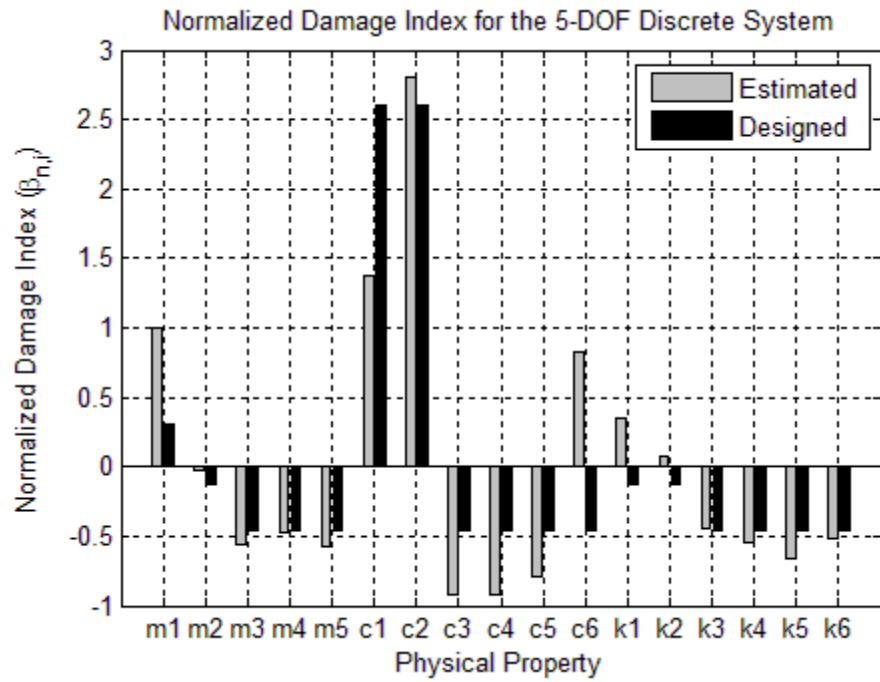


Figure 7.12. Normalized Averaged Damage Indices ( $\beta_{n,i}$ ) for 5-DOF Spring-Mass-Damper System with Noise-Polluted Accelerations (5% Noise, Ten Tests)

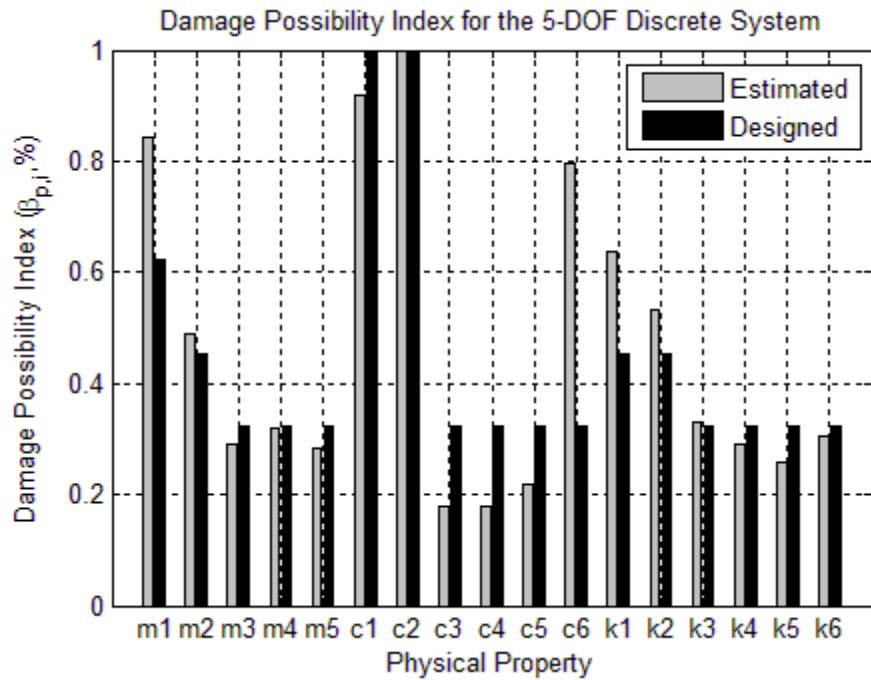


Figure 7.13. Probability Damage Indices ( $\beta_{p,i}$ ) for 5-DOF Spring-Mass-Damper System with Noise-Polluted Accelerations (5% Noise, Ten Tests)



### **7.3.3 Efficiency Study of Noise-Influence Reduction Based on Averaged Inputs**

In this subsection, the efficiency of noise-influence reduction based on averaged damage detection results will be studied using the 5-DOF spring-mass-damper system introduced in Case #6.2 in Section 6.2.2.

As introduced in the previous subsection, the numerical experiment will be simulated ten times. Before input each noise-polluted signals into the program, the ten groups of noise-polluted signals will be combined and averaged. The inputs for the program will be the averaged noise-polluted signals from the ten numerical experiments.

The estimated damage indices based on the averaged inputting signals and the designed damage indices for each physical property are listed in Table 7.3 and are plotted in Figure 7.14 and the related damage severities are plotted in Figure 7.15. The normalized damage indices are computed using Eq. 6.4 and are plotted in Figure 7.16. The damage possibility indices are plotted in Figure 7.17. Comparing the estimated damage indices with the designed damage indices, the accuracy of the damage indices has been obviously improved.

**Table 7.3. Damage Detection Results for the 5-DOF Spring-Mass-Damper System Based on Averaged Inputs (5% Noise Pollution, Ten Tests)**

<b>Property</b>	<b>Damage Index (<math>\beta_i</math>, Esimated)</b>	<b>Damage Severity (<math>\alpha_i</math>, Esimated)</b>	<b>Damage Index (<math>\beta_i</math>, Designed)</b>
$m_1$	1.25	-0.20	1.25
$m_2$	1.11	-0.10	1.11
$m_3$	1.00	0.00	1.00
$m_4$	1.00	0.00	1.00
$m_5$	1.00	0.00	1.00
$c_1$	2.20	-0.54	2.00
$c_2$	1.88	-0.47	2.00
$c_3$	0.98	0.02	1.00
$c_4$	1.00	0.00	1.00
$c_5$	1.04	-0.04	1.00
$c_6$	0.99	0.01	1.00
$k_1$	1.12	-0.11	1.11
$k_2$	1.11	-0.10	1.11
$k_3$	0.99	0.01	1.00
$k_4$	1.00	0.00	1.00
$k_5$	1.01	-0.01	1.00
$k_6$	1.00	0.00	1.00

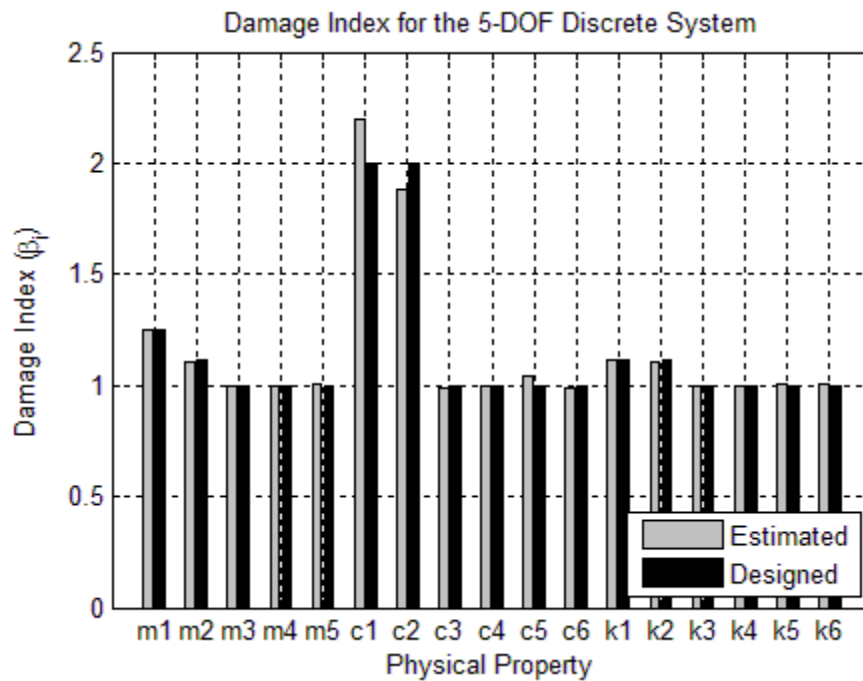


Figure 7.14. Damage Indices ( $\beta_i$ ) for 5-DOF Spring-Mass-Damper System with Averaged Noise-Polluted Accelerations (5% Noise, Ten Tests)

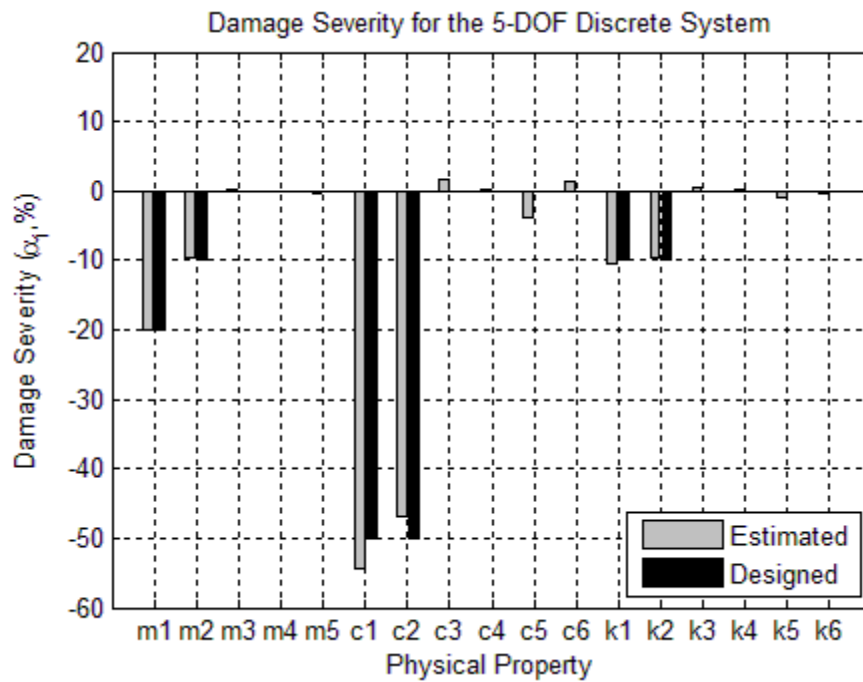


Figure 7.15. Damage Severities ( $\alpha_i$ ) for 5-DOF Spring-Mass-Damper System with Averaged Noise-Polluted Accelerations (5% Noise, Ten Tests)

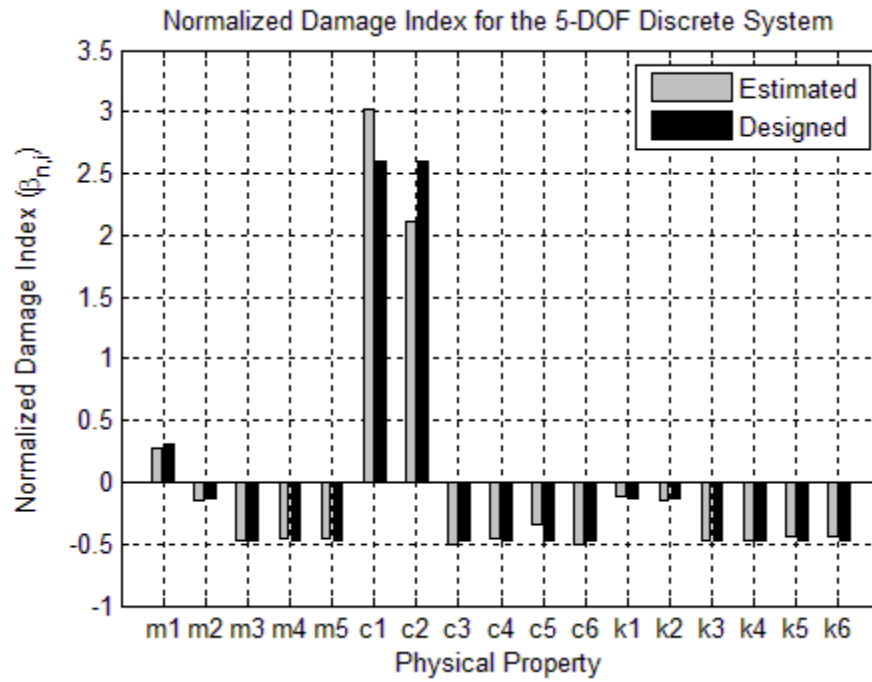


Figure 7.16. Normalized Damage Indices ( $\beta_{n,i}$ ) for 5-DOF Spring-Mass-Damper System with Averaged Noise-Polluted Accelerations (5% Noise, Ten Tests)

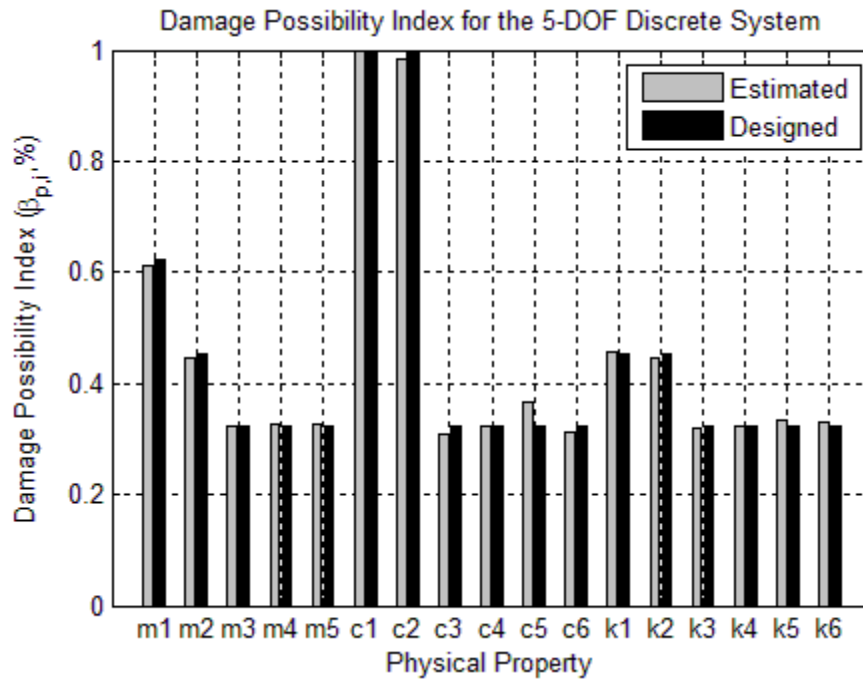


Figure 7.17. Probability Damage Indices ( $\beta_{p,i}$ ) for 5-DOF Spring-Mass-Damper System with Averaged Noise-Polluted Accelerations (5% Noise, Ten Tests)

#### **7.3.4 Summary**

In Subsection 7.3, ten numerical experiments with 5-DOF spring-mass-damper system were conducted. The noise polluted accelerations were simulated by mixing 5% white noise into the exact accelerations from each numerical experiment. The efficiency of noise-influence reduction of two methods was tested. According to the damage evaluation results, the method based on the averaged inputs had better performance.

### **7.4 STUDY OF DAMAGE DETECTION IN CONTINUOUS STRUCTURES WITH PROPORTIONAL DAMPING (CASE #7.3)**

#### **7.4.1 Introduction**

In this subsection, the damage detection in damped continuous structure will be studied. For simplicity purposes, the damping of the continuous structure will be modeled using Rayleigh Damping. In Subsection 7.4.2, the theory of Power Method for continuous structure with Rayleigh damping will be derived. In Subsection 7.4.3, the proposed theory will be validated using a fixed-fixed beam.

#### **7.4.2 Theory of Damage Detection in Continuous Structures with Proportional Damping**

The objective of this subsection is to complete the algorithms that are provided in Section 4, in which the damping damage detection in the continuous systems was not taken into consideration.

For completeness sake, both bending and axial motions will be considered in this case and the plain frame elements will be used. According to the finite element method, one frame structure can be meshed into several elements. From the free body diagram of Node  $i$ ,

shown in Figure 7.18, the dynamic equilibrium condition for Node  $i$  can be written as,

$$\{I^i\} + \{F_{s,i}\} + \{F_{s,i+1}\} + \{F_{c,i}\} + \{F_{c,i+1}\} = \{P^i\} \quad (7.25)$$

Where  $\{I^i\}$  is the inertial force vector at Node  $i$ ,  $\{F_{s,i}\}$  is the internal force from the positive end of Element  $i$  due to element stiffness;  $\{F_{c,i}\}$  is the internal force from the positive end of Element  $i$  due to element damping;  $\{P^i\}$  is the applied external load at Node  $i$ . Note that the positive end of Element  $i$  and the negative end of Element  $i+1$  share the same node.

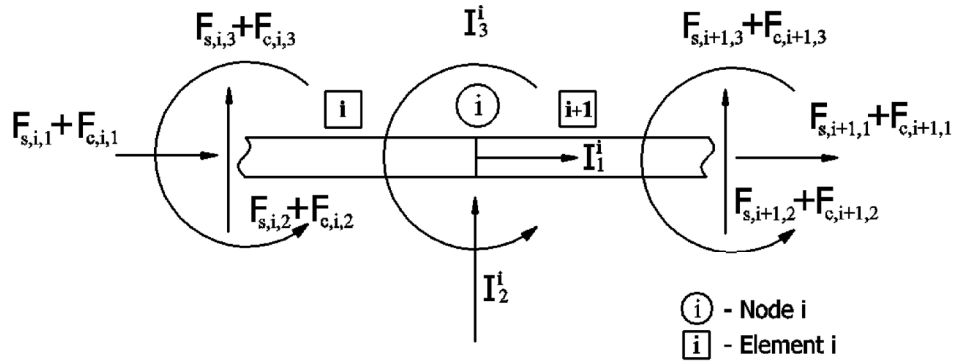


**Figure 7.18. Free Body Diagram of Node  $i$  Considering Axial, Shear Forces, and Bending Moment**

Similarly, for the damaged case, the dynamic equilibrium condition is,

$$\{I^{*i}\} + \{F_{s,i}^*\} + \{F_{s,i+1}^*\} + \{F_{c,i}^*\} + \{F_{c,i+1}^*\} = \{P^{*i}\} \quad (7.26)$$

Where the asterisk (“\*”) denotes the quantities from the damaged case.

Given any velocity vectors,  $\{\dot{\Delta}^i\}$  and  $\{\dot{\Delta}^{*i}\}$ , for the undamaged and damaged systems, the power performed by the external forces in the undamaged and damaged systems can be expressed as follows,

$$\{\dot{\Delta}^i\}^T \{I^i\} + \{\dot{\Delta}^i\}^T \{F_{s,i}\} + \{\dot{\Delta}^i\}^T \{F_{s,i+1}\} + \{\dot{\Delta}^i\}^T \{F_{c,i}\} + \{\dot{\Delta}^i\}^T \{F_{c,i+1}\} = \{\dot{\Delta}^i\}^T \{P^i\} \quad (7.27)$$

$$\{\dot{\Delta}^{*i}\}^T \{I^{*i}\} + \{\dot{\Delta}^{*i}\}^T \{F_{s,i}^*\} + \{\dot{\Delta}^{*i}\}^T \{F_{s,i+1}^*\} + \{\dot{\Delta}^{*i}\}^T \{F_{c,i}^*\} + \{\dot{\Delta}^{*i}\}^T \{F_{c,i+1}^*\} = \{\dot{\Delta}^{*i}\}^T \{P^{*i}\} \quad (7.28)$$

Assume that the applied external loads and the applied velocities used to compute power at Node  $i$  are the same for both the undamaged and damaged systems,

$$\{\dot{\Delta}^i\} = \{\dot{\Delta}^{*i}\} \quad (7.29)$$

$$\{P^i\} = \{P^{*i}\} \quad (7.30)$$

Substituting Eq. 7.29 and Eq. 7.30 into Eq. 7.28 yields,

$$\{\dot{\Delta}^{*i}\}^T \{I^{*i}\} + \{\dot{\Delta}^{*i}\}^T \{F_{s,i}^*\} + \{\dot{\Delta}^{*i}\}^T \{F_{s,i+1}^*\} + \{\dot{\Delta}^{*i}\}^T \{F_{c,i}^*\} + \{\dot{\Delta}^{*i}\}^T \{F_{c,i+1}^*\} = \{\dot{\Delta}^i\}^T \{P^i\} \quad (7.31)$$

Noticing the power done by the external load are the same for both the undamaged and damaged system. Substituting Eq.7.31 into Eq. 7.27 yields,

$$\begin{aligned} & \{\dot{\Delta}^i\}^T \{I^i\} + \{\dot{\Delta}^i\}^T \{F_{s,i}\} + \{\dot{\Delta}^i\}^T \{F_{s,i+1}\} + \{\dot{\Delta}^i\}^T \{F_{c,i}\} + \{\dot{\Delta}^i\}^T \{F_{c,i+1}\} \\ & = \{\dot{\Delta}^i\}^T \{I^{*i}\} + \{\dot{\Delta}^i\}^T \{F_{s,i}^*\} + \{\dot{\Delta}^i\}^T \{F_{s,i+1}^*\} + \{\dot{\Delta}^i\}^T \{F_{c,i}^*\} + \{\dot{\Delta}^i\}^T \{F_{c,i+1}^*\} \end{aligned} \quad (7.32)$$

Note, Eq. 7.32 is equivalent to Eq. 2.10.

In this case, the inertial forces for the undamaged system can be expressed using the following lumped mass matrix, (note that the inertial effect associated with any rotational degree of freedom is assumed can be neglected)

$$\{I^i\} = \left[ \left( \frac{\bar{m}_i L_i}{2} \right) + \left( \frac{\bar{m}_{i+1} L_{i+1}}{2} \right) \right] \begin{bmatrix} 1 & & \\ & 1 & \\ & & 0 \end{bmatrix}_i \begin{Bmatrix} \ddot{\delta}_1^i \\ \ddot{\delta}_2^i \\ \ddot{\delta}_3^i \end{Bmatrix} = m^i [M_o^i] \{\ddot{\delta}^i\} \quad (7.33)$$

Where  $\bar{m}_i$  is the linear mass of Element  $i$ ;  $\ddot{\delta}_1^i$  is the acceleration in axial direction at Node  $i$ ;  $\ddot{\delta}_2^i$  is the acceleration in transverse direction at Node  $i$  and  $\ddot{\delta}_3^i$  is the acceleration in bending rotation direction within the plain at Node  $i$ .

Similarly, for the damaged system,

$$\{I^{*i}\} = \left[ \left( \frac{\bar{m}_i^* L_i^*}{2} \right) + \left( \frac{\bar{m}_{i+1}^* L_{i+1}^*}{2} \right) \right] \begin{bmatrix} 1 & & \\ & 1 & \\ & & 0 \end{bmatrix}_i \begin{Bmatrix} \ddot{\delta}_1^{*i} \\ \ddot{\delta}_2^{*i} \\ \ddot{\delta}_3^{*i} \end{Bmatrix} = m^{*i} [M_o^{*i}] \{\ddot{\delta}^{*i}\} \quad (7.34)$$

The internal force vectors (i.e.  $\{F_{s,i}\}$ ,  $\{F_{s,i+1}\}$ ,  $\{F_{c,i}\}$ ,  $\{F_{c,i+1}\}$ ,  $\{F_{s,i}^*\}$ ,  $\{F_{s,i+1}^*\}$ ,  $\{F_{c,i}^*\}$ , and  $\{F_{c,i+1}^*\}$ ) in Eq. 7.32 can be computed as followings,



$$\begin{aligned}
\{F_{s,i}^+\} &= [K_i] \{\delta_i\} = \left( \frac{EI}{L^3} \right)_i \begin{bmatrix} -\frac{AL^2}{I} & 0 & 0 & \frac{AL^2}{I} & 0 & 0 \\ 0 & -12 & -6L & 0 & 12 & -6L \\ 0 & 6L & 2L^2 & 0 & -6L & 4L^2 \end{bmatrix}_i \begin{Bmatrix} \delta_{i,1}^- \\ \delta_{i,2}^- \\ \delta_{i,3}^- \\ \delta_{i,1}^+ \\ \delta_{i,2}^+ \\ \delta_{i,3}^+ \end{Bmatrix} \\
&= k_i [K_{o,i}] \{\delta_i\}
\end{aligned} \tag{7.35}$$

$$\begin{aligned}
\{F_{s,i+1}^-\} &= [K_{i+1}] \{\delta_{i+1}\} = \left( \frac{EI}{L^3} \right)_{i+1} \begin{bmatrix} \frac{AL^2}{I} & 0 & 0 & -\frac{AL^2}{I} & 0 & 0 \\ 0 & 12 & 6L & 0 & -12 & 6L \\ 0 & 6L & 4L^2 & 0 & -6L & 2L^2 \end{bmatrix}_{i+1} \begin{Bmatrix} \delta_{i+1,1}^- \\ \delta_{i+1,2}^- \\ \delta_{i+1,3}^- \\ \delta_{i+1,1}^+ \\ \delta_{i+1,2}^+ \\ \delta_{i+1,3}^+ \end{Bmatrix} \\
&= k_{i+1} [K_{o,i+1}] \{\delta_{i+1}\}
\end{aligned} \tag{7.36}$$

$$\begin{aligned}
\{F_{c,i}\} &= [C_i] \{\dot{\delta}_i\} = (a_{i,0}[M_i] + a_{i,1}[K_i]) \{\dot{\delta}_i\} = a_{i,0}[M_i] \{\dot{\delta}_i\} + a_{i,1}[K_i] \{\dot{\delta}_i\} \\
&= a_{i,0} \left( \frac{\overline{m}L}{2} \right)_i \begin{bmatrix} 0 & 0 & 0 & 1 & 0 & 0 \\ 0 & 0 & 0 & 0 & 1 & 0 \\ 0 & 0 & 0 & 0 & 0 & 0 \end{bmatrix}_i \begin{Bmatrix} \dot{\delta}_{i,1}^- \\ \dot{\delta}_{i,2}^- \\ \dot{\delta}_{i,3}^- \\ \dot{\delta}_{i,1}^+ \\ \dot{\delta}_{i,2}^+ \\ \dot{\delta}_{i,3}^+ \end{Bmatrix} \\
&\quad + a_{i,1} \left( \frac{EI}{L^3} \right)_i \begin{bmatrix} -\frac{AL^2}{I} & 0 & 0 & \frac{AL^2}{I} & 0 & 0 \\ 0 & -12 & -6L & 0 & 12 & -6L \\ 0 & 6L & 2L^2 & 0 & -6L & 4L^2 \end{bmatrix}_i \begin{Bmatrix} \dot{\delta}_{i,1}^- \\ \dot{\delta}_{i,2}^- \\ \dot{\delta}_{i,3}^- \\ \dot{\delta}_{i,1}^+ \\ \dot{\delta}_{i,2}^+ \\ \dot{\delta}_{i,3}^+ \end{Bmatrix} \\
&= a_{i,0} \left( \frac{\overline{m}L}{2} \right)_i \begin{bmatrix} 1 & 0 & 0 \\ 0 & 1 & 0 \\ 0 & 0 & 0 \end{bmatrix}_i \begin{Bmatrix} \dot{\delta}_{i,1}^+ \\ \dot{\delta}_{i,2}^+ \\ \dot{\delta}_{i,3}^+ \end{Bmatrix} \\
&\quad + a_{i,1} \left( \frac{EI}{L^3} \right)_i \begin{bmatrix} -\frac{AL^2}{I} & 0 & 0 & \frac{AL^2}{I} & 0 & 0 \\ 0 & -12 & -6L & 0 & 12 & -6L \\ 0 & 6L & 2L^2 & 0 & -6L & 4L^2 \end{bmatrix}_i \begin{Bmatrix} \dot{\delta}_{i,1}^- \\ \dot{\delta}_{i,2}^- \\ \dot{\delta}_{i,3}^- \\ \dot{\delta}_{i,1}^+ \\ \dot{\delta}_{i,2}^+ \\ \dot{\delta}_{i,3}^+ \end{Bmatrix} \\
&= a_{i,0} \frac{m_i}{2} [M_o^i] \{\dot{\delta}_i^+\} + a_{i,1} k_i [K_{o,i}] \{\dot{\delta}_i\}
\end{aligned}
\tag{7.37}$$

$$\begin{aligned}
\{F_{c,i+1}\} &= [C_{i+1}] \{\dot{\delta}_{i+1}\} = (a_{i+1,0}[M_{i+1}] + a_{i+1,1}[K_{i+1}]) \{\dot{\delta}_{i+1}\} = a_{i+1,0}[M_i] \{\dot{\delta}_i\} + a_{i+1,1}[K_i] \{\dot{\delta}_i\} \\
&= a_{i+1,0} \left( \frac{\bar{m}L}{2} \right)_{i+1} \left[ \begin{array}{cccccc} 1 & 0 & 0 & 0 & 0 & 0 \\ 0 & 1 & 0 & 0 & 0 & 0 \\ 0 & 0 & 0 & 0 & 0 & 0 \end{array} \right]_i \left\{ \begin{array}{c} \dot{\delta}_{i+1,1}^- \\ \dot{\delta}_{i+1,2}^- \\ \dot{\delta}_{i+1,3}^- \\ \dot{\delta}_{i+1,1}^+ \\ \dot{\delta}_{i+1,2}^+ \\ \dot{\delta}_{i+1,3}^+ \end{array} \right\} \\
&\quad + a_{i+1,1} \left( \frac{EI}{L^3} \right)_{i+1} \left[ \begin{array}{cccccc} \frac{AL^2}{I} & 0 & 0 & -\frac{AL^2}{I} & 0 & 0 \\ 0 & 12 & 6L & 0 & -12 & 6L \\ 0 & 6L & 4L^2 & 0 & -6L & 2L^2 \end{array} \right]_{i+1} \left\{ \begin{array}{c} \dot{\delta}_{i+1,1}^- \\ \dot{\delta}_{i+1,2}^- \\ \dot{\delta}_{i+1,3}^- \\ \dot{\delta}_{i+1,1}^+ \\ \dot{\delta}_{i+1,2}^+ \\ \dot{\delta}_{i+1,3}^+ \end{array} \right\} \\
&= a_{i+1,0} \left( \frac{\bar{m}L}{2} \right)_{i+1} \left[ \begin{array}{ccc} 1 & 0 & 0 \\ 0 & 1 & 0 \\ 0 & 0 & 0 \end{array} \right]_{i+1} \left\{ \begin{array}{c} \dot{\delta}_{i+1,1}^- \\ \dot{\delta}_{i+1,2}^- \\ \dot{\delta}_{i+1,3}^- \end{array} \right\} \\
&\quad + a_{i+1,1} \left( \frac{EI}{L^3} \right)_{i+1} \left[ \begin{array}{cccccc} \frac{AL^2}{I} & 0 & 0 & -\frac{AL^2}{I} & 0 & 0 \\ 0 & 12 & 6L & 0 & -12 & 6L \\ 0 & 6L & 4L^2 & 0 & -6L & 2L^2 \end{array} \right]_{i+1} \left\{ \begin{array}{c} \dot{\delta}_{i+1,1}^- \\ \dot{\delta}_{i+1,2}^- \\ \dot{\delta}_{i+1,3}^- \\ \dot{\delta}_{i+1,1}^+ \\ \dot{\delta}_{i+1,2}^+ \\ \dot{\delta}_{i+1,3}^+ \end{array} \right\} \\
&= a_{i+1,0} \frac{m_{i+1}}{2} [M_o^i] \{\dot{\delta}_{i+1}^-\} + a_{i+1,1} k_{i+1} [K_{o,i+1}] \{\dot{\delta}_{i+1}\}
\end{aligned} \tag{7.38}$$

For the damaged case,

$$\{F_{s,i}^*\} = \left(\frac{EI}{L^3}\right)_i^* \begin{bmatrix} -\frac{AL^2}{I} & 0 & 0 & \frac{AL^2}{I} & 0 & 0 \\ 0 & -12 & -6L & 0 & 12 & -6L \\ 0 & 6L & 2L^2 & 0 & -6L & 4L^2 \end{bmatrix}_i^* \begin{Bmatrix} \delta_{i,1}^{*-} \\ \delta_{i,2}^{*-} \\ \delta_{i,3}^{*-} \\ \delta_{i,1}^{*+} \\ \delta_{i,2}^{*+} \\ \delta_{i,3}^{*+} \end{Bmatrix} = k_i^* [K_{o,i}^*] \{\delta_i^*\} \quad (7.39)$$

$$\{F_{s,i+1}^*\} = \left(\frac{EI}{L^3}\right)_{i+1}^* \begin{bmatrix} \frac{AL^2}{I} & 0 & 0 & -\frac{AL^2}{I} & 0 & 0 \\ 0 & 12 & 6L & 0 & -12 & 6L \\ 0 & 6L & 4L^2 & 0 & -6L & 2L^2 \end{bmatrix}_{i+1}^* \begin{Bmatrix} \delta_{i+1,1}^{*-} \\ \delta_{i+1,2}^{*-} \\ \delta_{i+1,3}^{*-} \\ \delta_{i+1,1}^{*+} \\ \delta_{i+1,2}^{*+} \\ \delta_{i+1,3}^{*+} \end{Bmatrix} = k_{i+1}^* [K_{o,i+1}^*] \{\delta_{i+1}^*\} \quad (7.40)$$

$$\begin{aligned}
\{F_{c,i}^*\} &= [C_i^*] \{\dot{\delta}_i^*\} = (a_{i,0}^*[M_i^*] + a_{i,1}^*[K_i^*]) \{\dot{\delta}_i^*\} = a_{i,0}^*[M_i^*] \{\dot{\delta}_i^*\} + a_{i,1}^*[K_i^*] \{\dot{\delta}_i^*\} \\
&= a_{i,0}^* \left( \frac{\overline{m}L}{2} \right)_i^* \begin{bmatrix} 0 & 0 & 0 & 1 & 0 & 0 \\ 0 & 0 & 0 & 0 & 1 & 0 \\ 0 & 0 & 0 & 0 & 0 & 0 \end{bmatrix}_i \begin{Bmatrix} \dot{\delta}_{i,1}^{*-} \\ \dot{\delta}_{i,2}^{*-} \\ \dot{\delta}_{i,3}^{*-} \\ \dot{\delta}_{i,1}^{*+} \\ \dot{\delta}_{i,2}^{*+} \\ \dot{\delta}_{i,3}^{*+} \end{Bmatrix} \\
&\quad + a_{i,1}^* \left( \frac{EI}{L^3} \right)_i^* \begin{bmatrix} -\frac{AL^2}{I} & 0 & 0 & \frac{AL^2}{I} & 0 & 0 \\ 0 & -12 & -6L & 0 & 12 & -6L \\ 0 & 6L & 2L^2 & 0 & -6L & 4L^2 \end{bmatrix}_i \begin{Bmatrix} \dot{\delta}_{i,1}^{*-} \\ \dot{\delta}_{i,2}^{*-} \\ \dot{\delta}_{i,3}^{*-} \\ \dot{\delta}_{i,1}^{*+} \\ \dot{\delta}_{i,2}^{*+} \\ \dot{\delta}_{i,3}^{*+} \end{Bmatrix} \\
&= a_{i,0}^* \left( \frac{\overline{m}L}{2} \right)_i^* \begin{bmatrix} 1 & 0 & 0 \\ 0 & 1 & 0 \\ 0 & 0 & 0 \end{bmatrix}_i \begin{Bmatrix} \dot{\delta}_{i,1}^{*+} \\ \dot{\delta}_{i,2}^{*+} \\ \dot{\delta}_{i,3}^{*+} \end{Bmatrix} \\
&\quad + a_{i,1}^* \left( \frac{EI}{L^3} \right)_i^* \begin{bmatrix} -\frac{AL^2}{I} & 0 & 0 & \frac{AL^2}{I} & 0 & 0 \\ 0 & -12 & -6L & 0 & 12 & -6L \\ 0 & 6L & 2L^2 & 0 & -6L & 4L^2 \end{bmatrix}_i \begin{Bmatrix} \dot{\delta}_{i,1}^{*-} \\ \dot{\delta}_{i,2}^{*-} \\ \dot{\delta}_{i,3}^{*-} \\ \dot{\delta}_{i,1}^{*+} \\ \dot{\delta}_{i,2}^{*+} \\ \dot{\delta}_{i,3}^{*+} \end{Bmatrix} \\
&= a_{i,0}^* \frac{m_i^*}{2} [M_o^{*i}] \{\dot{\delta}_i^{*+}\} + a_{i,1}^* k_i^* [K_o^{*i}] \{\dot{\delta}_i^*\}
\end{aligned}
\tag{7.41}$$

$$\begin{aligned}
\{F_{c,i+1}^*\} &= [C_{i+1}^*] \{\dot{\delta}_{i+1}^*\} = (a_{i+1,0}^* [M_{i+1}^*] + a_{i+1,1}^* [K_{i+1}^*]) \{\dot{\delta}_{i+1}^*\} = a_{i+1,0}^* [M_i^*] \{\dot{\delta}_i^*\} + a_{i+1,1}^* [K_i^*] \{\dot{\delta}_i^*\} \\
&= a_{i+1,0}^* \left( \frac{\bar{m}L}{2} \right)_{i+1}^* \begin{bmatrix} 1 & 0 & 0 & 0 & 0 & 0 \\ 0 & 1 & 0 & 0 & 0 & 0 \\ 0 & 0 & 0 & 0 & 0 & 0 \end{bmatrix}_i \begin{Bmatrix} \dot{\delta}_{i+1,1}^{*-} \\ \dot{\delta}_{i+1,2}^{*-} \\ \dot{\delta}_{i+1,3}^{*-} \\ \dot{\delta}_{i+1,1}^{*+} \\ \dot{\delta}_{i+1,2}^{*+} \\ \dot{\delta}_{i+1,3}^{*+} \end{Bmatrix} \\
&\quad + a_{i+1,1}^* \left( \frac{EI}{L^3} \right)_{i+1}^* \begin{bmatrix} \frac{AL^2}{I} & 0 & 0 & -\frac{AL^2}{I} & 0 & 0 \\ 0 & 12 & 6L & 0 & -12 & 6L \\ 0 & 6L & 4L^2 & 0 & -6L & 2L^2 \end{bmatrix}_{i+1} \begin{Bmatrix} \dot{\delta}_{i+1,1}^{*-} \\ \dot{\delta}_{i+1,2}^{*-} \\ \dot{\delta}_{i+1,3}^{*-} \\ \dot{\delta}_{i+1,1}^{*+} \\ \dot{\delta}_{i+1,2}^{*+} \\ \dot{\delta}_{i+1,3}^{*+} \end{Bmatrix} \\
&= a_{i+1,0}^* \left( \frac{\bar{m}L}{2} \right)_{i+1}^* \begin{bmatrix} 1 & 0 & 0 \\ 0 & 1 & 0 \\ 0 & 0 & 0 \end{bmatrix} \begin{Bmatrix} \dot{\delta}_{i+1,1}^{*-} \\ \dot{\delta}_{i+1,2}^{*-} \\ \dot{\delta}_{i+1,3}^{*-} \end{Bmatrix} \\
&\quad + a_{i+1,1}^* \left( \frac{EI}{L^3} \right)_{i+1}^* \begin{bmatrix} \frac{AL^2}{I} & 0 & 0 & -\frac{AL^2}{I} & 0 & 0 \\ 0 & 12 & 6L & 0 & -12 & 6L \\ 0 & 6L & 4L^2 & 0 & -6L & 2L^2 \end{bmatrix}_{i+1} \begin{Bmatrix} \dot{\delta}_{i+1,1}^{*-} \\ \dot{\delta}_{i+1,2}^{*-} \\ \dot{\delta}_{i+1,3}^{*-} \\ \dot{\delta}_{i+1,1}^{*+} \\ \dot{\delta}_{i+1,2}^{*+} \\ \dot{\delta}_{i+1,3}^{*+} \end{Bmatrix} \\
&= a_{i+1,0}^* \frac{m_{i+1}^*}{2} [M_o^{*i}] \{\dot{\delta}_{i+1}^{*-}\} + a_{i+1,1}^* k_{i+1}^* [K_{o,i+1}^*] \{\dot{\delta}_{i+1}^{*+}\}
\end{aligned} \tag{7.42}$$

Where  $\dot{\delta}_1^i$  is the velocity in axial direction at Node  $i$ ;  $\dot{\delta}_2^i$  is the velocity in transverse direction at Node  $i$  and  $\dot{\delta}_3^i$  is the angular velocity within the plain at Node  $i$ .  $a_{i,0}$  and  $a_{i,1}$  are the damping coefficients for the proportional damping.

Substitute Eqs. 7.33 through 7.42 into Eq. 7.32 yields,

$$\begin{aligned}
& \{\dot{\Delta}^i\}^T m^i [M_o^i] \{\ddot{\delta}^i\} + \{\dot{\Delta}^i\}^T k_i [K_{o,i}] \{\delta_i\} + \{\dot{\Delta}^i\}^T k_{i+1} [K_{o,i+1}] \{\delta_{i+1}\} \\
& + \{\dot{\Delta}^i\}^T a_{i,0} \frac{m_i}{2} [M_o^i] \{\dot{\delta}_i^+\} + \{\dot{\Delta}^i\}^T a_{i,1} k_i [K_{o,i}] \{\dot{\delta}_i\} + \{\dot{\Delta}^i\}^T a_{i+1,0} \frac{m_{i+1}}{2} [M_o^i] \{\dot{\delta}_{i+1}^-\} \\
& + \{\dot{\Delta}^i\}^T a_{i+1,1} k_{i+1} [K_{o,i+1}] \{\dot{\delta}_{i+1}\} \\
& = \{\dot{\Delta}^i\}^T m^{*i} [M_o^{*i}] \{\ddot{\delta}^{*i}\} + \{\dot{\Delta}^i\}^T k_i^* [K_{o,i}^*] \{\delta_i^*\} + \{\dot{\Delta}^i\}^T k_{i+1}^* [K_{o,i+1}^*] \{\delta_{i+1}^*\} \\
& + \{\dot{\Delta}^i\}^T a_{i,0}^* \frac{m_i^*}{2} [M_o^{*i}] \{\dot{\delta}_i^{*+}\} + \{\dot{\Delta}^i\}^T a_{i,1}^* k_i^* [K_{o,i}^*] \{\dot{\delta}_i^*\} + \{\dot{\Delta}^i\}^T a_{i+1,0}^* \frac{m_{i+1}^*}{2} [M_o^{*i}] \{\dot{\delta}_{i+1}^{*-}\} \\
& + \{\dot{\Delta}^i\}^T a_{i+1,1}^* k_{i+1}^* [K_{o,i+1}^*] \{\dot{\delta}_{i+1}^*\}
\end{aligned} \tag{7.43}$$

Note that the positive end of Element  $i$ , the negative end of Element  $i+1$  and Node  $i$  shares the same node in the structure, thus,

$$\{\dot{\delta}_i^+\} = \{\dot{\delta}_{i+1}^-\} = \{\dot{\delta}^i\} \tag{7.44}$$

$$\{\dot{\delta}_i^{*+}\} = \{\dot{\delta}_{i+1}^{*-}\} = \{\dot{\delta}^{*i}\} \tag{7.45}$$

Substitute Eq. 7.44 and Eq. 7.45 into Eq. 7.43, yields,

$$\begin{aligned}
& \{\dot{\Delta}^i\}^T m^i [M_o^i] \{\ddot{\delta}^i\} + \{\dot{\Delta}^i\}^T k_i [K_{o,i}] \{\delta_i\} + \{\dot{\Delta}^i\}^T k_{i+1} [K_{o,i+1}] \{\delta_{i+1}\} \\
& + \{\dot{\Delta}^i\}^T a_{i,0} \frac{m_i}{2} [M_o^i] \{\dot{\delta}^i\} + \{\dot{\Delta}^i\}^T a_{i,1} k_i [K_{o,i}] \{\dot{\delta}_i\} + \{\dot{\Delta}^i\}^T a_{i+1,0} \frac{m_{i+1}}{2} [M_o^i] \{\dot{\delta}^i\} \\
& + \{\dot{\Delta}^i\}^T a_{i+1,1} k_{i+1} [K_{o,i+1}] \{\dot{\delta}_{i+1}\} \\
& = \{\dot{\Delta}^i\}^T m^{*i} [M_o^{*i}] \{\ddot{\delta}^{*i}\} + \{\dot{\Delta}^i\}^T k_i^* [K_{o,i}^*] \{\delta_i^*\} + \{\dot{\Delta}^i\}^T k_{i+1}^* [K_{o,i+1}^*] \{\delta_{i+1}^*\} \\
& + \{\dot{\Delta}^i\}^T a_{i,0}^* \frac{m_i^*}{2} [M_o^{*i}] \{\dot{\delta}^{*i}\} + \{\dot{\Delta}^i\}^T a_{i,1}^* k_i^* [K_{o,i}^*] \{\dot{\delta}_i^*\} + \{\dot{\Delta}^i\}^T a_{i+1,0}^* \frac{m_{i+1}^*}{2} [M_o^{*i}] \{\dot{\delta}^{*i}\} \\
& + \{\dot{\Delta}^i\}^T a_{i+1,1}^* k_{i+1}^* [K_{o,i+1}^*] \{\dot{\delta}_{i+1}^*\}
\end{aligned} \tag{7.46}$$

Rearranging the above equation yields,

$$\begin{aligned}
& \{\dot{\Delta}^i\}^T m^i [M_o^i] \{\ddot{\delta}^i\} + \{\dot{\Delta}^i\}^T k_i [K_{o,i}] \{\delta_i\} + \{\dot{\Delta}^i\}^T k_{i+1} [K_{o,i+1}] \{\delta_{i+1}\} \\
& + \{\dot{\Delta}^i\}^T \frac{a_{i,0} m_i + a_{i+1,0} m_{i+1}}{2} [M_o^i] \{\dot{\delta}^i\} + \{\dot{\Delta}^i\}^T a_{i,1} k_i [K_{o,i}] \{\dot{\delta}_i\} + \{\dot{\Delta}^i\}^T a_{i+1,1} k_{i+1} [K_{o,i+1}] \{\dot{\delta}_{i+1}\} \\
& = \{\dot{\Delta}^i\}^T m^{*i} [M_o^{*i}] \{\ddot{\delta}^{*i}\} + \{\dot{\Delta}^i\}^T k_i^* [K_{o,i}^*] \{\delta_i^*\} + \{\dot{\Delta}^i\}^T k_{i+1}^* [K_{o,i+1}^*] \{\delta_{i+1}^*\} \\
& + \{\dot{\Delta}^i\}^T \frac{a_{i,0}^* m_i^* + a_{i+1,0}^* m_{i+1}^*}{2} [M_o^{*i}] \{\dot{\delta}^{*i}\} + \{\dot{\Delta}^i\}^T a_{i,1}^* k_i^* [K_{o,i}^*] \{\dot{\delta}_i^*\} + \{\dot{\Delta}^i\}^T a_{i+1,1}^* k_{i+1}^* [K_{o,i+1}^*] \{\dot{\delta}_{i+1}^*\}
\end{aligned} \tag{7.47}$$

Note that the force vectors (i.e.  $\{I_i\}$ ,  $\{F_{s,i}\}$ ,  $\{F_{s,i+1}\}$ ,  $\{F_{c,i}\}$ ,  $\{F_{c,i+1}\}$ ,  $\{I_i^*\}$ ,  $\{F_{s,i}^*\}$ ,  $\{F_{s,i+1}^*\}$ ,  $\{F_{c,i}^*\}$ ,  $\{F_{c,i+1}^*\}$ ) can be summarized as the multiplication of property coefficients, configuration matrices and node displacement vectors. Because the designed damage are simulated by the changes of Young's modulus ( $E$ ), linear mass ( $\bar{m}$ ) and proportional damping coefficients  $a_{i,0}$  and  $a_{i,1}$ , other parameters, for example, the length of element ( $L$ ), the cross sectional area ( $A$ ) and the moment inertia of the cross section ( $I$ ), are not influenced by damage and remain the same for the undamaged and damaged elements. Consequently, the configuration matrices for the element stiffness and element mass are the same for both the damaged and undamaged elements. Namely,

$$[K_{o,i}^*] = [K_{o,i}] \tag{7.48}$$

$$[K_{o,i+1}^*] = [K_{o,i+1}] \tag{7.49}$$

$$[M_o^{*i}] = [M_o^i] \tag{7.50}$$

Substituting Eqs. 7.48 through 7.50 into Eq. 7.47 yields,



$$\begin{aligned}
& \{\dot{\Delta}^i\}^T m^i [M_o^i] \{\ddot{\delta}^i\} + \{\dot{\Delta}^i\}^T k_i [K_{o,i}] \{\delta_i\} + \{\dot{\Delta}^i\}^T k_{i+1} [K_{o,i+1}] \{\delta_{i+1}\} \\
& + \{\dot{\Delta}^i\}^T \frac{a_{i,0} m_i + a_{i+1,0} m_{i+1}}{2} [M_o^i] \{\dot{\delta}^i\} + \{\dot{\Delta}^i\}^T a_{i,1} k_i [K_{o,i}] \{\dot{\delta}_i\} + \{\dot{\Delta}^i\}^T a_{i+1,1} k_{i+1} [K_{o,i+1}] \{\dot{\delta}_{i+1}\} \\
& = \{\dot{\Delta}^i\}^T m^{*i} [M_o^i] \{\ddot{\delta}^{*i}\} + \{\dot{\Delta}^i\}^T k_i^* [K_{o,i}] \{\delta_i^*\} + \{\dot{\Delta}^i\}^T k_{i+1}^* [K_{o,i+1}] \{\delta_{i+1}^*\} \\
& + \{\dot{\Delta}^i\}^T \frac{a_{i,0}^* m_i^* + a_{i+1,0}^* m_{i+1}^*}{2} [M_o^i] \{\dot{\delta}^{*i}\} + \{\dot{\Delta}^i\}^T a_{i,1}^* k_i^* [K_{o,i}] \{\dot{\delta}_i^*\} + \{\dot{\Delta}^i\}^T a_{i+1,1}^* k_{i+1}^* [K_{o,i+1}] \{\dot{\delta}_{i+1}^*\}
\end{aligned} \tag{7.51}$$

Moving forward the property constant from each term into Eq. 7.51 and rearrange the equation yields,

$$\begin{aligned}
& m^i \{\dot{\Delta}^i\}^T [M_o^i] \{\ddot{\delta}^i\} + k_i \{\dot{\Delta}^i\}^T [K_{o,i}] \{\delta_i\} + k_{i+1} \{\dot{\Delta}^i\}^T [K_{o,i+1}] \{\delta_{i+1}\} \\
& + \frac{a_{i,0} m_i + a_{i+1,0} m_{i+1}}{2} \{\dot{\Delta}^i\}^T [M_o^i] \{\dot{\delta}^i\} + a_{i,1} k_i \{\dot{\Delta}^i\}^T [K_{o,i}] \{\dot{\delta}_i\} + a_{i+1,1} k_{i+1} \{\dot{\Delta}^i\}^T [K_{o,i+1}] \{\dot{\delta}_{i+1}\} \\
& - k_i^* \{\dot{\Delta}^i\}^T [K_{o,i}] \{\delta_i^*\} - k_{i+1}^* \{\dot{\Delta}^i\}^T [K_{o,i+1}] \{\delta_{i+1}^*\} - \frac{a_{i,0}^* m_i^* + a_{i+1,0}^* m_{i+1}^*}{2} \{\dot{\Delta}^i\}^T [M_o^i] \{\dot{\delta}^{*i}\} \\
& - a_{i,1}^* k_i^* \{\dot{\Delta}^i\}^T [K_{o,i}] \{\dot{\delta}_i^*\} - a_{i+1,1}^* k_{i+1}^* \{\dot{\Delta}^i\}^T [K_{o,i+1}] \{\dot{\delta}_{i+1}^*\} \\
& = m^{*i} \{\dot{\Delta}^i\}^T [M_o^i] \{\ddot{\delta}^{*i}\}
\end{aligned} \tag{7.52}$$

Dividing Eq. 7.52 by  $m^{*i}$  yields,

$$\begin{aligned}
& \frac{m^i}{m^{*i}} \{\dot{\Delta}^i\}^T [M_o^i] \{\ddot{\delta}^i\} + \frac{k_i}{m^{*i}} \{\dot{\Delta}^i\}^T [K_{o,i}] \{\delta_i\} + \frac{k_{i+1}}{m^{*i}} \{\dot{\Delta}^i\}^T [K_{o,i+1}] \{\delta_{i+1}\} \\
& + \frac{a_{i,0}m_i + a_{i+1,0}m_{i+1}}{2m^{*i}} \{\dot{\Delta}^i\}^T [M_o^i] \{\dot{\delta}^i\} + \frac{a_{i,1}k_i}{m^{*i}} \{\dot{\Delta}^i\}^T [K_{o,i}] \{\dot{\delta}_i\} + \frac{a_{i+1,1}k_{i+1}}{m^{*i}} \{\dot{\Delta}^i\}^T [K_{o,i+1}] \{\dot{\delta}_{i+1}\} \\
& - \frac{k_i^*}{m^{*i}} \{\dot{\Delta}^i\}^T [K_{o,i}] \{\delta_i^*\} - \frac{k_{i+1}^*}{m^{*i}} \{\dot{\Delta}^i\}^T [K_{o,i+1}] \{\delta_{i+1}^*\} - \frac{a_{i,0}^*m_i^* + a_{i+1,0}^*m_{i+1}^*}{2m^{*i}} \{\dot{\Delta}^i\}^T [M_o^i] \{\dot{\delta}^{*i}\} \\
& - \frac{a_{i,1}^*k_i^*}{m^{*i}} \{\dot{\Delta}^i\}^T [K_{o,i}] \{\dot{\delta}_i^*\} - \frac{a_{i+1,1}^*k_{i+1}^*}{m^{*i}} \{\dot{\Delta}^i\}^T [K_{o,i+1}] \{\dot{\delta}_{i+1}^*\} \\
& = \{\dot{\Delta}^i\}^T [M_o^i] \{\ddot{\delta}^{*i}\}
\end{aligned} \tag{7.53}$$

Define the following coefficients,

$$\beta_1 = \frac{m^i}{m^{*i}} \tag{7.54}$$

$$\beta_2 = \frac{k_i}{m^{*i}} \tag{7.55}$$

$$\beta_3 = \frac{k_{i+1}}{m^{*i}} \tag{7.56}$$

$$\beta_4 = \frac{a_{i,0}m_i + a_{i+1,0}m_{i+1}}{2m^{*i}} \tag{7.57}$$

$$\beta_5 = \frac{a_{i,1}k_i}{m^{*i}} \tag{7.58}$$

$$\beta_6 = \frac{a_{i+1,1}k_{i+1}}{m^{*i}} \tag{7.59}$$

$$\beta_7 = \frac{k_i^*}{m^{*i}} \tag{7.60}$$

$$\beta_8 = \frac{k_{i+1}^*}{m^{*i}} \quad (7.61)$$

$$\beta_9 = \frac{a_{i,0}^* m_i^* + a_{i+1,0}^* m_{i+1}^*}{2m^{*i}} \quad (7.62)$$

$$\beta_{10} = \frac{a_{i,1}^* k_i^*}{m^{*i}} \quad (7.63)$$

$$\beta_{11} = \frac{a_{i+1,1}^* k_{i+1}^*}{m^{*i}} \quad (7.64)$$

Substituting Eq. 7.54 through Eq. 7.64 to Eq. 7.53 yields,

$$\begin{aligned} & \beta_1 \{\dot{\Delta}^i\}^T [M_o^i] \{\ddot{\delta}^i\} + \beta_2 \{\dot{\Delta}^i\}^T [K_{o,i}] \{\delta_i\} + \beta_3 \{\dot{\Delta}^i\}^T [K_{o,i+1}] \{\delta_{i+1}\} + \beta_4 \{\dot{\Delta}^i\}^T [M_o^i] \{\dot{\delta}^i\} \\ & + \beta_5 \{\dot{\Delta}^i\}^T [K_{o,i}] \{\dot{\delta}_i\} + \beta_6 \{\dot{\Delta}^i\}^T [K_{o,i+1}] \{\dot{\delta}_{i+1}\} - \beta_7 \{\dot{\Delta}^i\}^T [K_{o,i}] \{\delta_i^*\} \\ & - \beta_8 \{\dot{\Delta}^i\}^T [K_{o,i+1}] \{\delta_{i+1}^*\} - \beta_9 \{\dot{\Delta}^i\}^T [M_o^i] \{\dot{\delta}^{*i}\} - \beta_{10} \{\dot{\Delta}^i\}^T [K_{o,i}] \{\dot{\delta}_i^*\} \\ & - \beta_{11} \{\dot{\Delta}^i\}^T [K_{o,i+1}] \{\dot{\delta}_{i+1}^*\} = \{\dot{\Delta}^i\}^T [M_o^i] \{\ddot{\delta}^{*i}\} \end{aligned} \quad (7.65)$$

Writing the Eq. 7.65 at different time point, yields the following groups of equations,

For  $t = t_0$ ,

$$\begin{aligned} & \beta_1 (\{\dot{\Delta}^i\}^T [M_o^i] \{\ddot{\delta}^i\})|_{t_0} + \beta_2 (\{\dot{\Delta}^i\}^T [K_{o,i}] \{\delta_i\})|_{t_0} + \beta_3 (\{\dot{\Delta}^i\}^T [K_{o,i+1}] \{\delta_{i+1}\})|_{t_0} \\ & + \beta_4 (\{\dot{\Delta}^i\}^T [M_o^i] \{\dot{\delta}^i\})|_{t_0} + \beta_5 (\{\dot{\Delta}^i\}^T [K_{o,i}] \{\dot{\delta}_i\})|_{t_0} + \beta_6 (\{\dot{\Delta}^i\}^T [K_{o,i+1}] \{\dot{\delta}_{i+1}\})|_{t_0} \\ & - \beta_7 (\{\dot{\Delta}^i\}^T [K_{o,i}] \{\delta_i^*\})|_{t_0} - \beta_8 (\{\dot{\Delta}^i\}^T [K_{o,i+1}] \{\delta_{i+1}^*\})|_{t_0} - \beta_9 (\{\dot{\Delta}^i\}^T [M_o^i] \{\dot{\delta}^{*i}\})|_{t_0} \\ & - \beta_{10} (\{\dot{\Delta}^i\}^T [K_{o,i}] \{\dot{\delta}_i^*\})|_{t_0} - \beta_{11} (\{\dot{\Delta}^i\}^T [K_{o,i+1}] \{\dot{\delta}_{i+1}^*\})|_{t_0} = (\{\dot{\Delta}^i\}^T [M_o^i] \{\ddot{\delta}^{*i}\})|_{t_0} \end{aligned} \quad (7.66)$$

For  $t = t_j$ ,

$$\begin{aligned}
& \beta_1(\{\dot{\Delta}\}^T[M_o^i]\{\ddot{\delta}^i\})|_{t_j} + \beta_2(\{\dot{\Delta}\}^T[K_{o,i}]\{\delta_i\})|_{t_j} + \beta_3(\{\dot{\Delta}\}^T[K_{o,i+1}]\{\delta_{i+1}\})|_{t_j} \\
& + \beta_4(\{\dot{\Delta}\}^T[M_o^i]\{\dot{\delta}^i\})|_{t_j} + \beta_5(\{\dot{\Delta}\}^T[K_{o,i}]\{\dot{\delta}_i\})|_{t_j} + \beta_6(\{\dot{\Delta}\}^T[K_{o,i+1}]\{\dot{\delta}_{i+1}\})|_{t_j} \\
& - \beta_7(\{\dot{\Delta}\}^T[K_{o,i}]\{\delta_i^*\})|_{t_j} - \beta_8(\{\dot{\Delta}\}^T[K_{o,i+1}]\{\delta_{i+1}^*\})|_{t_j} - \beta_9(\{\dot{\Delta}\}^T[M_o^i]\{\dot{\delta}^{*i}\})|_{t_j} \\
& - \beta_{10}(\{\dot{\Delta}\}^T[K_{o,i}]\{\dot{\delta}_i^*\})|_{t_j} - \beta_{11}(\{\dot{\Delta}\}^T[K_{o,i+1}]\{\dot{\delta}_{i+1}^*\})|_{t_j} = (\{\dot{\Delta}\}^T[M_o^i]\{\ddot{\delta}^{*i}\})|_{t_j}
\end{aligned} \tag{7.67}$$

For  $t = t_N$ ,

$$\begin{aligned}
& \beta_1(\{\dot{\Delta}\}^T[M_o^i]\{\ddot{\delta}^i\})|_{t_N} + \beta_2(\{\dot{\Delta}\}^T[K_{o,i}]\{\delta_i\})|_{t_N} + \beta_3(\{\dot{\Delta}\}^T[K_{o,i+1}]\{\delta_{i+1}\})|_{t_N} \\
& + \beta_4(\{\dot{\Delta}\}^T[M_o^i]\{\dot{\delta}^i\})|_{t_N} + \beta_5(\{\dot{\Delta}\}^T[K_{o,i}]\{\dot{\delta}_i\})|_{t_N} + \beta_6(\{\dot{\Delta}\}^T[K_{o,i+1}]\{\dot{\delta}_{i+1}\})|_{t_N} \\
& - \beta_7(\{\dot{\Delta}\}^T[K_{o,i}]\{\delta_i^*\})|_{t_N} - \beta_8(\{\dot{\Delta}\}^T[K_{o,i+1}]\{\delta_{i+1}^*\})|_{t_N} - \beta_9(\{\dot{\Delta}\}^T[M_o^i]\{\dot{\delta}^{*i}\})|_{t_N} \\
& - \beta_{10}(\{\dot{\Delta}\}^T[K_{o,i}]\{\dot{\delta}_i^*\})|_{t_N} - \beta_{11}(\{\dot{\Delta}\}^T[K_{o,i+1}]\{\dot{\delta}_{i+1}^*\})|_{t_N} = (\{\dot{\Delta}\}^T[M_o^i]\{\ddot{\delta}^{*i}\})|_{t_N}
\end{aligned} \tag{7.68}$$

Arranging the above linear equation group into matrix form, yields,

$$\mathbf{X}\boldsymbol{\beta} = \mathbf{Y} \tag{7.69}$$

Where the coefficient matrix of the linear equation group is given as following, (note, due to the limitation of the page size, the transposed form of the matrix is provided)

$$\begin{aligned}
\mathbf{X}^T = & \left[ \begin{array}{cccc}
(\{\dot{\Delta}^i\}^T[M_o^i]\{\ddot{\delta}^i\})|_{t_0} & \dots & (\{\dot{\Delta}^i\}^T[M_o^i]\{\ddot{\delta}^i\})|_{t_j} & \dots & (\{\dot{\Delta}^i\}^T[M_o^i]\{\ddot{\delta}^i\})|_{t_N} \\
(\{\dot{\Delta}^i\}^T[K_{o,i}]\{\dot{\delta}_i\})|_{t_0} & \dots & (\{\dot{\Delta}^i\}^T[K_{o,i}]\{\dot{\delta}_i\})|_{t_j} & \dots & (\{\dot{\Delta}^i\}^T[K_{o,i}]\{\dot{\delta}_i\})|_{t_N} \\
(\{\dot{\Delta}^i\}^T[K_{o,i+1}]\{\dot{\delta}_{i+1}\})|_{t_0} & \dots & (\{\dot{\Delta}^i\}^T[K_{o,i+1}]\{\dot{\delta}_{i+1}\})|_{t_j} & \dots & (\{\dot{\Delta}^i\}^T[K_{o,i+1}]\{\dot{\delta}_{i+1}\})|_{t_N} \\
(\{\dot{\Delta}^i\}^T[M_o^i]\{\dot{\delta}^i\})|_{t_0} & \dots & (\{\dot{\Delta}^i\}^T[M_o^i]\{\dot{\delta}^i\})|_{t_j} & \dots & (\{\dot{\Delta}^i\}^T[M_o^i]\{\dot{\delta}^i\})|_{t_N} \\
(\{\dot{\Delta}^i\}^T[K_{o,i}]\{\dot{\delta}_i\})|_{t_0} & \dots & (\{\dot{\Delta}^i\}^T[K_{o,i}]\{\dot{\delta}_i\})|_{t_j} & \dots & (\{\dot{\Delta}^i\}^T[K_{o,i}]\{\dot{\delta}_i\})|_{t_N} \\
(\{\dot{\Delta}^i\}^T[K_{o,i+1}]\{\dot{\delta}_{i+1}\})|_{t_0} & \dots & (\{\dot{\Delta}^i\}^T[K_{o,i+1}]\{\dot{\delta}_{i+1}\})|_{t_j} & \dots & (\{\dot{\Delta}^i\}^T[K_{o,i+1}]\{\dot{\delta}_{i+1}\})|_{t_N} \\
-(\{\dot{\Delta}^i\}^T[K_{o,i}]\{\dot{\delta}_i^*\})|_{t_0} & \dots & -(\{\dot{\Delta}^i\}^T[K_{o,i}]\{\dot{\delta}_i^*\})|_{t_j} & \dots & -(\{\dot{\Delta}^i\}^T[K_{o,i}]\{\dot{\delta}_i^*\})|_{t_N} \\
-(\{\dot{\Delta}^i\}^T[K_{o,i+1}]\{\dot{\delta}_{i+1}^*\})|_{t_0} & \dots & -(\{\dot{\Delta}^i\}^T[K_{o,i+1}]\{\dot{\delta}_{i+1}^*\})|_{t_j} & \dots & -(\{\dot{\Delta}^i\}^T[K_{o,i+1}]\{\dot{\delta}_{i+1}^*\})|_{t_N} \\
-(\{\dot{\Delta}^i\}^T[M_o^i]\{\dot{\delta}^{*i}\})|_{t_0} & \dots & -(\{\dot{\Delta}^i\}^T[M_o^i]\{\dot{\delta}^{*i}\})|_{t_j} & \dots & -(\{\dot{\Delta}^i\}^T[M_o^i]\{\dot{\delta}^{*i}\})|_{t_N} \\
-(\{\dot{\Delta}^i\}^T[K_{o,i}]\{\dot{\delta}_i^*\})|_{t_0} & \dots & -(\{\dot{\Delta}^i\}^T[K_{o,i}]\{\dot{\delta}_i^*\})|_{t_j} & \dots & -(\{\dot{\Delta}^i\}^T[K_{o,i}]\{\dot{\delta}_i^*\})|_{t_N} \\
-(\{\dot{\Delta}^i\}^T[K_{o,i+1}]\{\dot{\delta}_{i+1}^*\})|_{t_0} & \dots & -(\{\dot{\Delta}^i\}^T[K_{o,i+1}]\{\dot{\delta}_{i+1}^*\})|_{t_j} & \dots & -(\{\dot{\Delta}^i\}^T[K_{o,i+1}]\{\dot{\delta}_{i+1}^*\})|_{t_N}
\end{array} \right]
\end{aligned}
\tag{7.70}$$

The vector of unknown and the vector of known are given as,

$$\mathbf{\beta} = \left\{ \begin{array}{c} \beta_1 \\ \beta_2 \\ \beta_3 \\ \beta_4 \\ \beta_5 \\ \beta_6 \\ \beta_7 \\ \beta_8 \\ \beta_9 \\ \beta_{10} \\ \beta_{11} \end{array} \right\}
\tag{7.71}$$

$$\mathbf{Y} = \begin{Bmatrix} ((\dot{\Delta}^i)^T [M_o^i] \{\ddot{\delta}^{i*}\})|_{t_0} \\ \vdots \\ ((\dot{\Delta}^i)^T [M_o^i] \{\ddot{\delta}^{i*}\})|_{t_j} \\ \vdots \\ ((\dot{\Delta}^i)^T [M_o^i] \{\ddot{\delta}^{i*}\})|_{t_N} \end{Bmatrix} \quad (7.72)$$

Using the Least Square Method, the vector of unknown, ' $\boldsymbol{\beta}$ ', can be computed from the following equation,

$$\boldsymbol{\beta} = (\mathbf{X}^T \mathbf{X})^{-1} (\mathbf{X}^T \mathbf{Y}) \quad (7.73)$$

With the vector of unknown computed, the damage indices for stiffness, mass and damping can be computed as follows,

$$\beta_{m^i} = \frac{m^i}{m^{*i}} \quad (7.74)$$

$$\beta_{k_i} = \frac{k_i}{k_i^*} = \frac{\frac{k_i}{m^{*i}}}{\frac{k_i^*}{m^{*i}}} = \frac{\beta_2}{\beta_7} \quad (7.75)$$

$$\beta_{k_{i+1}} = \frac{k_{i+1}}{k_{i+1}^*} = \frac{\frac{k_{i+1}}{m^{*j}}}{\frac{k_{i+1}^*}{m^{*j}}} = \frac{\beta_3}{\beta_8} \quad (7.76)$$

$$\beta_{a_{i,1}} = \frac{a_{i,1}}{a_{i,1}^*} = \frac{\frac{a_{i,1} k_i}{m^{*i}}}{\frac{a_{i,1}^* k_i^*}{m^{*i}}} \cdot \frac{k_i}{k_i^*} = \frac{\beta_5}{\beta_{10}} \cdot \frac{1}{\beta_{k_i}} \quad (7.77)$$

$$\beta_{a_{i+1,1}} = \frac{a_{i+1,1}}{a_{i+1,1}^*} = \frac{\frac{a_{i+1,1} k_{i+1}}{m^{*i}}}{\frac{a_{i+1,1}^* k_{i+1}^*}{m^{*i}}} \cdot \frac{k_{i+1}^*}{k_{i+1}} = \frac{\beta_6}{\beta_{11}} \cdot \frac{1}{\beta_{k_{i+1}}} \quad (7.78)$$

Assume  $a_{i,0} \approx a_{i+1,0}$  and  $a_{i,0}^* \approx a_{i+1,0}^*$

$$\beta_{a_{i,0}} \approx \beta_{a_{i+1,0}} = \frac{a_{i+1,0}}{a_{i+1,0}^*} \approx \frac{a_{i,0}}{a_{i,0}^*} = \frac{a_{i,0}(m_i + m_{i+1})}{a_{i,0}^*(m_i^* + m_{i+1}^*)} \cdot \frac{m^{i*}}{m^i} \approx \frac{\frac{a_{i,0}m_i + a_{i+1,0}m_{i+1}}{2m^{*i}}}{\frac{a_{i,0}^*m_i^* + a_{i+1,0}^*m_{i+1}^*}{2m^{*i}}} \cdot \frac{m^{i*}}{m^i} = \frac{\beta_4}{\beta_9} \cdot \frac{1}{\beta_{m^i}} \quad (7.79)$$

### 7.4.3 Damage Evaluation for a Continuous System with Proportional Damping

In this subsection, a fixed-fixed beam is used to evaluate the performance of the proposed theory in dealing with damping damage detection. The geometry of the beam under consideration are indicated Figure 7.19. The detailed damage scenario is summarized in Table 7.4. The geometry of the cross-section of the beam is shown in 19. The modulus of elasticity (  $E$  ) of the material is 29,000 ksi. The mass density of the material is  $7.345 \times 10^{-7}$  kip•sec<sup>2</sup>/in<sup>4</sup>.

The fixed-fixed beam is meshed into 6 elements and has 7 equally spaced nodes. The length of each element is 12.0 inches. For illustrative purposes, typical elements are indicated in Figure 7.19.

For each node on the beam, a white noise,  $100 \times \text{random}(-1,1)$ , is used as node force and is applied in transverse direction. The five white-noise forces are the same as the one applied

in the above four cases and are plotted in Figure 6.2. Given the external load case, exact accelerations, velocities and displacements of the five nodes were computed at every  $1\text{E-}4$  seconds (10,000 Hz) for 0.2 seconds.

In this case, the velocity ( $\dot{x}(t)$ ) of each node in the undamaged case was used as the velocity used to compute power ( $\dot{\Delta}$ ) for both the undamaged and damaged cases. For every two nearby elements, the coefficient matrices (' $\mathbf{X}$ ') and known vector (' $\mathbf{Y}$ ') were constructed by substituting the acceleration ( $\ddot{x}(t)$ ), velocity ( $\dot{x}(t)$ ), displacement ( $x(t)$ ), and velocity used to compute power ( $\dot{\Delta}$ ) into Eq. 7.70 and Eq. 7.72. The coefficient damage index vector,  $\beta$ , related to the two nearby elements was computed using Eq. 7.73. Then the damage indices for nodal mass, element stiffness and element damping coefficients are computed using Eq. 7.74 through Eq. 7.79. The damage severities for stiffness are computed using Eq. 2.13. The damage indices for each property are shown in Table 7.5 and are plotted in Figure 7.23. The related damage severities are plotted in Figure 7.24



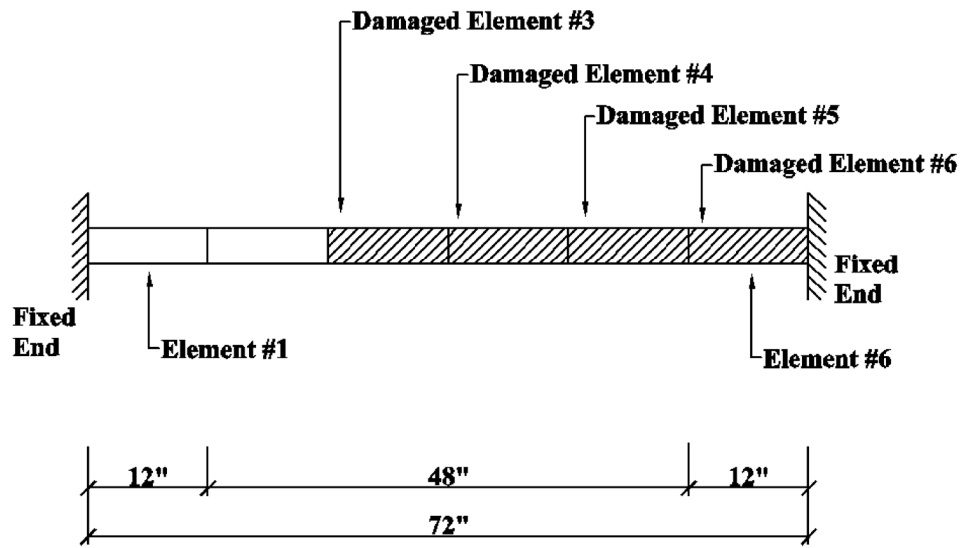
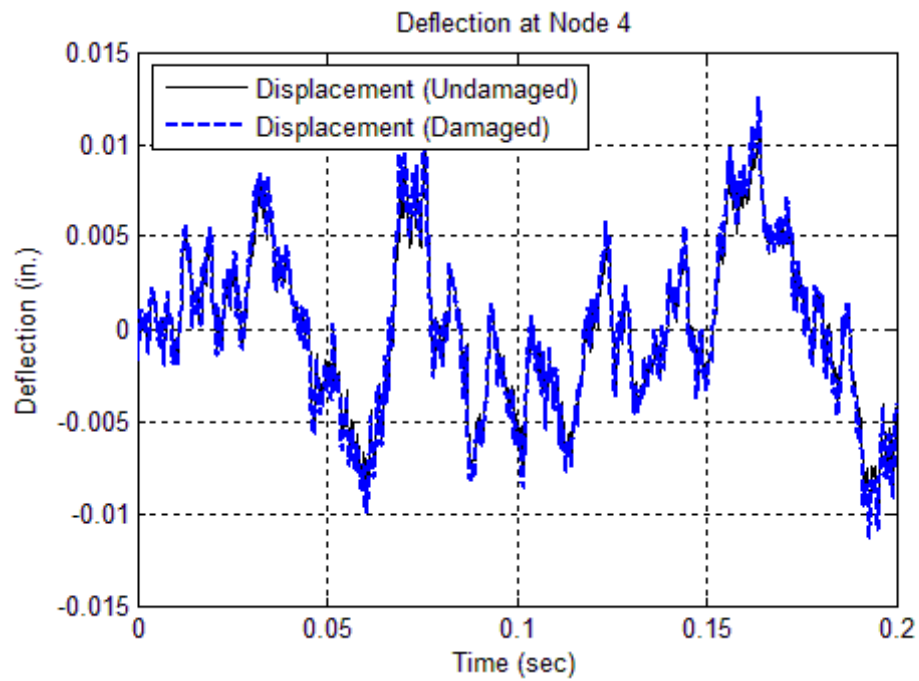


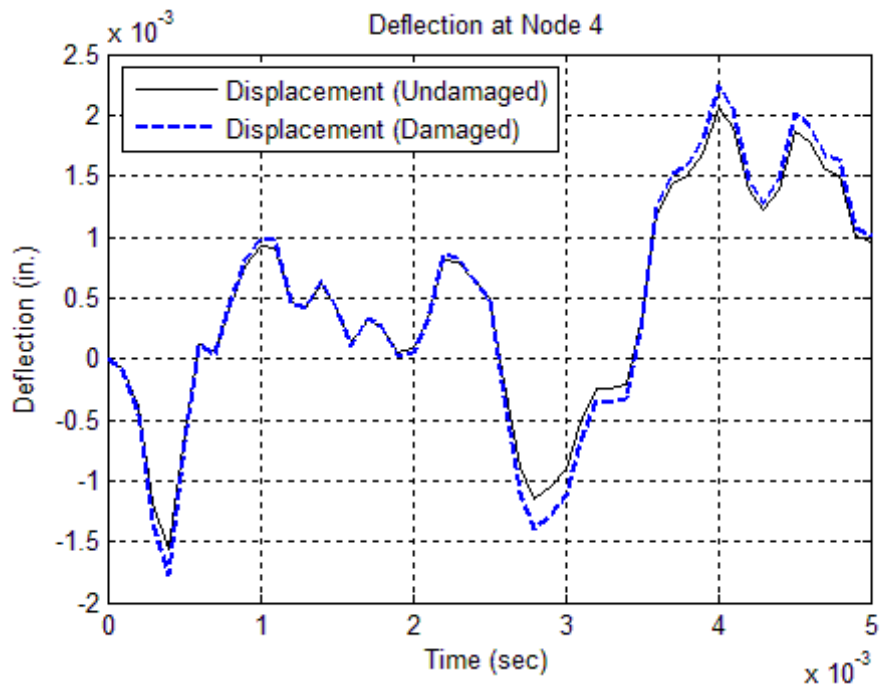
Figure 7.19. Geometry of the Fixed-Fixed Beam with Proportional Damping

Table 7.4. Designed Damage Scenario for the Fixed-Fixed Beam

Element Number	Element Stiffness	Element Mass	Designed Damage Severity (%)	
			Element Damping	
			$a_0$	$a_1$
#1	0	0	0	0
#2	0	0	0	0
#3	10	20	20	10
#4	10	20	20	10
#5	0	0	10	10
#6	0	0	10	10

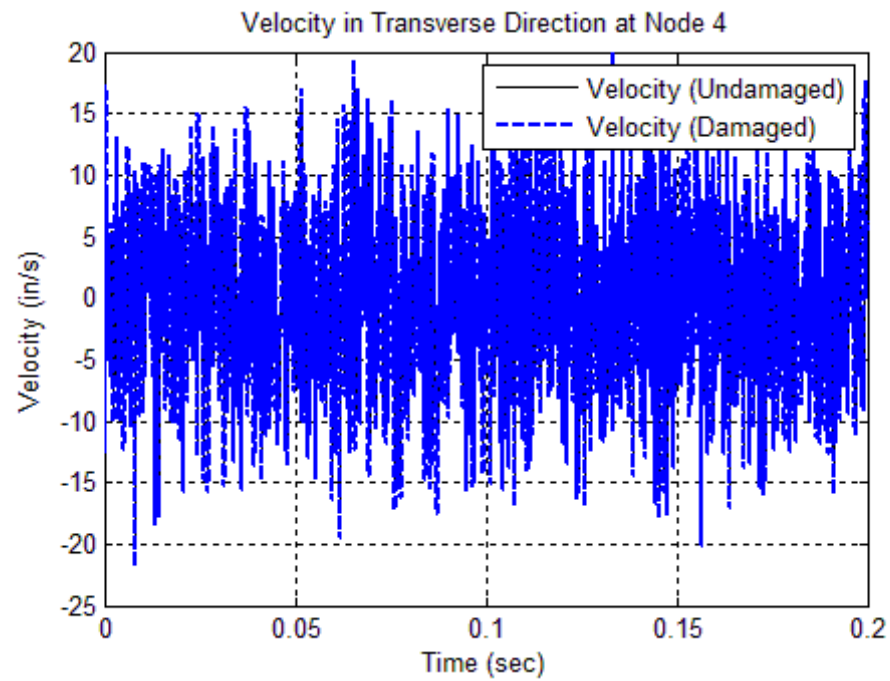


(a)

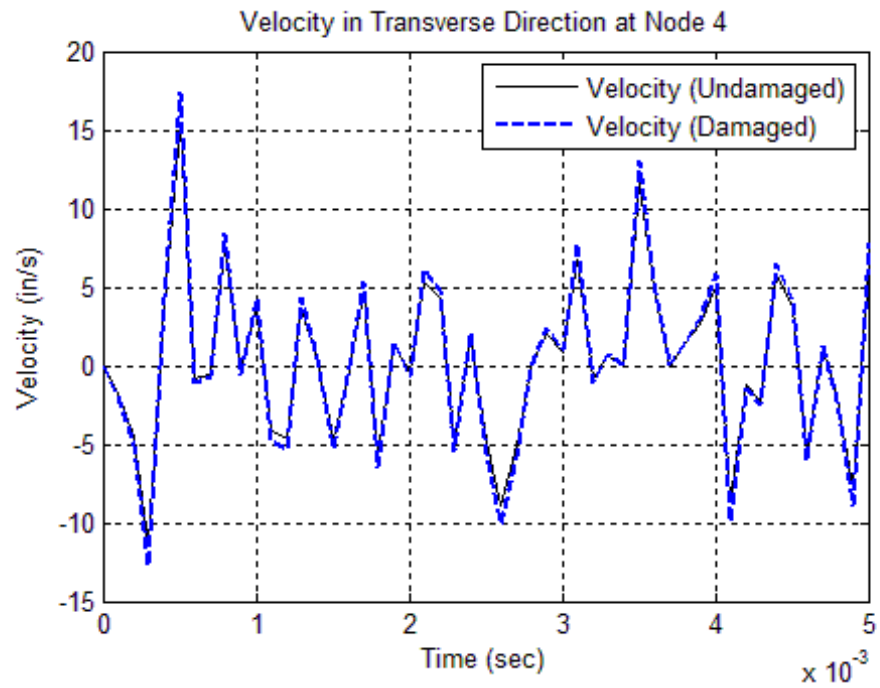


(b)

**Figure 7.20. Displacements in Transverse Direction of Node 4 of the Fixed-Fixed Beam under the Given External Load: (a) Full Plot and (b) Zoomed in Plot**

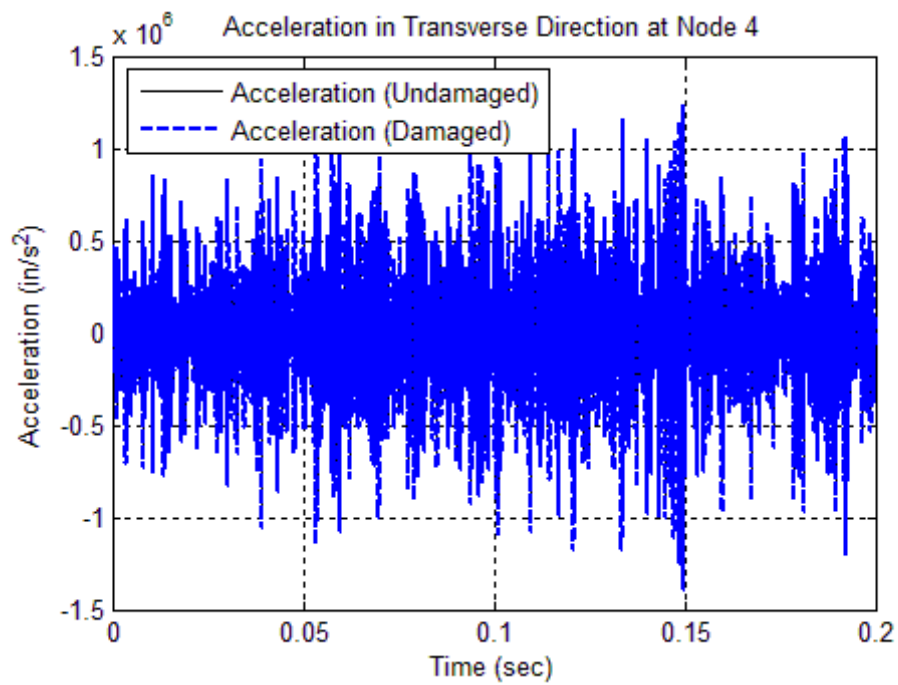


(a)

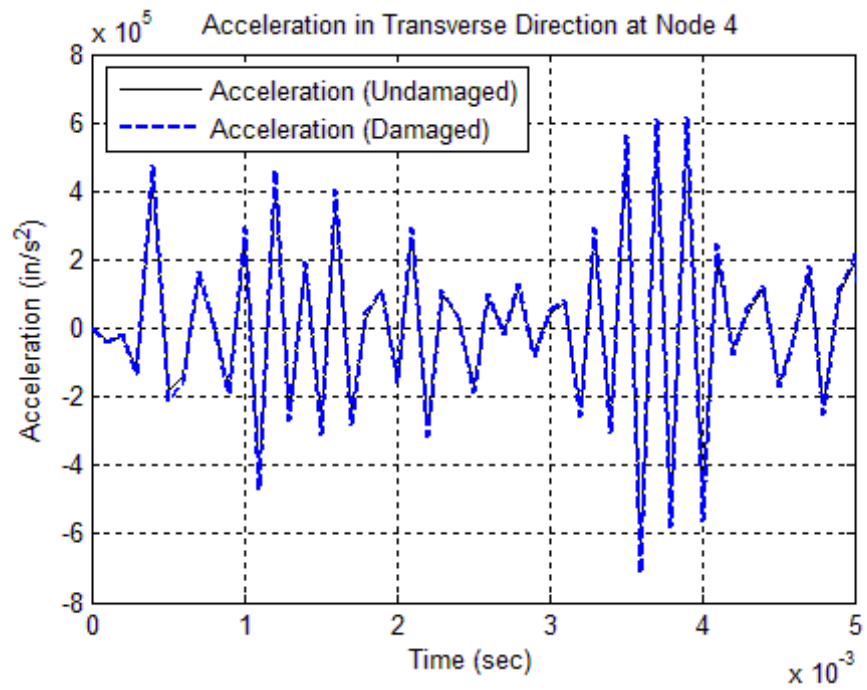


(b)

**Figure 7.21. Velocities in Transverse Direction of the Node 4 of the Fixed-Fixed Beam under the Given External Load: (a) Full Plot and (b) Zoomed in Plot**



(a)



(b)

Figure 7.22. Accelerations in Transverse Direction of Node 4 of the Fixed-Fixed Beam under the Given External Load: (a) Full Plot and (b) Zoomed in Plot

**Table 7.5. Damage Detection Results for the Fixed-Fixed Beam with Proportional Damping**

<b>Designed Damage Indices</b>			
<b>Property</b>	<b>System #1</b>	<b>System #2</b>	<b>System #3</b>
$m^i$	1.00	1.25	1.00
$k_i$	1.00	1.11	1.00
$k_{i+1}$	1.00	1.11	1.00
$a_{i,1}$	1.00	1.11	1.11
$a_{i+1,1}$	1.00	1.11	1.11
$a_{i,0}$	1.00	1.25	1.11
$a_{i+1,0}$	1.00	1.25	1.11

<b>Estimated Damage Indices</b>			
<b>Property</b>	<b>System #1</b>	<b>System #2</b>	<b>System #3</b>
$m^i$	1.00	1.25	1.00
$k_i$	1.00	1.11	1.00
$k_{i+1}$	1.00	1.11	1.00
$a_{i,1}$	1.00	1.11	1.11
$a_{i+1,1}$	1.00	1.11	1.11
$a_{i,0}$	1.00	1.25	1.11
$a_{i+1,0}$	1.00	1.25	1.11

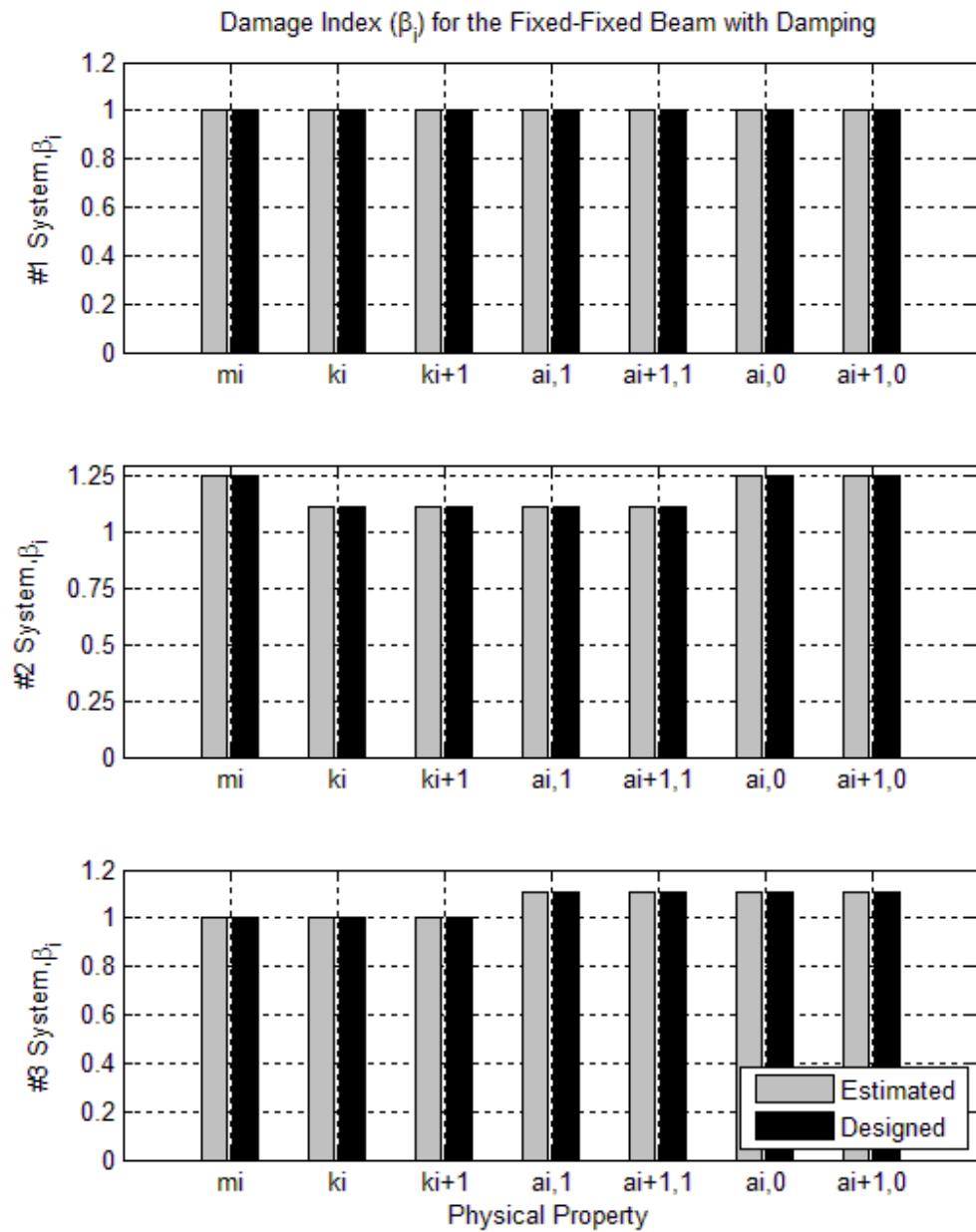


Figure 7.23. Damage Indices ( $\beta_i$ ) for the Fixed-Fixed Beam with Proportional Damping Using Isolated Beam Element Analysis Method

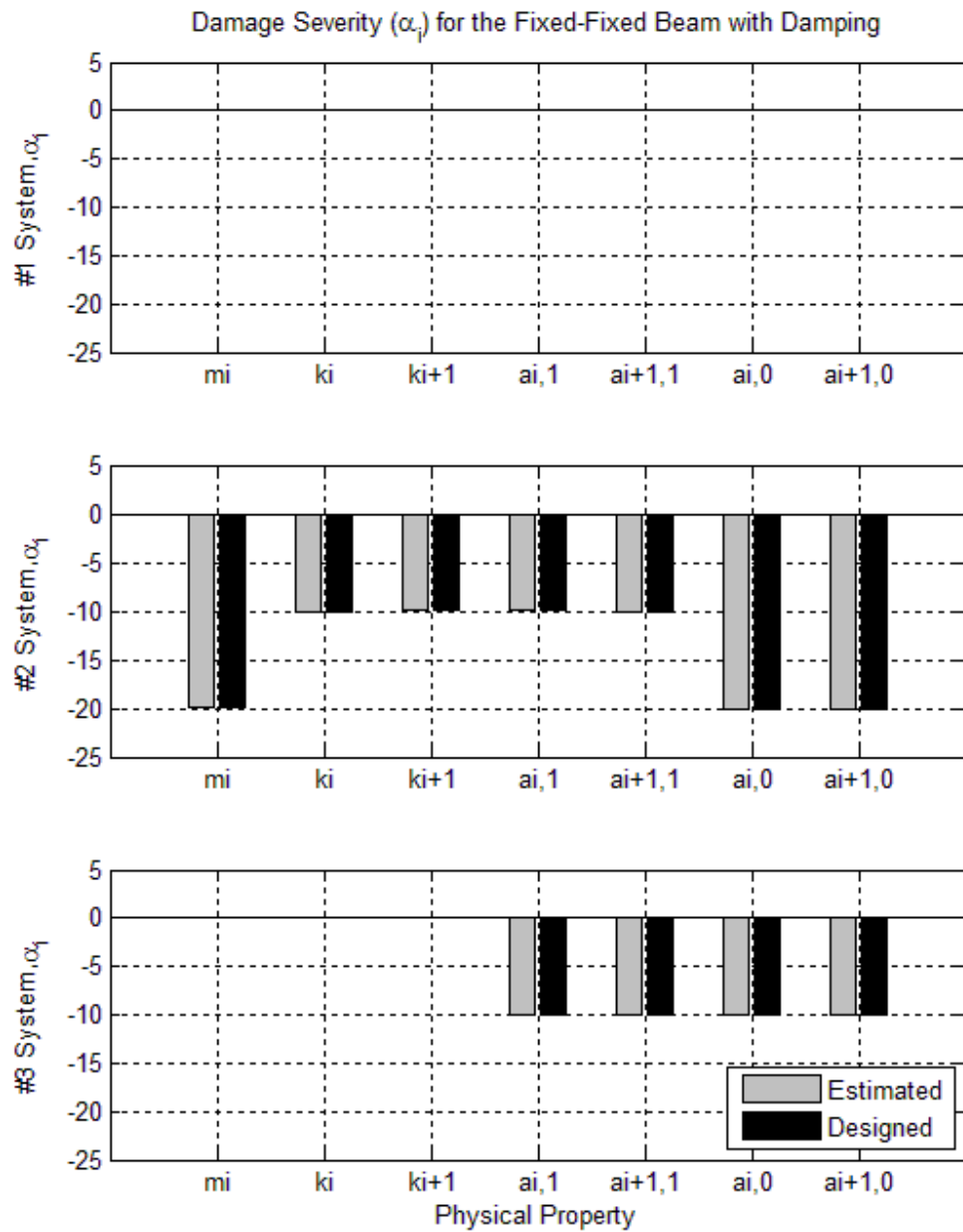


Figure 7.24. Damage Severities ( $\alpha_i$ ) for the Fixed-Fixed Beam with Proportional Damping Using Isolated Beam Element Analysis Method

#### **7.4.4 Summary**

In Subsection 7.4, the Power Method was developed to be able to detect damage in continuous system with damping, which was simulated by the proportional damping and a fixed-fixed beam is provided to validate the proposed theory. In the numerical case, damage in mass, stiffness, and damping were simulated and exact displacements, velocities, and accelerations were computed. According to the damage detection results, all the designed damage in masses, stiffness, and damping were located and evaluated accurately and neither false-positive damage index nor false-negative damage index was found.



## **8 APPLICATION OF THE METHOD TO SHAKE TABLE TESTS**

### **8.1 INTRODUCTION**

In this section, the performance of the proposed method in the real world will be studied using experimental data sets. The data sets were collected from a series of shake table tests of a bridge model conducted at the Caltrans Seismic Response Modification Devises facility at the University of California San Diego by Dr. Gianmario Benzoni, Dr. Noemi Bonessio, and Dr. Giuseppe Lomiento (Benzoni et al. 2012).

### **8.2 DESCRIPTION OF THE STRUCTURE AND TEST SETUP**

The bridge model tested on the shake table is a one-span steel frame composed by two columns, one deck and additional mass. The two columns of the bridge model are identical. The column is composed by four column portions and one cap beam which is prepared for the later installation of the viscous dampers between column and deck. Each of the four column portions is composed by one hollow rectangular section (HSS8×4×1/4) with four channel section (C4×7.25) on each side. The cap beam is composed by two 51 inches long plates with small plates in between. The height of each column portion is 17.5 inches and the height of the cap beam is 10 inches. The connections between two column portions and the connection between column portion and cap beam are both bolted connections. The deck of the bridge model is composed by two steel boxes and two longitudinal wide flange beams (W6×15) with six wide flange beams (W4×13) in between. Each of the steel boxes is seated on the top of each cap beam. The width of the deck is 64 inches and the length of the deck is 126 inches. Steel plates were put on the top of the deck as the additional mass to the bridge model to

reduce the natural frequencies of the bridge model. The total weight of the additional mass is 3,600 lbs. The bridge model and the global coordinate system are given in the photograph of Figure 8.1. The detailed dimensions of the structure are given in Figure 8.2. At different locations, tri-axial, single-axial accelerometers and string pots were installed to collect accelerations, and displacements in different directions. The locations of the accelerometers are indicated in the photograph of Figure 8.3. The locations of the string pots are indicated in the photograph of Figure 8.4. The acceleration and displacement data from the bridge model were collected at 0.002 second intervals.

Three types of white noise signals were used as inputs to excite the structure in global X, Y and Z directions. Input Type A is the reference input for X direction with frequency band 1-10 Hz. Input Type B is the reference input for Y direction with frequency band 1-10 Hz. Input Type C is the reference input for Z direction with frequency band 5-20 Hz. If the input intensity of the base vibration is risen up to 100%, the structure will be forced to reach its nominal capacity in the corresponding input direction of the base vibration. In case of any damage caused by extensive base vibration, the input intensity of the base vibration is limited up to 50%.

In the given data file, seventeen data sets were provided: Test #01, Test #03, and Test #05 through Test #19. Since Test#05, Test#06, Test#08, Test#09, Test#12, Test#13, Test#14, and Test#19 were not excited in the global X direction, these eight tests will not be taken into consideration in the following damage detection process. The remaining nine shake table tests were either excited solely in the global X direction or excited in the global X, Y, Z directions at the same time. Among these nine tests, the first five tests are undamaged cases and the remaining four tests are damaged cases:

- (1) Test #01 is an undamaged case and the structure is excited by 10% input Type A in global X direction only;
- (2) Test #03 is an undamaged case and the structure is excited by 25% input Type A in global X direction;
- (3) Test #07 is an undamaged case and the structure is excited by 50% input Type A in global X direction only;
- (4) Test #10 is an undamaged case and the structure is excited by 25% input Type A in global X direction, 25% input Type B in global Y direction, 25% input Type C in global Z direction;
- (5) Test #11 is an undamaged case and the structure is excited by 25% input Type A in global X direction only;
- (6) Test #15 is a damaged case and the structure is excited by 25% input Type A in global X direction, 25% input Type B in global Y direction, 25% input Type C in global Z direction. The damage is simulated by removing the south channel section from the lowest section of the north column;
- (7) Test #16 is a damaged case and the structure is excited by 25% input Type A in global X direction, 25% input Type B in global Y direction, 25% input Type C in global Z direction. The damage is simulated by (1) removing the south channel section from the lowest section of the north column and (2) removing the west channel section from the lowest section of the south column;
- (8) Test #17 is a damaged case and the structure is excited by 25% input Type A in global X direction, 25% input Type B in global Y direction, 25% input Type C in global Z direction. The damage in the model is simulated by (1) removing the south channel section from the lowest section of the north

column, (2) removing the west channel section from the lowest section of the south column and (3) removing the bottom beam component from central section of the west beam.

- (9) Test #18 is a damaged case and the structure is excited by 25% input Type A in global X direction. The damage is simulated by (1) removing the west channel section from the lowest section of the south column and (2) removing the bottom beam component from central section of the west beam.

To better illustrate the location of the damage, all the simulated damage in the structure are indicated in Figure 8.3.

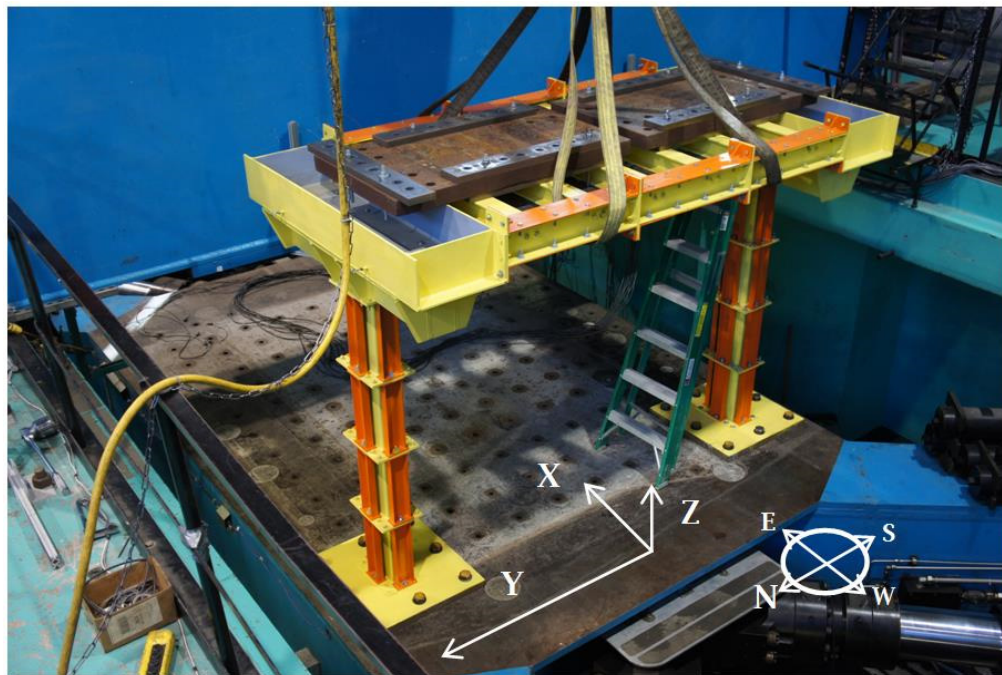


**Figure 8.1. Test Setup and Global Coordinate System (reprinted with permission from Benzon et al. 2012)**

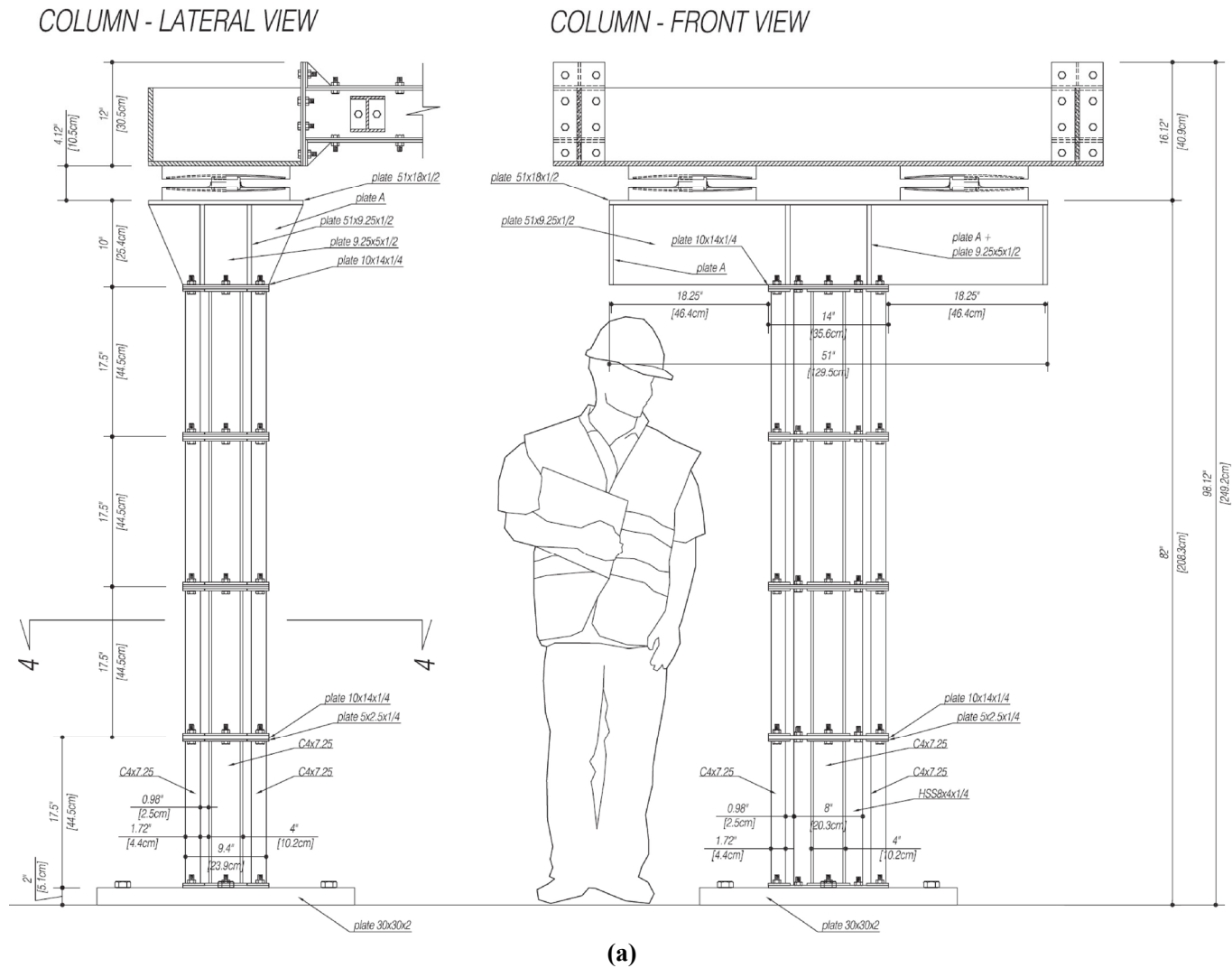
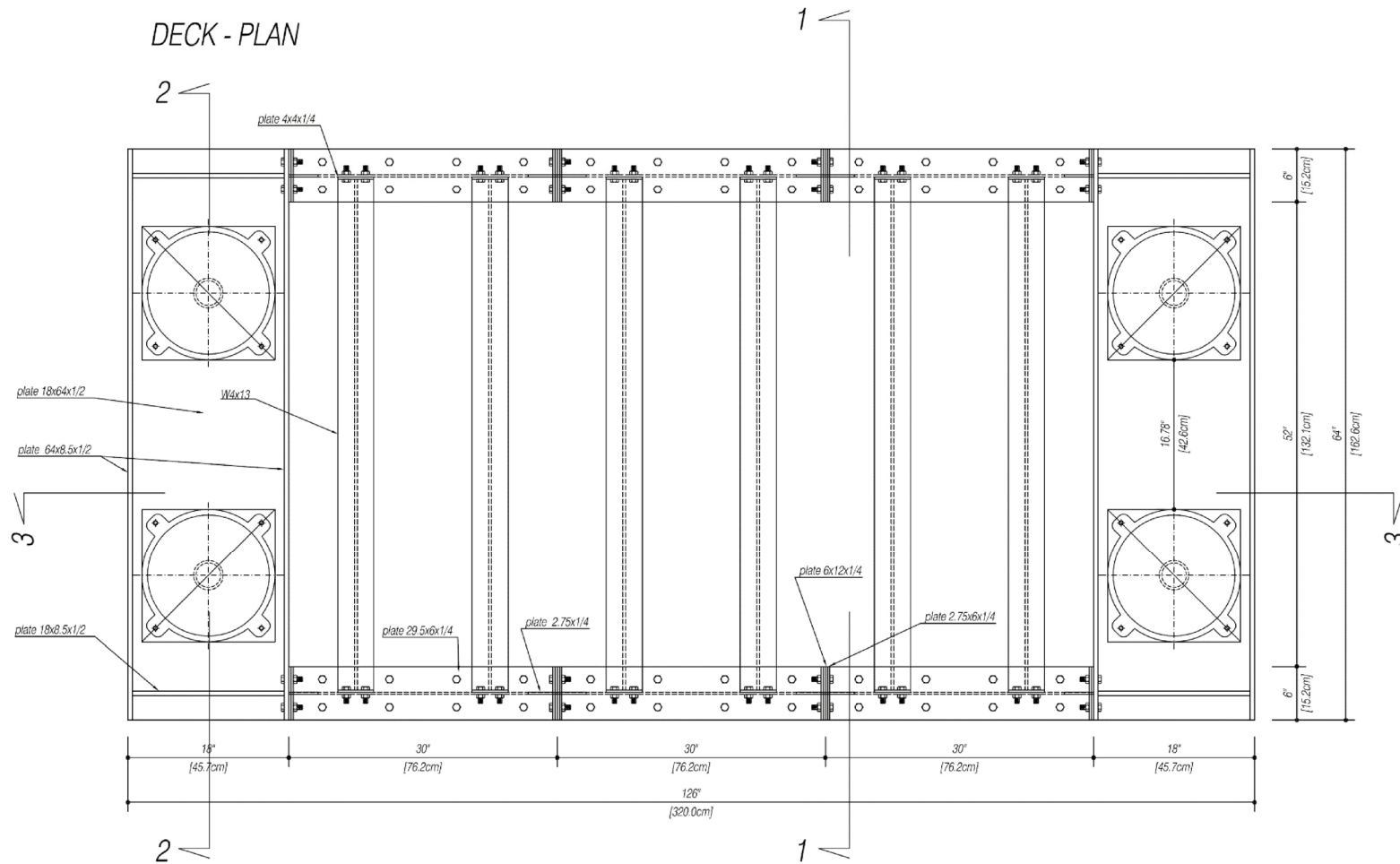


**Figure 8.2. Geometry of the Structure under Testing: (a) Geometry of Columns and (b) Geometry of Deck (reprinted with permission from Benzoni et al. 2012)**



(b)

Figure 8.2. Continued



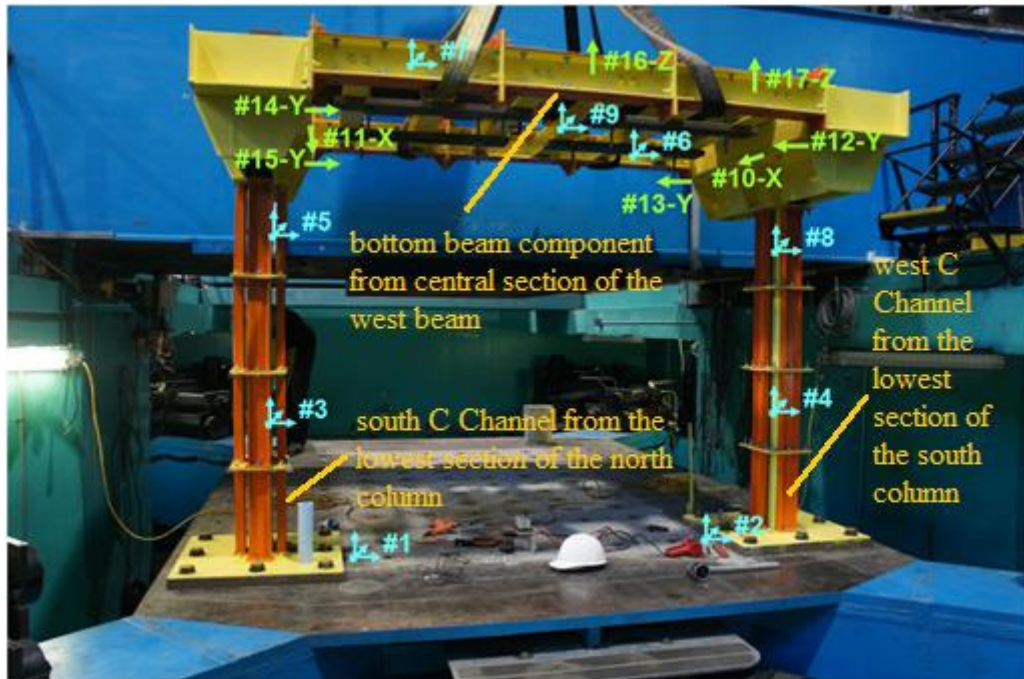


**Figure 8.3. Locations of Accelerometers and Damage Scenarios**

(Note, the original figure was copied from the report written by Dr. Benzoni et al. (2012).)

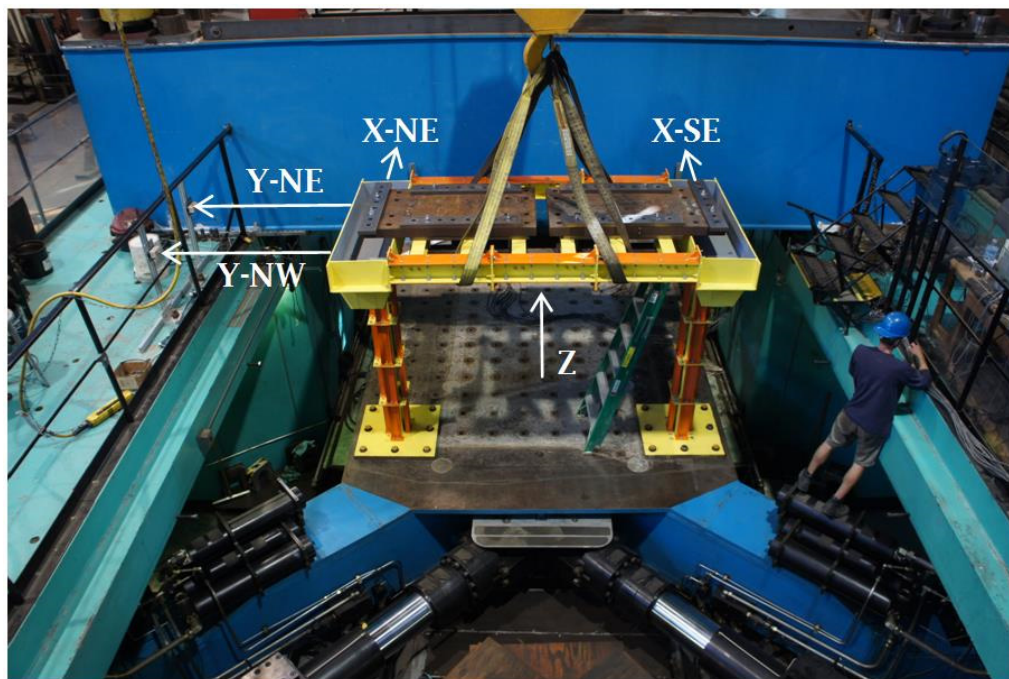


**Figure 8.4. Locations of String Pots (reprinted with permission from Benzoni et al. 2012)**

### **8.3 THEORY OF APPROACH**

From Figure 8.3, the Power Method can be applied using the data collected from tri-axial accelerometers. However, the noise level of the acceleration records from tri-axial accelerometers is much higher comparing with the noise level of the acceleration records from mono-axial accelerometers, which can be seen from Figure 8.5. The noise level of the acceleration records from tri-axial accelerometers is even higher than the acceptable noise level of the proposed method (5% to 10%). Thus, the damage detection results using the proposed method based on the data collected from the tri-axial accelerometers will be unstable and inaccurate.

From Figure 8.3, the Power Method can also be applied based on the data collected from mono-axial accelerometers. The noise level of the data collected from the mono-axial accelerometers is around 2% to 3%, which is acceptable and can be roughly seen from Figure 8.5. However, since the author has some doubt on the locations of the mono-axial accelerometers, the data collected from the mono-axial accelerometers will not be considered in the following damage detection process.

From Figure 8.4, the Power Method can also be applied based on the data collected from string pots. The noise level of the displacement records from the string pots are acceptable, which can be seen from Figure 8.10(a) and Figure 8.11(a).

Because only the data collected from the string pots at top ends of the two columns will be used to detect damage in the bridge model, the bridge model is simplified into the one-bay frame shown in Figure 8.6. The element number, joint number and element directions are also shown in Figure 8.6. Given the simplified model, the damage



detection algorithm is developed and is shown in the following paragraphs.

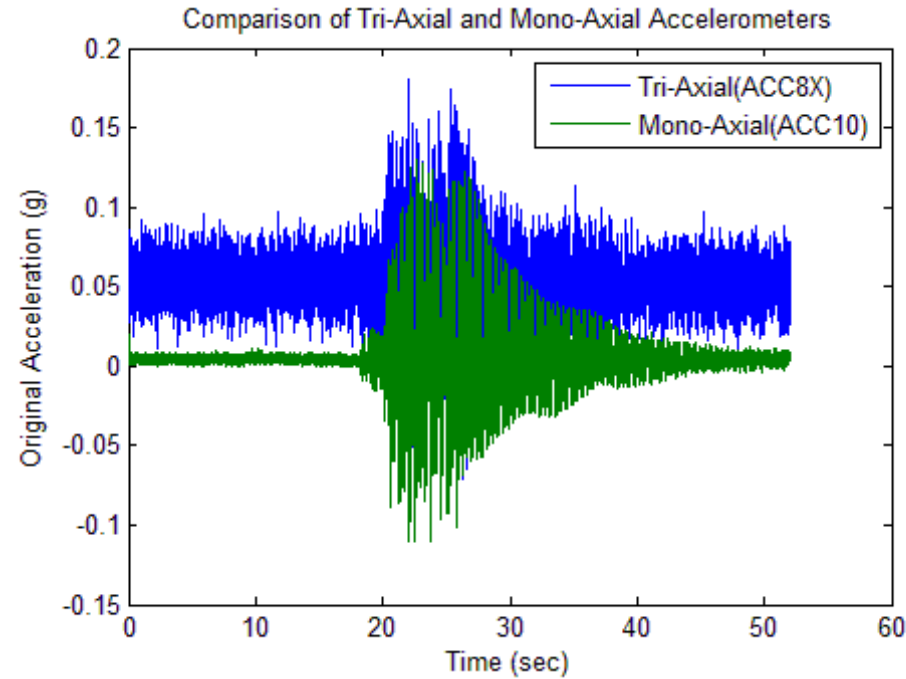


**Figure 8.5. Comparison of the Measured Accelerations from Tri-Axis and Single-Axis Accelerometers (Test #11)**

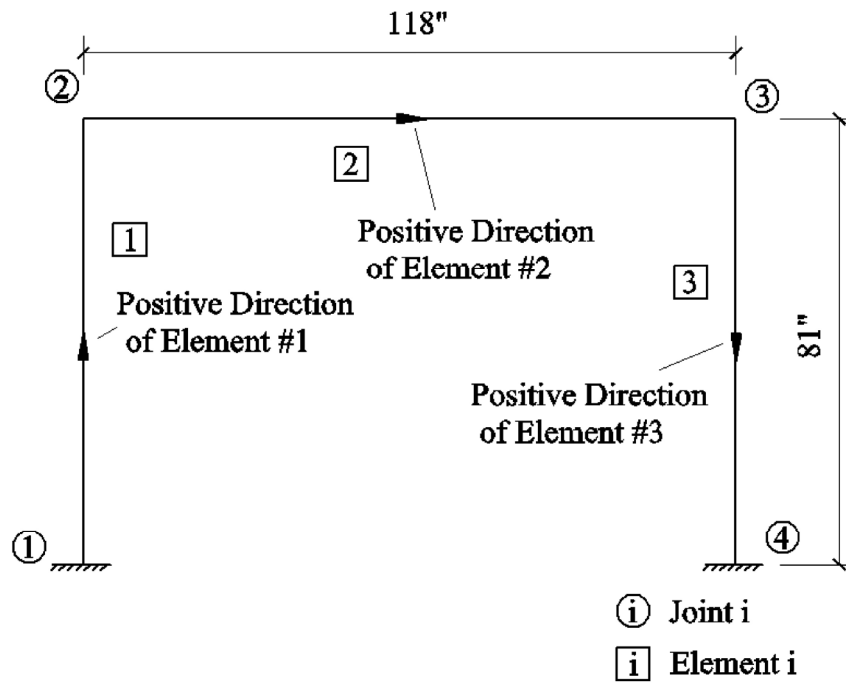


Figure 8.6. Simplified Numerical Model for the Bridge Model

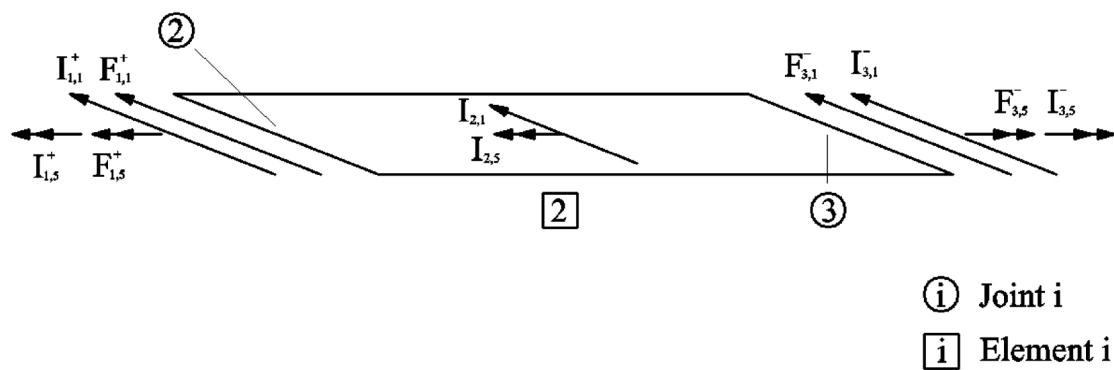


Figure 8.7. Free Body Diagram Analysis of the Deck (Element #2)

Since only the measurements of displacements in the global X direction at both ends of the columns in the bridge model satisfied the noise tolerance of the proposed method,

only the translational force and torsional moment of the deck can be estimated accurately. As shown in Figure 8.7, considering the translational force and torsional moment balance of the deck, gives

$$I_{1,1}^+ + F_{1,1}^+ + I_{2,1}^- + F_{3,1}^- = 0 \quad (8.1)$$

$$I_{1,5}^+ + F_{1,5}^+ + I_{2,5}^- - F_{3,5}^- = 0 \quad (8.2)$$

Where, the first subscript is the element number; the second subscript is the force direction: '1' represents the shear force in the global X direction and '5' represents the bending moment in the global Y direction. The superscript '+' indicates the positive end of the element and '-' indicates the negative end of the element. For example,  $I_{1,1}^+$  indicates the inertia force at the positive end of element #1 (north column) in shear force in the global X direction.

To avoid using the highly noise polluted acceleration data from the tri-axis accelerometer installed at the center of the deck, the inertia force for the deck is computed as the combination of the inertia force at the positive end of the deck and the inertia force at the negative end of the deck. Namely,

$$I_{2,1} = I_{2,1}^+ + I_{2,1}^- \quad (8.3)$$

$$I_{2,5} = I_{2,5}^+ - I_{2,5}^- \quad (8.4)$$

Note the above negative sign in Eq. 8.4 is due to the different positive direction defined for Joint 2 and Joint 3 around the global Y direction.

Substituting Eq. 8.3 and Eq. 8.4 into Eq. 8.1 and Eq. 8.2, respectively, yield,

$$I_{1,1}^+ + F_{1,1}^+ + I_{2,1}^- + I_{2,1}^+ + I_{3,1}^- + F_{3,1}^- = 0 \quad (8.5)$$

$$I_{1,5}^+ + F_{1,5}^+ + I_{2,5}^- - I_{2,5}^+ - I_{3,5}^- - F_{3,5}^- = 0 \quad (8.6)$$

The above two equations can be combined as following,

$$\begin{Bmatrix} I_{1,1}^+ \\ I_{1,5}^+ \end{Bmatrix} + \begin{Bmatrix} F_{1,1}^+ \\ F_{1,5}^+ \end{Bmatrix} + \begin{Bmatrix} I_{2,1}^- \\ I_{2,5}^- \end{Bmatrix} + \begin{bmatrix} 1 & 0 \\ 0 & -1 \end{bmatrix} \left( \begin{Bmatrix} I_{2,1}^+ \\ I_{2,5}^+ \end{Bmatrix} + \begin{Bmatrix} I_{3,1}^- \\ I_{3,5}^- \end{Bmatrix} + \begin{Bmatrix} F_{3,1}^- \\ F_{3,5}^- \end{Bmatrix} \right) = \begin{Bmatrix} 0 \\ 0 \end{Bmatrix} \quad (8.7)$$

The force components in the above expression can be computed as follows,

$$\begin{Bmatrix} I_{1,1}^+ \\ I_{1,5}^+ \end{Bmatrix} = \begin{bmatrix} m_{1,1}^+ & 0 \\ 0 & m_{1,5}^+ \end{bmatrix} \begin{Bmatrix} \ddot{\delta}_{1,1}^+ \\ \ddot{\delta}_{1,5}^+ \end{Bmatrix} \quad (8.8)$$

$$\begin{Bmatrix} I_{2,1}^- \\ I_{2,5}^- \end{Bmatrix} = \begin{bmatrix} m_{2,1}^- & 0 \\ 0 & m_{2,5}^- \end{bmatrix} \begin{Bmatrix} \ddot{\delta}_{2,1}^- \\ \ddot{\delta}_{2,5}^- \end{Bmatrix} \quad (8.9)$$

$$\begin{Bmatrix} I_{2,1}^+ \\ I_{2,5}^+ \end{Bmatrix} = \begin{bmatrix} m_{2,1}^+ & 0 \\ 0 & m_{2,5}^+ \end{bmatrix} \begin{Bmatrix} \ddot{\delta}_{2,1}^+ \\ \ddot{\delta}_{2,5}^+ \end{Bmatrix} \quad (8.10)$$

$$\begin{Bmatrix} I_{3,1}^- \\ I_{3,5}^- \end{Bmatrix} = \begin{bmatrix} m_{3,1}^- & 0 \\ 0 & m_{3,5}^- \end{bmatrix} \begin{Bmatrix} \ddot{\delta}_{3,1}^- \\ \ddot{\delta}_{3,5}^- \end{Bmatrix} \quad (8.11)$$

$$\begin{Bmatrix} F_{1,1}^+ \\ F_{1,5}^+ \end{Bmatrix} = \left( \frac{E_1 I_1}{L_1^3} \right) \begin{bmatrix} -12 & -6L_1 & 12 & -6L_1 \\ 6L_1 & 2L_1^2 & -6L_1 & 4L_1^2 \end{bmatrix} \begin{Bmatrix} \delta_{1,1}^- \\ \delta_{1,5}^- \\ \delta_{1,1}^+ \\ \delta_{1,5}^+ \end{Bmatrix} \quad (8.12)$$

$$\begin{Bmatrix} F_{3,1}^- \\ F_{3,5}^- \end{Bmatrix} = \left( \frac{E_3 I_3}{L_3^3} \right) \begin{bmatrix} 12 & 6L_3 & -12 & 6L_3 \\ 6L_3 & 4L_3^2 & -6L_3 & 2L_3^2 \end{bmatrix} \begin{Bmatrix} \delta_{3,1}^- \\ \delta_{3,5}^- \\ \delta_{3,1}^+ \\ \delta_{3,5}^+ \end{Bmatrix} \quad (8.13)$$

Where  $m_{i,1}^+$  and  $m_{i,1}^-$  represent the mass at the positive and negative ends of Element  $i$  along the global X axis direction, respectively;  $m_{i,5}^+$  and  $m_{i,5}^-$  represents the mass

moment of inertia at the positive and negative ends of Element  $i$  for the rotations about the global Y axis direction, respectively;  $\ddot{\delta}_{i,1}^+$  and  $\ddot{\delta}_{i,1}^-$  are the accelerations at the positive and negative ends of Element  $i$  along the global X axis direction, respectively;  $\ddot{\delta}_{1,5}^+$  and  $\ddot{\delta}_{1,5}^-$  are the angular accelerations at the positive and negative ends of Element  $i$  for the rotations about the global Y axis direction, respectively;  $\delta_{i,1}^+$  and  $\delta_{i,1}^-$  are the displacements at the positive and negative ends of Element  $i$  along the global X axis direction, respectively;  $\delta_{1,5}^+$  and  $\delta_{1,5}^-$  are the rotations at the positive and negative ends of Element  $i$  around the global Y axis direction, respectively.

Substituting Eq. 8.8 through Eq. 8.13 into Eq. 8.7 yields,

$$\begin{aligned}
& \begin{bmatrix} m_{1,1}^+ & 0 \\ 0 & m_{1,5}^+ \end{bmatrix} \begin{Bmatrix} \ddot{\delta}_{1,1}^+ \\ \ddot{\delta}_{1,5}^+ \end{Bmatrix} + \left( \frac{E_1 I_1}{L_1^3} \right) \begin{bmatrix} -12 & -6L_1 & 12 & -6L_1 \\ 6L_1 & 2L_1^2 & -6L_1 & 4L_1^2 \end{bmatrix} \begin{Bmatrix} \delta_{1,1}^- \\ \delta_{1,5}^- \\ \delta_{1,1}^+ \\ \delta_{1,5}^+ \end{Bmatrix} \\
& + \begin{bmatrix} m_{2,1}^- & 0 \\ 0 & m_{2,5}^- \end{bmatrix} \begin{Bmatrix} \ddot{\delta}_{2,1}^- \\ \ddot{\delta}_{2,5}^- \end{Bmatrix} + \begin{bmatrix} m_{2,1}^+ & 0 \\ 0 & -m_{2,5}^+ \end{bmatrix} \begin{Bmatrix} \ddot{\delta}_{2,1}^+ \\ \ddot{\delta}_{2,5}^+ \end{Bmatrix} + \begin{bmatrix} m_{3,1}^- & 0 \\ 0 & -m_{3,5}^- \end{bmatrix} \begin{Bmatrix} \ddot{\delta}_{3,1}^- \\ \ddot{\delta}_{3,5}^- \end{Bmatrix} \\
& + \left( \frac{E_3 I_3}{L_3^3} \right) \begin{bmatrix} 1 & 0 \\ 0 & -1 \end{bmatrix} \begin{bmatrix} 12 & 6L_3 & -12 & 6L_3 \\ 6L_3 & 4L_3^2 & -6L_3 & 2L_3^2 \end{bmatrix} \begin{Bmatrix} \delta_{3,1}^- \\ \delta_{3,5}^- \\ \delta_{3,1}^+ \\ \delta_{3,5}^+ \end{Bmatrix} = 0
\end{aligned} \tag{8.14}$$

Given the configuration of the structure, for  $i=1, 2$  and  $j=1, 5$ ,

$$\ddot{\delta}_{i,j}^+ = \ddot{\delta}_{i+1,j}^- = \ddot{\delta}_j^{i+1} \tag{8.15}$$

Where  $\ddot{\delta}_j^{i+1}$  is the acceleration at Node  $(i+1)$  along the direction indicated by the subscript “j”.

Substituting Eq. 8.15 into Eq. 8.14, yields,

$$\begin{aligned}
& \begin{bmatrix} m_{1,1}^+ + m_{2,1}^- & 0 \\ 0 & m_{1,5}^+ + m_{2,5}^- \end{bmatrix} \begin{Bmatrix} \ddot{\delta}_1^2 \\ \ddot{\delta}_5^2 \end{Bmatrix} + \left( \frac{E_1 I_1}{L_1^3} \right) \begin{bmatrix} -12 & -6L_1 & 12 & -6L_1 \\ 6L_1 & 2L_1^2 & -6L_1 & 4L_1^2 \end{bmatrix} \begin{Bmatrix} \delta_{1,1}^- \\ \delta_{1,5}^- \\ \delta_{1,1}^+ \\ \delta_{1,5}^+ \end{Bmatrix} \\
& + \begin{bmatrix} 1 & 0 \\ 0 & -1 \end{bmatrix} \begin{bmatrix} m_{2,1}^+ + m_{3,1}^- & 0 \\ 0 & m_{2,5}^+ + m_{3,5}^- \end{bmatrix} \begin{Bmatrix} \ddot{\delta}_1^3 \\ \ddot{\delta}_5^3 \end{Bmatrix} \\
& + \left( \frac{E_3 I_3}{L_3^3} \right) \begin{bmatrix} 1 & 0 \\ 0 & -1 \end{bmatrix} \begin{bmatrix} 12 & 6L_3 & -12 & 6L_3 \\ 6L_3 & 4L_3^2 & -6L_3 & 2L_3^2 \end{bmatrix} \begin{Bmatrix} \delta_{3,1}^- \\ \delta_{3,5}^- \\ \delta_{3,1}^+ \\ \delta_{3,5}^+ \end{Bmatrix} = 0
\end{aligned} \tag{8.16}$$

Define,

$$m_{1,1}^+ + m_{2,1}^- = m_1^2 \tag{8.17}$$

$$m_{1,5}^+ + m_{2,5}^- = m_5^2 \tag{8.18}$$

$$m_{2,1}^+ + m_{3,1}^- = m_1^3 \tag{8.19}$$

$$m_{2,5}^+ + m_{3,5}^- = m_5^3 \tag{8.20}$$

$$k_i = \left( \frac{E_i I_i}{L_i^3} \right) \tag{8.21}$$

$$[K_{o,1}] = \begin{bmatrix} -12 & -6L_1 & 12 & -6L_1 \\ 6L_1 & 2L_1^2 & -6L_1 & 4L_1^2 \end{bmatrix} \tag{8.22}$$

$$[K_{o,2}] = \begin{bmatrix} 12 & 6L_3 & -12 & 6L_3 \\ 6L_3 & 4L_3^2 & -6L_3 & 2L_3^2 \end{bmatrix} \tag{8.23}$$

$$\{\delta_i\} = \begin{Bmatrix} \delta_{i,1}^- \\ \delta_{i,5}^- \\ \delta_{i,1}^+ \\ \delta_{i,5}^+ \end{Bmatrix} \quad (8.24)$$

$$[R_3] = \begin{bmatrix} 1 & 0 \\ 0 & -1 \end{bmatrix} \quad (8.25)$$

Substituting Eq. 8.17 through Eq. 8.25 into Eq. 8.16, yields,

$$\begin{bmatrix} m_1^2 & 0 \\ 0 & m_5^2 \end{bmatrix} \begin{Bmatrix} \ddot{\delta}_1^2 \\ \ddot{\delta}_5^2 \end{Bmatrix} + k_1 [K_{o,1}] \{\delta_1\} + [R_3] \begin{bmatrix} m_1^3 & 0 \\ 0 & m_5^3 \end{bmatrix} \begin{Bmatrix} \ddot{\delta}_1^3 \\ \ddot{\delta}_5^3 \end{Bmatrix} + k_3 [R_3] [K_{o,2}] \{\delta_3\} = 0 \quad (8.26)$$

Ignore the mass moment of inertia in Eq. 8.26, yields,

$$\begin{bmatrix} m_1^2 & 0 \\ 0 & 0 \end{bmatrix} \begin{Bmatrix} \ddot{\delta}_1^2 \\ \ddot{\delta}_5^2 \end{Bmatrix} + k_1 [K_{o,1}] \{\delta_1\} + [R_3] \begin{bmatrix} m_1^3 & 0 \\ 0 & 0 \end{bmatrix} \begin{Bmatrix} \ddot{\delta}_1^3 \\ \ddot{\delta}_5^3 \end{Bmatrix} + k_3 [R_3] [K_{o,2}] \{\delta_3\} = 0 \quad (8.27)$$

Define

$$[M_o] = \begin{bmatrix} 1 & 0 \\ 0 & 0 \end{bmatrix} \quad (8.28)$$

Then Eq. 8.27 can be rewritten as,

$$m_1^2 [M_o] \{\ddot{\delta}^2\} + k_1 [K_{o,1}] \{\delta_1\} + m_1^3 [R_3] [M_o] \{\ddot{\delta}^3\} + k_3 [R_3] [K_{o,2}] \{\delta_3\} = 0 \quad (8.29)$$

Consider the following vector as the velocity vector used to compute power that will be used in the Power Method analysis.

$$\{\dot{\Delta}\} = \begin{Bmatrix} \dot{\Delta}_1^2 \\ \dot{\Delta}_1^3 \end{Bmatrix} \quad (8.30)$$

Multiplying Eq. 8.29 by the velocity vector used to compute power (i.e. Eq. 8.30) yields,

$$\begin{aligned} m_1^2 \{\dot{\Delta}\} [M_o] \{\ddot{\delta}^2\} + k_1 \{\dot{\Delta}\} [K_{o,1}] \{\delta_1\} + m_1^3 \{\dot{\Delta}\} [R_3] [M_o] \{\ddot{\delta}^3\} \\ + k_3 \{\dot{\Delta}\} [R_3] [K_{o,2}] \{\delta_3\} = 0 \end{aligned} \quad (8.31)$$

Rearrange the Eq. 8.31 yields,

$$\begin{aligned} m_1^2 \{\dot{\Delta}\} [M_o] \{\ddot{\delta}^2\} + k_1 \{\dot{\Delta}\} [K_{o,1}] \{\delta_1\} + k_3 \{\dot{\Delta}\} [R_3] [K_{o,2}] \{\delta_3\} \\ = -m_1^3 \{\dot{\Delta}\} [R_3] [M_o] \{\ddot{\delta}^3\} \end{aligned} \quad (8.32)$$

Dividing Eq. 8.32 by  $m_1^3$  yields,

$$\begin{aligned} \frac{m_1^2}{m_1^3} \{\dot{\Delta}\} [M_o] \{\ddot{\delta}^2\} + \frac{k_1}{m_1^3} \{\dot{\Delta}\} [K_{o,1}] \{\delta_1\} + \frac{k_3}{m_1^3} \{\dot{\Delta}\} [R_3] [K_{o,2}] \{\delta_3\} \\ = -\{\dot{\Delta}\} [R_3] [M_o] \{\ddot{\delta}^3\} \end{aligned} \quad (8.33)$$

Define the following coefficients,

$$\beta_1 = \frac{m_1^2}{m_1^3} \quad (8.34)$$

$$\beta_2 = \frac{k_1}{m_1^3} \quad (8.35)$$

$$\beta_3 = \frac{k_3}{m_1^3} \quad (8.36)$$

Substituting Eq. 8.34 through Eq. 8.36 into Eq. 8.33 yields,



$$\begin{aligned} & \beta_1 \{\dot{\Delta}\} [M_o] \{\ddot{\delta}^2\} + \beta_2 \{\dot{\Delta}\} [K_{o,1}] \{\delta_1\} + \beta_3 \{\dot{\Delta}\} [R_3] [K_{o,2}] \{\delta_3\} \\ & = -\{\dot{\Delta}\} [R_3] [M_o] \{\ddot{\delta}^3\} \end{aligned} \quad (8.37)$$

Writing the Eq. 8.37 at different time points yields the following groups of equations,

For  $t = t_0$ ,

$$\begin{aligned} & \beta_1 (\{\dot{\Delta}\} [M_o] \{\ddot{\delta}^2\})|_{t_0} + \beta_2 (\{\dot{\Delta}\} [K_{o,1}] \{\delta_1\})|_{t_0} + \beta_3 (\{\dot{\Delta}\} [R_3] [K_{o,2}] \{\delta_3\})|_{t_0} \\ & = -(\{\dot{\Delta}\} [R_3] [M_o] \{\ddot{\delta}^3\})|_{t_0} \end{aligned} \quad (8.38)$$

For  $t = t_j$ ,

$$\begin{aligned} & \beta_1 (\{\dot{\Delta}\} [M_o] \{\ddot{\delta}^2\})|_{t_j} + \beta_2 (\{\dot{\Delta}\} [K_{o,1}] \{\delta_1\})|_{t_j} + \beta_3 (\{\dot{\Delta}\} [R_3] [K_{o,2}] \{\delta_3\})|_{t_j} \\ & = -(\{\dot{\Delta}\} [R_3] [M_o] \{\ddot{\delta}^3\})|_{t_j} \end{aligned} \quad (8.39)$$

For  $t = t_N$ ,

$$\begin{aligned} & \beta_1 (\{\dot{\Delta}\} [M_o] \{\ddot{\delta}^2\})|_{t_N} + \beta_2 (\{\dot{\Delta}\} [K_{o,1}] \{\delta_1\})|_{t_N} + \beta_3 (\{\dot{\Delta}\} [R_3] [K_{o,2}] \{\delta_3\})|_{t_N} \\ & = -(\{\dot{\Delta}\} [R_3] [M_o] \{\ddot{\delta}^3\})|_{t_N} \end{aligned} \quad (8.40)$$

Arranging the above linear equation group into matrix form, yields,

$$\mathbf{X}\boldsymbol{\beta} = \mathbf{Y} \quad (8.41)$$

Where the coefficient matrix of the linear equation group is given as followings,

$$\mathbf{X} = \begin{bmatrix} (\{\dot{\Delta}\}[M_o]\{\ddot{\delta}^2\})|_{t_0} & (\{\dot{\Delta}\}[K_{o,1}]\{\delta_1\})|_{t_0} & (\{\dot{\Delta}\}[R_3][K_{o,2}]\{\delta_3\})|_{t_0} \\ \vdots & \vdots & \vdots \\ (\{\dot{\Delta}\}[M_o]\{\ddot{\delta}^2\})|_{t_j} & (\{\dot{\Delta}\}[K_{o,1}]\{\delta_1\})|_{t_j} & (\{\dot{\Delta}\}[R_3][K_{o,2}]\{\delta_3\})|_{t_j} \\ \vdots & \vdots & \vdots \\ (\{\dot{\Delta}\}[M_o]\{\ddot{\delta}^2\})|_{t_N} & (\{\dot{\Delta}\}[K_{o,1}]\{\delta_1\})|_{t_N} & (\{\dot{\Delta}\}[R_3][K_{o,2}]\{\delta_3\})|_{t_N} \end{bmatrix} \quad (8.42)$$

The vector of unknown and the vector of known are given as followings,

$$\boldsymbol{\beta} = \begin{Bmatrix} \beta_1 \\ \beta_2 \\ \beta_3 \end{Bmatrix} \quad (8.43)$$

$$\mathbf{Y} = \begin{Bmatrix} -(\{\dot{\Delta}\}[R_3][M_o]\{\ddot{\delta}^3\})|_{t_0} \\ \vdots \\ -(\{\dot{\Delta}\}[R_3][M_o]\{\ddot{\delta}^3\})|_{t_j} \\ \vdots \\ -(\{\dot{\Delta}\}[R_3][M_o]\{\ddot{\delta}^3\})|_{t_N} \end{Bmatrix} \quad (8.44)$$

Using the Least Square Method, the vector of unknown, ' $\boldsymbol{\beta}$ ', can be computed from the following equation,

$$\boldsymbol{\beta} = (\mathbf{X}^T \mathbf{X})^{-1} (\mathbf{X}^T \mathbf{Y}) \quad (8.45)$$

With the vector of unknown computed, the damage indices for stiffness, mass and damping can be computed as followings,

$$\beta_{m_1} = \frac{m_1^2}{m_1^3} = \beta_1 \quad (8.46)$$

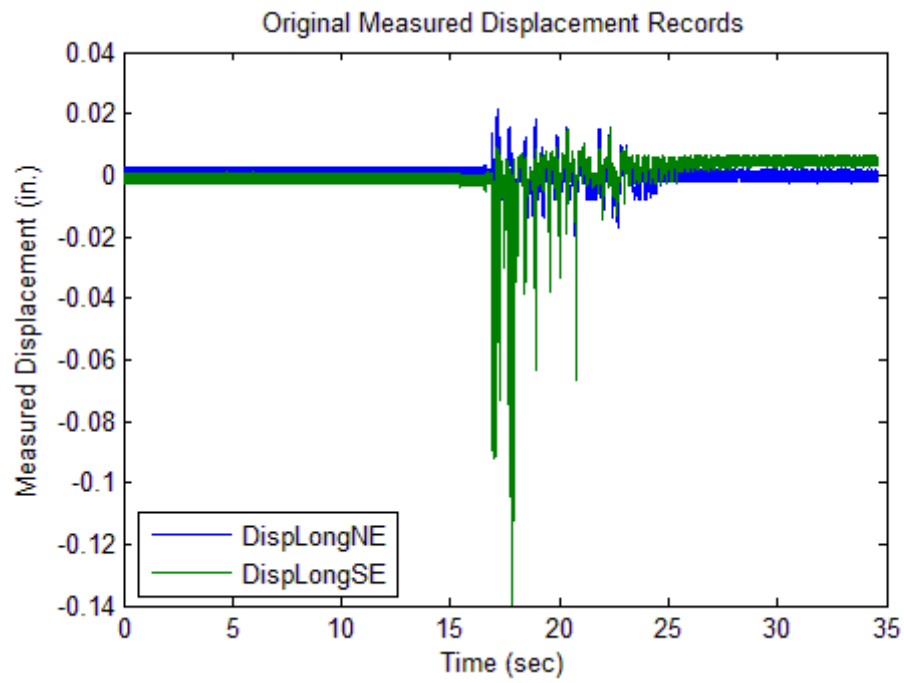
$$\beta_k = \frac{k_1}{k_3} = \frac{\frac{k_1}{m_1^3}}{\frac{k_3}{m_1^3}} = \frac{\beta_2}{\beta_3} \quad (8.47)$$

## 8.4 EXPERIMENTAL DATA PROCESSING

### 8.4.1 Introduction

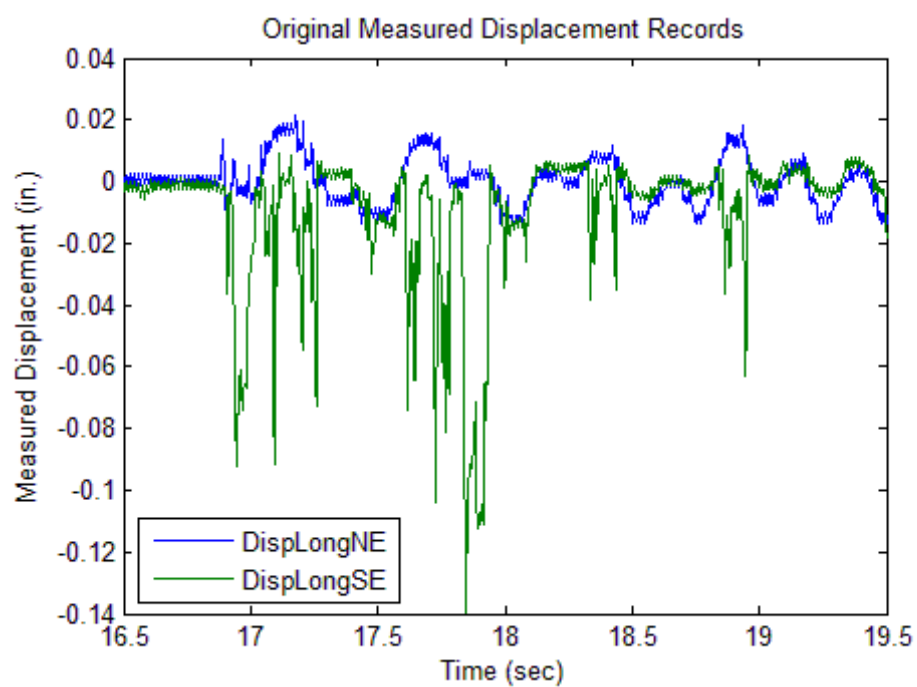
As stated previously, the data that will be used in the damage detection process is the data collected from the string pots at the top ends of the two columns. The displacement feedback from the shake table will be used as the base displacements of the two columns. For illustration purposes, the recorded displacement time histories from Test #01, Test #03, Test #07, and Test #16 are plotted in Figure 8.8 through Figure 8.11. From the Figure 8.8 and Figure 8.9, it's obvious that the displacement time histories from Test #01 and Test #03 are greatly influenced by noise. Consequently, Test #01 and Test #03 won't be taken into consideration for the later damage detection process. In the plotted displacement time histories, the noise level of one record can be seen from the beginning and ending of the plotted data, when the structure was in static situation. For example, the noise level of the displacements measured from Test #01 can be seen from the first fifteen seconds and the last 5 seconds in Figure 8.8(a). However, there might be other type of noise in the measured displacement records, which can be seen from the sudden changes of the measured displacement curve at the southeast corner of the desk in Figure 8.8(b) and Figure 8.9(b). Also from the plotted displacement time histories, the recorded time histories are observed to be shifted up or down by a small constant, which can be observed from Figure 8.8 (a). The constant mixed in the displacement records are considered to be initial zero setting problems. To reduce the noise levels and eliminate

the constant components from the measured displacement time histories, digital bandpass filters were used to process the data. To achieve better results, the average value will be deducted from each displacement record before the digital bandpass filter is applied.



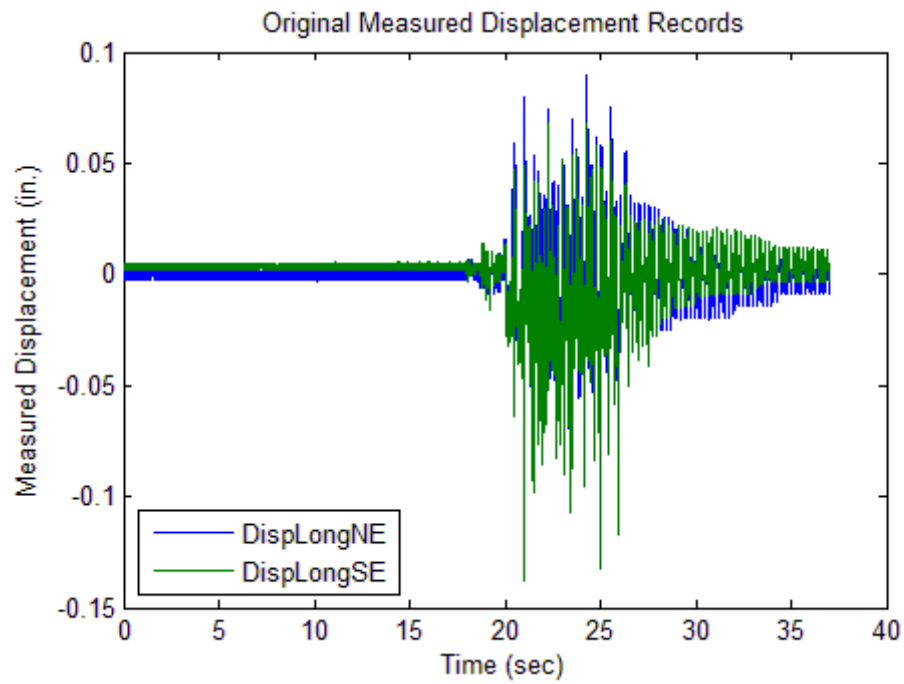
(a)

**Figure 8.8. Measured Displacement Time Histories by String Pots from Test #01: (a) Full Plot and (b) Zoomed in Plot**

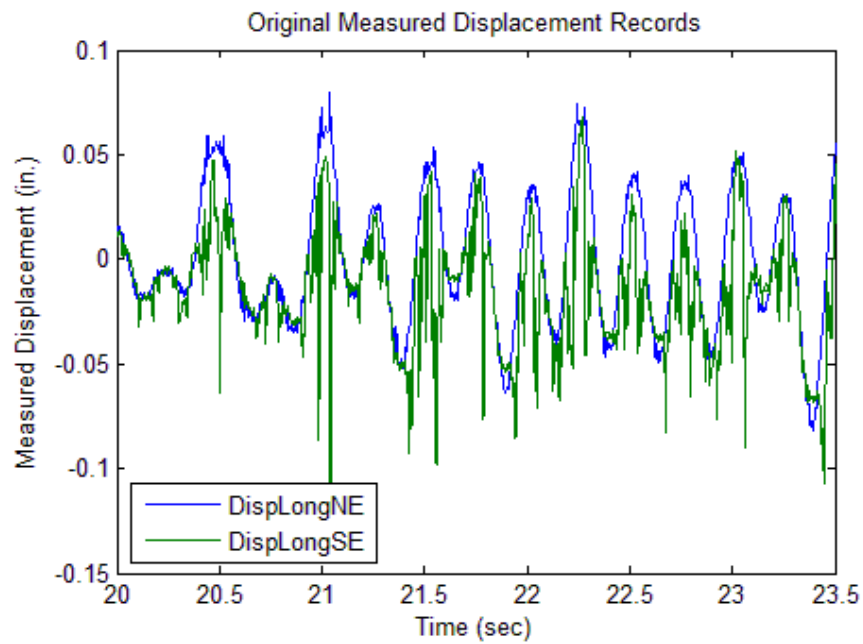


(b)

Figure 8.8. Continued

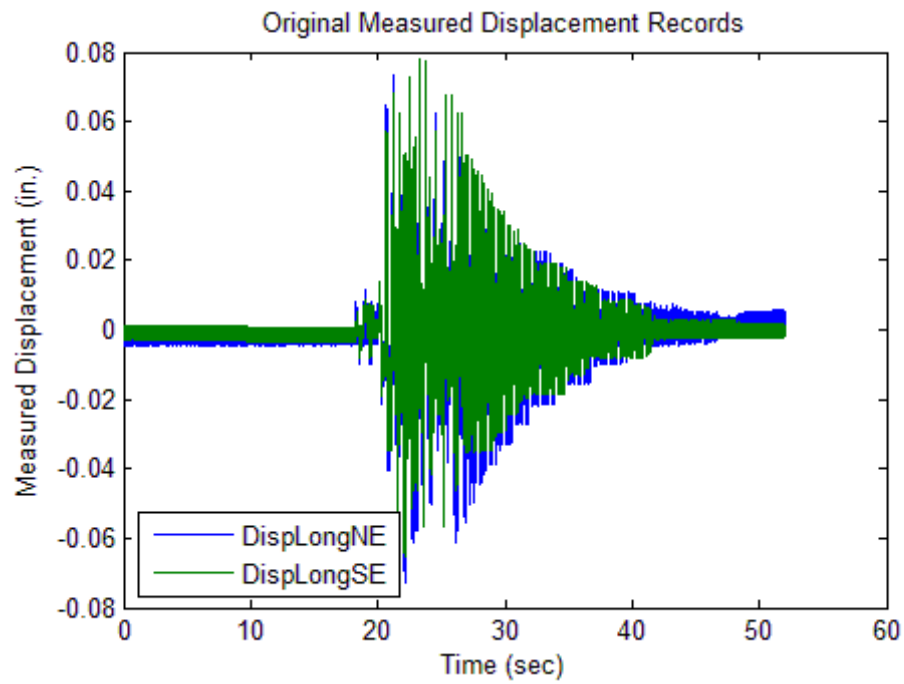


(a)

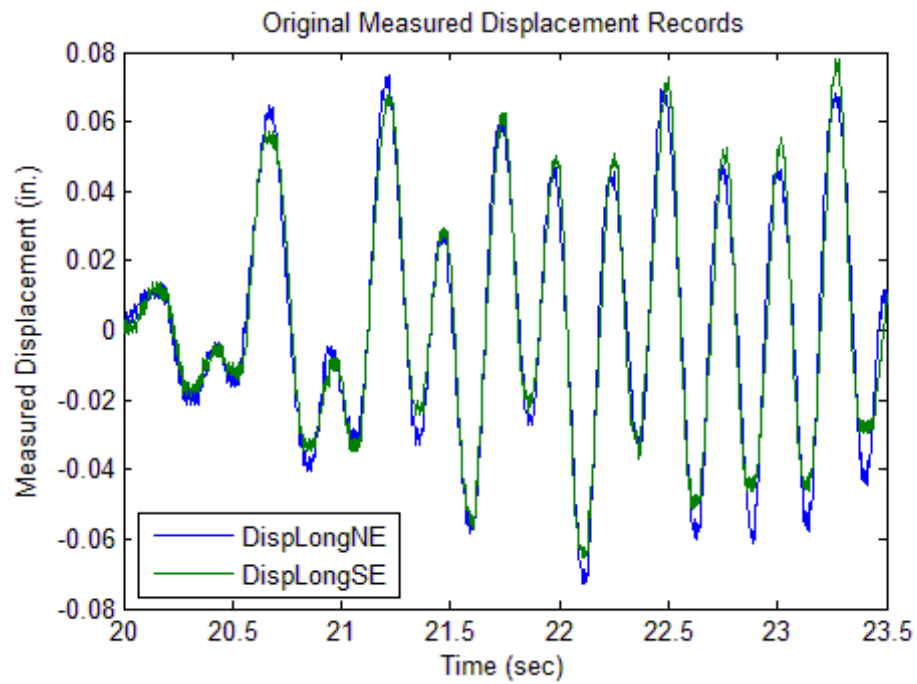


(b)

Figure 8.9. Measured Displacement Time Histories by String Pots from Test #03: (a) Full Plot and (b) Zoomed in Plot

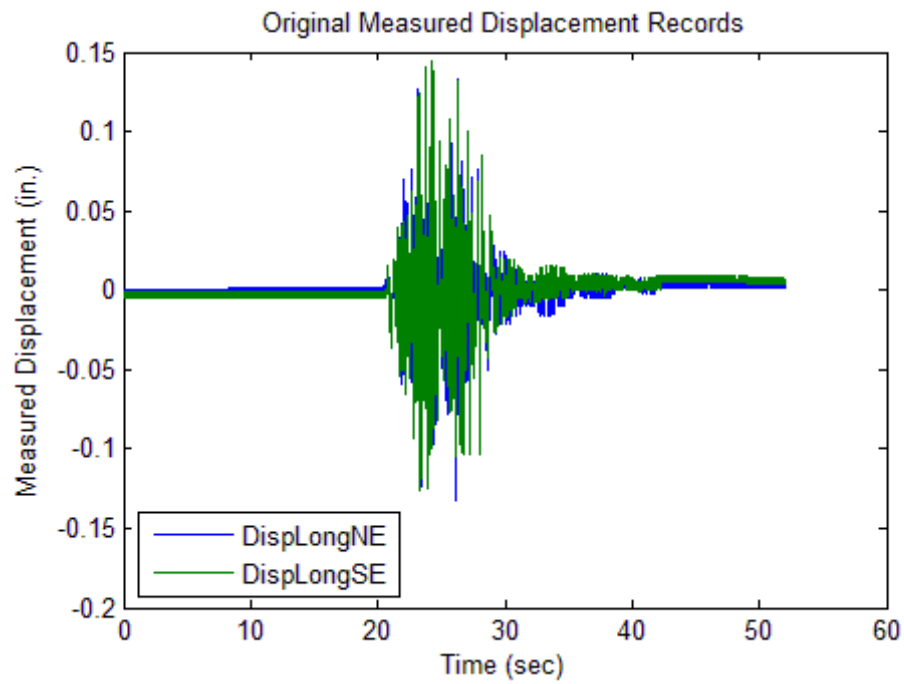


(a)

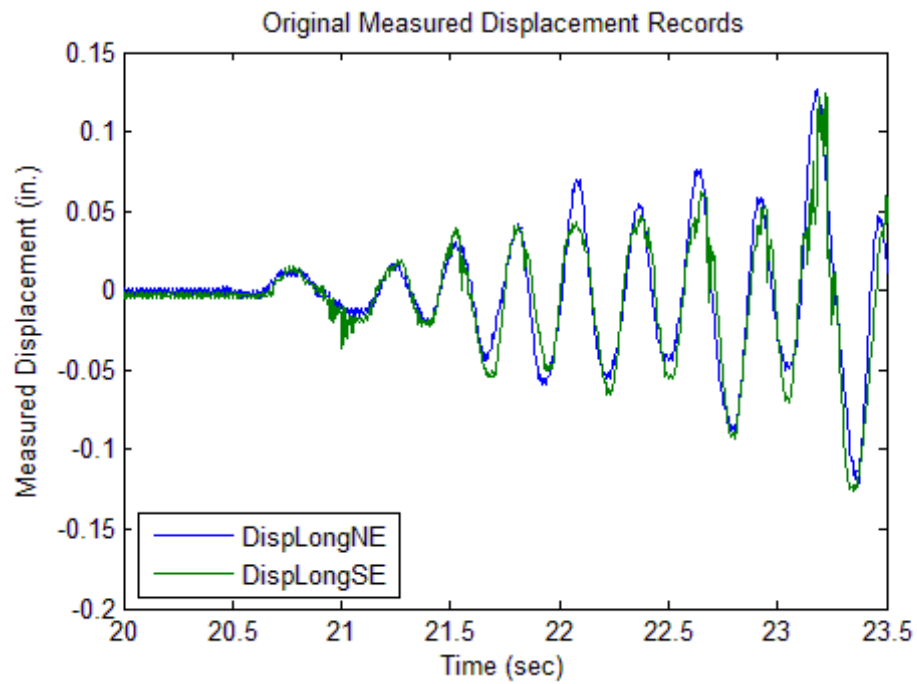


(b)

**Figure 8.10. Measured Displacement Time Histories by String Pots from Test #11: (a) Full Plot and (b) Zoomed in Plot**



(a)



(b)

**Figure 8.11. Measured Displacement Time Histories by String Pots from Test #16: (a) Full Plot and (b) Zoomed in Plot**



#### **8.4.2 Joint Motion Estimation**

To compute the shear forces and moments at the ends of the two columns, the following dynamic data at the top ends of the two columns are required: the joint rotations, joint angular velocities, joint angular accelerations around the global Y direction and joint translational displacements, joint translational velocities and joint translational accelerations in global X direction. However, only the joint translational displacements can be measured by the string pots at the northeast and southeast corners of the deck. The other joint motions will be estimated based on the measured displacement data at the two ends of the columns. Besides the author's doubt on the locations of the mono-axis accelerometers, the other reasons why the measured acceleration records are not used here are:

- (1) The locations of the accelerometers and string pots are not sufficiently close to each other; and
- (2) The noise within the measured accelerations and measured displacements are not the same due to the difference of the measuring instruments.

Due to the above two reasons, the damage indices based on the measured displacements and measured accelerations are not as stable as the damage indices based solely on measured displacements.

In order to compute joint angular velocities and joint angular accelerations, the joint translational velocities and joint translational accelerations should be estimated from measured displacement data. The joint translational velocity time histories are estimated based on the measured displacement time histories, using,

$$\dot{\delta}(t_1) = -\dot{\delta}(t_0) + \frac{2(\delta(t_1) - \delta(t_0))}{(t_1 - t_0)} \quad (8.48)$$

Where, the initial displacement and initial velocity are zeros for the shake table test.

Namely,  $\delta(0) = 0$ ,  $\dot{\delta}(0) = 0$ ,  $(t_1 - t_0) = dt = 0.002$  sec.

The joint translational acceleration time histories are estimated based on the joint translational velocity time histories using,

$$\ddot{\delta}(t_1) = -\ddot{\delta}(t_0) + \frac{2(\dot{\delta}(t_1) - \dot{\delta}(t_0))}{(t_1 - t_0)} \quad (8.49)$$

Where, the initial velocity and initial acceleration are zeros for the shake table test.

Namely,  $\dot{\delta}(0) = 0$ ,  $\ddot{\delta}(0) = 0$ ,  $(t_1 - t_0) = dt = 0.002$  sec.

Given the joint translational motions, the joint rotational motions can be estimated. In the current study, the joint rotational motions (i.e. joint rotations, joint angular velocities and joint angular accelerations) at the ends of the two columns are estimated using cubic interpolation and finite difference methods. To simulate the fixed bottom joints of the two columns, a pseudo joint, which shares the same motion (i.e. displacements, velocities and accelerations) as the base joint, is used and is assumed two inches beneath the base joint of each column. Given the joint translational motions at the pseudo joint, base joint and top end joint of each column, the deflection curve of each column at each time point is described using the cubic interpolation at each 0.05 inches. The joint rotations, joint angular velocities and joint angular accelerations at the top of the columns are estimated using the following finite difference equations based on the interpolated displacements, velocities and accelerations,

$$\delta_{1,5}\Big|_{z=L_1} = \frac{\delta_{1,1}\Big|_{z=L_1} - \delta_{1,1}\Big|_{z=L_1-dz}}{dz} = \delta_5^2 \quad (8.50)$$

$$\delta_{3,5}\Big|_{z=L_1} = -\frac{\delta_{3,1}\Big|_{z=L_1} - \delta_{3,1}\Big|_{z=L_1-dz}}{dz} = \delta_5^3 \quad (8.51)$$

$$\dot{\delta}_{1,5}\Big|_{z=L_1} = \frac{\dot{\delta}_{1,1}\Big|_{z=L_1} - \dot{\delta}_{1,1}\Big|_{z=L_1-dz}}{dz} = \dot{\delta}_5^2 \quad (8.52)$$

$$\dot{\delta}_{3,5}\Big|_{z=L_1} = -\frac{\dot{\delta}_{3,1}\Big|_{z=L_1} - \dot{\delta}_{3,1}\Big|_{z=L_1-dz}}{dz} = \dot{\delta}_5^3 \quad (8.53)$$

$$\ddot{\delta}_{1,5}\Big|_{z=L_1} = \frac{\ddot{\delta}_{1,1}\Big|_{z=L_1} - \ddot{\delta}_{1,1}\Big|_{z=L_1-dz}}{dz} = \ddot{\delta}_5^2 \quad (8.54)$$

$$\ddot{\delta}_{3,5}\Big|_{z=L_1} = -\frac{\ddot{\delta}_{3,1}\Big|_{z=L_1} - \ddot{\delta}_{3,1}\Big|_{z=L_1-dz}}{dz} = \ddot{\delta}_5^3 \quad (8.55)$$

Where  $dz$  is the interpolation spacing for the cubic interpolation and is set to be 0.05 inches in this case;  $L_1$  is the length of the column;  $\delta_{i,5}\Big|_z$ ,  $\dot{\delta}_{i,5}\Big|_z$ , and  $\ddot{\delta}_{i,5}\Big|_z$  are the joint rotation, joint angular velocity, and joint angular acceleration around the global Y direction (indicated by subscript ‘5’) of Element #i at the height of  $z$ ;  $\delta_{i,1}\Big|_z$ ,  $\dot{\delta}_{i,1}\Big|_z$ , and  $\ddot{\delta}_{i,1}\Big|_z$  are the translational displacement, velocity, and acceleration along the global X direction (indicated by subscript ‘1’) of Element #i at the height of  $z$ .

### 8.4.3 General Data Processing Procedures

In order to apply the proposed method to detect damage in the bridge model using only the measured displacement records at both ends of the columns, the measured displacement records need to be filtered and other joint motions, such as joint

translational acceleration and joint rotations, need to be estimated. The general data processing procedures, used in the current study, are summarized as follows,

- (1) Plot the power spectrum densities of the measured joint translational displacement time histories at both ends of each column and design the digital bandpass filter to filter out the first bending mode, which is indicated by the highest peak in the power spectrum densities plot;
- (2) Compute the filtered displacements by applying the designed filter from Step (1) to the measured displacement time histories;
- (3) Compute joint translational velocities using Eq. 8.48 and compute joint translational accelerations using Eq. 8.49;
- (4) Compute the filtered translational velocities and filtered translational acceleration using digital bandpass filters;
- (5) Compute joint rotations, joint angular velocities and joint angular accelerations using Eq. 8.50 to Eq. 8.55;
- (6) Input the computed filtered joint translational displacements, accelerations, joint rotations and joint angular accelerations into Eq. 8.42 and Eq. 8.44 and compute the coefficients of the linear equation group by using Eq. 8.45; and
- (7) Compute the damage indices for mass and stiffness using Eq. 8.46 and Eq. 8.47.

## **8.5 DAMAGE EVALUATION OF THE SHAKE TABLE TESTS**

According to the general data processing procedures introduced in Section 8.4.3, the power spectrum density for the original measured displacement time histories were plotted and passband of the digital filter were selected. For illustration purposes, the power spectrum densities of the measured displacement records from Test #11 are

plotted in Figure 8.12. If the displacement time histories are filtered at the highest peak shown in Figure 8.12, the filtered displacements at the tops of the north and south columns will be vibrating in the same direction with similar amplitudes. Based on the above observation, the highest peak is relative to the lateral bending mode in global X direction. The locations of the first bending mode in global X direction based on the displacement records for all the tests are reported in Table 8.1. The width of the pass band of the digital filters for all the tests are also provided in Table 8.1. Based on the observation of the frequency change of the bending modes from all tests, the frequency of bending mode will decrease for the damaged cases. However, based solely on the changes of the frequencies, the damage locations and damage severities cannot be detected and evaluated. As described in Steps (2) to (4) in Section 8.4.3, the filtered joint displacements, filtered joint velocities, filtered joint accelerations are computed. The filtered joint rotations, filtered joint angular velocities and filtered joint angular accelerations are computed as described in Step (5) in Section 8.4.3. For illustration purposes, the filtered joint displacement time histories at the top ends of the two columns for Test #11 are plotted in Figure 8.13. The filtered joint velocity time histories at the top ends of the two columns for Test #11 are plotted in Figure 8.14. The filtered joint acceleration time histories at the top ends of the two columns for Test #11 are plotted in Figure 8.15.

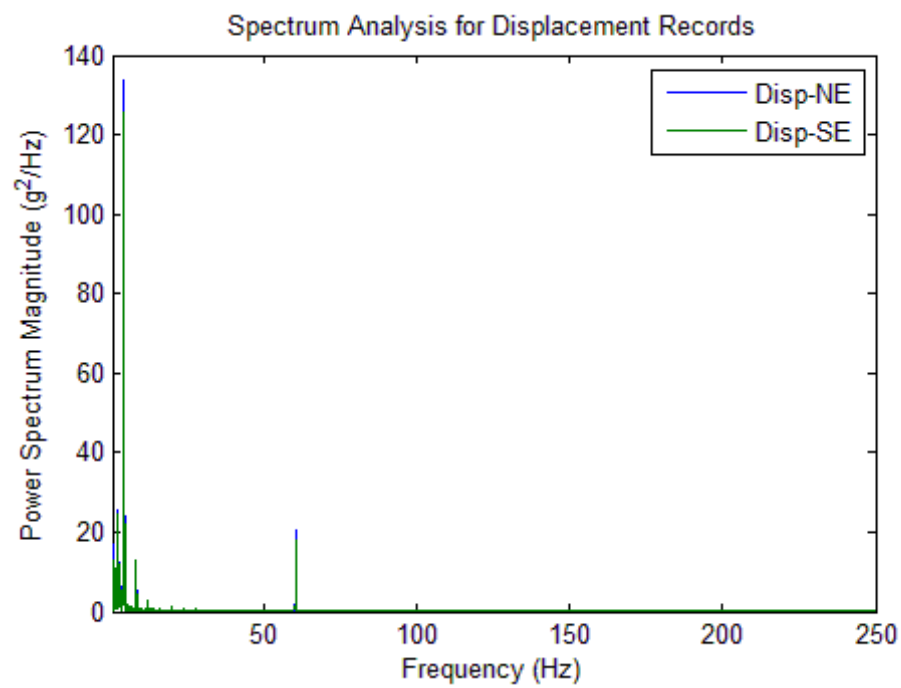
Due to the existence of noise in the measured displacement time histories, digital bandpass filters were adopted in: (1) filtering measured displacement time histories; (2) filtering estimated velocities; (3) filtering estimated accelerations. However, both the existence of noise and the filtering technique will cause a certain amount of loss of the damage information contained in the perfect displacement time histories. According to

experience acquired from detecting damage in noise-contained numerical models, two key points will assure the stable performance of the proposed method to the bridge model:

- (1) Use narrow bandpass filter. The main objective of using a digital bandpass filter is to increase the signal-to-noise ratio in the filtered displacement time histories. By applying a narrow bandpass filter right at the peak will enable most of the useful information to pass while most of useless noise to be filtered. The numerical error caused by an inappropriate narrow bandpass filter is obvious and can be modified by increase the width of the pass band appropriately.
- (2) Use relative displacements for the computation of member forces. Because the amplitude of base vibration is smaller than the vibration amplitude at each column top and the amplitude of noise in the base displacement time histories is the same, the signal-to-noise ratios of base displacement records are lower than the ones of the displacement records from column tops. By using the relative displacements, the base displacement records will become all zeros without any noise while the signal-to-noise ratios of the displacement records from column tops remain the same.

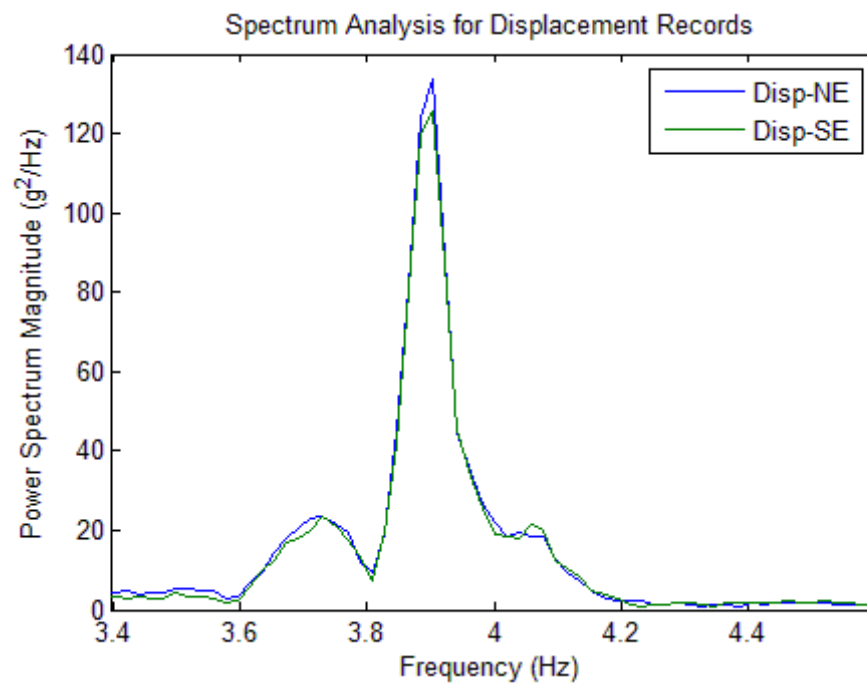
The coefficient matrix and known vector can be computed by substituting the computed joint absolute acceleration time histories and joint relative displacement time histories into Eq. 8.42 and Eq. 8.44. Then unknown coefficient vector shown in Eq. 8.43 can be computed using Eq. 8.45. The damage index of the joint translational masses and the damage index of the lateral stiffness of the columns can be computed using Eq. 8.46 and Eq. 8.47. The computed damage indices and damage severities for all the tests are listed

in Table 8.2.



(a)

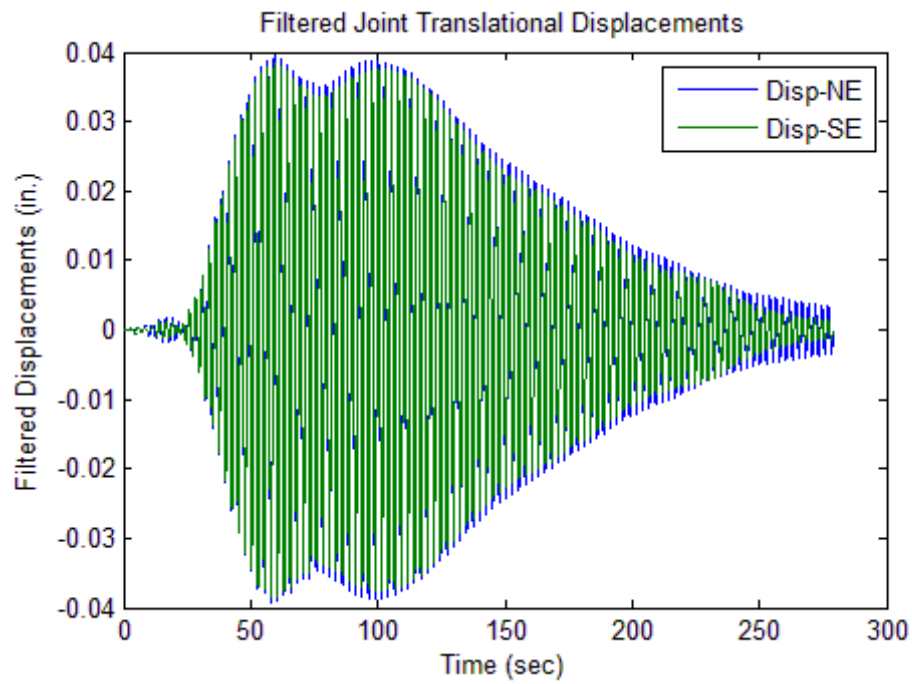
Figure 8.12. Power Spectrum Density Analysis of Displacements from String Pots from Test#11:  
(a) Full Plot and (b) Zoomed in Plot



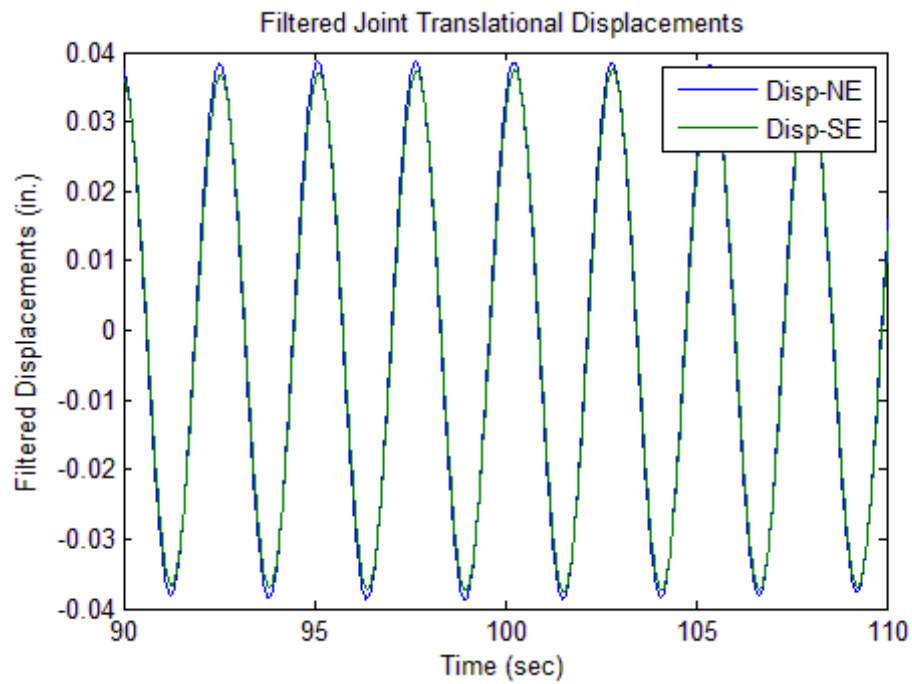
(b)

Figure 8.12. Continued



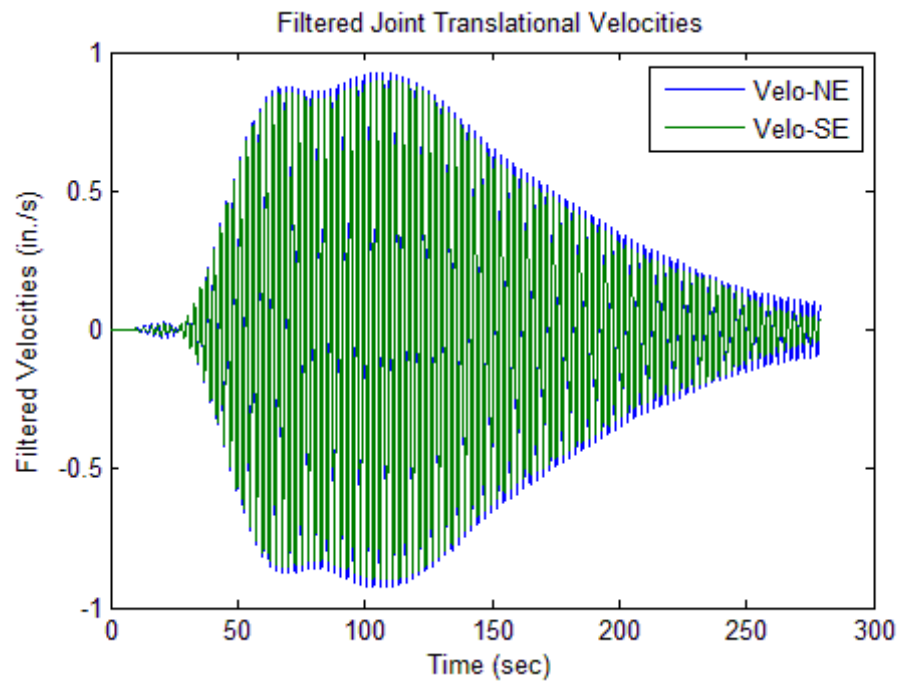


(a)

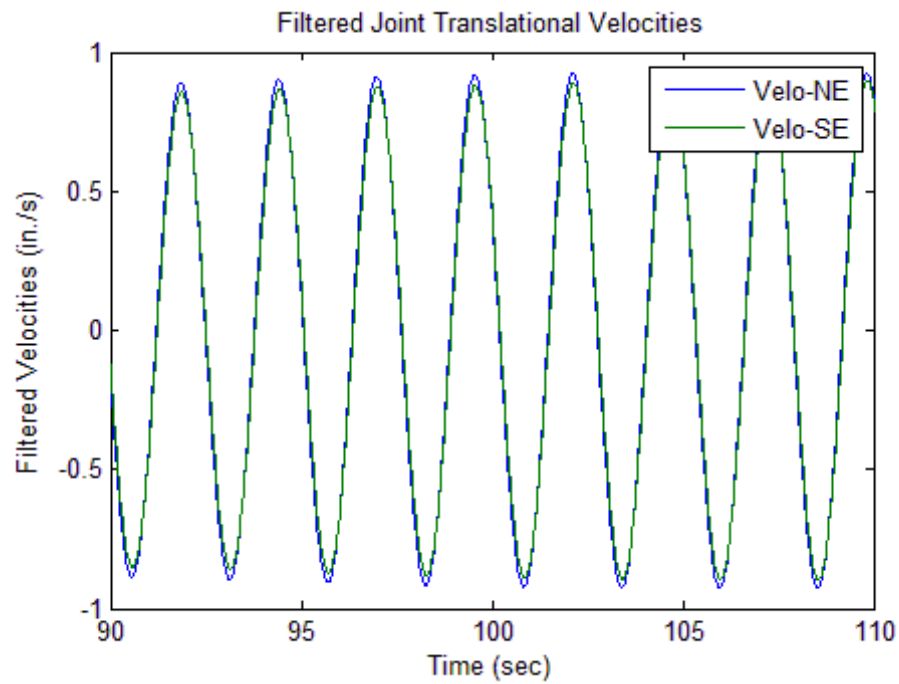


(b)

**Figure 8.13. Filtered Displacement Time Histories Recorded By String Pots from Test#11: (a) Full Plot and (b) Zoomed in Plot**

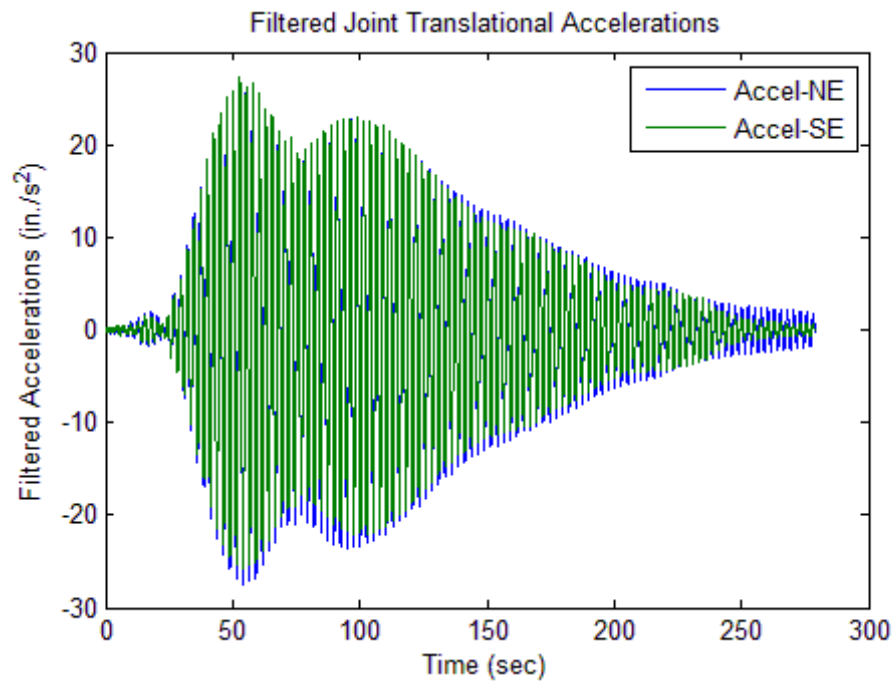


(a)

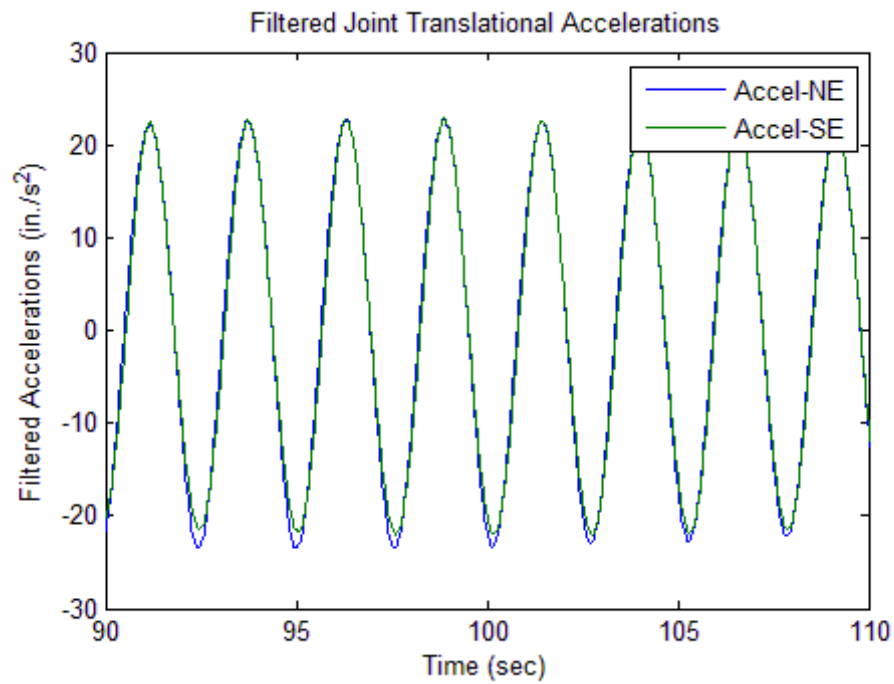


(b)

**Figure 8.14. Filtered Velocity Time Histories at the Locations of the String Pots from Test#11: (a) Full Plot and (b) Zoomed in Plot**



(a)



(b)

**Figure 8.15. Filtered Acceleration Time Histories at the Locations of the String Pots from Test#11: (a) Full Plot and (b) Zoomed in Plot**

**Table 8.1. Locations of Bending Mode and Selected Pass Band of Digital Filters**

Test Num.	Location of Bending Mode	Designed Pass Bands for
	Peak (Hz)	Digital Filters (Hz)
Test #07	3.8 ~ 4.3	3.83 ~ 3.93
Test #10	3.8 ~ 4.05	3.84 ~ 3.95
Test #11	3.8 ~ 4.2	3.83 ~ 4.00
Test #15	3.8 ~ 4.0	3.85 ~ 3.98
Test #16	3.45 ~ 3.75	3.53 ~ 3.68
Test #17	3.4 ~ 3.8	3.56 ~ 3.66
Test #18	3.3 ~ 3.8	3.61 ~ 3.7

**Table 8.2. Damage Indices and Damage Severities for the Bridge Model**

Test Num.	Damage Index		Damage Severity	
	$\beta_m$	$\beta_k$	$\alpha_m$	$\alpha_k$
Test #07	0.981	0.974	0.02	0.03
Test #10	1.000	0.994	0.00	0.01
Test #11	1.021	0.992	-0.02	0.01
Test #15	1.025	0.982	-0.02	0.02
Test #16	1.154	1.095	-0.13	-0.09
Test #17	1.195	1.109	-0.16	-0.10
Test #18	1.200	1.167	-0.17	-0.14

## 8.6 EVALUATION OF DESIGNED DAMAGE EXTENT

In this subsection, the designed damage extent regarding to the whole columns will be evaluated. The designed damage indices for the damaged portion of the column are easy to compute. However, as stated in the above analysis, each column will be treated as one

single element, thus the damage index for the whole column need to be computed. The computed designed damage index for the whole column will be used as a reference to check the accuracies of the damage detection results of the damaged column using the proposed method.

In order to compute the damage extent for the whole column, the damage extent for lowest section of the column needs to be evaluated. The layout of the cross section of the column is shown in Figure 8.16. The cross-sectional properties of the tube section and channel section are provided in Table 8.3. According to the given cross-sectional properties in Table 8.3, the moment of inertia of the undamaged column cross section can be computed as following,

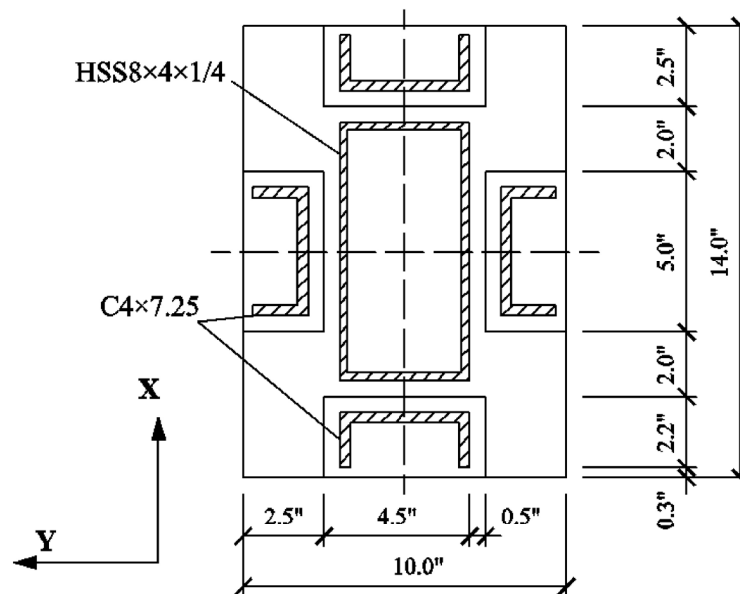
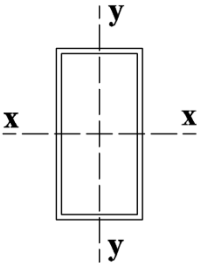
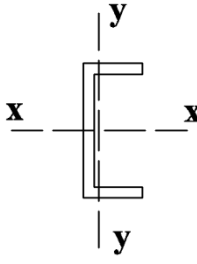
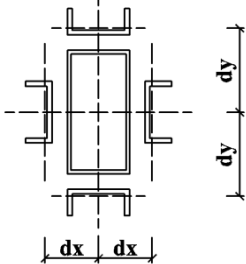


Figure 8.16. Layout of the Cross Section of the Column of the Bridge Model

**Table 8.3. Cross-Sectional Properties of the Tube and Channel Sections**

	<b>HSS8x4x0.25</b>	
	Cross-Sectional Area, $A_{HSS}$ (in <sup>2</sup> .)	5.24
	Moment of Inertia about Y axis, $I_{y,HSS}$ (in <sup>4</sup> .)	14.4
	Moment of Inertia about X axis, $I_{x,HSS}$ (in <sup>4</sup> .)	42.5
	<b>C4x7.25</b>	
	Cross-Sectional Area, $A_C$ (in <sup>2</sup> .)	2.13
	Moment of Inertia about Y axis, $I_{y,C}$ (in <sup>4</sup> .)	0.425
	Moment of Inertia about X axis, $I_{x,C}$ (in <sup>4</sup> .)	4.58
	Distance of the Paralleled Axes in Global X Direction, $d_x$ (in.)	5.439
	Distance of the Paralleled Axes in Global Y Direction, $d_y$ (in.)	3.439

(Note, x, y in the above table indicate the direction of local axes.)

The moment of inertia for bending around the global Y direction (note, the global directions are given in Figure 8.16),

$$I_y = I_{x,HSS} + 2I_{x,C} + 2(I_{y,C} + A_C d_y^2) \quad (8.56)$$

The moment of inertia for bending around the global X direction,

$$I_x = I_{y,HSS} + 2I_{x,C} + 2(I_{y,C} + A_C d_x^2) \quad (8.57)$$

The moment of inertia of the damaged column with the southern channel section removed bending around the global Y direction can be computed as (note, the southern channel section is the channel section on the right side of the tube section, which is shown in Figure 8.16),

$$I_y^{south} = I_{x,HSS} + I_{x,C} + 2(I_{y,C} + A_C d_y^2) \quad (8.58)$$

The moment of inertia of the damaged column with the southern channel section removed bending around the global X direction can be computed as,

$$I_x^{south} = I_{x,HSS} + 2I_{x,C} + (I_{y,C} + A_C d_x^2) \quad (8.59)$$

The moment of inertia of the damaged column with the western channel section removed bending around the global Y direction can be computed as (note, the western channel section is the channel section below the tube section, which is shown in Figure 8.16),

$$I_y^{west} = I_{x,HSS} + 2I_{x,C} + (I_{y,C} + A_C d_y^2) \quad (8.60)$$

The moment of inertia of the damaged column with the western channel section removed bending around the global X direction can be computed as,

$$I_x^{west} = I_{y,HSS} + I_{x,C} + 2(I_{y,C} + A_C d_x^2) \quad (8.61)$$

The computed moment of inertia from the above six cases are listed in Table 8.4. Given the moment of inertia in all the six cases and the modulus of elasticity (i.e.  $E = 29000$

ksi), six numerical cantilever models were built in SAP2000,

- (1) Undamaged column bending in global Y direction;
- (2) Undamaged column bending in global X direction;
- (3) Damaged column with southern channel section removed bending in global Y direction;
- (4) Damaged column with southern channel section removed bending in global X direction;
- (5) Damaged column with western channel section removed bending in global Y direction; and
- (6) Damaged column with western channel section removed bending in global X direction.

In SAP2000, one unit transverse load was added at the top ends of the cantilever beams and the static displacements at the top ends of the cantilever beam were outputted for the above six cases. The stiffness for each of the six cantilevers can be computed. Then the damage indices and damage severities are computed. The static displacements ('S' and 'S\*'), stiffness ('k' and 'k\*'), damage indices (' $\beta_k$ ') and damage severities (' $\alpha_k$ ') for the undamaged and damaged cases are listed in Table 8.5.

In Table 8.5,

- (1) **Case #1** compares the Y-direction bending stiffness between the damaged column with the southern channel section removed (' $I_y^{south}$ ') and the undamaged column (' $I_y$ '). Note that this case is relative to damage scenario in Test #15;



- (2) **Case #2** compares the Y-direction bending stiffness between damaged column with the southern channel section removed ( $I_y^{south}$ ) and damaged column with the western channel section removed ( $I_y^{west}$ ). Note that this case is relative to damage scenario in Test #16 and Test #17;
- (3) **Case #3** compares the Y-direction bending stiffness between the undamaged column ( $I_y$ ) and damaged column with the western channel section removed ( $I_y^{west}$ ). Note that this case is relative to damage scenario in Test #18;
- (4) **Case #4** compares the X-direction bending stiffness between undamaged column ( $I_x$ ) and damaged column with southern channel section removed ( $I_x^{south}$ ); and
- (5) **Case #5** compares the X-direction bending stiffness between the undamaged column ( $I_x$ ) and damaged column with western channel section removed ( $I_x^{west}$ ).

**Table 8.4. Moment of Inertia of the Cross Section of Column**

$I_x$ (in <sup>4</sup> .)	74.792
$I_y$ (in <sup>4</sup> .)	178.532
$I_x^{\text{south}}$ (in <sup>4</sup> .)	49.176
$I_y^{\text{south}}$ (in <sup>4</sup> .)	173.952
$I_x^{\text{west}}$ (in <sup>4</sup> .)	70.212
$I_y^{\text{west}}$ (in <sup>4</sup> .)	115.096

**Table 8.5. Evaluation of Damage Indices and Damage Severities**

Case (Test)	S (in.)	$S^*$ (in.)	k (kip/in.)	$k^*$ (kip/in.)	$\beta_k$	$\alpha_k$
Case #1 (T15)	0.0347	0.0342	28.82	29.24	0.986	0.015
Case #2 (T16,T17)	0.0347	0.044	28.82	22.73	1.268	-0.211
Case #3 (T18)	0.0342	0.044	29.24	22.73	1.287	-0.223
Case #4	0.0817	0.1037	12.24	9.64	1.269	-0.212
Case #5	0.0817	0.0844	12.24	11.85	1.033	-0.032

## 8.7 RESULTS DISCUSSION

According to Table 8.2, for Test #07, Test #10, and Test #11, where the tested structure is undamaged, the damage severities for mass damage are closed to zeros and stiffness damage are closed to zeros.

For Test #15, according to the damage index and damage severity of Case #1 in Table 8.5, due to the damage in the lower section of north column simulated by removing the southern channel section, the bending stiffness around global Y direction of the south column should be increased by 1.5% comparing with the damaged north column and the

translational mass should remain approximately the same. Comparing to the damaged north column, the computed damage severities for the stiffness is 2% increase and 2% decrease for the mass damage.

For Test #16 and Test #17, according to Case #2 in Table 8.5, the bending stiffness of the south column around the global Y direction is 21.1% decrease and the lumped mass of the south column should remain approximately the same with the one of the north column. Comparing to the north column, the computed damage severities for lumped mass of the south column are 13% for Test #16 and 16% for Test #17. The computed damage severities of the column bending stiffness are 9% decrease for Test #16 and 10% decrease for Test #17.

For Test #18, according to Case #3 in Table 8.5, the bending stiffness of the south column around the global Y direction is 22.3% decrease and the translational mass and mass moment of inertia of the south column should remain approximately the same with the ones of the north column. Comparing to the north column, the computed damage severities for lumped mass of the south column is 17% decrease. The computed damage severities of the column bending stiffness are 14% decrease.

The main reasons caused the errors in the damage detection results are,

- (1) Estimation of joint rotation at the top of the two columns. According to the analysis experience to the numerical models, the error in the estimation of joint rotations will underestimate the damage in column bending stiffness;
- (2) Estimation of joint translational accelerations. The estimation of the joint translational accelerations will cause inaccuracy in the mass damage

detection;

- (3) Noise in the measured displacement records. The noise in the measured displacements will cause the overall inaccuracy of the damage detection process; and
- (4) The application of digital bandpass filter. Although the application of the digital bandpass filter will reduce the noise influence, it will also cause the incompatibility among displacement, velocity, and acceleration time histories, which will cause the inaccuracy of damage detection results.

## **8.8 DAMAGE EVALUATION WITH ELEMENT DAMPING EFFECT**

For the steel members in the bridge model, it is inappropriate to consider damping in the level of individual structural members and it is impractical to determine the damping matrix in the same manner as the stiffness matrix is determined. Because the damping properties of materials are not well established and the significant amount of energy dissipation caused by effects other than material damping properties, such as the friction at the joint connections. The damping matrix for the structure should be determined from its modal damping ratios.

However, for experimental purposes, the damping properties of individual structural members will be considered in this subsection. For simplicity purposes, the Rayleigh damping model is used.

### **8.8.1 Theory of Approach**

According to Subsection 7.4.2, the damping forces can be computed as the Eq. 7.37. And the power done by the damping forces can be computed as Eq. 8.62. However, since the

displacement time histories were filtered by a narrow bandpass filter and the joint angular velocities were computed based on the filtered displacement time histories, the ‘ $\{\dot{\Delta}\}[M_o^i]\{\dot{\delta}_i\}$ ’ and ‘ $\{\dot{\Delta}\}[K_{o,i}]\{\dot{\delta}_i\}$ ’ parts become linearly dependent to each other, which will impact the performance of the least square method and force the damage detection results of  $a_{i,0}$  and  $a_{i,1}$  to be ones (i.e. “1” means undamaged). To overcome this dilemma, only the stiffness-proportional damping model will be used to simulate the element damping, which is given in Eq. 8.63.

$$\begin{aligned}
\{F_{c,i}\} &= [C_i] \{\dot{\delta}_i\} = (a_{i,0}[M_i] + a_{i,1}[K_i]) \{\dot{\delta}_i\} = a_{i,0}[M_i] \{\dot{\delta}_i\} + a_{i,1}[K_i] \{\dot{\delta}_i\} \\
&= a_{i,0} \left( \frac{\bar{m}L}{2} \right)_i \begin{bmatrix} -1 & 0 & 0 & 1 & 0 & 0 \\ 0 & -1 & 0 & 0 & 1 & 0 \\ 0 & 0 & 0 & 0 & 0 & 0 \end{bmatrix}_i \begin{Bmatrix} \dot{\delta}_{i,1}^- \\ \dot{\delta}_{i,2}^- \\ \dot{\delta}_{i,3}^- \\ \dot{\delta}_{i,1}^+ \\ \dot{\delta}_{i,2}^+ \\ \dot{\delta}_{i,3}^+ \end{Bmatrix} \\
&\quad + a_{i,1} \left( \frac{EI}{L^3} \right)_i \begin{bmatrix} -\frac{AL^2}{I} & 0 & 0 & \frac{AL^2}{I} & 0 & 0 \\ 0 & -12 & -6L & 0 & 12 & -6L \\ 0 & 6L & 2L^2 & 0 & -6L & 4L^2 \end{bmatrix}_i \begin{Bmatrix} \dot{\delta}_{i,1}^- \\ \dot{\delta}_{i,2}^- \\ \dot{\delta}_{i,3}^- \\ \dot{\delta}_{i,1}^+ \\ \dot{\delta}_{i,2}^+ \\ \dot{\delta}_{i,3}^+ \end{Bmatrix} \\
&= a_{i,0} \frac{m_i}{2} [M_o^i] \{\dot{\delta}_i\} + a_{i,1} k_i [K_{o,i}] \{\dot{\delta}_i\} \tag{7.37}
\end{aligned}$$

$$\{P_{c,i}\} = \{\dot{\Delta}\} \{F_{c,i}\} = \{\dot{\Delta}\} [C_i] \{\dot{\delta}_i\} = a_{i,0} \frac{m_i}{2} \{\dot{\Delta}\} [M_o^i] \{\dot{\delta}_i\} + a_{i,1} k_i \{\dot{\Delta}\} [K_{o,i}] \{\dot{\delta}_i\} \tag{8.62}$$

$$\{F_{c,i}\} = [C_i] \{\dot{\delta}_i\} = a_{i,1} k_i [K_{o,i}] \{\dot{\delta}_i\} \tag{8.63}$$

Substituting Eq. 8.63 into Eq. 8.29 yields,

$$\begin{aligned} m_1^2 [M_o] \{\ddot{\delta}^2\} + k_1 [K_{o,1}] \{\delta_1\} + a_{1,1} k_1 [K_{o,1}] \{\dot{\delta}_1\} + m_1^3 [R_3] [M_o] \{\ddot{\delta}^3\} \\ + k_3 [R_3] [K_{o,2}] \{\delta_3\} + a_{3,1} k_3 [R_3] [K_{o,2}] \{\dot{\delta}_3\} = 0 \end{aligned} \quad (8.64)$$

Multiplying Eq. 8.64 by the velocity vector used to compute power (i.e. Eq. 8.30) yields,

$$\begin{aligned} m_1^2 \{\dot{\Delta}\} [M_o] \{\ddot{\delta}^2\} + k_1 \{\dot{\Delta}\} [K_{o,1}] \{\delta_1\} + a_{1,1} k_1 \{\dot{\Delta}\} [K_{o,1}] \{\dot{\delta}_1\} \\ + m_1^3 \{\dot{\Delta}\} [R_3] [M_o] \{\ddot{\delta}^3\} + k_3 \{\dot{\Delta}\} [R_3] [K_{o,2}] \{\delta_3\} + a_{3,1} k_3 \{\dot{\Delta}\} [R_3] [K_{o,2}] \{\dot{\delta}_3\} = 0 \end{aligned} \quad (8.65)$$

Rearranging Eq. 8.65 yields,

$$\begin{aligned} m_1^2 \{\dot{\Delta}\} [M_o] \{\ddot{\delta}^2\} + k_1 \{\dot{\Delta}\} [K_{o,1}] \{\delta_1\} + a_{1,1} k_1 \{\dot{\Delta}\} [K_{o,1}] \{\dot{\delta}_1\} \\ + k_3 \{\dot{\Delta}\} [R_3] [K_{o,2}] \{\delta_3\} + a_{3,1} k_3 \{\dot{\Delta}\} [R_3] [K_{o,2}] \{\dot{\delta}_3\} = -m_1^3 \{\dot{\Delta}\} [R_3] [M_o] \{\ddot{\delta}^3\} \end{aligned} \quad (8.66)$$

Dividing Eq. 8.66 by  $m_1^3$  yields,

$$\begin{aligned} \frac{m_1^2}{m_1^3} \{\dot{\Delta}\} [M_o] \{\ddot{\delta}^2\} + \frac{k_1}{m_1^3} \{\dot{\Delta}\} [K_{o,1}] \{\delta_1\} + \frac{a_{1,1} k_1}{m_1^3} \{\dot{\Delta}\} [K_{o,1}] \{\dot{\delta}_1\} \\ + \frac{k_3}{m_1^3} \{\dot{\Delta}\} [R_3] [K_{o,2}] \{\delta_3\} + \frac{a_{3,1} k_3}{m_1^3} \{\dot{\Delta}\} [R_3] [K_{o,2}] \{\dot{\delta}_3\} = -\{\dot{\Delta}\} [R_3] [M_o] \{\ddot{\delta}^3\} \end{aligned} \quad (8.67)$$

Define the following coefficients,

$$\beta_1 = \frac{m_1^2}{m_1^3} \quad (8.68)$$

$$\beta_2 = \frac{k_1}{m_1^3} \quad (8.69)$$

$$\beta_3 = \frac{k_3}{m_1^3} \quad (8.70)$$

$$\beta_4 = \frac{a_{1,1}k_1}{m_1^3} \quad (8.71)$$

$$\beta_5 = \frac{a_{3,1}k_3}{m_1^3} \quad (8.72)$$

Substituting Eq. 8.68 through Eq. 8.72 into Eq. 8.67 yields,

$$\begin{aligned} & \beta_1 \{\dot{\Delta}\} [M_o] \{\ddot{\delta}^2\} + \beta_2 \{\dot{\Delta}\} [K_{o,1}] \{\delta_1\} + \beta_4 \{\dot{\Delta}\} [K_{o,1}] \{\dot{\delta}_1\} \\ & + \beta_3 \{\dot{\Delta}\} [R_3] [K_{o,2}] \{\delta_3\} + \beta_5 \{\dot{\Delta}\} [R_3] [K_{o,2}] \{\dot{\delta}_3\} = -\{\dot{\Delta}\} [R_3] [M_o] \{\ddot{\delta}^3\} \end{aligned} \quad (8.73)$$

Writing the Eq. 8.73 at different time point, yields the following groups of equations,

For  $t = t_0$ ,

$$\begin{aligned} & \beta_1 (\{\dot{\Delta}\} [M_o] \{\ddot{\delta}^2\})|_{t_0} + \beta_2 (\{\dot{\Delta}\} [K_{o,1}] \{\delta_1\})|_{t_0} + \beta_4 (\{\dot{\Delta}\} [K_{o,1}] \{\dot{\delta}_1\})|_{t_0} \\ & + \beta_3 (\{\dot{\Delta}\} [R_3] [K_{o,2}] \{\delta_3\})|_{t_0} + \beta_5 (\{\dot{\Delta}\} [R_3] [K_{o,2}] \{\dot{\delta}_3\})|_{t_0} = -(\{\dot{\Delta}\} [R_3] [M_o] \{\ddot{\delta}^3\})|_{t_0} \end{aligned} \quad (8.74)$$

For  $t = t_j$ ,

$$\begin{aligned} & \beta_1 (\{\dot{\Delta}\} [M_o] \{\ddot{\delta}^2\})|_{t_j} + \beta_2 (\{\dot{\Delta}\} [K_{o,1}] \{\delta_1\})|_{t_j} + \beta_4 (\{\dot{\Delta}\} [K_{o,1}] \{\dot{\delta}_1\})|_{t_j} \\ & + \beta_3 (\{\dot{\Delta}\} [R_3] [K_{o,2}] \{\delta_3\})|_{t_j} + \beta_5 (\{\dot{\Delta}\} [R_3] [K_{o,2}] \{\dot{\delta}_3\})|_{t_j} = -(\{\dot{\Delta}\} [R_3] [M_o] \{\ddot{\delta}^3\})|_{t_j} \end{aligned} \quad (8.75)$$

For  $t = t_N$ ,

$$\begin{aligned} & \beta_1 (\{\dot{\Delta}\} [M_o] \{\ddot{\delta}^2\})|_{t_N} + \beta_2 (\{\dot{\Delta}\} [K_{o,1}] \{\delta_1\})|_{t_N} + \beta_4 (\{\dot{\Delta}\} [K_{o,1}] \{\dot{\delta}_1\})|_{t_N} \\ & + \beta_3 (\{\dot{\Delta}\} [R_3] [K_{o,2}] \{\delta_3\})|_{t_N} + \beta_5 (\{\dot{\Delta}\} [R_3] [K_{o,2}] \{\dot{\delta}_3\})|_{t_N} = -(\{\dot{\Delta}\} [R_3] [M_o] \{\ddot{\delta}^3\})|_{t_N} \end{aligned} \quad (8.76)$$

Arranging the above linear equation group into matrix form, yields,

$$\mathbf{X}\boldsymbol{\beta} = \mathbf{Y} \quad (8.77)$$

Where the coefficient matrix of the linear equation group is given as following

$$\mathbf{X}^T = \begin{bmatrix} (\{\dot{\Delta}\}[M_o]\{\ddot{\delta}^2\})|_{t_0} & \cdots & (\{\dot{\Delta}\}[M_o]\{\ddot{\delta}^2\})|_{t_j} & \cdots & (\{\dot{\Delta}\}[M_o]\{\ddot{\delta}^2\})|_{t_N} \\ (\{\dot{\Delta}\}[K_{o,1}]\{\dot{\delta}_1\})|_{t_0} & \cdots & (\{\dot{\Delta}\}[K_{o,1}]\{\dot{\delta}_1\})|_{t_j} & \cdots & (\{\dot{\Delta}\}[K_{o,1}]\{\dot{\delta}_1\})|_{t_N} \\ (\{\dot{\Delta}\}[R_3][K_{o,2}]\{\dot{\delta}_3\})|_{t_0} & \cdots & (\{\dot{\Delta}\}[R_3][K_{o,2}]\{\dot{\delta}_3\})|_{t_j} & \cdots & (\{\dot{\Delta}\}[R_3][K_{o,2}]\{\dot{\delta}_3\})|_{t_N} \\ (\{\dot{\Delta}\}[K_{o,1}]\{\dot{\delta}_1\})|_{t_0} & \cdots & (\{\dot{\Delta}\}[K_{o,1}]\{\dot{\delta}_1\})|_{t_j} & \cdots & (\{\dot{\Delta}\}[K_{o,1}]\{\dot{\delta}_1\})|_{t_N} \\ (\{\dot{\Delta}\}[R_3][K_{o,2}]\{\dot{\delta}_3\})|_{t_0} & \cdots & (\{\dot{\Delta}\}[R_3][K_{o,2}]\{\dot{\delta}_3\})|_{t_j} & \cdots & (\{\dot{\Delta}\}[R_3][K_{o,2}]\{\dot{\delta}_3\})|_{t_N} \end{bmatrix} \quad (8.78)$$

The vector of unknown and the vector of known are given as follows,

$$\boldsymbol{\beta} = \begin{Bmatrix} \beta_1 \\ \beta_2 \\ \beta_3 \\ \beta_4 \\ \beta_5 \end{Bmatrix} \quad (8.79)$$

$$\mathbf{Y} = \begin{Bmatrix} -(\{\dot{\Delta}\}[R_3][M_o]\{\ddot{\delta}^3\})|_{t_0} \\ \vdots \\ -(\{\dot{\Delta}\}[R_3][M_o]\{\ddot{\delta}^3\})|_{t_j} \\ \vdots \\ -(\{\dot{\Delta}\}[R_3][M_o]\{\ddot{\delta}^3\})|_{t_N} \end{Bmatrix} \quad (8.80)$$

Using the Least Square Method, the vector of unknown, ' $\boldsymbol{\beta}$ ', can be computed from the following equation,

$$\boldsymbol{\beta} = (\mathbf{X}^T \mathbf{X})^{-1} (\mathbf{X}^T \mathbf{Y}) \quad (8.81)$$



With the vector of unknown computed, the damage indices for stiffness, mass and damping can be computed as follows,

$$\beta_{m_i} = \frac{m_1^2}{m_1^3} = \beta_1 \quad (8.82)$$

$$\beta_k = \frac{k_1}{k_3} = \frac{\frac{k_1}{m_1^3}}{\frac{k_3}{m_1^3}} = \frac{\beta_2}{\beta_3} \quad (8.83)$$

$$\beta_{a_i} = \frac{a_{1,1}}{a_{3,1}} = \frac{\frac{a_{1,1}k_1}{m_1^3}}{\frac{a_{3,1}k_3}{m_1^3}} \cdot \frac{k_3}{k_1} = \frac{\beta_4}{\beta_5} \cdot \frac{1}{\beta_k} \quad (8.84)$$

### 8.8.2 Damage Evaluation Results

According to Section 8.4.3, the filtered joint translational displacements, velocities, accelerations and the filtered joint rotations, angular velocities, angular accelerations are computed. Then the coefficient matrix is computed using Eq. 8.78 and the known vector is computed using Eq. 8.80. As stated in Section 8.5, the damping forces of columns are also computed using relative velocities. The unknown coefficient vector shown in Eq. 8.79 can be computed using Eq. 8.81. The damage indices of the joint translational masses, lateral stiffness of the columns and damping coefficients of the columns can be computed using Eq. 8.82 through Eq. 8.84. The computed damage indices and damage severities for all the tests are listed in Table 8.6.

**Table 8.6. Damage Indices and Damage Severities for the Bridge Model with Element Damping Effects**

Test Num.	Damage Index			Damage Severity		
	$\beta_{m, \text{shear}}$	$\beta_k$	$\beta_{a1}$	$\alpha_{m, \text{shear}}$	$\alpha_k$	$\alpha_{a1}$
Test #07	0.980	0.979	1.064	0.02	0.02	-0.06
Test #10	0.966	0.976	0.975	0.04	0.02	0.03
Test #11	0.958	0.960	1.165	0.04	0.04	-0.14
Test #15	0.937	0.952	0.972	0.07	0.05	0.03
Test #16	1.091	1.095	0.902	-0.08	-0.09	0.11
Test #17	1.163	1.204	0.829	-0.14	-0.17	0.21
Test #18	1.256	1.209	0.937	-0.20	-0.17	0.07

### 8.8.3 Results Discussion

According to Table 8.6, for Test #07, Test #10 and Test #11, where the tested structure is undamaged, the damage severities for mass and stiffness damage are closed to zeros. The damage severities for damping damage are not as stable as the ones for stiffness and mass damage.

For Test #15, according to Table 8.5, the designed damage severity for stiffness damage is +1.5%. From Table 8.6, the detected stiffness damage is +5%, which is higher than the ones from the undamaged cases (i.e. Test #07, Test #10 and Test #11). As expected, the damage severity for damping damage is around zero. This is because, as stated in Section 8.6, the damage in the north column has very small impact on the bending stiffness. Thus, the amplitudes of vibration velocities of the north and south columns are very similar.

For Test #16, Test #17 and Test #18, the designed damage severities for stiffness, according to Table 8.5, are around 20%. From Table 8.6, the detected damage severities for stiffness damage are 9% for Test #16 and 17% for both Test #17 and Test #18. The error in the estimation of the joint rotations, joint angular velocities, and joint angular accelerations contributed to the underestimation of the stiffness damage for Test #16, Test #17, and Test #18. According to Table 8.6, the damping effects for the south column are increased after damage for Test #16, Test #17 and Test #18. The increase of the damping effect can be explained by the increase of vibration amplitude of the damaged column.

The main reasons caused the errors in the damage detection results are,

- (1) Estimation of joint rotation at the top of the two columns. According to the analysis experience to the numerical models, the error in the estimation of joint rotations will underestimate the damage in column bending stiffness;
- (2) Estimation of joint translational accelerations. The estimation of the joint translational accelerations will cause inaccuracy in the mass damage detection;
- (3) Noise in the measured displacement records. The noise in the measured displacements will cause the overall inaccuracy of the damage detection process;
- (4) The application of digital bandpass filter. Although the application of the digital bandpass filter will reduce the noise influence, it will also cause the incompatibility among displacement, velocity, and acceleration time histories, which will cause the inaccuracy of damage detection results;
- (5) The application of the Rayleigh Damping as the element damping model. The

method in computing damping force in this section may cause the inaccuracy and instability in the damping damage detection; and

- (6) Estimation of the joint translational velocities and joint angular velocities.

These two factors will also contribute to the inaccuracy of the damping damage detection and will cause a certain influence to the damage detection results to mass and stiffness.

## **8.9 CONCLUSION**

According to the above analysis, the proposed theory could locate the damaged column and provide a close estimation the damage severities regarding to the whole column. And the accuracy of the estimation of the damage severities can be improved by providing more useful and less noise-polluted structural vibration measurements.

Note, the proposed method could locate and estimate the original designed damage in the lower portion of the column if less noise-polluted data could have been collected from the tri-axial accelerometers distributed on the north and south columns. Namely, more dense distribution of sensors is required in order to locate damage more accurately.

## **9 SUMMARY AND CONCLUSIONS**

### **9.1 SUMMARY**

In this dissertation, a new non-destructive evaluation method, named as the Power Method, was developed. The Power Method can be used to detect damage in both isolated structural components and the integral structures. To validate the proposed method, the method has been applied to different types of structures and the following sections were introduced,

In Section 2, the general form of the Power Method was developed. And also, the specific form of the proposed method for the 1-DOF, 2-DOF, N-DOF, and isolated spring-mass-damper systems were developed.

In Section 3, numerical examples for 1-DOF, 2-DOF, N-DOF, and isolated spring-mass-damper systems were developed and were used to validate the theories developed in Section 2. All the designed damage in masses, springs and dampers were located and evaluated accurately in each numerical model.

In Section 4, the specific form of the Power Method for rod, Euler-Bernoulli beam, plane frame, and space truss were developed.

In Section 5, numerical models of rod under axial and torsional vibrations, rod under axial vibration only, beam under bending vibration, plane frame under axial and bending vibrations, and space truss under axial vibration were simulated. All the designed damage

in masses and stiffness were located and evaluated accurately in each numerical experiment.

In Section 6, the performance of the proposed method to noise polluted inputs were evaluated for both the discrete and continuous systems. Two noise levels were considered for each numerical case. The proposed method was found to be able to accurately locate and evaluate multiple damage under the lower noise level (1% noise) and to be able to accurately locate damage and roughly evaluate damage under higher noise level (5% noise).

In Section 7, three possible technical issues were studied and solved. The three possible issues studied in this section are, (1) no external loads were applied within the structural components that were under damage detection; (2) the efficiency study of the two methods to reduce noise influence for the repeatable damage detection process; (3) the damping damage detection in continuous structures.

In Section 8, the proposed method was validated using experimental data from a shake table test made in University of California, San Diego. By using the displacement records at the top ends of the two columns, the designed damage in south column was detected and evaluated.

## **9.2 FINDINGS**

After finishing all the studies related to the Power Method, the followings were found,

From Section 2 and 3, the new findings are,

- (1) The Power Method can be applied to all kinds of linear discrete systems. For example, 1-DOF, 2DOF, and 5-DOF spring-mass-damper systems;
- (2) The Power Method can be applied to the whole discrete system and evaluate multiple structural components at one time, which makes the Power Method very efficient and economical;
- (3) The Power Method can be applied to isolated discrete systems and detect damage in the structural components that are within the isolated system; and
- (4) The advantages of the isolated system method is that it requires less motion information since fewer structural needs to be evaluated. Also, by using the isolated system method, the possibility of encountering a singularity problem during the application stage of least square method will become smaller. This is because less unknowns will be considered and solved.

From Section 4 and 5, the new findings are,

- (1) The Power Method can be applied to all kinds of linear continuous structural components. For example, rod, beam, frame and truss;
- (2) The Power Method can be applied to the whole continuous system and evaluate multiple structural components at one time;
- (3) The Power Method can be applied to isolated continuous systems and evaluate only the structural components within the isolated system;
- (4) When the Power Method is applied to the isolated system, dynamic information from different type of vibrations can be combined; and
- (5) Comparing to the static damage evaluation method based on structural curvatures, such as, Element Strain Energy method, the Power Method won't be influenced by the singularity problem caused by zero bending curvature

and force redistribution (secondary effect) of the statically indeterminate structures. This advantage makes the Power Method become superior to the damage detection methods based on static structural deformation.

From Section 6, the new findings are,

- (1) With 1% white noise, accurate damage evaluation can still be achieved by applying the proposed method;
- (2) With 5% white noise, the Power Method can accurately locate multiple damage. But the computed damage severities will become less reliable;
- (3) The Power Method requires only acceleration data. The velocity and displacement data can be computed based the given acceleration data; and
- (4) Comparing to the isolated system method, the integral system method will provide less false positives. This is because the integral system method will take all the dynamic inputs into consideration, the damage indices for all the undamaged elements will share similar values. Consequently, less damage indices for the undamaged elements will become false positives after the normalization process (i.e. defined in Eq. 6.4).

From Section 7, the new findings are,

- (1) The Power Method remains effective even no external loads are applied in the structural components that are under consideration;
- (2) For repeatable experiments, the proposed method based on the averaged inputs will yield better damage detection results; and
- (3) The Power Method can be used to detect damping damage in the continuous structural components.



From Section 8, the new findings are,

- (1) The Power Method can be used to detect damage in real structures; and
- (2) Because the Power Method requires only the structural vibration data, the damage detection process won't be restricted by the time and location of the engineers. After the recorded structural vibration data is uploaded online, with limited programming effort, the computer will be able to download the data and run the damage detection program automatically.

### **9.3 ORIGINALITY OF THIS WORK**

The originalities of the proposed method includes, but is not limited to,

- (1) The proposed method can be used to evaluate damage in mass, stiffness and damping simultaneously, while most of existing non-destructive evaluation methods will only be able to detect damage in stiffness, and a handful of non-destructive evaluation methods can be used to detect either damage in stiffness and mass or damage in stiffness and damping;
- (2) The proposed method can be used to evaluate damage in single structural component, multiple structural components, and the integral structure at one time;
- (3) The proposed method allows measurements from different types of vibration to be inputted in, the structural properties related to different vibrations will be analyzed at the same time;
- (4) The proposed method uses only the dynamic measurement directly from the structure. Thus, the proposed method can be easily applied to the real-world damage detection;

- (5) Because the proposed method is based on dynamic measurements not the modal or physical curvatures of the structure, singularity problems caused by zero bending curvatures will be out of concern;
- (6) This work introduced the procedures to detect damage in different discrete and continuous systems;
- (7) This work introduced the procedures to deal with the noise pollution within the real-world measurements and along with other approaches to handle some of the unfavorable situations; and
- (8) The damage detection process introduced in Section 8 set an example in the application of the proposed method and other similar methods to real-world data.

#### **9.4 CONTRIBUTION OF THIS WORK**

The dissertation will contribute to the following areas. Firstly, a new and powerful level III damage detection method is established and validated. As mentioned in the previous section, the Power Method is able to detect and evaluate damage in mass, stiffness and damping simultaneously. Moreover, the proposed method can not only detect damage in the whole system at one time but also evaluate damage using information from multiple types of vibrations. Secondly, the work recorded in this dissertation will be a good guidance for further studies and applications to help to reduce property losses and the maintenance cost of critical structures. The theories of the proposed method for various types of discrete and continuous systems were developed and validated using numerical examples and solutions for several unfavorable situations were provided as well. Finally, the idea of the Power Method which introduces new approaches to establish relationships between the undamaged and damaged structures will contribute to the developments of

other static and dynamic non-destructive evaluation methods.

## **9.5 CONCLUSION**

Most NDE methods proposed to date are only classified as Level I or Level II methods, which means only the presences of the damage, or at most, the locations of the damage can be detected. Moreover, most of these methods are limited in the detection of stiffness damage only and are not able to locate or evaluate mass damage and damping damage. The damage detection algorithm proposed in this work is a Level III method that has the following features:

- (1) It detects damage in local stiffness, mass and damping;
- (2) It provides clear indications to locate damage;
- (3) It locates tiny and obscure damage;
- (4) It provides accurate quantitative values of damage severities;
- (5) No analytical model of the structure is required;
- (6) The data from the field experiment can be directly used to complete the analyses;
- (7) The proposed method will still be able to accurately locate damage and provide referable estimations of damage severities with 5% noise;
- (8) The method is applicable to nearly all types of structures and cases with multiple damage locations; and
- (9) The computation process is straight-forward.

## **9.6 FUTURE WORK**

Although the Power Method is well developed and validated in this dissertation, the following issues are remain to be unsolved,

- (1) How to choose the velocity vector used to compute power to achieve better results. During the research process, the author found that, for the pure numerical cases, using the computed nodal velocity as the velocity vector used to compute power will yield better results than the results from using a constant vector as the velocity vector used to compute power. However, for the noise-polluted cases, the results from using a constant vector as the velocity vector used to compute power will be more stable and generally more accurate than the results from using the computed nodal velocity as the velocity vector used to compute power;
- (2) Extend the Power Method to solve for the structural components with unknown stiffness and mass matrices. For the current study cases, the stiffness, mass, and damping properties of one element can be expressed with well-known matrices. However, for the complex structural components and with limited number of sensors, the element matrices of the stiffness, mass, and damping might be unknown;
- (3) Development of the specific form of the Power Method for Timoshenko Beams. The proposed method can be easily applied to the damage detection in Timoshenko beams if the stiffness matrix of the Timoshenko beam is given. The detailed expression of the stiffness matrix of the Timoshenko beam can be found in relevant chapter in books related to finite element analysis. If only the differential equations were given, good ways to compute the partial differentiations of nodal displacements and nodal rotations should be found;
- (4) Development of the specific form of the Power Method for Kirchhoff-Love plates. Similarly, the proposed method can be applied to the damage detection in Kirchhoff-Love plates, if the stiffness matrix of the plate member is ready at

hand; and

- (5) Improve the noise tolerance capacity of the Power Method. Currently, the noise tolerance capacity of the proposed method is less than 10% of white noise. Although the noise in the input data is reduced using digital filters and the application of the least square method is also helpful in finding a good estimation of the real damage severities, the applications of the digital filters will introduce errors into the input data and the least square method is sensitive to input errors. Thus, more advanced techniques are needed to make the proposed method more robust to noise in the inputs.

## REFERENCES

- Adams, R. D., Walton, D., Flitcroft, J. E., and Short, D. (1975). "Vibration Testing as a Nondestructive Test Tool for Composite Materials." *Composite Reliability*, ASTM STP 580, Philadelphia, 159-175.
- Allemang, R. J. and Brown, D. L. (1982). "A Correlation Coefficient for Modal Vector Analysis." In *Proceedings of the 1st International Modal Analysis Conference*, Orlando, Florida, 110-116.
- Bighamian, R. and Mirdamadi, H. R. (2013). "Input/Output System Identification of Simultaneous Mass/Stiffness Damage Assessment Using Discrete - Time Pulse Responses, Differential Evolution Algorithm, and Equivalent Virtual Damped SDOF." *Structural Control and Health Monitoring*, 20(4), 576-592.
- Benzoni, G., Bonessio, N., and Lomiento, G. (2012). "Preliminary Shake Table Tests on the Bridge Model." Unpublished Manuscript, University of California San Diego, California, United States of America.
- Catbas, F. N., Brown, D. L., and Aktan, A. E. (2006). "Use of Modal Flexibility for Damage Detection and Condition Assessment: Case Studies and Demonstrations on Large Structures." *Journal of Structural Engineering*, 132(11), 1699-1712.
- Cawley, P. and Adams, R. D. (1979). "The Location of Defects in Structures from Measurements of Natural Frequencies." *Journal of Strain Analysis*, 14(2), 49-57.
- Cattarius, J. and Inman, D. J. (1997). "Time Domain Analysis for Damage Detection in Smart Structures." *Mechanical Systems and Signal Processing*, 11(3), 409-423.
- Choi, S. H. and Park, S. Y. (2003). "Nondestructive Damage Identification in a Truss Structure Using Time Domain Responses." *Journal of the Earthquake Engineering Society of Korea*, 7(4), 89-95.
- Choy, F. K., Liang, R., and Xu, P. (1995). "Fault Identification of Beams on Elastic Foundation." *Computers and Geotechnics*, 17(2), 157-176.

- Cornwell, P., Doebling, S. W., and Farrar, C. R. (1999). "Application of the Strain Energy Damage Detection Method to Plate-Like Structures." *Journal of Sound and Vibration*, 224(2), 359-374.
- Curadelli, R. O., Riera, J. D., Ambrosini, D., and Amani, M. G. (2008). "Damage Detection by Means of Structural Damping Identification." *Engineering Structures*, 30(12), 3497-3504.
- Doebling, S. W., Farrar, C. R., Prime, M. B., and Shevitz, D. W. (1996). "Damage Identification and Health Monitoring of Structural and Mechanical Systems from Changes in Their Vibration Characteristics: a Literature Review." Report No. LA-13070-MS, Los Alamos National Laboratory, New Mexico, United States of America.
- Farrar, C. R., Baker, W. E., Bell, T. M., Cone, K. M., Darling, T. W., Duffey, T. A., Eklund, A., and Migliori, A. (1994). "Dynamic Characterization and Damage Detection in the I-40 Bridge over the Rio Grande." Report No. LA-12767-MS, Los Alamos National Laboratory, New Mexico, United States of America.
- Farrar, C. and Jauregui, D. (1996). "Damage Detection Algorithms Applied to Experimental and Numerical Modal Data from the I-40 Bridge." Report No. LA-13074-MS, Los Alamos National Laboratory, New Mexico, United States of America.
- Frizzarin, M., Feng, M. Q., Franchetti, P., Soyoz, S., and Modena, C. (2010). "Damage Detection Based on Damping Analysis of Ambient Vibration Data." *Structural Control and Health Monitoring*, 17(4), 368-385.
- Gandomi, A. H., Sahab, M. G., and Rahai, A. (2011). "A Dynamic Nondestructive Damage Detection Methodology for Orthotropic Plate Structures." *Structural Engineering and Mechanics*, 39(2), 223-239.
- Gul, M. and Catbas, F. N. (2011). "Structural Health Monitoring and Damage Assessment Using a Novel Time Series Analysis Methodology with Sensor Clustering." *Journal of Sound and Vibration*, 330(6), 1196-1210.
- Hjelmstad, K. D. and Shin, S. (1996). "Crack Identification in a Cantilever Beam from Modal Response." *Journal of Sound and Vibration*, 198(5), 527-545.

- Huth, O., Feltrin, G., Maeck, J., Kilic, N., and Motavalli, M. (2005). "Damage Identification Using Modal Data: Experiences on a Prestressed Concrete Bridge." *Journal of Structural Engineering-ASCE*, 131(12), 1898-1910.
- Hyung, S. S. (2007). "Nondestructive Damage Detection by Simultaneous Identification of Stiffness and Damping." Doctoral Dissertation, Texas A&M University, College Station, Texas, United States of America.
- Johnson, E. A., Lam, H. F., Katafygiotis, L. S., and Beck, J. L. (2004). "Phase I IASC-ASCE Structural Health Monitoring Benchmark Problem Using Simulated Data." *Journal of Engineering Mechanics*, 130(1), 3-15.
- Just, F., Shafiq, B., Serrano, D., and Ortiz, M. (2006). "Damage Detection in Sandwich Composites Using Damping Matrix Identification." *Journal of the Mechanical Behavior of Materials*, 17(1), 17-30.
- Kang, J. S., Park, S. K., Shin, S., and Lee, H. S. (2005). "Structural System Identification in Time Domain Using Measured Acceleration." *Journal of Sound and Vibration*, 288(1), 215-234.
- Kiddy, J. and Pines, D. (1998). "Eigenstructure Assignment Technique for Damage Detection in Rotating Structures." *American Institute of Aeronautics and Astronautics Journal*, 36(9), 1680-1685.
- Ko, J. M., Wong, C. W., and Lam, H. F. (1994). "Damage Detection in Steel Framed Structures by Vibration Measurement Approach." In *Proceedings of the 12th International Modal Analysis*, 2251, 280-286.
- Lee, J. J., Lee, J. W., Yi, J. H., Yun, C. B., and Jung, H. Y. (2005). "Neural Networks-Based Damage Detection for Bridges Considering Errors in Baseline Finite Element Models." *Journal of Sound and Vibration*, 280(3), 555-578.
- Li, R. (2013). "Non-Destructive Damage Evaluation Based on Element Strain Energies." Master Thesis, Texas A&M University, College Station, Texas, United States of America.
- Lieven, N. A. J. and Ewins, D. J. (1988). "Spatial Correlation of Mode Shapes, the Co-Ordinate Modal Assurance Criterion (COMAC)." In *Proceedings of the 6th International Modal Analysis Conference*, 1, 690-695.



- Lin, S., Yang, J. N., and Zhou, L. (2005). "Damage Identification of a Benchmark Building For Structural Health Monitoring." *Smart Materials and Structures*, 14(3), S162.
- Lindner, D. K. and Kirby, G. (1994). "Location and Estimation of Damage in a Beam Using Identification Algorithms." In *Proceedings of 35th AIAA/ASME/ASCE/AHS/ASC Structures, Structural Dynamics and Materials Conference*, 192-198.
- Loland, O. and Dodds, C. J. (1976). "Experiences in Developing and Operating Integrity Monitoring System in North Sea." In *Proceedings of the 8th Annual Offshore Technology Conference 2*, OTC Paper No.2551, 313-319.
- Lopez, F. and Zimmerman, D. C. (2002). "Nonlinear Damage Detection Using a Time-Domain Minimum Rank Perturbation Theory." In *Proceedings SPIE, The International Society for Optical Engineering*, 4702, 179-190.
- Ma, T. W., Yang, H. T., and Chang, C. C. (2004). "Direct Damage Diagnosis of Structural Component Using Vibration Response." *NDE for Health Monitoring and Diagnostics*, 192-200.
- Majumder, L. and Manohar, C. S. (2003). "A Time-Domain Approach for Damage Detection in Beam Structures Using Vibration Data with a Moving Oscillator as an Excitation Source." *Journal of Sound and Vibration*, 268(4), 699-716.
- Pandey, A. K., Biswas, M., and Samman, M. M. (1991). "Damage Detection from Changes in Curvature Mode Shapes." *Journal of Sound and Vibration*, 145(2), 321-332.
- Pandey, A. K. and Biswas, M. (1994). "Damage Detection in Structures Using Changes in Flexibility." *Journal of Sound and Vibration*, 169(1), 3-17.
- Peterson, L. D., Alvin, K. F., Doebling, S. W., and Park, K. C. (1993). "Damage Detection Using Experimentally Measured Mass and Stiffness Matrices." In *Proceedings of 34th AIAA/ASME/ASCE/AHS/ASC Structures, Structural Dynamics, and Materials Conference*, 1, 1518-1528.

- Qu, W. and Peng, Q. (2007). "Damage Detection Method for Vertical Bars of Mast Structure in Time Domain." *Earthquake Engineering and Engineering Vibration-Chinese Edition*-, 27(5), 110.
- Raghavendrchar, M. and Aktan, A. E. (1992). "Flexibility by Multi-reference Impact Testing for Bridge Diagnostics." *ASCE Journal of Structural Engineering*, 118(8), 2186-2203.
- Rizos, P. F., Aspragathos, N., and Dimarogona, A. D. S. (1990). "Identification of Crack Location and Magnitude in a Cantilever Beam from the Vibration Modes." *Journal of Sound and Vibration*, 138(3), 381-388.
- Rytter, A. (1993). "Vibration Based Inspection of Civil Engineering Structures." Doctoral Dissertation, University of Aalborg, Aalborg, Denmark.
- Sheinman, I. (1996). "Damage Detection and Updating of Stiffness and Mass Matrices Using Mode Data." *Computers and Structures*, 59(1), 149-156.
- Shin, S. and Oh, S. H. (2007). "Damage Assessment of Shear Buildings By Synchronous Estimation Of Stiffness and Damping Using Measured Acceleration." *Smart Structures and Systems*, 3(3), 245-261.
- Shinozuka, M., Lee, S., Kim, S., and Chou, P. H. (2011). "Lessons from Two Field Tests on Pipeline Damage Detection Using Acceleration Measurement." *Smart Structures and Materials, Nondestructive Evaluation and Health Monitoring*, 7983, 798328-798328.
- Stubbs, N., Kim, J. T., and Topole, N. G. (1992). "An Efficient and Robust Algorithm for Damage Localization in Offshore Platforms." *10th Structures Congress*, San Antonio, Texas, 543-546.
- Stubbs, N. and Kim, J. T. (1996). "Damage Localization in Structures without Baseline Modal Parameters." *American Institute of Aeronautics and Astronautics Journal*, 34(8), 1644-1649.
- Trickey, S., Todd, M. D., Seaver, M. E., and Nichols, J. M. (2002). "Geometric Time-Domain Methods of Vibration-Based Damage Detection." *NDE for Health Monitoring and Diagnostics*, 113-121.

- Zhang, Z. and Aktan, A. E. (1995). "The Damage Indices for the Constructed Facilities." In Proceedings of the 13th International Modal Analysis Conference, 2, 1520-1529.
- Zhang, J., Xu, Y. L., Li, J., Xia, Y., and Li, J. C. (2013). "Statistical Moment-Based Structural Damage Detection Method in Time Domain." Earthquake Engineering and Engineering Vibration, 12(1), 13-23.
- Zhong, S., Oyadiji, S. O., and Ding, K. (2008). "Response-Only Method for Damage Detection of Beam-Like Structures Using High Accuracy Frequencies with Auxiliary Mass Spatial Probing." Journal of Sound and Vibration, 311(3), 1075-1099.
- Zimin, V. D. and Zimmerman, D. C. (2009). "Structural Damage Detection Using Time Domain Periodogram Analysis." Structural Health Monitoring, 8(2), 125-135.

## **APPENDIX**

### **NUMERICAL VALIDATION OF THE PROPOSED THEORY**

#### **A.1 INTRODUCTION**

The objective of the Appendix A is to verify the proposed process that was used to detect damage in the UCSD shake table tests. To verify this proposed process, a group of data was generated from the finite element model of the bridge model.

#### **A.2 DESCRIPTION OF THE FINITE ELEMENT MODEL**

In SAP2000, a one-bay frame was built and the properties of the cross sections of the frame were adjusted to simulate the real structure. The one-bay frame is plotted in Figure 8.6. The height of each column is 81 inches. The beam of the one-bay frame is designed to simulate the steel deck in the real structure and the length of the beam is 108 inches. In the finite element model, the moment of inertia of the cross section of the undamaged column is  $178.532 \text{ in}^4$  in X-direction and  $74.792 \text{ in}^4$  in Y-direction. The moment of inertia of cross section of the damaged portion in the south column is simulated as  $115.096 \text{ in}^4$  (around 35.5% reduction for the damaged section) in X-direction bending and  $70.212 \text{ in}^4$  (around 6.1% reduction for the damaged section) in Y-direction bending. The cross-sectional area of the undamaged column is  $13.76 \text{ in}^2$ . The cross-sectional area of the damaged portion of the south column is  $11.63 \text{ in}^2$  (around 15.5% reduction for the damaged section). The mass per unit length of the undamaged column is adjusted so that the total weight for the undamaged north column is around 0.891 kips. The total weight of the damaged south column is around 0.88 kips. The mass difference between the north column and the south column is caused by the removal of the lower west channel section

from the south column. The damping coefficients in the finite element model are assumed. The damping coefficients for the undamaged column portion are 0.025 for ' $C_m$ ' and 0.015 for ' $C_k$ '. The damping coefficients for the damaged column portion are 0.03 for ' $C_m$ ' and 0.02 for ' $C_k$ '.

The moment of inertia of the beam element in X direction bending is  $116.64 \text{ in}^4$  and the moment of inertia of the beam element in Z direction bending is  $12533.9 \text{ in}^4$ . The moment of inertia of the beam element is set according to the equivalent moment of inertia of the steel deck in the real bridge model. The cross-sectional area of the beam is  $8.86 \text{ in}^2$ . The total weight of the beam element is 5.835 kips (2.24 kips from the self-weight of the steel deck and 3.6 kips from the steel plates on the top of the steel deck).

Because the designed damage scenario is similar to the damage scenario of Test #18 from the shake table tests, the finite element model is excited using the base accelerations from Test #18 (i.e. Accelerations in the global X direction). Using the linear direction integration method within SAP2000, the displacement records at the top ends of the two columns can be outputted.

According to the modal analysis using the SAP2000, the first mode of the finite element model is the bending mode in the global X direction at 8.40 Hz; the second mode of the finite element model is the torsional mode around the global Z direction at 9.47 Hz; the third mode is the bending mode in the global Y direction at 10.26 Hz. The natural frequencies detected for the finite element model are larger than the real bridge model. The natural frequencies detected for the real bridge model by researchers in UCSD are: (1) around 3.5 Hz for the bending mode in the global X direction; (2) around 3.9 Hz for

the bending mode in the global Y direction; (3) around 7.5 Hz for the torsional mode around the global Z direction. The differences between the natural frequencies from the finite element model and the natural frequencies from the real bridge model might be caused by the following factors:

- (1) The finite element model built within SAP2000 is a simplified equivalent bar-joint model instead of a detailed 3D model with shell elements.
- (2) The parts in real bridge model are connected with bolts. However, it is hard to simulate these bolted connections even in the very detailed finite element model.

### A.3 NOISE SIMULATION

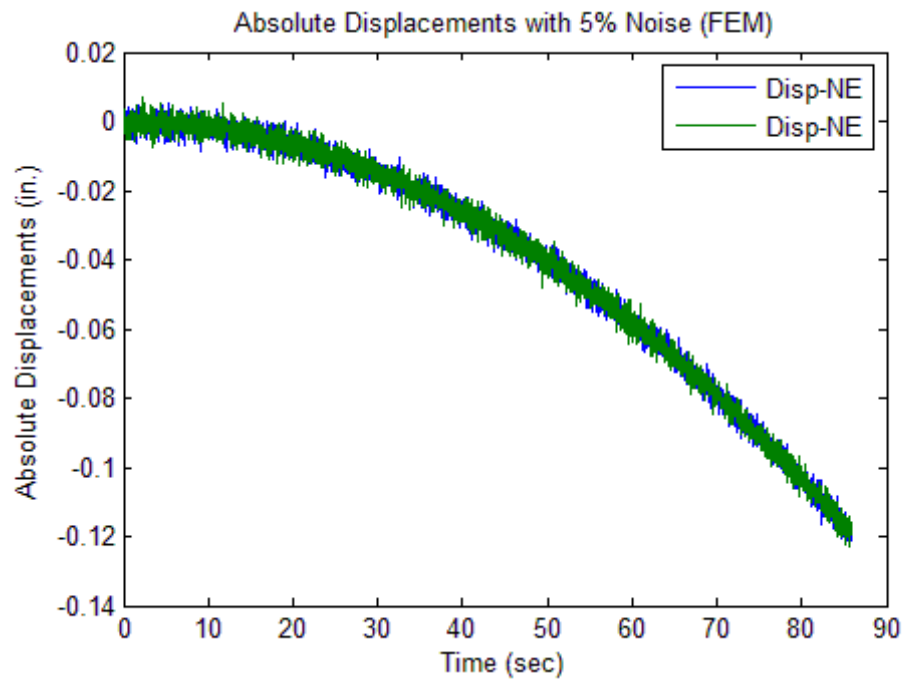
One of the main objectives of the Appendix A is to test the noise-tolerant capacity of the proposed process. According to the computation in Section 8, the noise levels in the displacement records from shake table tests are around 3%. To simulate the noise in the displacement records, 6% of white noise was superimposed into the exact displacement records which are directly outputted from SAP2000.

The noise-polluted displacements are computed using the following equation,

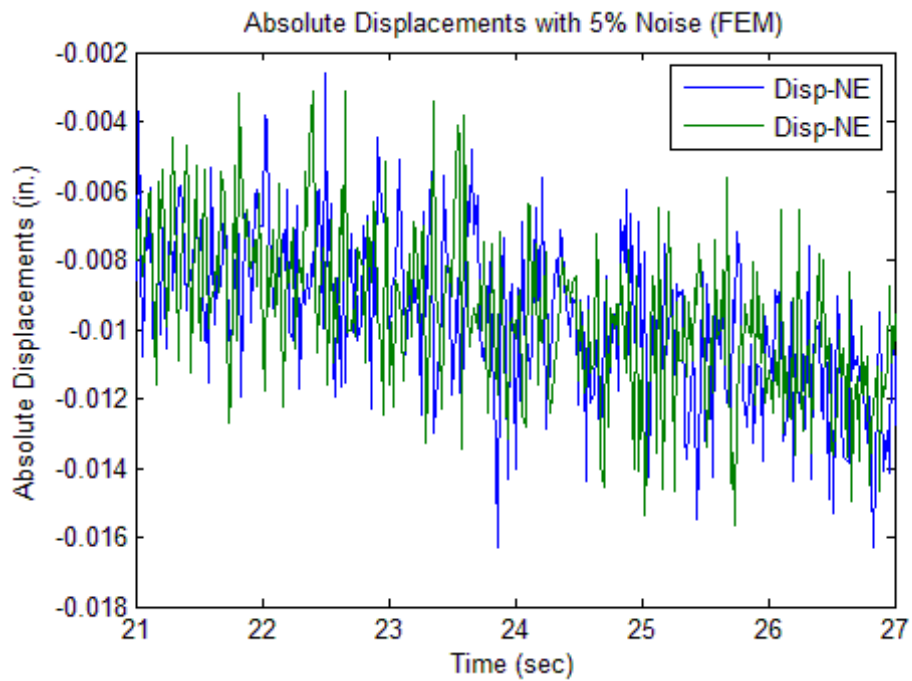
$$S_{noise}(t_i) = S_{pure}(t_i) + w(t_i) \cdot \rho \cdot \frac{std(S_{pure})}{std(w)} \quad (A.1)$$

Where  $S_{noise}(t_i)$  is the noise-polluted displacement at time  $t_i$ ;  $S_{pure}(t_i)$  is the exact displacement at time  $t_i$ ;  $w(t_i)$  is the random white noise at time  $t_i$ ;  $\rho$  is the percent of noise selected to add into the pure acceleration data;  $std(x)$  indicates the standard deviation of vector  $x$ .

However, due to the limitation of the capacity of the personal computer, only the behavior of the model within the first 8.58 seconds was computed. The displacements at the top ends of the two columns are closed to parabolas and are quite close to each other, which are given in Figure A.1. If the 6% white noise is directly superimposed onto the absolute displacement records, the noise level will be too big comparing to the real case, which is shown in Figure A.2. However, if we add the 6% white noise into the relative displacement records, which is shown in Figure A.3, then numerical case will match the real case better. Thus two groups of 6% white noise were superimposed onto the relative displacement records at the two top ends of the north and south columns. For comparison purposes, the relative displacement records from the real bridge model measured from Test #18 are plotted in Figure A.4.



(a)



(b)

**Figure A.1. The Absolute Displacements at the Top Ends of the North and South Columns with 6% White Noise from Finite Element Model: (a) Full Plot and (b) Zoomed in Plot**



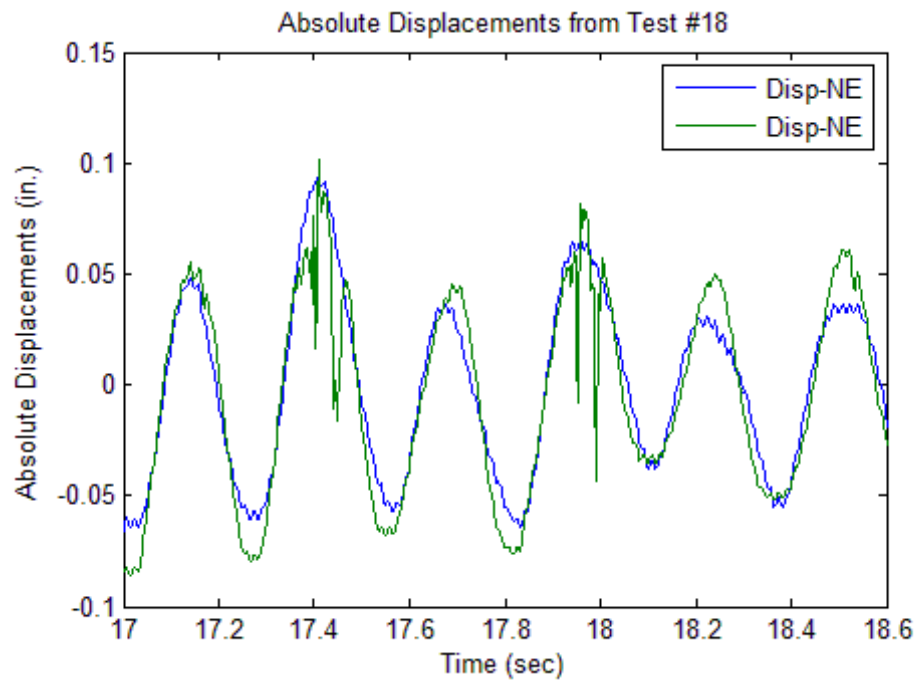
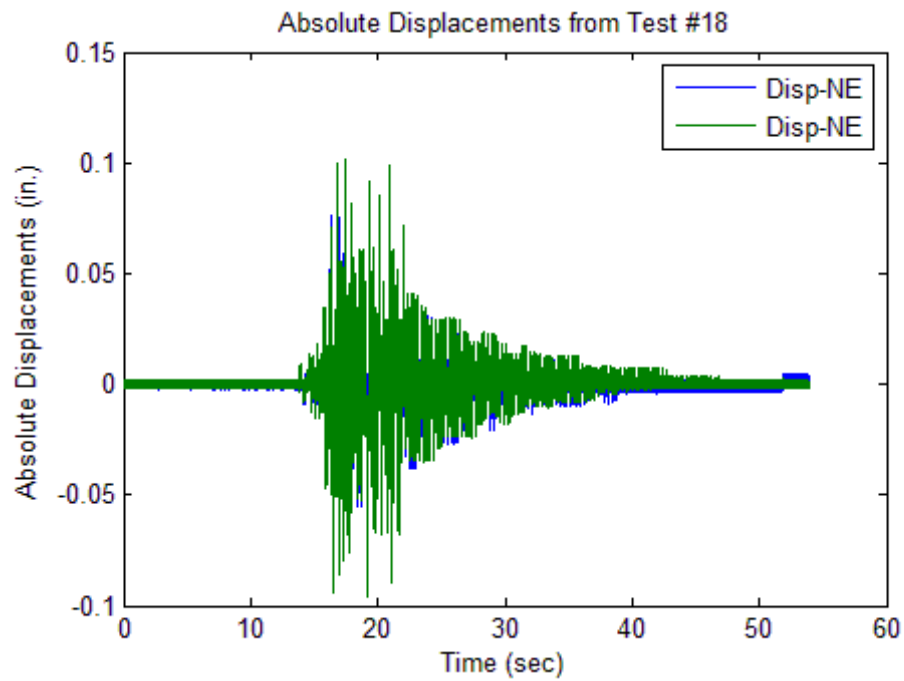
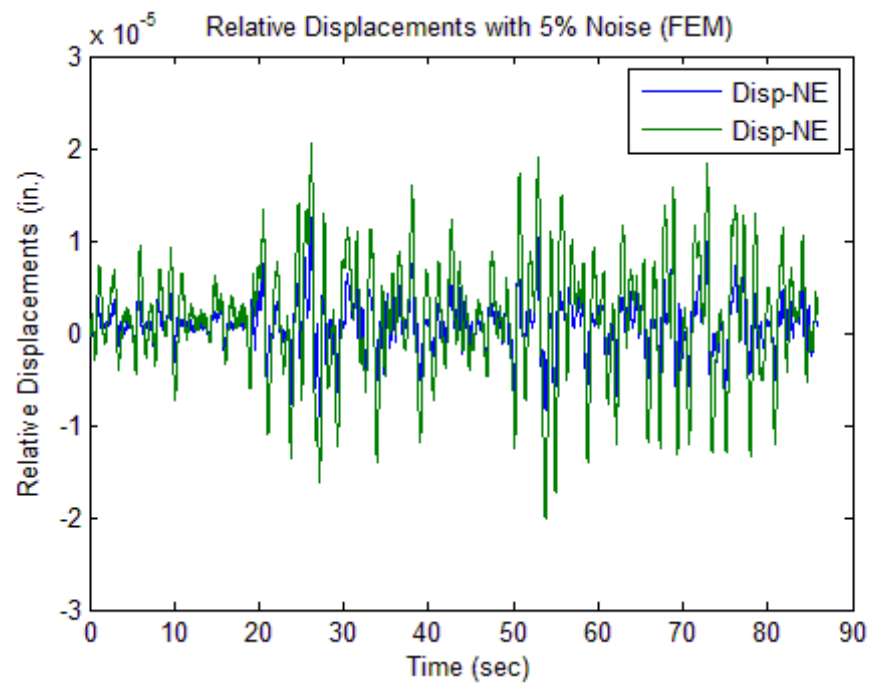
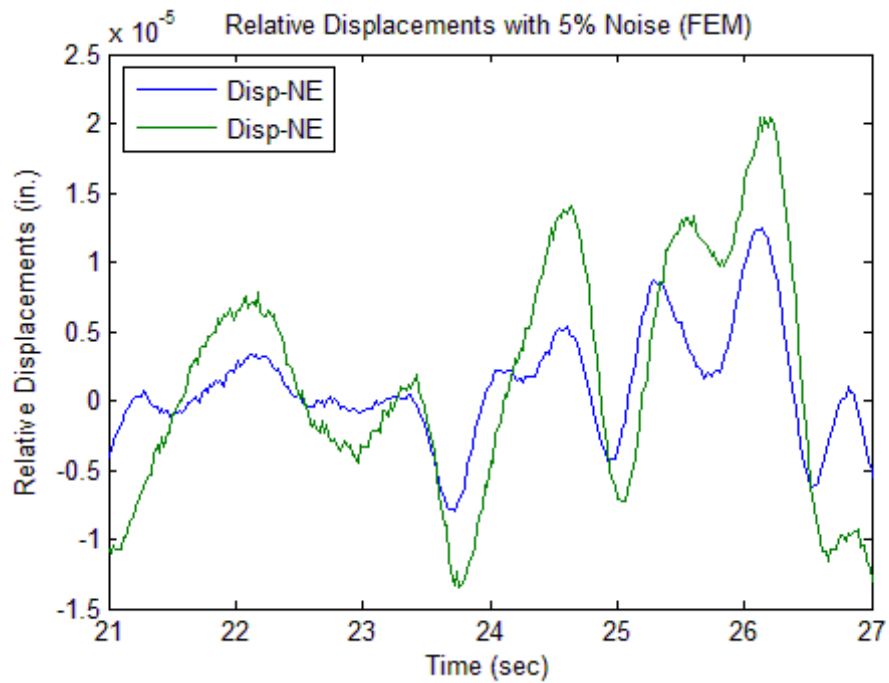


**Figure A.2. The Absolute Displacements at the Top Ends of the North and South Columns from Test #18 of the Shake Table Tests: (a) Full Plot and (b) Zoomed in Plot**

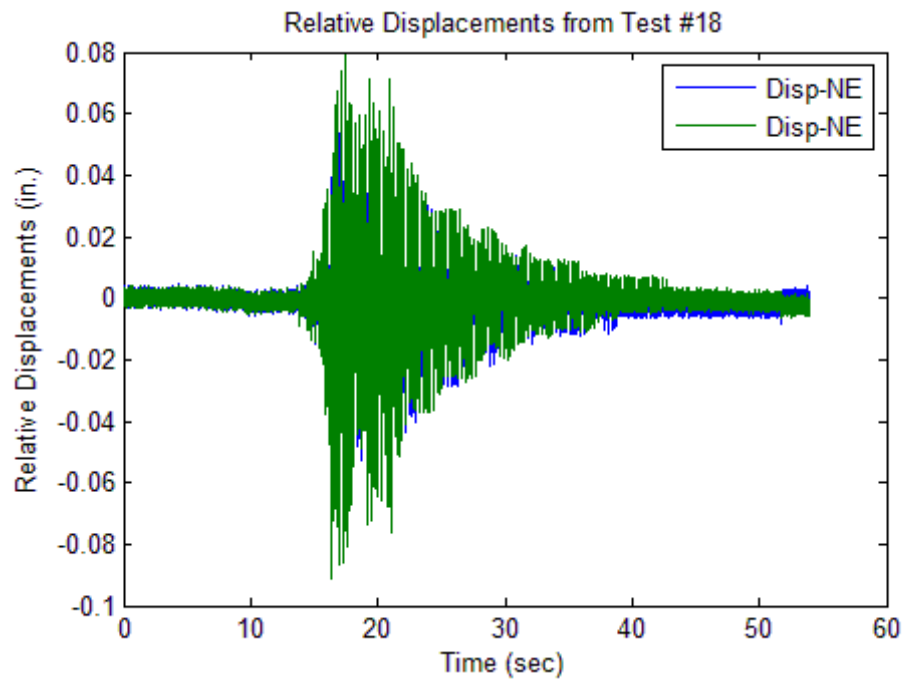


(a)

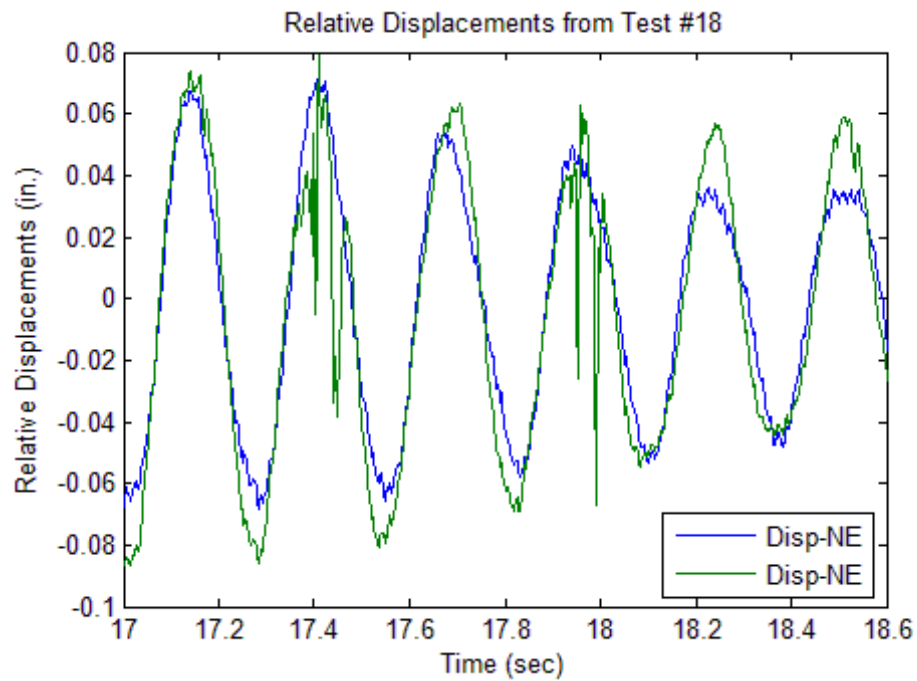


(b)

**Figure A.3. The Relative Displacements at the Top Ends of the North and South Columns with 6% White Noise from Finite Element Model: (a) Full Plot and (b) Zoomed in Plot**



(a)



(b)

**Figure A.4. The Relative Displacements at the Top Ends of the North and South Columns from Test #18 of the Shake Table Tests: (a) Full Plot and (b) Zoomed in Plot**

Note that the sudden changes shown in Figure A.4(b) will only appears at limited peaks of the displacement records, thus, the influence of these sudden changes can be reduced by the application of the digital bandpass filters.

#### **A.4 DAMAGE EVALUATION RESULTS**

Firstly, the theory of approach introduced in Section 8.3 and data processing techniques introduced in Section 8.4 were used to detect damage in the finite element model described in Section A.2. When the white noise level is 6%, ten groups of results are computed and are shown in Table A.1.

Secondly, the theory of approach introduced in Section 8.8.1 and data processing techniques introduced in Section 8.4 were used to detect damage in the finite element model described in Section A.2. When the white noise level is 6%, ten groups of results are computed and are shown in Table A.2.

**Table A.1. Damage Detection Results without Considering Element Damping**

Expr. Num.	Damage Index		Damage Severity	
	$\beta_m$	$\beta_k$	$\alpha_m$	$\alpha_k$
Expr. 1	1.021	1.269	-0.02	-0.21
Expr. 2	1.012	1.245	-0.01	-0.20
Expr. 3	1.019	1.268	-0.02	-0.21
Expr. 4	1.009	1.231	-0.01	-0.19
Expr. 5	1.020	1.264	-0.02	-0.21
Expr. 6	1.017	1.253	-0.02	-0.20
Expr. 7	1.017	1.253	-0.02	-0.20
Expr. 8	1.019	1.270	-0.02	-0.21
Expr. 9	1.018	1.265	-0.02	-0.21
Expr. 10	1.015	1.255	-0.02	-0.20

**Table A.2. Damage Detection Results with Element Damping**

Expr. Num.	Damage Index			Damage Severity		
	$\beta_m$	$\beta_k$	$\beta_{ak}$	$\alpha_m$	$\alpha_k$	$\alpha_{ak}$
Expr. 1	1.022	1.301	0.958	-0.02	-0.23	0.04
Expr. 2	1.016	1.284	0.958	-0.02	-0.22	0.04
Expr. 3	1.017	1.279	0.943	-0.02	-0.22	0.06
Expr. 4	1.016	1.291	0.979	-0.02	-0.23	0.02
Expr. 5	1.019	1.279	0.947	-0.02	-0.22	0.06
Expr. 6	1.022	1.297	0.960	-0.02	-0.23	0.04
Expr. 7	1.022	1.297	0.960	-0.02	-0.23	0.04
Expr. 8	1.022	1.302	0.953	-0.02	-0.23	0.05
Expr. 9	1.020	1.307	0.969	-0.02	-0.24	0.03
Expr. 10	1.020	1.295	0.954	-0.02	-0.23	0.05

## **A.5 RESULTS DISCUSSION**

According to Table A.1, the damage severity of the stiffness of the right column is stable at 20% to 21% decrease and the damage severity of the mass of the right column is stable at 1% to 2% decrease. According to the third row in Table 8.5, the designed damage severity of the stiffness of the right column is 22.3% decrease. The results from Table A.1 provide an accurate estimation to the designed damage.

According to Table A.2, the damage severity of the stiffness of the right column is stable at 22% to 23% decrease, the damage severity of the mass of the right column is stable at 2% decrease and the damage severity of the damping of the right column is stable at 4% to 6% increase. According to the third row in Table 8.5, the designed damage severity of the stiffness of the right column is 22.3%. The influence of the designed damage to the mass of right column can be ignored. According to the settings of the physical properties of the frame in Section A.2, the damping coefficient related to column stiffness ( $C_k$ ) is increased from 0.15 to 0.2 after damage. Thus the designed damage severity for the damaged portion of the column is a 33.3% increase. However, since the theory introduced in Section 8.8.1 considers the damping damage for the whole south column, the designed damping damage severity of the whole column should be smaller than 33.3%. Also the noise superimposed into the displacement data may also contribute to the reduction of the damage severity of damping coefficient. Thus, the detected damping damage, which is 4% to 6%, can be reasonable. Thus, the results from Table A.2 provide an accurate estimation to the designed damage.

## **A.6 SENSITIVITY ANALYSIS**

In this subsection, the sensitivity of the proposed method to white noise will be studied.

For the given numerical model, the exact displacement time histories will be computed from SAP2000. By mixing with different white noise, the noise-polluted displacement data is generated. The white noise level varies from 2% to 20% with 2% increment.

Then the theory of approach introduced in Section 8.3 and data processing techniques introduced in Section 8.4 were used to detect damage using the noise-polluted displacement data. For each noise level, damage detection results from ten numerical experiments were collected. Under the designed different noise level, the damage detection results using a constant combination velocity vector (i.e.  $[1,1,1]$  in this case) are reported in Table A.3. Under the designed different noise level, the damage detection results using a variable combination velocity vector (i.e.  $[1, \text{transverse velocity at the top of the north column, transverse velocity at the top of the south column}]$  in this case) are reported in Table A.4. According to the summary of the damage detection results from Table A.5 and Table A.6, the following noise sensitivity figure is plotted.

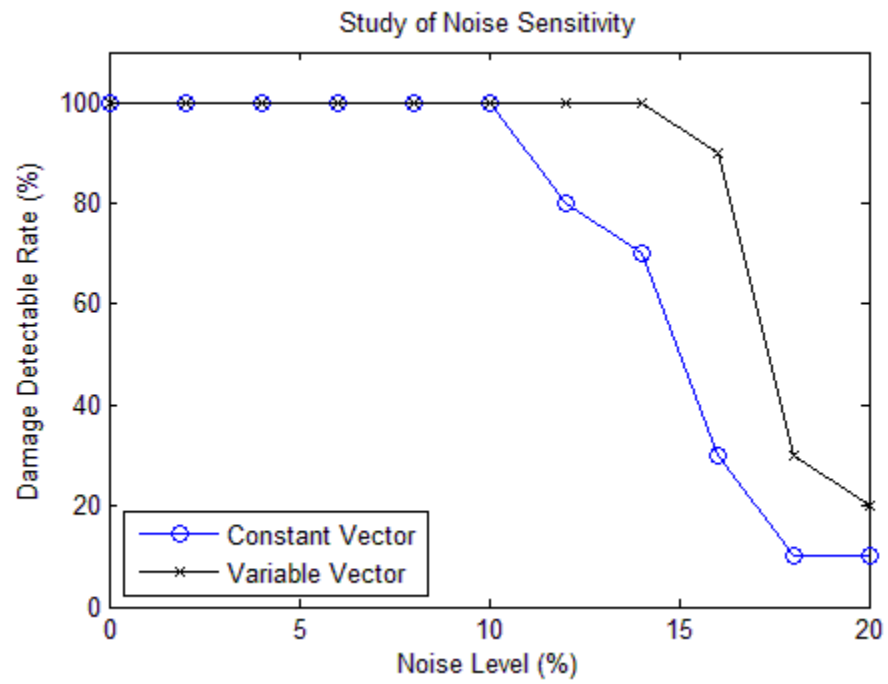


**Figure A.5. Study of the Noise Sensitivity of the Power Method**



**Table A.7. Damage Detection Results with Different Noise Level Using Constant Velocity Vector**

Noise Level	2%		4%		6%		8%		10%	
Expr. Num.	$\beta_m$	$\beta_k$	$\beta_m$	$\beta_k$	$\beta_m$	$\beta_k$	$\beta_m$	$\beta_k$	$\beta_m$	$\beta_k$
Expr. 1	0.9698	1.3112	0.9747	1.3020	0.9717	1.3063	0.9920	1.2344	1.0048	1.1813
Expr. 2	0.9723	1.3035	0.9749	1.2966	0.9733	1.3061	0.9948	1.2356	1.0073	1.1683
Expr. 3	0.9759	1.2959	0.9721	1.3064	0.9730	1.3047	0.9951	1.2291	0.9997	1.2069
Expr. 4	0.9725	1.3061	0.9706	1.3100	0.9743	1.3027	0.9984	1.2179	1.0114	1.1769
Expr. 5	0.9727	1.3063	0.9699	1.3115	0.9711	1.3076	0.9915	1.2425	1.0125	1.1352
Expr. 6	0.9744	1.2986	0.9721	1.3075	0.9710	1.3075	0.9740	1.3021	0.9717	1.3067
Expr. 7	0.9706	1.3087	0.9733	1.3059	0.9721	1.3077	0.9703	1.3104	0.9709	1.3103
Expr. 8	0.9697	1.3132	0.9729	1.3045	0.9715	1.3099	0.9699	1.3103	0.9707	1.3077
Expr. 9	0.9727	1.3059	0.9727	1.3067	0.9735	1.3052	0.9746	1.3007	0.9699	1.3107
Expr. 10	0.9720	1.3054	0.9704	1.3090	0.9744	1.3028	0.9720	1.3070	0.9758	1.2992
Damage Detectable Rate	10/10		10/10		10/10		10/10		10/10	

Noise Level	12%		14%		16%		18%		20%	
Expr. Num.	$\beta_m$	$\beta_k$	$\beta_m$	$\beta_k$	$\beta_m$	$\beta_k$	$\beta_m$	$\beta_k$	$\beta_m$	$\beta_k$
Expr. 1	1.0237	1.0138	1.0336	0.8608	1.0338	0.9644	1.0593	0.2975	1.0718	0.4899
Expr. 2	1.0187	1.0845	1.0285	1.0036	1.0365	0.8249	1.0398	0.9928	1.0557	0.7335
Expr. 3	1.0253	0.9845	1.0218	1.0836	1.0346	0.9450	1.0674	1.7576	1.0786	4.3967
Expr. 4	1.0238	0.9452	1.0228	1.0615	1.0386	0.7957	1.0534	0.4363	1.0515	0.8548
Expr. 5	1.0122	1.1569	1.0295	0.9228	1.0376	0.9708	1.0553	0.4099	1.0519	0.7644
Expr. 6	1.0184	1.0874	1.0243	1.1019	1.0258	1.0788	1.0489	0.6487	1.0508	0.8908
Expr. 7	1.0196	1.0681	1.0351	0.8412	1.0327	1.0690	1.0448	0.8948	1.0607	0.2352
Expr. 8	1.0207	1.0712	1.0267	1.0046	1.0260	1.0630	1.0647	0.3579	1.0586	0.5737
Expr. 9	1.0090	1.1619	1.0249	1.0346	1.0392	0.8565	1.0517	0.7059	1.0623	0.6329
Expr. 10	1.0138	1.1150	1.0252	1.0104	1.0402	0.7298	1.0511	0.7313	1.0542	0.6612
Damage Detectable Rate	8/10		7/10		3/10		1/10		1/10	

**Table A.8. Damage Detection Results with Different Noise Level Using Variable Velocity Vector**

Noise Level	2%		4%		6%		8%		10%	
Expr. Num.	$\beta_m$	$\beta_k$	$\beta_m$	$\beta_k$	$\beta_m$	$\beta_k$	$\beta_m$	$\beta_k$	$\beta_m$	$\beta_k$
Expr. 1	0.9736	1.2871	0.9774	1.2784	0.9738	1.2864	0.9798	1.2598	1.0013	1.1846
Expr. 2	0.9754	1.2811	0.9781	1.2720	0.9766	1.2810	0.9867	1.2475	0.9981	1.1931
Expr. 3	0.9794	1.2712	0.9741	1.2851	0.9747	1.2857	0.9962	1.2016	0.9887	1.2383
Expr. 4	0.9749	1.2851	0.9736	1.2859	0.9775	1.2788	0.9865	1.2507	1.0067	1.1707
Expr. 5	0.9752	1.2845	0.9734	1.2879	0.9743	1.2850	0.9875	1.2394	1.0067	1.1538
Expr. 6	0.9759	1.2808	0.9752	1.2841	0.9751	1.2823	0.9765	1.2798	0.9759	1.2802
Expr. 7	0.9735	1.2872	0.9773	1.2795	0.9744	1.2872	0.9747	1.2841	0.9735	1.2889
Expr. 8	0.9750	1.2849	0.9738	1.2877	0.9741	1.2876	0.9758	1.2800	0.9738	1.2857
Expr. 9	0.9745	1.2870	0.9755	1.2836	0.9757	1.2834	0.9781	1.2767	0.9740	1.2856
Expr. 10	0.9758	1.2806	0.9745	1.2848	0.9761	1.2829	0.9755	1.2827	0.9768	1.2807
Damage Detectable Rate	10/10		10/10		10/10		10/10		10/10	
Noise Level	12%		14%		16%		18%		20%	
Expr. Num.	$\beta_m$	$\beta_k$	$\beta_m$	$\beta_k$	$\beta_m$	$\beta_k$	$\beta_m$	$\beta_k$	$\beta_m$	$\beta_k$
Expr. 1	1.0164	1.0719	1.0189	1.0499	1.0209	1.0629	1.0391	0.8471	1.0592	0.1266
Expr. 2	1.0061	1.1580	1.0105	1.1296	1.0204	1.0434	1.0305	1.0312	1.0349	0.9918
Expr. 3	1.0036	1.1718	1.0094	1.1453	1.0241	1.0170	1.0482	0.4292	1.0397	0.7989
Expr. 4	1.0091	1.1185	1.0118	1.1381	1.0296	0.9339	1.0454	0.5464	1.0389	0.9230
Expr. 5	1.0007	1.1988	1.0100	1.1239	1.0152	1.1230	1.0335	0.9308	1.0340	0.9436
Expr. 6	1.0110	1.1305	1.0149	1.1177	1.0106	1.1540	1.0311	0.9585	1.0361	1.0003
Expr. 7	1.0054	1.1691	1.0239	1.0199	1.0280	1.0867	1.0210	1.0897	1.0221	1.0165
Expr. 8	1.0135	1.1098	1.0143	1.1077	1.0137	1.1268	1.0414	0.7777	1.0316	0.9528
Expr. 9	1.0022	1.1738	1.0187	1.0647	1.0238	1.0203	1.0364	0.9481	1.0421	0.9113
Expr. 10	1.0047	1.1631	1.0002	1.1821	1.0197	1.0503	1.0263	1.0280	1.0436	0.7512
Damage Detectable Rate	10/10		10/10		9/10		3/10		2/10	

## **A.7 CONCLUSION**

According to the analysis in Subsection A.4 and Subsection A.5, the proposed theory in Section 8 can be used to locate the damaged column and provide a close estimation the damage severities regarding to the whole column in the finite element model of the bridge model with 6% noise.

According to the analysis in Subsection A.6, the proposed theory will be able to locate damages under the given conditions up to 10% to 14% white noise depending the selected combination velocity vector, which is used to compute power. However, the sensitivity plot in Figure A.6 may not be generally ture for each situation. The sensitivity of the proposed method may vary from case to case. To find the general sensitivity of the proposed method, futher study is needed.